The Impact of Crohn's Disease on the Expression of Intestine Drug Metabolising Enzymes and Transporters - Implications in Oral Drugs Disposition

A thesis submitted to the University of Manchester for the degree of

Doctor of Philosophy

in the Faculty of Biology, Medicine and Health

2021

Sarah Alrubia

School of Health Sciences
Division of Pharmacy & Optometry

Contents

Word Count: 60,172

List of figures

List of supplementary figures

List of tables

List of supplementary tables

Abbreviations

% => Percent
ºC => Degrees Centigrade
ABC => ATP-binding Cassette Transporter Protein
ADH => Alcohol Dehydrogenase
ADME => Absorption, Distribution, Metabolism and Excretion
ADAM => Advanced Dissolution Absorption and Metabolism
α-1AGP => Alpha-1-Acid GlycoProtein
ALDH => Aldehyde Dehydrogenase
ALT => Alanine Aminotransferase
ALP => Alkaline Phosphatase
ALPI => Intestinal alkaline phosphatase
AmBic => Ammonium Bicarbonate
AOX => Aldehyde Oxidase
AQUA => Absolute Quantification Standards
ASBT => Apical Sodium-dependent Bile acid Transporter
AST => Aspartate Aminotransferase
ATP1A1 => ATPase Subunit Alpha-1
AUC => Area under the Plasma Concentration-time Curve
$AUC_{0-\infty}$ => Area under the Curve from Time 0 to Infinity
BCA => Bicinchoninic Acid
BCRP => Breast Cancer Resistance Protein
BMI => Body Mass Index
BSA => Body Surface Area
BSA => Bovine Serum Albumin
BSEP => Bile Salt Export Pump
BWT => Bowel Wall Thickness
CAR => Constitutive Androstane Receptor
CCR => Cytochrome C Reductase
CD => Crohn's Disease
CDH => Cadherin
CES => Carboxylesterase
CI => Confidence Interval
CI => Cardiac Index
CL => Clearance
$Cl_{int,H}$ => Hepatic Intrinsic Clearance
CL_H => Hepatic Clearance
CL_R => Renal Clearance
C_{max} => Maximum Plasma Concentration
CSH => Charged Surface Hybrid
Csys => Systemic Concentration
CNT2 => Concentrative Nucleoside Transporter
CO => Cardiac Output

CV => Coefficient of Variation
CYP => Cytochrome P450
Da => Dalton
DDA => Data-Dependent Acquisition
DDI => Drug-Drug Interaction
DDIs => Disease-Drug Interactions
DIA => Data-Independent Acquisition
DMEs => Drug Metabolising Enzymes
DMETs => Drug Metabolising Enzymes and Transporters
DTT => Dithiothreitol
EDTA => EthyleneDiamineTetraacetic Acid
E_G => Gut Extracted Ratio
E_H => Hepatic Extraction Ratio
ENT => Equilibrative Nucleoside Transporter
ENS => Enteric Nervous System
ESR => Erythrocyte Sedimentation Rate
ER => Extraction Ratio
EPHX => Epoxide Hydrolase
F => bioavailability
FASP => Filter Aided Sample Preparation
FDA => US Food and Drug Administration
FDR => False Discovery Rate
F_H => Drug Fraction Absorbed Through the Liver
F_{GI} => Drug Fraction Absorbed Through the Gut
FMO => Flavin-containing Monooxygenase
fu => fraction unbound
fu_B => blood fraction unbound
g => Gram
g => Gravity
GSA => Global Sensitivity Analysis
GIT => Gastrointestinal Tract
GST => Glutathione S-Transferase
GPX => Glutathione Peroxidase
h => Hour
HEPES => 4-(2-hydroxyethyl)-1-piperazineethenesulfonic Acid
HiN => High Ion Intensity Approach
HIM => Human Intestine Microsomes
HN-CD => Histologically Normal Crohn's Disease
HNF4α => Hepatocyte Nuclear Factor 4α
HSA => Human Serum Albumin
HPLC => High-performance Liquid Chromatography
HV => Healthy Volunteers
IAA => Iodoacetamide
IBD => Inflammatory Bowel Disease

I-CD => Inflamed Crohn's Disease
IEC => Intestine Epithelial Cells
IL => Interleukin
INF => Interferon
iTRAQ => Isobaric Tags for Relative and Absolute Quantitation
IV => Intravenous
IVIVE => *In Vitro-In Vivo* Extrapolation
kDa => Kilo Dalton
Kp => Partition Coefficient
KinCAT => Concatemer of Standard Peptides from Human Receptor Tyrosine Kinases
LC => Liquid Chromatography
LC-MS => Liquid Chromatography-Mass Spectrometry
LIT => Linear Ion Trap
LLOQ => Lower Limit of Quantification
LysC => Lysine C
M-ADAM => Multilayer-Advanced Dissolution Absorption and Metabolism
MAO => Monoamine Oxidase
MATE => Multidrug and Toxin Extrusion Protein
MCT1 => Monocarboxylate Transporter 1
MDR => Multidrug Resistance Protein
MDZ => Mdazolam
MetCAT => Concatemer of Standard Peptides from Human Drug Metabolizing Enzymes
MGST => Microsomal Glutathione S-Transferase
min => Minute
MIPD => Model-Informed Precision Dosing
µM => Millimolar
MRM => Multiple Reaction Monitoring
mRNA => Messenger Ribonucleic Acid
MRP => Multidrug Resistance-associated Protein
MS/MS => Tandem Mass Spectrometry
MS => Mass Spectrometry
MS^E => Mass Spectrometry by Collision Energy Alternation
MWt => Molecular Weight
MWCO => Molecular Weight Cut Off
m/z => Mass-to-charge Ratio
n => Number of observations
NAT => N-acetyltransferase
NNOP => Non-naturally Occurring Peptide
NTCP => Sodium-dependent Uptake Transporter
Nrf2 => Transcription Factor Nuclear Factor E2-Related Factor 2
NuncCAT => Non-UGT Non-CYP Metabolic Enzymes QconCAT
OAT => Organic Anion Transporter Protein
OATP => Organic Anion Transporting Polypeptide
OCT => Organic Cation Transporter Protein

OCTN => Organic Cation/Carnitine Transporter
OST => Organic Solute Transporter
p= albumin concentration
P-gp => P-glycoprotein
PBPK => Physiology-Based Pharmacokinetics
PCA => Principal Components Analysis
PD => Pharmacodynamics
PEPT1 => Peptide transporter 1
pI => Isoelectric Point
PI => Protease Inhibitors
PIP => Percentage Identical Peptides
PIPr => Percentage Identical Proteins
PK => Pharmacokinetics
pKa => Acid Dissociation Constant at Logarithmic Scale
pmol => Picomole
PMI => Post Mortem Interval
PO => Oral
POR => NADPH-cytochrome P450 Reductase
ppm => Parts per Million
PSAQ => Protein Standards for Absolute Quantification
PTM => Post-Translational Modification
PXR => Pregnancy X Receptor
Q => Quadrupole
QC => Quality Control
QconCAT => Concatemer of Standard Peptides
QH => Hepatic blood flow
QSP => Quantitative Systems Pharmacology
RA => Rheumatoid Arthritis
rpm => Revolutions per Minute
SD => Standard Deviation
SDS => Sodium Dodecyl Sulfate
SI=> Small Intestine
SIL => Stable Isotope Labelled
SILAC => Stable Isotope Labelling in Cell Culture
SITT => Small Intestine-Transit Time
SLC => Solute Carrier Transporter Protein
SLCO => Solute Carrier Organic Ion Transporter Protein
SMA => Superior mesenteric artery
SNP => Single Nucleotide Polymorphism
S-Trap => Suspension Trapping
SRM => Selected Reaction Monitoring
SULT => Sulfotransferase
SWATH => Sequential Window Acquisition of All Theoretical Fragment Mass Spectra
TFA => Trifluoroacetic Acid

TJ => Tight Junction
T_{max} => Time at which Maximum Plasma Concentration
TMT => Tandem Mass Tags
TNF => Tumour Necrosis Factor
TOF => Time-of-flight
TPA => Total Protein Approach
TPMT => Thiopurine Methyltransferase
TXN => Thioredoxin
TransCAT => Concatemer of Standard Peptides from Human Transporters
UGT => Uridine 5′-diphospho-glucuronosyltransferase
VIP => Vasoactive Intestinal Polypeptide
Vss => Volume of Distribution
v/v => Volume by Volume
w/v => Weight by Volume

Amino Acids Abbreviations

Amino Acid	Abbreviation	
	Three Letters	One Letter
Alanine	Ala	A
Arginine	Arg	R
Asparagine	Asn	N
Aspartic Acid	Asp	D
Cysteine	Cys	C
Glutamic Acid	Glu	E
Glutamine	Gln	Q
Glycine	Gly	G
Histidine	His	H
Isoleucine	Ile	I
Leucine	Leu	L
Lysine	Lys	K
Methionine	Met	M
Phenylalanine	Phe	F
Proline	Pro	P
Serine	Ser	S
Threonine	Thr	T
Tryptophan	Trp	W
Tyrosine	Tyr	Y
Valine	Val	V

Abstract

Background: Crohn's disease (CD) is a chronic inflammatory bowel disease that impacts the intestine function; the drug metabolism enzymes and transporters (DMETs) are part of the affected variables. The observed inflammation effect on the enzymes and transporters causes alteration of the intestine absorption and metabolism capacity, hence, oral drug bioavailability. Dosing guidance and regulations for CD population are lacking. Importance of such practice implementation can be carried out via *in silico* physiologically-based pharmacokinetic (PBPK) modelling. The CD population is a heterogenic population, as different system parameters are altered differently in the active and remission phases of the disease.

Methods: Literature gap analysis was performed to collect the available information of system parameters that impact oral drug pharmacokinetics (PK) and identify the gaps hindering appropriate PBPK predictions in CD patients utilising Simcyp simulator. By experimentation, LC-MS/MS-based label free proteomics was carried out to generate *in vitro* abundance data of DMETs in CD tissue samples. The desired proteins were quantified in 8 and 12 diseased ileum and colon samples respectively, compared to 10 healthy samples. The determined proteins level were integrated into the created CD PBPK models to assess oral drug PK in CD population.

Results: The protein abundance of 61 and 48 DMETs in ileum and colon, respectively, decreased in inflamed and histologically normal homogenate samples of CD relative to healthy samples. The reduction of cytochrome P450 (CYP), UDP-glucuronosyltransferase (UGT) and non-CYP non-UGT enzymes, ATP-binding cassette (ABC) transporters and Solute Carriers (SLC) abundance in the tissues derived from CD subjects were comparable with varying levels of significance. Abundance values of proteins relevant to budesonide and midazolam were used in the created PBPK models of CD population to validate their predictive performance. Moreover, the PBPK models were used to investigate the PK profile of 10 oral drugs, where celecoxib, dabigatran etexilate, gemfibrozil, ritonavir, valsartan and verapamil demonstrated >2 fold change in their exposure in CD compared with healthy population.

Conclusion: To our knowledge, the work carried out in this thesis provides for the first time, direct protein abundance data of DMETs in histologically normal and inflamed ileum and colon tissues from individual CD patients. This proteomics data supports the development of CD PBPK models, which highlight the importance of using special population data to aid in guiding dose adjustments.

Declaration

Chapter Two has also been submitted in support of an application for another PhD qualification of The University of Manchester by Areti Maria Vasilogianni and Eman El-Khateeb (PhD students, University of Manchester). This is a published chapter, and the first three authors share the first-authorship:

El-Khateeb, E., Vasilogianni, A. M., **Alrubia, S**., Al-Majdoub, Z. M., Couto, N., Howard, M., Barber, J., Rostami-Hodjegan, A., & Achour, B. **(2019**). Quantitative mass spectrometry-based proteomics in the era of model-informed drug development: applications in translational pharmacology and recommendations for best practice. *Pharmacol Ther* **203**:107397.

No other portion of the work referred to in the thesis has been submitted in support of an application for another degree of qualification of this or any other university or other institute of learning.

Copyright statement

i. The author of this thesis (including any appendices and/or schedules to this thesis) owns certain copyright or related rights in it (the "Copyright") and she has given the University of Manchester certain rights to use such Copyright, including for administrative purposes.

ii. Copies of this thesis, either in full or in extracts and whether in hard or electronic copy, may be made **only** in accordance with the Copyright, Designs and Patents Act 1988 (as amended) and regulations issued under it or, where appropriate, in accordance with licensing agreements which the University has from time to time. This page must form part of any such copies made.

iii. The ownership of certain Copyright, patents, designs, trademarks and other intellectual property (the "Intellectual Property") and any reproductions of copyright works in the thesis, for example graphs and tables ("Reproductions"), which may be described in this thesis, may not be owned by the author and may be owned by third parties. Such Intellectual Property and Reproductions cannot and must not be made available for use without the prior written permission of the owner(s) of the relevant Intellectual Property and/or Reproductions.

iv. Further information on the conditions under which disclosure, publication and commercialisation of this thesis, the Copyright and any Intellectual Property and/or Reproductions described in it may take place is available at the University IP Policy (see https://documents.manchester.ac.uk/DocuInfo.aspx?DocID=24420), in any relevant Thesis restriction declarations deposited in the University Library, The University Library's regulations (see http://library.manchester.ac.uk/about/regulations/) and in The University's Policy on Presentation of Theses.

Dedication

To my mum Lubna, thank you for always believing in me.

I hope I do you proud.

Acknowledgments

At first, I would like to thank my supervisors, Dr. Jill barber and Prof. Amin Rostami- Hodjegan for their continuous support and guidance. I'm especially thankful for their encouragement to keep updated and connected with the industrial perspective of the work, which had made me gain confidence and opened new aspects for me during this PhD and in the future. I'm thankful to the government of the Kingdom of Saudi Arabia and King Saud University for funding this PhD. The faculty of Pharmaceutical Chemistry Department in KSU has helped me in sourcing and obtaining this scholarship and for that I'm grateful, especially for Prof. Nourh Alzoman. A special thank for my friend and work colleague Hanan Alshibl, one of the kindest people I've met, for helping me through the process and keeping me in contact with the department. Also, I am thankful for all the collaborators who provided the samples and the LC-MS analysis.

I started this PhD with two extraordinary colleagues who are now my dear friends, Dr. Areti Maria Vasilogianni and Dr. Eman El-Khateeb. Without their emotional and professional support, things would've been much harder and less fun. I was lucky to work alongside expert researchers within the Centre for Applied Pharmacokinetics Research (CAPKR). A special thanks to Dr. Zubida Al-Majdoub and Dr. Brahim Achour for providing advice, assistance and training throughout the PhD. I'm extremely appreciative to my Manchester friend Dr. Amira Alghamdi, who created a home away from home atmosphere, with her heart and house warmth.

I'm extremely grateful to my brother Abdullah for taking a big step and getting out of his comfort zone to make things easier for me. It was always enjoyable to have long philosophical discussions with my youngest brother Ahmed. Difficult moments are always easier when shared, for that I'm blessed to be surrounded by my sisters' team the strongest support network anyone can ask for. Mariam, Asmaa, Alaa and Maha and my dearest friends Shada and Lama. Our long calls and ceaseless texting created an unconditional vent for me at all times. The unplanned long calls Maha made where all of my sisters joined at some point made me feel at home and not very far away. The short catch-up calls interrupted by work gave me the energy to work so I can go back home and enjoy our long evenings. My mum's endless love and her satisfaction look made all the hardship I've been through worthwhile.

Last but not least, I'm indebted to my soulmate Bob, words can't express my gratitude for his support through the whole process. I couldn't have done it without you, you added the element of lightness to this journey. We have been through many unexpected and unusual events during

the four years of the PhD, and I was always your priority which greatly helped me to carry on when it felt unbearable anymore. For that, thank you for always being there for me, for your patience in listening to me complain about the lab work and my back pain countless times, for waiting for me when I had to work very late which warmed Manchester's cold nights, for taking the time and effort to accompany me in San Francisco for my internship, for being next to me during Covid19 pandemic assuring me during hard and uncertain times and for making me smile during the darkest moments in this PhD especially when there were no results and I thought I don't have a project. You had faith in me when I lost my faith and eased my stress which allowed me to deliver.

Preface

The work in this thesis is presented in the journal format. This format allows each section incorporated to be a potential publication in peer-reviewed journals. Thus far, this thesis consists of six separate but linked chapters, where two of the chapters are submitted to journals and some of the rest are yet to follow. This format maximises the possibility of publishing the research undertaken over the course of this PhD. The thesis consist of six research papers of which the thesis author is also the lead author. A declaration at the start of each chapter highlights the contribution of each author. The structure of the thesis is outlined below.

Crohn's disease (CD) is a chronic inflammatory bowel disease that predominantly affects the mucosal layer of ileum and colon segments. Most CD cases are diagnosed before the age of 30. CD patients receive many different drugs beyond those used for the disease itself. Oral drug bioavailability is influenced by the integrity of the intestine and abundance of intestinal drug metabolising enzymes and transporters (DMETs). Therefore, understanding the potential variations of these proteins in CD patients is essential. The heterogeneity of CD population complicate defining the alterations in the physiological parameters related to oral drug bioavailability encountered during the active and inactive phases of the disease. CD patients demonstrated variable responses in drug pharmacokinetics (PK), high rate of patient's relapse and treatment failure either due to drug's intolerable adverse events or inefficacy. Creation of model-informed precision dosing can aid in addressing such treatment limitations utilising *in vitro-in vivo* extrapolation (IVIVE) techniques and physiologically-based pharmacokinetic (PBPK) modelling. No designated PK studies on inflammatory bowel diseases (IBD) population are involved in the process of oral drug development. At the meantime, the regulatory authorities are supporting the inclusion of diverse patient populations in the clinical studies. In order to create a reliable *in silico* model, drug and population specific system parameters are crucial. Thus, this research project aims to identify the available oral drug related systems parameters and fill the gaps that hinders building a PBPK model for CD patients. This was done with a focus on the ileum and colon intestine segments' proteomic profile.

Firstly, a gap analysis (Chapter One) was conducted and aimed to gather the current available in-vitro and in-vivo knowledge of the adult CD population concerning potential differences from healthy individuals or non-CD patients. Assessment of the availability of drug

independent system parameters concerning intestinal drug disposition, and identification of the gaps that can be filled by this project was the primary objective to fulfil the aim of building a mechanistic model to predict the fate of oral drugs in CD population. In the literature, there is no wide coverage of the DMETs abundance in the intestine of CD patients. Therefore, the main focus of this PhD research is on generating DMETs abundance data using LC-MS based proteomics quantitative analysis. The feasibility of the proteomics experimental work and generation of the required data was evaluated. This was done firstly by conducting a comprehensive review (Chapter Two) of the available LC-MS proteomics methods and their applications in drug development. The information gathered in this review assisted with the selection of the appropriate LC-MS based quantitative proteomic method to be used for the intended purpose of this PhD. This was followed by an experimental examination (Chapter Three) of the different techniques that can be applied with the different proteomics methodology steps. The experimental evaluation included determination of the quality and type of information (Chapter Four and Five) that can be produced and expected when the proteomic work is conducted on a larger number of the intestine tissue samples with varying histological sources and properties. Finally, quantification of DMETs (Chapter Six) was done and the change in the abundance between CD and healthy donors was established. The generated abundance values were used in the created PBPK model to predict the fate of the investigated oral drugs in Crohn's disease population.

The steps described above were necessary to define and fulfil the research aims of this PhD. More specifically, the aims of the project were to:

- Collect and identify the available drug related systems parameters to build for the first time an active and inactive Crohn's disease PBPK model. This is important to assess the contribution extent of the identified altered systems parameters on oral drug bioavailability and to guide the following steps to be taken in order to fill the major gaps hampering a reliable and reproducible prediction of oral drug pharmacokinetics.

- Establish for the first time the absolute abundance of relevant drug metabolising enzymes and transporter proteins in the ileum and colon of active Crohn's disease patients. To incorporate the generated abundance data in the created active Crohn's disease PBPK model to bridge the gap between the in vitro and in vivo data of oral drug bioavailability.

- Measure the effect of inflammation on the expression of the drug metabolising enzymes and transporter proteins in the ileum and colon inflamed and histologically normal tissue samples from Crohn's disease patients.

- Investigate for the first time the impact of the observed alterations of the relevant drug metabolising enzymes and transporter proteins in active Crohn's disease population on oral drug pharmacokinetics utilising PBPK simulations based on the created active Crohn's disease population model and highlight future work needed to be defined in order to optimise the PBPK model prediction and drug dosing regimens.

Overall, this project aims to define and provide for the first time intestine system parameters specific for Crohn's disease population, to build a PBPK model that assesses the prediction of oral drug pharmacokinetics behaviour.

Chapter one: *In Vitro* and *In Vivo* Literature Gap Analysis to Build a Mechanistic Model to Predict the Fate and Source of Altered Bioavailability of Oral Substrates in Crohn Disease Population

Declaration

Sarah Alrubia, Jialin Mao, Yuan Chen, Jill Barber and Amin Rostami-Hodjegan.

I carried out the literature search, generation and analysis of data, contributed to the study design and wrote the manuscript. Dr Jialin Mao guided the data collection and generation. Prof. Amin Rostami-Hodjegan guided the PBPK modelling and was consulted on the data collection and generation. Dr Jialin Mao reviewed and suggested edits to the manuscript. Prof. Amin Rostami-Hodjegan and Dr. Yuan Chen contributed in to the study design and provided guidance. I retained editorial control.

1.1.Abstract

Crohn's disease (CD) is a chronic inflammatory bowel disease that predominantly affects the mucosal layer of ileum and colon segments. Most CD cases are diagnosed before the age of 30. Hence, these patients receive many different drugs beyond those used for CD itself. Oral drug bioavailability is influenced by the integrity of the intestine and abundance of intestinal drug metabolising enzymes and transporters (DMETs). Therefore, understanding the potential variations of these proteins in CD patients is essential. The current gap analysis aimed to gather the current available *in-vitro* and *in-vivo* knowledge of the human CD population concerning potential differences from healthy individuals or non-CD patients. The primary objectives were to assess the availability of drug independent system parameters concerning intestinal drug disposition, and the feasibility of building a mechanistic model to predict the fate of oral drugs in the CD population. We found that the number of published DMETs proteomic studies on CD human intestine are lacking, focusing mainly on P-gp transporter and CYP3A4 enzyme isoform. Moreover, all the assays were based on mRNA expression, which is a poor indicator for protein abundance, and may not reflect actual differences in CD vs non-CD populations. The ileum is studied less than the colon in the CD population, despite a more dominant role in oral drug absorption. Available clinical pharmacokinetic (PK) studies in CD population are also sparse and show uncertainties in separating the impact of the intestine from other systems like the liver on the observed alteration in the drug disposition. Quantitative analysis of the reported data was done to separate the roles of intestine and liver in first-pass clearance and oral bioavailability. The explanation of the PK difference in CD compared to healthy was not adequate to withdraw the line between the involvement of the intestine and other body systems. The current gap analysis concerning the drug disposition in CD indicates multiple interesting observations on the role of the liver and intestine. However, there is currently inadequate proteomic data to furnish the systems parameters and enable predictive models within the physiologically-based pharmacokinetics paradigm. Understanding changes to system parameters in CD (e.g. quantification of CYPs, UGTs, ABCs and SLCs proteins in ileum, colon and liver) is warranted for predictive models of drug disposition in CD and avoiding dedicated studies for every drug in this population.

1.2.Introduction

Crohn's disease (CD) is a chronic inflammatory bowel disease (IBD) which is a characterised by excessive release of the inflammatory mediators at the site of injury, which can lead to tissue damage, hemodynamic changes, and eventually organ failure. It predominantly affects the mucosal layer of the intestine, ileum and colon segments.[1] Most of the CD cases are diagnosed before the age of 30. In general, IBD patients are more susceptible to cancer, arthritis, as well as cardiovascular, respiratory, kidney and liver diseases.[2,3] Hence, these patients received many different drugs beyond those used for CD itself.

1.1.1. The intestine involvement

The small intestine represented by duodenum, jejunum, and ileum, plays a major role in drug absorption as it consist of large surface area due to the abundant presence of villi and microvilli.[4,5] On the other hand, the large intestine represented by cecum, colon, and rectum, contributes to drug absorption and metabolism in a more restrained manner as it mainly absorbs nutrients, salts and water in addition to some special formulation drugs that extendedly released in the colon.[6] The intestine mucosa is lined with the epithelium layer which contains multiple intestinal cells. The enterocytes are the most important cells out of Intestine Epithelial Cells (IEC) for oral drugs as they represent the absorptive units in the intestine. It consist of two membranes: the apical membrane from the gut lumen side and the basolateral, which is from the tissue blood supply side.[7]

Drug metabolizing enzymes and transporters (DMETs) lie within and limited to the enterocyte, representing a small fraction of the intestine.[8] DMETs participates in the diffusion and absorption process of xenobiotic hence their bioavailability.[9] In general, sugars and amino acids are passively and actively absorbed to the bloodstream while, lipid degradation products are absorbed by active transportation mechanism.[10] During CD, the epithelial cells encounter morphological and functional change where, absorption decreases, and secretion increases and leads to initiation and progress of the inflammation.[1,11] Inflammation causes loss of the tissue function, which might lead to other complications like infection, increase of permeability due to the disruption of the tight junctions, leukocyte dysregulation, and release of the inflammatory mediators. Enterocytes as part of the epithelial cells witness changes that causes alteration of oral drug absorption and metabolism.[1,12]

1.1.2. Effect of inflammation on DMETs expression

Drug metabolizing enzymes (DMEs) present in all segments of the intestine are of two sources: mammalian which is more abundant in the upper small intestine segments and bacterial which is more abundant in the ileum and colon.[13]

The general trend of the reported DMETs expression in healthy population literature data shows that the jejunum represents the segment with the highest abundance of DMETs, while the colon has the lowest DMETs abundance. Yet these data have some discrepancy in the reported protein expression level in one segment compared to the others or its detection in all of the samples examined. This data conflict occurs among mRNA, immunoblotting and LC/MS-MS reported results or between the different techniques. Also the number of the samples examined, the segments utilized and subjects' variability (ethnicity, age, sex, medical history, etc.) plays an un-negligible role in creating variation sources. List of the reported detected metabolizing enzymes of CYPs and UGTs in different intestinal segments by different technique in healthy population summarized in supplementary Table S1.1 and S1.2.

1.1.2.1. Cytochrome P450 (CYPs)

As a conclusion from the reported relative and absolute metabolizing enzymes abundance data in Table S1.1, CYP3A4 and CYP2C9 represent the most abundant isoforms of CYPs and CYP (1A1, 2C8, 2J2, 2B6) were reported to be detected but in a very low concentration or not detected in all of the examined samples regardless of the studied segment. Interestingly, only one study has studied metabolizing enzymes absolute abundance quantification difference along the length of the human intestine. *Drozdzik et al. 2019,*[14] reported data on adult Caucasian showed that CYP3A4 is the dominant CYP isoform in all the intestine segments followed by CYP2C9.

1.1.2.2. UDP Glucosyltransferases (UGTs)

Just like CYP enzymes UGTs shows a non-uniform pattern of distribution but to less extent.[13] As a general take out of the different available studies in Table S1.2, UGT 1A5, UGT1A7-9, and UGT2B4 isoforms reported low expression level or below the detection level in different intestine segments. While on average, UGT1A1, 1A10, 2B7 & 2B17 has shown to have the highest expression levels of Phase II enzymes in all the intestine segments with UGT1A10 exhibiting a

similar concentration in all segments in multiple studies. The colon shows a lower level of glucuronidation activity compared to the small intestine regions.

The UGTs absolute count based on *Drozdzik et al. 2019*,[14] showed that UGT1A1 is the most abundant in all studied region of the small intestine. Its abundance was significantly higher in the jejunum compared to the other segments. Following the same pattern, UGT2B7 concentration has shown a significant increase from duodenum to jejunum, and then decreased to ileum. On the other hand, UGT1A1 and UGT2B7 protein content were not detected in the colon, which does not correlate with the mRNA expression findings.

1.1.2.3. Drug Transporters in the intestine

Transporters in the intestine influence the bioavailability of oral dosage forms by modulating the number of drugs crossing the gut membrane and the amount passing to the hepatocyte.[15] The efflux transporters P-gp, MRP2 and BCRP are the most studied transporters in the human intestine by immunoblotting technique. In addition, the intestinal uptake transporters play an essential part in oral drug absorption, distribution and drug-drug interaction process.[16]

Furthermore, the knowledge of apical or basolateral localization of the transporters is important in order to determine their effect on drug bioavailability, for example, efflux transporters localized in the apical side of the enterocytes can limit the intestinal absorption of drugs by pumping them from the enterocytes back to the intestinal lumen.[17–19] This function has been studied for apical membrane transporters [20,21] but for the basolateral membrane transporters, more data should be generated to establish better knowledge on their role and effect.[22] Generally, most of the transporters expressed on the apical membrane of the enterocyte; Figure 1.1 illustrates the localization of the expressed transporters in the intestine.

The abundance of the solute carrier (SLC) and ATP-binding cassette (ABC) transporters in the different segments of the intestine of healthy population have been reported in many relative and absolute quantification published articles, which are listed in Table S1.3. Focusing on the absolute quantification data, the concentration of drug transporters is higher in small intestine segments compared to the colon. This general finding has some exceptions as MRP2 and MRP3 found more abundantly in the colon compared to other small intestine segments while OATP2B1, OCT1, and OCT3 were found to have the same and low distribution in all segments, with no detection of

ASBT and PEPT1 in the colon. This was reported specifically in a study that compared the transporters expression in all the intestine segments.[23] Recently a meta-analysis was published on intestine absolute transporters abundance by *Harwood et al. 2019* [24] on healthy Caucasian adults. Considering the segments transporters profile, PEPT1 represents the highest expressed SLC transporter in jejunum and ileum while ASBT was the lowest in jejunum and OCT3 the lowest in ileum. MRP2 is the highest expressed ABC transporter in jejunum and MRP3 in ileum while BCRP is the lowest in both. Furthermore, the colon transporters expression is as follows MRP3 > MRP1 ≈ P-gp > MRP2.[24]

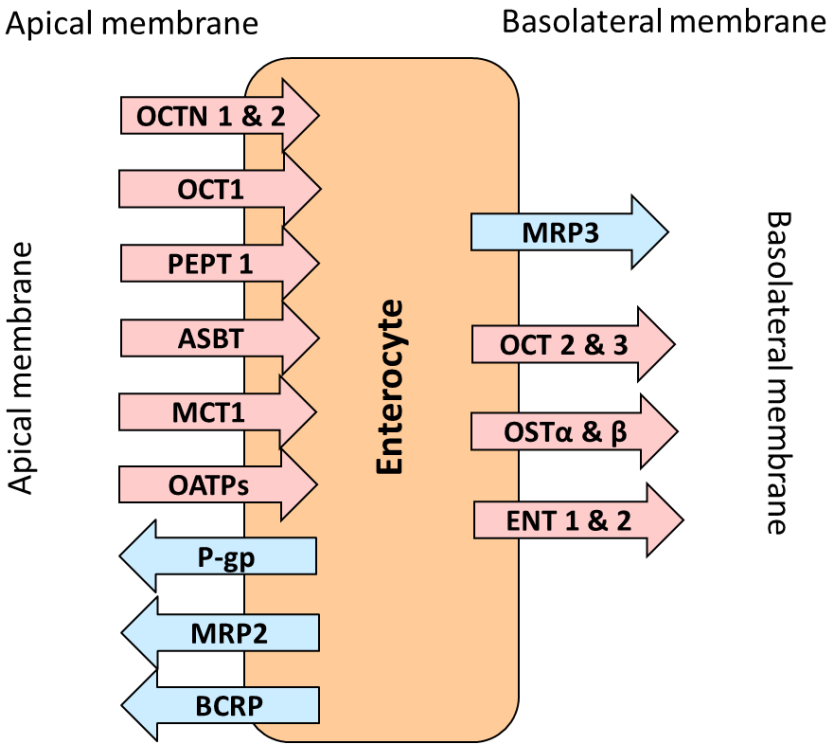

Figure 1.1. *Expression of major intestinal uptake (pink) and efflux (blue) transporters in the basolateral and apical membrane of the enterocyte.*

DMETs expression has been reported to be influenced by the inflammation caused by different disease conditions other than CD.[25–28] The underlying cause of the expression alteration can be generally divided based on disease factors and drug factors illustrated in Figure (1.2).

Inflammation caused by CD can lead to several Disease-Drug Interactions (DDIs) that can influence the pharmacokinetics (PK) of oral drug either by affecting the DMETs levels in the intestine or other major metabolising organs like the liver. Further analysis and highlight of the literature reported data is reported in this study.

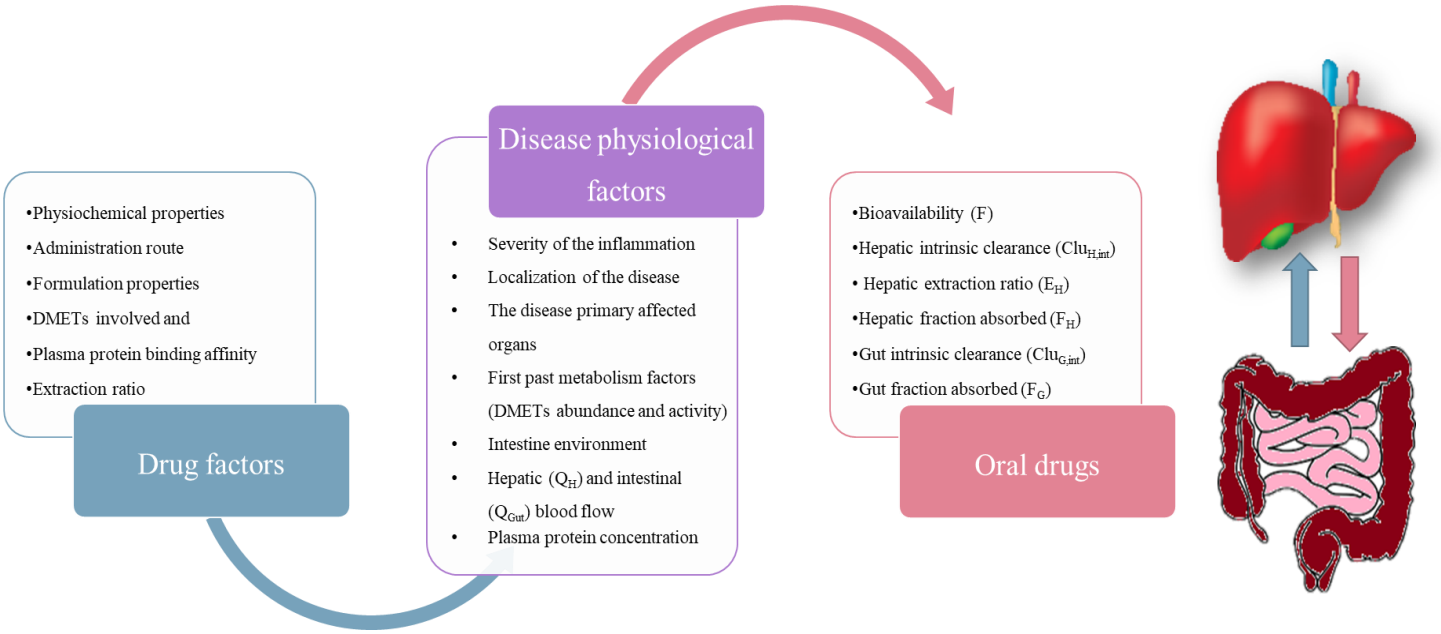

Figure 1.2. *Illustrative representation of drug and disease physiological factors driving oral drugs bioavailability and clearance values.*

1.1.3. Liver in inflammation

Inflammation caused by CD can affect other major metabolising organs like the liver by altering DMETs activity levels or abundance. A suppressive effect on hepatic CYP450 was reported in relation to elevation of IL-6,[29–34] IL-1β, tumour necrosis factor α, and interferon-α and γ inflammatory biomarkers during inflammatory conditions other than CD.[35,36] Increase in theses biomarkers are known to be associated with CD.[37,38] Also 4β-OH-cholesterol and C-reactive protein are reported to increase in CD in response to inflammation and are reported to be associated with reduction of hepatic CYP3A activity.[39–41]

Liver function enzymes ALT, AST, ALP and bilirubin reported to increase in CD patients as indication of liver injury. Abnormal liver function tests are found in approximately 20% to 30%

of individuals with IBD.[42] They can be as a result of extra-intestinal manifestations of the disease process, related to medication toxicity, or the result of an underlying primary hepatic disorder unrelated to IBD.[43,44] The increase production of different enzymes and inflammatory biomarkers by the liver during CD inflammation can cause alteration in CYP3A4 release by hepatocytes. The only measurement of liver DMEs expression reported reduction of CYP1A2, 2E1, CYP3A2, CYP2C11 in rat induced colitis.[45]

1.1.4. Effect of inflammation on drug pharmacokinetics (PK)

The effect of inflammation causing PK alteration is more pronounced in oral drug formulation that is a substrate of more than one DMETs. This is specifically noticeable from clinical data of CYP3A4 and P-gp substrates like verapamil and budesonide in CD,[46,47] verapamil and simvastatin in rheumatoid arthritis (RA),[33,48] erythromycin in cancer,[26] and cyclosporine and erythromycin in acute inflammatory conditions.[49,50] Propranolol which is a CYP (2C9, 1A2, 2D6) and P-gp substrates has shown a significant alteration in its PK profile in CD and RA.[51] Other inflammatory conditions reported PK change in oral CYP substrates but it showed less variation.[28,29] Other non-CYPs and P-gp DMETs substrates like mesalamine (NAT enzyme substrate) PK profile in CD has shown to be changed.[52] Further highlight of the liver impact, intestine DMETs expression and oral dugs PK alteration in CD is reviewed and discussed as part of this analysis focus.

Other intestine environment parameters encounter pathological change in CD patients which can affect oral drug PK. For example, many of prodrugs activation and modified release drugs of some of the enteric-coated formulations depends on the intestinal pH and/or metabolised by the bacterial enzymes to release its active moiety. Thus, change in the intestinal luminal pH can cause alteration in drugs releases and their active metabolites.[53]

1.1.5. Importance of Physiological based pharmacokinetics (PBPK) modelling

IBD patients to a large extent can encounter deterioration of the disease state after reaching to remission phase despite the availability of several treatment options and drugs with various formulations and administration routs. This complicates the disease control and results in introducing multiple novel drugs to the market in the past few years.[54] This necessitate the focus on precision dosing in clinical practice which is becoming a challenge for CD treatment.

Physiological based pharmacokinetics (PBPK) approach can be applied to determine the effect of inflammation on DMETs activity in disease states that haven't been heavily studied *in-vivo* or *in-vitro* due to several limitations: availability of large number of subjects to be recruited, difficulty in sourcing multi organ tissues from the same donor or different donors, funding, time, variability of physiological contributors in oral drug PK, which is the case in CD.

There are several PBPK platforms in use in the applications of drug discovery and development. The most common and widely used are, GastroPlus (Simulation Plus, Inc.), Simcyp Simulator (Certara UK) and PK-Sim.[55] Their popularity is mainly connected to the availability of a graphical user interface and a library of predefined models and databases for the user to choose from. In addition, the possibility of creating and testing complex scenarios to predict the clinical outcome adds to their popularity and makes it appealing to unexperienced users. A review was carried out to assess the different PBPK tools relative contributions in PBPK publications over the last 20 years.[55] The relative contribution of Simcyp showed an increase (from 35% to 55%). While PK-Sim showed an increase from 3% to 6% but its relative contribution remained the lowest when compared with GastroPlus and Simcyp.

The first CD PBPK population model published,[56] while it has achieved its aim the model still didn't put in consideration the differences between active and inactive CD stages it rather built a model based on highest and lowest reported values of the system parameters. In addition, the blood flow of both liver and intestine was not considered although budesonide was the modelled drug which is a high extraction ration drug. As mentioned in the publication, the level and performance of hepatic and gut CYP3A4 was based on the measured hepatic and intestine extraction ratio of CYP3A4 in CD subjects as direct reflection of CYP3A4 abundance in the two organs. Furthermore, the study did not distinguish between the studies where budesonide bioavailability in CD population is reported to be significantly different or not which doesn't achieve the goal of this study to investigate the causative factors of differences observed in oral drug PK in CD population.

The aim of this gap analysis is to explain the influence of CD on oral drug metabolism and absorption and the extent of the intestine, liver and other physiological parameters' involvement. This is carried out by conducting a thorough literature search and analysis to build a PBPK CD

population model, which is achieved by characterising the influence of CD on CYP3A-mediated oral drugs metabolism. By building a compound profile for budesonide and midazolam utilising the gathered current available *in-vitro* and *in-vivo* knowledge of adult human CD population. Using the selected drugs to demonstrate that the PBPK will be available to reflect the PK difference in healthy individuals or non-CD patients' vs CD. To evaluate the model applicability on other oral drugs differ in their formulation or PK nature.

Assessing the availability of drug independent system parameters concerning intestinal drug disposition and assessing the feasibility of building a mechanistic model to predict the fate of oral drugs in CD population, were the two prime objectives.

1.3. Methodology: Crohn's disease (CD) PBPK population model development framework

1.3.1. Step 1: Physiological characterisation and system parameters data collection

To develop a Crohn's disease population a literature search was conducted to extract data related to physiological and anatomical changes of the intestine and whole body system parameters during the course of CD. The identified physiological aspects that can alter oral drug bioavailability and known to have an effect on their PK based on drugs' nature, physiochemical properties and formulation are summarised in Table 1.1. The collected information where based on different segments of the intestine, differentiation between active and inactive disease state, female and male and fed and fasted conditions is considered whenever possible. Inadequate or incomplete information is highlighted in each aspect where it can limits and/or compromises the accuracy of the PBPK model to identify the gaps to be filled by future work to allow for better prediction of the fate of oral drugs in CD population.

The literature search was run in PubMed using the terms in Table 1.1 in combination with "Crohn's disease". Screening of titles and abstracts was carried out to identify the studies with a clear indication of the required information in Crohn's disease patients. No time frame of the research was applied. Inclusion of data was restricted to original articles, studies that provided information where determination of the mean, SD and CI is possible, studies that reported the level of the parameter at the baseline (before the treatment intervention), availability of both CD and healthy (HV) subjects in the same study when possible to minimize the variability from different methods and settings. If there were no studies where both population are recruited then different studies for each population are used with similar methodology settings as possible to calculate the overall mean value for HV and CD.[51,57–59] Only adult population and English publications are considered for all of the reviewed parameters. In some cases studies included none-IBD patients as the control group instead of healthy subjects, when such studies are included in the analysis; due the low number of the available studies in regard to the investigated parameter, it is indicated in the results section.

For drug metabolising enzymes and transporters (DMETs) expression, all studies are included without distinguishing between inflamed or non-inflamed tissue if a fold change of CD value to

control is reported or can be determined. The differentiation was based on active or inactive CD phase if possible. If it was not clearly indicated in the study if the patients are active or inactive then they are considered mixed (active & inactive).

The percent increase or decrease in the mean value of CD subjects compared to HV is used as the input value in Simycp simulator to build the CD population model. In some cases, the published article on CD population would use a reference value for HV instead of including healthy subjects, which is mentioned in the results when this is used as the comparison method.[60–63] When the difference between CD and HV group is reported to be significant in the original study, it is highlighted in the results for each system parameter.

The collected physiological parameters in HV and CD population from different studies analysed by calculating the weighted mean (WX) and overall standard deviation (SD) from the reported mean (x) and SD (Equation 1, 2 & 3) whenever possible based on each study number of observations (n). Then a percentage of the change between the CD and the HV population was estimated from the ratio CD/HV.

$$WX = \sum_{i=1}^{n} ni * xi / \sum_{i=1}^{n} ni \qquad \textbf{(1)}$$

$$Overall\ SD = \sqrt{overall\ sum\ of\ squares/n} \qquad \textbf{(2)}$$

$$Overall\ sum\ of\ squares = \sum_{i=1}^{n} [\{(SDi)2 + (xi)2\} * ni] - n * WX2 \qquad \textbf{(3)}$$

Some publications provided only the median and the upper and lower range values, from which the mean (X) and the SD were calculated using Equation 4 and 5. [64]

$$X \approx a + 2m + b/4 \qquad \textbf{(4)}$$

Where; *a* is the upper limit, *b* is the lower limit and m is the median.

$$SD \approx b - a/\xi(n) \qquad \textbf{(5)}$$

Where; ξ (n) values are computed in Table1 in the reference [64] up to 50 n (sample size) and ξ (n) = 6 when n > 70. [64]

The extracted data were used to create two virtual CD populations active and inactive. To be verified using the *in vivo* data which did not count for the physiological difference in the two disease state that would affect the drug bioavailability. The mean value of active and inactive CD is taken with the percent change from HV. The identified system parameters were altered in the existing healthy volunteer population of Simcyp® Simulator Version 19 (Certara, Sheffield, UK) according to the percent change of the active and inactive state, alternately, to test the extent of capturing the clinical data by the developed CD based-PBPK population models. The created active and inactive CD population performance was evaluated against the selected oral drugs PK profile in healthy model outcome and validated by its similarity to the observed *in vivo* PK data.

Table 1.1. Healthy volunteers (HV) and Crohn's disease (CD) (active and inactive) physiological parameters evaluated to be incorporated as system parameters in CD-PBPK population model.

pH (fasted)	Proximal small intestine pH Terminal small intestine pH Large intestine pH
Small intestine and colonic transit time (hr)	Fasted small intestine-transit time (SITT) Fed small intestine-transit time (SITT) Fed colonic transit time
Gastric emptying time (hr)	Fasted Gastric emptying time Fed Gastric emptying time
Vascularity and hemodynamic	Superior mesenteric artery (SMA) blood flow (ml/min) Regional intestine blood flow (ml/min*100g) Thickness of the intestine wall (mm)
Intestine DMETs abundance	Cytochrome P450 (CYPs) ATP-binding cassettes (ABCs) Solute carrier transporters (SLCs)
Blood Proteins (g/L)	Human serum Albumin levels α1-Acid glycoprotein levels
Hepatic function (linked to IL-6)	DMETs abundance

1.3.2. Step 2: Drugs with available clinical information in CD population

As part of the identification process of the causes of oral drug PK alteration, a systematic review of the reported oral drugs bioavailability and IV drugs clearance in CD population in comparison to HV population is carried out. The included drugs data weren't restricted to studies where PK parameters are measured in both CD and HV population in the same study, fed or fasted state, sample size or any other factor due to scarcity of the available data in this disease population. The only consideration was the similarity of the trial methodology and normalisation of the doses to avoid verities of the results based on such diversities.

The area under the curve (AUC) of the drugs in both CD and HV was the parameter from where the relative bioavailability between the CD and HV is calculated, AUC= (CD/HV). While IV drugs clearance (CL) was the parameter from where the relative clearance is calculated, CL= (CD/HV)

with employing a 95% Confidence Interval (CI). Whenever the two populations are not present in the same study, then a HV study for the drug was searched and the comparison is based on the matched AUC (AUC 0-∞, AUC-ss, and AUC-t) and normalisation of the AUC in both groups is applied if required. Whenever there is no matched AUC in HV to the CD then the drug is excluded since the bioavailability comparison is not possible.

The calculation applied was based on Fieller's Theorem [65–67] where the details of the calculation method and the relative bioavailability of oral drugs and clearance of IV drugs studies between CD and HV populations reported in the literature is in Table S1.4 and S1.5.

1.3.3. Step 3: Drugs selected to build compound files and evaluate the CD-PBPK population

To explain and identify the major influential system parameters two CYP3A-substrates midazolam (MDZ) and budesonide are investigated by means of PBPK modelling utilizing The Simcyp® Simulator M-ADAM absorption model, a presenter of the gut wall multilayer incorporated into the dissolution, absorption, and metabolism (ADAM) model.[68] This is to help in verifying the built CD population with all relevant known physiological differences in intestine and other body systems. The study design taken from each study was used for building and validating the drug model for budesonide IV [69] and oral Entocort® [47] dose and midazolam IV and oral dose [70] in healthy volunteers. The healthy population used is the default Simcyp® Simulator V19 healthy population. Age range, female to male proportion, fed or fasted and dosage regimen are based on the HV subjects in each study.

Budesonide and midazolam are chosen for the PBPK model, as both drugs are primarily metabolized by CYP3A4 that is the most important metabolising enzyme as it represent 15-30% of expressed cytochromes in human liver and around 80% of small intestine CYP3A enzymes.[8] In addition, it counts for 30-40% of xenobiotic metabolism.[71,72] Moreover, CYP3A4 is the most clinically studied in CD population where validation of the model can be carried out based on reported data not only based on the simulation outcome. This is important to consider as it allows better identification of the gaps in the current knowledge to build a CD population model.

MDZ is a CYP3A4 probe which will allow to investigate the influence of liver and intestine based on CYP3A4 expression in the two organs. It is given in solution formulation allowing for investigation of the intestine upper segments involvement in CD. Budesonide is a CYP3A4, CYP2C9, CYP1A2 and P-gp substrate which allows to investigate the synergistic effect influence. It is a high extraction ratio drug (ER=0.9)[73] which will allow to investigate the liver and intestine blood flow (cardiac output) impact. It is given in controlled release formulation where its release triggered by pH 5.5 allowing for investigation of the intestine lower segments involvement. The two drugs are highly bound to albumin (80-90%). Both drugs showed significant alteration in their oral bioavailability in CD subjects vs HV. They are clinically relevant to CD patients as MDZ used before endoscopy procedures as an anxiolytic while budesonide is used for treatment of CD.

Furthermore, both have available clinical intravenous and oral data in CD subjects where a significant alteration in their bioavailability after oral (PO) dose administration is demonstrated in CD subjects in relation to healthy subjects. To allow investigating the physiological changes accompanied with the disease which causes the observed PK behaviour alteration. Budesonide has at least four clinical trials on CD population to determine its PK profile under different conditions.[47,63,74,75] Our focus is on the study that showed a significant difference [47] in budesonide bioavailability in CD compared to HV population. While MDZ has one study that recorded its bioavailability difference in CD. [75]

1.3.4. Step 4: Data generation and evaluation of CD-PBPK model

The initial evaluation of the drug models is carried out utilising the HV population where the drug specific parameters of budesonide are mainly taken from (*Effinger A, 2020*).[56] For MDZ the available Simcyp drug model was used. Both drug profiles has the following key modification; the absorption model used is M-ADAM and the distribution model used is full PBPK which is based on HV *in vivo* IV and oral data for budesonide [47,69] and MDZ.[70] Whenever information are missing from the literature, Simcyp parameter estimation function was used to estimate the best value that fits the clinical outcome. Detailed modified and estimated input parameter used in Simcyp simulator for building budesonide and MDZ drug profile are summarised in Table S1.6 and S1.7, respectively.

.

The created drug profiles of budesonide and MDZ were evaluated by the similarity of the predicted relative mean values of C_{max}, AUC0-∞ and T_{max} to the observed values in HV population. Simulation of budesonide IV and PO plasma concentration time profile shown in Figure S1.1 and MDZ in Figure S1.2. The mean values of predicted and observed PK parameters are in Table S1.8. The PK parameters of budesonide and MDZ are derived from the clinical studies under investigation for both HV and CD subjects using GetData Graph Digitizer 2.26 to create parameter estimation template to evaluate the simulated results by overlaying it on the clinical results.

The difference between female and male in CYP3A4 abundance was enabled in Simcyp simulator throughout all simulations, as the gender difference is reported to affect the outcome of CYP3A4 substrates clearance [76] which would be reflected on the built model when simulating a study with a different gender ratio. All trial designs are based on 100 subject (10 subjects in 10 trials), age range, female to male proportion, fed or fasted and dosage regimen are based on the CD subjects and study design from each study investigated. Simulating the oral drugs in CD for budesonide controlled release [47] and for midazolam (MDZ).[75] Details of the trial design data in Table 1.2.

Table 1.2. Demographics of the virtual individuals of budesonide and midazolam implemented in the PBPK-based simulation workflow and their corresponding trial design parameters.

Trial parameter	**Budesonide** [47,69]	**Midazolam** [70,75]
Oral Dose	18 mg	100 µg
IV Dose	0.5 mg for 9 minutes	1 µg (HV) & 0.5 µg (CD) for 5 minutes
Oral Formulation	Controlled release capsule	Solution
CD population age range	21–63 years	25–65 years
CD female / male	50% female (3 / 3) 3 active and 3 inactive	87% (7/1) all active
HV population age	40–53 years	18–60 years
HV female / male	All male	50% (8/8)
Fed/ fasted	Fed	Fasted

To build the PBPK model and mechanically determine the involvement and influence of the two main metabolising and disposition organs; the liver and the intestine, functional applications are applied using the available information from the *in-vivo* CD studies under investigation for MDZ and budesonide. This data are used when no other data are available from the literature to support

the observed changes. The equations deriving the extrapolation of system-specific, combined system-specific and drug-specific parameters in CD PBPK model for budesonide and MDZ are in Table 1.3 and 1.4, respectively.

Table 1.3. Equations and functions used for the extrapolation of system-specific and combined system-specific and drug-specific model parameters in the PBPK model of Crohn's disease for budesonide controlled release oral formulation.[47,69]

Equation and units	Abbreviation	Comments
$\boldsymbol{BSA\ (m2) = weight\ (kg)0.425 * height\ (cm)0.725 * 0.007184}$	BSA= Body surface area	The BSA is known to be better correlated with many physiological functions, organ sizes and blood flows than height or weight alone. It was calculated based on Du Bois method.[77]
$\boldsymbol{CI\ (L/min/m2) = 3 + (-0.01(age(years) - 20))}$	CI = Cardiac Index for age >20 years [78]	Normal range for CI (2.5 to 4 L/min/m^2)
$\boldsymbol{CO\left(\frac{L}{min}\right) = CI\left(\frac{\frac{L}{min}}{m2}\right) * BSA\ (m2)}$	CO= Cardiac Output[78]	Normal range for CO (4 to 8 L/min)
$\boldsymbol{QH\left(\frac{L}{min}\right) = 0.26 * CO\left(\frac{L}{min}\right)}$	Q_H = Hepatic blood flow CO= cardiac output	Q_H represent 26% of CO (average of female 27% and male 25.5 %)[79]
fu_P in disease state $= \mathbf{1/(1 + (1 - fu) * [pi]/[p] * fu)}$ [79]	*pi = albumin concentration in CD* *p= albumin concentration in HV* *fu= drug unbound fraction in HV*	Albumin HV= 40.6 g/L [52,81] Albumin CD= 32.1 g/L [58,60]
$Cl_{int,H}$	$Cl_{int,H}$ = hepatic intrinsic clearance	Predicted using Simcyp simulator Retrograde model after creating the drug compound profile by applying the Q_H, fu_P and CL_{IV} values from the

		clinical study [47] for the HV and CD population.
$\boldsymbol{FH = QH/(QH + fuB * Clint)}$ $\boldsymbol{FGI = F/FH}$ [81]	F_H= drug fraction absorbed through the liver F_{GI}= drug fraction absorbed through the gut	

Table 1.4. Equations and functions used for the extrapolation of system-specific and combined system-specific and drug-specific model parameters in the PBPK model of Crohn's disease for midazolam oral formulation. [70,75]

Equation and units	Abbreviation	Comments
$\boldsymbol{QH\ (L/min) = CL/EH}$ [82]	CL = systemic clearance E_H = hepatic extraction ratio	CL (L/min) in CD= 0.12 CL (L/min) in HV= 0.44 E_H CD = 0.11 E_H HV = 0.4 Mean values from MDZ study
fu_P in disease state $\boldsymbol{= 1/(1 + (1 - fu) * [pi]/[p] * fu)}$ [80]	*pi = albumin concentration in CD* *p= albumin concentration in healthy* *fu= unbound fraction in healthy*	Albumin HV= 40.6 g/L [52,81] Albumin CD= 32.1 g/L [58,60]
$\boldsymbol{CLH\left(\frac{L}{MIN}\right) = CL - CLR}$ [82]	CL_H= hepatic clearance CL_R = renal clearance	CL_R≈ 0.5% of systemic [83]
$\boldsymbol{CLint,H\left(\frac{L}{MIN}\right) = QH * \frac{CLH}{fuB(QH - CLH)}}$	$Cl_{int,H}$ = hepatic intrinsic clearance fu_B= blood fraction unbound	From CL_H well-stirred' liver model equation Where: *fu_B* HV =0.05, CD=0.08 Q_H (L/min) HV = 1.06, CD =1.18 CL_H HV= 0.4, CD = 0.12
$\boldsymbol{FH = \frac{QH}{QH + fuB * Clint}}$ $\boldsymbol{FH = 1 - E_H}$	F_H= hepatic absorbed fraction	E_H CD = 0.11 E_H HV = 0.4

$\boldsymbol{FG = 1 - EG}$ $\mathbf{FG = F/FH}$ [82]	E_G= extracted fraction from gut F_{GI}= gut absorbed fraction F = bioavailability	E_G CD = 0. 64 E_G HV = 0. 53

1.3.5. Step 5: Global sensitivity analysis (GSA)

The impact of the identified system parameters in Table 1.1 on the PK properties of the oral drugs of interest is investigated utilising Global Sensitivity Analysis (GSA) function within Simcyp. GSA is important as the effect of the physiological alterations encountered by CD patients varies per drug based on several disease and drug factors. Determination of the impact spectrum and identification of the key parameters was performed based on budesonide and MDZ nature and the integrated system data in CD population framework. The distributions of the investigated system parameters values was based on uniform distribution. The applied range of the lower bound and upper bound was based on the collected literature system parameters in HV and active CD population. GSA Morris method was selected where it define the parameters impact based on their influence on the output variable. It also accounts partly for the interaction between the investigated parameters.[84]

The influence of the different system parameters on the altered bioavailability is reflected on the simulated PK properties C_{max}, AUC and T_{max} of budesonide and MDZ oral formulations based on their trials specifications. The influential parameters determined by the GSA were compared with the extracted available literature data to identify the gaps in the key parameters to guide the decision for future research needed to be carried out to fill these gaps. To allow for a reliable predictive active and inactive CD PBPK population models.

1.4.Results

1.4.1. Step 1: system parameters of CD population (intestine)

1.4.1.1. pH

The reports of the CD population pH are not consistence; differences can be seen during and within the active and inactive phases of CD subjects. Four studies [81,85–87] had HV and CD group where the pH of Proximal SI (Small Intestine) (Figure 1.3), Terminal SI (Figure 1.4) and Large intestine (Figure 1.5) values are reported in fasted state. Only two studies provided the pH values for the active group separately allowing distinguish between the two disease states. Details of each pH study results included are in Table S1.9. For the Proximal and Terminal SI pH none of these studies reported a significant difference between the CD population and HV population.

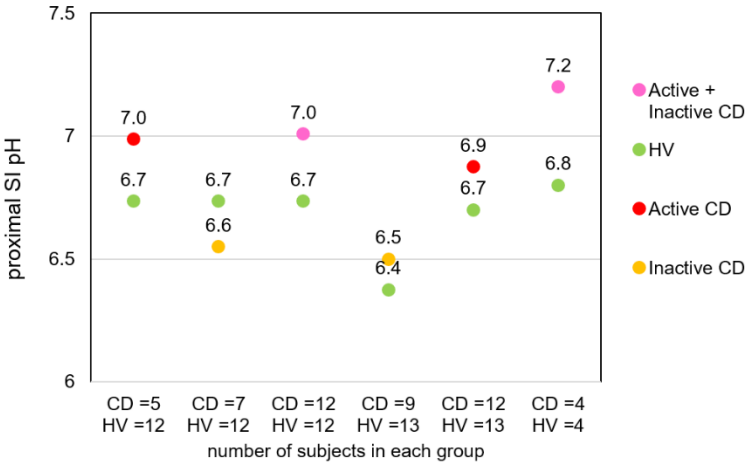

Figure 1.3. *Mean pH value of the proximal small intestine (SI) in active and inactive Crohn's disease (CD) population compared to healthy volunteers (HV) in fasted state.*

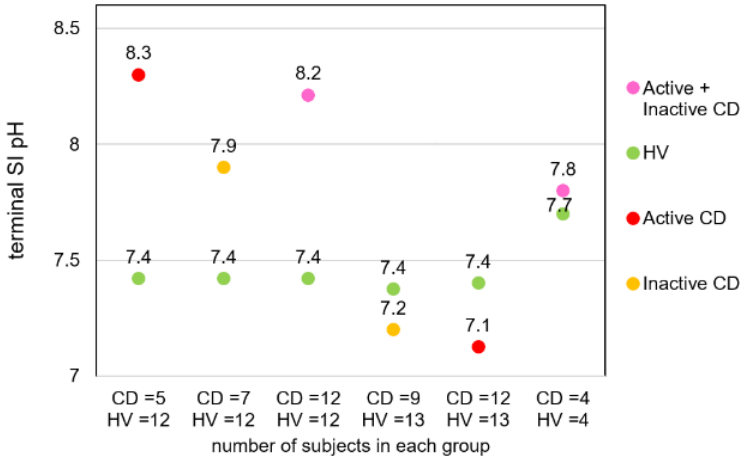

Figure 1.4. *Mean pH value of the terminal small intestine (SI) in active and inactive Crohn's disease (CD) population compared to healthy volunteers (HV) in fasted state.*

As for the pH of the large intestine in CD population compared to HV, only one study with mixed active and inactive (three active and 1 inactive) CD subjects reported significantly lower pH than HV.[87] In Figure S1.3, the results of each segment pH for each group are combined to highlight the

differences observed. No pH data in CD reported in fed state, but there are studies where the fed state pH value is reported in a mix of IBD patients.

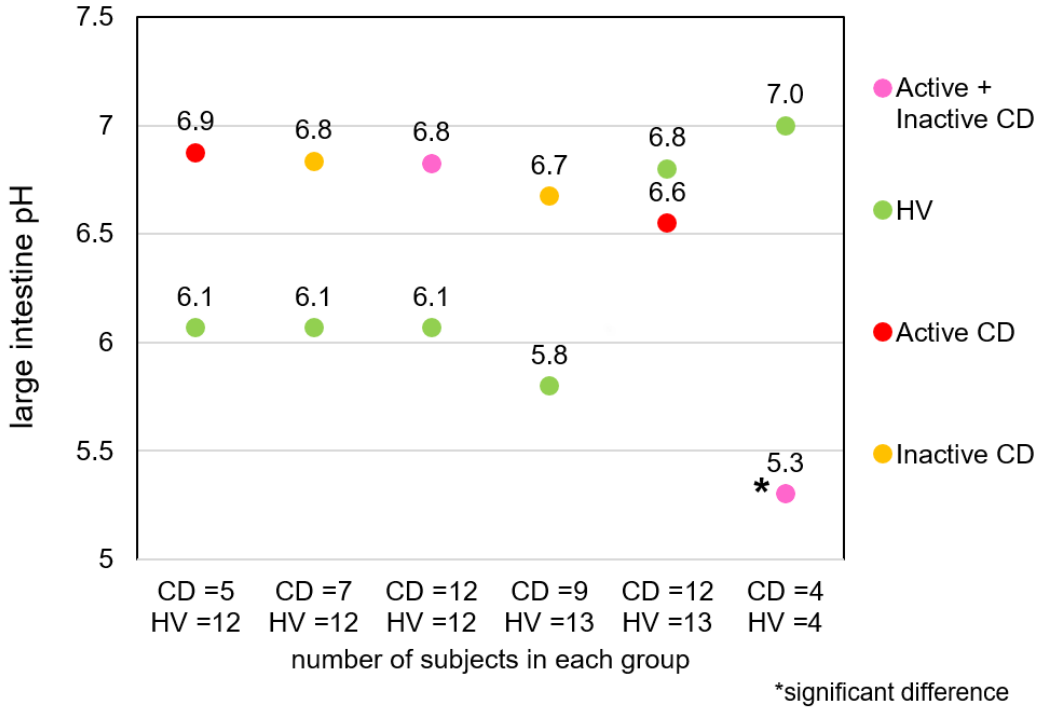

Figure 1.5. *Mean pH value of the large intestine in active and inactive Crohn's disease (CD) population compared to healthy volunteers (HV) in fasted state.*

1.4.1.2. Intestine transit time and motility

Small Intestine-Transit Time (SITT) was reported in three studies [81,88,89] for HV and CD group under fasted condition (Figure 1.6) two of which provided SITT for active CD separately where both showed significantly higher SITT compared to HV. One study was done under fed conditions[47] (Figure 1.7). Only one study provided the colonic transit time for the active CD group and showed a significantly lower transit time compared to HV [47] (Figure 1.7). Details of each transit time study results included are in Table S1.10. One study with mixed active and inactive CD subjects where all underwent an ileocecal resection surgery reported significant decrease in SITT compared to HV.[81] In Figure S1.4, the results of each segment transit time for each group under fasted and fed conditions are combined to highlight the differences observed.

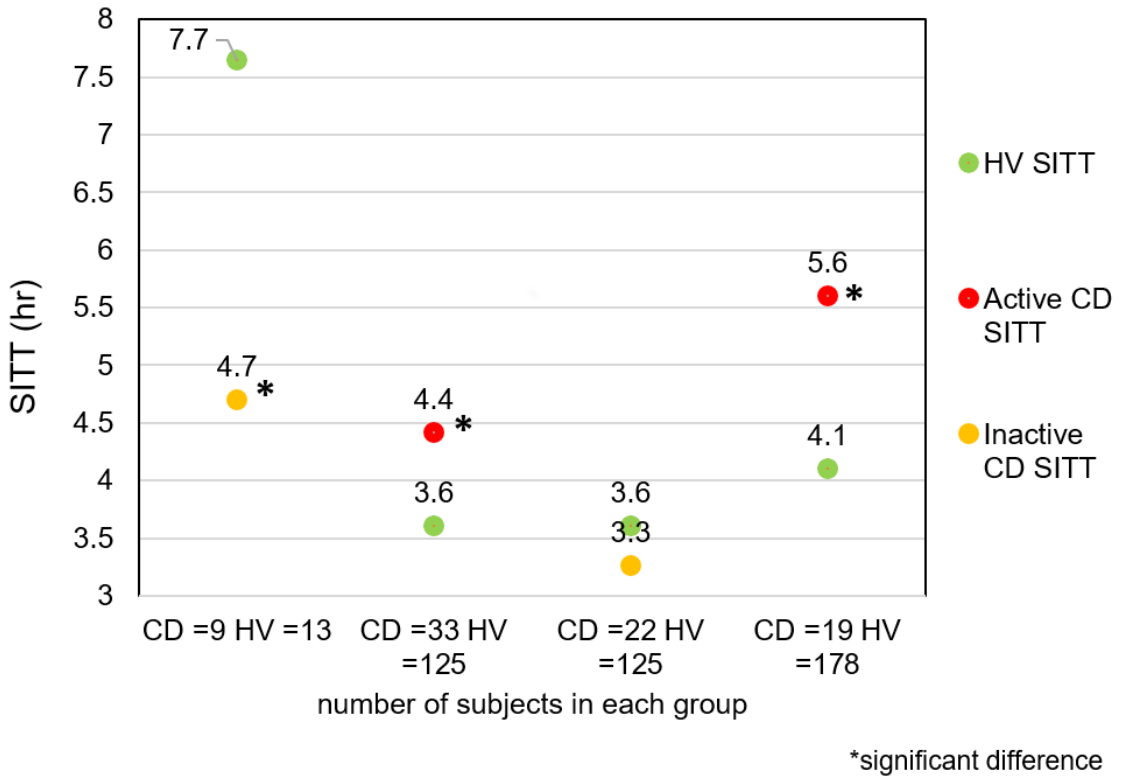

Figure 1.6. *Mean small intestine transit time (SITT) in active and inactive Crohn's disease (CD) population compared to healthy volunteers (HV) in fasted state.*

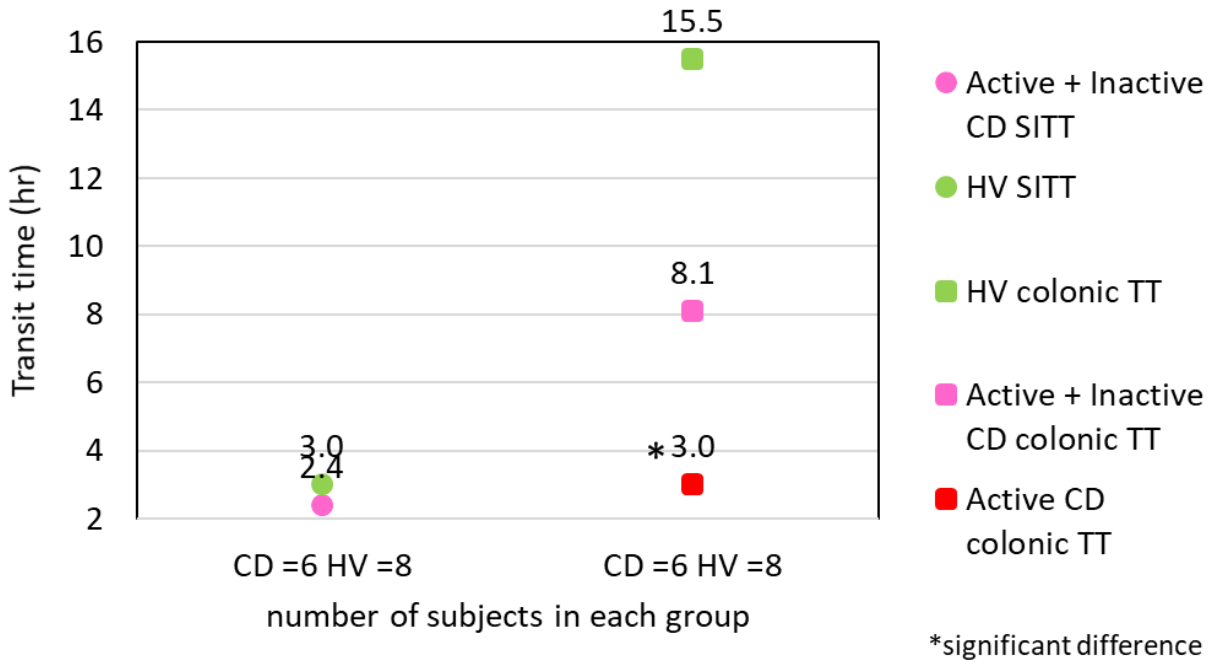

Figure 1.7. *Mean small intestine and colonic transit time in active and inactive Crohn's disease (CD) population compared to healthy volunteers (HV) in fed state.*

The intestinal motility is reported to be reduced under fasted and fed conditions during the course of CD this might be due to muscular or neurological dysfunction because of the inflammation and cytokines effect on hindering the contraction ability of the smooth muscles.[90,91] The duodeno-jejunal contractions significantly reduced by 28% in 26 inactive CD vs 18 controls. The antral contractions significantly reduced by 47% in 16 inactive CD vs 18 controls.[92] In another study, six ileum and 10 colon from UC and CD tissues vs 10 ileum and 10 colon histologically normal (HN) tissues, the contractility of ileum and colon significantly reduced by 17-33% and 3-26%, respectively, in CD compared to HN.[93]

1.4.1.3. Gastric emptying time

Three studies [47,89,94] reported gastric emptying time in HV and CD subjects (Figure 1.8), one in fasted and 2 in-fed state. Only one the studies provided the gastric emptying time for the active group separately. Details of each study gastric emptying time results used are in Table S1.11. One study with mixed active and inactive CD subjects (3 active and 3 inactive) showed significant increase of gastric emptying time compared to HV under fed conditions. [47]

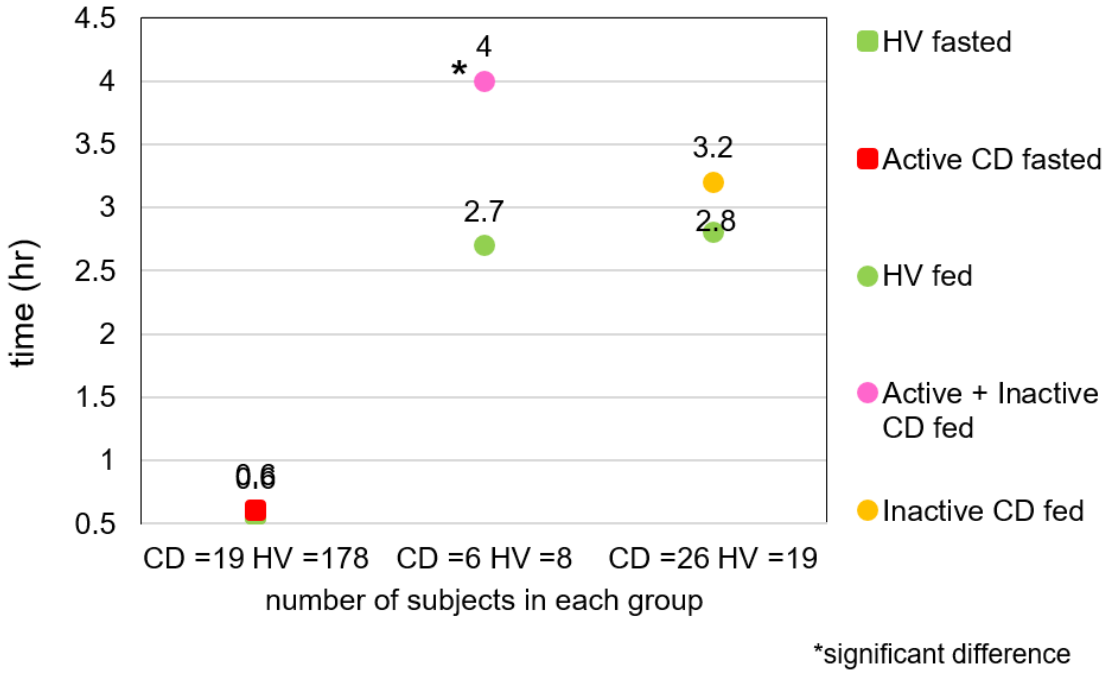

Figure 1.8. *Mean gastric emptying time in active and inactive Crohn's disease (CD) population compared to healthy volunteers (HV) in fasted and fed state.*

1.4.1.4. Vascularity and hemodynamic

The intestine morphology and vascularity differ in the acute stage of the disease where the inflammation is active and in the chronic stage where the inflammation is controlled. The key identified differences linked to the gut blood flow, hence, oral drug PK in the early stage of acute CD are; dilation of the blood vessels diameter,[95] increase in the superior mesenteric artery (SMA) blood flow, volume, rate and diameter,[96] increase the intestine vascularity,[97,98] increases of the intestine blood perfusion,[97–99] and thickness of the intestine wall >4mm.[95,96,99] For the late stage long standing chronic CD, the identified changes are: decrease the intestine vascularity,[98,100] decrease the intestine blood flow and perfusion,[97,98,100,101] submucosal fibrosis and muscularisation[98] and the intestine wall becomes wrapped in fat.[102]

The SMA blood flow which represent an important aspect for oral drug with high extraction ratio has shown to significantly increase in active CD compared to in active and HV [96,103,104] as in Figure 1.9. Another aspect is the intestine regional blood flow, which showed to differ between intestine regions based on the activity of the disease.[105] The colonic blood flow significantly increased in active stage while the ileum blood flow significantly decreased in inactive stage compared to HV as shown in Figure 1.10. The bowel wall significantly thickens in active stage to exceed 4mm compared to 2.7mm in HV while no significant change observed in inactive stage.[99] Details of the blood flow and bowel wall studies results are in Table S1.12, S1.13 and S1.14.

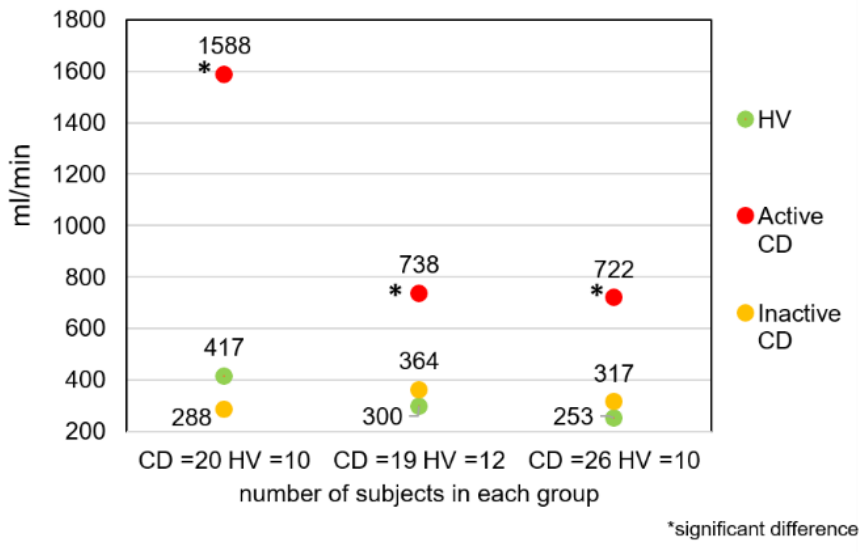

Figure 1.9. *Mean superior mesenteric artery (SMA) blood flow in active and inactive Crohn's disease (CD) population compared to healthy volunteers (HV).*

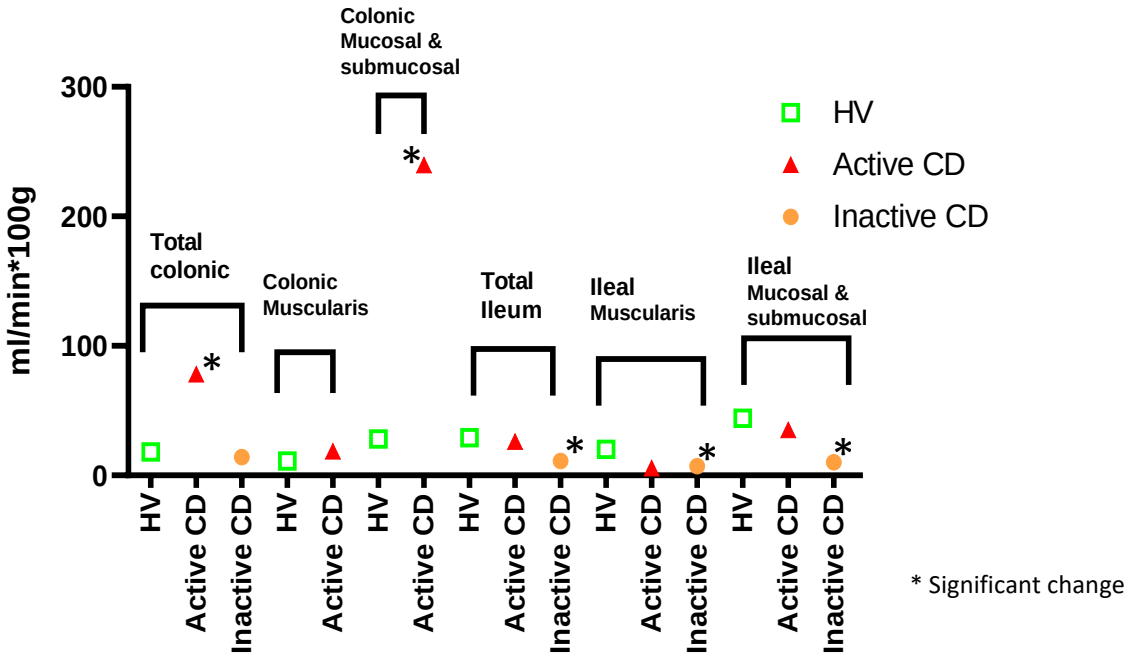

Figure 1.10. *Mean regional intestine blood flow in active and inactive Crohn's disease (CD) population compared to healthy volunteers (HV).*

1.4.1.5. Intestine DMETs abundance

The effect of CD inflammation on DMETs expression is not extensively studied; DMETs proteomics studies are limited in number and prospective. In total, we found 13 publications seven studied DMEs, [41,106–111] seven studied ABC transporters [41,106–110,112,113] and six reported SLC and/or SLOC expression.[41,110,114–117] Most of the available proteomics data only reported relative abundance or mRNA gene expression levels and no direct measurement of the protein abundance by LC/MS-MS technique is reported. Six of these publications had healthy subjects as the control group [108,114,117] while the rest had non-IBD patients as the control group. The ileum, which is known to have more dominant role in oral drug, was studied in six of these studies. While the upper intestine segments (duodenum, jejunum), which are rarely affected by direct inflammation due to CD has no reported DMETs expression information.

All the reported significant changes in CYP enzymes (Figure 1.11), ABC transporters (Figure 1.12) and SLCs (Figure 1.13) expression in active CD compared to HV populations are presented in fold change difference (CD/HV). Details of the studied DMETs abundance are summarised in

Table S1.15, only studies that recruited a control group were included to be able to report the relative expression levels. The reported relative abundance data shows high variability in the reported changes during CD for example, one study showed 10 times fold decrease of CYP3A4 [106] while another showed two fold increases [107] in CD patients. The expression of some of these protein in remission state was reported separately in one study [41] while in tow other study the expression of active and inactive disease state was reported undifferentiated [109,114] with indicating that disease activity showed no effect on the reported expression of CYP3A4 and p-gp.[109] one study reported multiple DMETs expression of HN tissue from CD patients.[108]

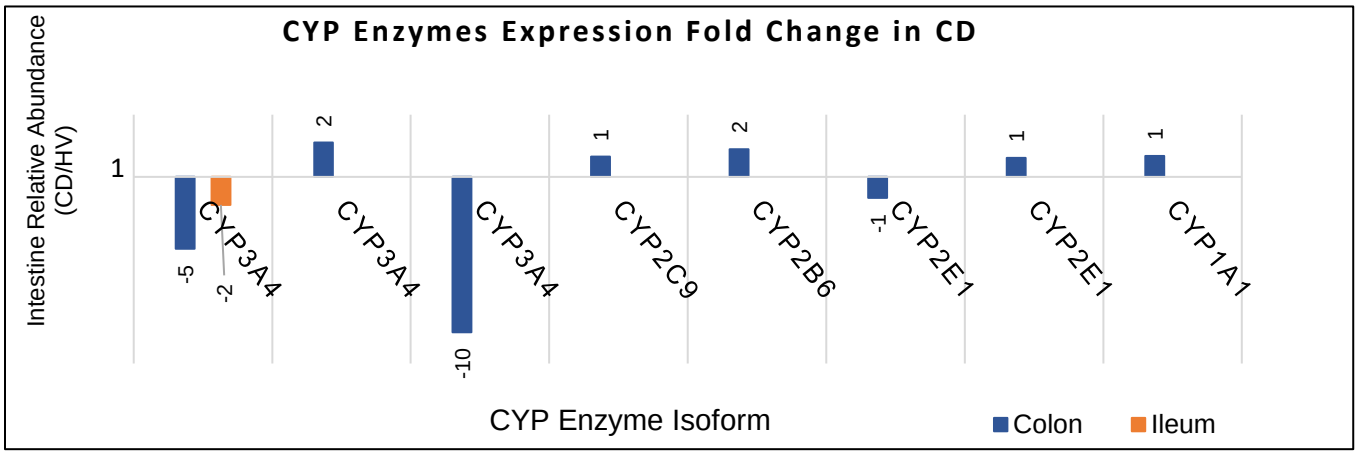

Figure 1.11. *CYP450 enzymes expression in active Crohn's disease (CD) population relative to healthy volunteers (HV).*

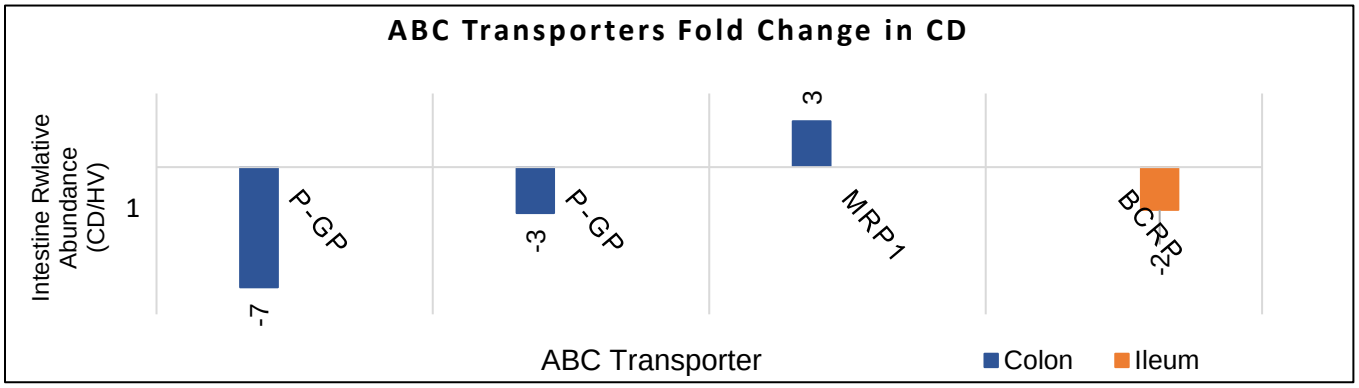

Figure 1.12. *ABC transporters expression in active Crohn's disease (CD) population relative to healthy volunteers (HV).*

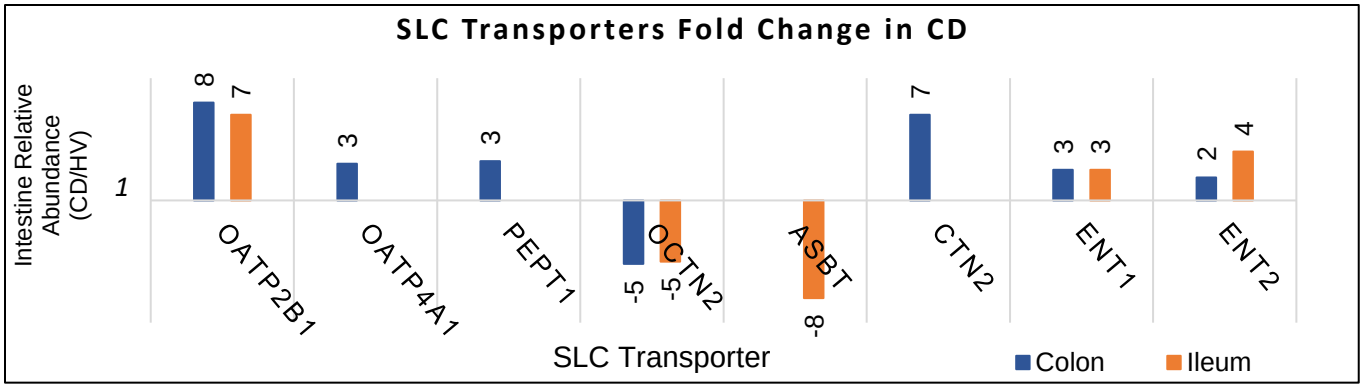

***Figure 1.13**. SLCs expression in active Crohn's disease (CD) population relative to healthy volunteers (HV).*

In general, limited number of DMETs isoforms were studied and only CYP3A4, CYP2E1, P-gp, MRP3, ASBT, PEPT1 and MCT1 expression was reported in more than one publication, UGTs and other important intestines ADME proteins have no published expression data in inflamed tissue from CD. In addition, there is no *in vitro* activity data on human CD population.

1.4.2. Step 2: system parameters of CD population (other body systems)

1.4.2.1. Liver DMETs abundance

There are no available direct information of DMETs abundance or activity of CD liver. Only one study measured the hepatic (E_H) and intestinal (E_G) extraction ratio in eight active CD patients using midazolam as a CYP3A4 probe.[75] The measured E_H= 0.11 in CD showed a 76.6% decrease from the mean HV E_H= 0.47. In CD, E_G=0.64 showed a 42.2% increase from the mean HV E_G= 0.45 when compared to the referenced literature values of HV.

Other than this study, the approach used to investigate the liver CYP3A4 involvement in the alteration of oral drug bioavailability in CD has followed the impact of inflammatory biomarkers (specifically IL-6) on liver protein abundance during inflammatory conditions. Like other inflammation associated conditions CD is coupled with disturbance of cytokines inflammatory biomarkers levels from which IL-6 release is reported to be elevated.[37,38]

The focus on IL-6 in this gap analysis is related to its pro-inflammatory mechanisms that causes alteration of the CYP450 iso-enzymes, P-gp and albumin, hence, their substrates' PK. A

suppressive effect of inflammation on hepatic CYP450 was reported in relation to IL-6 increase during inflammatory conditions other than CD.[29–34] This has not being reported yet specifically in CD liver, but building the assumption that CYPs level is affected in CD liver in the same way as in other inflammatory conditions can explain the change of the observed difference in the PK of oral drug studied in CD; which are predominantly metabolised by CYPs proteins. Moreover, one study established a PBPK model for cytokine related DDIs that simulated the impact of IL-6 increase on CYPs in the liver of rheumatoid arthritis, neuromyelitis optica (NMO) or NMO spectrum disorder subjects.[118] This PBPK simulation predicted moderated interaction with CP3A4 substrates, mild with CYP2C9, 2C19 and 2D6 while no interaction was noticed with CYP1A2 substrates.

Elevation of inflammatory biomarkers with increase of the disease severity might explain the observed difference in oral drug PK between different CD activity states. This is observed when the subjects with more active disease (based on Harvey-Bradshaw index (HBI) which is a subjective index not objective [119]) has higher oral verapamil pharmacodynamics (PD) and PK difference compared to the subjects with lower CD activity and healthy subjects.[46]

1.4.2.2. Blood Proteins (Albumin & α1-AGP)

Human Serum Albumin (HSA) and α1-AGP levels has witnessed dysregulation during CD. Dysregulation of drug-blood protein binding levels would affect the drug bioavailability based on the extent of drug-protein binding affinity.

α1-AGP reported data in active and inactive CD compared to HV, showed that active CD has a significantly higher level compared to inactive CD and HV (Figure 1.14).[40] Details of the α1-AGP levels reported is summarised in Table S1.16.

On the other hand, albumin level was significantly lower when the same set of CD patients were examined in active state and after remission (Figure 1.15).[58] The results of this study are in agreement with other publications where only active CD showed significant drop in albumin compared to inactive CD patients.[52,81,120] Differentiation between the albumin level of female and male of active CD patients showed higher drop of albumin in female patients than male, with both being significantly lower than HV (Figure 1.16).[60]

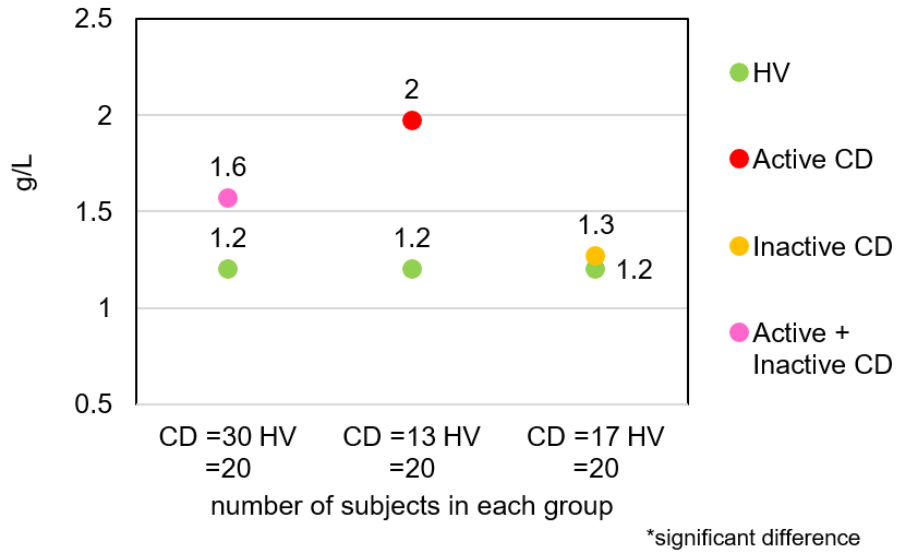

Figure 1.14. *Mean levels of α1-AGP in active and inactive Crohn's disease (CD) population compared to healthy volunteers (HV).*

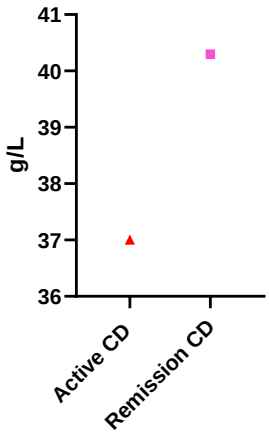

Figure 1.15. *Mean albumin level of 39 Crohn's disease (CD) patients during active phase and after remission.*

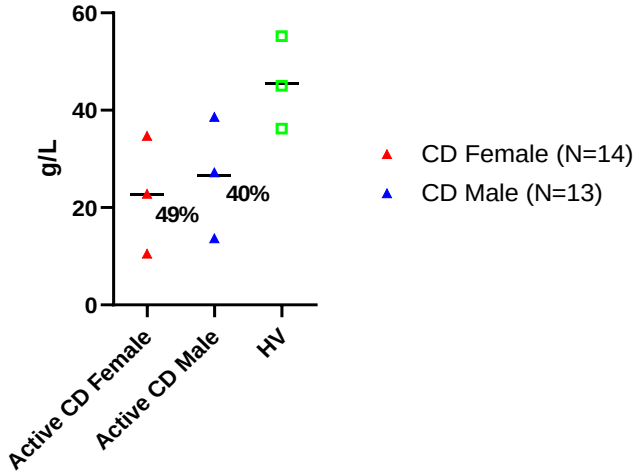

Figure 1.16. *Mean albumin level in active male and female Crohn's disease (CD) patients and percent of its drop compared to healthy volunteers (HV).*

It is important not to assume that albumin level is always low in active CD population, as reported by two large-scale publication of 117 [61] and 6082 [62] active CD subjects. The percent of the patients who encountered severe drop of their albumin during active inflammation did not exceed 22% (Figure 1.17). This to some extent help to explain the bioavailability differences seen when the

same oral drug is given to the same CD patient in different stages of the disease. Details of albumin level studies in CD patients are summarised in Table S1.17.

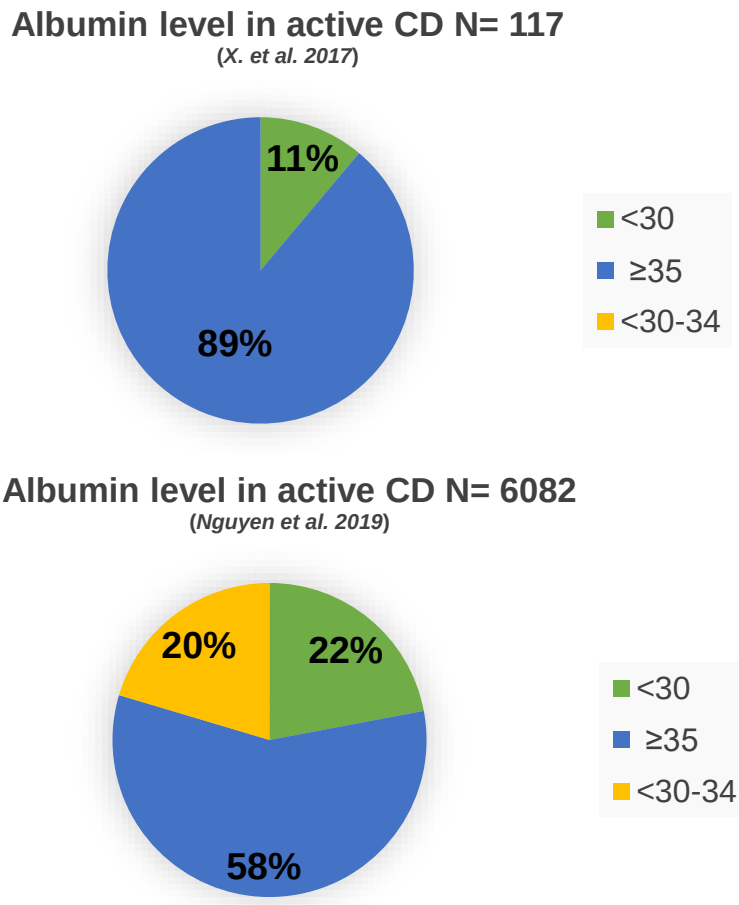

Figure 1.17. *Percent of albumin level; < 30 g/L, <30-34 g/L and ≥35 g/L level in 177 and 6082 active Crohn's disease (CD) patients.*

1.4.1. Step 3: Drugs with available clinical information in CD population

A systematic review was carried out to determine the bioavailability of oral drugs in CD population relative to healthy (Figure 1.18). The observed bioavailability difference in CD can be due to different factors related to the diseased group and/or the drug characteristics. These differences are not consistent for the drugs that are substrates of the same enzyme. Substrates of CYP3A (midazolam, verapamil and budesonide) has shown a significant difference in their bioavailability in some studies.[46,47,75] Although S-verapamil shows the highest deviation in bioavailability (8.7) and maximum blood concentration (Cmax) (9.55) in CD patients compared to healthy subjects

(Table S1.4) there is no available IV data in CD population. Therefore, midazolam and budesonide are chosen for the PBPK application as they also have a significant deviation of their bioavailability (5.25 and 1.89, respectively) with available IV clinical data in CD and healthy population. The IV PK data along with the PO are required to build the compound profile and validate the created CD population. Also this will allow for a better differentiation between the liver and the intestine impact in CD.

Other studies showed similar bioavailability profile in CD patients to HV, regardless of the formulation influence, this was seen with budesonide, prednisolone and cyclosporine.[63,74,121,122] The formulation can also be the reason as seen with mesalamine (5-ASA), the enteric coated formulation showed higher relative bioavailability [52] while the multiparticulate coated formulation showed lower relative bioavailability[123] in CD patients, but the difference observed is not significant. This difference can be translated by the different physiological changes encountered during the active and remission phases of the disease based on the drug properties and how it can be influenced accordingly. Where these drugs were applied on active CD subjects only or mixed active and inactive CD subjects in the different studies.

Other enzymes' substrates showed no significant difference of their bioavailability in CD compared to healthy[75,124] with the exception of propranolol. In propranolol study,[51] the plasma concertation of a single oral dose was examined between Rheumatoid Arthritis (RA), CD and healthy subjects. The results showed that Erythrocyte Sedimentation Rate (ESR) (its elevation used as a nonspecific inflammation indicator[125]) was connected with the observed change in propranolol concentration in the three groups, where higher ESR was associated with higher propranolol concentration. When ESR was low the concentration of propranolol in RA patients was similar to healthy group concentration, but this was not the case in CD group as the concentration remained significantly higher compared to healthy levels. This might be attributed to the fact that the intestine is the primary absorption organ of propranolol and it is the organ directly affected by CD inflammation causing its altered absorption rate, while for RA the inflammation does not primarily occur in the intestine affecting all major organs evenly, thus, their DMETS proteins.

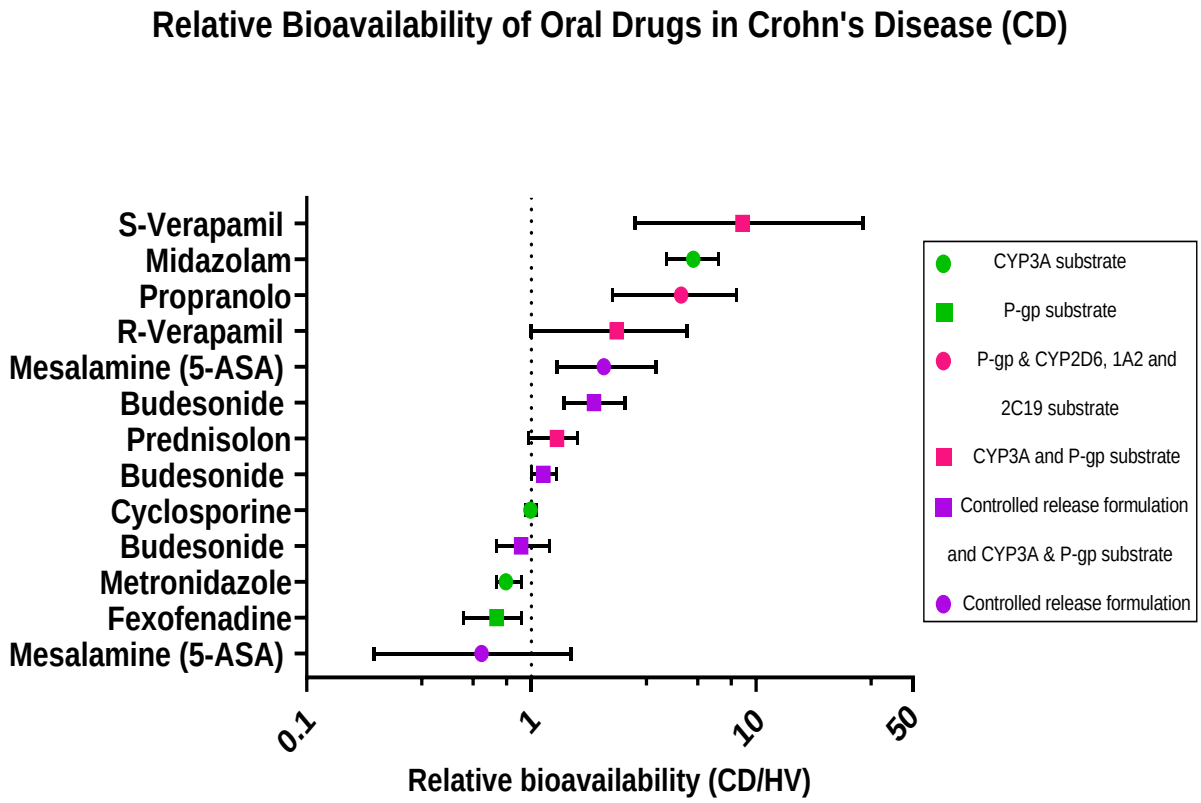

Figure 1.18. *Relative bioavailability (CD/HV) of orally administered drugs in Crohn's disease.*

The reported clearance of the intravenous (IV) drugs in CD relative to HV population showed no significant difference in the clearance ratio except for midazolam (Figure 1.19).

The available information from the IV and PO drugs studied in CD population is not sufficient to withdraw a clear and final conclusion on the behaviour and reasons causing the observed alteration in the drugs bioavailability, with their variable characteristics. Furthermore, it does not give a clear indication of the expected bioavailability profile of drugs that are metabolised and/or absorbed by other DMETs, when given to CD population.

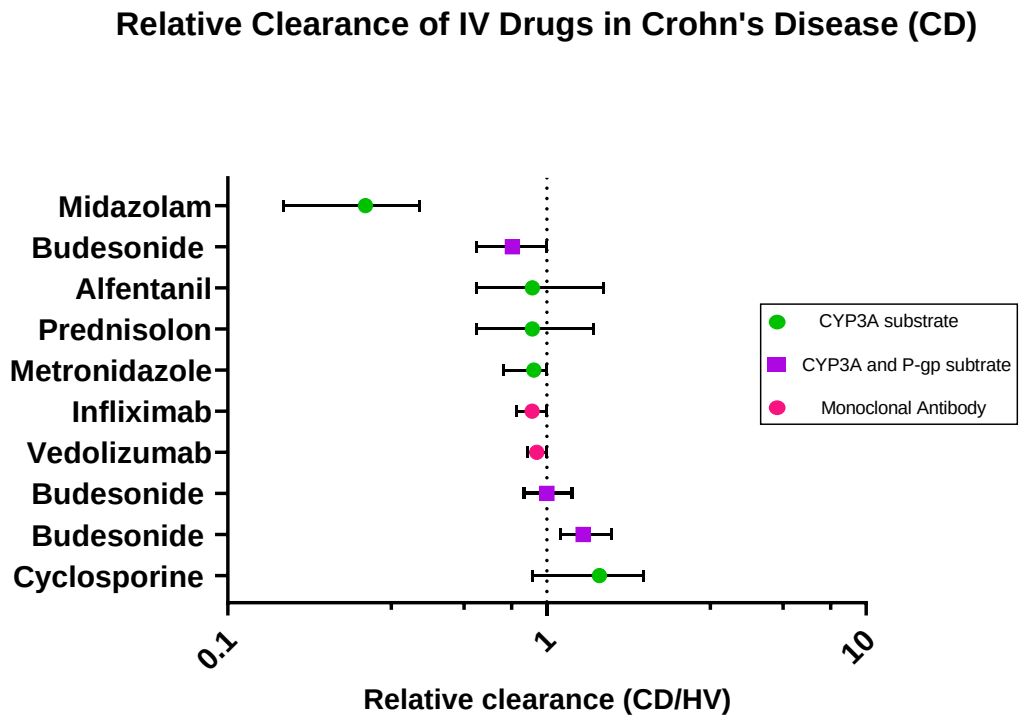

Figure 1.19. *Relative clearance (CD/HV) of drugs administered by intravenous (IV) route in Crohn's disease patients.*

1.4.2. Step 4: Data generation and evaluation of CD-PBPK model

The calculated PBPK model information of budesonide and MDZ extracted from the *in vivo* study in CD are presented in Table 1.5.

Table 1.5. System-specific, combined system-specific and drug-specific model parameters in the PBPK model of Crohn's disease for budesonide controlled release [47] and midazolam oral formulation. [75]

Parameter	Budesonide PBPK results mean Values	MDZ PBPK results mean Values
Body surface area (BSA)	HV= 2.05 m^2 CD= 1.76 m^2	———
Cardiac Index (CI)	HV= 2.74 L/min/m^2 CD= 2.81 L/min/m^2	———

Cardiac output (CO)	HV= 5.62 L/min CD= 4.94 L/min CO (CD/HV) = 12% decrease	____
Hepatic blood flow (Q_H)	HV= 1.46 L/min CD= 1.29 L/min Q_H (CD/HV) = 12% decrease	HV= 1.06 L/min CD= 1.18 L/min Q_H (CD/HV) = 11.3% increase
Drug plasma fraction unbound (fu_P)	HV= 0.15 g/L [56] CD= 0.18 g/L fu_P (CD/HV) = 20% increase	HV= 0.032 g/L CD= 0.041 g/L fu_P (CD/HV) = 28% increase
Hepatic Clearance (CL_H)	____	HV= 0.44 L/min CD= 0.12 L/min CL_H (CD/HV) = 73% decrease
Hepatic intrinsic clearance ($Cl_{int,H}$)	HV= 14.45 L/min CD= 10.2 L/min $Cl_{int,H}$ (CD/HV) = 29.4% decrease	HV= 11.3 L/min CD= 2.02 L/min $Cl_{int,H}$ (CD/HV) = 82% decrease
F_H	The CL_{IV} in both CD and HV populations was reported to be similar (1.3 L/min) and the upper and lower limits of the confidence interval were not far from the mean value. Prober calculation and estimation of CL_H to differentiate between the contribution of intestine F_G and liver F_H in the observed increase of the drug bioavailability in CD population is not possible.	HV= 0.6 CD= 0.9 F_H (CD/HV) = 52% increase From the resulted F_H in CD, it shows that the liver clearance (CYP3A4 activity) has decreased and MDZ absorption has increased by ~50% compared to HV.
F_G	It is noticed from the reported $t_{1/2}$ in HV that it is 10 % lower than CD and the calculated Q_H is 12 % lower in CD suggesting that CD population witness ~10% reduction in budesonide clearance, as it is a high extraction ratio drug (ER= 0.9) which makes it very dependent and affected by the change in Q_H.	HV= 0.5 CD= 0.36 F_G (CD/HV) = 28% decrease On the opposite of what is expected the intestine MDZ absorption F_G decreased by ~30% in CD compared to HV.

From all the above literature-collected system parameters, a population can be created for active, inactive and mixed (active and inactive) CD. This is done based on the overall mean form the above studies for each physiological parameter and their percent change from healthy/control population (Table 1.6). Reduction of Liver CYP3A4 expression by 50 % was based on the F_H increase of MDZ in Crohn's subject as there is no other available data in CD population.[75]

Table 1.6. Summary of identified system parameters and their alterations in active and inactive CD population in relation to healthy/control population, based on literature collected data and extracted data form budesonide [47] and MDZ [75] *in-vivo* studies.

Physiological parameter	**Active CD (Mean ± SD), 90% CI**	**Inactive CD (Mean ± SD), 90% CI**	**CD % mean change from HV mean based on the collected literature data**		**Mixed active and inactive (Mean ± SD), 90% CI**
pH Proximal SI (fasted)	7 ±0.63 (5.98-8.05)	6.5 ±0.34 (5.98-7.09)	**Active**	6.1% increase	6.9 ±0.6, (5.93-7.89) 4.55% increase
			Inactive	1.5% decrease	
pH Terminal SI (fasted)	7.5 ±0.7 (6.44-8.74)	7.6 ±0.6 (6.72-8.64)	**Active**	1.4% increase	7.6 ±0.61, (6.6-8.62) 2.7% increase
			Inactive	2.7% increase	
pH Large intestine (fasted)	6.7 ±0.71 (5.29-7.63)	6.8 ±0.43 (6.06-7.48)	**Active**	1.6% increase	6.5 ±0.61 (5.59-7.58) 3.2% increase
			Inactive	8% increase	
SITT (hr) (fasted)	4.9 ±0.87 (3.57-6.41)	4.7 ±1.62 (2.56-7.71)	**Active**	11% decrease	4.4 ±1.14, (2.81-6.5) 19.1% decrease
			Inactive	14.6% decrease	
SITT (hr) (fed)	5.33±3.8, (1.5-12.45)	—	**Active**	13.4% increase	4.4±3.06, (1.26-10.1) 7.23% decrease
			Inactive	7.23% decrease	
Colonic transit time (hr) (fed)	3 ± 3.54 (9-0.42)	—	**Active**	82.4% decrease	8.1±8, (1.4-14.8) 95% CI 52.5% decrease
			Inactive	52.5% decrease	
	5.9 ±3.59	3.2 ±0.13	**Active**	110.7% increase	3.8±1.83,

Gastric emptying time (hr) (fed)	(2-12.69)	(3-3.42)	**Inactive**	14.3% increase	(1.62-7.27) 38% increase
Gastric emptying time (hr) (fasted)	0.61±0.75, (0.08-1.87)	N/A*	**Active**	3.4% increase	___
			Inactive	___	
Bowel Wall Thickness (BWT) (µm)	8.2 ±2.14, (5.2-12.1)	N/A* [(a)]	**Active**	203.7% increase	___
			Inactive	___	
Superior Mesenteric artery (SMA) blood flow (ml/min)	997.6 ±573.8, (2083.44-359)	321 ±105.3 (516-180.33)	**Active**	209.8% increase	654 ±531, (157.5-1637) 103.14% increase
			Inactive	0.31% decrease	
Local intestine segments blood flow (ml/min*100 g)	Colonic = 78 ±20 Ileum = 26 ±5	Colonic = 14 ±11.8 Ileum = 11 ±1	**Active**	Colon 333% increase	Colon= 54 ± 35.53, (16.82-120.98) 200% increase Ileum= 19.1 ± 8.36, (8.77-34.8) 34% decrease
				Ileum 10.4% decrease	
			Inactive	Colon 22% decrease	
				Ileum 62% decrease	
Intestine DMETs expression	See Table S1.15		**Active**	Table S1.15	___
			Inactive		
Liver CYP3A4	Only available data is based on hepatic extraction ration E_H = 0.11 [(b)]	N/A*	**Active**	50% decrease	___
			Inactive	___	
Serum Albumin (g/L)	32.1±7.6, (21.25-45.85)	40±2.5, (36.04-44.15)	**Active**	20.94% decrease	36.7±6.42, (27.2-48.1) 9.61 % decrease
			Inactive	1.5% decrease	
α1-AGP (g/L)	1.97 ±0.35, (1.45-2.59)	1.27 ±0.2, (0.97-1.62)	**Active**	65.55% increase	1.57 ±0.46, (0.94-2.42) 31.93% increase
			Inactive	6.7% increase	

* N/A; no available data

[(a)] The individual values of the inactive CD group BWT are not reported and the only one showed a change was the active CD; [(b)] Based on MDZ study, F_H increase in active CD patients by 50%.[75]

Based on the % increase or decrease in Table 1.6 of the relevant system parameters for budesonide and MDZ for active and inactive CD compared to healthy values, the change was applied on Simcyp HV population to create the active (Table 1.7) and inactive (Table 1.8) CD population framework. The only exception was the reduction of HSA, it was derived from the only study that reported the albumin level of male and female separately in active subjects. [60] The HSA reduced by 49% in female and 40% in male relative of healthy subjects' level. Furthermore, the reduction of albumin was not assumed to be the definite state of CD patients, thus, the simulation of active CD was carried out once with reduced HSA and once with normal HSA levels. When there is no differentiation between the active and inactive phase the percent change of the mixed CD group is used for both populations.

Table 1.7. Summary of the system parameters input into the Simcyp V19 Simulator for the development of the active CD population for oral budesonide and MDZ.

Physiological parameter	**Budesonide (mix active and inactive CD subjects) (fed)**	**MDZ (active CD subjects) (fasted)**
pH Proximal SI	Unaltered from normal values [(a)]	Duodenum=6.8 Jejunum I & II =6.9 & 7
pH Terminal SI	Unaltered from normal values [(a)]	Ileum(I-IV)= 7, 7.1, 7.2 & 7.4
pH Large intestine	Unaltered from normal values [(a)]	Colon = 6.7
SITT (hr)	5.4	2.96
Colonic transit time (hr)	Male= 6.6 Female = 9.82	Unaltered from normal values [(a)]
Gastric emptying time (hr)	2.5	0.41
Small Intestine blood flow (% of cardiac output)	Male= 31 Female = 34	
Intestine CYP3A4	SI = 36.4 (nmol/SI) Colon = 0.43 (nmol/colon)	

Intestine CYP3A5 [(b)] CYP1A2, [(c)] CYP2C9 [(c)]	SI CYP1A2 and CYP2C9 Unaltered from normal values[(a)] SI CYP2C9 = 13.7 (nmol/SI) Colon CYP2C9 Simcyp value = 0	SI and Colon CYP3A5 Unaltered from normal values[(a)]
Intestine P-gp [(c)]	Duodenum= 0.33, Jejunum I-II = 0.94 and Ileum I-IV = 0.974 (nmol/SI) Colon = 0.18 (nmol/colon)	Not applicable
Liver blood flow (Q_H) (% of cardiac output)	Male= 25 Female = 27 (based on the increase of the intestine blood flow the liver will increase accordingly)	
Liver CYP3A4 [pmol/mg protein] [(d)]	Male = 63 Female = 91.5	
Liver CYP3A5, CYP1A2 and CYP2C9 [(a)]	Unaltered from normal values	
Serum Albumin (g/L) [(e)]	Unaltered from normal values in one simulation Female = 25.2 Male = 30.13	

[(a)] No available information that support their alteration from normal values, so Simcyp HV population values are used; [(b)] used with MDZ only ; [(c)] used with Budesonide only; [(d)] Based on MDZ study F_H increase in active CD patients by 50% [75]; [(e)] Only around 20 % of CD population suffer from albumin drop based on the collected literature data so two simulations are carried out once with reduced albumin level and once with normal albumin level.

Table 1.8. Summary of the system parameters input into the Simcyp V19 Simulator for the development of the inactive CD population for oral budesonide and MDZ.

Physiological parameter	**Budesonide (mix active and inactive CD subjects) (fed)**	**MDZ (active CD subjects) (fasted)**
pH Proximal SI	Unaltered from normal values [(a)]	Duodenum=6.3 Jejunum I & II =6.4 & 6.5
pH Terminal SI	Unaltered from normal values [(a)]	Ileum(I-IV)= 7.1, 7.2, 7.3 & 7.5
pH Large intestine	Unaltered from normal values [(a)]	Colon = 7.1

SITT (hr)	4.4	2.84
Colonic transit time (hr)	Male= 17.8 Female = 26.5	Unaltered from normal values [a]
Gastric emptying time (hr)	1.35	Unaltered from normal values [a]
Small Intestine blood flow (% of cardiac output)	Male= 9.97 Female = 10.97	
Intestine CYP3A4	SI = 36.4 (nmol/SI) Colon = 0.43 (nmol/colon)	
Intestine CYP3A5, CYP1A2 and CYP2C9 [a]	Unaltered from normal values except SI CYP2C9 = 13.7 (nmol/SI)	
Intestine P-gp [b]	Duodenum= 0.15, Jejunum I-II = 0.42 and Ileum I-IV = 0.43 (nmol/SI) Colon = 0.18 (nmol/colon)	Not applicable
Liver blood flow (Q_H) (% of cardiac output)	Male= 18.9 Female = 21.4 (based on the increase of the intestine blood flow the liver will increase accordingly)	
Liver CYP3A4, CYP3A5, CYP1A2 and CYP2C9 [a]	Unaltered from normal values	
Serum Albumin (g/L)	Unaltered from normal values in one simulation Female = 48.6 Male = 49.6	

[a] No available information that support their alteration from normal values, so Simcyp HV population values are used; [b] used with Budesonide only.

The two created CD populations were alternately applied on budesonide and MDZ. The simulations of budesonide in Figure 1.20 and MDZ in Figure 1.21, shows the overlay of plasma concentration time profile of Simcyp HV, active and inactive CD populations models on the

observed clinical data in CD. The predicted and observed PK parameters based on CD population models are presented in Table 1.9, 1.10 and 1.11.

Table 1.9. Comparison of the predicted and observed PK parameters of oral MDZ and Budesonide based on in active CD population with reduced albumin level.

Parameter	**Midazolam oral solution, fasted**			**Parameter**	**Budesonide controlled release, fed**		
	Predicted	Observed Mean ±SD	Predicted/ Observed		Predicted	Observed Mean, 95% CI	Predicted/ Observed
$AUC_{0-\infty}$ (nM*h)	3.6	14±6.38	0.26	$AUC_{0-\infty}$ (nmol*h/L)	194	114, (81.4-159.5)	1.7
Cmax (nM)	2.08	8.4±5.13	0.25	Cmax (nM)	22.3	14.3, (6-13.7)	1.56
Tmax (h)	0.35	0.53± 1.3	0.66	Tmax (h)	5.37	6, (3-8)	0.89
F %	28	31±22	0.9	F %	22	20.5, (8.8-15)	1.07

Table 1.10. Comparison of the predicted and observed PK parameters of oral MDZ and Budesonide in active CD populations with normal albumin level.

Parameter	**Midazolam oral solution, fasted**			**Parameter**	**Budesonide controlled release, fed**		
	Predicted	Observed Mean ±SD	Predicted/ Observed		Predicted	Observed Mean, 95% CI	Predicted/ Observed
$AUC_{0-\infty}$ (nM*h)	6.7	14±6.38	0.48	$AUC_{0-\infty}$ (nM*h)	233.9	114, (81.4-159.5)	2.05
Cmax (nM)	2.97	8.4±5.13	0.35	Cmax (nM)	28.46	14.3, (6-13.7)	1.99
Tmax (h)	0.45	0.53± 1.3	0.85	Tmax (h)	5.23	6, (3-8)	0.87
F %	36.8	31±22	1.19	F %	30	20.5, (8.8-15)	1.46

Table 1.11. Comparison of the predicted and observed PK parameters of oral MDZ and Budesonide in inactive CD populations.

Parameter	**Midazolam oral solution, fasted**			**Parameter**	**Budesonide controlled release, fed**		
	Predicted	Observed Mean ±SD	Predicted/ Observed		Predicted	Observed Mean, 95% CI	Predicted/ Observed
$AUC_{0-\infty}$ (nM*h)	3.06	14±6.38	0.22	$AUC_{0-\infty}$ (nM*h)	51.4	114, (81.4-159.5)	0.45
Cmax (nM)	1.63	8.4±5.13	0.2	Cmax (nM)	7.02	14.3, (6-13.7)	0.49
Tmax (h)	0.42	0.53± 1.3	0.79	Tmax (h)	4.72	6, (3-8)	0.79
F %	27	31±22	0.87	F %	11.5	20.5, (8.8-15)	0.56

As seen from the overlay of the created populations and the PK parameters predicted/observed ratio, that the inactive did not capture the observed clinical outcome. While the simulation of budesonide is better than MDZ, the included subjects in budesonide study where mix of active and inactive CD patients. The active CD population, showed better capture of the observed clinical outcome with both budesonide and MDZ. For budesonide simulation, the reduction of albumin seems to give a relatively closer prediction (within 2 fold) compared to the simulation with normal albumin level. A better simulation of MDZ clinical data is seen with the active CD population when the albumin level is kept to normal values. Nevertheless, these model cannot be relied on as reproducible PBPK model for CD population. Therefore, a global sensitivity analysis was carried out to identify the literature gaps that primarily participate in the observed alteration of the bioavailability in CD subjects.

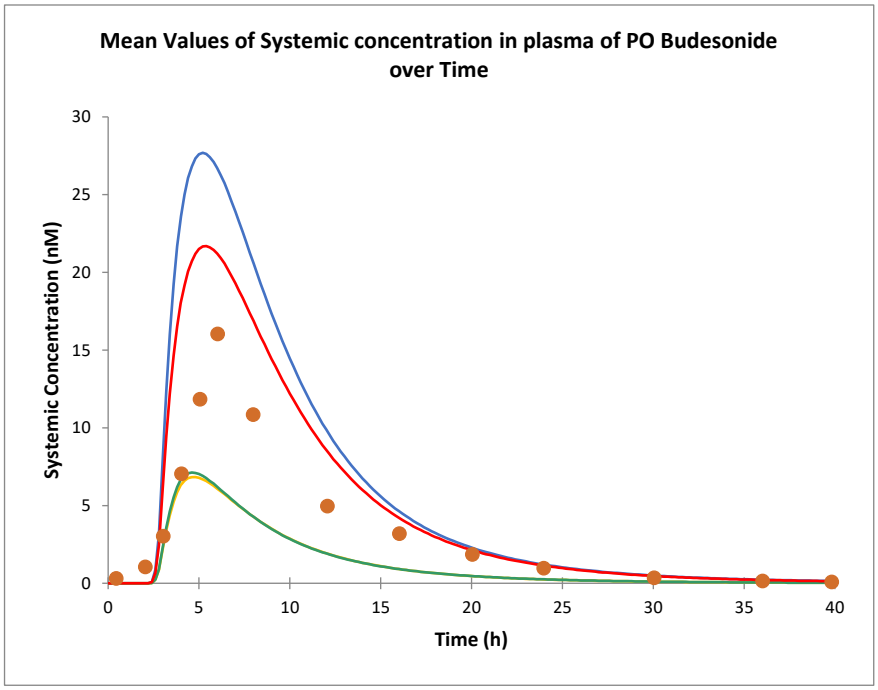

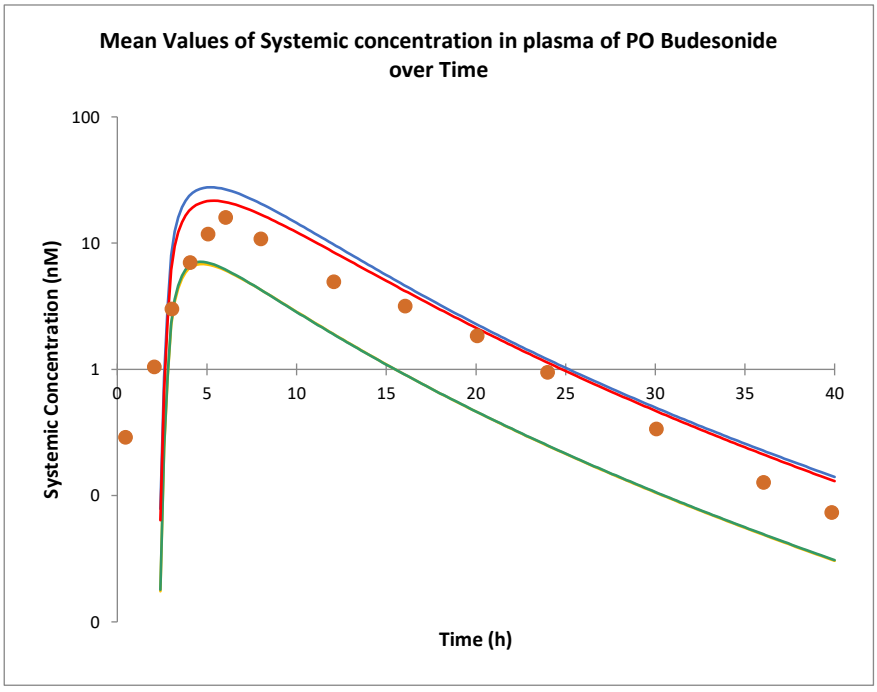

Figure 1.20. *Simulation of budesonide plasma concentration in active and inactive Crohn's disease (CD) patients after administration of 18 mg controlled release oral (PO) formulation in the fed state compared with the observed values from (Edsbäcker et al. 2003).*[47]

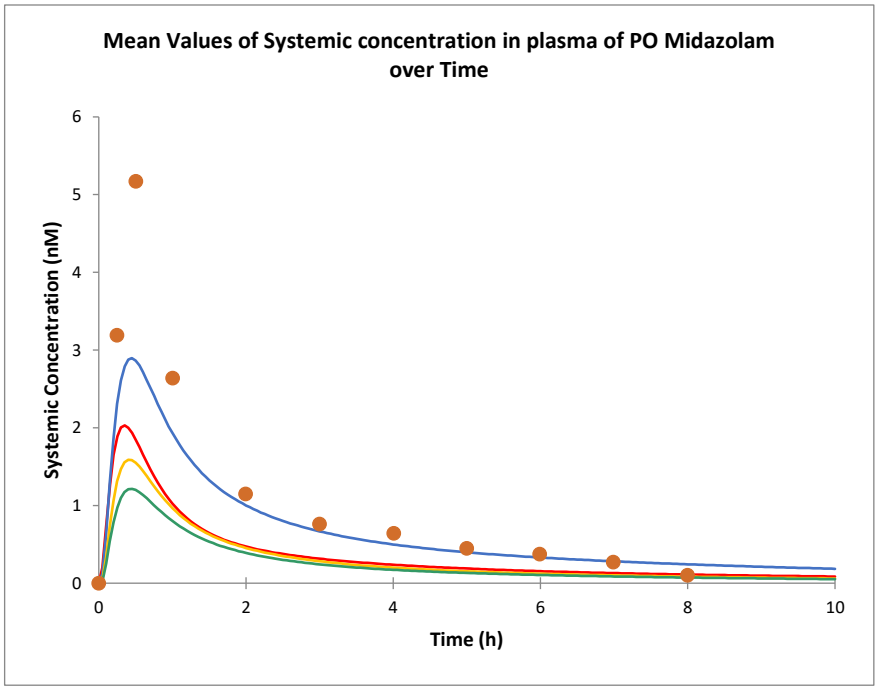

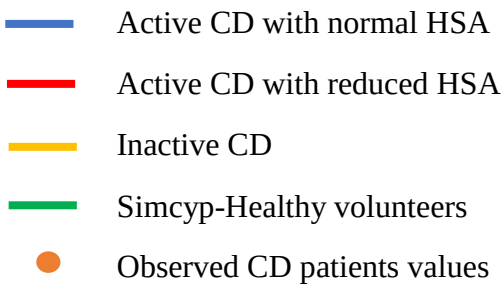

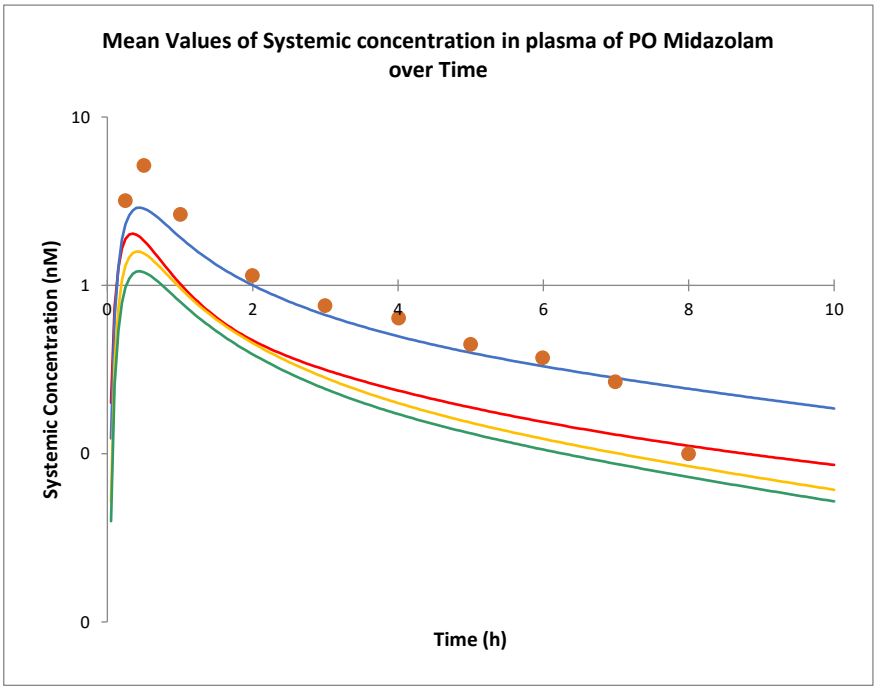

Figure 1.21. *Simulation of midazolam plasma concentration for active and in active Crohn's disease (CD) patients after administration of 0.1 mg oral (PO) solution formulation in the fasted state compared with the observed values from (Wilson, Tirona, and Kim 2017).* [75]

1.4.3. Step 5: Global sensitivity analysis (GSA)

The extent of system parameters involvement in the observed PK difference of CD population investigated. All the identified system parameters that are altered during the course of CD were included in the GSA. But only the parameters that showed the highest influence on the PK parameter investigated are shown. The other parameters with low impact are excluded from the presented output data.

Budesonide global sensitivity index for AUC, Cmax and Tmax are shown in Figure 1.22. The cardiac output is found to have the highest influence on AUC, Cmax and Tmax. HSA comes second for AUC and Cmax and third for Tmax. Mean residence time (MRT) of stomach fluid is one of the highest contributors in Cmax and Tmax observation. When it comes to CYP influence, the liver CYP3A4 is the most impactful on all the three investigated parameters. While the small intestine CYP3A4 abundance has its highest impact on Tmax.

MDZ global sensitivity analysis index is shown in Figure 1.23. The small intestine CYP3A4 abundance is found to be the major influencer on MDZ AUC and Cmax. While gastric emptying time is Tmax major influencer. The liver CYP3A4 abundance comes second for AUC and Tmax, and the cardiac output for Cmax. The jejunum pH and the small intestine transit time participates in the observations of the three investigated PK parameters with varying influence.

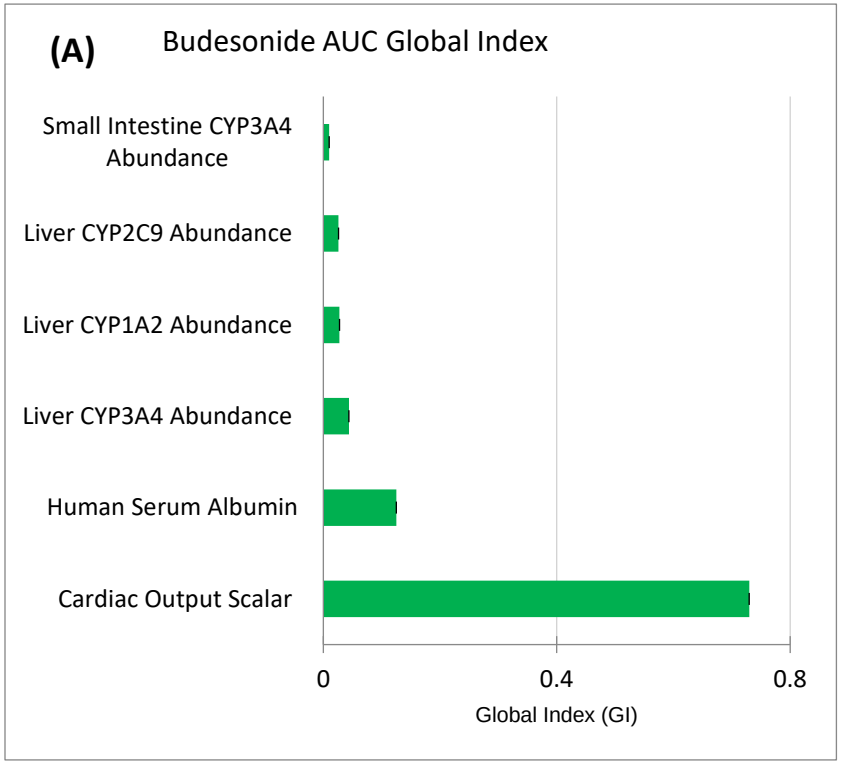

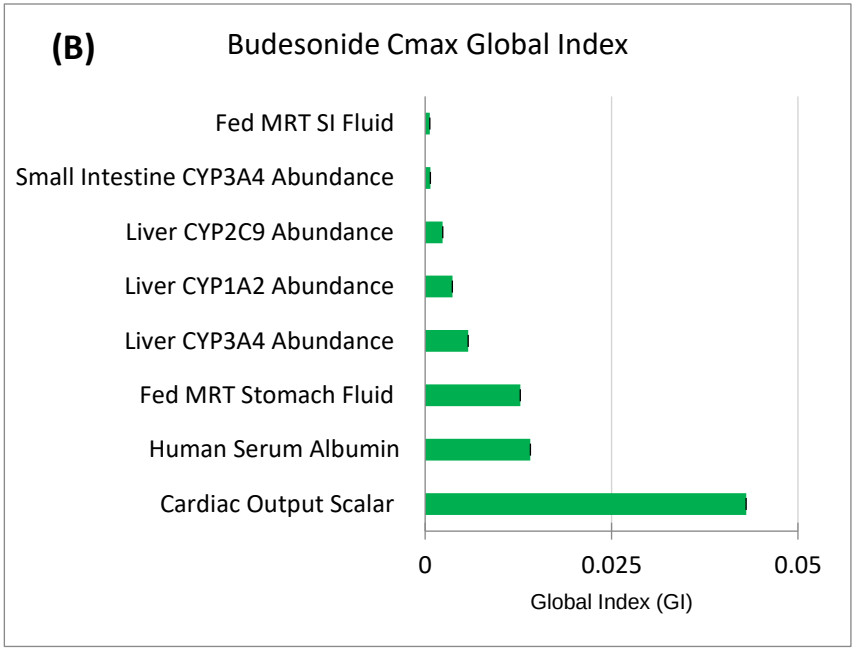

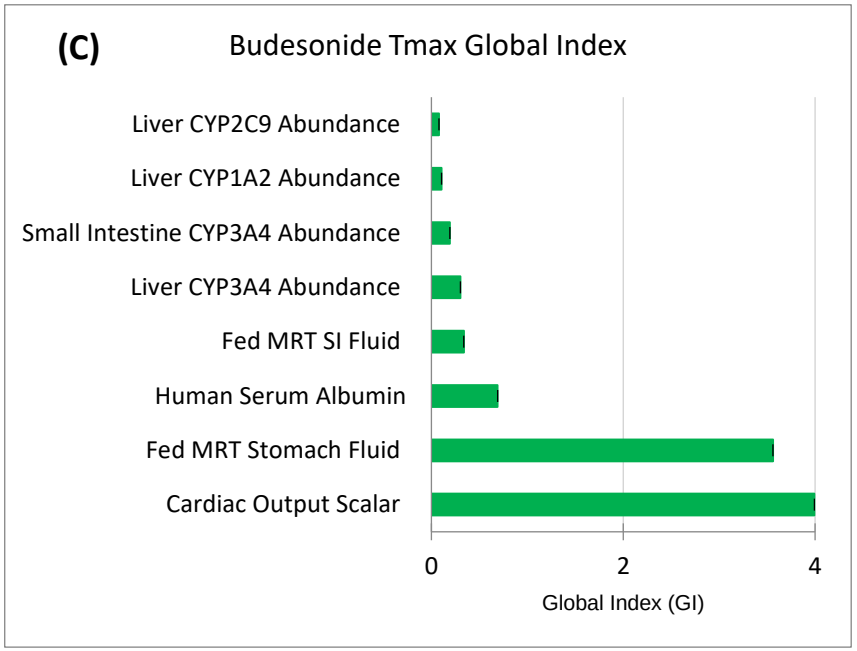

Figure 1.22. *Relative sensitivity of budesonide pharmacokinetic (PK) variables: (A) AUC (B) C_{max} and (C) T_{max} to the system parameters selected for sensitivity analysis in Crohn's disease (CD) population.*

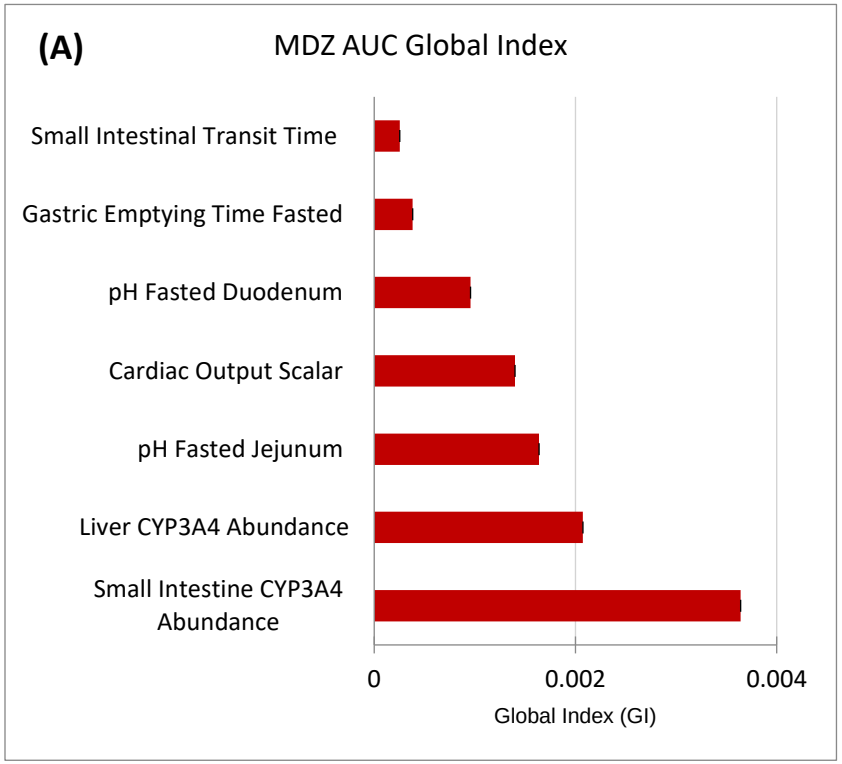

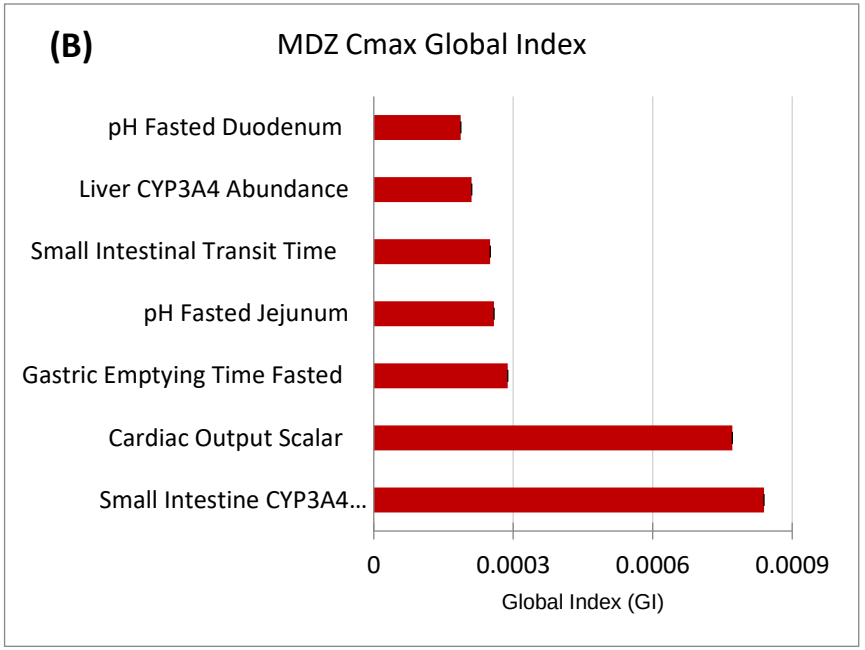

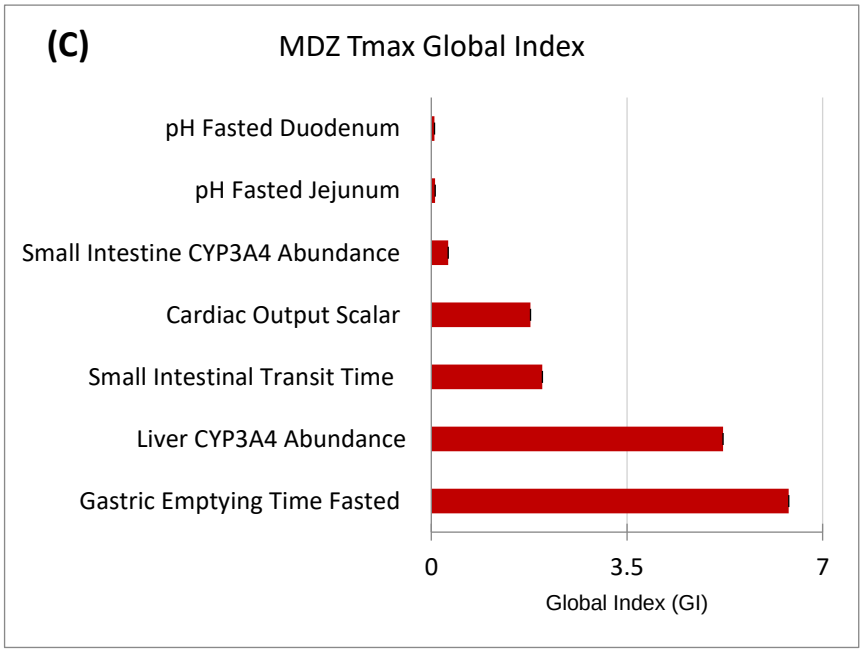

Figure 1.23. *Relative sensitivity of MDZ pharmacokinetic (PK) variables: (A) AUC (B) C_{max} and (C) T_{max} to the system parameters selected for sensitivity analysis in Crohn's disease (CD) population.*

1.5.Discussion

Differentiation between active and inactive Crohn's disease should be made as it can make a big impact when it comes to oral drug pharmacokinetics behaviour. This is identified from the collected literature data of the system parameters, the drug specific parameters and from the PBPK model output simulations. Due to the multifactorial physiological alterations of active and inactive CD, attempts to explain observed changes to oral bioavailability in CD population using single attributes of drugs or simplified modelling is not successful. Available *in vitro* and *in vivo* literature data showed some variations when attempting to build the CD population.

This is specifically pronounced with DMETs abundance data since the gene expression analysis using mRNA relative values does not have a high correlation with direct protein expression measurements for all proteins.[126,127] This was seen with P-gp,[128–130] BCRP, OATP2B1, while MRP2[131–135] mRNA levels are shown to be relatively consistent with the direct protein expression.[136] The UGTs absolute count showed that UGT1A1 and UGT2B7 absolute protein content were not detected in the colon, which does not correlate with the mRNA expression findings.[14] Establishing a relationship that would reflect the correlation between protein mRNA expression and direct concentration is challenging as it was found that around 60% of proteins mRNA levels does not highly correlate to their abundance.[137] In Vitro data are missing in CD population, this data would allow to identify the intestine intrinsic clearance and the microsomal fraction unbound to enable reproducible and more accurate prediction for oral drug PK and differentiation between the involvements of the main metabolising organs.

The developed model analysis was able to capture the major physiological influencers and the gaps to be filled by future research. The liver seems to play a considerable role in several aspects not only as major metabolising organ. It also contributes to the concentration levels of albumin and release of inflammatory cytokines. In inflammatory conditions, albumin synthesis by the liver can be shifted as a result of one or more pathological factors such as protein undernutrition, increased losses due to increases in vascular permeability, maldistribution between intravascular and extravascular spaces and hepatic protein synthesis may be diverted toward other inflammatory cytokines.[138,139] Albumin reduction will affect the drug fraction unbound in the plasma (fu_P). This will affect drug disposition and lead to increase of free drug plasma concentration. The volume of

distribution (Vss) and clearance are sensitive to fu_P values.[140,141] Under prediction of fu_P can lead to under prediction of clearance and hinder the prediction accuracy of drugs with high protein binding affinity.[142,143]

Correlation between albumin reduction and IL-6 elevation is reported in relation to inflammation caused by several conditions. IL-6 reduction along with albumin elevation levels were measured as an indicator of medication effectiveness and reaching to remission state in CD patients.[58] Cultured human hepatocytes were utilized to study the IL-6 suppressing effect on albumin synthesis, the results showed a dose dependent reduction of albumin secretion with increasing IL-6 level.[144,145] In IBD patients (CD and UC), a significant correlation between increased IL-6 and the severity of the disease indicated by its clinical and biochemical manifestations where albumin reduction was detected.[59]

The intestine permeability is another major player in the observed changes. Inflammatory biomarkers elevation is linked to change in the intestine permeability during the course of CD by affecting Vasoactive Intestinal Polypeptide (VIP). VIP is a neuro modulator that participate in increasing the tight junction, thus, reducing the intestine permeability,[146] where it reduces IL-1β, IL-6, and IL-12 and increases IL-10 cytokine inflammatory biomarkers production.[147,148] VIP expression reduction is reported in active CD as part of CD effect on the Enteric Nervous System (ENS) which leads to compromising its functionality in CD population. From several studied inflammatory modulators in CD, IL-6 was the only one found to cause VIP expression reduction in ESN and treating active CD with anti-IL-6 antibody causes elevation of VIP expression.[149] Furthermore, Ileal biopsies taken from elderly subjects with elevated IL-6 [150] and Caco-2 cells [151] were utilized to test IL-6 effect on permeability. IL-6 showed marked positive association between its high level and claudin-2 expression induction, a protein that decreases the tightness of epithelial cells Tight Junction (TJ),[152] which in turn decreases the trans epithelial electric resistance (TEER)[150] and increases TJ [151], thus, increasing the permeability.

The liver effect and its connection to other physiological factors can explain the significant difference seen with MDZ and to some extent budesonide clearance and bioavailability in CD population regardless of their different nature and formulation. If the liver activity is hindered due to liver damage caused by the inflammation then the PK of the drug does not count for a big

difference as seen in liver damaged due to other causes.[153,154] The clearance of the drug is affected despite its PK properties because of two main factors; reduced drug uptake and metabolising enzymes abundance.[154] Livre DMETs alteration will cause a considerable change in drug clearance as it is the major xenobiotic metabolising organ.[155] CYP enzymes are most abundantly present in hepatocytes compared to other metabolising organs.[156] Other non CYP DMEs also contribute largely to drug clearance as they metabolise about 30% of approved drugs.[157] Undesired drug disease interaction can occur of such changes which might result in several complication and delay of the disease control. Thus, more focus should be drawn to it.

Another aspect influenced by the deterioration of the liver function and has no relation with the drug formulation is the displacement of the drug form binding plasma proteins as a result of reduction of albumin synthesis by the liver [158] or as a form of drug-drug interaction.[154] Thus, high extraction ratio drugs like budesonide will be affected by the liver activity deterioration by the same magnitude of low extraction ratio drugs. In addition, counting for oral fraction unbound is different from the IV, and knowing the unbound concentration of the oral formula in CD population is important to judge the change in oral drugs despite their PK nature.

The case of oral budesonide requires further investigation as the different studies reported its bioavailability in CD didn't show significant variation from HV [63,74,75] except for one.[47] The different studies has followed different dose regimens under different fed and fasted conditions but this was reported to carry no significant effect on the drug PK. The sample size in all budesonide studies is small (6-8 subjects), the male to female proportion and the inclusion of active and inactive subjects varies which can contribute to the noticed difference. Another factor is the nature of the drug as it is a high extraction ratio drug highly affected by the blood flow, which is subjected to individual variability due to several conditions. From which is the fed and fasted state, since the fed state results in increasing the splanchnic blood flow (blood flow to the small intestine and liver) which leads to increase their absorption.[159] Increase in the splanchnic blood flow for both liver and intestine has been incorporated in a PBPK model based on a time-variant fed state which captured the elevation extent of two drugs exposure in healthy population.[159] This observed changed indicates that when an oral high extraction drug is under investigation many different factors contribute to its PK behaviour and these factors are changeable specifically in a disease situation; where the change is caused by a combination of organs dysfunction and

alteration in physiological factors all together in the same time. The influence of blood flow sought to be overcame by a multimatrix formulation (MMX®) which is developed to decrease the variation in budesonide PK.[160]

When it comes to the formulation effect, the immediate release and the enteric-coated formulation had similar systemic bioavailability indicating that the site of absorption does not influence budesonide metabolism despite the fact that CYP3A4 present dominantly in the upper parts of the intestine.[47] Assuming that the intestine is treated as a whole organ without considering its different segments and their different properties and functions. This should not be the case as the intestine segments showed to exhibit different absorption effect on budesonide, where ketoconazole used to inhibit intestinal CYP3A4 in jejunum, ileum and colon, which lead to double budesonide plasma concentration in the first two segments while no difference observed in the colon.[161] It rather can be linked to the fact that budesonide is a CYP3A4 and P-gp substrate where they are suggested to function in synergy as a barrier for drugs absorption.[162,163] This assumption is built on their close location in the enterocyte villous tips, the extent of the substrate affinity to each, and coordination between transporter and metabolic enzyme.[164] Both *in-silico* modelling [165–168] and *in vitro* experiments [169,170] have supported the additive relationship of CYP3A4 and P-gp. The difference between immediate release and controlled release formulation for combined CYP3A4 and P-gp substrates was examined by means of PBPK modelling under different scenarios.[67] The reported outcome data showed no significant differences on the AUC between the two formulations compared to when they were examined separately as a CYP3A4 and P-gp substrate. Therefore oral budesonide can't be explained by the liver factors alone or intestine factors alone. this is seen in the *in vivo* experiment in CD where MDZ and fexofenadine used as CYP3A4 and P-gp probe, respectively, showing that only 25% of budesonide PK behaviour can be explained by CYP3A and P-gp abundance.[75]

In relation to the first published CD PBPK model [56] which has a different focus angle from this work our PBPK CD population model has covered more detailed insight of the system parameters (including liver and intestine blood flow, α1-AGP levels) that are not only connected to the investigated drugs (MDZ and budesonide). This allows a wider applicability of the model on oral drug development and precision dosing in CD population. Analysis was applied on all the available system data to identify the gaps, which warrants generation of proteomic and activity data of

intestine and liver DMETs in CD population. To identify the actual magnitude of the two organs impact on drug clearance and bioavailability considering the drugs' various nature and formulations, further investigation of the liver role was implemented in this study to see the extent of its effect based on the different drugs' nature. The liver should be a focused on as no many studies provided direct information on its impact. A distinguish should be made between patients with active disease and in remission state when addressing the physiological status of CD population. The severity of the disease correlate with the deterioration of the physiological parameters which necessitate more focus on the disease activity and severity.

To confirm this findings a GSA was performed which showed variation in the effect intensity of the influencer physiological parameter on MDZ and budesonide. This variation is attributed to different factors related to the drug nature and formulation. Also the activity state of the disease participates in this variability. This is noticed when comparing the GSA of budesonide with MDZ outcomes as the CD subjects participated in budesonide study are a mixture of active and inactive state. While MDZ study had only active state participants.

In conclusion, out of the system parameters that highly influence bioavailability of the two investigated drugs in CD population the expression/activity of liver and intestine enzymes lack reliable literature data. This literature gap stands between the creation of reproducible and predictive CD population PBPK model. The fact that two major elements scarce the required information makes it more challenging to create a model by only relaying on best fit approach. Therefore, an urge for such information generation should be priorities to allow simulation of the fate of oral drugs in CD patients with less uncertainties. Additionally, the two CD populations based on the activity stage were necessary to build separately due to lack of segregation between the two groups in PK related clinical studies in CD population with the noticeable differences in their physiological parameters.

1.6.References

1. Chen L., Deng H., Cui H., Fang J., Zuo Z., Deng J., et al. Inflammatory responses and inflammation-associated diseases in organs. *Oncotarget* 2018. Doi: 10.18632/oncotarget.23208.

2. Xu F., Dahlhamer JM., Zammitti EP., Wheaton AG., Croft JB. Health-Risk Behaviors and Chronic Conditions Among Adults with Inflammatory Bowel Disease — United States, 2015 and 2016. *MMWR Morb Mortal Wkly Rep* 2018;**67**(6):190–5. Doi: 10.15585/mmwr.mm6706a4.

3. Feuerstein JD., Cheifetz AS. Crohn Disease: Epidemiology, Diagnosis, and Management. *Mayo Clin Proc* 2017;**92**(7):1088–103. Doi: 10.1016/j.mayocp.2017.04.010.

4. Doherty MM., M., Pang KS. First-Pass Effect: Significance of the Intestine for Absorption and Metabolism. *Drug Chem Toxicol* 1997;**20**(4):329–44. Doi: 10.3109/01480549709003891.

5. Kiela PR., Ghishan FK. Physiology of Intestinal Absorption and Secretion. *Best Pract Res Clin Gastroenterol* 2016;**30**(2):145–59. Doi: 10.1016/j.bpg.2016.02.007.

6. Gujral N. Celiac disease: Prevalence, diagnosis, pathogenesis and treatment. *World J Gastroenterol* 2012;**18**(42):6036. Doi: 10.3748/wjg.v18.i42.6036.

7. Ballad ST. The Regulation of Tight Junction Permeability During Nutrient Absorption Across the Intestinal Epithelium. *Annu Rev Nutr* 1995;**15**(1):35–55. Doi: 10.1146/annurev.nutr.15.1.35.

8. Paine MF., Hart HL., Ludington SS., Haining RL., Rettie AE., Zeldin DC. THE HUMAN INTESTINAL CYTOCHROME P450 “PIE.” *Drug Metab Dispos* 2006;**34**(5):880–6. Doi: 10.1124/dmd.105.008672.

9. Giacomini KM., Huang S-M. Transporters in Drug Development and Clinical Pharmacology. *Clin Pharmacol Ther* 2013;**94**(1):3–9. Doi: 10.1038/clpt.2013.86.

10. Stevens BR., Kaunitz JD., Wright EM. Intestinal Transport of Amino Acids and Sugars: Advances Using Membrane Vesicles. *Annu Rev Physiol* 1984;**46**(1):417–33. Doi: 10.1146/annurev.ph.46.030184.002221.

11. Barbara G., Stanghellini V., Cremon C., De Giorgio R., Corinaldesi R. What is the effect of inflammation on intestinal function? *Inflamm Bowel Dis* 2008. Doi: 10.1002/ibd.20701.

12. Sartor RB. Current concepts of the etiology and pathogenesis of ulcerative colitis and Crohn’s disease. *Gastroenterol Clin North Am* 1995.

13. Lin JH., Chiba M., Baillie T a. Is the role of the small intestine in first-pass metabolism overemphasized? *Pharmacol Rev* 1999;**51**(2):135–58.

14. Drozdzik M., Busch D., Lapczuk J., Müller J., Ostrowski M., Kurzawski M., et al. Protein Abundance of Clinically Relevant Drug-Metabolizing Enzymes in the Human Liver and Intestine: A Comparative Analysis in Paired Tissue Specimens. *Clin Pharmacol Ther* 2019;**105**(5):1204–12. Doi: 10.1002/cpt.967.

15. Shugarts S., Benet LZ. The Role of Transporters in the Pharmacokinetics of Orally Administered Drugs. *Pharm Res* 2009;**26**(9):2039–54. Doi: 10.1007/s11095-009-9924-0.

16. Tamai I., Nakanishi T. OATP transporter-mediated drug absorption and interaction. *Curr Opin Pharmacol* 2013;**13**(6):859–63. Doi: 10.1016/j.coph.2013.09.001.

17. Huang SM., Zhang L., Giacomini KM. The international transporter consortium: A collaborative group of scientists from academia, industry, and the FDA. *Clin Pharmacol Ther* 2010;**87**(1):32–6. Doi: 10.1038/clpt.2009.236.

18. Estudante M., Morais JG., Soveral G., Benet LZ. Intestinal drug transporters: An overview. *Adv Drug Deliv Rev* 2013;**65**(10):1340–56. Doi: 10.1016/j.addr.2012.09.042.

19. Müller J., Keiser M., Drozdzik M., Oswald S. Expression, regulation and function of intestinal drug transporters: an update. *Biol Chem* 2017;**398**(2):175–92. Doi: 10.1515/hsz-2016-0259.

20. König J., Müller F., Fromm MF. Transporters and Drug-Drug Interactions: Important Determinants of Drug Disposition and Effects. *Pharmacol Rev* 2013;**65**(3):944–66. Doi: 10.1124/pr.113.007518.

21. Nakanishi T., Tamai I. Interaction of Drug or Food with Drug Transporters in Intestine and Liver. *Curr Drug Metab* 2015;**16**(9):753–64. Doi: 10.2174/1389200216091512011135 37.

22. Oswald S. Organic Anion Transporting Polypeptide (OATP) transporter expression, localization and function in the human intestine. *Pharmacol Ther* 2019;**195**:39–53. Doi: 10.1016/j.pharmthera.2018.10.007.

23. Drozdzik M., Gröer C., Penski J., Lapczuk J., Ostrowski M., Lai Y., et al. Protein Abundance of Clinically Relevant Multidrug Transporters along the Entire Length of the Human Intestine. *Mol Pharm* 2014;**11**(10):3547–55. Doi: 10.1021/mp500330y.

24. Harwood MD., Zhang M., Pathak SM., Neuhoff S. The Regional-Specific Relative and Absolute Expression of Gut Transporters in Adult Caucasians: A Meta-Analysis. *Drug Metab Dispos* 2019;**47**(8):854–64. Doi: 10.1124/dmd.119.086959.

25. Petrovic V., Teng S., Piquette-Miller M. Regulation of Drug Transporters: During Infection and Inflammation. *Mol Interv* 2007;**7**(2):99–111. Doi: 10.1124/mi.7.2.10.

26. Slaviero KA., Clarke SJ., Rivory LP. Inflammatory response: an unrecognised source of variability in the pharmacokinetics and pharmacodynamics of cancer chemotherapy. *Lancet Oncol* 2003;**4**(4):224–32. Doi: 10.1016/S1470-2045(03)01034-9.

27. Dumais G., Iovu M., du Souich P. Inflammatory reactions and drug response: importance of cytochrome P450 and membrane transporters. *Expert Rev Clin Pharmacol* 2008;**1**(5):627–47. Doi: 10.1586/17512433.1.5.627.

28. Morgan ET., Goralski KB., Piquette-Miller M., Renton KW., Robertson GR., Chaluvadi MR., et al. Regulation of Drug-Metabolizing Enzymes and Transporters in Infection, Inflammation, and Cancer. *Drug Metab Dispos* 2008;**36**(2):205–16. Doi: 10.1124/dmd.107.018747.

29. Frye RF., Schneider VM., Frye CS., Feldman AM. Plasma levels of TNF-α and IL-6 are inversely related to cytochrome P450-dependent drug metabolism in patients with congestive heart failure. *J Card Fail* 2002;**8**(5):315–9. Doi: 10.1054/jcaf.2002.127773.

30. Rivory LP., Slaviero KA., Clarke SJ. Hepatic cytochrome P450 3A drug metabolism is reduced in cancer patients who have an acute-phase response. *Br J Cancer* 2002;**87**(3):277–80. Doi: 10.1038/sj.bjc.6600448.

31. Sunman JA., Hawke RL., LeCluyse EL., Kashuba ADM. Kupffer Cell-Mediated IL-2 Suppression of CYP3A Activity in Human Hepatocytes. *Drug Metab Dispos* 2004;**32**(3):359–63. Doi: 10.1124/dmd.32.3.359.

32. Aitken AE., Morgan ET. Gene-Specific Effects of Inflammatory Cytokines on Cytochrome P450 2C, 2B6 and 3A4 mRNA Levels in Human Hepatocytes. *Drug Metab Dispos* 2007;**35**(9):1687–93. Doi: 10.1124/dmd.107.015511.

33. Schmitt C., Kuhn B., Zhang X., Kivitz AJ., Grange S. Disease–Drug–Drug Interaction Involving Tocilizumab and Simvastatin in Patients With Rheumatoid Arthritis. *Clin Pharmacol Ther* 2011;**89**(5):735–40. Doi: 10.1038/clpt.2011.35.

34. Dickmann LJ., Patel SK., Rock DA., Wienkers LC., Slatter JG. Effects of Interleukin-6 (IL-6) and an Anti-IL-6 Monoclonal Antibody on Drug-Metabolizing Enzymes in Human Hepatocyte Culture. *Drug Metab Dispos* 2011;**39**(8):1415–22. Doi: 10.1124/dmd.111.038679.

35. Aitken AE., Richardson TA., Morgan ET. REGULATION OF DRUG-METABOLIZING ENZYMES AND TRANSPORTERS IN INFLAMMATION. *Annu Rev Pharmacol Toxicol* 2006;**46**(1):123–49. Doi: 10.1146/annurev.pharmtox.46.120604.141059.

36. Morgan E. Impact of Infectious and Inflammatory Disease on Cytochrome P450–Mediated Drug Metabolism and Pharmacokinetics. *Clin Pharmacol Ther* 2009;**85**(4):434–8. Doi: 10.1038/clpt.2008.302.

37. Korolkova OY., Myers JN., Pellom ST., Wang L., M'koma AE. Characterization of Serum Cytokine Profile in Predominantly Colonic Inflammatory Bowel Disease to Delineate Ulcerative and Crohn's Colitides. *Clin Med Insights Gastroenterol* 2015;**8**:CGast.S20612. Doi: 10.4137/CGast.S20612.

38. Gombošová L., Lazúrová I., Zakuciová M., Čurová K., Kmeťová M., Petrášová D., et

al. Genes of intestinal Escherichia coli and their relation to the inflammatory activity in patients with ulcerative colitis and Crohn's disease. *Folia Microbiol (Praha)* 2011;**56**(5):367–72. Doi: 10.1007/s12223-011-0051-z.

39. Diczfalusy U., Nylén H., Elander P., Bertilsson L. 4β-hydroxycholesterol, an endogenous marker of CYP3A4/5 activity in humans. *Br J Clin Pharmacol* 2011;**71**(2):183–9. Doi: 10.1111/j.1365-2125.2010.03773.x.

40. Ricci G., Ambrosi A., Resca D., Masotti M., Alvisi V. Comparison of serum total sialic acid, C-reactive protein, α1-acid glycoprotein and β2-microglobulin in patients with non-malignant bowel diseases. *Biomed Pharmacother* 1995;**49**(5):259–62. Doi: 10.1016/0753-3322(96)82632-1.

41. Jahnel J., Fickert P., Hauer AC., Högenauer C., Avian A., Trauner M. Inflammatory Bowel Disease Alters Intestinal Bile Acid Transporter Expression. *Drug Metab Dispos* 2014;**42**(9):1423–31. Doi: 10.1124/dmd.114.058065.

42. Silva J., Brito BS., Silva IN de N., Nóbrega VG., da Silva MCSM., Gomes HDDN., et al. Frequency of Hepatobiliary Manifestations and Concomitant Liver Disease in Inflammatory Bowel Disease Patients. *Biomed Res Int* 2019;**2019**:7604939. Doi: 10.1155/2019/7604939.

43. Cappello M., Randazzo C., Bravatà I., Licata A., Peralta S., Craxì A., et al. Liver Function Test Abnormalities in Patients with Inflammatory Bowel Diseases: A Hospital-based Survey. *Clin Med Insights Gastroenterol* 2014;**7**:CGast.S13125. Doi: 10.4137/CGast.S13125.

44. Parisi I., O'Beirne J., Rossi RE., Tsochatzis E., Manousou P., Theocharidou E., et al. Elevated liver enzymes in inflammatory bowel disease. *Eur J Gastroenterol Hepatol* 2016;**28**(7):786–91. Doi: 10.1097/MEG.0000000000000624.

45. Masubuchi Y., Horie T. Endotoxin-mediated disturbance of hepatic cytochrome P450 function and development of endotoxin tolerance in the rat model of dextran sulfate sodium-induced experimental colitis. *Drug Metab Dispos* 2004;**32**(4):437–41. Doi: 10.1124/dmd.32.4.437.

46. Sanaee F., Clements JD., Waugh AWG., Fedorak RN., Lewanczuk R., Jamali F. Drug−disease interaction: Crohn's disease elevates verapamil plasma concentrations but reduces response to the drug proportional to disease activity. *Br J Clin Pharmacol* 2011;**72**(5):787–97. Doi: 10.1111/j.1365-2125.2011.04019.x.

47. Edsbäcker S., Bengtsson B., Larsson P., Lundin P., Nilsson Å., Ulmius J., et al. A pharmacoscintigraphic evaluation of oral budesonide given as controlled-release (Entocort) capsules. *Aliment Pharmacol Ther* 2003;**17**(4):525–36. Doi: 10.1046/j.1365-2036.2003.01426.x.

48. Mayo PR., Skeith K., Russell AS., Jamali F. Decreased dromotropic response to verapamil despite pronounced increased drug concentration in rheumatoid arthritis. *Br J Clin Pharmacol* 2008;**50**(6):605–13. Doi: 10.1046/j.1365-2125.2000.00314.x.

49. Schultz K., Nevill T., Balshaw R., Toze C., Corr T., Currie C., et al. Effect of gastrointestinal inflammation and age on the pharmacokinetics of oral microemulsion cyclosporin A in the first month after bone marrow transplantation. *Bone Marrow Transplant* 2000;**26**(5):545–51. Doi: 10.1038/sj.bmt.1702545.

50. Haas CE., Kaufman DC., Jones CE., Burstein AH., Reiss W. Cytochrome P450 3A4 activity after surgical stress. *Crit Care Med* 2003;**31**(5):1338–46. Doi: 10.1097/01.CCM.0000063040.24541.49.

51. Schneider R., Bishop H., Hawkins C. Plasma propranolol concentrations and the erythrocyte sedimentation rate. *Br J Clin Pharmacol* 1979;**8**(1):43–7. Doi: 10.1111/j.1365-2125.1979.tb05907.x.

52. Norlander B., Gotthard R., Strom M. Pharmacokinetics of a 5-aminosalicylic acid enteric-coated tablet in patients with Crohn's disease or ulcerative colitis and in healthy volunteers. *Aliment Pharmacol Ther* 1990;**4**(5):497–505. Doi: 10.1111/j.1365-2036.1990.tb00496.x.

53. NUGENT SG. Intestinal luminal pH in inflammatory bowel disease: possible determinants and implications for therapy with aminosalicylates and other drugs. *Gut* 2001;**48**(4):571–7. Doi: 10.1136/gut.48.4.571.

54. Chen P., Zhou G., Lin J., Li L., Zeng Z., Chen M., et al. Serum Biomarkers for Inflammatory Bowel Disease. *Front Med* 2020;**7**:123. Doi: 10.3389/fmed.2020.00123.

55. El-Khateeb E., Burkhill S., Murby S., Amirat H., Rostami-Hodjegan A., Ahmad A. Physiological-based pharmacokinetic modeling trends in pharmaceutical drug development over the last 20-years; in-depth analysis of applications, organizations, and platforms. *Biopharm Drug Dispos* 2021;**42**(4):107–17. Doi: 10.1002/bdd.2257.

56. Effinger A., O'Driscoll CM., McAllister M., Fotaki N. Predicting budesonide performance in healthy subjects and patients with Crohn's disease using biorelevant in vitro dissolution testing and PBPK modeling. *Eur J Pharm Sci* 2020:105617. Doi: 10.1016/j.ejps.2020.105617.

57. HARDY JG., HEALEY JNC., REYNOLDS JR. Evaluation of an enteric-coated delayed-release 5-aminosalicylic acid tablet in patients with inflammatory bowel disease. *Aliment Pharmacol Ther* 1987;**1**(4):273–80. Doi: 10.1111/j.1365-2036.1987.tb00627.x.

58. Suzuki Y., Matsui T., Ito H., Ashida T., Nakamura S., Motoya S., et al. Circulating Interleukin 6 and Albumin, and Infliximab Levels Are Good Predictors of Recovering Efficacy After Dose Escalation Infliximab Therapy in Patients with Loss of Response to Treatment for Crohn's Disease. *Inflamm Bowel Dis* 2015;**21**(9):2114–22. Doi: 10.1097/MIB.0000000000000475.

59. Takac B., Mihaljević S., Stefanić M., Glavas-Obrovac L., Kibel A., Samardzija M. Importance of interleukin 6 in pathogenesis of inflammatory bowel disease. *Coll Antropol* 2014;**38**(2):659–64.

60. Jarnum S., Jensen KB. Fecal Radioiodide Excretion Following Intravenous Injection of 131I-Albumin and 125I-Immunoglobulin G in Chronic Inflammatory Bowel Disease. *Gastroenterology* 1975;**68**(6):1433–44. Doi: 10.1016/S0016-5085(75)80129-6.

61. Liu X., Wu X., Zhou C., Hu T., Ke J., Chen Y., et al. Preoperative hypoalbuminemia is associated with an increased risk for intra-abdominal septic complications after primary anastomosis for Crohn's disease. *Gastroenterol Rep* 2017;**5**(4):298–304. Doi: 10.1093/gastro/gox002.

62. Nguyen GC., Du L., Chong RY., Jackson TD. Hypoalbuminaemia and Postoperative Outcomes in Inflammatory Bowel Disease: the NSQIP Surgical Cohort. *J Crohn's Colitis* 2019;**13**(11):1433–8. Doi: 10.1093/ecco-jcc/jjz083.

63. Lundin PDP., Edsbäcker S., Bergstrand M., Ejderhamn J., Linander H., Högberg L., et al. Pharmacokinetics of budesonide controlled ileal release capsules in children and adults with active Crohn's disease. *Aliment Pharmacol Ther* 2003. Doi: 10.1046/j.1365-2036.2003.01386.x.

64. Wan X., Wang W., Liu J., Tong T. Estimating the sample mean and standard deviation from the sample size, median, range and/or interquartile range. *BMC Med Res Methodol* 2014;**14**(1):135. Doi: 10.1186/1471-2288-14-135.

65. Fieller EC. Some Problems in Interval Estimation. *J R Stat Soc Ser B* 1954;**16**(2):175–85. Doi: 10.1111/j.2517-6161.1954.tb00159.x.

66. Motulsky H. *Intuitive Biostatistics: A Nonmathematical Guide to Statistical Thinking*. 2010.

67. Olivares-Morales A., Kamiyama Y., Darwich AS., Aarons L., Rostami-Hodjegan A. Analysis of the impact of controlled release formulations on oral drug absorption, gut wall metabolism and relative bioavailability of CYP3A substrates using a physiologically-based pharmacokinetic model. *Eur J Pharm Sci* 2015;**67**:32–44. Doi: 10.1016/j.ejps.2014.10.018.

68. Jamei M., Turner D., Yang J., Neuhoff S., Polak S., Rostami-Hodjegan A., et al. Population-Based Mechanistic Prediction of Oral Drug Absorption. *AAPS J* 2009;**11**(2):225–37. Doi: 10.1208/s12248-009-9099-y.

69. Thorsson L., Edsbäcker S., Conradson T-B. Lung deposition of budesonide from Turbuhaler® is twice that from a pressurized metered-dose inhaler P-MDI. *Eur Respir J* 1994;**7**(10):1839–44. Doi: 10.1183/09031936.94.07101839.

70. Hohmann N., Kocheise F., Carls A., Burhenne J., Haefeli WE., Mikus G. Midazolam microdose to determine systemic and pre-systemic metabolic CYP3A activity in humans. *Br J Clin Pharmacol* 2015;**79**(2):278–85. Doi: 10.1111/bcp.12502.

71. Klein K., Zanger UM. Pharmacogenomics of Cytochrome P450 3A4: Recent Progress Toward the "Missing Heritability" Problem. *Front Genet* 2013;**4**. Doi: 10.3389/fgene.2013.00012.

72. Xie F., Ding X., Zhang Q-Y. An update on the role of intestinal cytochrome P450 enzymes in drug disposition. *Acta Pharm Sin B* 2016;**6**(5):374–83. Doi: 10.1016/j.apsb.2016.07.012.

73. Pharmacology C. Entocort EC. *Metab Clin Exp* 2005:3–17.

74. Lundin P., Naber T., Nilsson M., Edsbacker S. Effect of food on the pharmacokinetics of budesonide controlled ileal release capsules in patients with active Crohn's disease. *Aliment Pharmacol Ther* 2001. Doi: 10.1046/j.1365-2036.2001.00910.x.

75. Wilson A., Tirona RG., Kim RB. CYP3A4 Activity is Markedly Lower in Patients with Crohn's Disease. *Inflamm Bowel Dis* 2017;**23**(5):804–13. Doi: 10.1097/MIB.0000000000001062.

76. Chetty M., Mattison D., Rostami-Hodjegan A. Sex differences in the clearance of CYP3A4 substrates: exploring possible reasons for the substrate dependency and lack of consensus. *Curr Drug Metab* 2012;**13**(6):778–86. Doi: 10.2174/138920012800840464.

77. Du Bois D., Du Bois E. A formula to estimate the approximate surface area if height and body mass be known. *Arch Intern Med* 1916.

78. Guyton A., Hall J. Textbook of medical physiology. *Am Heart J* 1966;**71**(5):722. Doi: 10.1016/0002-8703(66)90334-6.

79. Valentin J. Basic anatomical and physiological data for use in radiological protection: reference values. A report of age- and gender-related differences in the anatomical and physiological characteristics of reference individuals. ICRP Publication 89. *Ann ICRP* 2002;**32**(3–4):5–265. Doi: 10.1016/S0146-6453(03)00002-2.

80. Cristea S., Krekels EHJ., Rostami-Hodjegan A., Allegaert K., Knibbe CAJ. The Influence of Drug Properties and Ontogeny of Transporters on Pediatric Renal Clearance through Glomerular Filtration and Active Secretion: a Simulation-Based Study. *AAPS J* 2020;**22**(4):87. Doi: 10.1208/s12248-020-00468-7.

81. Fallingborg J., Pedersen P., Jacobsen BA. Small intestinal transit time and intraluminal pH in ileocecal resected patients with Crohn's disease. *Dig Dis Sci* 1998;**43**(4):702–5. Doi: 10.1023/a:1018893409596.

82. Benet LZ., Zia-Amirhosseini P. Basic Principles of Pharmacokinetics. *Toxicol Pathol* 1995;**23**(2):115–23. Doi: 10.1177/019262339502300203.

83. Allonen H., Ziegler G., Klotz U. Midazolam kinetics. *Clin Pharmacol Ther* 1981;**30**(5):653–61. Doi: 10.1038/clpt.1981.217.

84. Liu D., Li L., Rostami-Hodjegan A., Bois FY., Jamei M. Considerations and Caveats when Applying Global Sensitivity Analysis Methods to Physiologically Based Pharmacokinetic Models. *AAPS J* 2020;**22**(5):93. Doi: 10.1208/s12248-020-00480-x.

85. Press AG., Hauptmann IA., Hauptmann L., Fuchs B., Fuchs M., Ewe K., et al.

Gastrointestinal pH profiles in patients with inflammatory bowel disease. *Aliment Pharmacol Ther* 1998;**12**(7):673–8. Doi: 10.1046/j.1365-2036.1998.00358.x.

86. Ewe K., Schwartz S., Petersen S., Press AG. Inflammation does not decrease intraluminal pH in chronic inflammatory bowel disease. *Dig Dis Sci* 1999;**44**(7):1434–9. Doi: 10.1023/a:1026664105112.

87. Sasaki Y., Hada R., Nakajima H., Fukuda S., Munakata A. Improved localizing method of radiopill in measurement of entire gastrointestinal pH profiles: colonic luminal pH in normal subjects and patients with Crohn's disease. *Am J Gastroenterol* 1997;**92**(1):114–8.

88. Fischer M., Siva S., Wo JM., Fadda HM. Assessment of Small Intestinal Transit Times in Ulcerative Colitis and Crohn's Disease Patients with Different Disease Activity Using Video Capsule Endoscopy. *AAPS PharmSciTech* 2017;**18**(2):404–9. Doi: 10.1208/s12249-016-0521-3.

89. Niv E., Fishman S., Kachman H., Arnon R., Dotan I. Sequential capsule endoscopy of the small bowel for follow-up of patients with known Crohn's disease. *J Crohn's Colitis* 2014;**8**(12):1616–23. Doi: 10.1016/j.crohns.2014.03.003.

90. Vermillion DL., Huizinga JD., Riddell RH., Collins SM. Altered small intestinal smooth muscle function in Crohn's disease. *Gastroenterology* 1993;**104**(6):1692–9. Doi: 10.1016/0016-5085(93)90647-U.

91. Vrees MD., Pricolo VE., Potenti FM., Cao W. Abnormal motility in patients with ulcerative colitis: the role of inflammatory cytokines. *Arch Surg* 2002;**137**(4):439–45; discussion 445-6. Doi: 10.1001/archsurg.137.4.439.

92. Annese V., Bassotti G., Napolitano G., Usai P., Andriulli A., Vantrappen G. Gastrointestinal Motility Disorders in Patients with Inactive Crohn's Disease. *Scand J Gastroenterol* 1997;**32**(11):1107–17. Doi: 10.3109/00365529709002989.

93. Hellström, A. Al-Saffar PM. Contractile Responses to Natural Tachykinins and Selective Tachykinin Analogs in Normal and Inflamed Ileal and Colonic Muscle. *Scand J Gastroenterol* 2001;**36**(5):485–93. Doi: 10.1080/00365520117439.

94. Nóbrega ACM., Ferreira BRS., Oliveira GJ., Sales KMO., Santos AA., Nobre e Souza MÂ., et al. Dyspeptic symptoms and delayed gastric emptying of solids in patients with inactive Crohn's disease. *BMC Gastroenterol* 2012;**12**(1):175. Doi: 10.1186/1471-230X-12-175.

95. Lunderquist A., Knutsson H. Angiography in Crohn's disease of the small bowel and colon. *Am J Roentgenol Radium Ther Nucl Med* 1967;**101**(2):338–44. Doi: 10.2214/ajr.101.2.338.

96. Yekeler E., Danalioglu A., Movasseghi B., Yilmaz S., Karaca C., Kaymakoglu S., et al. Crohn disease activity evaluated by Doppler ultrasonography of the superior mesenteric artery and the affected small-bowel segments. *J Ultrasound Med* 2005;**24**(1):59–65.

Doi: 10.7863/jum.2005.24.1.59.

97. Bacaner MB. Quantitative measurement of regional colon blood flow in the normal and pathological human bowel. *Gastroenterology* 1966;**51**(5):764–77. Doi: 10.1016/S0016-5085(19)34333-1.

98. Angerson WJ., Allison MC., Baxter JN., Russell RI. Neoterminal ileal blood flow after ileocolonic resection for Crohn's disease. *Gut* 1993;**34**(11):1531–4. Doi: 10.1136/gut.34.11.1531.

99. Di Sabatino A., Fulle I., Ciccocioppo R., Ricevuti L., Tinozzi FP., Tinozzi S., et al. Doppler Enhancement After Intravenous Levovist Injection in Crohn's Disease. *Inflamm Bowel Dis* 2002;**8**(4):251–7. Doi: 10.1097/00054725-200207000-00003.

100. Brahme F. Mesenteric Angiography in Regional Enterocolitis. *Radiology* 1966;**87**(6):1037–42. Doi: 10.1148/87.6.1037.

101. Su KC., Leung FW., Guth PH. Assessment of mucosal hemodynamics in normal human colon and patients with inflammatory bowel disease. *Gastrointest Endosc* 1989;**35**(1):22–7. Doi: 10.1016/S0016-5107(89)72680-8.

102. Sheehan AL., Warren BF., Gear MWL., Shepherd NA. Fat-wrapping in Crohn's disease: Pathological basis and relevance to surgical practice. *Br J Surg* 1992;**79**(9):955–8. Doi: 10.1002/bjs.1800790934.

103. van Oostayen JA., Wasser MNJM., van Hogezand RA., Griffioen G., de Roos A. Activity of Crohn disease assessed by measurement of superior mesenteric artery flow with Doppler US. *Radiology* 1994;**193**(2):551–4. Doi: 10.1148/radiology.193.2.7972778.

104. van Oostayen J. Diagnosis of Crohn's ileitis and monitoring of disease activity: value of Doppler ultrasound of superior mesenteric artery flow. *Am J Gastroenterol* 1998;**93**(1):88–91. Doi: 10.1016/S0002-9270(97)00029-4.

105. Hultén L., Lindhagen J., Lundgren O., Fasth S., Ahrén C. Regional intestinal blood flow in ulcerative colitis and Crohn's disease. *Gastroenterology* 1977;**72**(3):388–96. Doi: 10.1016/S0016-5085(77)80245-X.

106. Thörn M., Finnström N., Lundgren S., Rane A., Lööf L. Expression of cytochrome P450 and MDR1 in patients with proctitis. *Ups J Med Sci* 2007;**112**(3):303–12. Doi: 10.3109/2000-1967-203.

107. Plewka D., Plewka A., Szczepanik T., Morek M., Bogunia E., Wittek P., et al. Expression of selected cytochrome P450 isoforms and of cooperating enzymes in colorectal tissues in selected pathological conditions. *Pathol - Res Pract* 2014;**210**(4):242–9. Doi: 10.1016/j.prp.2013.12.010.

108. Langmann T., Moehle C., Mauerer R., Scharl M., Liebisch G., Zahn A., et al. Loss of detoxification in inflammatory bowel disease: dysregulation of pregnane X receptor target genes. *Gastroenterology* 2004;**127**(1):26–40. Doi: 10.1053/j.gastro.2004.04.019.

109. Wilson A., Urquhart BL., Ponich T., Chande N., Gregor JC., Beaton M., et al. Crohn's Disease Is Associated with Decreased CYP3A4 and P-Glycoprotein Protein Expression. *Mol Pharm* 2019;**16**(9):4059–64. Doi: 10.1021/acs.molpharmaceut.9b00459.

110. Takayama K., Ito K., Matsui A., Yamashita T., Kawakami K., Hirayama D., et al. In Vivo Gene Expression Profile of Human Intestinal Epithelial Cells: From the Viewpoint of Drug Metabolism and Pharmacokinetics. *Drug Metab Dispos* 2021;**49**(3):221–32. Doi: 10.1124/dmd.120.000283.

111. Klotz U., Hoensch H., Schütz T., Beaune P., Zanger U., Bode JC., et al. Expression of intestinal drug-metabolizing enzymes in patients with chronic inflammatory bowel disease. *Curr Ther Res* 1998;**59**(8):556–63. Doi: 10.1016/S0011-393X(98)85095-9.

112. Blokzijl H., Borght S Vander., Bok LIH., Libbrecht L., Geuken M., van den Heuvel FAJ., et al. Decreased P-glycoprotein (P-gp/MDR1) expression in inflamed human intestinal epithelium is independent of PXR protein levels. *Inflamm Bowel Dis* 2007;**13**(6):710–20. Doi: 10.1002/ibd.20088.

113. Blokzijl H., van Steenpaal A., Borght S Vander., Bok LIH., Libbrecht L., Tamminga M., et al. Up-regulation and Cytoprotective Role of Epithelial Multidrug Resistance-associated Protein 1 in Inflammatory Bowel Disease. *J Biol Chem* 2008;**283**(51):35630–7. Doi: 10.1074/jbc.M804374200.

114. Wojtal KA., Eloranta JJ., Hruz P., Gutmann H., Drewe J., Staumann A., et al. Changes in mRNA Expression Levels of Solute Carrier Transporters in Inflammatory Bowel Disease Patients. *Drug Metab Dispos* 2009;**37**(9):1871–7. Doi: 10.1124/dmd.109.027367.

115. Thibault R., De Coppet P., Daly K., Bourreille A., Cuff M., Bonnet C., et al. Down-Regulation of the Monocarboxylate Transporter 1 Is Involved in Butyrate Deficiency During Intestinal Inflammation. *Gastroenterology* 2007;**133**(6):1916–27. Doi: 10.1053/j.gastro.2007.08.041.

116. Jung D. Human ileal bile acid transporter gene ASBT (SLC10A2) is transactivated by the glucocorticoid receptor. *Gut* 2004;**53**(1):78–84. Doi: 10.1136/gut.53.1.78.

117. Girardin M., Dionne S., Goyette P., Rioux J., Bitton A., Elimrani I., et al. Expression and functional analysis of intestinal organic cation/l-carnitine transporter (OCTN) in Crohn's Disease. *J Crohn's Colitis* 2012;**6**(2):189–97. Doi: 10.1016/j.crohns.2011.08.003.

118. Machavaram KK., Endo-Tsukude C., Terao K., Gill KL., Hatley OJ., Gardner I., et al. Simulating the Impact of Elevated Levels of Interleukin-6 on the Pharmacokinetics of Various CYP450 Substrates in Patients with Neuromyelitis Optica or Neuromyelitis Optica Spectrum Disorders in Different Ethnic Populations. *AAPS J* 2019;**21**(3):42. Doi: 10.1208/s12248-019-0309-y.

119. Zittan E., Kabakchiev B., Kelly OB., Milgrom R., Nguyen GC., Croitoru K., et al. Development of the Harvey-Bradshaw Index-pro (HBI-PRO) Score to Assess

Endoscopic Disease Activity in Crohn's Disease. *J Crohn's Colitis* 2016:jjw200. Doi: 10.1093/ecco-jcc/jjw200.

120. Vagianos K., Bector S., McConnell J., Bernstein CN. Nutrition Assessment of Patients With Inflammatory Bowel Disease. *J Parenter Enter Nutr* 2007;**31**(4):311–9. Doi: 10.1177/0148607107031004311.

121. Milsap RL., George DE., Szefler SJ., Murray KA., Lebenthal E., Jusko WJ. Effect of inflammatory bowel disease on absorption and disposition of prednisolone. *Dig Dis Sci* 1983;**28**(2):161–8. Doi: 10.1007/BF01315146.

122. Flückiger SS., Schmidt C., Meyer A., Kallay Z., Johnston A., Kutz K. Pharmacokinetics of Orally Administered Cyclosporine in Patients with Crohn's Disease. *J Clin Pharmacol* 1995;**35**(7):681–7. Doi: 10.1002/j.1552-4604.1995.tb04108.x.

123. Gionchetti P., Campieri M., Belluzzi A., Boschi S., Brignola C., Miglioli M., et al. Bioavailability of single and multiple doses of a new oral formulation of 5-ASA in patients with inflammatory bowel disease and healthy volunteers. *Aliment Pharmacol Ther* 1994;**8**(5):535–40. Doi: 10.1111/j.1365-2036.1994.tb00327.x.

124. Melander A., Kahlmeter G., Kamme C., Ursing B. Bioavailability of metronidazole in fasting and non-fasting healthy subjects and in patients with Crohn's disease. *Eur J Clin Pharmacol* 1977;**12**(1):69–72. Doi: 10.1007/BF00561408.

125. Alende-Castro V., Alonso-Sampedro M., Vazquez-Temprano N., Tuñez C., Rey D., García-Iglesias C., et al. Factors influencing erythrocyte sedimentation rate in adults. *Medicine (Baltimore)* 2019;**98**(34):e16816. Doi: 10.1097/MD.0000000000016816.

126. Picotti P., Bodenmiller B., Mueller LN., Domon B., Aebersold R. Full Dynamic Range Proteome Analysis of S. cerevisiae by Targeted Proteomics. *Cell* 2009;**138**(4):795–806. Doi: 10.1016/j.cell.2009.05.051.

127. Ohtsuki S., Uchida Y., Kubo Y., Terasaki T. Quantitative targeted absolute proteomics-based ADME research as a new path to drug discovery and development: Methodology, advantages, strategy, and prospects. *J Pharm Sci* 2011;**100**(9):3547–59. Doi: 10.1002/jps.22612.

128. Mouly S., Paine MF. P-Glycoprotein Increases from Proximal to Distal Regions of Human Small Intestine. *Pharm Res* 2003;**20**(10):1595–9. Doi: 10.1023/A:1026183200740.

129. Bruyère A., Declèves X., Bouzom F., Ball K., Marques C., Treton X., et al. Effect of variations in the amounts of P-glycoprotein (ABCB1), BCRP (ABCG2) and CYP3A4 along the human small intestine on PBPK models for predicting intestinal first pass. *Mol Pharm* 2010;**7**(5):1596–607. Doi: 10.1021/mp100015x.

130. Thorn M., Finnstrom N., Lundgren S., Rane A., Loof L. Cytochromes P450 and MDR1 mRNA expression along the human gastrointestinal tract. *Br J Clin Pharmacol* 2005;**60**(1):54–60. Doi: 10.1111/j.1365-2125.2005.02389.x.

131. Nakamura T., Sakaeda T., Ohmoto N., Tamura T., Aoyama N., Shirakawa T., et al. Real-Time Quantitative Polymerase Chain Reaction for MDR1, MRP1, MRP2, and CYP3A-mRNA Levels in Caco-2 Cell Lines, Human Duodenal Enterocytes, Normal Colorectal Tissues, and Colorectal Adenocarcinomas. *Drug Metab Dispos* 2002;**30**(1):4–6. Doi: 10.1124/dmd.30.1.4.

132. Zimmermann C., Gutmann H., Hruz P., Gutzwiller J-P., Beglinger C., Drewe J. Mapping of multidrug resistance gene 1 and multidrug resistance-associated protein isoform 1 to 5 mRNA expression along the human intestinal tract. *Drug Metab Dispos* 2005;**33**(2):219–24. Doi: 10.1124/dmd.104.001354.

133. Englund G., Rorsman F., Rönnblom A., Karlbom U., Lazorova L., Gråsjö J., et al. Regional levels of drug transporters along the human intestinal tract: Co-expression of ABC and SLC transporters and comparison with Caco-2 cells. *Eur J Pharm Sci* 2006;**29**(3–4):269–77. Doi: 10.1016/j.ejps.2006.04.010.

134. Seithel A., Karlsson J., Hilgendorf C., Björquist A., Ungell A-L. Variability in mRNA expression of ABC- and SLC-transporters in human intestinal cells: Comparison between human segments and Caco-2 cells. *Eur J Pharm Sci* 2006;**28**(4):291–9. Doi: 10.1016/j.ejps.2006.03.003.

135. Hilgendorf C., Ahlin G., Seithel A., Artursson P., Ungell A-L., Karlsson J. Expression of Thirty-six Drug Transporter Genes in Human Intestine, Liver, Kidney, and Organotypic Cell Lines. *Drug Metab Dispos* 2007;**35**(8):1333–40. Doi: 10.1124/dmd.107.014902.

136. Harwood MD., Neuhoff S., Carlson GL., Warhurst G., Rostami-Hodjegan A. Absolute abundance and function of intestinal drug transporters: a prerequisite for fully mechanistic in vitro-in vivo extrapolation of oral drug absorption. *Biopharm Drug Dispos* 2013;**34**(1):2–28. Doi: 10.1002/bdd.1810.

137. Vogel C., Marcotte EM. Insights into the regulation of protein abundance from proteomic and transcriptomic analyses. *Nat Rev Genet* 2012;**13**(4):227–32. Doi: 10.1038/nrg3185.

138. Soeters PB., Wolfe RR., Shenkin A. Hypoalbuminemia: Pathogenesis and Clinical Significance. *J Parenter Enter Nutr* 2019;**43**(2):181–93. Doi: 10.1002/jpen.1451.

139. Powell-Tuck J. Protein metabolism in inflammatory bowel disease. *Gut* 1986;**27**(Suppl 1):67–71. Doi: 10.1136/gut.27.Suppl_1.67.

140. Ye M., Nagar S., Korzekwa K. A physiologically based pharmacokinetic model to predict the pharmacokinetics of highly protein-bound drugs and the impact of errors in plasma protein binding. *Biopharm Drug Dispos* 2016;**37**(3):123–41. Doi: 10.1002/bdd.1996.

141. Wilkinson GR., Shand DG. Commentary: a physio-logical approach to hepatic drug clearance. *Clin Pharmacol Ther* 1975;**18**:377–90.

142. Obach RS. Prediction of human clearance of twenty-nine drugs from hepatic microsomal intrinsic clearance data: An examination of in vitro half-life approach and nonspecific binding to microsomes. *Drug Metab Dispos* 1999;**27**(11):1350–9.

143. Baker M., Parton T. Kinetic determinants of hepatic clearance: Plasma protein binding and hepatic uptake. *Xenobiotica* 2007;**37**(10–11):1110–34. Doi: 10.1080/00498250701658296.

144. Li Y., Liu F-Y., Liu ZH., Huang YF., Li LS., Zhang X., et al. Effect of tacrolimus and cyclosporine A on suppression of albumin secretion induced by inflammatory cytokines in cultured human hepatocytes. *Inflamm Res* 2006;**55**(5):216–20. Doi: 10.1007/s00011-006-0074-0.

145. Castell J V., Gómez-lechón MJ., David M., Fabra R., Trullenque R., Heinrich PC. Acute-phase response of human hepatocytes: Regulation of acute-phase protein synthesis by interleukin-6. *Hepatology* 1990;**12**(5):1179–86. Doi: 10.1002/hep.1840120517.

146. Neunlist M., Toumi F., Oreschkova T., Denis M., Leborgne J., Laboisse CL., et al. Human ENS regulates the intestinal epithelial barrier permeability and a tight junction-associated protein ZO-1 via VIPergic pathways. *Am J Physiol Liver Physiol* 2003;**285**(5):G1028–36. Doi: 10.1152/ajpgi.00066.2003.

147. Ekblad E., Bauer AJ. Role of vasoactive intestinal peptide and inflammatory mediators in enteric neuronal plasticity. *Neurogastroenterol Motil* 2004;**16**(s1):123–8. Doi: 10.1111/j.1743-3150.2004.00487.x.

148. Abad C., Juarranz Y., Martinez C., Arranz A., Rosignoli F., García-Gómez M., et al. cDNA Array Analysis of Cytokines, Chemokines, and Receptors Involved in the Development of TNBS-Induced Colitis: Homeostatic Role of VIP. *Inflamm Bowel Dis* 2005;**11**(7):674–84. Doi: 10.1097/01.MIB.0000171872.70738.58.

149. Soufflet F., Biraud M., Rolli-Derkinderen M., Lardeux B., Trang C., Coron E., et al. Modulation of VIPergic phenotype of enteric neurons by colonic biopsy supernatants from patients with inflammatory bowel diseases: Involvement of IL-6 in Crohn's disease. *Neurogastroenterol Motil* 2018;**30**(2):e13198. Doi: 10.1111/nmo.13198.

150. Man AL., Bertelli E., Rentini S., Regoli M., Briars G., Marini M., et al. Age-associated modifications of intestinal permeability and innate immunity in human small intestine. *Clin Sci* 2015;**129**(7):515–27. Doi: 10.1042/CS20150046.

151. Suzuki T., Yoshinaga N., Tanabe S. Interleukin-6 (IL-6) Regulates Claudin-2 Expression and Tight Junction Permeability in Intestinal Epithelium. *J Biol Chem* 2011;**286**(36):31263–71. Doi: 10.1074/jbc.M111.238147.

152. Van Itallie CM., Holmes J., Bridges A., Gookin JL., Coccaro MR., Proctor W., et al. The density of small tight junction pores varies among cell types and is increased by expression of claudin-2. *J Cell Sci* 2008;**121**(3):298–305. Doi: 10.1242/jcs.021485.

153. Orlando R. Cytochrome P450 1A2 is a major determinant of lidocaine metabolism in vivo: effects of liver function. *Clin Pharmacol Ther* 2004;**75**(1):80–8. Doi: 10.1016/j.clpt.2003.09.007.

154. Orlando R., De Martin S., Pegoraro P., Quintieri L., Palatini P. Irreversible CYP3A Inhibition Accompanied by Plasma Protein–Binding Displacement: A Comparative Analysis in Subjects With Normal and Impaired Liver Function. *Clin Pharmacol Ther* 2009;**85**(3):319–26. Doi: 10.1038/clpt.2008.216.

155. Couto N., Al-Majdoub ZM., Achour B., Wright PC., Rostami-Hodjegan A., Barber J. Quantification of Proteins Involved in Drug Metabolism and Disposition in the Human Liver Using Label-Free Global Proteomics. *Mol Pharm* 2019;**16**(2):632–47. Doi: 10.1021/acs.molpharmaceut.8b00941.

156. Gundert-Remy U., Bernauer U., Blömeke B., Döring B., Fabian E., Goebel C., et al. Extrahepatic metabolism at the body's internal-external interfaces. *Drug Metab Rev* 2014;**46**(3):291–324. Doi: 10.3109/03602532.2014.900565.

157. Cerny MA. Prevalence of Non-Cytochrome P450-Mediated Metabolism in Food and Drug Administration-Approved Oral and Intravenous Drugs: 2006-2015. *Drug Metab Dispos* 2016;**44**(8):1246–52. Doi: 10.1124/dmd.116.070763.

158. Bernardi M., Angeli P., Claria J., Moreau R., Gines P., Jalan R., et al. Albumin in decompensated cirrhosis: new concepts and perspectives. *Gut* 2020;**69**(6):1127–38. Doi: 10.1136/gutjnl-2019-318843.

159. Rose RH., Turner DB., Neuhoff S., Jamei M. Incorporation of the Time-Varying Postprandial Increase in Splanchnic Blood Flow into a PBPK Model to Predict the Effect of Food on the Pharmacokinetics of Orally Administered High-Extraction Drugs. *AAPS J* 2017;**19**(4):1205–17. Doi: 10.1208/s12248-017-0099-z.

160. Brunner M., Ziegler S., Di Stefano AFD., Dehghanyar P., Kletter K., Tschurlovits M., et al. Gastrointestinal transit, release and plasma pharmacokinetics of a new oral budesonide formulation. *Br J Clin Pharmacol* 2006;**61**(1):31–8. Doi: 10.1111/j.1365-2125.2005.02517.x.

161. Edsb??cker S., Andersson T. Pharmacokinetics of Budesonide (Entocort??? EC) Capsules for Crohn???s Disease. *Clin Pharmacokinet* 2004;**43**(12):803–21. Doi: 10.2165/00003088-200443120-00003.

162. Watkins P. The barrier function of CYP3A4 and P-glycoprotein in the small bowel. *Adv Drug Deliv Rev* 1997;**27**(2–3):161–70. Doi: 10.1016/S0169-409X(97)00041-0.

163. Benet LZ., Wu C-Y., Hebert MF., Wacher VJ. Intestinal drug metabolism and antitransport processes: A potential paradigm shift in oral drug delivery. *J Control Release* 1996;**39**(2–3):139–43. Doi: 10.1016/0168-3659(95)00147-6.

164. Benet LZ. The Drug Transporter−Metabolism Alliance: Uncovering and Defining the Interplay. *Mol Pharm* 2009;**6**(6):1631–43. Doi: 10.1021/mp900253n.

165. S. Darwich A., Neuhoff S., Jamei M., Rostami-Hodjegan A. Interplay of Metabolism and Transport in Determining Oral Drug Absorption and Gut Wall Metabolism: A Simulation Assessment Using the "Advanced Dissolution, Absorption, Metabolism (ADAM)" Model. *Curr Drug Metab* 2010;**11**(9):716–29. Doi: 10.2174/138920010794328913.

166. Badhan R., Penny J., Galetin A., Houston JB. Methodology for development of a physiological model incorporating CYP3A and P-glycoprotein for the prediction of intestinal drug absorption. *J Pharm Sci* 2009;**98**(6):2180–97. Doi: 10.1002/jps.21572.

167. Ito K., Kusuhara H., Sugiyama Y. Effects of intestinal CYP3A4 and P-glycoprotein on oral drug absorption--theoretical approach. *Pharm Res* 1999;**16**(2):225–31. Doi: 10.1023/a:1018872207437.

168. Watanabe T., Maeda K., Nakai C., Sugiyama Y. Investigation of the Effect of the Uneven Distribution of CYP3A4 and P-Glycoprotein in the Intestine on the Barrier Function against Xenobiotics: A Simulation Study. *J Pharm Sci* 2013;**102**(9):3196–204. Doi: 10.1002/jps.23623.

169. Cummins CL., Jacobsen W., Benet LZ. Unmasking the Dynamic Interplay between Intestinal P-Glycoprotein and CYP3A4. *J Pharmacol Exp Ther* 2002;**300**(3):1036–45. Doi: 10.1124/jpet.300.3.1036.

170. Cummins CL., Jacobsen W., Christians U., Benet LZ. CYP3A4-Transfected Caco-2 Cells as a Tool for Understanding Biochemical Absorption Barriers: Studies with Sirolimus and Midazolam. *J Pharmacol Exp Ther* 2004;**308**(1):143–55. Doi: 10.1124/jpet.103.058065.

1.7.Supplementary material-Methodology

Calculation method of oral drugs relative bioavailability and IV drugs relative clearance and its 95% confidence interval (CI)

The relative bioavailability and clearance between CD and HV populations was calculated from the mean AUC and clearance data reported for the different studies collated from the literature.

For the estimation of the ratio between CD and HV populations, $\frac{a}{b}$, and its 95% confidence interval (CI), an approximation of the Fieller's theorem [1–3] was employed as per Equation 1.

$$CI_{\frac{a}{b}(1-\alpha)} = \frac{a}{b \times (1-g)} \pm t_{\alpha,df} SE_{\frac{a}{b}} \qquad \textbf{(1)}$$

Where; a is the mean AUC for the CD population and b is the mean AUC for the HV population, $t_{\alpha,df}$ is the inverse of the cumulative t distribution (two tailed) for a significance level of α (0.05) and degrees of freedom (df) is equal to n_a+n_b-2, n_a and n_b are the number of subjects in the study for the estimation of a and b, respectively, and $SE\frac{a}{b}$ is the combined. Standard error for the ratio $\frac{a}{b}$ and it is calculated from Equation 2.

$$SE_{\frac{a}{b}} = \frac{a}{b \times (1-g)} \sqrt{(1-g) \times \frac{SE_a{}^2}{a^2} + \frac{SE_b{}^2}{b^2}} \qquad \textbf{(2)}$$

Where; the quantity g is given by Equation 3, and SE_a and SE_b are the standard error of the means a and b, respectively.

$$g = \frac{t^2{}_{\alpha,df} \times SE_b{}^2}{b^2} \qquad \textbf{(3)}$$

When the standard deviation (SD) is not provided in a study to enable calculation of SE it is calculated from CI upper and lower limits [4] following Equation 4.

$$SD = \sqrt{N} * (upper\ limit - lower\ limit)/t\ distribution \qquad \textbf{(4)}$$

Table S1.1. CYP450 enzymes expression in healthy population along the human intestine.

CYPs	mRNA & immunoblotting studies	LCMS studies
Jejunum **mRNA:** [5–12] **LC/MS:** [13–17]	*CYP3A subfamily* CYP3A4, CYP3A5, CYP3A7 *CYP2C subfamily* CYP2C9, CYP2C19 *Other CYPs isoforms* CYP1A1, CYP2D6, CYP2J2	*CYP3A subfamily* CYP3A4, CYP3A5, CYP3A7. *CYP2C subfamily* CYP2C9, CYP2C19, CYP2C8, CYP2C18. *Other CYPs isoforms* CYP2D6, CYP2J2, CYP2B6, CYP1A2, CYP2E1, CYP1A21, CYP2J2.
Duodenum **mRNA:** [5,9,11,18–21] **LC/MS:** [16]	*CYP3A subfamily* CYP3A4, CYP3A5, CYP3A7 *CYP2C subfamily* CYP2C8, CYP2C9, CYP2C18, CYP2C19 *Other CYPs isoforms* CYP2D6, CYP2B6, CYP2E1, CYP2J2	
Ileum **mRNA:** [5,8,10,11,22] **LC/MS:** [16,17]	*CYP3A subfamily* CYP3A4, CYP3A5, CYP3A7 *CYP2C subfamily* CYP2C9, CYP2C18, CYP2C19 *Other CYPs isoforms* CYP2B6, CYP2J2	
Colon **mRNA:** [10,20,22–26] **LC/MS:** [16]	*CYP3A subfamily* CYP3A4, CYP3A5 *CYP2C subfamily* CYP2C8, CYP2C9, CYP2C18, CYP2C19 *Other CYPs isoforms* CYP2E1, CYP2B6, CYP2J2	
Small intestine **mRNA:** [18,27,28]	*CYP3A subfamily* CYP3A4, CYP3A5 *CYP2C subfamily* CYP2C8, CYP2C9, CYP2C18, CYP2C19 *Other CYPs isoforms* CYP1A1, CYP2D6, CYP2E1, CYP2J2, CYP2B6	

Table S1.2. UGT enzymes expression in healthy population along the human intestine.

UGTs	mRNA studies	Absolute abundance
Jejunum **mRNA:** [29–31] **LC/MS:** [13–17]	*UGT1A subfamily* UGT1A1, UGT1A3, UGT1A4, UGT1A6, UGT1A10 *UGT2B subfamily* UGT2B4, UGT2B7, UGT2B15, UGT2B17	*UGT1A subfamily* UGT1A1, UGT1A3, UGT1A4, UGT1A6, UGT1A8. *UGT2B subfamily* UGT2B4, UGT2B7, UGT2B15, UGT2B17.
Duodenum **mRNA:** [21,30,31] **LC/MS:** [16]	*UGT1A subfamily* UGT1A1, UGT1A3, UGT1A4, UGT1A6, UGT1A10 *UGT2B subfamily* UGT2B4, UGT2B7, UGT2B15, UGT2B17	
Ileum **mRNA:** [22,29–31] **LC/MS:** [16,17]	*UGT1A subfamily* UGT1A1, UGT1A4, UGT1A5, UGT1A6, UGT1A8, UGT1A9, UGT1A10 *UGT2B subfamily* UGT2B4, UGT2B7, UGT2B15, UGT2B17	
Colon **mRNA:** [22,31–33] **LC/MS:** [16]	*UGT1A subfamily* UGT1A1, UGT1A4, UGT1A5, UGT1A6, UGT1A8, UGT1A9, UGT1A10 *UGT2B subfamily* UGT2B7, UGT2B17	

Table S1.3. Drug SLC and ABC transporters expression in human intestine.

SLC Uptake transporters	mRNA studies	LCMS studies
Jejunum **mRNA:** [17,34–37] **LC/MS:** [12,15,17,38,39]	*SLC, Uptake transporters*	*SLC, Uptake transporters*

	PEPT1, OCTN2, MCT1, OATP2B1, OCT1, OCT2, OCT3, OSTα/β	PEPT1, MCT1, OSTα/β, OATP2B1, OCTN1, CNT2, OCT1, OCT3, OATP1A2
Duodenum **mRNA:** [34,37,40–42] **LC/MS:** [39]	*SLC, Uptake transporters* PEPT1, OCTN1, OCTN2, OCT1, MCT1, OATP2B1, CNT1, CNT2, ASBT	*SLC, Uptake transporters* PEPT1, OATP2B1, OCT1, OCT3
Ileum **mRNA:** [17,22,34,37,40–43] **LC/MS:** [17,38,39,44]	*SLC, Uptake transporters* PEPT1, MCT1, OATP2B1, OCT1, OCT2, OCT3, OCTN1, OCTN2, ASBT, CNT2, CNT1, ENT1, ENT2, OATP4A1, OSTα/β	*SLC, Uptake transporters* PEPT1, MCT1, OATP2B1, OSTα/β, OCT1, OCT2, OCT3, ASBT, OCNT1, OCNT2, OATP1A2
Colon **mRNA:** [22,34–37,40–43] **LC/MS:** [39]	*SLC, Uptake transporters* MCT1, OATP2B1, OCT1, OCT2, OCT3, OCTN1, OCTN2, CNT2, ENT1, ENT2, OATP4A1	*SLC, Uptake transporters* OATP2B1, OCT1, OCT3, OCT2, OCNT1, OCNT2, OSTα/β * PEPT1 and ASBT (not present)
ABC Efflux transporters	**mRNA studies**	**LCMS studies**
Jejunum **mRNA:** [8,10,11,17,34–37,45] **LC/MS:** [12,14,17,38,39,44,46,47]	*ABC, Efflux transporters* P-gp, BCRP, MRP1, MRP2, MRP3	*ABC, Efflux transporters* P-gp, BCRP, MRP1, MRP2, MRP3
Duodenum **mRNA:** [11,19,20,25,34,37,40,45,48–50] **LC/MS:** [39]	*ABC, Efflux transporters* P-gp, BCRP, MRP1, MRP2, MRP3	*ABC, Efflux transporters* P-gp, BCRP, MRP2, MRP3
Ileum **mRNA:** [8,10,11,17,22,34,37,40,45,50] **LC/MS:** [17,38,39,44,46,47]	*ABC, Efflux transporters* P-gp, BCRP, MRP1, MRP2, MRP3	*ABC, Efflux transporters* P-gp, BCRP, MRP1, MRP2, MRP3 * MRP2 wasn't detected in *one study* [44]
Colon **mRNA:** [10,22,34–37,40,49,50] **LC/MS:** [39]	*ABC, Efflux transporters* P-gp, BCRP, MRP1, MRP2, MRP3 *mRNA expression of MRP2 in the colon was not detected in two studies.[36,40]	*ABC, Efflux transporters* P-gp, BCRP, MRP1, MRP2, MRP3

Table S1.4. Relative bioavailability studies between Crohn's disease (CD) and healthy volunteers (HV) populations reported in the literature.

Oral Compound	AUC_{CD} (μg×h/mL)	SD	N_{CD}	AUC_{HV} (μg×h/mL)	SD	N_{HV}	Relative (AUC_{CD}/AUC_{HV})	Lower 95% CI	Upper 95% CI	Relative C_{max} (CD/HV)	Reference
Metronidazole	0.37	0.05	9	0.49	150	10	0.77	0.7	0.9	1.1	[51]
Propranolol	0.37	0.34	16	0.08	0.013	13	4.64	2.32	8.17	N/A	[52]
Prednisolone [a]	2.8	0.7	7	2.2	0.34	7	1.3	0.97	1.6	N/A	[53]
Mesalamine (5-ASA) EC [b]	6.95	2.9	9	3.35	1.95	10	2.1	1.3	3.6	1.23	[54]
Mesalamine (5-ASA) EC [b]	0.9	0.8	9	1.5	0.88	6	0.6	0.2	1.5	0.33	[55]
Cyclosporine	4.61	1.39	19	4.54	1.3	23	0.99	0.94	1.05	0.9	[56]
Budesonide EC [b c]	0.012	0.0002	8	0.013	0.009	8	0.9	0.7	1.2	0.85	[57,58]
Budesonide EC [b c]	0.02	0.01	6	0.013	0.009	8	1.13	1	1.3	1.33	[58,59]
Budesonide EC [b]	0.05	0.02	6	0.026	0.009	8	1.9	1.4	2.6	1.6	[58]
S-Verapamil	0.54	0.6	14	0.06	0.06	9	8.7	2.9	30	9.55	[60]
R-Verapamil	1.72	1.7	14	0.72	0.45	9	2.4	1	4.9	2.	[60]
Midazolam [c]	0.005	0.01	8	0.001	0.0003	16	5.25	4	6.8	0.8	[61,62]
Fexofenadine [c]	2.2	0.77	8	3.25	0.43	12	0.7	0.5	0.9	0.8	[61,63]

AUC_{CD}, mean AUC for Crohn's disease population; **AUC_{HV}**, mean AUC for healthy volunteers population; **N_{CD}**, number of subjects employed for the calculation of AUC_{CD}**;** **N_{HV}**, number of subjects employed for the calculation of AUC_{HV}; **C_{max}**, maximum concentration in blood; EC, enteric coated; 5-ASA, 5 aminosalicylic acid; **N/A**, no available data.

[a] the pateint group were mixed active Crohn;s disease and Ulcerative coloitis and it was not compared to HV it was compared to remession group.

[b] duplicated compounds in different studies. [c] Crohn's disease and healthy volunteer group are not from the same study.

Table S1.5. Relative clearance studies between Crohn's disease (CD) and healthy volunteers (HV) populations reported in the literature.

IV Compound	**CL_{CD}** (ml/min)	**SD**	**N_{CD}**	**CL_{HV}** (ml/min)	**SD**	**N_{HV}**	**Ratio** (CL_{CD}/CL_{HV})	Lower 95% CI	Upper 95% CI	**Relative C_{max}** (CD/HV)	**Reference**
Prednisolon [a]	178	70	7	197	66	7	0.9	0.77	0.903	N/A	[53]
Metronidazole [c]	3.24	0.53	7	3.56	0.68	18	0.91	0.89	0.91	0.89	[64,65]
Cyclosporine [c]	462	275	12	317	51	10	1.46	1.35	1.54	N/A	[66,67]
Alfentanil	342	120	12	384	216	10	0.9	0.702	0.834	1.8	[68]
Budesonide EC [b c]	1710	96	8	1300	299	8	1.3	1.26	1.3	N/A	[57,58]
Budesonide EC [b c]	1020	150	5	1300	299	8	0.78	0.74	0.78	N/A	[58,59]
Budesonide EC [b]	1300	48	6	1300	299	8	1	0.954	0.98	N/A	[58]
Infliximab [c]	9.8	2	25	10.9	2.95	53	0.9	089	0.9	0.92	[69,70]
Midazolam [c]	117	72	8	428	55	16	0.27	0.24	0.292	0.27	[61,62]
Vedolizumab	0.155	0.044	209	0.166	0.033	41	0.93	0.93	0.933	N/A	[71]

AUC_{CD}, mean AUC for Crohn's disease population; **AUC_{HV}**, mean AUC for healthy volunteers population; **N_{CD}**, number of subjects employed for the calculation of AUC_{CD}; **N_{HV}**, number of subjects employed for the calculation of AUC_{HV}; **C_{max}**, maximum concentration in blood; EC, enteric coated; 5-ASA, 5 aminosalicylic acid; **N/A**, no available data.

[a] the pateint group were mixed active Crohn;s disease and Ulcerative coloitis and it was not compared to HV it was compared to remession group.

[b] duplicated compounds in different studies.

[c] Crohn's disease and healthy volunteer group are not from the same study.

Table S1.6. Budesonide drug profile input parameters for Simcyp simulations.

Parameter	*Value*	*Reference/comments*
Molecular weight (g/mol)	430.5	[72]
LogP (octanol:water)	2.62	
Ionic class	Neutral	
Fraction unbound in plasma	0.15	
Blood plasma ratio (B:P)	0.8	
Distribution model	Full PBPK, Method 2	
Kp scaler [1]	0.235	Estimated based on best fit to the observed IV data in healthy population [73]
Elimination	Enzyme kinetics (Recombinant)	
CL_{IV} (L/hr)	63	Based on the HV study [73] best fit CL value (range 56.4-118.8 which adjusted based on Simcyp by * BP (0.8) giving 45.12-95.04 L/hr range)
$CL_{Int,H}$ [2] **(µL/min/pmol of isoform)**	CYP3A4 = 8.4	Calculated with Simcyp retrograde model based on 63 L/h systemic clearance and Simcyp healthy population
	CYP1A2 = 1.37	
	CYP2C9 = 0.946	
Difference in male/female CYP3A4 abundance activated		
Transport (permeability limited organ) [1]	Intestine ABCB1 (P-gp) **Jmax** = 93 **Km**= 9.4	Estimated based on best fit to the observed PO data in healthy population [58]
Absorption model	Multiple layer gut wall within ADAM (M-ADAM)	User-defined effective passive permeability
Apical Ptrans,0 (10^{-6} cm/s)	Duodenum, jejunum I & II =1.9 Ileum I-IV = 3.4 and Colon= 0.59	[74]
Basolateral Ptrans Ptrans,0 (10-6 cm/s) [1]	Duodenum= 13, jejunum I & II =9, Ileum I-IV = 6 and Colon= 18	Predicted based on the LogP value, the apical Ptrans and observed PO data in healthy population. As is this membrane

		has a relatively higher permeability compared to the apical membrane.
Paracellular Ptrans,0 (10-6 cm/s) [1]	100 for all segments	Predicted based on best fit in relation to the apical and Basolateral Ptrans.
Capillary bed permeability-surface area product (L/hr)	40 Default value	Low values indicates significant absorption via lymph which is not known about budesonide.
***fu*$_{ubl}$ and Lymphatic reflection coefficient**	1 Default value	
Formulation	Solid controlled release formulation	[58]
	Dispersible system using Weibull function for release profile [1]	Weibull function parameters estimated based on best fit to the observed PO data in healthy population
Intrinsic solubility (mg/mL)	0.028	[75]
Segregated transit time model activated with permitting mean residence and lag time		

IV*; Intravenous dose.* ***PO****; Oral dose.*

[1]Parameter fitted to experimental data.

[2]Calculated with retrograde model enzyme kinetics using the percentage of enzymatic contribution from published reactive CYP 450 phenotyping experiments and the clearance after intravenous administration of budesonide.

Table S1.7. Midazolam (MDZ) drug profile input parameters for the Simcyp simulations.

Parameter	***Value***	***Reference/comments***
Molecular weight (g/mol)	325.8	Simcyp compound
LogP (octanol:water)	3.53	
Ionic class	Monoprotic base	
pka	6	
Fraction unbound in plasma	0.032	
Blood plasma ratio (B:P)	0.603	
Distribution model	Full PBPK, Method 2	
Kp scaler [1]	0.27	Estimated based on best fit to the observed IV data in healthy population [62]

Elimination	Enzyme kinetics (Recombinant)	Simcyp compound
CYP3A4, 1-OH pathway	**Vmax=** 5.23, **Km=** 2.16	
CYP3A4, 4-OH pathway	**Vmax=** 5.2, **Km=** 31.8	
CYP3A5, 1-OH pathway	**Vmax=** 19.7, **Km=** 4.16	
CYP3A5, 4-OH pathway	**Vmax=** 4.03.2, **Km=** 38.4	
CYP3A4/3A5 correlation activated		
Difference in male/female CYP3A4 abundance activated		
Absorption model	Multiple layer gut wall within ADAM (M-ADAM)	Mechanistic passive regional Permeability predictor (Mech Peff) model
Mech Peff Ptrans,0 (10-6 cm/s) [1]	160	Estimated based on best fit to the observed PO data in healthy population[62]
Capillary bed permeability-surface area product (L/hr)	2.2	Estimated based on best fit to the observed PO data in healthy population[62]
***fu*$_{ubl}$ and Lymphatic reflection coefficient**	Default value = 1	
Formulation	Oral solution	[61] [62]

IV*; Intravenous dose.* ***PO****; Oral dose;* [1]Parameter fitted to experimental data.

Table S1.8. Comparison of predicted and observed pharmacokinetics (PK) parameters and their fold change in healthy volunteers (HV) populations of oral midazolam and budesonide.

Parameter	**Midazolam oral solution, fasted**			**Parameter**	**Budesonide controlled release, fed**		
	Predicted	Observed Mean, (95% CI)	Predicted/Observed		Predicted	Observed Mean, (95% CI)	Predicted/ Observed
$AUC_{0-\infty}$ (nM*h)	0.09	0.082, (0.069- 0.097)	1.1	$AUC_{0-\infty}$ (nM*h/)	59.77	60.4, (45.1-80.8)	0.99
Cmax (nM)	0.035	0.037, (0.028-0.042)	0.95	Cmax (nM)	8.42	9.1, (8.9-22.9)	0.93
Tmax (h)	0.59	0.5, (0.25–0.75)	1.18	Tmax (h)	4.68	6, (6-16)	0.78
F %	23.1	23.4, (20, 27.3)	0.99	F %	11	11.5, (8.8-15)	0.96

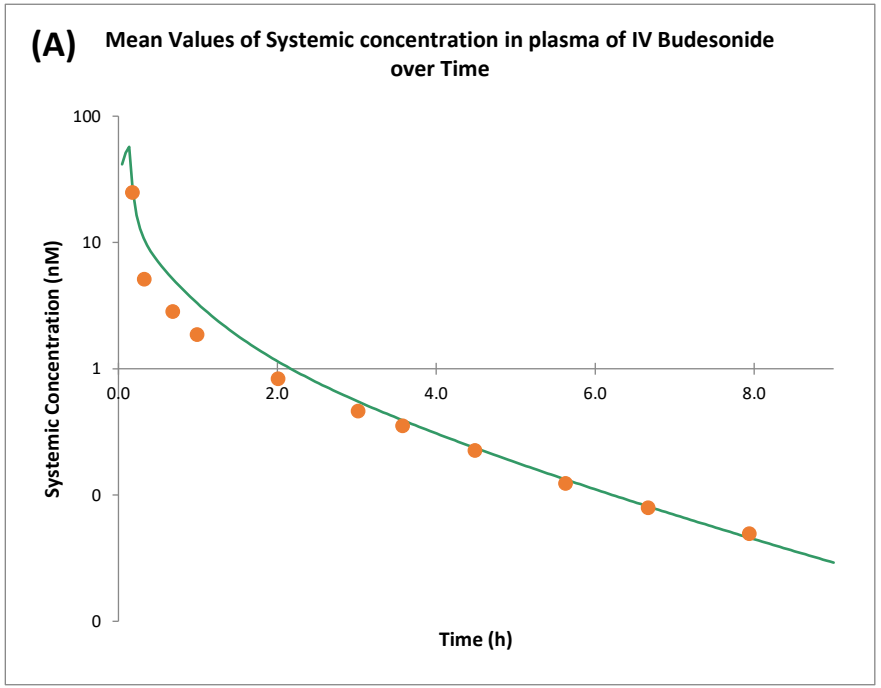

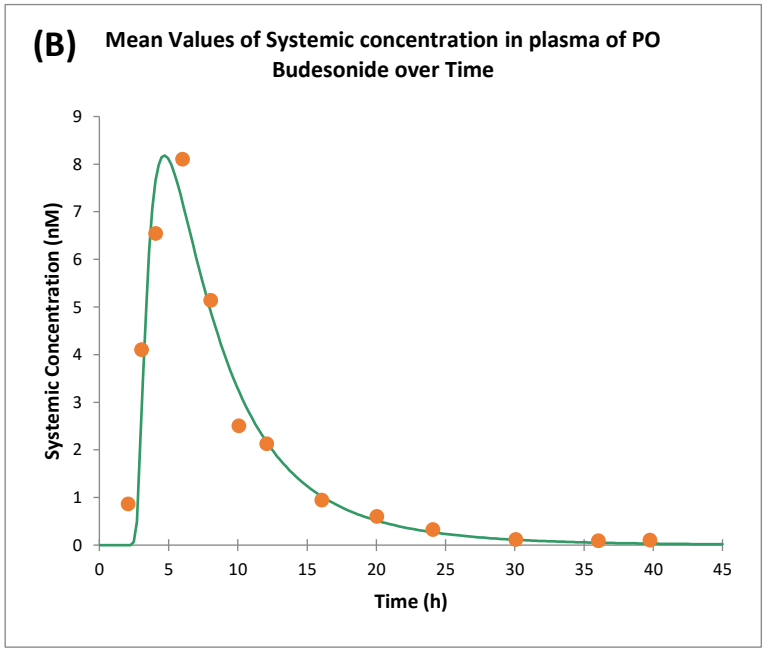

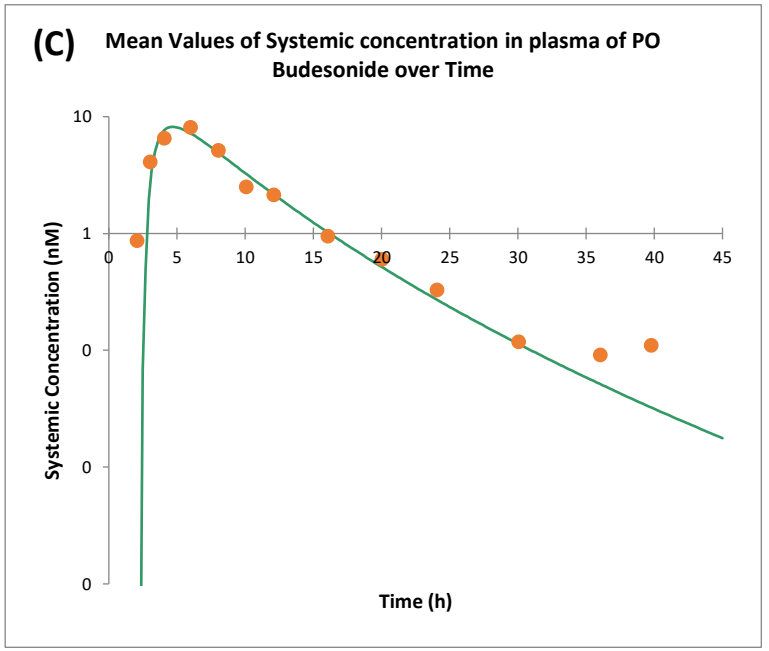

Figure S1.1. *Prediction of budesonide plasma concentration for healthy subjects after administration of* ***(A)*** *systemic 0.5 mg intravenous (IV) dose with observed values from (Thorsson, Edsbäcker, and Conradson 1994)* [73] *and* ***(B)*** *18 mg oral (PO) solution and* ***(C)*** *18 mg oral (PO) solution log scale with observed values from (Edsbäcker et al. 2003)* [58] *in the fed state.*

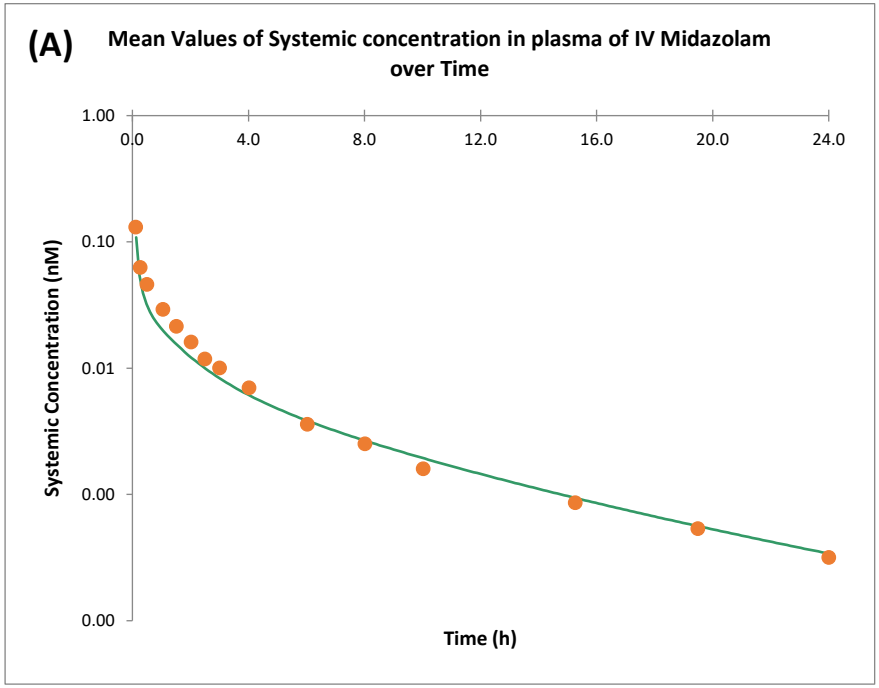

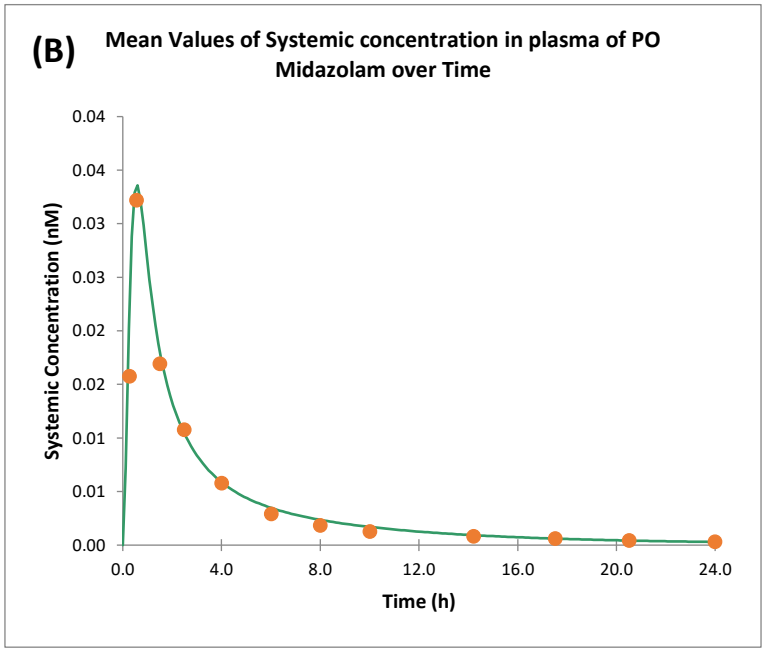

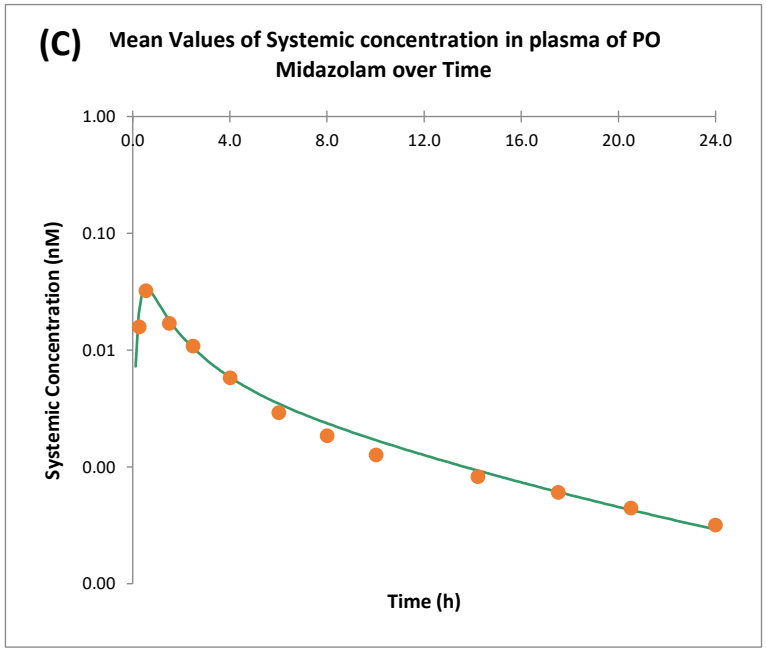

Figure S1.2. *Prediction of midazolam plasma concentration for healthy subjects after administration of* ***(A)*** *systemic 0.001 mg intravenous (IV) dose with observed values from* [62] *(Hohmann et al. 2015) and* ***(B)*** *0.003 mg oral (PO) solution and* ***(C)*** *0.003 mg oral (PO) solution log scale with observed values from* [62] *(Hohmann et al. 2015) in the fasted state.*

1.8.Supplementary material-Results

Table S1.9. Mean ± SD pH value of the proximal and terminal small intestine (SI) and large intestine in fasted state of Crohn's disease (CD) and healthy volunteers (HV) population measured in the same study.

Fasted pH	**Number of subjects (N)**	**Proximal SI (mean ± SD)**	**Terminal SI (mean ± SD)**	**Large intestine (mean ± SD)**
HV (control group)	12 [76]	(6.7 ±0.37)	(7.4 ±0.33)	(6.1±0.57)
	13 [77]	(6.4 ±0.27)	(7.4 ±0.45)	(5.8 ±0.3)
	13 [78]	(6.7 ±0.36)	(7.4 ±0.36)	(6.8 ±0.24)
	4 [79 a]	(6.8 ±0.34)	(7.7 ±0.24)	(7 ±0.3)
	HV Overall means, SD, 90% CI	6.6 ±0.37, (6.03-7.25)	7.4 ±0.38, (6.81-8.08)	6.3 ±0.6, (5.36-7.34)
CD (all active unless if mentioned otherwise)	12 (5 active) (7 inactive) [76]	Active (7 ±1.01) Inactive (6.55 ±0.33) Both (7±0.78)	Active (8.3 ±0.69) Inactive (7.9 ±0.15) Both (8.2 ±0.44)	Active (6.9 ±0.73) Inactive (6.8 ±0.7) Both (6.8 ±0.58)
	9 (inactive, ileocecal resection less than 100 cm of terminal ileum) [77]	(6.5 ±0.34)	(7.2 ±0.13)	(6.7 ±0.24)
	12 [78]	(6.9 ±0.46)	(7.1 ±0.46)	(6.6 ±0.25)
	4 (3 active) (1 inactive) [79]	(7.2 ±0.34)	(7.8 ±0.24)	(5.3 ±0.5)*
	Overall means ± overall SD, 90% CI	6.9 ±0.6, (5.93-7.89)	7.6 ±0.61, (6.6-8.62)	6.5 ±0.61 (5.59-7.58)
	pH % change CD/HV	4.55% increase	2.7% increase	3.2% increase
	Active CD Overall means ± overall SD, 95% CI	7 ±0.63, (5.98-8.05)	7.5 ±0.7, (6.44-8.74)	6.4 ±0.71 (5.29-7.63)
	pH % change CD/HV	6.1% increase	1.35% increase	1.6% increase
	Inactive CD Overall means ± overall SD, 95% CI	6.5 ±0.34, (5.98-7.09)	7.6 ±0.6, (6.72-8.64)	6.8 ±0.43 (6.06-7.48)
	pH % change CD/HV	1.5% decrease	2.7% increase	8 % increase

*reported significant difference; [a] not mentioned if Fasted or not.

Table S1.10. Mean ± SD Small intestine and colonic transit time value in fasted and fed state of Crohn's disease (CD) and healthy volunteers (HV) population measured in the same study.

Study group	**Number of subjects (N)**	**Fasted (SI) Small intestine Transit Time (hr) (mean ± SD)**	**Number of subjects (N)**	**Fed Small intestine Transit time (SITT) (hr) (mean ± SD)**	**Fed colonic Transit time (hr) (mean ± SD)**
HV (control group)	13 [77]	(7.7 ±1.68)	8 [58]	(3±1.56)	(15.5±6.94)
	125 (non IBD patients) [80]	(3.6 ±0.45)	20 [81]	(5.4 ±1.31)	(17.7 ±11.14)
	178 (non IBD patients) [82]	(4.1 ±1.4)	**HV** Overall means ± overall SD, 95% CI	4.7 ±1.54, (2.64-7.56)	17 ±9.46, (6.34-34.95)
	HV Overall means ± overall SD, 95% CI	5.5 ±2.32, (2.57-9.82)			
CD (all active unless if mentioned otherwise)	9 (inactive, ileocecal resection) [77]	(4.7 ±1.62)*	5 [83]	(6.72 ±3.22)	N/A
	33 [80]	(4.4 ±0.57)*	6 (3 active and 3 inactive) [58]	(2.4±1.43)	Active (3 ± 3.54)* Both (8.1±8)
	22 (inactive) [80]	(3.3 ±0.46)	Overall means± overall SD, 95% CI	4.4±3.06, (1.26-10.1)	8.1±8, 95% CI (1.4-14.8)
	19 [82]	(5.6 ±0.78)*	Transit time % change CD/HV	7.23% decrease	52.46% decrease
	Overall means ± overall SD, 95% CI	4.4 ±1.14, (2.81-6.5)	**Active** CD Overall means ± overall SD, 95% CI	5.33±3.8, (1.5-12.45)	3 ± 3.54,* (9-0.42)
	SITT % change CD/HV	19.1% decrease	Transit time % change CD/HV	13.4% increase	82.4% decrease
	Active CD Overall means ± overall SD, 95% CI	4.9 ±0.87, (3.57-6.41)	**Inactive** CD Overall means ± overall SD, 95% CI	No only inactive values (mixed is applied)	No only inactive values (mixed is applied)

	SITT % change CD/HV	11% decrease			
	Inactive CD Overall means ± overall SD, 95% CI	4.7 ±1.62, (2.56-7.71)			
	SITT % change CD/HV	14.55% decrease			

*reported significant difference.

Table S1.11. Mean ± SD Gastric emptying time value in fasted and fed state of Crohn's disease (CD) and healthy volunteers (HV) population measured in the same study.

Study group	**Number of subjects (N)**	**Fed Gastric emptying time (hr) (mean ± SD)**	**Fasted Gastric emptying time (hr) (mean ± SD)**
HV (control group)	8 [58]	(2.7, 95% CI 2.1-3.2)	(0.8, 95% CI 0.3-1.3)
	19 [84]	(2.8 ±0.11)	N/A
	178 [82]	N/A	(0.6±0.29)
	HV Overall means ± overall SD, 95% CI	2.8±0.1, (2.6-2.92)	0.59±0.29, (0.25-1.13)
CD (all active unless if mentioned otherwise)	7 [83]	(5.9 ±3.59)	N/A
	6 (3 active and 3 inactive) [58]	(4, 95% CI 3.3-4.7)*	N/A
	26 (inactive) [84]	(3.2 ±0.13)	N/A
	19 [82]	N/A	(0.6±0.75)
	Overall means ± overall SD, 95% CI	3.8±1.83, (1.62-7.27)	N/A
	Gastric emptying % change CD/HV	38% increase	N/A
	Active CD Overall means ± overall SD, 95% CI	5.9 ±3.59 (2-12.69)	0.61±0.75, (0.08-1.87)
	Gastric emptying % change CD/HV	110.7% increase	3.4% increase
	Inactive CD Overall means ± overall SD, 95% CI	3.2 ±0.13 (3-3.42)	N/A
	Gastric emptying % change CD/HV	14.3% increase	N/A

*reported significant difference.

Table S1.12. Mean ± SD Superior Mesenteric artery blood flow value of Crohn's disease (CD) and healthy volunteers (HV) population measured in the same study.

Study group	**Number of subjects (N)**	**Superior Mesenteric artery (SMA) blood flow (ml/min)**
HV	10 [85]	(417 ±147)
	12 [86]	(300 ± 91)
	10 [87]	(253 ± 101)
	HV Overall means ± overall SD, 95% CI	322 ±132.4, (155.33-570.44)
CD (all active unless if mentioned otherwise)	10 active 10 inactive [85]	Active (1588 ±576)* Inactive (288 ±113)
	10 active 9 inactive [86]	Active (738 ± 411)* Inactive (364 ± 101)
	12 active 14 inactive [87]	Active (722 ± 195)* Inactive (317 ± 92)
	Overall means ± overall SD, 95% CI	654.12 ±531.14, (157.5-1637)
	SAM % change CD/HV	103.14% increase
	Active CD Overall means ± overall SD, 95% CI	997.6 ±573.8, (359-2083.44)
	SAM % change CD/HV	209.8% increase
	Inactive CD Overall means ± overall SD, 95% CI	321 ±105.3, (180.33-516)
	SAM % change CD/HV	0.31% decrease
	Overall means ± overall SD, 95% CI	322 ±132.4, (155.33-570.44)

*reported significant difference.

Table S1.13. Mean ± SD ileum and colon local blood flow value of CD and HV population measured in the same study.

Study group	**Number of subjects (N)**	**Total Colonic blood flow (ml/min*100 g)**	**Colonic Mucosal & submucosal blood flow (ml/min*100 g)**	**Colonic muscularis blood flow (ml/min*100 g)**	**Ileum Mucosal & submucosal blood flow (ml/min*100 g)**	**Ileum muscularis blood flow (ml/min*100 g)**	**Ileum total blood flow (ml/min*100 g)**
HV [88]	8	(18 ± 2)	(28 ± 5)	(11 ± 1)	(44 ± 7)	(20 ± 2)	(29 ± 3)
CD [88]	5 active colonic CD	(78 ±20)*	(239.5± 111.9)*	(18.5± 2.62)	(35 ±5)	(5.7±6.63)*	(26 ±5)
	Active Intestine blood flow % change CD/HV	333% increase	755% increase	68.2% increase	20.5% decrease	71.5% decrease	10.4% decrease
	3 Inactive CD	(14 ±11.8)	N/A	N/A	(10 ±4)*	(7 ±1)*	(11 ±1)*
	Inactive Intestine blood flow % change CD/HV	22% decrease	N/A	N/A	77.3% decrease	65% decrease	62% decrease
	Overall means ± overall SD, 95% CI	54 ± 35.53, (16.82-120.98)	N/A	N/A	22.5 ± 13.3, (7.87-47.65)	6.35 ± 4.8, (1.68-15.28)	19.1 ± 8.36, (8.77-34.8)
	Intestine blood flow % change CD/HV	200% increase	N/A	N/A	49% decrease	68.3% decrease	34% decrease

*reported significant difference; NA. no available information.

Table S1.14. Mean ± SD bowel wall thinking value of Crohn's disease (CD) and healthy volunteers (HV) population measured in the same study.

Study group	**Number of subjects (N)**	**bowel wall thinking BWT (mm)** **(mean ± SD)**
HV [89]	20	(2.7 ±0.43)
	HV Overall means ± overall SD, 95% CI	2.7 ±0.43, (2.06-3.46)
CD [89]	31, 18 active 13 inactive	22 CD patients had a bowel wall thinking BWT >4 mm, 16 active CD. 2 active CD patients with BWT <4mm. 7 inactive CD with BWT <4mm 6 inactive CD had normal BWT. CD BWT (8.2 ±2.14)*
	Overall means ± overall SD, 95% CI	8.2 ±2.14,* (5.2-12.1)
	BWT % change CD/HV	203.7% increase
	Active CD Overall means ± overall SD, 95% CI	8.2 ±2.14, (5.2-12.1)
	BWT % change CD/HV	203.7% increase
	Inactive CD Overall means ± overall SD,	N/A

*reported significant difference

Table S1.15. Intestine mean DMETs expression in Crohn's disease (CD) compared to healthy volunteers (HV) population measured in the same study.

Drug Metabolizing Enzymes (DMEs)	HV (control, non-inflamed)	CD (active, inflamed)	CD (inactive)
CYP % of mRNA expression and/or relative expression values			
CYP3A4	N= 11 (rectum) 45 %, (0.0004) [90]	N= 2 18 %, (0.00004)* [90] CD/HV=90% decrease	___
	N= 40 (colon) (82.4±7.4) [91]	N= 40 (182.4±20.8)* [91] CD/HV=121.4% increase	N= 40 (182.4±20.8)* [91] CD/HV=121.4% increase
	N= 37 (colon & ileum) (0.37 ± 0.34 & 0.72 ± 0.33) [92]	N= 23 (colon & ileum) (0.08 ± 0.08 & 0.40 ± 0.35)* [92 (a)] Colon CD/HV=78.4% decrease Ileum CD/HV=44.4% decrease	N= 23 (colon & ileum) (0.08 ± 0.08 & 0.40 ± 0.35)* [92 (a)] Colon CD/HV=78.4% decrease Ileum CD/HV=44.4% decrease
	N= 14 (colon & ileum)[93]	N= 9 Colon CD/HV=68.8% decrease Ileum CD/HV= 30 % increase	N= 9 Colon CD/HV=68.8% decrease Ileum CD/HV= 30 % increase
Overall average of the % CD/HV since the expression is not similar	Colon 33.6% decrease Ileum 23.5% decrease		Colon 33.6% decrease Ileum 23.5% decrease
CYP3A5 (rectum)[90]	100 %, (0.0027)	100 %, (0.0034) CD/HV=26% increase	___
CYP3A7 (colon & ileum) [93]	N= 14	N= 9 Ileum FC= 1.2 increase Colon FC= 1.7 reduction	N= 9 Ileum FC= 1.2 increase Colon FC= 1.7 reduction
CYP2C9	N= 14 (colon & ileum) [93]	N= 9 Ileum CD/HV = 10% increase	= 9 Ileum CD/HV = 10% increase

		Colon CD/HV = 56.5% reduction	Colon CD/HV = 56.5% reduction
	N= 40 (colon) (127.1±11.3) [91]	N= 40 (164.6±14.1)* CD/HV=29.5% increase	—
CYP2B6 (colon)[91]	(94.2±11.1)	(168.2±14.3) *	—
CYP2E1	N= 11 (rectum) 90 %, (0.6731) [90]	N=2 81%, (0.4996)*	—
	N= 40 (colon) (88.7±4.1) [91]	N= 40 (108.2±7.3)*	
CYP1A1 (colon)[91]	(120±8.9)	(160.5±10.8) *	—
Others DMEs % of mRNA expression and/or relative expression values			
CES (colon & ileum) [93]	N= 14	N= 9 Ileum FC= 1.1 increase Colon FC= 2.1 reduction	N= 9 Ileum FC= 1.1 increase Colon FC= 2.1 reduction
UGT1A3 (colon & ileum) [93]	N= 14	N= 9 Ileum FC= 2.3 reduction Colon FC= 3.4 reduction	N= 9 Ileum FC= 2.3 reduction Colon FC= 3.4 reduction
UDP-GT (colon)[91]	(126.6±11.3)	(170.7±15.8) *	
GSTA1 (colon & ileum) [93]	N= 14	N= 9 Ileum FC= 1.4 increase Colon FC= 2 reduction	N= 9 Ileum FC= 1.4 increase Colon FC= 2 reduction
GSTM4 (colon & ileum) [93]	N= 14	N= 9 Ileum FC= 1.3 increase Colon FC= 1.4 reduction	N= 9 Ileum FC= 1.3 increase Colon FC= 1.4 reduction
GSTT1 (colon & ileum) [93]	N= 14	N= 9 Ileum FC= 1.1 reduction Colon FC= 1.1 reduction	N= 9 Ileum FC= 1.1 reduction Colon FC= 1.1 reduction
SULT1A1 (colon & ileum) [93]	N= 14	N= 9 Ileum FC= 1.2 increase	N= 9 Ileum FC= 1.2 increase

		Colon FC= 1.1 reduction	Colon FC= 1.1 reduction
SULT1A2 (colon & ileum) [93]	N= 14	N= 9 Ileum FC= 1.1 increase Colon FC= 1.4 reduction	N= 9 Ileum FC= 1.1 increase Colon FC= 1.4 reduction
SULT1A3 (colon & ileum) [93]	N= 14	N= 9 Ileum FC= 1 Colon FC= 2 reduction	N= 9 Ileum FC= 1 Colon FC= 2 reduction
SULT2A1	N= 9 (ileum)[94]	N= 14 69 % reduction* FC in mRNA expression (CD/HV) ~0.3	N= 7 FC in mRNA expression (CD/HV) ~1
	N= 14 (colon & ileum) [93]	N= 9 Ileum FC= 3 increase Colon FC= 1.6 reduction	N= 9 Ileum FC= 3 increase Colon FC= 1.6 reduction
SULT2B1 (colon & ileum) [93]	N= 14	N= 9 Ileum FC= 1.3 reduction Colon FC= 3.5 reduction	N= 9 Ileum FC= 1.3 reduction Colon FC= 3.5 reduction
Drug Transporters	**HV (non-inflamed tissue)**	**CD (active)**	**CD (inactive)**
ABC % of mRNA expression and/or relative expression values			
P-gp (ABCB1)	N= 11 (rectum) 90%, (0.0014) [90]	N= 2 90 %, (0.0003) [90] %CD/HV=78.6% decrease	___
	N= 10 (colon & ileum) (0.9 & 3.5) [95]	N= 20 (colon & ileum) (0.4 & 1)* [95 (a)] Colon CD/HV=55.6% decrease Ileum CD/HV=71.4% decrease	N= 20 (colon & ileum) (0.4 & 1)* [95 (a)] Colon CD/HV=55.6% decrease Ileum CD/HV=71.4% decrease
	N= 20 (colon) (1) [96]	N= 20 (0.4)* [96] Colon CD/HV=60% decrease	___
	N= 9 (ileum) [94]	N= 14 FC in mRNA expression (CD/HV)	N= 7

		~0.8 [94] Ileum CD/HV=20% decrease	FC in mRNA expression (CD/HV) ~0.9 [94] Similar to control
	N= 37 (colon & ileum) (0.17 ± 0.2 & 0.11 ± 0.09) [92]	N= 23 (colon & ileum) (0.026 ± 0.029 & 0.095 ± 0.10)* [92(a)] Colon CD/HV=84.7% decrease Ileum CD/HV=13.6% decrease	——
	N= 14 (colon & ileum)[93]	N= 9 Colon CD/HV = 50% reduction Ileum CD/HV = 30% increase	N= 9 Colon CD/HV = 50% reduction Ileum CD/HV = 30% increase
Overall average of the % CD/HV since the expression is not similar	Colon 65% decrease Ileum 27% decrease		Colon =54% decrease Ileum =41.4% decrease
MRP1 (colon) [95]	N=20 (0.9)	N=20 (2)*	——
MRP (2,4,5 & 6) (colon) [96]	N=2 (1)	N= 2 Not significant	——
MRP2 (colon & ileum)[93]	N= 14	N= 9 Ileum FC= 1.6 reduction Colon FC= 2.6 reduction	N= 9 Ileum FC= 1.6 reduction Colon FC= 2.6 reduction
MRP3	N= 20 (colon) (1) [96]	N= 2 Not significant [96]	——
	N= 9 (ileum) [94]	N= 14 FC in mRNA expression (CD/HV) ~1.3 [94]	N= 7 FC in mRNA expression (CD/HV) ~1.2 [94]
	N= 14 (colon & ileum)[93]	N= 9 Ileum FC= 2 reduction Colon FC= 1.2 increase	N= 9 Ileum FC= 2 reduction Colon FC= 1.2 increase
BCRP (ileum)[94]	N=9	N= 14	N= 7

		43 % reduction* FC in mRNA expression (CD/HV) ~0.6	33 % reduction* FC in mRNA expression (CD/HV) ~0.7
SLC % of mRNA expression and/or relative expression values			
OSTα/β (ileum) [94]	N=9	N= 14 FC in mRNA expression (CD/HV) (α≈ 1.2),(β≈ 0.8)	N= 7 FC in mRNA expression (CD/HV) (α≈ 1),(β≈ 0.7)
OATP2B1 [97 (b)]	N= 23 (ileum & colon) (0.01±0.01)	N= 49, (ileum & colon) (0.07±0.07 & 0.08±0.07)*	___
OATP4A1 [97 (b)]	(0.002±0.003 & 0.01±0.01)	(0.01±0.009 & 0.03±0.06)*	___
PEPT1 [97 (b)]	(7.44±4.33 & 0.18±0.23)	(10.02±6.39 & 0.58±0.63*)	___
OCTN1	N= 23 (ileum & colon) (2±1.28 & 0.53±0.53) [97 (b)]	N= 53 (ileum & colon) (2.32±1.39 & 0.76±0.8) [97 (b)]	___
	N= 9 (ileum), 7 (colon)[43]	N= 17 (ileum) (~3.7%), 7 (colon) (~6.9%) Ileum FC~ 1.3 reduction Colon FC~ 1	N= 17 (ileum) (~3.7%), 7 (colon) (~6.9%) Ileum FC~ 1.3 reduction Colon FC~ 1
OCTN2	N= 23 (ileum & colon) (0.1±0.05 & 0.26±0.14)[97 (b)]	N= 53 (ileum & colon) (0.02±0.01 & 0.05±0.04)*	___
	N= 10 (ileum), 11 (colon)[43]	N= 19 (ileum) (~4.5%), 7 (colon) (~0.8%) Ileum FC~ 1.6 reduction Colon FC~ 1.2 increase	N= 19 (ileum) (~4.5%), 7 (colon) (~0.8%) Ileum FC~ 1.6 reduction Colon FC~ 1.2 increase
ASBT	N= 23 (ileum & colon) (0.96±0.85 & 0.007±0.008) [97]	N= 53 (ileum & colon) (0.12±0.12 & 0.0002±0.0005)* [97 (b)]	___
	N= 9 (ileum) [94]	N= 14 64 % * reduction FC in mRNA expression (CD/HV)	N= 7 47 % * reduction

		~0.4 [94]	FC in mRNA expression (CD/HV) ~0.5 [94]
	N=10 (ileum) (1.27) [98]	N= 16 (0.88) FC= 1.44 reduction	N= 16 (0.88) FC= 1.44 reduction
CTN1 [97 (b)]	(0.15±0.09 & 0.001±0.001)	(0.25±0.15 & 0.001±0.0006)*	—
CTN2 [97 (b)]	(0.85±0.63 & 0.05±0.05)	(0.76±0.57 & 0.35±0.42*)	—
ENT1 [97 (b)]	(0.008±0.01 & 0.02±0.02)	(0.02±0.02 & 0.05±0.06)*	—
ENT2 [97 (b)]	(0.01±0.01 & 0.09±0.11)	(0.04±0.03 & 0.17±0.07)*	—
MCT1 [99]	N= 10, (colon) (2.9-1) Fluorescence intensity (70.5±36.5)	N= 14, (colon) (0.1-0.4)* Fluorescence intensity (28.5 ±17.5)*	—

*reported significant difference; ** all are colon expression data unless if its specified otherwise; [(a)]relative expression values of CD subjects are based on mix of active and remission stage participants and no effect of disease activity on the expression was recorded; [(b)]relative expression values of CD subjects are based on mix of active and remission stage participants.

Table S1.16. Mean ± SD α1- acid glycoprotein level in Crohn's disease (CD) and healthy volunteers (HV) population measured in the same study.

Study group	**Number of subjects (N)**	**α1-AGP (g/L)**
HV [100]	20	(1.19±0.29)
	HV Overall means ± overall SD, 95% CI	1.19±0.29, (0.78-1.72)
CD [100]	30, (13 active & 17 inactive)	Total (1.57 ±0.46) Active (1.97 ±0.35)* Inactive (1.27 ±0.2)
	Overall means ± overall SD, 95% CI	1.57 ±0.46, (0.94-2.42)
	α1-AGP % change CD/HV	31.93% increase
	Active CD Overall means ± overall SD, 95% CI	1.97 ±0.35, (1.45-2.59)
	α1-AGP % change CD/HV	65.55% increase
	Inactive CD Overall means ± overall SD, 95% CI	1.27 ±0.2, (0.97-1.62)
	α1-AGP % change CD/HV	6.7% increase

*reported significant difference.

Table S1.17. Mean ±SD human serum albumin level in Crohn's disease (CD) and healthy volunteers (HV) population measured in the same study.

Study group	Number of subjects (N)	Human Serum Albumin (HAS) (g/L)		
HV	Reference values [101]	Range: 36.2-55.2 Male CD/HV= 25.4-51.1 % decrease Female CD/HV= 36.5-58.3 % decrease Overall CD/HV= 30.9-54.7 % decrease		
	13 (7 female) [77]	(38 ±3.6) Inactive CD/HV= 9.2 % increase		
	Reference values [102]	Normal (≥35) CD/HV= 14.3% decrease		
	Reference values [103]	Normal ≥35 Modest hypoalbuminemia, (30 – 34), Severe hypoalbuminemia (<30)		
	10 [54]	(44 ±3.25) Inactive CD/HV= 15.9% decrease		
	HV Overall means ± overall SD, 95% CI	40.6±4.56, (33.6-48.5) [1]		
Study group	**Number of subjects (N)**	**All**	**Female**	**Male**
CD (all active unless if mentioned otherwise)	27 (15 non operated & 12 operated subjects; removal of intestine parts) (13 male & 14 female) [101]	(25 ±7.03)	(23 ±7.1)	(27±7.46)
	9 (6 female) (inactive, ileocecal resection)[77]	(41.5 ±2.02)*	N/A	N/A
	84 (32% active and 52% inactive) (52 female) [104]	(38 ±5.1)	N/A	N/A
	117 (25 female) [102]	Only 13 <30 104 ≥35	N/A	N/A

	6082 (54% female) [103]	1340 <30, 1240 <30-34, 3502 ≥35		
	39 (10 female) (18 were operated) [105]	Active (37 ±2.09) Inactive (after remission) (40.3 ±1.63)		
	32 [106]	(39.4 ±5.97)		
	9 inactive or low activity [54]	(37 ±3.37)		
	Overall means ± overall SD, 95% CI	36.7±6.42, (27.2-48.1)		
	Serum Albumin % change CD/HV	9.61 % decrease		
	Active CD Overall means ± overall SD, 95% CI	32.1±7.6, [2] (21.25-45.85)	23 ±7.1	27±7.46
	HSA % change CD/HV	20.94 % decrease	**Female = 49% decrease**	**Male = 40 % decrease**
	Inactive CD Overall means ± overall SD, 95% CI	40±2.5, (36.04-44.15)		
	HSA % change CD/HV	1.5 % decrease		

*reported significant difference.

[1] Most of the studies did not have a healthy population to compare to but rather used a reference healthy albumin value to be ≥35, while the ones that have a HV population reported 35 to be lower than the HV value and their mean is calculated as the HV overall mean. This value is only used to compared between with inactive and overall (active +inactive) since there is a study of active Female and male CD with direct comparison to HV.

[2] only studies that reported a HV group to compare with are included in the mean calculation of the CD group.

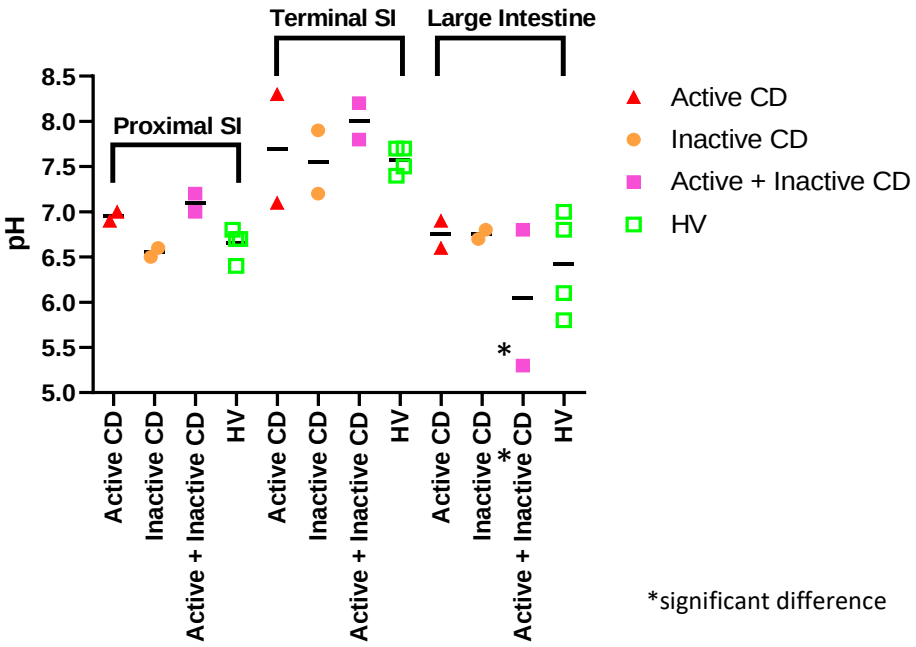

Figure S1.3. *Mean pH of proximal small intestine (SI), terminal SI and large intestine in active and inactive Crohn's disease population compared to healthy volunteers (HV) in fasted state.*

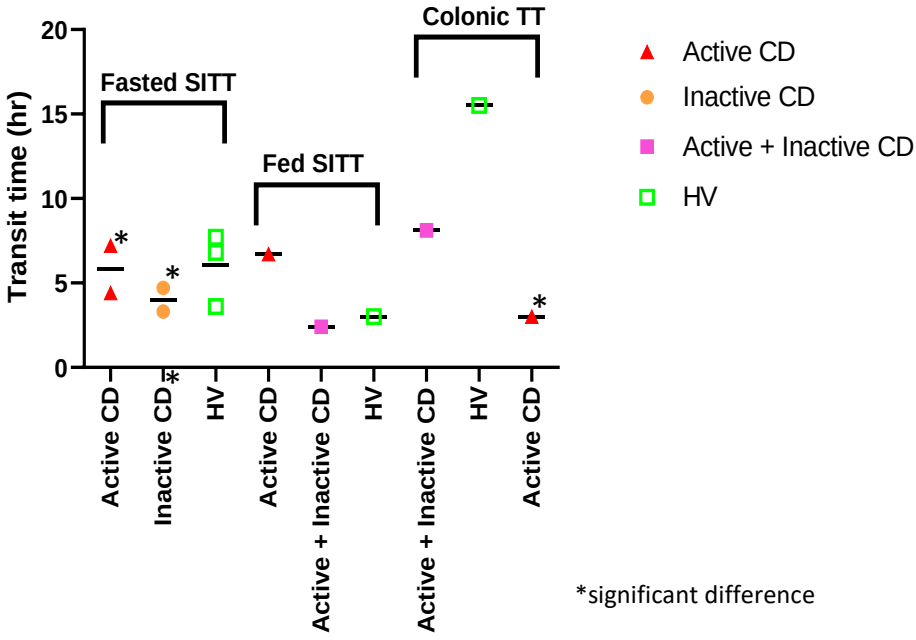

Figure S1.4. *Mean small intestine (SITT) and colonic transit time (TT) in in active and inactive Crohn's disease population compared to healthy volunteers (HV) in fasted and fed state.*

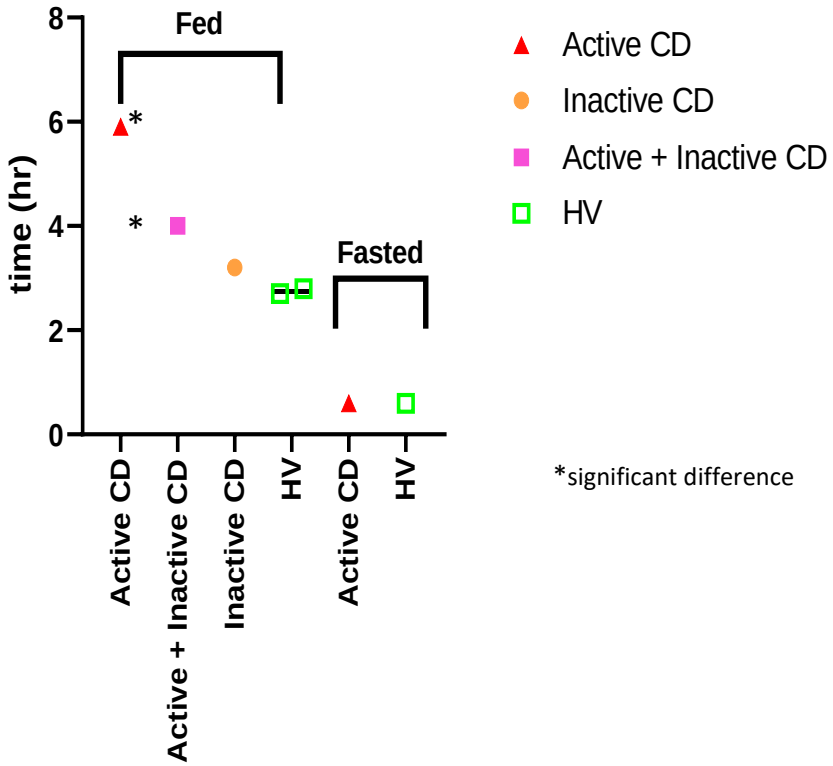

Figure S1.5. *Mean gastric emptying time in active and inactive Crohn's disease population compared to healthy volunteers (HV) in fasted and fed state.*

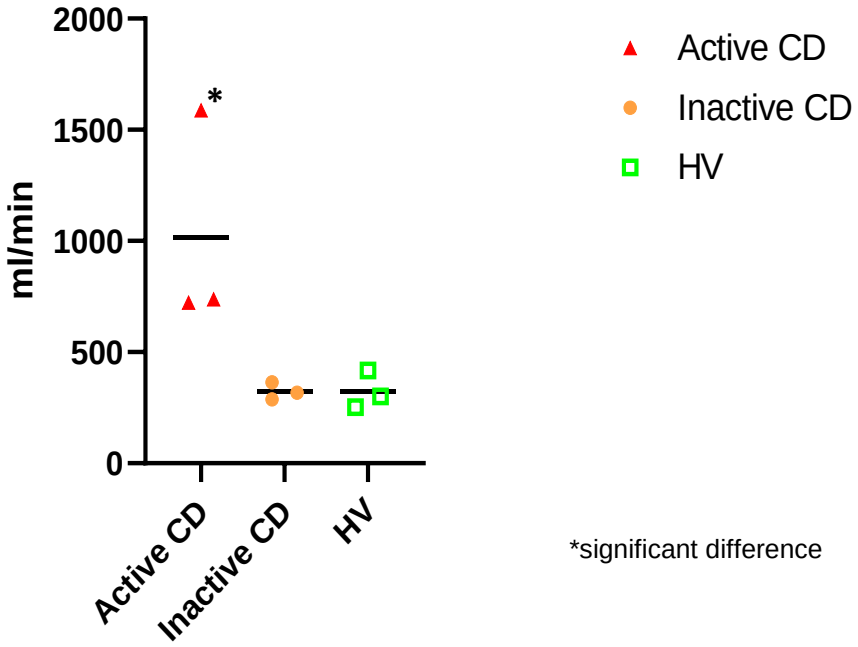

Figure S1.6. *Mean superior mesenteric artery (SMA) blood flow in active and inactive Crohn's disease population compared to healthy volunteers (HV) in fasted and fed state.*

1.9.References

1. Fieller EC. Some Problems in Interval Estimation. *J R Stat Soc Ser B* 1954;**16**(2):175–85. Doi: 10.1111/j.2517-6161.1954.tb00159.x.

2. Motulsky H. *Intuitive Biostatistics: A Nonmathematical Guide to Statistical Thinking*. 2010.

3. Olivares-Morales A., Kamiyama Y., Darwich AS., Aarons L., Rostami-Hodjegan A. Analysis of the impact of controlled release formulations on oral drug absorption, gut wall metabolism and relative bioavailability of CYP3A substrates using a physiologically-based pharmacokinetic model. *Eur J Pharm Sci* 2015;**67**:32–44. Doi: 10.1016/j.ejps.2014.10.018.

4. Higgins JPT., Thomas J., Chandler J., Cumpston M., Li T., Page MJ., et al. *Cochrane Handbook for Systematic Reviews of Interventions*. Wiley; 2019.

5. Paine MF., Khalighi M., Fisher JM., Shen DD., Kunze KL., Marsh CL., et al. Characterization of interintestinal and intraintestinal variations in human CYP3A-dependent metabolism. *J Pharmacol Exp Ther* 1997;**283**(3):1552–62.

6. Madani S., Paine MF., Lewis L., Thummel KE., Shen DD. Comparison of CYP2D6 content and metoprolol oxidation between microsomes isolated from human livers and small intestines. *Pharm Res* 1999;**16**(8):1199–205. Doi: 10.1023/a:1018989211864.

7. Obach RS., Zhang QY., Dunbar D., Kaminsky LS. Metabolic characterization of the major human small intestinal cytochrome P450S. *Drug Metab Dispos* 2001;**29**(3):347–52.

8. Canaparo R., Finnström N., Serpe L., Nordmark A., Muntoni E., Eandi M., et al. Expression of CYP3A Isoforms and P-Glycoprotein in Human Stomach, Jejunum and Ileum. *Clin Exp Pharmacol Physiol* 2007;**34**(11):1138–44. Doi: 10.1111/j.1440-1681.2007.04691.x.

9. Paine MF., Hart HL., Ludington SS., Haining RL., Rettie AE., Zeldin DC. The Human Intestinal Cytochrome P450 "PIE." *Drug Metab Dispos* 2006;**34**(5):880–6. Doi: 10.1124/dmd.105.008672.

10. Berggren S., Gall C., Wollnitz N., Ekelund M., Karlbom U., Hoogstraate J., et al. Gene and Protein Expression of P-Glycoprotein, MRP1, MRP2, and CYP3A4 in the Small and Large Human Intestine. *Mol Pharm* 2007;**4**(2):252–7. Doi: 10.1021/mp0600687.

11. Bruyère A., Declèves X., Bouzom F., Ball K., Marques C., Treton X., et al. Effect of variations in the amounts of P-glycoprotein (ABCB1), BCRP (ABCG2) and CYP3A4 along the human small intestine on PBPK models for predicting intestinal first pass. *Mol Pharm* 2010;**7**(5):1596–607. Doi: 10.1021/mp100015x.

12. Vaessen SFC., van Lipzig MMH., Pieters RHH., Krul CAM., Wortelboer HM., van de Steeg E. Regional Expression Levels of Drug Transporters and Metabolizing Enzymes along the Pig and Human Intestinal Tract and Comparison with Caco-2 Cells. *Drug Metab Dispos* 2017;**45**(4):353–60. Doi: 10.1124/dmd.116.072231.

13. Gröer C., Busch D., Patrzyk M., Beyer K., Busemann A., Heidecke CD., et al. Absolute protein quantification of clinically relevant cytochrome P450 enzymes and UDP-glucuronosyltransferases by mass spectrometry-based targeted proteomics. *J Pharm Biomed Anal* 2014;**100**:393–401. Doi: 10.1016/j.jpba.2014.08.016.

14. Lloret-Linares C., Miyauchi E., Luo H., Labat L., Bouillot JL., Poitou C., et al. Oral Morphine Pharmacokinetic in Obesity: The Role of P-Glycoprotein, MRP2, MRP3, UGT2B7, and CYP3A4 Jejunal Contents and Obesity-Associated Biomarkers. *Mol Pharm* 2016;**13**(3):766–73. Doi: 10.1021/acs.molpharmaceut.5b00656.

15. Miyauchi E., Tachikawa M., Declèves X., Uchida Y., Bouillot JL., Poitou C., et al. Quantitative Atlas of Cytochrome P450, UDP-Glucuronosyltransferase, and Transporter Proteins in Jejunum of Morbidly Obese Subjects. *Mol Pharm* 2016;**13**(8):2631–40. Doi: 10.1021/acs.molpharmaceut.6b00085.

16. Bradbury M., Stamler D., Baillie T., Sidhu S., Wood SG., Teva IS., et al. Protein abundance of pharmacokinetically relevant transporter proteins and metabolizing enzymes along the human intestine and in the liver: A comparative intra-subject study. *Drug Metab Pharmacokinet* 2018;**33**(1):S76–7. Doi: 10.1016/j.dmpk.2017.11.252.

17. Couto N., Al-Majdoub ZM., Gibson S., Davies PJ., Achour B., Harwood MD., et al. Quantitative Proteomics of Clinically Relevant Drug-Metabolizing Enzymes and Drug Transporters and Their Intercorrelations in the Human Small Intestine. *Drug Metab Dispos* 2020;**48**(4):245–54. Doi: 10.1124/dmd.119.089656.

18. Klose TS., Blaisdell JA., Goldstein JA. Gene structure ofCYP2C8 and extrahepatic distribution of the human CYP2Cs. *J Biochem Mol Toxicol* 1999;**13**(6):289–95. Doi: 10.1002/(SICI)1099-0461(1999)13:6<289::AID-JBT1>3.0.CO;2-N.

19. Lindell M., Karlsson MO., Lennernäs H., Påhlman L., Lang MA. Variable expression of CYP and Pgp genes in the human small intestine. *Eur J Clin Invest* 2003;**33**(6):493–9. Doi: 10.1046/j.1365-2362.2003.01154.x.

20. Thorn M., Finnstrom N., Lundgren S., Rane A., Loof L. Cytochromes P450 and MDR1 mRNA expression along the human gastrointestinal tract. *Br J Clin Pharmacol* 2005;**60**(1):54–60. Doi: 10.1111/j.1365-2125.2005.02389.x.

21. Shin H-C., Kim H-R., Cho H-J., Yi H., Cho S-M., Lee D-G., et al. Comparative gene expression of intestinal metabolizing enzymes. *Biopharm Drug Dispos* 2009;**30**(8):411–21. Doi: 10.1002/bdd.675.

22. Bourgine J., Billaut-Laden I., Happillon M., Lo-Guidice J-M., Maunoury V., Imbenotte M., et al. Gene Expression Profiling of Systems Involved in the Metabolism and the Disposition of Xenobiotics: Comparison between Human Intestinal Biopsy Samples and Colon Cell Lines. *Drug Metab Dispos* 2012;**40**(4):694–705. Doi: 10.1124/dmd.111.042465.

23. Gervot L., Carrière V., Costet P., Cugnenc P-H., Berger A., Beaune PH., et al. CYP3A5 is the major cytochrome P450 3A expressed in human colon and colonic cell lines. *Environ Toxicol Pharmacol* 1996;**2**(4):381–8. Doi: 10.1016/S1382-6689(96)00075-0.

24. Waziers I d., Cugnenc PH., Berger A., Leroux J-P., Beaune PH. Drug-metabolizing enzyme expression in human normal, peritumoral and tumoral colorectal tissue samples. *Carcinogenesis* 1991;**12**(5):905–9. Doi: 10.1093/carcin/12.5.905.

25. Nakamura T., Sakaeda T., Ohmoto N., Tamura T., Aoyama N., Shirakawa T., et al. Real-Time Quantitative Polymerase Chain Reaction for MDR1, MRP1, MRP2, and CYP3A-mRNA Levels in Caco-2 Cell Lines, Human Duodenal Enterocytes, Normal Colorectal Tissues, and Colorectal Adenocarcinomas. *Drug Metab Dispos* 2002;**30**(1):4–6. Doi: 10.1124/dmd.30.1.4.

26. Bergheim I., Bode C., Parlesak A. Distribution of cytochrome P450 2C, 2E1, 3A4, and 3A5 in human colon mucosa. *BMC Clin Pharmacol* 2005;**5**(1):4. Doi: 10.1186/1472-6904-5-4.

27. Zhang QY., Dunbar D., Ostrowska A., Zeisloft S., Yang J., Kaminsky LS. Characterization of human small intestinal cytochromes P-450. *Drug Metab Dispos* 1999;**27**(7):804–9.

28. Nishimura M., Yaguti H., Yoshitsugu H., Naito S., Satoh T. Tissue Distribution of mRNA Expression of Human Cytochrome P450 Isoforms Assessedby High-Sensitivity Real-Time Reverse Transcription PCR. *YAKUGAKU ZASSHI* 2003;**123**(5):369–75. Doi: 10.1248/yakushi.123.369.

29. Radominska-Pandya A., Little JM., Pandya JT., Tephly TR., King CD., Barone GW., et al. UDP-glucuronosyltransferases in human intestinal mucosa. *Biochim Biophys Acta - Lipids Lipid Metab* 1998;**1394**(2–3):199–208. Doi: 10.1016/S0005-2760(98)00115-5.

30. Strassburg CP., Kneip S., Topp J., Obermayer-Straub P., Barut A., Tukey RH., et al. Polymorphic Gene Regulation and Interindividual Variation of UDP-glucuronosyltransferase Activity in Human Small Intestine. *J Biol Chem* 2000;**275**(46):36164–71. Doi: 10.1074/jbc.M002180200.

31. Wu B., Kulkarni K., Basu S., Zhang S., Hu M. First-Pass Metabolism via UDP-Glucuronosyltransferase: a Barrier to Oral Bioavailability of Phenolics. *J Pharm Sci* 2011;**100**(9):3655–81. Doi: 10.1002/jps.22568.

32. Strassburg CP., Manns MP., Tukey RH. Expression of the UDP-glucuronosyltransferase 1A Locus in Human Colon. *J Biol Chem* 1998;**273**(15):8719–26. Doi: 10.1074/jbc.273.15.8719.

33. Ohno S., Nakajin S. Determination of mRNA Expression of Human UDP-Glucuronosyltransferases and Application for Localization in Various Human Tissues by Real-Time Reverse Transcriptase-Polymerase Chain Reaction. *Drug Metab Dispos* 2009;**37**(1):32–40. Doi: 10.1124/dmd.108.023598.

34. Terada T., Shimada Y., Pan X., Kishimoto K., Sakurai T., Doi R., et al. Expression profiles of various transporters for oligopeptides, amino acids and organic ions along the human digestive tract. *Biochem Pharmacol* 2005;**70**(12):1756–63. Doi: 10.1016/j.bcp.2005.09.027.

35. Seithel A., Karlsson J., Hilgendorf C., Björquist A., Ungell A-L. Variability in mRNA expression of ABC- and SLC-transporters in human intestinal cells: Comparison between human segments and Caco-2 cells. *Eur J Pharm Sci* 2006;**28**(4):291–9. Doi: 10.1016/j.ejps.2006.03.003.

36. Hilgendorf C., Ahlin G., Seithel A., Artursson P., Ungell A-L., Karlsson J. Expression of Thirty-six Drug Transporter Genes in Human Intestine, Liver, Kidney, and Organotypic Cell Lines. *Drug Metab Dispos* 2007;**35**(8):1333–40. Doi: 10.1124/dmd.107.014902.

37. Klaassen CD., Aleksunes LM. Xenobiotic , Bile Acid , and Cholesterol Transporters : *Pharmacol Rev* 2010;**62**(1):1–96. Doi: 10.1124/pr.109.002014.1.

38. Gröer C., Brück S., Lai Y., Paulick A., Busemann A., Heidecke CD., et al. LC–MS/MS-based quantification of clinically relevant intestinal uptake and efflux transporter proteins. *J Pharm Biomed Anal* 2013;**85**:253–61. Doi: 10.1016/j.jpba.2013.07.031.

39. Drozdzik M., Gröer C., Penski J., Lapczuk J., Ostrowski M., Lai Y., et al. Protein Abundance of Clinically Relevant Multidrug Transporters along the Entire Length of the Human Intestine. *Mol Pharm* 2014;**11**(10):3547–55. Doi: 10.1021/mp500330y.

40. Englund G., Rorsman F., Rönnblom A., Karlbom U., Lazorova L., Gråsjö J., et al. Regional levels of drug transporters along the human intestinal tract: Co-expression of ABC and SLC transporters and comparison with Caco-2 cells. *Eur J Pharm Sci* 2006;**29**(3–4):269–77. Doi: 10.1016/j.ejps.2006.04.010.

41. Meier Y., Eloranta JJ., Darimont J., Ismair MG., Hiller C., Fried M., et al. Regional Distribution of Solute Carrier mRNA Expression Along the Human Intestinal Tract. *Drug Metab Dispos* 2007;**35**(4):590–4. Doi: 10.1124/dmd.106.013342.

42. Tamai I. Oral drug delivery utilizing intestinal OATP transporters. *Adv Drug Deliv Rev* 2012;**64**(6):508–14. Doi: 10.1016/j.addr.2011.07.007.

43. Girardin M., Dionne S., Goyette P., Rioux J., Bitton A., Elimrani I., et al. Expression and functional analysis of intestinal organic cation/l-carnitine transporter (OCTN) in Crohn's Disease. *J Crohn's Colitis* 2012;**6**(2):189–97. Doi: 10.1016/j.crohns.2011.08.003.

44. Harwood MD., Achour B., Russell MR., Carlson GL., Warhurst G., Rostami-Hodjegan A. Application of an LC-MS/MS method for the simultaneous quantification of human intestinal transporter proteins absolute abundance using a QconCAT technique. *J Pharm Biomed Anal* 2015;**110**:27–33. Doi: 10.1016/j.jpba.2015.02.043.

45. Mouly S., Paine MF. P-Glycoprotein Increases from Proximal to Distal Regions of Human Small Intestine. *Pharm Res* 2003;**20**(10):1595–9. Doi: 10.1023/A:1026183200740.

46. Oswald S., Gröer C., Drozdzik M., Siegmund W. Mass Spectrometry-Based Targeted Proteomics as a Tool to Elucidate the Expression and Function of Intestinal Drug Transporters. *AAPS J* 2013;**15**(4):1128–40. Doi: 10.1208/s12248-013-9521-3.

47. Harwood MD., Achour B., Neuhoff S., Russell MR., Carlson G., Warhurst G., et al. In Vitro-In Vivo Extrapolation Scaling Factors for Intestinal P-glycoprotein and Breast Cancer Resistance Protein: Part I: A Cross- Laboratory Comparison of Transporter Protein Abundances and Relative Expression Factors in Human Intestine and Caco-2 Cell. *Drug Metab Dispos* 2016;**44**(3):297–307. Doi: 10.1124/dmd.115.067371.

48. Tucker TGHA., Milne AM., Fournel-Gigleux S., Fenner KS., Coughtrie MWH. Absolute immunoquantification of the expression of ABC transporters P-glycoprotein, breast cancer resistance protein and multidrug resistance-associated protein 2 in human liver and duodenum. *Biochem Pharmacol* 2012;**83**(2):279–85. Doi: 10.1016/j.bcp.2011.10.017.

49. Gutmann H., Hruz P., Zimmermann C., Beglinger C., Drewe J. Distribution of breast cancer resistance protein (BCRP/ABCG2) mRNA expression along the human GI tract. *Biochem Pharmacol* 2005;**70**(5):695–9. Doi: 10.1016/j.bcp.2005.05.031.

50. Zimmermann C., Gutmann H., Hruz P., Gutzwiller J-P., Beglinger C., Drewe J. Mapping of multidrug resistance gene 1 and multidrug resistance-associated protein isoform 1 to 5 mRNA expression along the human intestinal tract. *Drug Metab Dispos* 2005;**33**(2):219–24. Doi: 10.1124/dmd.104.001354.

51. Melander A., Kahlmeter G., Kamme C., Ursing B. Bioavailability of metronidazole in fasting and non-fasting healthy subjects and in patients with Crohn's disease. *Eur J Clin Pharmacol* 1977;**12**(1):69–72. Doi: 10.1007/BF00561408.

52. Schneider R., Bishop H., Hawkins C. Plasma propranolol concentrations and the erythrocyte sedimentation rate. *Br J Clin Pharmacol* 1979;**8**(1):43–7. Doi: 10.1111/j.1365-2125.1979.tb05907.x.

53. Milsap RL., George DE., Szefler SJ., Murray KA., Lebenthal E., Jusko WJ. Effect of inflammatory bowel disease on absorption and disposition of prednisolone. *Dig Dis Sci* 1983;**28**(2):161–8. Doi: 10.1007/BF01315146.

54. Norlander B., Gotthard R., Strom M. Pharmacokinetics of a 5-aminosalicylic acid enteric-coated tablet in patients with Crohn's disease or ulcerative colitis and in healthy volunteers. *Aliment Pharmacol Ther* 1990;**4**(5):497–505. Doi: 10.1111/j.1365-2036.1990.tb00496.x.

55. Gionchetti P., Campieri M., Belluzzi A., Boschi S., Brignola C., Miglioli M., et al. Bioavailability of single and multiple doses of a new oral formulation of 5-ASA in patients with inflammatory bowel disease and healthy volunteers. *Aliment Pharmacol Ther* 1994;**8**(5):535–40. Doi: 10.1111/j.1365-2036.1994.tb00327.x.

56. Flückiger SS., Schmidt C., Meyer A., Kallay Z., Johnston A., Kutz K. Pharmacokinetics of Orally Administered Cyclosporine in Patients with Crohn's Disease. *J Clin Pharmacol* 1995;**35**(7):681–7. Doi: 10.1002/j.1552-4604.1995.tb04108.x.

57. Lundin P., Naber T., Nilsson M., Edsbacker S. Effect of food on the pharmacokinetics of budesonide controlled ileal release capsules in patients with active Crohn's disease. *Aliment Pharmacol Ther* 2001. Doi: 10.1046/j.1365-2036.2001.00910.x.

58. Edsbäcker S., Bengtsson B., Larsson P., Lundin P., Nilsson Å., Ulmius J., et al. A pharmacoscintigraphic evaluation of oral budesonide given as controlled-release (Entocort) capsules. *Aliment Pharmacol Ther* 2003;**17**(4):525–36. Doi: 10.1046/j.1365-2036.2003.01426.x.

59. Lundin PDP., Edsbäcker S., Bergstrand M., Ejderhamn J., Linander H., Högberg L., et al. Pharmacokinetics of budesonide controlled ileal release capsules in children and adults with active Crohn's disease. *Aliment Pharmacol Ther* 2003. Doi: 10.1046/j.1365-2036.2003.01386.x.

60. Sanaee F., Clements JD., Waugh AWG., Fedorak RN., Lewanczuk R., Jamali F. Drug−disease interaction: Crohn's disease elevates verapamil plasma concentrations but reduces response to the drug proportional to disease activity. *Br J Clin Pharmacol* 2011;**72**(5):787–97. Doi: 10.1111/j.1365-2125.2011.04019.x.

61. Wilson A., Tirona RG., Kim RB. CYP3A4 Activity is Markedly Lower in Patients with Crohn's Disease. *Inflamm Bowel Dis* 2017;**23**(5):804–13. Doi: 10.1097/MIB.0000000000001062.

62. Hohmann N., Kocheise F., Carls A., Burhenne J., Haefeli WE., Mikus G. Midazolam microdose to determine systemic and pre-systemic metabolic CYP3A activity in humans. *Br J Clin Pharmacol* 2015;**79**(2):278–85. Doi: 10.1111/bcp.12502.

63. Dresser GK., Kim RB., Bailey DG. Effect of Grapefruit Juice Volume on the Reduction

of Fexofenadine Bioavailability: Possible Role of Organic Anion Transporting Polypeptides*. *Clin Pharmacol Ther* 2005;**77**(3):170–7. Doi: 10.1016/j.clpt.2004.10.005.

64. Shaffer J., Kershaw A., Houston J. Disposition of metronidazole and its effects on sulphasalazine metabolism in patients with inflammatory bowel disease. *Br J Clin Pharmacol* 1986;**21**(4):431–5. Doi: 10.1111/j.1365-2125.1986.tb05218.x.

65. Sprandel KA., Schriever CA., Pendland SL., Quinn JP., Gotfried MH., Hackett S., et al. Pharmacokinetics and Pharmacodynamics of Intravenous Levofloxacin at 750 Milligrams and Various Doses of Metronidazole in Healthy Adult Subjects. *Antimicrob Agents Chemother* 2004;**48**(12):4597–605. Doi: 10.1128/AAC.48.12.4597-4605.2004.

66. Brynskov J., Freund L., Campanini MC., Kampmann JP. Cyclosporin Pharmacokinetics after Intravenous and Oral Administration in Patients with Crohn's Disease. *Scand J Gastroenterol* 1992;**27**(11):961–7. Doi: 10.3109/00365529209000171.

67. Ducharme MP., Warbasse LH., Edwards DJ. Disposition of intravenous and oral cyclosporine after administration with grapefruit juice*. *Clin Pharmacol Ther* 1995;**57**(5):485–91. Doi: 10.1016/0009-9236(95)90032-2.

68. Gesink-van der Veer BJ., Burm AG., Vletter AA., Bovill JG. Influence of Crohn's disease on the pharmacokinetics and pharmacodynamics of alfentanil. *Br J Anaesth* 1993;**71**(6):827–34. Doi: 10.1093/bja/71.6.827.

69. Schwab M., Klotz U. Pharmacokinetic Considerations in the Treatment of Inflammatory Bowel Disease. *Clin Pharmacokinet* 2001;**40**(10):723–51. Doi: 10.2165/00003088-200140100-00003.

70. Shin D., Kim Y., Kim YS., Körnicke T., Fuhr R. A Randomized, Phase I Pharmacokinetic Study Comparing SB2 and Infliximab Reference Product (Remicade®) in Healthy Subjects. *BioDrugs* 2015;**29**(6):381–8. Doi: 10.1007/s40259-015-0150-5.

71. Rosario M., Dirks NL., Milch C., Parikh A., Bargfrede M., Wyant T., et al. A Review of the Clinical Pharmacokinetics, Pharmacodynamics, and Immunogenicity of Vedolizumab. *Clin Pharmacokinet* 2017;**56**(11):1287–301. Doi: 10.1007/s40262-017-0546-0.

72. Effinger A., O'Driscoll CM., McAllister M., Fotaki N. Predicting budesonide performance in healthy subjects and patients with Crohn's disease using biorelevant in vitro dissolution testing and PBPK modeling. *Eur J Pharm Sci* 2020:105617. Doi: 10.1016/j.ejps.2020.105617.

73. Thorsson L., Edsbäcker S., Conradson T-B. Lung deposition of budesonide from Turbuhaler® is twice that from a pressurized metered-dose inhaler P-MDI. *Eur Respir*

J 1994;**7**(10):1839–44. Doi: 10.1183/09031936.94.07101839.

74. Sjögren E., Dahlgren D., Roos C., Lennernäs H. Human in vivo regional intestinal permeability: Quantitation using site-specific drug absorption data. *Mol Pharm* 2015;**12**(6):2026–39. Doi: 10.1021/mp500834v.

75. Effinger A., M O'Driscoll C., McAllister M., Fotaki N. Gastrointestinal diseases and their impact on drug solubility: Ulcerative Colitis. *Eur J Pharm Sci* 2020;**152**:105458. Doi: 10.1016/j.ejps.2020.105458.

76. Press AG., Hauptmann IA., Hauptmann L., Fuchs B., Fuchs M., Ewe K., et al. Gastrointestinal pH profiles in patients with inflammatory bowel disease. *Aliment Pharmacol Ther* 1998;**12**(7):673–8. Doi: 10.1046/j.1365-2036.1998.00358.x.

77. Fallingborg J., Pedersen P., Jacobsen BA. Small intestinal transit time and intraluminal pH in ileocecal resected patients with Crohn's disease. *Dig Dis Sci* 1998;**43**(4):702–5. Doi: 10.1023/a:1018893409596.

78. Ewe K., Schwartz S., Petersen S., Press AG. Inflammation does not decrease intraluminal pH in chronic inflammatory bowel disease. *Dig Dis Sci* 1999;**44**(7):1434–9. Doi: 10.1023/a:1026664105112.

79. Sasaki Y., Hada R., Nakajima H., Fukuda S., Munakata A. Improved localizing method of radiopill in measurement of entire gastrointestinal pH profiles: colonic luminal pH in normal subjects and patients with Crohn's disease. *Am J Gastroenterol* 1997;**92**(1):114–8.

80. Fischer M., Siva S., Wo JM., Fadda HM. Assessment of Small Intestinal Transit Times in Ulcerative Colitis and Crohn's Disease Patients with Different Disease Activity Using Video Capsule Endoscopy. *AAPS PharmSciTech* 2017;**18**(2):404–9. Doi: 10.1208/s12249-016-0521-3.

81. Haase AM., Gregersen T., Christensen LA., Agnholt J., Dahlerup JF., Schlageter V., et al. Regional gastrointestinal transit times in severe ulcerative colitis. *Neurogastroenterol Motil* 2016;**28**(2):217–24. Doi: 10.1111/nmo.12713.

82. Niv E., Fishman S., Kachman H., Arnon R., Dotan I. Sequential capsule endoscopy of the small bowel for follow-up of patients with known Crohn's disease. *J Crohn's Colitis* 2014;**8**(12):1616–23. Doi: 10.1016/j.crohns.2014.03.003.

83. Hardy JG., Healey JNC., Reynolds JR. Evaluation of an enteric-coated delayed-release 5-aminosalicylic acid tablet in patients with inflammatory bowel disease. *Aliment Pharmacol Ther* 1987;**1**(4):273–80. Doi: 10.1111/j.1365-2036.1987.tb00627.x.

84. Nóbrega ACM., Ferreira BRS., Oliveira GJ., Sales KMO., Santos AA., Nobre e Souza MÂ., et al. Dyspeptic symptoms and delayed gastric emptying of solids in patients with

inactive Crohn's disease. *BMC Gastroenterol* 2012;**12**(1):175. Doi: 10.1186/1471-230X-12-175.

85. van Oostayen JA., Wasser MNJM., van Hogezand RA., Griffioen G., de Roos A. Activity of Crohn disease assessed by measurement of superior mesenteric artery flow with Doppler US. *Radiology* 1994;**193**(2):551–4. Doi: 10.1148/radiology.193.2.7972778.

86. van Oostayen J. Diagnosis of Crohn's ileitis and monitoring of disease activity: value of Doppler ultrasound of superior mesenteric artery flow. *Am J Gastroenterol* 1998;**93**(1):88–91. Doi: 10.1016/S0002-9270(97)00029-4.

87. Yekeler E., Danalioglu A., Movasseghi B., Yilmaz S., Karaca C., Kaymakoglu S., et al. Crohn disease activity evaluated by Doppler ultrasonography of the superior mesenteric artery and the affected small-bowel segments. *J Ultrasound Med* 2005;**24**(1):59–65. Doi: 10.7863/jum.2005.24.1.59.

88. Hultén L., Lindhagen J., Lundgren O., Fasth S., Ahrén C. Regional intestinal blood flow in ulcerative colitis and Crohn's disease. *Gastroenterology* 1977;**72**(3):388–96. Doi: 10.1016/S0016-5085(77)80245-X.

89. Di Sabatino A., Fulle I., Ciccocioppo R., Ricevuti L., Tinozzi FP., Tinozzi S., et al. Doppler Enhancement After Intravenous Levovist Injection in Crohn's Disease. *Inflamm Bowel Dis* 2002;**8**(4):251–7. Doi: 10.1097/00054725-200207000-00003.

90. Thörn M., Finnström N., Lundgren S., Rane A., Lööf L. Expression of cytochrome P450 and MDR1 in patients with proctitis. *Ups J Med Sci* 2007;**112**(3):303–12. Doi: 10.3109/2000-1967-203.

91. Plewka D., Plewka A., Szczepanik T., Morek M., Bogunia E., Wittek P., et al. Expression of selected cytochrome P450 isoforms and of cooperating enzymes in colorectal tissues in selected pathological conditions. *Pathol - Res Pract* 2014;**210**(4):242–9. Doi: 10.1016/j.prp.2013.12.010.

92. Wilson A., Urquhart BL., Ponich T., Chande N., Gregor JC., Beaton M., et al. Crohn's Disease Is Associated with Decreased CYP3A4 and P-Glycoprotein Protein Expression. *Mol Pharm* 2019;**16**(9):4059–64. Doi: 10.1021/acs.molpharmaceut.9b00459.

93. Langmann T., Moehle C., Mauerer R., Scharl M., Liebisch G., Zahn A., et al. Loss of detoxification in inflammatory bowel disease: dysregulation of pregnane X receptor target genes. *Gastroenterology* 2004;**127**(1):26–40. Doi: 10.1053/j.gastro.2004.04.019.

94. Jahnel J., Fickert P., Hauer AC., Högenauer C., Avian A., Trauner M. Inflammatory Bowel Disease Alters Intestinal Bile Acid Transporter Expression. *Drug Metab Dispos* 2014;**42**(9):1423–31. Doi: 10.1124/dmd.114.058065.

95. Blokzijl H., Borght S Vander., Bok LIH., Libbrecht L., Geuken M., van den Heuvel FAJ., et al. Decreased P-glycoprotein (P-gp/MDR1) expression in inflamed human intestinal epithelium is independent of PXR protein levels. *Inflamm Bowel Dis* 2007;**13**(6):710–20. Doi: 10.1002/ibd.20088.

96. Blokzijl H., van Steenpaal A., Borght S Vander., Bok LIH., Libbrecht L., Tamminga M., et al. Up-regulation and Cytoprotective Role of Epithelial Multidrug Resistance-associated Protein 1 in Inflammatory Bowel Disease. *J Biol Chem* 2008;**283**(51):35630–7. Doi: 10.1074/jbc.M804374200.

97. Wojtal KA., Eloranta JJ., Hruz P., Gutmann H., Drewe J., Staumann A., et al. Changes in mRNA Expression Levels of Solute Carrier Transporters in Inflammatory Bowel Disease Patients. *Drug Metab Dispos* 2009;**37**(9):1871–7. Doi: 10.1124/dmd.109.027367.

98. Jung D. Human ileal bile acid transporter gene ASBT (SLC10A2) is transactivated by the glucocorticoid receptor. *Gut* 2004;**53**(1):78–84. Doi: 10.1136/gut.53.1.78.

99. Thibault R., De Coppet P., Daly K., Bourreille A., Cuff M., Bonnet C., et al. Down-Regulation of the Monocarboxylate Transporter 1 Is Involved in Butyrate Deficiency During Intestinal Inflammation. *Gastroenterology* 2007;**133**(6):1916–27. Doi: 10.1053/j.gastro.2007.08.041.

100. Ricci G., Ambrosi A., Resca D., Masotti M., Alvisi V. Comparison of serum total sialic acid, C-reactive protein, α1-acid glycoprotein and β2-microglobulin in patients with non-malignant bowel diseases. *Biomed Pharmacother* 1995;**49**(5):259–62. Doi: 10.1016/0753-3322(96)82632-1.

101. Jarnum S., Jensen KB. Fecal Radioiodide Excretion Following Intravenous Injection of 131I-Albumin and 125I-Immunoglobulin G in Chronic Inflammatory Bowel Disease. *Gastroenterology* 1975;**68**(6):1433–44. Doi: 10.1016/S0016-5085(75)80129-6.

102. Liu X., Wu X., Zhou C., Hu T., Ke J., Chen Y., et al. Preoperative hypoalbuminemia is associated with an increased risk for intra-abdominal septic complications after primary anastomosis for Crohn's disease. *Gastroenterol Rep* 2017;**5**(4):298–304. Doi: 10.1093/gastro/gox002.

103. Nguyen GC., Du L., Chong RY., Jackson TD. Hypoalbuminaemia and Postoperative Outcomes in Inflammatory Bowel Disease: the NSQIP Surgical Cohort. *J Crohn's Colitis* 2019;**13**(11):1433–8. Doi: 10.1093/ecco-jcc/jjz083.

104. Vagianos K., Bector S., McConnell J., Bernstein CN. Nutrition Assessment of Patients With Inflammatory Bowel Disease. *J Parenter Enter Nutr* 2007;**31**(4):311–9. Doi: 10.1177/0148607107031004311.

105. Suzuki Y., Matsui T., Ito H., Ashida T., Nakamura S., Motoya S., et al. Circulating

Interleukin 6 and Albumin, and Infliximab Levels Are Good Predictors of Recovering Efficacy After Dose Escalation Infliximab Therapy in Patients with Loss of Response to Treatment for Crohn's Disease. *Inflamm Bowel Dis* 2015;**21**(9):2114–22. Doi: 10.1097/MIB.0000000000000475.

106. Takac B., Mihaljević S., Stefanić M., Glavas-Obrovac L., Kibel A., Samardzija M. Importance of interleukin 6 in pathogenesis of inflammatory bowel disease. *Coll Antropol* 2014;**38**(2):659–64.

Chapter Two: Quantitative Mass Spectrometry-Based Proteomics in the Era of Model-Informed Drug Development: Applications in Translational Pharmacology and Recommendations for Best Practice

Declaration

This chapter constitutes a published article.

El-Khateeb, E., Vasilogianni, A. M., **Alrubia, S**., Al-Majdoub, Z. M., Couto, N., Howard, M., Barber, J., Rostami-Hodjegan, A., & Achour, B. (2019). Quantitative mass spectrometry-based proteomics in the era of model-informed drug development: applications in translational pharmacology and recommendations for best practice. Pharmacology & Therapeutics, 203, 107397 (online publication).

The manuscript was written equally by the first three authors who share the first-authorship. Dr Zubida M. Al-Majdoub, Dr Narciso Couto, Dr Martyn Howard, Dr Jill Barber, Prof Amin Rostami-Hodjegan provided guidance and suggested edits to the manuscript. Dr Brahim Achour outlined the structure of the review, edited the manuscript, and retained editorial control through the journal's invitation.

2.1.Abstract

Quantitative translation of the fate and action of a drug in the body is facilitated by models that allow extrapolation of *in vitro* measurements (such as the rate of metabolism, active transport across membranes, inhibition of enzymes and receptor occupancy) to *in vivo* consequences (intensity and duration of drug effects). These models use various physiological parameters, including data that describe the expression levels of pharmacologically relevant enzymes, transporters and receptors in tissues and *in vitro* systems. Immunoquantification approaches have traditionally been used to determine protein expression levels, generally providing relative quantification data with compromised selectivity and reproducibility. More recently, the development of several quantitative proteomic techniques, fuelled by advances in state-of-the-art mass spectrometry, has led to generating a wealth of qualitative and quantitative data. These data are currently used for various quantitative systems pharmacology applications, with the ultimate goal of conducting virtual clinical trials to inform clinical studies, especially when assessments are difficult to conduct on patients. In this review, we explore available quantitative proteomic methods, discuss their main applications in translational pharmacology and offer recommendations for selecting and implementing proteomic techniques.

2.2.Introduction

Translational pharmacology requires extrapolation of *in vitro* observations to predict the outcome of therapy *in vivo* using various scaling factors measured in tissues and relevant *in vitro* systems.[1] When extrapolating measurements made *in vitro* (e.g. Km, Vmax, Jmax), functional data may be used as scalars when selective probes are available, for example in the case of several cytochrome P450 (CYP)[2] and uridine 5′-diphospho-glucuronosyltransferase (UGT) enzymes. [3,4] However, owing to a lack of specific substrates for many enzymes and for the majority of transporters and receptors, the use of abundance data remains the preferred approach for *in vitro-in vivo* extrapolation (IVIVE), facilitated by analytical methods that can quantify the levels of individual proteins in heterogeneous biological matrices. Over the past two decades, quantitative proteomics based on liquid chromatography in conjunction with mass spectrometry (LC-MS) has replaced traditional immunoquantitative methods, such as Western blotting and enzyme-linked immunosorbent assays (ELISA),[5] mainly because traditional techniques require purified protein standards and specific antibodies for each target, which are not always available.

Pharmacologically active enzymes and transporters tend to have high sequence homology and most of these proteins are found at very low amounts within the membranes of tissues and cellular systems.[6] Highly selective and sensitive mass spectrometry techniques are therefore ideal for implementation in pharmacology applications.[7,8] LC-MS analysis offers various other advantages including reproducibility, high throughput and the ability to multiplex measurements. This allows simultaneous detection and quantification of dilute amounts of a large number of proteins (hundreds to thousands) in complex biological systems.[9] Quantitative proteomic techniques have therefore been implemented by different laboratories worldwide for various pharmacology applications, leading to improved extrapolation of drug pharmacokinetics[10,11] and better understanding of the effects various factors, including age,[12,13] ethnicity, [13–15] and genetics [14,16,17] on the expression of enzymes and transporters.

The typical aim of a proteomic experiment is to characterize the entire set of proteins expressed in a particular system (global proteomics) or to target a specified set of proteins for quantification (targeted proteomics).[18] These two types of proteomic analysis require specific considerations for robust analysis to be achieved.[19] In this review, we explore state-of-the-art mass spectrometry-based proteomic methods, both global and targeted, used for the characterization of drug metabolizing and transporting proteins as well as drug targets, and

discuss their advantages, limitations, caveats for implementation and their main applications in translational pharmacokinetics (PK) and pharmacodynamics (PD).

2.3.Overview of a typical quantitative proteomic experiment

The quantitative proteomic workflow can be customized for the type of biological sample and the target proteins to be quantified; however, routinely applied bottom-up methods tend to follow generally similar steps (Figure 2.1 A). A biological sample (tissues, cell lines or biofluids) is processed by cell lysis or homogenization, often followed by enrichment of specific fractions (e.g. microsomes, cytosol, S9, plasma membrane, mitochondrial fraction) (Figure 2.1 B) prior to protein solubilisation and digestion.[20–22] The variable array of available samples requires consideration of the effects of the type of sample and subsequent processing on end-point protein abundance.[23]

Whole cell lysates or tissue homogenates can be used for the quantification of various pharmacologically relevant proteins.[24] When enriched systems are required, the localization of the target protein is critical to the decision of which fraction to use.[22] Cytosolic proteins (e.g. alcohol/aldehyde dehydrogenases, sulfotransferases) are best quantified in cytosol or S9 fractions.[25] Membrane-bound reticular proteins (e.g. CYPs and UGTs) are enriched in microsomal membrane fractions.[26] Enzymes localized in the reticular lumen (e.g. carboxylesterases) can be quantified in microsomes; however, a proportion of these proteins is expected to be lost into the cytosol during sample processing and therefore these proteins are quantified more accurately in S9 fractions (consisting of microsomes and cytosol) provided the target proteins are sufficiently abundant.[25,27] Transporters and PD-relevant targets, such as receptors, protein phosphatases and kinases, can be found in the plasma membrane,[28,29] and therefore cell membrane-enriched fractions can be used for these applications. Detailed sub-cellular location information can be found in various databases, including Gene Ontology (www.geneontology.org) and UniProt (www.uniprot.org).

Bottom-up proteomic techniques rely on quantitative analysis of unique (proteotypic) peptides used as surrogates for target proteins.[18] Sample proteins are digested using specific proteases, typically trypsin or lysyl endopeptidase (LysC), independently or in combination.[30,31] Other proteases, such as chymotrypsin, can be used for specific applications, such as increased depth and reproducibility of analysis.[32] Sample digestion can be done in gel, in solution or using filter-aided sample preparation (FASP).[33–35] Complementary data is expected to be generated

when several protein preparation workflows are used.[36,37] After digestion, peptides are desalted, enriched, separated by liquid chromatography (LC) and analysed using mass spectrometry (MS). Additional separation prior to mass spectrometry can be performed using ion mobility.[38,39] Multiple quantitative MS and data acquisition approaches can be used (Figure 2.1 C), depending on the aim of the experiment and the availability of instrumentation.[40] Targeted and global methodologies are routinely used to identify and quantify expression levels of pharmacologically-relevant proteins. Standards are added at different stages of the proteomic workflow (Figure 2.1 A). Data acquisition is followed by data analysis and interpretation, often facilitated by vendor or open-source software. Assessment of the performance of various software packages used for targeted and global proteomics was previously reported.[41–43]

Several quality control (QC) steps are required at certain stages of the experiment. Assessment of the quality of sample processing during homogenization and fractionation is required to ensure maximum recovery of protein, normally using colorimetric/fluorometric protein assays. Assessment of the digestion efficiency is done before LC-MS analysis; this is achieved by evaluating time-dependent release of peptides in targeted experiments or by monitoring the rate of missed cleavage in global experiments. Finally, the reliability of the proteomic quantification technique depends on the performance of the LC-MS system, which can be assessed using internal standards and well-characterized QC samples.[19,23]

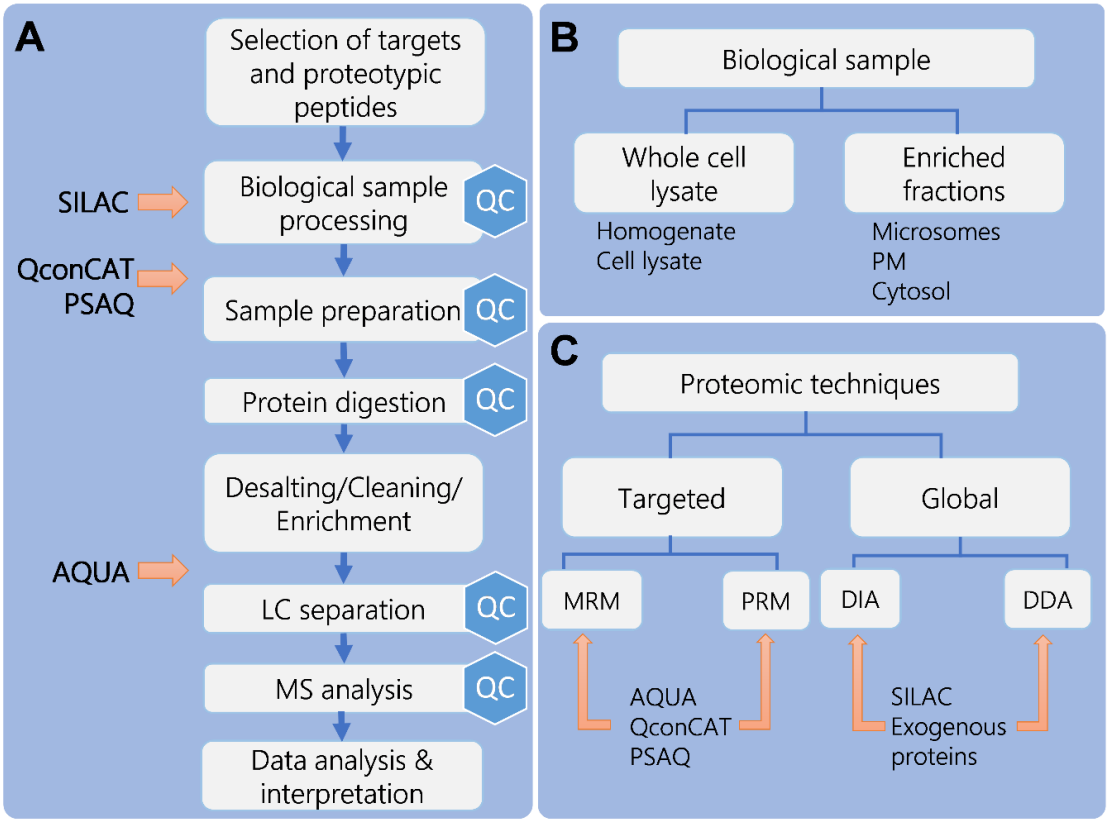

Figure 2.1. Overview of the experimental quantitative proteomic workflow. A. *Basic proteomic strategy starting from selection of targets and sample preparation, followed by LC-MS analysis, and finally data analysis/interpretation. Protein digestion relies on proteases, such as trypsin and lysyl endopeptidase (LysC), and can be done in solution, in gel or using filter-aided sample preparation (FASP). Standards are added at different stages of sample preparation. SILAC mixtures represent isotopically labeled proteomes; QconCAT and PSAQ protein standards are added to samples prior to protein digestion; AQUA peptide standards are added before LC-MS analysis. Several quality control (QC) steps are required throughout the workflow.* ***B.*** *The two main types of samples used to generate proteomic data, whole cell lysates (cell and tissue homogenates) and enriched fractions (e.g. microsomes, plasma membrane, cytosol, mitochondrial fractions or S9 fractions).* ***C.*** *The main types of proteomic techniques (targeted and global) and data acquisition methods (MRM/PRM for targeted proteomics and DDA/DIA for global proteomics). Red arrows show the steps where standards are introduced. Abbreviations: AQUA, absolute quantification peptide standards; DDA, data-dependent acquisition; DIA, data-independent acquisition; MRM; multiple reaction monitoring; QC, quality control; QconCAT, quantitative concatemers; PM, plasma membrane; PRM, parallel reaction monitoring; PSAQ, protein standards for absolute quantification; SILAC, stable isotope labeling by amino acids in cell culture.*

2.4.Targeted quantitative proteomic methods

Targeted methods are in many ways superior to global methods for the quantification of specific proteins of interest that are known to be expressed in a particular system. The use of targeted proteomics with enriched fractions (e.g. plasma membrane, microsomes) offers highly reproducible measurements of proteins expressed at low levels. The workflow of quantification using these methods starts with identifying the target proteins of interest, followed by selection of proteotypic peptides used as surrogates to quantify the selected targets. These methods require stable isotope labeled (SIL) internal standards for absolute quantification. Generally, MS platforms used for targeted techniques include triple quadrupole (QqQ), quadrupole/time-of-flight (Q-TOF) and hybrid Orbitrap mass spectrometers. Table 2.1 summarizes the advantages and limitations of targeted proteomic methods. The types of targeted acquisition methods are discussed below.

Table 2.1. The overall aims, advantages and limitations of various proteomic data acquisition methods: targeted (MRM, PRM), global data-dependent acquisition (DDA) and data-independent acquisition (DIA) techniques.

Method	Advantages	Disadvantages
Targeted techniques (MRM, PRM) **Aim: Robust quantification of a selected set of proteins, known to be expressed in a particular system**	• High sensitivity and reproducibility • Simple data analysis • Allows relative and absolute quantification; SIL standards address matrix effects • High resolution instruments are not required for MRM • High selectivity with PRM	• Limited resolution and selectivity with MRM • Limited number of target proteins (10-50 targets per single analysis) • Requirement of prior knowledge of target proteins • Requirement for synthesis of internal standards • Targeted methods cannot be used for discovery of novel targets or pathways
Global data-dependent acquisition (DDA) techniques **Aim: discovery proteomics and proteome-wide quantification**	• Simple method setup • High proteome coverage • Internal SIL standards are not needed • Allows relative and absolute quantification (with spiked standards or TPA approach) • PTMs can be characterized using global data	• Bias toward highly expressed proteins and compromised reproducibility for low abundance proteins • Sensitive to changes in LC-MS conditions due to longer runs required • Absolute quantification is relatively less reliable than targeted methods

	• Data can provide guidance for targeted quantification	• Requirement of instrument with high-end specifications • Selectivity and sensitivity are compromised
Global data-independent acquisition (DIA) techniques **Aim: discovery proteomics and proteome-wide quantification. In the case of sequential window methods (SWATH), the aim can also be set to the quantification of a limited number of target proteins**	• Moderate/high precision of peptide quantification. • Wide breadth of peptide identification and quantification leading to high target coverage (typically higher than DDA) • Amenable to discovery and quantitative applications • Provides rich data for targeted methods, including peptide information, fragment information, PTMs and potentially SNPs	• Complex and convoluted data • SWATH requires multiple steps to compile spectral libraries, with many parameters to optimize • Requirement of instrument with high-end specifications • Requirement for specialist software and high computational power for analysis

PTM, post-translational modifications; SNP, single-nucleotide polymorphism; TPA, total protein approach

2.4.1. Selected/multiple reaction monitoring (SRM/MRM)

Selected or multiple reaction monitoring (SRM/MRM) is the most commonly used targeted proteomic method in biological and pharmacological research.[44,45] In MRM, a peptide and a selected set of its fragment ions (transitions) are monitored by mass filtering on a triple quadrupole instrument.[46] The technique is routinely used with internal SIL standards, and heavy (standard) and light (analyte) ions are analyzed simultaneously. This technique offers several advantages including multiplexed analysis, high throughput, reproducibility, sensitivity and wide dynamic range.[5,46] The sensitivity achieved by this method makes it ideal when samples are small, e.g. biopsies.[47] The limitations of targeted techniques include the requirement for extensive method development and the selection of suitable targets. Low abundance analyte proteins are not accurately quantifiable and interference can occur due to the use of pre-defined mass filters and low resolution mass analyzers.[44,45]

Several applications of this technique have been reported including determination of inter-individual variability in drug-metabolizing enzymes and transporters,[48–50] prediction of variability in clearance [51] and drug-drug interactions (DDIs),[11] determination of inter-species differences of transporter expression at the blood-brain barrier,[37,52] characterization of various hepatocyte-based in vitro systems,[53,54] region-specific transporter expression in the brain,[55] kidney [56] and intestine,[20] region-specific enzyme expression in the kidney,[57] quantification of biomarkers in biological fluids, such as plasma and urine [58] and assessment of the effects of disease on different organs.[25,59,60]

2.4.2. Parallel reaction monitoring (PRM)

Parallel reaction monitoring (PRM) is a recently introduced targeted method with higher specificity than MRM[61,62] because of the use of high-end mass spectrometers, such as Orbitrap[63,64] and quadrupole/time-of-flight [65] platforms, offering high resolution and high mass accuracy. The principle of PRM is based on simultaneous monitoring of all (precursor ion/fragment ion) transitions of a targeted peptide arising from both standard and sample, in parallel at the MS and tandem MS (MS/MS) levels. By contrast, the MRM approach monitors only pre-defined fragments. The combination of full scan mode, high resolution and high mass accuracy makes PRM a very attractive method, especially for the analysis of complex biological matrices. PRM requires less time for method development and is less prone to interference than MRM owing to the availability of a higher number of quantifiable

fragments.[66,67] Because of the large number of monitored transitions, the sensitivity of PRM is sometimes reduced relative to MRM, and the requirement of high resolving power makes the technique less widely applicable.[67] Comparable performance by MRM and PRM has recently been demonstrated.[66,68] Reported applications of PRM-MS include plasma biomarker analysis,[69] quantification of enzyme variants,[70] and characterization of liver, kidney and intestine pools.[68]

2.4.3. Accurate mass and retention time (AMRT)

Quantification (relative or absolute) based on accurate mass and retention time (AMRT) is a simple and rapid method.[71] This method is less widely used than MRM and PRM techniques and relies on measurement of precursor ion intensity of analyte and standard peptides at a predefined mass (*m/z* ratio) and retention time. Confirmation of the peptides identities is carried out after fragmentation at the MS/MS level. This method can be used in conjunction with global proteomic methods to quantify selected targets in proteome-wide analyses. Because AMRT relies on the parent ion intensity in the MS scan, its efficiency is dependent on reproducible peptide separation (by LC) and the use of high resolution mass analyzers (MS). In addition, only a limited number of moderate to high abundance proteins can be quantified. This technique was applied to measuring protein abundance in human serum[71] and assessment of disease perturbations in the expression of transporters at the blood-brain barrier.[60]

2.5.Standards for targeted proteomics

Absolute quantification is typically achieved by targeted techniques that use SIL peptides or proteins as standards or calibrants.[72] These standards represent heavy versions of the surrogate peptides selected to quantify the target proteins. Standards are synthesized chemically or biologically and incorporate a heavy isotope (^{13}C, ^{15}N), which allows distinction between analyte (light) and standard (heavy) by mass spectrometry. The types of standards routinely used in targeted quantitative proteomics include absolute quantification (AQUA) peptides, quantitative concatemers (QconCAT) and protein standards for absolute quantification (PSAQ). A summary of the characteristics of these standards is shown in Table 2.2.

Table 2.2. Characteristics of standards used in targeted proteomic methods (AQUA, QconCAT and PSAQ) and their analytical performance.

	AQUA	**QconCAT**	**PSAQ**
Description	Chemically synthesized isotope labeled peptides	Biologically synthesized sequence of isotope labeled peptides	Intact isotopically labeled recombinant protein
Commercial availability	Available	Available	Available
Digestion evaluation	Necessary	Necessary	Not Necessary but desirable
Number of target proteins	One for each standard	Up to 50 per standard protein	One for each standard
Cost	Low, depending on the number of targets	Moderate	High
Considerations for synthesis	Subject to stability issues during the chemical synthesis	Subject to failure of expression	Subject to failure of expression
Addition in the experimental workflow	Post-digestion	Before solubilization and digestion	Before solubilization and digestion
Compatible proteomic techniques	MRM	MRM	MRM

	PRM	PRM AMRT	PRM
Performance of targeted methods	Highly reproducible Multiplexed	Highly reproducible Multiplexed Ideal for stoichiometric analysis	Highly reproducible Accurate
SNP and stoichiometric analysis	Possible; requires QC	Yes	No
Analysis of PTMs	Yes	No	No

AMRT, accurate mass and retention time mass spectrometry; MRM, multiple reaction monitoring; PRM, parallel reaction monitoring; PTM, post-translational modifications; QC, quality control; SNP, single-nucleotide polymorphism

The selection of standard peptide sequences is a critical step and follows previously reported criteria.[73] These criteria can also be applied to select surrogate peptides in global proteomic methods.[19] Generally accepted requirements include:

- **Proteotypic sequence:** unique to the protein of interest with distinct mass (*m/z*) and fragmentation pattern (MS/MS); isobaric and isomeric sequences are avoided.
- **Cleavable by proteases used in quantitative proteomics:** the sequence should not be mapped to transmembrane domains; absence of closely occurring cleavage sites in the target protein sequence (e.g. arginine (R) and lysine (K) in the case of trypsin).
- **Detectable by LC-MS:** optimal hydrophobicity (LC) and ionizability (MS); absence of known single nucleotide polymorphism (SNP) and post-translational modification (PTM); optimal length (7-25 amino acids depending on the MS platform).
- **Stable:** not susceptible to chemical modification during storage and handling including oxidation of methionine (M) and deamidation of asparagine/glutamine (N/Q).

These general selection criteria can be customized for different biological applications. For example, peptides with known PTMs and SNPs are targeted if the biological question requires such stoichiometric analysis. Allele-specific protein quantification was demonstrated recently for the assessment of significant genetic variations in CYP and UGT enzymes.[70,74]

2.5.1. Absolute quantification (AQUA) peptide standards

SIL peptides or AQUA standards are chemically synthesized isotope labeled standard peptides with sequences specific to the target proteins. High quality and high purity peptides are available commercially in isotopically labeled form, making them easily accessible for large scale studies.[75,76] A known amount of the AQUA peptide is introduced into the sample at a late stage of sample preparation, usually after protein digestion. AQUA standards can be applied with MRM or PRM techniques, making these targeted techniques very useful when screening a specific protein in a large number of samples as a clinical test or when the quantification of a small set of proteins is desirable.[40] AQUA can also be applied to the elucidation of PTMs, such as phosphorylation.[76] However, synthesis and quantification of standards for large scale studies is expensive and time-consuming.[77] The need to store peptides can be limiting as they tend to precipitate during long-term storage and lead to inconsistent quantification.[78] AQUA peptides are normally added to the sample directly before LC-MS analysis and the accuracy of quantification by the AQUA method can therefore be affected by analyte peptide loss during sample preparation.[79] We recommend addition of standards to the samples before pre-

fractionation and desalting so that equal loss of standard and analyte peptides is incurred from the mixture.

The AQUA-MRM approach is the most widely used quantification method in pharmacokinetic research and has been used to quantify various enzymes and transporters in different human tissues. Quantified enzymes include CYP and UGT enzymes in liver,[17,25,29,80–84] intestine[50,81,85,86] and Kidney.[57,81,85] In brain, the AQUA-MRM workflow was used to quantify CYPs, glutathione S-transferases (GSTs) and catechol O-methyltransferase (COMT).[87] Non-CYP and non-UGT drug-metabolizing enzymes quantified by this method include liver flavin-containing monooxygenases (FMOs), sulfotransferases (SULTs), aldehyde oxidase 1 and alcohol and aldehyde dehydrogenases.[26,88–90] In additions, drug transporters were successfully quantified using this quantitative strategy in various tissues, including liver,[24,91] intestine,[20,92] kidney,[56] brain[55,87,93] and lung.[94]

2.5.2. Quantitative concatemers (QconCAT)

QconCAT is a concatenated set of peptides expressed recombinantly from an artificial gene. The host organism is usually *E. coli* grown in culture media, supplemented with labeled amino acids, usually $^{13}C_6$-lysine and $^{13}C_6$-arginine. QconCATs are available commercially but can also be expressed in-house at relatively reasonable costs.[74] The QconCAT protein is added to the sample at a known concentration (estimated using an unlabeled peptide corresponding to a standard peptide within the QconCAT) prior to digestion and can be used with several targeted techniques (MRM, PRM, AMRT). A single QconCAT can be designed to quantify several proteins (up to 50), making it amenable to multiplexing and achieving higher coverage of protein targets. QconCAT ensures a strict 1:1 stoichiometry making it particularly advantageous in determining polymorphisms [70,74] and establishing protein-protein inter-correlations.[95] The development of QconCAT constructs is time-consuming and most worthwhile when a significant number of proteins (10-50) are to be quantified in a large number of samples. The QconCAT-MRM workflow has been successfully used to quantify hepatic drug-metabolizing enzymes[27,70,95,96] as well as transporters in liver,[24] intestine[97,98] and brain microvessels.[37,60]

Complete cleavage of peptides in the digestion process is, of course, essential, and there has been some interest in the use of ‘flanking’ sequences to make the environment of the peptides more analyte-like so that incomplete digestion will better resemble digestion efficiency of the

target proteins.[99,100] Although this idea is attractive in theory, the claim of comparable digestion efficiency between standard and analyte proteins is yet to be tested. We have preferred to optimize the digestion process so that there is complete release of peptides from the QconCAT and as far as possible of the target proteins.[101,102]

There is always the possibility of expression failure of a QconCAT, and this has been addressed in several ways.[74,102] Experience indicates that smaller QconCATs are generally expressed more efficiently than larger constructs and ideally QconCATs should be below 100 kDa in size.[103] The use of a small, insoluble tag, such as a ribosomal construct [101] can force a QconCAT to express in insoluble form in inclusion bodies, from which it may be readily isolated.[74] More radically, to address the issue of low yield and expression failure of larger QconCATs, multiplexed efficient expression of recombinant QconCATs (MEERCAT) was recently introduced to serve as standard for large scale protein quantification. The QconCATs are expressed in cell-free medium, with advantages such as expression efficiency, cost-effectiveness and ability to monitor the number of expressed QconCATs.[104]

2.5.3. Protein standards for absolute quantification (PSAQ)

A PSAQ standard is similar in concept to a QconCAT, but consists of an intact isotopically labeled recombinant protein added at a known concentration to the sample under investigation early in the sample preparation workflow. When a PSAQ standard is employed to quantify an unmodified protein, it can control for solubilization efficiency, digestion and LC-MS conditions; digestion discrepancies are avoided as PSAQ conserves the native context of the target peptides.[105] This approach is particularly advantageous when quantifying low abundance, soluble targets in clinical samples.[106,107] However, PSAQ is only applicable to a small number of proteins; the development of such standards is prohibitively expensive and requires rigorous quality control.[77] This technique is not useful for assessing PTMs, identifying inter-correlations or multiplexed quantification of a large number of targets.[40] The application of PSAQ in the quantification of drug-metabolizing enzymes and drug transporters in human tissue is yet to be reported. In biomarker research, this method was successfully used to quantify enzymes useful as indicators of cardiovascular disease[108] and acute kidney injury[109] in biological fluids.

2.6.Global quantitative proteomic methods

Global untargeted proteomic approaches are routinely used for assessment of protein expression profiles, biomarker discovery, and identification and quantification of a large number of target proteins. Global approaches offer a wide dynamic range and broad proteome coverage while targeted approaches offer higher precision and accuracy. Proteome-wide quantification by global methods is routinely performed either by stable isotope labeling of sample proteins or peptides, e.g. stable isotope labeling by amino acids in cell culture (SILAC) and isobaric tags for relative and absolute quantitation (iTRAQ),[110,111] or by label-free analysis of the entire identifiable proteome.[6,112]

In metabolic labeling methods, such as SILAC, samples are labeled with amino acids (e.g. arginine, lysine or leucine) carrying a stable isotope label (^{13}C, ^{15}N) and pooled before further sample processing, thus minimizing bias due to handling. The ratios of light to heavy peptide signals at defined retention times are used to relatively quantify protein expression differences between control and treatment conditions. Recent developments in labeling technology increased the ability of SILAC to multiplex from 2 samples to 6 samples.[113] SILAC is best suited for induction studies, elucidation of drug effects on protein expression,[114,115] and analysis of post-translational modifications, such as relative quantification of phosphorylated proteins and identification of novel phosphorylation sites.[116] In addition, SILAC has been used to prepare labeled standard mixtures for targeted proteomics.[117] These labeled standards are added to analyte samples before protein digestion (Figure 2.1 A), demonstrating similar performance to AQUA standards.[118] Metabolic labeling of whole animals, such as rodents, represents a recent extension of SILAC, with various applications in pharmacology research, such as the direct quantification of liver drug-metabolizing enzymes.[119]

Chemical labeling methods, such as iTRAQ and tandem mass tags (TMT), are used at the peptide level after proteolytic digestion of sample proteins. Chemical tags react with amine groups and unique reporter ions are released upon fragmentation in MS/MS analysis.[120] Unlike SILAC, chemical labeling can be used to analyze up to 8 samples and 11 samples in the same pool using iTRAQ and TMT reagents, respectively. Chemical labeling methods in conjunction with global proteomics demonstrated comparable performance to targeted AQUA-MRM methodology.[121] Applications of chemical labeling include quantification of hepatic drug-metabolizing enzymes and drug transporters [121], characterization of plasma proteins in acute renal rejection,[122] biomarker identification for breast cancer,[123] eye disease[124] and gum

disease,[125] and relative quantification of proteins in Alzheimer's disease.[126] It is worth noting that proteome-wide labeling methods (SILAC/iTRAQ/TMT) are more aligned with applications that require relative quantification.

In label-free methods, normalization of measurements uses either unlabeled exogenous protein references or the total protein approach (TPA). Exogenous proteins include various protein standards distinct from the target proteome; for example, quantification of human enzymes can employ bovine serum albumin or yeast alcohol dehydrogenase at known concentrations.[112] The TPA method uses the total intensity of peptide peaks belonging to a certain protein relative to the total intensity of all quantifiable peptides in the proteome.[127] Both methods have previously been used to quantify human liver enzymes and transporters.[6,38,128]

Global proteomic techniques are generally carried out using Q-TOF or Orbitrap instruments. To correct for changes in MS conditions over long analyses, sophisticated correction and chromatographic alignment procedures are used to compensate for retention time shifts and to avoid mismatching peptide peaks across runs.[129] Data acquisition methods used in global proteomics include data-dependent acquisition (DDA) and data-independent acquisition (DIA). DDA represents the standard shotgun approach widely used for whole-proteome analysis.[130] On the other hand, the more recent DIA approach can generate more depth of analysis and broader proteome coverage, especially when window acquisition approaches, such as sequential window acquisition of all theoretical fragment mass spectra (SWATH), are used.[40,131] A summary of the advantages and limitations of global proteomic methods is presented in Table 2.1.

2.6.1. Data-dependent acquisition (DDA)

In DDA, the initial scan of peptide peaks is used for the selection of peptides for fragmentation depending on their ion intensity, with the most abundant ions being selected preferentially. The main advantages of DDA are its flexibility and broad proteome coverage compared to targeted methods. DDA proteomics can identify thousands of proteins and provide reliable relative quantification across samples.[131] DDA can also be used for absolute quantification using suitable exogenous protein standards.[112] However, this method is less precise in comparison with targeted quantitative methods as low abundance peptides are not detected reproducibly, leading to bias toward high abundance proteins.[24,131,132] The performance of this method declines as sample complexity increases.[130,133]

Q-TOF or Orbitrap mass analyzers are normally used and data are interpreted using software packages, such as MaxQuant, Progenesis or Peaks. DDA data analysis can be performed either by spectral counting or by ion abundance/intensity,[112,134] with ion intensity preferred owing to its higher accuracy and reproducibility.[19,39] Importantly, to ensure robust quantification, consistency in sample preparation and stability of LC-MS conditions are required. DDA shotgun methodology was successfully used for the quantification of transporters and receptors at the blood-brain barrier[60] and for profiling various enzymes and transporters in liver tissue[6,24,32,121,128] and hepatocyte-based *in vitro* systems.[6,135]

2.6.2. Data-independent acquisition (DIA)

DIA was proposed to address the limitations of DDA in relation to limited depth of analysis and biased quantification. In DIA, all precursor ions within a selected mass range are fragmented and analysed.[131] Theoretically, this method identifies all detectable peptides within the selected mass range and is therefore less biased towards high abundance proteins. However, the generated data tend to be highly complex and specialized software is required for data deconvolution post-acquisition.[129] DIA combines the advantage of broad proteome coverage offered by DDA methods and highly reproducible quantification, typically achieved by targeted techniques.[18,131] The most widely used DIA approaches include MS^E [39,112] and SWATH.[136] MS^E is a collision energy alternation method that uses a range of collision energies over a *m/z* window, leading to high- and low-energy fragmentation.[39] The deconvoluted spectra are searched against a protein database for identification, while quantification can be done using an unlabeled standard protein. The applications of MS^E include relative and absolute label-free quantification of proteins [133]. For example, this method was successfully used for quantitative profiling of various drug-metabolizing enzymes in human liver.[38]

In methods that use fragmentation windows, such as SWATH-MS, instead of fragmenting the entire set of precursor ions in a particular scan, small *m/z* windows can be selected for fragmentation and acquisition.[136] This potentially reduces the complexity of data and theoretically improves analytical depth and coverage. SWATH is widely applied using Q-TOF and Orbitrap mass analyzers, and data are processed by sophisticated pipelines, such as the open-source, cross-platform software OpenSWATH.[43] The main advantages of SWATH are its compatibility with the analysis of low abundance sub-proteomes and PTMs, such as acetylation and glycosylation,[137] and its high reproducibility and consistency owing to peptide-centric scoring analysis.[129] SWATH is therefore particularly applicable when wide proteome

coverage, high consistency and accurate quantification are required. Post-acquisition interrogation of selected data yields high quality quantification of target proteins comparable to targeted MRM analyses.[136] SWATH has only recently been introduced and therefore it has not been widely used in pharmacology research; reported applications include profiling of hepatic drug-metabolizing enzymes[138] and quantification of enzymes and transporters in pooled liver, intestine and kidney microsomes.[68] Importantly, the utility of SWATH has recently been demonstrated in digital biobanking of tissue proteomic maps in health and disease.[139]

2.7.Key pharmacology applications of proteomic data

The interaction between various intrinsic and extrinsic factors that affect patient populations can result in variability in the expression levels of PK-relevant proteins and PD targets, leading to variations in drug exposure and response profiles (Figure 2.2 A). Proteomic methods are used to assess the effects of these factors, including age,[12,16,140,141] disease,[25,49,59,60,142] ethnicity,[14,15] and genetics,[14,16,91] individually or in combination, on protein expression profiles. Changes in abundance associated with perturbed systems relative to control are then used to predict effects on the fate of drugs (Figure 2.2 B).[25,121,142–145]

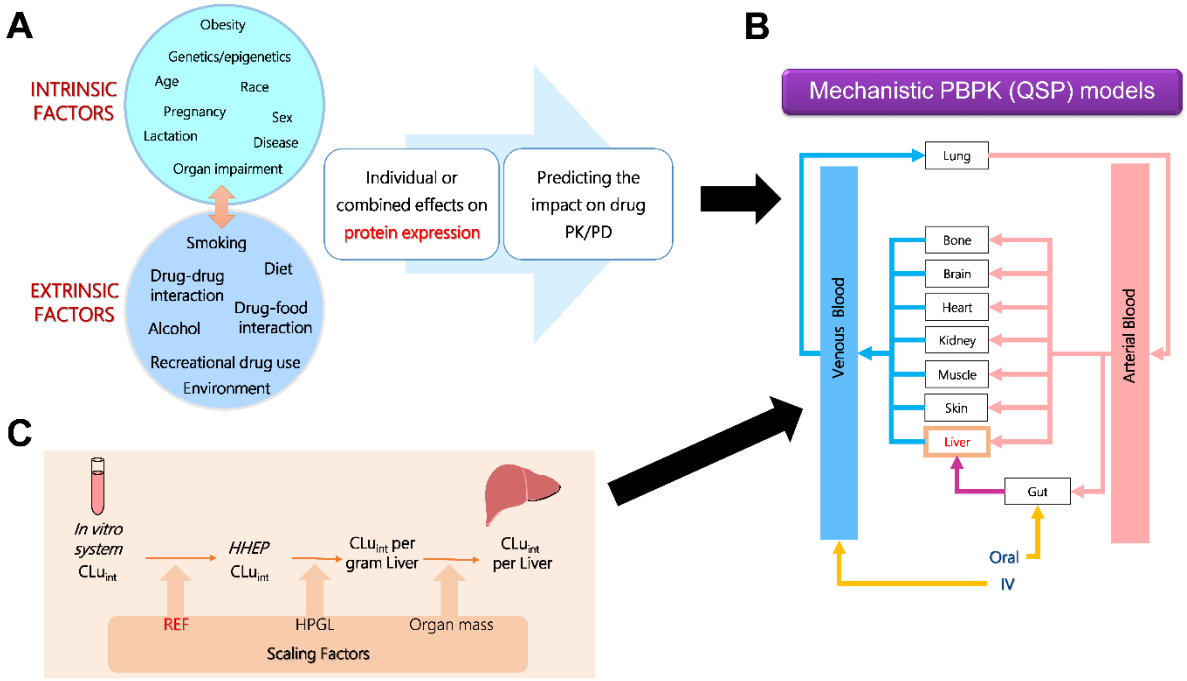

Figure 2.2. The use of proteomic data in PBPK prediction of drug exposure. A. *Several intrinsic and extrinsic factors can affect the abundance of proteins which in turn can affect drug PK and PD.* ***B.*** *Effects of intrinsic and extrinsic factors can be simulated using QSP (PBPK) models that incorporate physiological parameters (e.g. abundance) and drug data.* ***C.*** *The process of extrapolation from in vitro measurements in hepatocytes to the prediction of clearance in human liver; the process of IVIVE is used in combination with PBPK (or QSP) models (B) to predict drug PK (or PD) in a population of interest. Scaling factors used in IVIVE from hepatocytes are REF = Abundance in tissue/Abundance in the in vitro system, HPGL and liver mass. Abbreviations: CLu_{int}, intrinsic clearance of unbound drug; HHEP, human hepatocytes; HPGL, hepatocytes per gram liver; IV, intra-venous administration; PBPK, physiology-based pharmacokinetics; PD, pharmacodynamics; PK, pharmacokinetics; QSP, quantitative systems pharmacology; REF, relative expression factor measured using abundance data.*

Ideally, measurement of the effects on abundance and activity of functional proteins should be carried out and used to achieve robust predictions; however, specific substrates and optimized functional assays are still lacking for enzymes and transporters, with the exception of several CYP and UGT enzymes.[2,4,146] Abundance is commonly used as a surrogate for activity; correlation between protein abundance and activity was demonstrated for various hepatic and renal drug-metabolizing enzymes, such as CYPs, UGTs, carboxylesterase 1, aldehyde oxidase 1, flavin-containing monooxygenases and sulfotransferases.[3,26,27,29,49,57,90,147,148] This was also

demonstrated for certain transporters, such as P-gp and BCRP.[48,149] *In vitro* measurements are therefore routinely extrapolated to *in vivo* activity (IVIVE) using scaling factors that rely on abundance measurements (Figure 2.2 C).[98,150] In addition to scaling, measuring the abundance of pharmacologically relevant proteins also allows evaluation of the sources of variability in activity rates; inter-individual variation is driven by variability in the level of expression, alterations in intrinsic protein activity, or a combination of these factors.[151] Below is a brief account of the main pharmacology applications of proteomic data. Each application requires a different level of proteomic analysis (absolute quantification, relative quantification or discovery/identification) as illustrated in Figure 2.3.

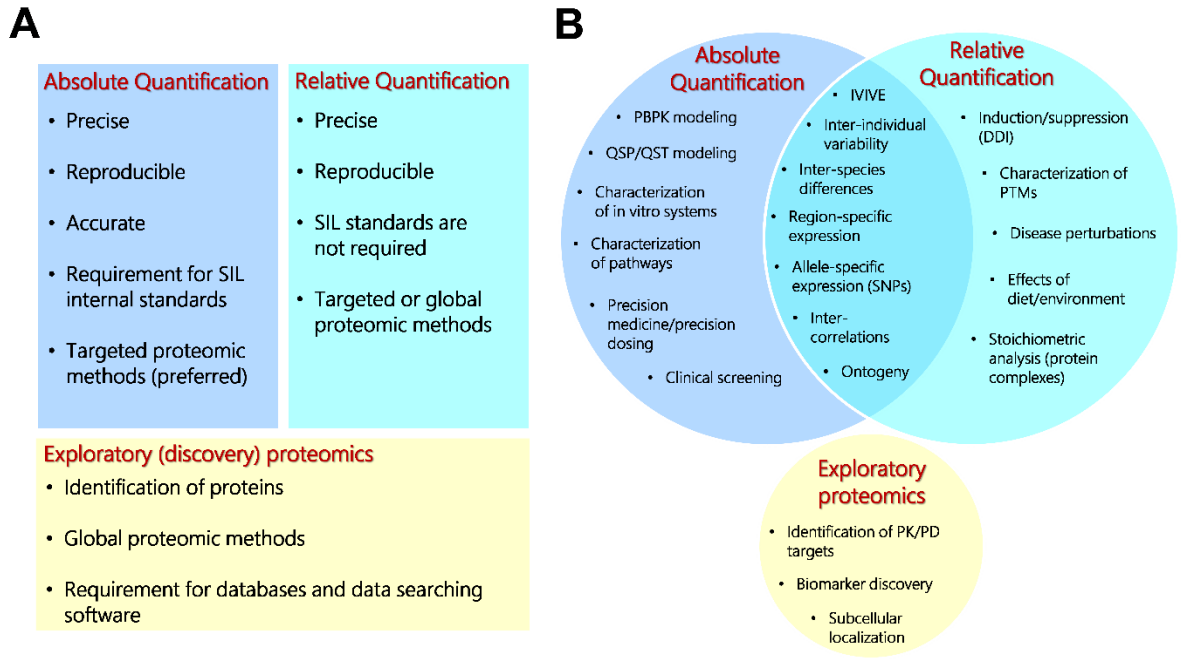

Figure 2.3. The characteristics and applications of absolute quantification, relative quantification and discovery proteomic approaches. A. *The requirements and characteristics of different levels of quantitative proteomic analysis. Absolute quantification requires assays that are accurate and precise; relative quantification requires reproducibility.* ***B.*** *Applications of data generated using absolute quantification, relative quantification and exploratory proteomics in translational PK and PD research. Several applications overlap between absolute and relative quantification. Abbreviations: DDI, drug-drug interaction; PBPK, physiology-based pharmacokinetics; PD, pharmacodynamics; PK, pharmacokinetics; PTM, post-translational modification; QSP, quantitative systems pharmacology; QST, quantitative systems toxicology; SIL, stable isotope label; SNP, single nucleotide polymorphism.*

2.7.1. Physiology-based pharmacokinetic (PBPK) modeling and IVIVE

The use of PBPK models has now become firmly embedded in practices within the pharmaceutical industry and evidence from these models is used in different phases of drug development.[152,153] PBPK modeling has gained wide acceptance with regulatory agencies,[154] with PBPK data being used in the labels of 21% of new drug applications approved by US Food and Drug Administration (FDA) in 2015.[155] Modeling is commonly used for prediction of human pharmacokinetic parameters and evaluation of the effects of factors affecting a patient population, such as genetics and lifestyle.[7,156] PBPK models are built by integrating drug profiles with physiological data, including blood flow, organ size, protein binding, and abundances of enzymes and transporters (Figure 2.2).[157] Various commercial and non-commercial platforms, e.g. Simcyp, GastroPlus, and PK-Sim, have facilitated the use of PBPK modeling,[158] but all require data describing protein abundance and population variability, and such data are still in short supply.[7] Key areas where PBPK models suffer from limited data include non-CYP and non-UGT metabolic pathways, extra-hepatic drug-metabolism and disposition, effects of differences in special populations (e.g. hepatically/renally-impaired, pediatric and geriatric patients) and inter-species variability. These limitations have started to be addressed in recent years mainly because of increased availability of (biopsy and surgical) tissue samples, advances in sample preparation methods and increased application of LC-MS proteomic techniques.

The use of IVIVE has extended the utility of PBPK modeling and made biosimulation more widely usable by linking modeling to *in vitro* studies using animal and human systems.[159] The application of IVIVE-PBPK requires integration of absolute abundance data in tissue relative to the *in vitro* system and system-specific scaling factors (e.g. microsomal protein content or hepatocellularity) with various patient-derived physiological parameters[150] to predict pharmacokinetic profiles and account for metabolic differences among specific populations.[1] A recent systematic survey of the literature showed that the majority of PBPK models are used for the assessment of clinical pharmacokinetics and DDIs.[159] Recently reported PBPK models that used proteomic data were developed for an array of applications, such as the prediction of variability in clearance,[10,121,160] variability in DDIs,[11] impact of formulation,[161] effects of liver disease [25,142] and kidney impairment[162] on drug pharmacokinetics, and predicting drug kinetics in paediatrics,[13,161,163] older patients[164] and during pregnancy.[165–167] In addition to these applications, PBPK models represent a valuable tool for learning and internal decision making

in the pharmaceutical industry as well as storing and integrating compound-specific information throughout drug discovery and development.

2.7.2. Quantitative systems pharmacology (QSP) models

Models with broader pharmacological applications include QSP models which represent new tools for drug development,[168] with several applications, including prediction of the effects of therapeutic agents, mechanisms of interaction between therapeutic targets and elucidating the biological processes underlying disease and resistance to drugs.[169–171] The US FDA has recently adopted the use of these models and the first case was the assessment of a novel parathyroid hormone replacement biologic.[172] The use of QSP models for supporting new drug submissions is therefore expected to increase.[173] In particular, a promising application of QSP models is the assessment of pharmacodynamics DDI potential by probing the mechanisms of interaction of a drug combination in the system and exploring the outcomes of target perturbations, as reported recently for the interaction between glibenclamide and the glucose-insulin-glucagon system in Type 2 diabetes.[174] The requirement for multi-omic data is emphasized for building pharmacology and toxicology models with the essential role of pharmaco- and toxico-proteomics in identifying and quantifying critical proteins in pathways affected by drug, chemical and environmental exposure.[175] This normally follows a strategy consisting of a discovery method followed by robust targeted quantification.[18] Proteomic data were previously used as the basis for developing QSP models to predict the effects of drugs, such as gemcitabine and birinapant in pancreatic cancer[176] and 5-flurouracil in colorectal cancer.[177]

2.7.3. Disease perturbation

Disease perturbation models are QSP models that aim to simulate disease progression and assess the effects of different drug regimens on a diseased population. Modeling disease perturbations requires relative abundance data for the diseased tissue compared to a healthy set of samples used as control. Disease-scale models have been applied to several disease states, including cirrhosis and different types of cancer. Cirrhosis is a disease of the liver that significantly affects drug metabolism and disposition and hence disease modeling can help with tailoring dosage regimens that are both safe and efficacious. Liver fibrosis generally leads to a reduction in expression of phase I and phase II enzymes (including CYPs, UGTs and sulfotransferases), and consequently, progressive decline in their abundance and activity is

observed as the disease advances.[178,179] Proteomic evidence of changes in the abundance of CYPs, UGTs and other hepatic enzymes was reported in cirrhotic livers and was shown to be dependent on the cause of cirrhosis.[25] Phase I metabolizing enzymes are reported to be more influenced by disease progression than phase II pathways which can be attributed to shortage in blood supply reaching the scarred tissue.[180] Incorporating proteomic data into disease-scale PBPK models has led to improved model performance in cirrhosis as reported for zidovudine, morphine,[25] repaglinide, bosentan, telmisartan, valsartan and olmesartan.[142,181]

Applications of disease models have also been highlighted for different malignancies, including breast cancer [182] and colon cancer.[177] These models were mainly used to predict the prognosis in certain populations and assess the effect of anti-cancer regimens at different stages of the disease. Because of the difficulty in recruiting cancer patient populations in clinical studies and the ethical issues related to the exposure of healthy subjects to toxic anti-cancer drugs, PBPK models are better accepted in oncology drug development compared to other disease states.[183] There is currently a lack of abundance data in cancer, and LC-MS proteomics is set to address this gap by providing quantitative measurements of enzymes and transporters from biopsies and archived surgical samples.[156]

2.7.4. Protein inter-correlations

Inter-individual variation in drug PK and PD can largely be predicted by integration of known sources of variability, including demographic factors (e.g. age and ethnicity) and physiological parameters (e.g. blood flow, levels of enzymes and transporters).[184] *In silico* approaches, such as PBPK models, can simulate the interaction between different covariates, such as changes in enzyme/transporter abundance, and predict their effects on clearance and DDIs.[11,185] Considering the inter-correlation between the expression levels of pharmacologically active proteins, and indeed between other physiological parameters (e.g. liver size and blood flow), can lead to more plausible parameter combinations when sampling from a population distribution.[186] Multiplexed quantitative proteomics can measure multiple enzymes and transporters in individual biological samples simultaneously, allowing robust assessment of inter-correlations between these proteins.[19,187] Due to the nature of correlation analysis, technical bias can in some cases lead to apparent relationships in protein expression and therefore caution should be exercised in order to use only verified biological inter-correlations in modeling applications.[7]

While various inter-correlations between drug-metabolizing enzymes and transporters have been confirmed both at the RNA[151,188,189] and protein levels,[95,128,190,191] the quantitative impact of such relationships on pharmacokinetic outcomes has only recently started to be explored, with models incorporating inter-correlations outperforming those that do not.[11,192] It is expected that the use of more realistic combinations of physiological parameters will be widely practiced in PK and PD modeling and simulation.[185]

2.7.5. Precision dosing

Model-informed precision dosing (MIPD) aims to predict the right dose of a drug for a specific patient based on individual characteristics. This is expected to lead to improved efficacy and reduced toxicity and pave the way to individualized therapy.[193] This approach is most applicable to drugs with a narrow therapeutic index and for special populations, such as pediatrics, geriatrics and patients with hepatic and renal impairment.[194] Multi-omic approaches and recent developments in 'liquid biopsy' assays [195] are expected to facilitate the construction of 'virtual twins' as a useful strategy to enable precision dosing. A 'virtual twin' is an *in silico* model that represents an individual patient, created by integrating system parameters (i.e. demographic, clinical and enzyme/transporter abundance data) from the patient in order to simulate individualized drug response.[196] This requires collection of absolute and relative expression data [194] measured in individual patients using innovative sampling techniques, such as the use of biofluids.[197]

2.7.6. Ontogeny

The process of growth and maturation is thought to be the main contributor to observed differences in drug PK profiles across the pediatric population age range and when compared to adult populations.[198] For example, physiological changes, such as gastric pH and emptying and intestinal motility that occur from birth to adulthood affect the rate of drug absorption. This is particularly evident in neonates in which absorption is generally delayed.[199,200] In addition, the ontogeny of drug-metabolizing enzymes, such as CYPs and UGTs, and transporter proteins within the liver and other organs contributes to variable rates of drug metabolism and excretion,[12,16,89,141,201] with consequences for toxicity and efficacy profiles.[199,202]

Current drug dosing regimens for pediatrics are based on allometric scaling from adult populations or reliant on local guidance and clinician experience because of lack of data from clinical trials.[203] Regulators are increasingly supportive of mechanistic PBPK models to inform

drug labels in lieu of clinical trials in pediatric applications.[204,205] There is still, however, a paucity of data to feed these paediatric models, in large part because pediatric samples are obtained opportunistically.[206,207]

Despite the difficulties of sample collection, there is consensus that the abundance and function of the majority of enzyme and transporter proteins are comparatively low in fetal and neonatal samples, increasing at varying rates as a function of age toward adult equivalent levels.[26,191,201,208] For example, CYP3A4, UGT2B7 and P-gp are present in small amounts in neonatal samples, increasing toward or surpassing adult equivalent levels by 1-3 years of age.[12,16,209] Conversely, CYP3A7 abundance is relatively high in fetal and neonatal samples, decreasing rapidly toward adult equivalent levels within 1 year.[209,210] Incorporation of ontogeny profiles with *in silico* models led to useful pharmacokinetic predictions for several drugs, such as theophylline,[211] propofol,[212] tramadol [213] and valproic acid,[214] in children.

2.7.7. Characterization of polymorphisms

Most drug-metabolizing enzymes, particularly CYPs, and transporters, such as organic anion transporting polypeptides, are polymorphic with a range of clinical consequences.[215,216] Various genetic polymorphisms are non-synonymous and can be characterized at the protein level, while polymorphisms occurring in the regulatory region of a gene can affect gene expression and mRNA stability in a particular tissue but do not result in modifications to the protein sequence. The effect of polymorphism becomes significant when it causes variability to an extent that necessitates a change in the administered dose of a specific drug;[217] a case in point is CYP2C9 polymorphism and its effects on the required dose of the anti-coagulant warfarin. Our group has previously developed an allele-specific proteomic workflow that can distinguish different polymorphic variants of CYP2B6.[74,95] Shi et al. (2018)[70] showed applicability of this approach to UGT2B15 with the aim of elucidating the regulatory mechanisms of UGT expression. Although relative quantification is as applicable to studying polymorphisms as absolute quantification, this application requires accurate and reproducible assessment of the stoichiometry of target enzymes (or transporters), and therefore targeted proteomic methods that employ a QconCAT standard are especially suitable.[218]

2.7.8. Disease biomarker discovery

Identification of biomarkers assists in understanding the pathophysiology of a disease and its progression, as well as monitoring patient response during therapy.[177,219] This is applicable not

only to traditional drugs but also to testing the efficacy of new candidates and comparing them to already available therapeutic agents. Often more than one biomarker is necessary to characterize a disease state, where the synergy between several targets in the same (or related) disease pathway makes a composite test more effective than monitoring a single biomarker of disease.[220] A rigorous discovery proteomics workflow should consist of a preliminary discovery phase using global proteomics, such as shotgun DDA or SWATH profiling, followed by verification or validation of target proteins using more quantitative targeted techniques, such as MRM or PRM. The settings of the targeted experiment will depend on information collected in the discovery phase.[19]

The initial step can be performed on a small set of well-characterized samples from patients with the relevant disease state relative to control with the aim of identifying differentially expressed proteins.[18,219] Global proteomics has led to the discovery of various diagnostic biomarkers, such as proteins related to resistance to cancer chemotherapy, and biomarkers for monitoring treatment.[221,222] These biomarkers are normally associated with critical cell function pathways, such as survival, proliferation,[223] apoptosis[177] and post-translational modification of proteins.[224] After conclusive identification of a set of biomarkers, targets are quantified in samples from different populations, such as patients at different stages of the disease, and a healthy cohort.[225,226]

A promising application of global proteomics showed differences in expression profiles between Crohn's disease and ulcerative colitis, which are symptomatically very similar but require entirely different treatment regimens.[227] In cancer, a wide range of signalling pathways can be perturbed, including the function of protein kinases and phosphatases, which can be monitored as disease biomarkers and targeted by novel drug therapies.[228,229] Recently characterized cancer biomarkers for the assessment of prognosis and therapy-related considerations include HER2 for decision-making in cancer treatment,[170] cAMP-CREB1 axis as a key mechanism associated with resistance to platinum-based therapy,[171] caspase networks associated with prognosis of colorectal cancer,[177] Stathmin-1 in relation to cell migration in colon cancer metastasis,[230] and protein Z as an early biomarker for the detection of ovarian cancer.[222]

2.8.Recommendations for best practice in applying proteomic techniques

With the recent expansion in the use of proteomic techniques in clinical and pharmacology research, robust guidelines have become crucially required for choosing the most appropriate method for a specific application. The decision-making process tends to be complex and will depend on multiple factors including the biological question, the type of sample, the number of samples, the number of targets, and the available budget. Figure 2.4 shows a simplified decision tree intended to guide the choice of proteomic methods used for pharmacology applications. In the same line, a workshop was recently held by the International Society for the Study of Xenobiotics (ISSX), with the aim of reaching a consensus on the use of proteomics in translational pharmacology research. Various recommendations for the choice and application of different techniques were proposed but a general consensus was not achieved.[19]

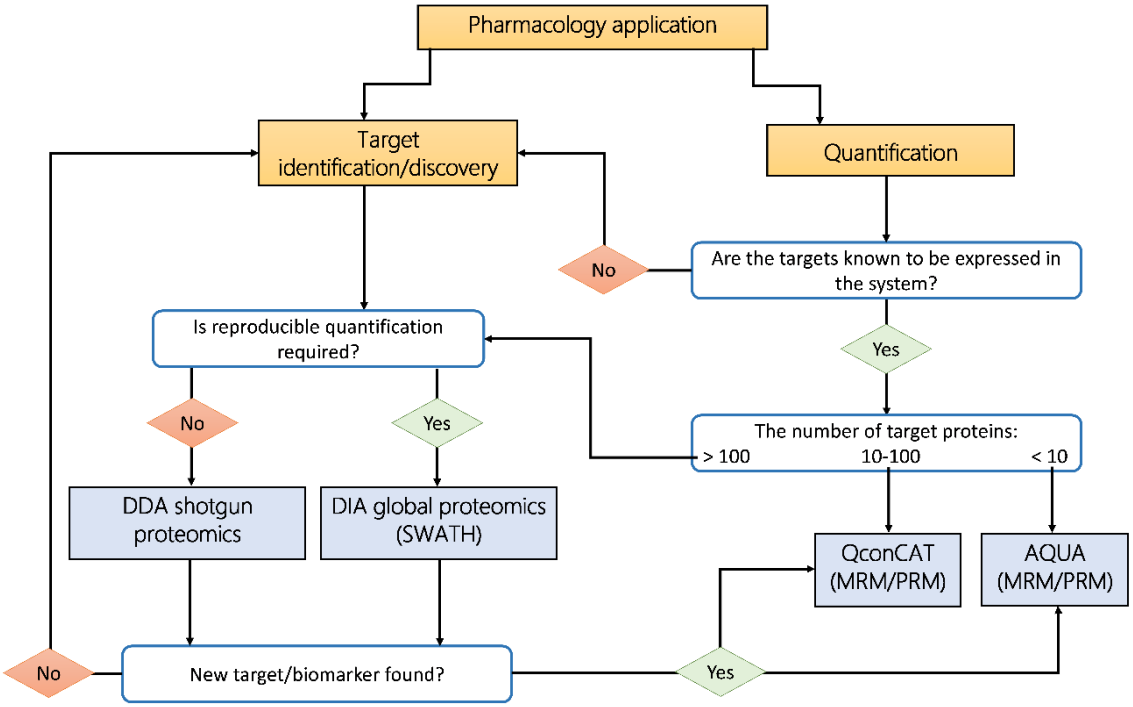

Figure 2.4. Decision tree for choosing suitable proteomic techniques intended for pharmacology applications. *A typical number of samples (~30) is used as input for the decision tree. The application can be hypothesis-driven and focused on quantification or hypothesis-generating and intended for discovery. If the application is focused on discovery, global proteomics are most suitable, with preference for data-independent acquisition when reproducible quantification of differential expression is required. When a target or a biomarker is discovered, more accurate quantification is achieved with targeted proteomics. If the target proteins are known to be expressed in the system and are well-defined, targeted proteomics are preferred. If the number of targets is small (< 10), AQUA-based methods (in conjunction with MRM or PRM techniques) are cost-effective. When the number of targets is higher (10-100), QconCAT methodology is preferred. Quantification of larger numbers of targets (> 100) and characterization of proteomes is better achieved using global proteomics. Orange boxes denote applications and blue boxes represent proteomic methods.*

Considerations for choosing a technique will generally differ for targeted and global proteomic methods. In targeted analysis, isotopically labeled standards are used to improve precision and accuracy of measurements and reduce bias caused by variations in sample preparation and matrix effects.[23] This is desirable when accurate quantification of inter-individual variability is required for QSP models and MIPD. Techniques recommended for these applications include MRM applied on triple quadrupole instruments and PRM conducted on higher resolution

platforms, such as Orbitraps and Q-TOF instruments. Both methods can be used for multiplexed quantification and they offer a wide dynamic range, typically two orders of magnitude, and therefore spiking of standards should be guided by the range of targeted proteins. One of the main advantages of targeted analysis is possibly its unparalleled sensitivity achieved even in the presence of a complex biological matrix.[231] Therefore, recommended practice is to quantify protein expressed at very low abundance in a targeted manner. MRM is currently the 'gold standard' in clinical and pharmacological research,[46] and recent guidelines by the Clinical Proteomic Tumor Analysis Consortium (CPTAC) provides recommendations and standard operating procedures (SOPs) for the development, application and reporting of MRM assays.[232,233] Large-scale cross-laboratory assessment of plasma proteins showed improved quantification when harmonized SOPs are followed.[58] Triple quadrupole instruments used for MRM are less expensive than higher resolution mass spectrometers and the use of scheduled MRM improves the reproducibility of the data and increases the number of peptides that can be analyzed in one experiment,[234] thus reducing the cost and time of analysis. PRM methodology offers advantages in selectivity, resolution and sensitivity while requiring a lower level of method development compared to MRM.[63] Orbitrap and Q-TOF instruments tend to be expensive but they represent versatile platforms capable of targeted (PRM) and global analyses.[63,65]

Targeted techniques rely on the use of labeled standards and the choice of suitable standards depends on the type of experiment and available budget and expertise. Isotope-labeled internal standards tends to be expensive, but they provide better quality quantification (higher precision and accuracy) than label-free methods. AQUA peptides are ideal for screening applications where a small number of proteins (< 10) are monitored in a large number of samples. QconCATs are more applicable when higher numbers of proteins are targeted and for applications that require strict stoichiometry, such as allele-specific proteomics.[70,218] QconCAT standards have the advantage of sustainability and transferability across laboratories;[74] a plasmid can be shared by different groups with access to protein expression facilities. We have previously developed a cost-benefit framework to assess the use of quantitative proteomic methods based on cost and application.[77] This assessment showed that the high cost of PSAQ standards hinders their application when a considerable set of proteins are targeted.

For applications that aim to identify novel proteins or quantify a large number of targets (> 100 proteins), the method of choice is global proteomics. Shotgun global proteomics, in conjunction

with the TPA approach, can be cheaper than targeted methods because they do not require the use of labeled standards. This method is applied with Q-TOF and Orbitrap instruments and has a wide range of hypothesis-generating applications, including proteome-wide analysis, assessment of disease perturbations and biomarker discovery. Data-independent methods, such as SWATH, offer increased depth of analysis and quantitative reproducibility,[136] making them very suitable for generating protein network data for systems pharmacology applications. Their use is however still restricted to core facilities, and sophisticated bioinformatics tools are required for data analysis and interpretation.[39,43] A combined discovery-quantification strategy is recommended when characterizing a novel target or disease pathway.[18] This requires using global analysis (e.g. SWATH) on well-defined (disease and control) samples followed by targeted (MRM or PRM) quantification.

The concept of a 'proteomic map of disease' has recently been proposed,[139,235] supported by highly reproducible sample preparation and global proteomic workflows. We recommend that major academic centres should conduct harmonized efforts to generate and share similar proteomic maps in health and disease for available biopsy and surgical samples from different tissues, as demonstrated recently.[236] This will likely require the use of highly reproducible methods capable of wide proteome coverage, such as SWATH-MS,[136] and these digital maps can be interrogated retrospectively by various groups for future applications.

2.9.Conclusion

Quantitative proteomic measurements can make a significant contribution to the advance of quantitative systems pharmacology and can be relatively quickly translated into the clinic, where they directly benefit patients. These measurements are powerful, providing selectivity and sensitivity unparalleled by other protein-level techniques. The disadvantage of the unparalleled sensitivity is that independent orthogonal verification of a measurement is often challenging. Further, the cost of these experiments and small sample sizes preclude extensive sample sharing and cross-laboratory analyses. Prasad et al. (2019)[19] have highlighted the difficulty in obtaining consensus as to appropriate protocols for different measurements, especially as the most thorough approaches are beyond the budgets of many laboratories.

We can however make a number of broad observations. Firstly, targeted methods are preferred where a specific, poorly expressed set of proteins is to be quantified, whereas global methods are better adapted to gaining a general picture of the functional proteome in a cell. Secondly,

while there is merit in terms of accuracy in analyzing unfractionated samples, the loss of precision and sensitivity compared with the use of fractions is often critical. Thirdly, neither QconCAT proteins nor AQUA peptides are ideal as standards for targeted proteomics; QconCATs are favorable where large numbers of similar samples are to be analyzed for several proteins, whereas AQUA peptides are effective for small numbers of target proteins. When a decision is made, the minimal requirement is that the use of a particular quantitative proteomic technique should be 'fit for purpose'. Ultimately, the selected method and the level of proteomic quantification will have a substantial impact on the quality and validity of model-informed predictions.

2.10. References

1. Rostami-Hodjegan A. Physiologically Based Pharmacokinetics Joined With In Vitro–In Vivo Extrapolation of ADME: A Marriage Under the Arch of Systems Pharmacology. *Clin Pharmacol Ther* 2012;**92**(1):50–61. Doi: 10.1038/clpt.2012.65.

2. Walsky RL., Obach RS. Validated assays for human cytochrome P450 activities. *Drug Metab Dispos* 2004;**32**(6):647–60. Doi: 10.1124/dmd.32.6.647.

3. Achour B., Dantonio A., Niosi M., Novak JJ., Fallon JK., Barber J., et al. Quantitative characterization of major hepatic UDP-glucuronosyltransferase enzymes in human liver microsomes: Comparison of two proteomic methods and correlation with catalytic activity. *Drug Metab Dispos* 2017;**45**(10):1102–12. Doi: 10.1124/dmd.117.076703.

4. Walsky RL., Bauman JN., Bourcier K., Giddens G., Lapham K., Negahban A., et al. Optimized assays for human UDP-glucuronosyltransferase (UGT) activities: Altered alamethicin concentration and utility to screen for UGT inhibitors. *Drug Metab Dispos* 2012;**40**(5):1051–65. Doi: 10.1124/dmd.111.043117.

5. Aebersold R., Burlingame AL., Bradshaw RA. Western blots versus selected reaction monitoring assays: time to turn the tables? *Mol Cell Proteomics* 2013;**12**(9):2381–2. Doi: 10.1074/mcp.E113.031658.

6. Vildhede A., Wiśniewski JR., Norén A., Karlgren M., Artursson P. Comparative Proteomic Analysis of Human Liver Tissue and Isolated Hepatocytes with a Focus on Proteins Determining Drug Exposure. *J Proteome Res* 2015;**14**(8):3305–14. Doi: 10.1021/acs.jproteome.5b00334.

7. Heikkinen AT., Lignet F., Cutler P., Parrott N. The role of quantitative ADME proteomics to support construction of physiologically based pharmacokinetic models for use in small molecule drug development. *Proteomics - Clin Appl* 2015;**9**(7–8):732–44. Doi: 10.1002/prca.201400147.

8. Al Feteisi H., Achour B., Rostami-Hodjegan A., Barber J. Translational value of liquid chromatography coupled with tandem mass spectrometry-based quantitative proteomics for in vitro – in vivo extrapolation of drug metabolism and transport and considerations in selecting appropriate techniques . *Expert Opin Drug Metab Toxicol* 2015;**11**(9):1357–69. Doi: 10.1517/17425255.2015.1055245.

9. Ong S-E., Mann M. Mass spectrometry-based proteomics turns quantitative. *Nat Chem Biol* 2005;**1**(5):252–62. Doi: 10.1038/nchembio736.

10. Kumar V., Yin J., Billington S., Prasad B., Brown CDA., Wang J., et al. The Importance of Incorporating OCT2 Plasma Membrane Expression and Membrane Potential in IVIVE of Metformin Renal Secretory Clearance. *Drug Metab Dispos* 2018;**46**(10):1441–5. Doi: 10.1124/dmd.118.082313.

11. Doki K., Darwich AS., Achour B., Tornio A., Backman JT., Rostami-Hodjegan A. Implications of intercorrelation between hepatic CYP3A4-CYP2C8 enzymes for the evaluation of drug-drug interactions: a case study with repaglinide. *Br J Clin Pharmacol* 2018;**84**(5):972–86. Doi: 10.1111/bcp.13533.

12. van Groen BD., van de Steeg E., Mooij MG., van Lipzig MMH., de Koning BAE., Verdijk RM., et al. Proteomics of human liver membrane transporters: A focus on fetuses and newborn infants. *Eur J Pharm Sci* 2018;**124**:217–27. Doi: 10.1016/j.ejps.2018.08.042.

13. Ladumor MK., Bhatt DK., Gaedigk A., Sharma S., Thakur A., Pearce RE., et al. Ontogeny of hepatic sulfotransferases and prediction of age-dependent fractional contribution of sulfation in acetaminophen metabolism. *Drug Metab Dispos* 2019;**47**(8):818–31. Doi: 10.1124/dmd.119.086462.

14. Peng K., Bacon J., Zheng M., Guo Y., Wang MZ. Ethnic variability in the expression of hepatic drug transporters: absolute quantification by an optimized targeted quantitative proteomic approach. *Drug Metab Dispos* 2015;**43**(7):1045–55. Doi: 10.1124/dmd.115.063362.

15. Kawakami H., Ohtsuki S., Kamiie J., Suzuki T., Abe T., Terasaki T. Simultaneous Absolute Quantification of 11 Cytochrome P450 Isoforms in Human Liver Microsomes by Liquid Chromatography Tandem Mass Spectrometry with In Silico Target Peptide Selection. *J Pharm Sci* 2011;**100**(1):341–52. Doi: 10.1002/JPS.22255.

16. Bhatt DK., Mehrotra A., Gaedigk A., Chapa R., Basit A., Zhang H., et al. Age- and Genotype-Dependent Variability in the Protein Abundance and Activity of Six Major Uridine Diphosphate-Glucuronosyltransferases in Human Liver. *Clin Pharmacol Ther* 2019;**105**(1):131–41. Doi: 10.1002/cpt.1109.

17. Weiß F., Hammer HS., Klein K., Planatscher H., Zanger UM., Norén A., et al. Direct quantification of cytochromes P450 and drug transporters - A rapid, targeted mass spectrometry-based immunoassay panel for tissues and cell culture lysates. *Drug Metab Dispos* 2018;**46**(4):387–96. Doi: 10.1124/dmd.117.078626.

18. Gillet LC., Leitner A., Aebersold R. Mass Spectrometry Applied to Bottom-Up Proteomics: Entering the High-Throughput Era for Hypothesis Testing. *Annu Rev Anal Chem* 2016;**9**(1):449–72. Doi: 10.1146/annurev-anchem-071015-041535.

19. Prasad B., Achour B., Artursson P., Hop CECA., Lai Y., Smith PC., et al. Toward a Consensus on Applying Quantitative Liquid Chromatography-Tandem Mass Spectrometry Proteomics in Translational Pharmacology Research: A White Paper. *Clin Pharmacol Ther* 2019;**106**(3):525–43. Doi: 10.1002/cpt.1537.

20. Drozdzik M., Gröer C., Penski J., Lapczuk J., Ostrowski M., Lai Y., et al. Protein Abundance of Clinically Relevant Multidrug Transporters along the Entire Length of

the Human Intestine. *Mol Pharm* 2014;**11**(10):3547–55. Doi: 10.1021/mp500330y.

21. Harwood MD., Russell MR., Neuhoff S., Warhurst G., Rostami-Hodjegan A. Lost in centrifugation: Accounting for transporter protein losses in quantitative targeted absolute proteomics. *Drug Metab Dispos* 2014;**42**(10):1766–72. Doi: 10.1124/dmd.114.058446.

22. Wiśniewski JR., Wegler C., Artursson P. Subcellular fractionation of human liver reveals limits in global proteomic quantification from isolated fractions. *Anal Biochem* 2016;**509**:82–8. Doi: 10.1016/j.ab.2016.06.006.

23. Bhatt DK., Prasad B. Critical Issues and Optimized Practices in Quantification of Protein Abundance Level to Determine Interindividual Variability in DMET Proteins by LC-MS/MS Proteomics. *Clin Pharmacol Ther* 2018;**103**(4):619–30. Doi: 10.1002/cpt.819.

24. Wegler C., Gaugaz FZ., Andersson TB., Wiśniewski JR., Busch D., Gröer C., et al. Variability in Mass Spectrometry-based Quantification of Clinically Relevant Drug Transporters and Drug Metabolizing Enzymes. *Mol Pharm* 2017;**14**(9):3142–51. Doi: 10.1021/acs.molpharmaceut.7b00364.

25. Prasad B., Bhatt DK., Johnson K., Chapa R., Chu X., Salphati L., et al. Abundance of Phase 1 and 2 Drug-Metabolizing Enzymes in Alcoholic and Hepatitis C Cirrhotic Livers: A Quantitative Targeted Proteomics Study. *Drug Metab Dispos* 2018;**46**(7):943–52. Doi: 10.1124/dmd.118.080523.

26. Chen Y., Zane NR., Thakker DR., Wang MZ. Quantification of Flavin-containing Monooxygenases 1, 3, and 5 in Human Liver Microsomes by UPLC-MRM-Based Targeted Quantitative Proteomics and Its Application to the Study of Ontogeny. *Drug Metab Dispos* 2016;**44**(7):975–83. Doi: 10.1124/dmd.115.067538.

27. Wang X., Shi J., Zhu H-J. Functional Study of Carboxylesterase 1 Protein Isoforms. *Proteomics* 2019;**19**(4):1800288. Doi: 10.1002/pmic.201800288.

28. Batth TS., Papetti M., Pfeiffer A., Tollenaere MAX., Francavilla C., Olsen J V. Large-Scale Phosphoproteomics Reveals Shp-2 Phosphatase-Dependent Regulators of Pdgf Receptor Signaling. *Cell Rep* 2018;**22**(10):2784–96. Doi: 10.1016/j.celrep.2018.02.038.

29. Ohtsuki S., Schaefer O., Kawakami H., Inoue T., Liehner S., Saito A., et al. Simultaneous Absolute Protein Quantification of Transporters, Cytochrome P450s and UDP-glucuronosyltransferases as a Novel Approach for the Characterization of Individual Human Liver: Comparison with mRNA Levels and Activities. *Drug Metab Dispos* 2012;**40**(1):83–92. Doi: 10.1124/dmd.111.042259.

30. Achour B., Barber J. The activities of Achromobacter lysyl endopeptidase and Lysobacter lysyl endoproteinase as digestive enzymes for quantitative proteomics. *Rapid Commun Mass Spectrom* 2013;**27**(14):1669–72. Doi: 10.1002/rcm.6612.

31. Wiśniewski JR., Mann M. Consecutive Proteolytic Digestion in an Enzyme Reactor Increases Depth of Proteomic and Phosphoproteomic Analysis. *Anal Chem* 2012;**84**(6):2631–7. Doi: 10.1021/ac300006b.

32. Wiśniewski JR., Wegler C., Artursson P. Multiple-Enzyme-Digestion Strategy Improves Accuracy and Sensitivity of Label- and Standard-Free Absolute Quantification to a Level That Is Achievable by Analysis with Stable Isotope-Labeled Standard Spiking. *J Proteome Res* 2019;**18**(1):217–24. Doi: 10.1021/acs.jproteome.8b00549.

33. Langenfeld E., Zanger UM., Jung K., Meyer HE., Marcus K. Mass spectrometry-based absolute quantification of microsomal cytochrome P450 2D6 in human liver. *Proteomics* 2009;**9**(9):2313–23. Doi: 10.1002/pmic.200800680.

34. Wiśniewski JR., Zougman A., Nagaraj N., Mann M. Universal sample preparation method for proteome analysis. *Nat Methods* 2009;**6**(5):359–62. Doi: 10.1038/nmeth.1322.

35. Fallon JK., Harbourt DE., Maleki SH., Kessler FK., Ritter JK., Smith PC. Absolute quantification of human uridine-diphosphate glucuronosyl transferase (UGT) enzyme isoforms 1A1 and 1A6 by tandem LC-MS. *Drug Metab Lett* 2008;**2**:210–22. Doi: 10.2174/187231208785425764.

36. Choksawangkarn W., Edwards N., Wang Y., Gutierrez P., Fenselau C. Comparative study of workflows optimized for In-gel, In-solution, and on-filter proteolysis in the analysis of plasma membrane proteins. *J Proteome Res* 2012;**11**(5):3030–4. Doi: 10.1021/pr300188b.

37. Al Feteisi H., Al-Majdoub ZM., Achour B., Couto N., Rostami-Hodjegan A., Barber J. Identification and quantification of blood-brain barrier transporters in isolated rat brain microvessels. *J Neurochem* 2018;**146**(6):670–85. Doi: 10.1111/jnc.14446.

38. Achour B., Al Feteisi H., Lanucara F., Rostami-Hodjegan A., Barber J. Global Proteomic Analysis of Human Liver Microsomes: Rapid Characterization and Quantification of Hepatic Drug-Metabolizing Enzymes. *Drug Metab Dispos* 2017;**45**(6):666–75. Doi: 10.1124/dmd.116.074732.

39. Distler U., Kuharev J., Navarro P., Levin Y., Schild H., Tenzer S. Drift time-specific collision energies enable deep-coverage data-independent acquisition proteomics. *Nat Methods* 2014;**11**(2):167–70. Doi: 10.1038/nmeth.2767.

40. Smith BJ., Martins-De-Souza D., Fioramonte M. A Guide to Mass Spectrometry-Based Quantitative Proteomics. *Methods in Molecular Biology*. 2019.

41. Cox J., Mann M. MaxQuant enables high peptide identification rates, individualized p.p.b.-range mass accuracies and proteome-wide protein quantification. *Nat Biotechnol*

2008;**26**(12):1367–72. Doi: 10.1038/nbt.1511.

42. Tommi V., Suomi T., Elo LL. A comprehensive evaluation of popular proteomics software workflows for label-free proteome quantification and imputation. *Brief Bioinform* 2018;**19**(6):1344–55. Doi: 10.1093/bib/bbx054.

43. Röst HL., Rosenberger G., Navarro P., Gillet L., Miladinoviä SM., Schubert OT., et al. OpenSWATH enables automated, targeted analysis of data-independent acquisition MS data. *Nat Biotechnol* 2014;**32**(3):219–23. Doi: 10.1038/nbt.2841.

44. Kitteringham NR., Jenkins RE., Lane CS., Elliott VL., Park BK. Multiple reaction monitoring for quantitative biomarker analysis in proteomics and metabolomics. *J Chromatogr B* 2009;**877**(13):1229–39. Doi: 10.1016/j.jchromb.2008.11.013.

45. Gillette MA., Carr SA. Quantitative analysis of peptides and proteins in biomedicine by targeted mass spectrometry. *Nat Methods* 2013;**10**(1):28–34. Doi: 10.1038/nmeth.2309.

46. Carr SA., Abbatiello SE., Ackermann BL., Borchers C., Domon B., Deutsch EW., et al. Targeted Peptide Measurements in Biology and Medicine: Best Practices for Mass Spectrometry-based Assay Development Using a Fit-for-Purpose Approach. *Mol Cell Proteomics* 2014;**13**(3):907–17. Doi: 10.1074/mcp.M113.036095.

47. Vrana M., Whittington D., Nautiyal V., Prasad B. Database of Optimized Proteomic Quantitative Methods for Human Drug Disposition-Related Proteins for Applications in Physiologically Based Pharmacokinetic Modeling. *CPT Pharmacometrics Syst Pharmacol* 2017;**6**(4):267–76. Doi: 10.1002/psp4.12170.

48. Kumar V., Prasad B., Patilea G., Gupta A., Salphati L., Evers R., et al. Quantitative transporter proteomics by liquid chromatography with tandem mass spectrometry: addressing methodologic issues of plasma membrane isolation and expression-activity relationship. *Drug Metab Dispos* 2015;**43**(2):284–8. Doi: 10.1124/DMD.114.061614.

49. Margaillan G., Rouleau M., Fallon JK., Caron P., Villeneuve L., Turcotte V., et al. Quantitative profiling of human renal UDP-glucuronosyltransferases and glucuronidation activity: a comparison of normal and tumoral kidney tissues. *Drug Metab Dispos* 2015;**43**(4):611–9. Doi: 10.1124/dmd.114.062877.

50. Gröer C., Busch D., Patrzyk M., Beyer K., Busemann A., Heidecke CD., et al. Absolute protein quantification of clinically relevant cytochrome P450 enzymes and UDP-glucuronosyltransferases by mass spectrometry-based targeted proteomics. *J Pharm Biomed Anal* 2014;**100**:393–401. Doi: 10.1016/j.jpba.2014.08.016.

51. Vildhede A., Mateus A., Khan EK., Lai Y., Karlgren M., Artursson P., et al. Mechanistic Modeling of Pitavastatin Disposition in Sandwich-Cultured Human Hepatocytes: A Proteomics-Informed Bottom-Up Approach. *Drug Metab Dispos* 2016;**44**(4):505–16. Doi: 10.1124/dmd.115.066746.

52. Hoshi Y., Uchida Y., Tachikawa M., Inoue T., Ohtsuki S., Terasaki T. Quantitative Atlas of blood-brain barrier transporters, receptors, and tight junction proteins in rats and common marmoset. *J Pharm Sci* 2013;**102**(9):3343–55. Doi: 10.1002/jps.23575.

53. Kumar V., Salphati L., Hop CECA., Xiao G., Lai Y., Mathias A., et al. A Comparison of Total and Plasma Membrane Abundance of Transporters in Suspended, Plated, Sandwich-Cultured Human Hepatocytes Versus Human Liver Tissue Using Quantitative Targeted Proteomics and Cell Surface Biotinylation. *Drug Metab Dispos* 2019;**47**(4):350–7. Doi: 10.1124/dmd.118.084988.

54. Schaefer O., Ohtsuki S., Kawakami H., Inoue T., Liehner S., Saito A., et al. Absolute quantification and differential expression of drug transporters, cytochrome P450 enzymes, and UDP-glucuronosyltransferases in cultured primary human hepatocytes. *Drug Metab Dispos* 2012;**40**(1):93–103. Doi: 10.1124/dmd.111.042275.

55. Billington S., Salphati L., Hop CECA., Chu X., Evers R., Burdette D., et al. Interindividual and Regional Variability in Drug Transporter Abundance at the Human Blood–Brain Barrier Measured by Quantitative Targeted Proteomics. *Clin Pharmacol Ther* 2019;**106**(1):228–37. Doi: 10.1002/cpt.1373.

56. Prasad B., Johnson K., Billington S., Lee C., Chung GW., Brown CDA., et al. Abundance of Drug Transporters in the Human Kidney Cortex as Quantified by Quantitative Targeted Proteomics. *Drug Metab Dispos* 2016;**44**(12):1920–4. Doi: 10.1124/dmd.116.072066.

57. Knights KM., Spencer SM., Fallon JK., Chau N., Smith PC., Miners JO. Scaling factors for the in vitro-in vivo extrapolation (IV-IVE) of renal drug and xenobiotic glucuronidation clearance. *Br J Clin Pharmacol* 2016;**81**(6):1153–64. Doi: 10.1111/bcp.12889.

58. Abbatiello SE., Schilling B., Mani DR., Zimmerman LJ., Hall SC., MacLean B., et al. Large-Scale Interlaboratory Study to Develop, Analytically Validate and Apply Highly Multiplexed, Quantitative Peptide Assays to Measure Cancer-Relevant Proteins in Plasma. *Mol Cell Proteomics* 2015;**14**(9):2357–74. Doi: 10.1074/mcp.M114.047050.

59. Billington S., Ray AS., Salphati L., Xiao G., Chu X., Humphreys WG., et al. Transporter Expression in Noncancerous and Cancerous Liver Tissue from Donors with Hepatocellular Carcinoma and Chronic Hepatitis C Infection Quantified by LC-MS/MS Proteomics. *Drug Metab Dispos* 2018;**46**(2):189–96. Doi: 10.1124/dmd.117.077289.

60. Al-Majdoub ZM., Al Feteisi H., Achour B., Warwood S., Neuhoff S., Rostami-Hodjegan A., et al. Proteomic Quantification of Human Blood–Brain Barrier SLC and ABC Transporters in Healthy Individuals and Dementia Patients. *Mol Pharm* 2019;**16**(3):1220–33. Doi: 10.1021/acs.molpharmaceut.8b01189.

61. Gallien S., Duriez E., Demeure K., Domon B. Selectivity of LC-MS/MS analysis:

Implication for proteomics experiments. *J Proteomics* 2013;**81**:148–58. Doi: 10.1016/j.jprot.2012.11.005.

62. Schiffmann C., Hansen R., Baumann S., Kublik A., Nielsen PH., Adrian L., et al. Comparison of targeted peptide quantification assays for reductive dehalogenases by selective reaction monitoring (SRM) and precursor reaction monitoring (PRM). *Anal Bioanal Chem* 2014;**406**(1):283–91. Doi: 10.1007/s00216-013-7451-7.

63. Peterson AC., Russell JD., Bailey DJ., Westphall MS., Coon JJ. Parallel Reaction Monitoring for High Resolution and High Mass Accuracy Quantitative, Targeted Proteomics. *Mol Cell Proteomics* 2012;**11**(11):1475–88. Doi: 10.1074/mcp.O112.020131.

64. Gallien S., Duriez E., Crone C., Kellmann M., Moehring T., Domon B. Targeted Proteomic Quantification on Quadrupole-Orbitrap Mass Spectrometer. *Mol Cell Proteomics* 2012;**11**(12):1709–23. Doi: 10.1074/mcp.O112.019802.

65. Schilling B., MacLean B., Held JM., Sahu AK., Rardin MJ., Sorensen DJ., et al. Multiplexed, Scheduled, High-Resolution Parallel Reaction Monitoring on a Full Scan QqTOF Instrument with Integrated Data-Dependent and Targeted Mass Spectrometric Workflows. *Anal Chem* 2015;**87**(20):10222–9. Doi: 10.1021/acs.analchem.5b02983.

66. Ronsein GE., Pamir N., von Haller PD., Kim DS., Oda MN., Jarvik GP., et al. Parallel reaction monitoring (PRM) and selected reaction monitoring (SRM) exhibit comparable linearity, dynamic range and precision for targeted quantitative HDL proteomics. *J Proteomics* 2015;**113**:388–99. Doi: 10.1016/j.jprot.2014.10.017.

67. Gallien S., Bourmaud A., Kim SY., Domon B. Technical considerations for large-scale parallel reaction monitoring analysis. *J Proteomics* 2014;**100**:147–59. Doi: 10.1016/j.jprot.2013.10.029.

68. Nakamura K., Hirayama-Kurogi M., Ito S., Kuno T., Yoneyama T., Obuchi W., et al. Large-scale multiplex absolute protein quantification of drug-metabolizing enzymes and transporters in human intestine, liver, and kidney microsomes by SWATH-MS: Comparison with MRM/SRM and HR-MRM/PRM. *Proteomics* 2016;**16**(15–16):2106–17. Doi: 10.1002/pmic.201500433.

69. Kim YJ., Gallien S., El-Khoury V., Goswami P., Sertamo K., Schlesser M., et al. Quantification of SAA1 and SAA2 in lung cancer plasma using the isotype-specific PRM assays. *Proteomics* 2015;**15**(18):3116–25. Doi: 10.1002/pmic.201400382.

70. Shi J., Wang X., Zhu H., Jiang H., Wang D., Nesvizhskii A., et al. Determining Allele-Specific Protein Expression (ASPE) Using a Novel Quantitative Concatamer Based Proteomics Method. *J Proteome Res* 2018;**17**(10):3606–12. Doi: 10.1021/acs.jproteome.8b00620.

71. Silva JC., Denny R., Dorschel CA., Gorenstein M., Kass IJ., Li GZ., et al. Quantitative proteomic analysis by accurate mass retention time pairs. *Anal Chem* 2005;**77**(7):2187–200. Doi: 10.1021/ac048455k.

72. Calderón-Celis F., Encinar JR., Sanz-Medel A. Standardization approaches in absolute quantitative proteomics with mass spectrometry. *Mass Spectrom Rev* 2018;**37**(6):715–37. Doi: 10.1002/mas.21542.

73. Kamiie J., Ohtsuki S., Iwase R., Ohmine K., Katsukura Y., Yanai K., et al. Quantitative atlas of membrane transporter proteins: Development and application of a highly sensitive simultaneous LC/MS/MS method combined with novel in-silico peptide selection criteria. *Pharm Res* 2008;**25**(6):1469–83. Doi: 10.1007/S11095-008-9532-4.

74. Russell MR., Achour B., Mckenzie EA., Lopez R., Harwood MD., Rostami-Hodjegan A., et al. Alternative Fusion Protein Strategies to Express Recalcitrant QconCAT Proteins for Quantitative Proteomics of Human Drug Metabolizing Enzymes and Transporters. *J Proteome Res* 2013;**12**(12):5934–42. Doi: 10.1021/pr400279u.

75. Kirkpatrick DS., Gerber SA., Gygi SP. The absolute quantification strategy: A general procedure for the quantification of proteins and post-translational modifications. *Methods* 2005. Doi: 10.1016/j.ymeth.2004.08.018.

76. Kettenbach AN., Rush J., Gerber SA. Absolute quantification of protein and post-translational modification abundance with stable isotope-labeled synthetic peptides. *Nat Protoc* 2011;**6**(2):175–86. Doi: 10.1038/nprot.2010.196.

77. Al Feteisi H., Achour B., Barber J., Rostami-Hodjegan A. Choice of LC-MS Methods for the Absolute Quantification of Drug-Metabolizing Enzymes and Transporters in Human Tissue: a Comparative Cost Analysis. *AAPS J* 2015;**17**(2):438–46. Doi: 10.1208/s12248-014-9712-6.

78. Mirzaei H., McBee JK., Watts J., Aebersold R. Comparative evaluation of current peptide production platforms used in absolute quantification in proteomics. *Mol Cell Proteomics* 2008;**7**(4):813–23. Doi: 10.1074/mcp.M700495-MCP200.

79. Havliš J., Shevchenko A. Absolute quantification of proteins in solutions and in polyacrylamide gels by mass spectrometry. *Anal Chem* 2004;**76**(11):3029–36. Doi: 10.1021/ac035286f.

80. Fallon JK., Neubert H., Hyland R., Goosen TC., Smith PC. Targeted quantitative proteomics for the analysis of 14 UGT1As and -2Bs in human liver using NanoUPLC-MS/MS with selected reaction monitoring. *J Proteome Res* 2013;**12**(10):4402–13. Doi: 10.1021/pr4004213.

81. Sato Y., Nagata M., Tetsuka K., Tamura K., Miyashita A., Kawamura A., et al. Optimized methods for targeted peptide-based quantification of human uridine 59-

diphosphate-glucuronosyltransferases in biological specimens using liquid chromatography-tandem mass spectrometry. *Drug Metab Dispos* 2014;**42**(5):885–9. Doi: 10.1124/dmd.113.056291.

82. Hansen J., Palmfeldt J., Pedersen KW., Funder AD., Frost L., Hasselstrøm JB., et al. Postmortem protein stability investigations of the human hepatic drug-metabolizing cytochrome P450 enzymes CYP1A2 and CYP3A4 using mass spectrometry. *J Proteomics* 2019;**194**(November):125–31. Doi: 10.1016/j.jprot.2018.11.024.

83. Sato Y., Nagata M., Kawamura A., Miyashita A., Usui T., Kawamura A., et al. Protein quantification of UDP-glucuronosyltransferases 1A1 and 2B7 in human liver microsomes by LC-MS/MS and correlation with glucuronidation activities. *Xenobiotica* 2012;**42**(9):823–9. Doi: 10.3109/00498254.2012.665950.

84. Cieślak A., Kelly I., Trottier J., Verreault M., Wunsch E., Milkiewicz P., et al. Selective and sensitive quantification of the cytochrome P450 3A4 protein in human liver homogenates through multiple reaction monitoring mass spectrometry. *Proteomics* 2016;**16**(21):2827–37. Doi: 10.1002/pmic.201500386.

85. Harbourt DE., Fallon JK., Ito S., Baba T., Ritter JK., Glish GL., et al. Quantification of human uridine-diphosphate glucuronosyl transferase 1A isoforms in liver, intestine, and kidney using nanobore liquid chromatography-tandem mass spectrometry. *Anal Chem* 2012:98–105. Doi: 10.1021/ac201704a.

86. Drozdzik M., Busch D., Lapczuk J., Müller J., Ostrowski M., Kurzawski M., et al. Protein Abundance of Clinically Relevant Drug-Metabolizing Enzymes in the Human Liver and Intestine: A Comparative Analysis in Paired Tissue Specimens. *Clin Pharmacol Ther* 2018;**104**(3):515–24. Doi: 10.1002/cpt.967.

87. Scherrmann J-M., Dauchy S., Couraud P-O., Daumas-Duport C., Shawahna R., Chassoux F., et al. Transcriptomic and Quantitative Proteomic Analysis of Transporters and Drug Metabolizing Enzymes in Freshly Isolated Human Brain Microvessels. *Mol Pharm* 2011;**8**(4):1332–41. Doi: 10.1021/mp200129p.

88. Yoshitake S., McKay-Daily M., Tanaka M., Huang Z. Quantification of Sulfotransferases 1A1 and 1A3/4 in Tissue Fractions and Cell Lines by Multiple Reaction Monitoring Mass Spectrometry. *Drug Metab Lett* 2017. Doi: 10.2174/1872312811666170731170153.

89. Bhatt DK., Gaedigk A., Pearce RE., Leeder JS., Prasad B. Age-dependent protein abundance of cytosolic alcohol and aldehyde dehydrogenases in human liver. *Drug Metab Dispos* 2017;**45**(9):1044–8. Doi: 10.1124/dmd.117.076463.

90. Fu C., Di L., Han X., Soderstrom C., Snyder M., Troutman MD., et al. Aldehyde Oxidase 1 (AOX1) in Human Liver Cytosols: Quantitative Characterization of AOX1 Expression Level and Activity Relationship. *Drug Metab Dispos* 2013;**41**(10):1797–

804. Doi: 10.1124/dmd.113.053082.

91. Prasad B., Evers R., Gupta A., Hop CECA., Salphati L., Shukla S., et al. Interindividual variability in hepatic organic anion-transporting polypeptides and P-glycoprotein (ABCB1) protein expression: quantification by liquid chromatography tandem mass spectroscopy and influence of genotype, age, and sex. *Drug Metab Dispos* 2013;**42**(1):78–88. Doi: 10.1124/dmd.113.053819.

92. Gröer C., Brück S., Lai Y., Paulick A., Busemann A., Heidecke CD., et al. LC–MS/MS-based quantification of clinically relevant intestinal uptake and efflux transporter proteins. *J Pharm Biomed Anal* 2013;**85**:253–61. Doi: 10.1016/j.jpba.2013.07.031.

93. Uchida Y., Ohtsuki S., Katsukura Y., Ikeda C., Suzuki T., Kamiie J., et al. Quantitative targeted absolute proteomics of human blood–brain barrier transporters and receptors. *J Neurochem* 2011;**117**(2):333–45. Doi: 10.1111/J.1471-4159.2011.07208.X.

94. Fallon JK., Houvig N., Booth-Genthe CL., Smith PC. Quantification of membrane transporter proteins in human lung and immortalized cell lines using targeted quantitative proteomic analysis by isotope dilution nanoLC-MS/MS. *J Pharm Biomed Anal* 2018;**154**:150–7. Doi: 10.1016/j.jpba.2018.02.044.

95. Achour B., Russell MR., Barber J., Rostami-Hodjegan A. Simultaneous Quantification of the Abundance of Several Cytochrome P450 and Uridine 5′-Diphospho-Glucuronosyltransferase Enzymes in Human Liver Microsomes Using Multiplexed Targeted Proteomics. *Drug Metab Dispos* 2014;**42**(4):500–10. Doi: 10.1124/dmd.113.055632.

96. Wang H., Zhang H., Li J., Wei J., Zhai R., Peng B., et al. A new calibration curve calculation method for absolute quantification of drug metabolizing enzymes in human liver microsomes by stable isotope dilution mass spectrometry. *Anal Methods* 2015. Doi: 10.1039/c5ay00664c.

97. Harwood MD., Achour B., Russell MR., Carlson GL., Warhurst G., Rostami-Hodjegan A. Application of an LC-MS/MS method for the simultaneous quantification of human intestinal transporter proteins absolute abundance using a QconCAT technique. *J Pharm Biomed Anal* 2015;**110**:27–33. Doi: 10.1016/j.jpba.2015.02.043.

98. Harwood MD., Achour B., Neuhoff S., Russell MR., Carlson G., Warhurst G., et al. In Vitro-In Vivo Extrapolation Scaling Factors for Intestinal P-Glycoprotein and Breast Cancer Resistance Protein: Part I: A Cross-Laboratory Comparison of Transporter-Protein Abundances and Relative Expression Factors in Human Intestine and Caco-2 Cells. *Drug Metab Dispos* 2016;**44**(3):297–307. Doi: 10.1124/dmd.115.067371.

99. Kito K., Ota K., Fujita T., Ito T. A synthetic protein approach toward accurate mass spectrometric quantification of component stoichiometry of multiprotein complexes. *J Proteome Res* 2007. Doi: 10.1021/pr060447s.

100. Cheung CSF., Anderson KW., Wang M., Turko I V. Natural Flanking Sequences for Peptides Included in a Quantification Concatamer Internal Standard. *Anal Chem* 2015;**87**(2):1097–102. Doi: 10.1021/ac503697j.

101. Al-Majdoub ZM., Carroll KM., Gaskell SJ., Barber J. Quantification of the Proteins of the Bacterial Ribosome Using QconCAT Technology. *J Proteome Res* 2014;**13**(3):1211–22. Doi: 10.1021/pr400667h.

102. Achour B., Al-Majdoub ZM., Al Feteisi H., Elmorsi Y., Rostami-Hodjegan A., Barber J. Ten years of QconCATs: Application of multiplexed quantification to small medically relevant proteomes. *Int J Mass Spectrom* 2015;**391**:93–104. Doi: 10.1016/j.ijms.2015.08.003.

103. Brownridge P., Holman SW., Gaskell SJ., Grant CM., Harman VM., Hubbard SJ., et al. Global absolute quantification of a proteome: Challenges in the deployment of a QconCAT strategy. *Proteomics* 2011;**11**(15):2957–70. Doi: 10.1002/pmic.201100039.

104. Takemori N., Beynon RJ., Endo Y., Hurst JL., Tanaka Y., Gómez-Baena G., et al. MEERCAT: Multiplexed Efficient Cell Free Expression of Recombinant QconCATs For Large Scale Absolute Proteome Quantification. *Mol Cell Proteomics* 2017. Doi: 10.1074/mcp.ra117.000284.

105. Chen B., Liu L., Ho H., Chen Y., Yang Z., Liang X., et al. Strategies of Drug Transporter Quantitation by LC-MS: Importance of Peptide Selection and Digestion Efficiency. *AAPS J* 2017;**19**(5):1469–78. Doi: 10.1208/s12248-017-0106-4.

106. Dupuis A., Hennekinne JA., Garin J., Brun V. Protein Standard Absolute Quantification (PSAQ) for improved investigation of staphylococcal food poisoning outbreaks. *Proteomics* 2008. Doi: 10.1002/pmic.200800326.

107. Adrait A., Lebert D., Trauchessec M., Dupuis A., Louwagie M., Masselon C., et al. Development of a Protein Standard Absolute Quantification (PSAQ^{TM}) assay for the quantification of Staphylococcus aureus enterotoxin A in serum. *J Proteomics* 2012. Doi: 10.1016/j.jprot.2011.11.031.

108. Ghaleb B., Garin J., Brun V., Lebert D., Le Corvoisier P., Bruley C., et al. Accurate Quantification of Cardiovascular Biomarkers in Serum Using Protein Standard Absolute Quantification (PSAQ^{TM}) and Selected Reaction Monitoring. *Mol Cell Proteomics* 2011;**11**(2):M111.008235. Doi: 10.1074/mcp.m111.008235.

109. Gilquin B., Louwagie M., Jaquinod M., Cez A., Picard G., El Kholy L., et al. Multiplex and accurate quantification of acute kidney injury biomarker candidates in urine using Protein Standard Absolute Quantification (PSAQ) and targeted proteomics. *Talanta* 2017;**164**(November 2016):77–84. Doi: 10.1016/j.talanta.2016.11.023.

110. Ong S-E., Blagoev B., Kratchmarova I., Kristensen DB., Steen H., Pandey A., et al.

Stable isotope labeling by amino acids in cell culture, SILAC, as a simple and accurate approach to expression proteomics. *Mol Cell Proteomics* 2002;**1**(5):376–86.

111. Wiese S., Reidegeld KA., Meyer HE., Warscheid B. Protein labeling by iTRAQ: a new tool for quantitative mass spectrometry in proteome research. *Proteomics* 2007;**7**(3):340–50. Doi: 10.1002/pmic.200600422.

112. Silva JC., Gorenstein M V., Li G-Z., Vissers JPC., Geromanos SJ. Absolute Quantification of Proteins by LCMSE: a virtue of parallel MS acquisition. *Mol Cell Proteomics* 2006;**5**(1):144–56. Doi: 10.1074/mcp.M500230-MCP200.

113. Merrill AE., Hebert AS., MacGilvray ME., Rose CM., Bailey DJ., Bradley JC., et al. NeuCode labels for relative protein quantification. *Mol Cell Proteomics* 2014;**13**(9):2503–12. Doi: 10.1074/mcp.M114.040287.

114. Zhang F., Xiao Y., Wang Y. SILAC-Based Quantitative Proteomic Analysis Unveils Arsenite-Induced Perturbation of Multiple Pathways in Human Skin Fibroblast Cells. *Chem Res Toxicol* 2017;**30**(4):1006–14. Doi: 10.1021/acs.chemrestox.6b00416.

115. Kurokawa N., Kishimoto T., Tanaka K., Kondo J., Takahashi N., Miura Y. New approach to evaluating the effects of a drug on protein complexes with quantitative proteomics, using the SILAC method and bioinformatic approach. *Biosci Biotechnol Biochem* 2019:DOI: 10.1080/09168451.2019.1637244. Doi: 10.1080/09168451.2019.1637244.

116. Ibarrola N., Kalume DE., Gronborg M., Iwahori A., Pandey A. A Proteomic Approach for Quantitation of Phosphorylation Using Stable Isotope Labeling in Cell Culture. *Anal Chem* 2003;**75**(22):6043–9. Doi: 10.1021/ac034931f.

117. Geiger T., Cox J., Ostasiewicz P., Wisniewski JR., Mann M. Super-SILAC mix for quantitative proteomics of human tumor tissue. *Nat Methods* 2010;**7**(5):383–5. Doi: 10.1038/nmeth.1446.

118. Prasad B., Unadkat JD. Comparison of Heavy Labeled (SIL) Peptide versus SILAC Protein Internal Standards for LC-MS/MS Quantification of Hepatic Drug Transporters. *Int J Proteomics* 2014;**2014**:1–11. Doi: 10.1155/2014/451510.

119. MacLeod AK., Fallon PG., Sharp S., Henderson CJ., Wolf CR., Huang JT-J. An enhanced in vivo stable isotope labeling by amino acids in cell culture (SILAC) model for quantification of drug metabolism enzymes. *Mol Cell Proteomics* 2015;**14**(3):750–60. Doi: 10.1074/mcp.M114.043661.

120. Ross PL., Huang YN., Marchese JN., Williamson B., Parker K., Hattan S., et al. Multiplexed Protein Quantitation in *Saccharomyces cerevisiae* Using Amine-reactive Isobaric Tagging Reagents. *Mol Cell Proteomics* 2004;**3**(12):1154–69. Doi: 10.1074/mcp.M400129-MCP200.

121. Vildhede A., Nguyen C., Erickson BK., Kunz RC., Jones R., Kimoto E., et al. Comparison of Proteomic Quantification Approaches for Hepatic Drug Transporters: Multiplexed Global Quantitation Correlates with Targeted Proteomic Quantitation. *Drug Metab Dispos* 2018;**46**(5):692–6. Doi: 10.1124/dmd.117.079285.

122. Freue GVC., Sasaki M., Meredith A., Günther OP., Bergman A., Takhar M., et al. Proteomic Signatures in Plasma during Early Acute Renal Allograft Rejection. *Mol Cell Proteomics* 2010;**9**(9):1954–67. Doi: 10.1074/mcp.M110.000554.

123. Meiqun C., Zifan G., Kehuan S., Zhengzhi W. Application of iTRAQ quantitative proteomics in identification of serum biomarkers in breast cancer. *4th International Conference on Biomedical Engineering and Informatics*. IEEE; 2011. p. 1658–63.

124. Linghu D., Guo L., Zhao Y., Liu Z., Zhao M., Huang L., et al. iTRAQ-based quantitative proteomic analysis and bioinformatics study of proteins in pterygia. *Proteomics – Clin Appl* 2017;**11**(7–8):1600094. Doi: 10.1002/prca.201600094.

125. Tsuchida S., Satoh M., Kawashima Y., Sogawa K., Kado S., Sawai S., et al. Application of quantitative proteomic analysis using tandem mass tags for discovery and identification of novel biomarkers in periodontal disease. *Proteomics* 2013;**13**(15):2339–50. Doi: 10.1002/pmic.201200510.

126. Morales AG., Lachén-Montes M., Ibáñez-Vea M., Santamaría E., Fernández-Irigoyen J. Application of Isobaric Tags for Relative and Absolute Quantitation (iTRAQ) to Monitor Olfactory Proteomes During Alzheimer's Disease Progression. *Current Proteomic Approaches Applied to Brain Function*. 2017. p. 29–42.

127. Wiśniewski JR., Ostasiewicz P., Duś K., Zielińska DF., Gnad F., Mann M. Extensive quantitative remodeling of the proteome between normal colon tissue and adenocarcinoma. *Mol Syst Biol* 2012;**8**(1):611. Doi: 10.1038/msb.2012.44.

128. Couto N., Al-Majdoub ZM., Achour B., Wright PC., Rostami-Hodjegan A., Barber J. Quantification of Proteins Involved in Drug Metabolism and Disposition in the Human Liver Using Label-Free Global Proteomics. *Mol Pharm* 2019;**16**(2):632–47. Doi: 10.1021/acs.molpharmaceut.8b00941.

129. Ludwig C., Gillet L., Rosenberger G., Amon S., Collins BC., Aebersold R. Data-independent acquisition-based SWATH-MS for quantitative proteomics: a tutorial. *Mol Syst Biol* 2018;**14**(8):e8126. Doi: 10.15252/msb.20178126.

130. Geromanos SJ., Vissers JPC., Silva JC., Dorschel CA., Li GZ., Gorenstein M V., et al. The detection, correlation, and comparison of peptide precursor and product ions from data independent LC-MS with data dependant LC-MS/MS. *Proteomics* 2009;**9**(6):1683–95. Doi: 10.1002/pmic.200800562.

131. Hu A., Noble WS., Wolf-Yadlin A. Technical advances in proteomics: new

developments in data-independent acquisition. *F1000Research* 2016;**5**:419. Doi: 10.12688/f1000research.7042.1.

132. Michalski A., Cox J., Mann M. More than 100,000 detectable peptide species elute in single shotgun proteomics runs but the majority is inaccessible to data-dependent LC-MS/MS. *J Proteome Res* 2011;**10**(4):1785–93. Doi: 10.1021/pr101060v.

133. Bilbao A., Varesio E., Luban J., Strambio-De-Castillia C., Hopfgartner G., Müller M., et al. Processing strategies and software solutions for data-independent acquisition in mass spectrometry. *Proteomics* 2015;**15**(5–6):964–80. Doi: 10.1002/pmic.201400323.

134. Ishihama Y., Oda Y., Tabata T., Sato T., Nagasu T., Rappsilber J., et al. Exponentially Modified Protein Abundance Index (emPAI) for Estimation of Absolute Protein Amount in Proteomics by the Number of Sequenced Peptides per Protein. *Mol Cell Proteomics* 2005;**4**(9):1265–72. Doi: 10.1074/mcp.M500061-MCP200.

135. Wiśniewski JR., Vildhede A., Norén A., Artursson P. In-depth quantitative analysis and comparison of the human hepatocyte and hepatoma cell line HepG2 proteomes. *J Proteomics* 2016;**136**:234–47. Doi: 10.1016/j.jprot.2016.01.016.

136. Gillet LC., Navarro P., Tate S., Röst H., Selevsek N., Reiter L., et al. Targeted Data Extraction of the MS/MS Spectra Generated by Data-independent Acquisition: A New Concept for Consistent and Accurate Proteome Analysis. *Mol Cell Proteomics* 2012;**11**(6):O111.016717. Doi: 10.1074/mcp.O111.016717.

137. Keller A., Bader SL., Kusebauch U., Shteynberg D., Hood L., Moritz RL. Opening a SWATH Window on Posttranslational Modifications: Automated Pursuit of Modified Peptides. *Mol Cell Proteomics* 2016;**15**(3):1151–63. Doi: 10.1074/mcp.m115.054478.

138. Jamwal R., Barlock BJ., Adusumalli S., Ogasawara K., Simons BL., Akhlaghi F. Multiplex and Label-Free Relative Quantification Approach for Studying Protein Abundance of Drug Metabolizing Enzymes in Human Liver Microsomes Using SWATH-MS. *J Proteome Res* 2017;**16**(11):4134–43. Doi: 10.1021/acs.jproteome.7b00505.

139. Guo T., Kouvonen P., Koh CC., Gillet LC., Wolski WE., Röst HL., et al. Rapid mass spectrometric conversion of tissue biopsy samples into permanent quantitative digital proteome maps. *Nat Med* 2015;**21**(4):407–13. Doi: 10.1038/nm.3807.

140. Prasad B., Gaedigk A., Vrana M., Gaedigk R., Leeder JS., Salphati L., et al. Ontogeny of Hepatic Drug Transporters as Quantified by LC-MS/MS Proteomics. *Clin Pharmacol Ther* 2016;**100**(4):362–70. Doi: 10.1002/cpt.409.

141. Boberg M., Vrana M., Mehrotra A., Pearce RE., Gaedigk A., Bhatt DK., et al. Age-dependent absolute abundance of hepatic carboxylesterases (CES1 and CES2) by LC-MS/MS proteomics: Application to PBPK modeling of oseltamivir in vivo

pharmacokinetics in infants. *Drug Metab Dispos* 2017;**45**(2):216–23. Doi: 10.1124/dmd.116.072652.

142. Wang L., Collins C., Kelly EJ., Chu X., Ray AS., Salphati L., et al. Transporter expression in liver tissue from subjects with alcoholic or hepatitis C cirrhosis quantified by targeted quantitative proteomics. *Drug Metab Dispos* 2016;**44**(11):1752–8. Doi: 10.1124/dmd.116.071050.

143. Ishida K., Ullah M., Tóth B., Juhasz V., Unadkat JD. Successful Prediction of In Vivo Hepatobiliary Clearances and Hepatic Concentrations of Rosuvastatin Using Sandwich-Cultured Rat Hepatocytes, Transporter-Expressing Cell Lines, and Quantitative Proteomics. *Drug Metab Dispos* 2018;**46**(1):66–74. Doi: 10.1124/dmd.117.076539.

144. Bi Y., Qiu X., Rotter CJ., Kimoto E., Piotrowski M., Varma M V., et al. Quantitative assessment of the contribution of sodium-dependent taurocholate co-transporting polypeptide (NTCP) to the hepatic uptake of rosuvastatin, pitavastatin and fluvastatin. *Biopharm Drug Dispos* 2013;**34**(8):452–61. Doi: 10.1002/bdd.1861.

145. Vildhede A., Karlgren M., Svedberg EK., Wisniewski JR., Lai Y., Norén A., et al. Hepatic uptake of atorvastatin: influence of variability in transporter expression on uptake clearance and drug-drug interactions. *Drug Metab Dispos* 2014;**42**(7):1210–8. Doi: 10.1124/dmd.113.056309.

146. den Braver-Sewradj SP., den Braver MW., Baze A., Decorde J., Fonsi M., Bachellier P., et al. Direct comparison of UDP-glucuronosyltransferase and cytochrome P450 activities in human liver microsomes, plated and suspended primary human hepatocytes from five liver donors. *Eur J Pharm Sci* 2017;**109**:96–110. Doi: 10.1016/j.ejps.2017.07.032.

147. Venkatakrishnan K., von Moltke LL., Court MH., Harmatz JS., Crespi CL., Greenblatt DJ. Comparison between cytochrome P450 (CYP) content and relative activity approaches to scaling from cDNA-expressed CYPs to human liver microsomes: ratios of accessory proteins as sources of discrepancies between the approaches. *Drug Metab Dispos* 2000;**28**(12):1493–504.

148. Xie C., Yan T., Chen J., Li X., Zou J., Zhu L., et al. LC-MS/MS quantification of sulfotransferases is better than conventional immunogenic methods in determining human liver SULT activities: implication in precision medicine. *Sci Rep* 2017;**7**(1):3858. Doi: 10.1038/s41598-017-04202-w.

149. Harwood MD., Neuhoff S., Rostami-Hodjegan A., Warhurst G. Breast Cancer Resistance Protein Abundance, but Not mRNA Expression, Correlates with Estrone-3-Sulfate Transport in Caco-2. *J Pharm Sci* 2016;**105**(4):1370–5. Doi: 10.1016/j.xphs.2016.01.018.

150. Barter Z., Bayliss M., Beaune P., Boobis A., Carlile D., Edwards R., et al. Scaling

Factors for the Extrapolation of In Vivo Metabolic Drug Clearance From In Vitro Data: Reaching a Consensus on Values of Human Micro-somal Protein and Hepatocellularity Per Gram of Liver. *Curr Drug Metab* 2007;**8**(1):33–45. Doi: 10.2174/138920007779315053.

151. Zhang H-F., Wang H-H., Gao N., Wei J-Y., Tian X., Zhao Y., et al. Physiological Content and Intrinsic Activities of 10 Cytochrome P450 Isoforms in Human Normal Liver Microsomes. *J Pharmacol Exp Ther* 2016;**358**(1):83–93. Doi: 10.1124/jpet.116.233635.

152. Jamei M. Recent Advances in Development and Application of Physiologically-Based Pharmacokinetic (PBPK) Models: a Transition from Academic Curiosity to Regulatory Acceptance. *Curr Pharmacol Reports* 2016;**2**(3):161–9. Doi: 10.1007/s40495-016-0059-9.

153. Huang S-M., Abernethy DR., Wang Y., Zhao P., Zineh I. The utility of modeling and simulation in drug development and regulatory review. *J Pharm Sci* 2013;**102**(9):2912–23. Doi: 10.1002/jps.23570.

154. Rowland M., Lesko LJ., Rostami-Hodjegan A. Physiologically based pharmacokinetics is impacting drug development and regulatory decision making. *CPT Pharmacometrics Syst Pharmacol* 2015;**4**(6):313–5. Doi: 10.1002/psp4.52.

155. Marsousi N., Desmeules JA., Rudaz S., Daali Y. Usefulness of PBPK Modeling in Incorporation of Clinical Conditions in Personalized Medicine. *J Pharm Sci* 2017;**106**(9):2380–91. Doi: 10.1016/j.xphs.2017.04.035.

156. Prasad B., Vrana M., Mehrotra A., Johnson K., Bhatt DK. The Promises of Quantitative Proteomics in Precision Medicine. *J Pharm Sci* 2017;**106**(3):738–44. Doi: 10.1016/j.xphs.2016.11.017.

157. Jones HM., Rowland-Yeo K. Basic Concepts in Physiologically Based Pharmacokinetic Modeling in Drug Discovery and Development. *CPT Pharmacometrics Syst Pharmacol* 2013;**2**(8):e63. Doi: 10.1038/psp.2013.41.

158. Kuepfer L., Niederalt C., Wendl T., Schlender JF., Willmann S., Lippert J., et al. Applied Concepts in PBPK Modeling: How to Build a PBPK/PD Model. *CPT Pharmacometrics Syst Pharmacol* 2016;**5**(10):516. Doi: 10.1002/PSP4.12134.

159. Sager JE., Yu J., Ragueneau-Majlessi I., Isoherranen N. Physiologically Based Pharmacokinetic (PBPK) Modeling and Simulation Approaches: A Systematic Review of Published Models, Applications, and Model Verification. *Drug Metab Dispos* 2015;**43**(11):1823–37. Doi: 10.1124/dmd.115.065920.

160. Harwood MD., Achour B., Neuhoff S., Russell MR., Carlson G., Warhurst G., et al. In Vitro-In Vivo Extrapolation Scaling Factors for Intestinal P-glycoprotein and Breast

Cancer Resistance Protein: Part II. The Impact of Cross-Laboratory Variations of Intestinal Transporter Relative Expression Factors on Predicted Drug Disposition. *Drug Metab Dispos* 2016;**44**(3):476–80. Doi: 10.1124/dmd.115.067777.

161. Johnson TN., Zhou D., Bui KH. Development of physiologically based pharmacokinetic model to evaluate the relative systemic exposure to quetiapine after administration of IR and XR formulations to adults, children and adolescents. *Biopharm Drug Dispos* 2014;**35**(6):341–52. Doi: 10.1002/bdd.1899.

162. Zhao P., Vieira M de LT., Grillo JA., Song P., Wu T-C., Zheng JH., et al. Evaluation of Exposure Change of Nonrenally Eliminated Drugs in Patients With Chronic Kidney Disease Using Physiologically Based Pharmacokinetic Modeling and Simulation. *J Clin Pharmacol* 2012;**52**(S1):91S-108S. Doi: 10.1177/0091270011415528.

163. Jiang X-L., Zhao P., Barrett JS., Lesko LJ., Schmidt S. Application of Physiologically Based Pharmacokinetic Modeling to Predict Acetaminophen Metabolism and Pharmacokinetics in Children. *CPT Pharmacometrics Syst Pharmacol* 2013;**2**(10):e80. Doi: 10.1038/psp.2013.55.

164. Polasek TM., Patel F., Jensen BP., Sorich MJ., Wiese MD., Doogue MP. Predicted metabolic drug clearance with increasing adult age. *Br J Clin Pharmacol* 2013;**75**(4):1019–28. Doi: 10.1111/j.1365-2125.2012.04446.x.

165. Ke AB., Nallani SC., Zhao P., Rostami-Hodjegan A., Isoherranen N., Unadkat JD. A Physiologically Based Pharmacokinetic Model to Predict Disposition of CYP2D6 and CYP1A2 Metabolized Drugs in Pregnant Women. *Drug Metab Dispos* 2013;**41**(4):801–13. Doi: 10.1124/dmd.112.050161.

166. Ke AB., Nallani SC., Zhao P., Rostami-Hodjegan A., Unadkat JD. Expansion of a PBPK model to predict disposition in pregnant women of drugs cleared via multiple CYP enzymes, including CYP2B6, CYP2C9 and CYP2C19. *Br J Clin Pharmacol* 2014;**77**(3):554–70. Doi: 10.1111/bcp.12207.

167. Gaohua L., Abduljalil K., Jamei M., Johnson TN., Rostami-Hodjegan A. A pregnancy physiologically based pharmacokinetic (p-PBPK) model for disposition of drugs metabolized by CYP1A2, CYP2D6 and CYP3A4. *Br J Clin Pharmacol* 2012;**74**(5):873–85. Doi: 10.1111/j.1365-2125.2012.04363.x.

168. Danhof M. Systems pharmacology -- Towards the modeling of network interactions. *Eur J Pharm Sci* 2016;**94**:4–14. Doi: 10.1016/j.ejps.2016.04.027.

169. Kirouac DC. How Do We "Validate" a QSP Model? *CPT Pharmacometrics Syst Pharmacol* 2018;**7**(9):547–8. Doi: 10.1002/psp4.12310.

170. Kirouac DC., Lahdenranta J., Du J., Yarar D., Onsum MD., Nielsen UB., et al. Model-Based Design of a Decision Tree for Treating HER2+ Cancers Based on Genetic and

Protein Biomarkers. *CPT Pharmacometrics Syst Pharmacol* 2015;**4**(3):e00019. Doi: 10.1002/psp4.19.

171. Dimitrova N., Nagaraj AB., Razi A., Singh S., Kamalakaran S., Banerjee N., et al. InFlo: A novel systems biology framework identifies cAMP-CREB1 axis as a key modulator of platinum resistance in ovarian cancer. *Oncogene* 2017;**36**(17):2472–82. Doi: 10.1038/onc.2016.398.

172. Peterson MC., Riggs MM. FDA advisory meeting clinical pharmacology review utilizes a quantitative systems pharmacology (QSP) model: A watershed moment? *CPT Pharmacometrics Syst Pharmacol* 2015;**4**(3):189–92. Doi: 10.1002/psp4.20.

173. Niu J., Straubinger RM., Mager DE. Pharmacodynamic Drug–Drug Interactions. *Clin Pharmacol Ther* 2019;**105**(6):1395–406. Doi: 10.1002/cpt.1434.

174. Choy S., Hénin E., van der Walt J-S., Kjellsson MC., Karlsson MO. Identification of the primary mechanism of action of an insulin secretagogue from meal test data in healthy volunteers based on an integrated glucose-insulin model. *J Pharmacokinet Pharmacodyn* 2013;**40**(1):1–10. Doi: 10.1007/s10928-012-9281-1.

175. Wetmore BA., Merrick BA. Invited Review: Toxicoproteomics: Proteomics Applied to Toxicology and Pathology. *Toxicol Pathol* 2004;**32**(6):619–42. Doi: 10.1080/01926230490518244.

176. Zhu X., Shen X., Qu J., Straubinger RM., Jusko WJ. Multi-Scale Network Model Supported by Proteomics for Analysis of Combined Gemcitabine and Birinapant Effects in Pancreatic Cancer Cells. *CPT Pharmacometrics Syst Pharmacol* 2018;**7**(9):549–61. Doi: 10.1002/psp4.12320.

177. Hector S., Rehm M., Schmid J., Kehoe J., McCawley N., Dicker P., et al. Clinical application of a systems model of apoptosis execution for the prediction of colorectal cancer therapy responses and personalisation of therapy. *Gut* 2012;**61**(5):725–33. Doi: 10.1136/gutjnl-2011-300433.

178. Fisher CD., Lickteig AJ., Augustine LM., Ranger-Moore J., Jackson JP., Ferguson SS., et al. Hepatic Cytochrome P450 Enzyme Alterations in Humans with Progressive Stages of Nonalcoholic Fatty Liver Disease. *Drug Metab Dispos* 2009;**37**(10):2087–94. Doi: 10.1124/dmd.109.027466.

179. Hardwick RN., Ferreira DW., More VR., Lake AD., Lu Z., Manautou JE., et al. Altered UDP-Glucuronosyltransferase and Sulfotransferase Expression and Function during Progressive Stages of Human Nonalcoholic Fatty Liver Disease. *Drug Metab Dispos* 2013;**41**(3):554–61. Doi: 10.1124/dmd.112.048439.

180. Yang LQ., Li SJ., Cao YF., Man XB., Yu WF., Wang HY., et al. Different alterations of cytochrome P450 3A4 isoform and its gene expression in livers of patients with

chronic liver diseases. *World J Gastroenterol* 2003;**9**(2):359–63. Doi: 10.3748/wjg.v9.i2.359.

181. Li R., Barton H., Maurer T. A Mechanistic Pharmacokinetic Model for Liver Transporter Substrates Under Liver Cirrhosis Conditions. *CPT Pharmacometrics Syst Pharmacol* 2015;**4**(6):338–49. Doi: 10.1002/psp4.39.

182. Hodgkinson VC., Agarwal V., ELFadl D., Fox JN., McManus PL., Mahapatra TK., et al. Pilot and feasibility study: comparative proteomic analysis by 2-DE MALDI TOF/TOF MS reveals 14-3-3 proteins as putative biomarkers of response to neoadjuvant chemotherapy in ER-positive breast cancer. *J Proteomics* 2012;**75**(9):2745–52. Doi: 10.1016/j.jprot.2012.03.049.

183. Yoshida K., Budha N., Jin JY. Impact of physiologically based pharmacokinetic models on regulatory reviews and product labels: Frequent utilization in the field of oncology. *Clin Pharmacol Ther* 2017;**101**(5):597–602. Doi: 10.1002/CPT.622.

184. Jamei M., Dickinson GL., Rostami-Hodjegan A. A framework for assessing inter-individual variability in pharmacokinetics using virtual human populations and integrating general knowledge of physical chemistry, biology, anatomy, physiology and genetics: A tale of "bottom-up" vs "top-down" recognition . *Drug Metab Pharmacokinet* 2009;**24**(1):53–75.

185. Melillo N., Darwich AS., Magni P., Rostami-Hodjegan A. Accounting for inter-correlation between enzyme abundance: a simulation study to assess implications on global sensitivity analysis within physiologically-based pharmacokinetics. *J Pharmacokinet Pharmacodyn* 2019;**46**(2):137–54. Doi: 10.1007/s10928-019-09627-6.

186. Tsamandouras N., Wendling T., Rostami-Hodjegan A., Galetin A., Aarons L. Incorporation of stochastic variability in mechanistic population pharmacokinetic models: handling the physiological constraints using normal transformations. *J Pharmacokinet Pharmacodyn* 2015;**42**(4):349–73. Doi: 10.1007/s10928-015-9418-0.

187. Achour B., Barber J., Rostami-Hodjegan A. Expression of hepatic drug-metabolizing cytochrome P450 enzymes and their intercorrelations: A meta-analysis. *Drug Metab Dispos* 2014;**42**(8):1349–56.

188. Izukawa T., Nakajima M., Fujiwara R., Yamanaka H., Fukami T., Takamiya M., et al. Quantitative analysis of UGT1A and UGT2B expression levels in human livers. *Drug Metab Dispos* 2009;**37**(8):1759–68. Doi: 10.1124/dmd.109.027227.

189. Wortham M., Czerwinski M., He L., Parkinson A., Wan YJY. Expression of constitutive androstane receptor, hepatic nuclear factor 4α, and P450 oxidoreductase genes determines interindividual variability in basal expression and activity of a broad scope of xenobiotic metabolism genes in the human liver. *Drug Metab Dispos* 2007;**35**(9):1700–10. Doi: 10.1124/dmd.107.016436.

190. Mooij MG., Van De Steeg E., Van Rosmalen J., Windster JD., De Koning BAE., Vaes WHJ., et al. Proteomic analysis of the developmental trajectory of human hepatic membrane transporter proteins in the first three months of life. *Drug Metab Dispos* 2016;**44**(7):1005–13. Doi: 10.1124/dmd.115.068577.

191. Cheung KWK., Groen BD., Spaans E., Borselen MD., Bruijn ACJM., Simons-Oosterhuis Y., et al. A Comprehensive Analysis of Ontogeny of Renal Drug Transporters: mRNA Analyses, Quantitative Proteomics, and Localization. *Clin Pharmacol Ther* 2019;**106**(5):1083–92. Doi: 10.1002/cpt.1516.

192. Barter ZE., Perrett HF., Yeo KR., Allorge D., Lennard MS., Rostami-Hodjegan A. Determination of a quantitative relationship between hepatic CYP3A5*1/*3 and CYP3A4 expression for use in the prediction of metabolic clearance in virtual populations. *Biopharm Drug Dispos* 2010;**31**(8–9):516–32. Doi: 10.1002/bdd.732.

193. Darwich AS., Ogungbenro K., Vinks AA., Powell JR., Reny JL., Marsousi N., et al. Why has model-informed precision dosing not yet become common clinical reality? lessons from the past and a roadmap for the future. *Clin Pharmacol Ther* 2017;**101**(5):646–56. Doi: 10.1002/cpt.659.

194. Polasek TM., Shakib S., Rostami-Hodjegan A. Precision dosing in clinical medicine: present and future. *Expert Rev Clin Pharmacol* 2018;**11**(8):743–6. Doi: 10.1080/17512433.2018.1501271.

195. Rowland A., Ruanglertboon W., van Dyk M., Wijayakumara D., Wood LS., Meech R., et al. Plasma extracellular nanovesicle (exosome)-derived biomarkers for drug metabolism pathways: a novel approach to characterize variability in drug exposure. *Br J Clin Pharmacol* 2019;**85**(1):216–26. Doi: 10.1111/bcp.13793.

196. Patel N., Wiśniowska B., Jamei M., Polak S. Real Patient and its Virtual Twin: Application of Quantitative Systems Toxicology Modelling in the Cardiac Safety Assessment of Citalopram. *AAPS J* 2018;**20**(1):6. Doi: 10.1208/s12248-017-0155-8.

197. Boukouris S., Mathivanan S. Exosomes in bodily fluids are a highly stable resource of disease biomarkers. *Proteomics - Clin Appl* 2015;**9**(3–4):358–67. Doi: 10.1002/prca.201400114.

198. Fernandez E., Perez R., Hernandez A., Tejada P., Arteta M., Ramos JT. Factors and mechanisms for pharmacokinetic differences between pediatric population and adults. *Pharmaceutics* 2011;**3**(1):53–72. Doi: 10.3390/pharmaceutics3010053.

199. Batchelor HK., Marriott JF. Paediatric pharmacokinetics: Key considerations. *Br J Clin Pharmacol* 2015;**79**(3):395–404. Doi: 10.1111/bcp.12267.

200. Lu H., Rosenbaum S. Developmental pharmacokinetics in pediatric populations. *J Pediatr Pharmacol Ther* 2014;**19**(4):262–76. Doi: 10.5863/1551-6776-19.4.262.

201. Badée J., Fowler S., de Wildt SN., Collier AC., Schmidt S., Parrott N. The Ontogeny of UDP-glucuronosyltransferase Enzymes, Recommendations for Future Profiling Studies and Application Through Physiologically Based Pharmacokinetic Modelling. *Clin Pharmacokinet* 2019;**58**(2):189–211. Doi: 10.1007/s40262-018-0681-2.

202. Elmorsi Y., Barber J., Rostami-Hodjegan A. Ontogeny of Hepatic Drug Transporters and Relevance to Drugs Used in Pediatrics. *Drug Metab Dispos* 2016;**44**(7):992–8. Doi: 10.1124/dmd.115.067801.

203. Calvier EAM., Krekels EHJ., Välitalo PAJ., Rostami-Hodjegan A., Tibboel D., Danhof M., et al. Allometric Scaling of Clearance in Paediatric Patients: When Does the Magic of 0.75 Fade? *Clin Pharmacokinet* 2017;**56**(3):273–85. Doi: 10.1007/s40262-016-0436-x.

204. Jones HM., Chen Y., Gibson C., Heimbach T., Parrott N., Peters SA., et al. Physiologically based pharmacokinetic modeling in drug discovery and development: a pharmaceutical industry perspective. *Clin Pharmacol Ther* 2015;**97**(3):247–62. Doi: 10.1002/cpt.37.

205. Miller NA., Reddy MB., Heikkinen AT., Lukacova V., Parrott N. Physiologically Based Pharmacokinetic Modelling for First-In-Human Predictions: An Updated Model Building Strategy Illustrated with Challenging Industry Case Studies. *Clin Pharmacokinet* 2019;**58**(6):727–46. Doi: 10.1007/s40262-019-00741-9.

206. Templeton IE., Jones NS., Musib L. Pediatric Dose Selection and Utility of PBPK in Determining Dose. *AAPS J* 2018;**20**(2):31. Doi: 10.1208/s12248-018-0187-8.

207. Howard M., Barber J., Alizai N., Rostami-Hodjegan A. Dose adjustment in orphan disease populations: the quest to fulfill the requirements of physiologically based pharmacokinetics. *Expert Opin Drug Metab Toxicol* 2018;**14**(12):1315–30. Doi: 10.1080/17425255.2018.1546288.

208. Upreti V V., Wahlstrom JL. Meta-analysis of hepatic cytochrome P450 ontogeny to underwrite the prediction of pediatric pharmacokinetics using physiologically based pharmacokinetic modeling. *J Clin Pharmacol* 2016;**56**(3):266–83. Doi: 10.1002/jcph.585.

209. Mehrotra A., Boberg M., Vrana M., Gaedigk A., Pearce RE., Leeder S., et al. Age-dependent Expression Analysis of Major Drug Metabolizing Enzymes in Human Liver. *FASEB J* 2015;**30**(1 Supplement):713.11.

210. Leeder JS., Meibohm B. Challenges and opportunities for increasing the knowledge base related to drug biotransformation and pharmacokinetics during growth and development. *Drug Metab Dispos* 2016;**44**(7):916–23. Doi: 10.1124/dmd.116.071159.

211. Ginsberg G., Hattis D., Russ A., Sonawane B. Physiologically based pharmacokinetic

(PBPK) modeling of caffeine and theophylline in neonates and adults: implications for assessing children's risks from environmental agents. *J Toxicol Environ Heal Part A* 2004;**67**(4):297–329. Doi: 10.1080/15287390490273550.

212. Michelet R., Van Bocxlaer J., Allegaert K., Vermeulen A. The use of PBPK modeling across the pediatric age range using propofol as a case. *J Pharmacokinet Pharmacodyn* 2018;**45**(6):765–85. Doi: 10.1007/s10928-018-9607-8.

213. T'jollyn H., Snoeys J., Vermeulen A., Michelet R., Cuyckens F., Mannens G., et al. Physiologically Based Pharmacokinetic Predictions of Tramadol Exposure Throughout Pediatric Life: an Analysis of the Different Clearance Contributors with Emphasis on CYP2D6 Maturation. *AAPS J* 2015;**17**(6):1376–87. Doi: 10.1208/s12248-015-9803-z.

214. Ogungbenro K., Aarons L. A physiologically based pharmacokinetic model for Valproic acid in adults and children. *Eur J Pharm Sci* 2014;**63**:45–52. Doi: 10.1016/j.ejps.2014.06.023.

215. Zhou Y., Ingelman-Sundberg M., Lauschke VM. Worldwide Distribution of Cytochrome P450 Alleles: A Meta-analysis of Population-scale Sequencing Projects. *Clin Pharmacol Ther* 2017;**102**(4):688–700. Doi: 10.1002/cpt.690.

216. Oswald S. Organic Anion Transporting Polypeptide (OATP) transporter expression, localization and function in the human intestine. *Pharmacol Ther* 2019;**195**:39–53. Doi: 10.1016/j.pharmthera.2018.10.007.

217. Gentry PR., Hack CE., Haber L., Maier A., Clewell HJ. An approach for the quantitative consideration of genetic polymorphism data in chemical risk assessment: Examples with warfarin and parathion. *Toxicol Sci* 2002;**70**(1):120–39. Doi: 10.1093/toxsci/70.1.120.

218. Achour B., Rostami-Hodjegan A., Barber J. Response to "Determining Allele-Specific Protein Expression (ASPE) Using a Novel Quantitative Concatamer Based Proteomics Method". *J Proteome Res* 2019;**18**(1):574–574. Doi: 10.1021/acs.jproteome.8b00871.

219. O'Dwyer D., Ralton LD., O'Shea A., Murray GI. The proteomics of colorectal cancer: identification of a protein signature associated with prognosis. *PLoS One* 2011;**6**(11):e27718. Doi: 10.1371/journal.pone.0027718.

220. Russell MR., Graham C., D'Amato A., Gentry-Maharaj A., Ryan A., Kalsi JK., et al. A combined biomarker panel shows improved sensitivity for the early detection of ovarian cancer allowing the identification of the most aggressive type II tumours. *Br J Cancer* 2017;**117**(5):666–74. Doi: 10.1038/bjc.2017.199.

221. Srivastava A., Creek DJ. Discovery and Validation of Clinical Biomarkers of Cancer: A Review Combining Metabolomics and Proteomics. *Proteomics* 2019;**19**(10):1700448. Doi: 10.1002/pmic.201700448.

222. Russell MR., Walker MJ., Williamson AJK., Gentry-Maharaj A., Ryan A., Kalsi J., et al. Protein Z: A putative novel biomarker for early detection of ovarian cancer. *Int J Cancer* 2016;**138**(12):2984–92. Doi: 10.1002/ijc.30020.

223. Shruthi BS., Vinodhkumar P., Selvamani M. Proteomics: A new perspective for cancer. *Adv Biomed Res* 2016;**5**:67. Doi: 10.4103/2277-9175.180636.

224. Held JM., Danielson SR., Behring JB., Atsriku C., Britton DJ., Puckett RL., et al. Targeted quantitation of site-specific cysteine oxidation in endogenous proteins using a differential alkylation and multiple reaction monitoring mass spectrometry approach. *Mol Cell Proteomics* 2010;**9**(7):1400–10. Doi: 10.1074/mcp.M900643-MCP200.

225. Elschenbroich S., Ignatchenko V., Clarke B., Kalloger SE., Boutros PC., Gramolini AO., et al. In-Depth Proteomics of Ovarian Cancer Ascites: Combining Shotgun Proteomics and Selected Reaction Monitoring Mass Spectrometry. *J Proteome Res* 2011;**10**(5):2286–99. Doi: 10.1021/pr1011087.

226. Sjöström M., Ossola R., Breslin T., Rinner O., Malmström L., Schmidt A., et al. A Combined Shotgun and Targeted Mass Spectrometry Strategy for Breast Cancer Biomarker Discovery. *J Proteome Res* 2015;**14**(7):2807–18. Doi: 10.1021/acs.jproteome.5b00315.

227. Starr AE., Deeke SA., Ning Z., Chiang CK., Zhang X., Mottawea W., et al. Proteomic analysis of ascending colon biopsies from a paediatric inflammatory bowel disease inception cohort identifies protein biomarkers that differentiate Crohn's disease from UC. *Gut* 2017;**66**(9):1573–83. Doi: 10.1136/gutjnl-2015-310705.

228. Bollu LR., Mazumdar A., Savage MI., Brown PH. Molecular pathways: Targeting protein tyrosine phosphatases in cancer. *Clin Cancer Res* 2017;**23**(9):2136–42. Doi: 10.1158/1078-0432.CCR-16-0934.

229. Bhullar KS., Lagarón NO., McGowan EM., Parmar I., Jha A., Hubbard BP., et al. Kinase-targeted cancer therapies: progress, challenges and future directions. *Mol Cancer* 2018;**17**(1):48. Doi: 10.1186/s12943-018-0804-2.

230. Tan HT., Wu W., Ng YZ., Zhang X., Yan B., Ong CW., et al. Proteomic analysis of colorectal cancer metastasis: Stathmin-1 revealed as a player in cancer cell migration and prognostic marker. *J Proteome Res* 2012;**11**(2):1433–45. Doi: 10.1021/pr2010956.

231. Holman SW., Sims PFG., Eyers CE. The use of selected reaction monitoring in quantitative proteomics. *Bioanalysis* 2012;**4**:1763–86. Doi: 10.4155/bio.12.126.

232. Abbatiello SE., Ackermann BL., Borchers C., Bradshaw RA., Carr SA., Chalkley R., et al. New Guidelines for Publication of Manuscripts Describing Development and Application of Targeted Mass Spectrometry Measurements of Peptides and Proteins. *Mol Cell Proteomics* 2017;**16**(3):327–8. Doi: 10.1074/mcp.E117.067801.

233. Whiteaker JR., Halusa GN., Hoofnagle AN., Sharma V., MacLean B., Yan P., et al. CPTAC Assay Portal: a repository of targeted proteomic assays. *Nat Methods* 2014;**11**(7):703–4. Doi: 10.1038/nmeth.3002.

234. Oswald S., Gröer C., Drozdzik M., Siegmund W. Mass Spectrometry-Based Targeted Proteomics as a Tool to Elucidate the Expression and Function of Intestinal Drug Transporters. *AAPS J* 2013;**15**(4):1128–40. Doi: 10.1208/s12248-013-9521-3.

235. Xu J., Patassini S., Rustogi N., Riba-Garcia I., Hale BD., Phillips AM., et al. Regional protein expression in human Alzheimer's brain correlates with disease severity. *Commun Biol* 2019;**2**(1):43. Doi: 10.1038/s42003-018-0254-9.

236. Uhlen M., Fagerberg L., Hallstrom BM., Lindskog C., Oksvold P., Mardinoglu A., et al. Tissue-based map of the human proteome. *Science (80-)* 2015;**347**(6220):1260419–1260419. Doi: 10.1126/science.1260419.

Chapter Three: Development of a Methodology for Absolute Quantification of Enzymes and Transporters Using Liquid-Chromatography-Coupled to Tandem Mass Spectrometry (LC-MS/MS) for Normal and Crohn's Disease Human Intestine Tissue

Declaration

Sarah Alrubia, Zubida M. Al-Majdoub, Narciso Couto, Amin Rostami-Hodjegan, Jill Barber

I carried out the literature search, generation and analysis of data, contributed to the study design and wrote the manuscript. Dr Zubida M. Al-Majdoub and Dr Narciso Couto were consulted on experimental methodology. Dr Zubida M. Al-Majdoub reviewed and suggested edits to the manuscript. Dr Jill Barber and Prof. Amin Rostami-Hodjegan contributed to the study design and provided guidance. I retained editorial control.

3.1.Abstract

Background and Aims: Various methodology techniques are applied in different stages of preparation of intestine tissue sample using liquid-chromatography coupled to tandem mass spectrometry (LC-MS/MS) based quantitative proteomics analysis. Moreover, advances in these techniques are introduced, which causes variation in the outcomes of the proteins abundance levels. The most appropriate technique to use with our set of intestine samples (histologically normal and Crohn's disease) is being developed and investigated. This is to determine their impact on the intestine drug metabolising enzymes and transporters abundance and to produce a more reliable and less variable proteomics data. Additionally, Quantitative Concatemers (QconCAT) is a gold standard provides reliable proteins abundance quantification. Isotopically labelled concatenated surrogate peptides based on the specific intestine transporters were developed and characterised.

Methods: Histologically normal and diseased adult human ileum and colon tissues have been utilised. Enterocytes were isolated by calcium chelation elution and scraping methods. Filter-aided sample preparation (FASP) and suspension trapping (S-Trap) were used to digest proteins. The extracted homogenate and S9 fractions were compared. LC-MS/MS Orbitrap Elite and Q-Exactive proteome coverage is assessed. The number of identified protein and their abundance values served as the comparison criteria between the methods in each step. Incorporation of several transporters into the TransCAT includes Apical Na+/dependent Bile acid Transporter (ASBT), H+/Peptide Cotransporters (PEPT1), MonoCarboxylate Transporter1 (MCT1) and Organic Anion Transporter 4A1 (OATP4A1) and Alkaline Phosphatase enzymes (ALPI) was carried out. Characterisation of the built TranCAT is tested as well as its purity and suitability for LC-MS/MS targeted quantitative proteomics analysis.

Results: The elution and scarping methods were used to harvest enterocytes from the underlying lamina propria, but the elution method was determined to be superior based on the amount and expression of enzymes and transporters. FASP and S-Trap proteins digestion showed comparable profile of proteins expression levels but the number of the detected proteins was higher when applying FASP digestion protocol. Expression of transporters and most of non-cytosolic enzymes was higher in homogenate compared to the S9 fraction, which had a better profile for the cytosolic proteins. The Q-Exactive LC-MS instrument provides better proteome coverage compared to the Orbitrap Elite. Successful expression of the designed transporters in the constructed QconCAT is achieved by high labelling efficiency (98.5% with

lysine peptides and 95.5% arginine peptides), purity and high recovery of the surrogate peptides (92%).

Conclusion: Assessment of enterocytes isolation, proteins digestion, subcellular fractions and LC-MS instrument steps of ileum and colon samples preparation was performed. Each step identifies the most suitable methods to be used with our healthy, normal and inflamed intestine samples. The expression levels and detection of phase I & II metabolising enzymes as well as uptake & influx transporters were superior in samples prepared by EDTA elution, FASP proteolytic digestion, homogenate fraction, and Q-Exactive mass spectrometer. QconCAT was generated to be used in targeted LC-MS/MS proteomics study of drug metabolising enzymes and transporters.

3.2.Introduction

As intestine drug metabolising enzymes and transporters (DMETs) have a dominant effect on oral drug pharmacokinetics (PK), their expression levels provide data essential for developing of physiologically based pharmacokinetic (PBPK) models.[1,2]

This is particularly crucial for disease populations where the expression regulation is affected and unfavourable clinical outcomes can occur. Literature data for DMETs expression were available for healthy[3], non-diseased (histologically normal)[4] and diseased tissue[5] which enable better prediction of oral dosage forms utilising physiological based pharmacokinetics (PBPK) modelling.[6–8] The available literature data indicate that DMETs expression, activity, and regulation show substantial variations, which can be attributed to different factors (e.g. origin of the isolated tissue, disease condition, demographic data, and genetic polymorphism)[9–11] and differences in sample preparation and analysis methodology steps and techniques used in each step.[12–15]

Proteomics analysis of DMETs by liquid-chromatography coupled with tandem mass spectrometry (LC-MS/MS) has been able to quantify the desired protein abundance. The field has been advancing its various techniques to enhance protein quantification and identification.

Proteomics analysis of intestine proteomes involves a variety of methodologies including: subcellular fractionation such as enterocytes isolation, homogenization, proteins digestion, LC-MS/MS and data analysis. To identify and quantify enzymes (cytosolic, mitochondrion, and microsomal) and transporters (membrane and mitochondria) in different subcellular localization in the mucosal layer of the enterocytes, the complexity of intestine tissue needs to be reduced.[16,17] The intestine heterogeneity adds to the difficulty of quantifying the necessary proteins. Due to differences in the structure and function of each segment, differences in enzyme, transporter expression and distribution are found between the upper and lower segments[4,18–20]

The enterocytes line the intestine lumen and the presence of DMETs improves their function as absorptive units altering xenobiotic bioavailability.[16,17] Enterocytes isolation from the mucosal layer is physically performed either by scraping[21,22], crushing[4,23] or by calcium chelation to chemically elute the cells.[24,25] The nature and size of the intestine starting material, the harvested material amount and the targeted proteins all play a role in determining the best approach.

The scraping is an aggressive procedure that exposes the content to proteolytic enzymes, compromising the reproducibility, quantity, and integrity of proteins in the isolated cell. However, this can be overcome by using a cocktail of protease inhibitors (PI).[26] The elution methods requires longer time and larger tissue sizes to provide a good mucosal surface area and in many situations, the procedure was carried out with specialised physical tools that are not easily available in laboratory settings.[24,25,27] These two procedures were mostly used on a healthy human or animal intestinal tissue.

To measure specific proteins abundances, a further reduction in sample complexity is required based on their subcellular location as their presence in fractions other than their specific ones can be relatively low. The predominant phase 1 and 2 metabolising enzymes represented by Cytochrome P450 (CYPs) isoforms and UDP Glucosyltransferases (UGTs) are localised in the endoplasmic reticulum. Other metabolising enzymes found in in the cytoplasm and the mitochondria include Glutathione S-Transferase (GSTs) and Sulfotransferases (STs).[28–30] Drug Transporters are mainly localized in the enterocyte membrane where they execute uptake or efflux roles. Solute carriers (SLCs) are the most common uptake transporters, while ATP-binding cassette (ABCs) are the most common efflux transporters. After the cell isolation, differential centrifugation is performed to remove contaminants and achieve sample enrichment and separation, resulting in a more purified fraction.[31] Homogenate is a very complex fraction as it consist of all cellular components which can mask the desired proteins abundance level if it's not abundantly expressed. The S9 fraction is a post-mitochondrial fraction consist of a mixture of microsomal and cytosolic proteins, although the amount and enrichment of transporters is not well established. Microsomal enzymes and transporter abundances have been measured in human intestinal homogenate[25], S9 fractions[32–34] and in other organs[14,34–36] with varying levels. As a result, determining the most appropriate fraction in terms of the primary targeted DMETs is important as choosing the incorrect fraction can result in the enrichment of some targets while causing the loss of others.

For quantitative LC-MS/MS-based proteomic analysis, complete protein digestion is crucial. Proteins are digested into peptides by means of proteolytic enzymes such as trypsin and lysyl endopeptidase (Lys-C). Proteomics solution-based digestion methods include filter-aided sample preparation (FASP), eFASP[37,38] and a recently introduced suspension trapping (S-Trap) methods.[39] In the field of proteomics, FASP is a well-established and commonly applied method. Proteins are retained on a molecular-weight filter membrane which enables their

digestion, adequate purification and peptides recovery through centrifugation prior to LC-MS/MS analysis.[37,40] The main disadvantages of this method are been tedious and time consuming due to repetitive and prolong centrifugation.[41] On the other hand, S-Trap is a new developed method that has been demonstrated to produce reliable and reproducible results while also reducing the overall preparation time, as the centrifugation steps are short and less frequent.[39]

There is no such thing as the best digesting method or conditions as different outcomes have been reported with the same conditions depending on the biological sample's origin and the sources of the peptides being studied.[23,42–47] FASP protocol has been successfully used with human intestine tissue for quantitative proteomics analysis.[4,48] While S-Trap has showed promising positive results from a variety of samples other than the intestine.[49–51]

LC-MS/MS absolute proteomics quantification of multiple proteins simultaneously is achieved by addition of stable isotope labelled (SIL) peptides as internal standard to the biological sample. Same amino acid sequence peptides (heavy isotopes (^{13}C, ^{15}N)) as the targeted peptides (light form (^{12}C, ^{14}N)) are included in these standards. The surrogate peptides will co-elute with the targeted peptides from the analyte sample and detected at the same retention time with a mass shift allowing absolute quantification by comparing the peaks intensities area ratios (heavy and light).[52] Biologically synthetized labelled stable isotopes expressed within Escherichia coli known as Quantification Concatemer (QconCAT) allow a relatively large number of targets to be incorporated (up to 20 proteins).[53] Usually, two to three surrogate peptides are concatenated per target protein. To enable quantification of the QconCAT, a non-naturally occurring peptides (NNOP) is incorporated into the construct.[54,55] QconCAT concatenated peptides are spiked to the sample mixture in a known concentration prior to LC-MS/MS analysis. This enables simultaneous digestion and peptides release of the sample proteins and the QconCAT. Several QconCATs have been designed where the selection of the surrogate peptides covers most of the targeted phase I and II DMEs (MetCAT)[56] and transporters (TransCAT).[54]

LC-MS/MS mass analyser are used in proteomics analysis, where the Q-Exactive (QE) and Orbitrap Elite are the ones available to be used with our intestine samples. The two instruments have been successfully used with biological proteomes samples by our research group.[57,58] Orbitrap Elite and QE are Orbitap mass analysers with many common features between the two systems. The major difference between them is the ion selection and the fragmentation.[59–

[64] The Elite dual linear ion trap (LIT) isolation system fill the trap before isolating the ions which makes it less suitable for complex biological samples. This is because the high abundance proteins will control the trap fill times covering the detection of the low abundance proteins.[59–61] The QE quadrupole mass isolation system can enrich low abundance proteins which provides low detection limits of proteins in complex proteomes.[61,62]

Here, we aimed to assess several methodology steps involved in the LC-MS/MS based quantitative proteomics analysis workflow, illustrated in Figure 3.1, to ensure the success of samples preparation and data generation to identify and quantify DMETs from Crohn's disease (CD), histologically normal (HN) and healthy ileum and colon tissue samples. Thus, we carried out a differential comparison to investigate the impact of enterocyte isolation, subcellular fraction, protein digestion, and LC-MS/MS instrument on DMETs based on our samples nature, size and laboratory facilities. The key evaluation criteria are the number of peptides and proteins identified and their absolute quantification, relevance to drug metabolising enzymes and transporters proteins.

Additionally, because the previous constructed QconCATs were done based on the primary DMETs in organs other than the intestine, several intestine transporters were not included, thus, in this chapter, addition of these proteins to the already designed QconCAT is carried out.

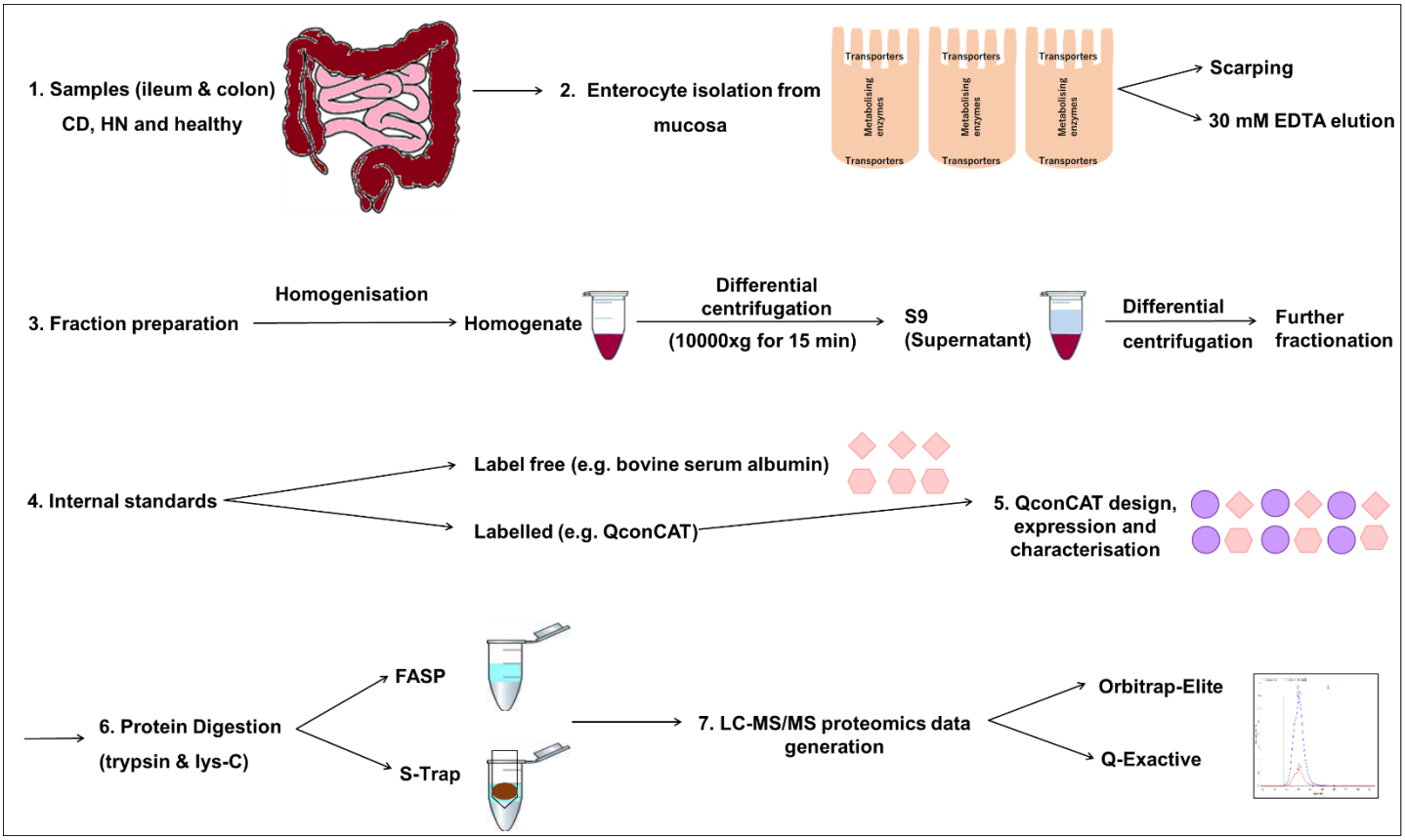

Figure 3.1. *Scheme describing the general intestine sample preparation steps for LC-MS/MS based quantitative proteomics analysis. CD; Crohn's disease, HN; histologically normal, FASP; filter-aided sample preparation, S-Trap; suspension trapping.*

3.3.Materials and methods

3.3.1. Materials

Unless otherwise indicated, all chemicals were supplied by Sigma-Aldrich (Poole, UK). All solvents were high performance liquid chromatography (HPLC) grade and supplied by Thermo Fisher Scientific (Paisley, UK). Lysyl endopeptidase (Lys-C) was purchased from Wako (Osaka, Japan). Sequencing-grade modified trypsin was supplied by Promega (Southampton, UK). Complete Mini, EDTA-free protease inhibitor cocktail tablets were supplied by Roche (Mannheim, Germany). BCA protein concentration measuring kit was obtained from ThermoFisher Scientific (Hemel Hempstead, UK).

3.3.2. Human intestinal tissue

Three fresh frozen human tissues from ileum and colon were used to carry out the methodology development workflow. Details of the samples, their histological nature and in which step of the method they were used is listed in Table 3.1. Samples were obtained after informed consent from patients and supplied by Manchester Biomedical Research Centre (BRC) Biobank, Manchester University NHS Foundation Trust, Manchester, UK. Prior ethics approval was granted by NRES Committee North West - Haydock (19/NW/0644). The tissue samples used were chosen based on their accessibility, size and suitability for the purpose.

Table 3.1. Demographic and tissue details of samples used in the different methodology steps.

Sample	ID	Age	Gender	Ethnicity	Segment	Methodology Step
Histologically normal (HN)	2077	59	Female	White - British	Ileum (adenocarcinoma)	Enterocyte isolation, Proteolytic digestion, and LC-MS/MS instrument
Crohn's disease (CD)	2055	30	Male	Pakistani	Colon	Determination of the subcellular fraction with the highest detected number of proteins of interest.
Histologically normal (HN)	2097	55	Male	White - British	Ileum (adenocarcinoma)	

Due to the fact that the Crohn's disease (CD) samples are precious with limited availability (only one supplier were able to provide CD samples), small tissue size (CD colon; 30-570 mg and CD ileum; 20-270 mg), the healthy samples are expensive (n=10 ~ £10,000), relatively small (500 mg) and previous studies have only been tested on healthy tissues the procedures are carried out utilising histologically normal samples from cancer patients (HN-cancer) since they are more readily available in larger sizes and can be used to evaluate the conditions on an intestinal tissue from a diseased subject, Unless the results need to be proved in CD tissue then a CD tissue is used.

3.3.3. Enterocyte isolation method

A macroscopically normal ileum tissue is used to assess the effect of enterocyte isolation by scraping versus elution by chelation on protein abundance based on the nature and the size of the different available intestinal samples. The same tissue was cut into two equal pieces and prepared by elution and scrapping, two typical methods for isolating enterocytes from the mucosal layer. The procedures were carried out on ice, and all solutions were pH 7.4 equilibrated. Microscopical examination of the isolated enterocytes by the two methods was performed before and after homogenisation step as a quality control step to determine successful isolation of the enterocytes.

Elution by EDTA-calcium chelation was adapted from (*Harwood et al. 2015*)[24] with few modifications. The base buffer for all solutions used was 112 mM NaCl, 5 mM KCl, 20 mM HEPES along with addition of protease inhibitor cocktail (PI) to prevent the inhibitory effect of the released intestine proteases (e.g. a serine proteases) on DMETs yield during isolation process.[65,66] The mucosa was washed twice in the base buffer and immersed for 30 min in 27 mM sodium citrate solution, a mild chelating agent which ease and pre-prepare the tissue cells for dissociation,[67,68] then incubated in EDTA buffer (30 mM EDTA, 10 U/mL heparin (to decrease protein mucus trapping), and 1 mM dithiothreitol (DTT)) with stirring at 250 rpm for 40 min to initiate chelation. EDTA mediates enterocytes release from mucosa lamina propria by disrupting the cells calcium dependent adhesion.[69] The chelated enterocytes were collected from the mucosa by repeated flushing with EDTA buffer. The formed material was washed by centrifugation twice at 2000 *xg* for 10 min to reduce mucus contamination. The resulting enterocyte pellet was weighted (mucosal weight) then re-suspended in homogenisation buffer (10 mM Tris–HCl, 250 mM sucrose, 0.1 mM EGTA, 0.5 mM $MgCl_2$, 5 mM histidine and 0.2% sodium dodecyl sulfate (SDS)) at 3 ml per g of cells. Homogenisation was carried out with a

Dounce hand-held homogeniser for a minimum of 75 strokes, followed by treatment with an ultrasonication probe (30 W) for two 10s bursts to disrupt cell membranes. The formed homogenate fraction was stored in aliquots at -80°C until further processing.

To separate the mucosal layer by scarping method, a glass spatula was scraped across the defrosted ileum tissue. The isolated mucosa was weighted then homogenised with the same homogenisation buffer and procedure as the elution. After homogenisation, any big fragments were removed then re-homogenised for a minimum of 75 strokes. Ultrasonication, centrifugation and storage was carried out as with elution method.

3.3.4. Proteolytic digestion method

The protein content of the homogenate from the sample used in elution protocol was measured in triplicate using BCA assay using bovine serum albumin (BSA) as a standard. An amount equivalent to 50 µg of homogenate protein was used for the two digestion methods, filter aided sample preparation (FASP) and suspension traps (S-Trap). The FASP was carried out as previously described [70] using Amicon Ultra 0.5 mL centrifugal filters at 10-kDa molecular weight cut-off (MWCO) (Merck Millipore, Nottingham, UK). Briefly, homogenate proteins were solubilised and denatured with 10% (w/v) sodium deoxycholate by incubation at room temperature for 10 min. Followed by disulfide bonds reduction with 100 mM DTT by incubation at 56°C for 30 min in a thermomixer. After conditioning the filter units by 100 mM Tris-HCl buffer (pH 8.5) the sample was transferred to the filter unit, then centrifuged at 14000*xg* at room temperature for 30 min. The sample was incubated with 100 µl of 50 mM iodoacetamide (IAA) in the dark for 30 min at room temperature to alkylate the reduced cysteine and prevent reformation of disulphide bonds. To remove sodium deoxycholate the sample was washed twice with 200 µl of 8 M urea in the 0.1M Tris buffer (pH 8.5). To reduce urea concentration a buffer exchange step was performed by two washes with 200 µl of 1 M urea in 50 mM ammonium bicarbonate (AmBic) (pH 8.5). For each wash centrifugation at 14000*xg* at room temperature for 20 min was carried out. The filtrate was transferred into a new collection tube and 80 µl 1 M urea in 50 mM AmBic was added to it to prevent sample evaporation during digestion standing time. Protein digestion was achieved by adding Lys C (enzyme to protein ratio 1:50, for 3-4 hours, at 30°C) prior to trypsin as it cleaves only at lysine residues and may facilitate digestion to completeness in combination with trypsin. Later trypsin was added (enzyme to protein ratio 1:25 for 12 hours at 37°C). After digestion completed peptides were recovered from the filter unit by centrifugation at 14000*xg* for 20 min followed

by addition of 100 µl of 500 mM sodium chloride to the filter and centrifuged (14000 *xg*, 20 min) for a second collection. The collected peptides were acidified with trifluoroacetic acid, then desalted using C18 spin columns according to the manufacturer's instructions (Nest group, USA). The peptides were lyophilised to dryness using a vacuum concentrator at 30ºC and with vacuum in aqueous mode then stored at −80°C until mass spectrometric analysis.

S-Trap method was carried out using Spin columns (Protifi, NY, USA) and adapted from the manufacturer's procedure and (*Zougman et al. 2014*)[39] with some modifications. Briefly, homogenate proteins were reduced using 20 mM DTT for 1 h at 37 °C then alkylated with 50 mM IAA for 15 min incubated in the dark. Lysis buffer SDS (5% (w/v) final concentration) and 50mM Tris/HCl (pH 7.6) was added to the sample. Phosphoric acid solution (1.2% final concentration) was added to the sample. In the Spin column, binding buffer 90% methanol and 100 mM Tris/HCl (pH 7.1) was added in 6:1 ratio to the acidified sample. The sample was loaded into the spin column and centrifuged at 2800 *xg* for 2 min. The flow-through collected and reloaded, the step was repeated three times. Washing with 100 µl of the binding buffer and centrifuging (2800 *xg* for 2 min) was performed three times. 50 mM AmBic solution was added to the spin column and centrifuged at 2800 *xg* for 1 min. For proteins digestion Lys C (1:50 ratio) was added for 2 hours at 30°C. Then trypsin (ratio 1:25) was added for 12 hours at 37°C. The spin column was centrifuged at 2300 *xg* for 2 min and the filtrate was collected according to the manufacturer's elution procedure. The eluted peptides were lyophilised to dryness using a vacuum concentrator and stored at −80°C until further analysis.

3.3.5. Subcellular fractionation

3.3.5.1. Homogenate and S9 fractions

In order to determine the appropriate fraction for the targeted proteins in in-vitro CD models, the expression profiles of DMETs in homogenate and S9 fractions were analysed. This was done utilising one inflamed CD colon sample and one HN-cancer ileum sample (Table 3.1). Homogenate fractions were generated based on the previously mentioned elution method. The S9 fractions were generated by further ultracentrifugation (OptimaTM L-100, Beckman Coulter, Inc., Fullerton, CA) of a portion of the homogenate at 10,000 *xg* for 15 min at 4°C. The resultant supernatant representing the S9 fraction was collected, while the formed pellet representing the mitochondria, peroxisomes, intact cells lysosomes and nuclei was discarded. Homogenate and S9 samples were stored at -80°C for further processing. Both fractions were digested by FASP method as mentioned above to be analysed by LC-MS/MS.

3.3.5.2. Activity of cytochrome P450 enzymes

Furthermore, cytochrome C reductase (CCR) activity assay was used to indicate the kinetic activity of cytochrome P450 enzymes in the homogenate and the S9 fractions produced by elution and scraping enterocytes isolation methods. CCR assay measures the cytochrome P450 reductase activity by converting the oxidised form of cytochrome C to the reduced form via the donation of hydrogen from NADPH creating NADP. The assay was carried out as per the kit instructions. In brief, cytochrome c working solution was prepared by mixing the assay buffer (300 mM potassium phosphate buffer (pH 7.8) and 0.1mM EDTA) with cytochrome C and amount of the homogenate and S9 fraction from each isolation method equivalent to 1 mg of tissue at 25ºC. The reaction was started by adding 100 µL of 0.85 mg/mL NADPH. Absorbance was measured at 10sec interval over 7 minutes (the first 2 minutes were to establish the baseline before adding NADPH) at 550 nm on a kinetic mode using a Jenway 7315 UV-Visible spectrophotometer (Thermo Fisher Scientific).

3.3.6. QconCAT design and characterization

3.3.6.1. TransCAT design

Intestine related transporters (Apical Sodium-dependent Bile acid Transporter (ASBT), H+/Peptide Cotransporters (PEPT1), MonoCarboxylate Transporter1 (MCT1) and Organic Anion Transporter 4A1 (OATP4A1)) and Alkaline Phosphatase enzymes (ALPI and ALPL) were designed and added to previously designed membrane proteins QconCATs.[54,71] The peptides were chosen based on previous studies on intestine tissue, the changes in protein expression among the intestinal segments, and the *2018 International Transporter Consortium* recommendations.[72] The TransCAT includes transporters related to other organs such as the liver, which are also relevant to the intestine. Table S3.1 contains a complete list of TransCAT transporters as well as their unique peptides. The QconCAT is being designed so that it can be used as an internal standard in future targeted proteomic works of CD and healthy intestinal tissues to quantify the targeted DMETs.

The criteria for designing and selecting surrogate peptide are carried out as in (*Russell et al. 2013*)[54] and (*Prasad and Unadkat. 2014*)[73]. In summary, the Uniprot Knowledge Base Human (http://www.uniprot.org/) was used to extract the desired proteins' accession, sequences and their cellular localisation. Protein *in silico* digestion was carried out using Protein Prospector (MS Digest) (http://prospector.ucsf.edu/). Uniqueness of the surrogate peptides to human were

checked by Peptide uniqueness checker (https://www.nextprot.org/tools/peptide-uniqueness-checker). Peptides presence in bacteria was double checked using Uniprot BLAST (http://blast.ncbi.nlm.nih.gov/Blast.cgi), this is important for the intestine as a contamination might occur due to the bacterial flora in the gut. Post-translational modifications (PTM) was checked using Expasy peptide mass (https://www.expasy.org/). Isoelectric point and the molecular weight for each peptide was determine using (http://isoelectric.org/calculate.php).

The suitability of surrogate peptides for quantification and detection determines their selection, thus, the following criteria were used. Peptide length between 6 and 22 amino acids, transmembrane regions are excluded by checking topology in Uniprot input, PTM should be avoided because they change the peptide mass (potential phosphorylation checked in http://www.cbs.dtu.dk/services/NetPhos/, N-glycosylation in http://www.cbs.dtu.dk/services/NetNGlyc/ and O-glycosylation in http://www.cbs.dtu.dk/services/NetOGlyc/), genetic polymorphism was checked in https://www.ncbi.nlm.nih.gov/snp and if allele frequency is lower than 1% then its excluded. Peptides with methionine (M) (susceptible to oxidation) and cysteine (C) (susceptible to alkylation) were excluded. Peptide sequence with adjacent arginine (K) or lysine (R), close to the site of cleavage such as KK, RR, KR, & RK was also excluded as it might cause incomplete trypsin digestion. Sequence contains KP & RP was also excluded as it is not cleaved by trypsin. Additionally, some extra exclusion criteria were applied whenever possible (see supplementary material).

Based on the above steps and criteria two peptides (except PEPT 1, three peptides) were selected as a surrogate peptides to be introduced in the TransCAT (Table 3.2).

Table 3.2. List of the added TransCAT proteins, their substrate, and their surrogate peptides.

Target	Surrogate Peptides	Substrate
ASBT (SLC10A2)[74,75]	IAGLPWYR	Fatty acids and cholesterol based drugs.
	LWIIGTIFPVAGYSLGFLLAR	
PEPT1 (SLC15A1)[76,77]	GNEVQIK	β-lactam antibiotics, angiotensin-converting enzyme inhibitors, thrombin inhibitors, thyrotropic-releasing hormone, aminocephalosporins, amino lactam antibiotics, acetylcholinesterase inhibitors,
	TLPVFPK	
	HTLLVWAPNHYQVVK	

		bestatin, renin inhibitors, prodrug of acyclovir, and valcyclovir.
MCT1 (SLC16A1)[78–80]	SITVFFK	Salicylic acid, valproic acid, statin acid, NSIDs, and fluoroquinolones.
	DLHDANTDLIGR	
OATP4A1 (SLCO4A1)[81]	YEVELDAGVR	Oestrogens, prostaglandins, thyroid hormones, taurocholate, benzylpenicillin, and unoprostone.
	ILGGIPGPIAFGWVIDK	
ALPI[82–85]	GFYLFVEGGR	Estramustine phosphate, etoposide phosphate, oxymethylphosphate prdrugs for lopinavir & ritonavir, benzimidazole phosphate, fosamprenavir phosphate prodrug of amprenavir, and dinitrobenzamide mustards (DNBM) are a prodrug group for anticancer medications.
	NLILFLGDGLGVPTVTATR	
ALPL	LDGLDLVDTWK	
	ANEGTVGVSAATER	

For TransCAT quantification, non-naturally occurring peptide (NNOP) (VGFLPDGVIK) and GluFib peptide EGVNDNEEGFFSAR[54] were added. An Escherichia coli ribosomal core was fused to the QconCAT sequence for improved expression and a His-affinity tag was added for purification as described previously.[86] The designed TransCAT Mw and average isoelectric point (IP) was 100 kDa and 6, respectively. The TransCAT was expressed and purified by PolyQuant® (GmbH, Germany (http://www.polyquant.com/)) as previously described.[87]

3.3.6.2. Characterization of the TransCAT

One-dimensional sodium dodecyl sulphate-polyacrylamide gel electrophoresis (1D-SDS-PAGE) was used to determine the purity of the synthesised TransCAT. 10 µl of the TransCAT and 5 µl of the molecular weight marker (Precision Plus ProteinTM Standards) were separately mixed with loading buffer (500 mM DTT, NuPAGE and water) and loaded onto 5% stacking gel (30% acryl-bisacrylamide, 1.5 M Tris-HCl (pH 6.8), 10% SDS, 10% ammonium persulfate, 1 µl/ml TEMED and water) and overlaid on 12% resolving gel (pH 8.8), resolved using a mini-Protean 3 system (Bio-Rad). Staining of the gel was done with 0.1 % Coomassie Brilliant Blue (Sigma, UK) to view the protein bands. Total protein content of TransCAT was determined using Bradford assay (ThermoFisher Scientific, Hemel Hempstead, UK) in triplicate following manufacturer protocol.[88] Then TransCAT was subjected to FASP protocol (using 10 µg of TransCAT and diluted NNOP 1:5 from 1 nmol/µl stock concentration), this followed by LC-

MS/MS analysis. Sequence coverage of TransCAT and labelling efficiency of the incorporated R and K was determined by the intensity ratios of the light (unlabelled) to the heavy (labelled) peptide. Finally, TransCAT concentration (mg/ml) calculated from the following equation (1):

$$[QconcAT](mg\ /\ ml) = \frac{\left(\frac{H}{L}\right) \times pmol\ of\ NNOP \times Mwt}{V} \qquad \textbf{(1)}$$

Where (H/L); is the intensity ratio of the heavy NNOP incorporated in TransCAT to the light NNOP added after correction based on its labelling efficiency, *Mwt*; is the molecular weight of the TransCAT in kDa, *V* is the digestion volume used.

3.3.7. Liquid Chromatography Tandem Mass Spectrometry (LC-MS/MS)

Homogenate digest prepared by enterocyte elution method from histologically normal ileum tissue, was analysed by two mass spectrometers. Lyophilised peptides re-suspended in 3% (v/v) acetonitrile in water with 0.1% (v/v) formic acid were analysed by Orbitrap Elite and QExactive HF Hybrid Quadrupole-Orbitrap (QE) mass spectrometers over a 90 min gradient.

For the Elite mass spectrometer, analysis was executed using an UltiMate 3000 Rapid Separation LC RSLC, Dionex Corporation, Sunnyvale, CA, USA) coupled to an Orbitrap Elite mass spectrometer (Thermo Fisher Scientific, Waltham, MA). Peptides from 1 µl of the sample were separated using a multistep gradient from 95% mobile phase A (0.1% formic acid in water) and 5% mobile phase B (0.1% formic acid in acetonitrile) to 7% B at 1 min, 22% B at 58 min, 30% B at 73 min and 60% B at 75 min at 300 nl/min, on a Charged Surface Hybrid (CSH) C18 analytical column (75 mm x 250 µm i.d., 1.7 µm particle size) (Waters, UK). Peptides were selected for fragmentation automatically by data-dependant acquisition (DDA). DDA MS scan mass window was set at 350−1500 m/z, and top three peptides with 2^+, 3^+ charge state ions were selected for fragmentation. Dynamic precursor ion exclusion was used with duration of 60 seconds.

For the QE mass spectrometer, peptides were analysed utilising an UltiMate® 3000 Rapid Separation LC (RSLC, Dionex Corporation, Sunnyvale, CA) coupled to a Q-Exactive HF Hybrid Quadrupole-Orbitrap mass spectrometer (Thermo Fisher Scientific, Waltham, MA). Mobile phase A (0.1% formic acid in water) and mobile phase B (0.1% formic acid in acetonitrile), and peptides were eluted on CSH C18 analytical column (75 mm x 250 µm inner diameter, 1.7 µm particle size) (Waters, UK). A 1 µl aliquot of the sample was transferred to a

5 µl loop and loaded onto the column at a flow rate of 300 nl/min for 5 min at 5% B. The loop was then taken out of line and the flow was reduced from 300 nl/min to 200 nl/min in 0.5 min. Peptides were separated using a gradient from 5% to 18% B in 63.5 min, then from 18% to 27% B in 8 min, and finally from 27% B to 60% B in 1 min. The column was washed at 60% B for 3 min before re-equilibration to 5% B in 1 min. At 85 min, the flow was increased to 300 nl/min until the end of the run. Peptides were selected for fragmentation automatically by DDA with an MS scan window between 300 to 1750 m/z. The top 12 peptides with a charge state of 2^+, 3^+ were selected with dynamic exclusion set at 15 seconds.

3.3.8. Data analysis and protein identification and quantification

Data analysis was carried out using MaxQuant version 1.6.1.0. (Max Planck Institute for Biochemistry, Munich, Germany). The peptide MS/MS database search was applied against a UniProtKB human proteome fasta file of 74788 protein entries including the TransCAT peptides (UniProt, May 2017 (http://www.uniprot.org/)). The total protein approach (TPA) was used for quantification of the detected DMETs. This was done by assigning proteins to their unique detected peptides. The total signal intensity of the peptides assigned for each protein was used to quantify the protein abundance according to Equation (2).

$$[\text{Protein}](\text{pmol/mg}) = \frac{\left(\sum_{p=1}^{n} Ip \Big/ \sum Isample\right)}{Mwt} \qquad \textbf{(2)}$$

Where I*p*; is the sum of all peptides intensities of a desired protein relative to Isample; the sum of all peptides intensities in the sample (expressed in parts per million (PPM)). Each desired protein PPM value is normalised by its Mwt (molecular weight in kDa) to give abundance value in (pmol/mg).

In order to unify the units and rectify the abundance value of the required DMETs in the ileum if loss occurred owing to enterocyte extraction by elution and scraping procedures, [89,90] scaling up of the proteins expression was performed by scaling back the homogenate weight to the initial mucosal weight. Equation (3) was used to calculate the total abundance of DMETs in the small intestine in each homogenate portion.[89]

$$Protein\ content\ (nmol) = \frac{\begin{matrix} Homogenate\ protein\ expression\ (pmol/mg\ protein) \\ \times\ Protein\ content\ of\ enterocyte\ homogenate\ (mg/g\ mucosa) \\ \times\ Weight\ of\ enterocytes\ (720\ g) \end{matrix}}{1000} \quad \textbf{(3)}$$

Where 720 g; the weight of enterocytes in the small intestine when a total volume of enterocytes of 720 ml^3 and a density of 1 g/mL are assumed.

The number of identified DMETs and their abundance level after correction (if applicable) was used to compare between the various methods/instruments used in each step. In addition, activity of cytochrome P450 enzymes in the homogenate and S9 subcellular fractions prepared by elution and scraping enterocytes isolation methods were measured and compared. For the proteolytic digestion methods used (FASP and S-Trap), percentage of misscleaved peptides produced in each method was also compared. Statistical data analyses, proteins quantification and abundance comparisons (relative ratios) were performed using Microsoft Excel v16.23.

3.4.Results

3.4.1. Enterocyte isolation method

The histologically normal ileum tissue was visually inspected under the microscope (Figure S3.1), the images showed that enterocytes integrity was successfully disrupted from the lamina propria and released their content by scraping and elution by chelation.

To investigate whether different methods of enterocytes isolation alter DMETs abundance, both protocols (elution and scraping) were applied on the same human ileum tissue. The homogenate total protein content was measured (Figure 3.2), where homogenate by scraping showed higher protein content than elution. The total number of identified peptides in homogenate prepared by elution was 13384 after LC-MS analysis, compared to 14667 by scraping. The total number of identified proteins in homogenate prepared by elution was 2335 compared to 2639 by scraping. However, when just the identified DMETs were considered, 35 metabolising enzymes (21 CYPs & UGTs and 14 non-CYP-non-UGT) were identified in homogenate prepared by elution vs 28 (10 CYPs & UGTs and 18 non-CYP-non-UGT) prepared by scraping. While 67 transporters were identified in homogenate prepared by elution compared to 55 by scraping.

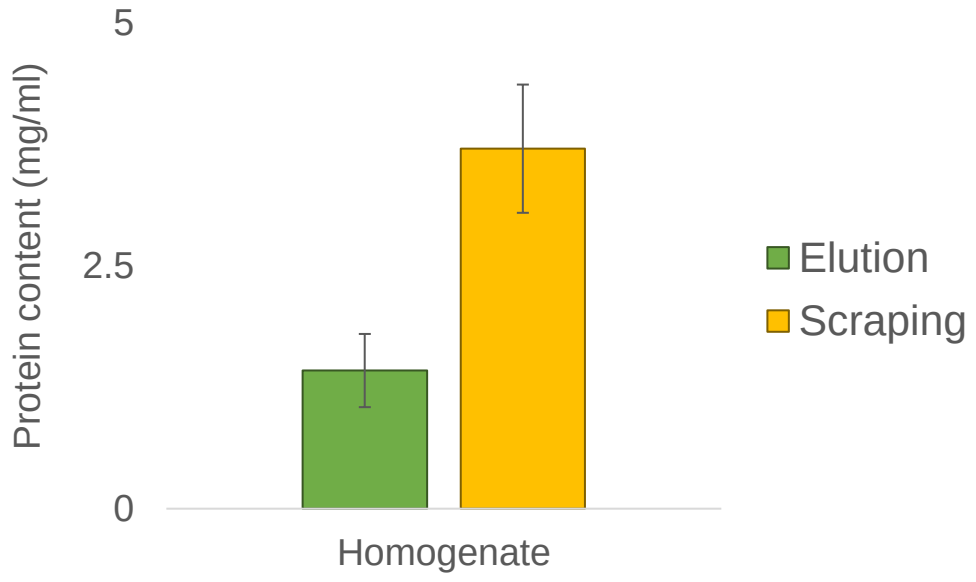

Figure 3.2. *The protein content (mg/ml) of the homogenate generated by enterocytes elution and scraping approaches from the same histologically normal ileum sample. The data was obtained after a BCA assay prepared in triplicate. The values are given as Mean±SD.*

DMETs abundance scaled back to be per mg of mucosal tissue rather than per mg of homogenate to unify the measurement by the two methods and correct for loss if occurred in isolation by scraping or elution. The expression level difference before and after correction for each isolation method is shown in Figure 3.3. After applying the small intestine total protein content, the mean relative difference of DMETs expression in homogenate prepared by elution to homogenate prepared by scraping was 9 before scaling up and 3 after scaling up. CYP3A4 abundance showed the highest difference in its expression between the two methods. The relative difference of CYP3A4 expression in homogenate by elution (32.6 nmol) to homogenate by scraping (1.9 nmol) was ~17 after scaling up and ~57 (4 and 0.07 nmol by elution and scraping, respectively) before scaling up. As a result, the expression difference between the two methods' ratios before applying the correction lower by ~ 3.4 times for CYP3A4 and lower by 3 times on average of all other DMETs. Total content difference of quantified DMETs in homogenate generated by mucosal scraping or enterocyte elution provided in Figure 3.4 after being scaled up. The majority of the DMETs displayed a higher abundance after enterocyte elution by chelation compared to mucosal scraping.

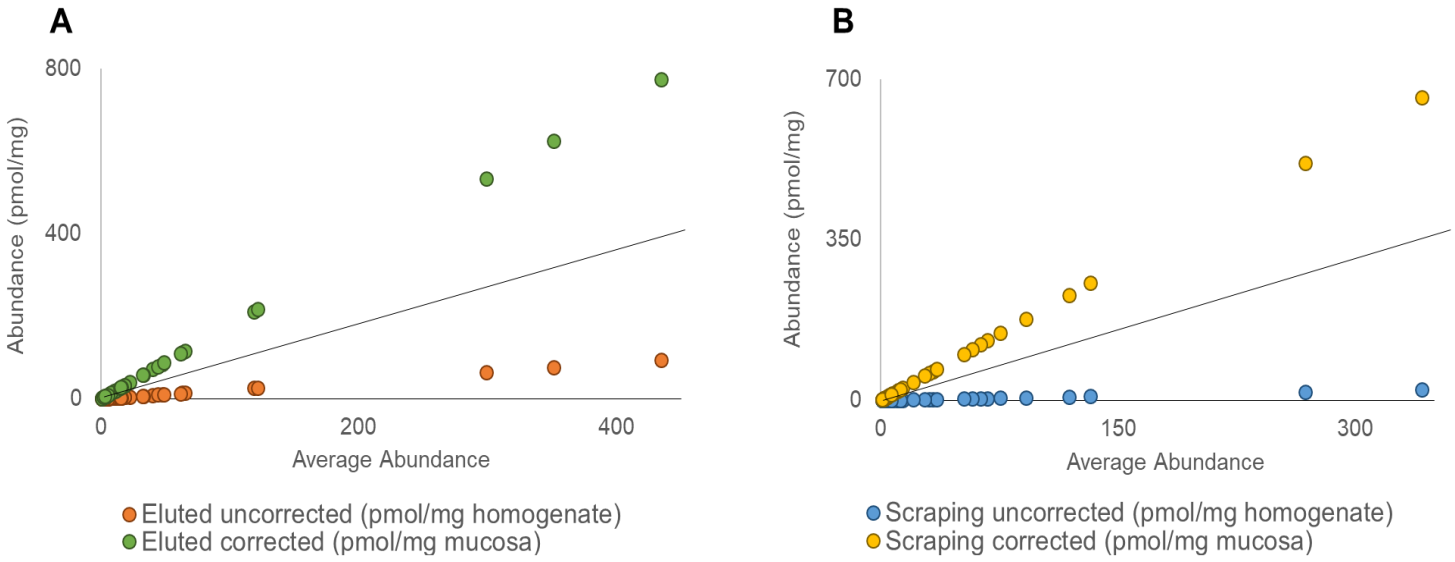

Figure 3.3. *Comparison of protein expression levels (pmol/mg) of detected DMETs before and after scaling up of homogenate fraction prepared by* ***(A)*** *enterocytes elution by EDTA chelation and by* ***(B)*** *mucosal scraping from the same histologically normal ileum sample*

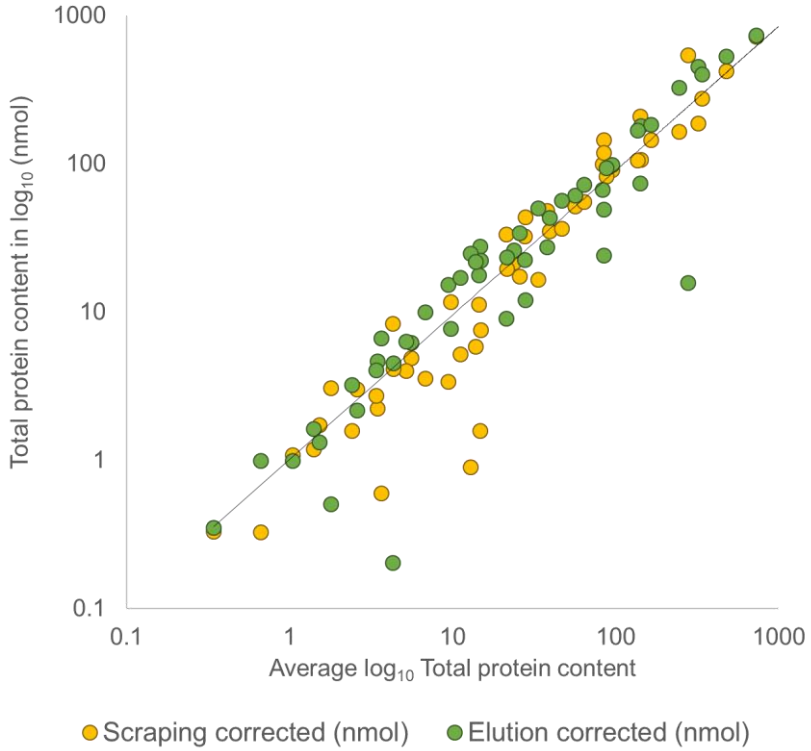

Figure 3.4. *Comparison of total protein content (nmol) after scaling up the abundance of DMETs in homogenate samples prepared by enterocytes elution and by mucosal scraping from the same histologically normal ileum sample.*

3.4.2. Proteolytic digestion method

Using the same homogenate fraction from HN-ileum, we investigated the effects of FASP and S-Trap protein digestion methods on the abundance of the discovered DMETs. The total number of identified peptides and proteins in FASP-digested sample was higher (18024 and 2938, respectively) than in the S-Trap (14106 and 2274, respectively) after LC-MS analysis (Figure 3.5). Similarly, FASP displayed higher number of detected DMETs, 44 metabolising enzymes (25 CYPs & UGTs and 19 non-CYP-non-UGT) were identified compared to 38 (20 CYPs & UGTs and 18 non-CYP-non-UGT) in the homogenate digested by S-Trap. In homogenate digested by FASP, 58 transporters were identified, compared to 46 by S-Trap. Moreover, with the FASP method, 17% of the detected peptides were misscleaveged and 37% with S-Trap. For quantification, DMETs abundance did not show a high difference between the two methods for most of the proteins (Figure 3.6). Generally, FASP had generally higher expression levels but this was seen with only small number of the targets.

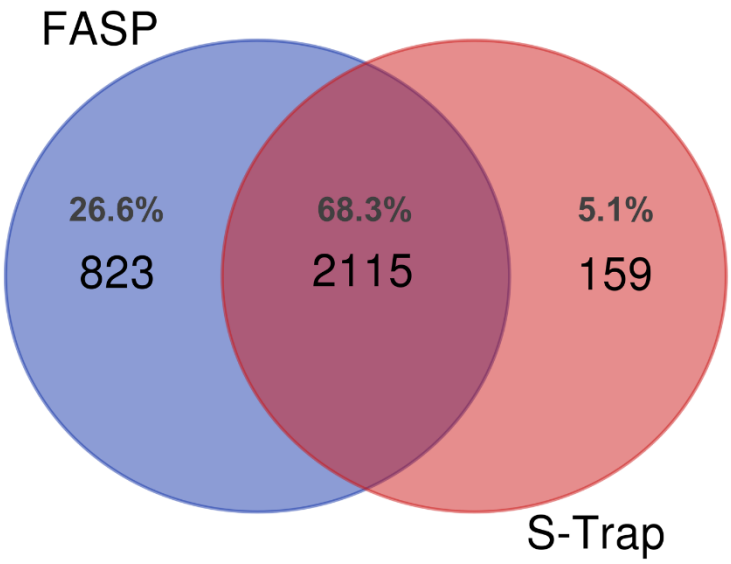

Figure 3.5. *Comparison of identified proteins generated from FASP and S-Trap methodologies of digested homogenate from the same histologically normal ileum tissue.*

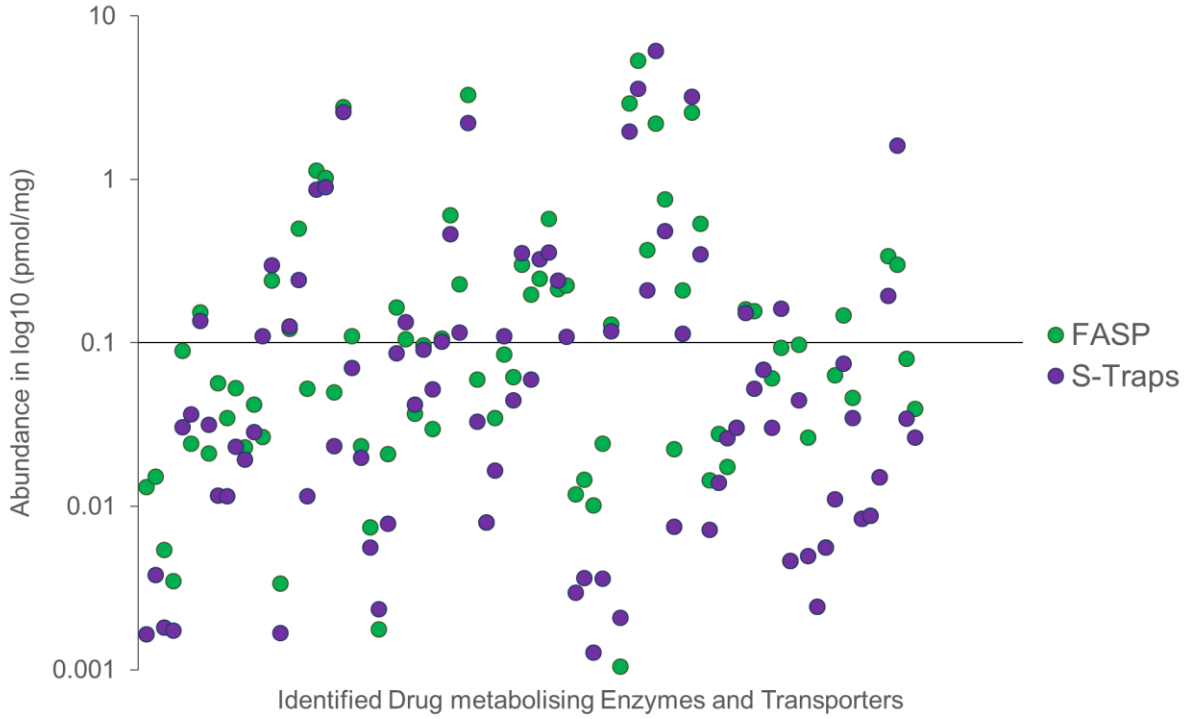

Figure 3.6. *Comparison of protein abundance values (pmol/mg) of detected DMETs in homogenate samples digested by FASP and S-Trap from the same histologically normal ileum sample.*

3.4.3. Subcellular fractionation

A homogenate and S9 fraction extracted from the same HN-ileum and CD-colon mucosa were compared to see if different subcellular fractions would yield better results of the identified DMETs. The protein content of the homogenate and the S9 for the ileum and the colon samples by the EDTA chelation method are shown in Figure 3.7.

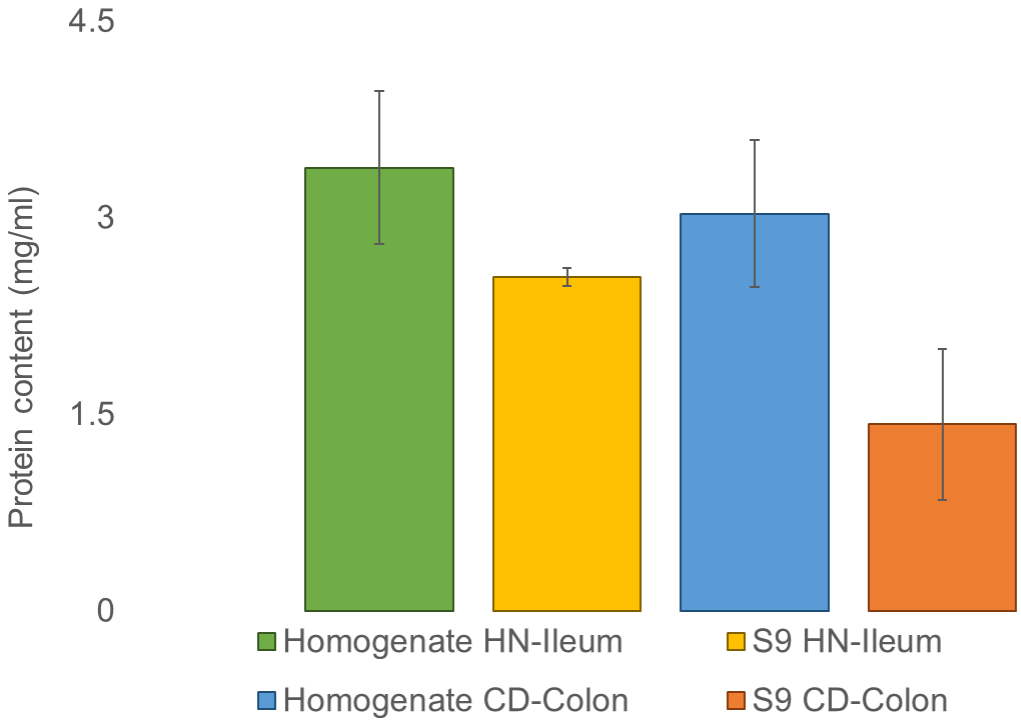

Figure 3.7. *The protein content (mg/ml) of the homogenate and S9 fractions generated by enterocytes elution by EDTA chelation from one histologically normal ileum sample (HN-Ileum) and one Crohn's disease colon sample (CD-Colon). The data was obtained after a BCA assay prepared in triplicate. The values are given as Mean±SD.*

The number of identified peptides and proteins in the starting homogenate for HN-ileum were slightly lower than the S9 fraction (6362 peptides and 1521 proteins in homogenate; 6430 peptides and 1544 proteins in S9). While a higher number of DMETs were identified in the homogenate fraction; 32 enzymes (18 CYPs &UGTs and 14 non-CYP-non-UGT) and 40 transporters compared to the S9; 29 enzymes (18 CYPs &UGTs and 11 non-CYP-non-UGT) and 37 transporters. For the CD-colon sample, the number of identified peptides was slightly

higher in the S9 compared to the homogenate fraction (7244 and 7192, respectively). While the number of proteins was higher in the homogenate compared to the S9 fraction (1757 and 1722, respectively). Also, homogenate consisted of a slightly higher number of enzymes (10 CYPs &UGTs and 10 non-CYP-non-UGT) and 38 transporters compared to the S9 (8 CYPs &UGTs and 10 non-CYP-non-UGT) and 34 transporters.

The expression level of the identified DMETs in the two fractions was compared, a higher abundance levels of the microsomal and membrane proteins were observed, while, cytosolic proteins showed low expression in the homogenate compared to the S9 in the HN-ileum sample (Figure 3.8) and in the CD-colon sample (Figure 3.9).

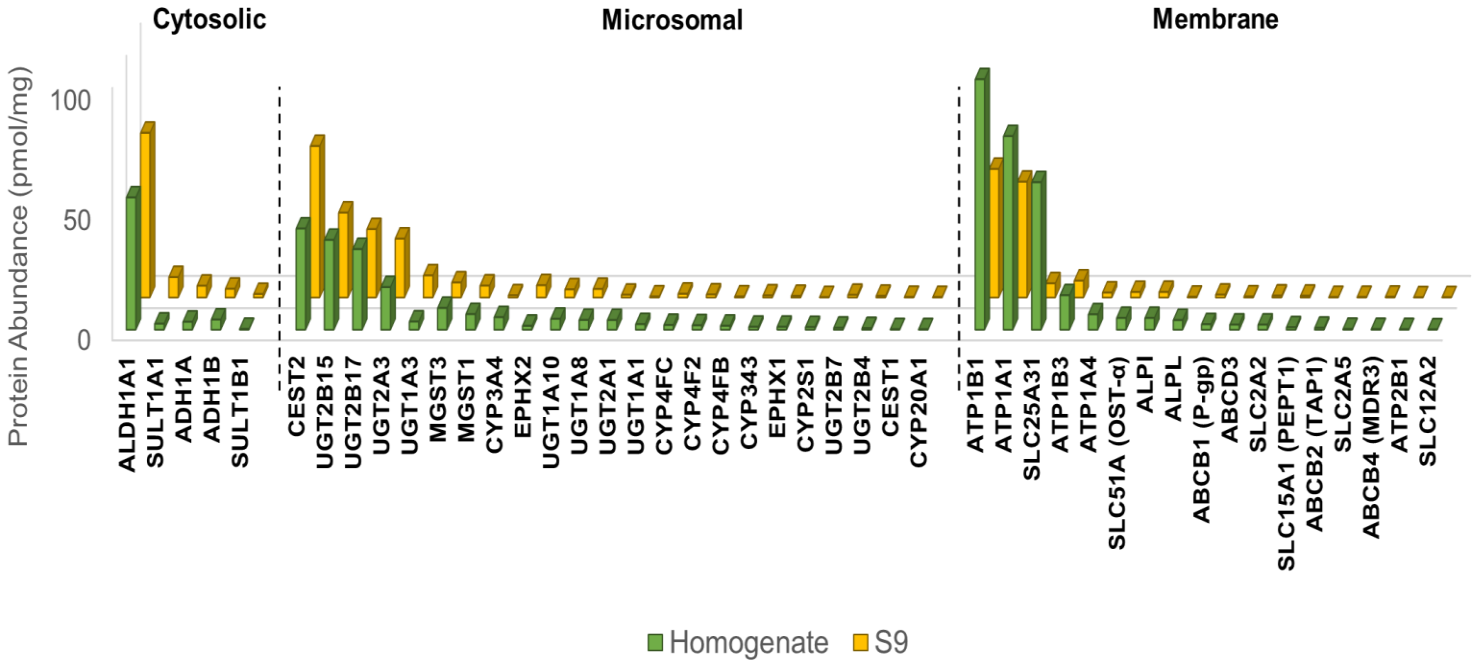

Figure 3.8. *Comparison of protein abundance (pmol/mg total protein) of detected DMETs in the homogenate and S9 fractions generated by enterocytes elution from the same histologically normal ileum sample. Only cytosolic, microsomal and membrane enzymes and transporters detected in both fractions are included in the figure. Mitochondrial, nuclear and peroxisome enzymes and transporters are excluded as the S9 fraction only contain traces of them.*

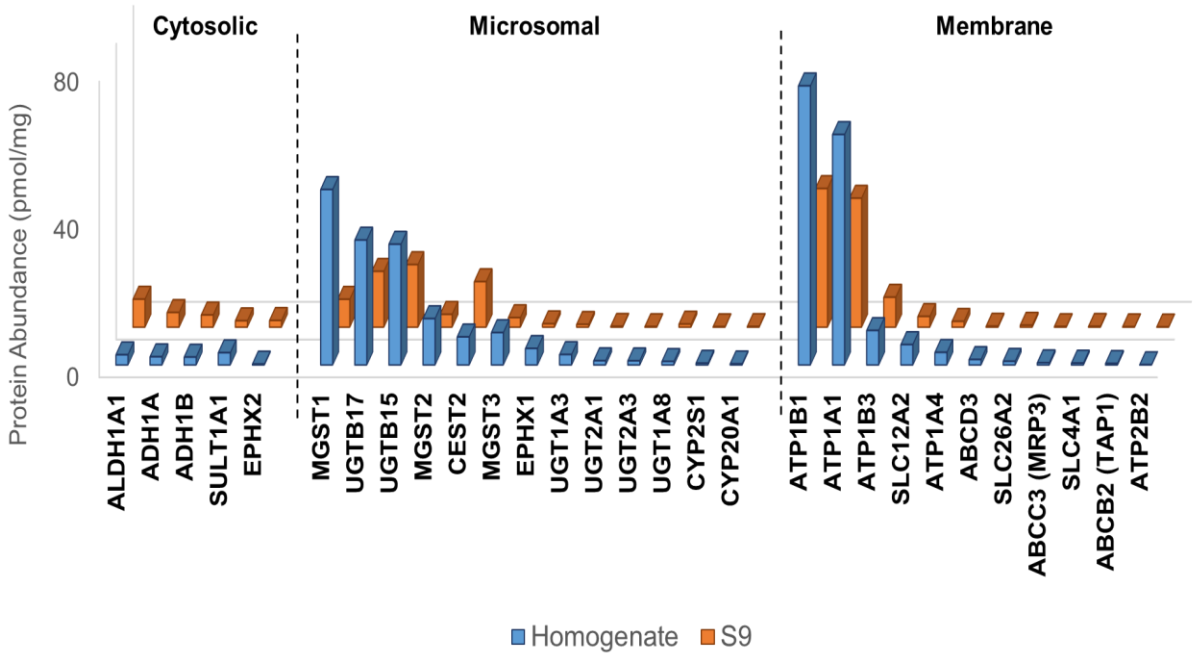

Figure 3.9. *Comparison of protein abundance (pmol/mg total protein) of detected DMETs in the homogenate and S9 fractions generated by enterocytes elution from the same Crohn's disease colon sample. Only cytosolic, microsomal and membrane enzymes and transporters detected in both fractions are included. Mitochondrial, nuclear and peroxisome enzymes and transporters are excluded as the S9 fraction only contain traces of them.*

Additionally, cytochrome P450 activity was determined by means of CYP reductase assay in both the homogenate and the S9 fraction extracted from HN-ileum tissue by elution and scraping methods. In comparison to scraping, cytochrome P450 activity was higher (~ 2 fold) in homogenate and S9 fraction prepared using elution method (Figure 3.10). The activity to assess cytochrome P450 enrichment within the S9 fraction from starting homogenates extracted by elution protocol showed a mean fold increase of 1.05 ± 0.75 in the S9 fraction versus the homogenate fraction. Homogenate fraction showed a mean fold increase of cytochrome P450 activity 1.13 ± 1.95 versus the S9 fraction in scraped sample.

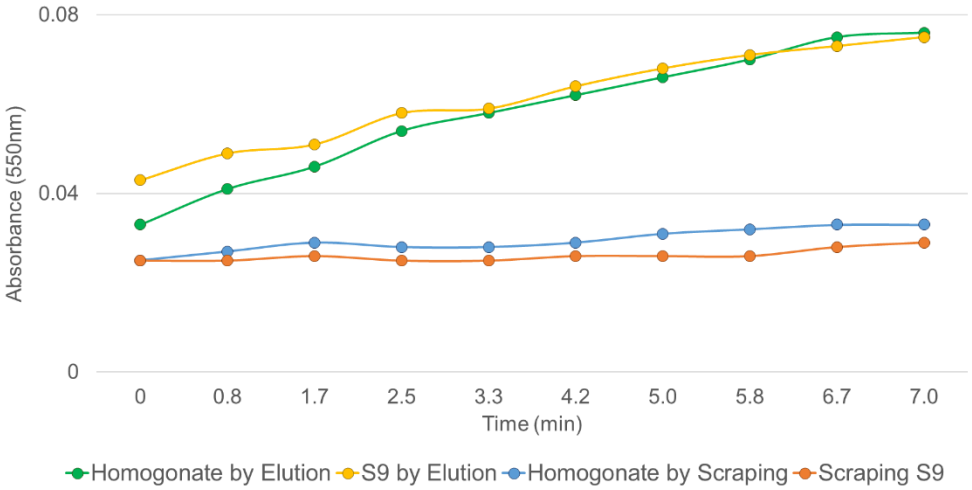

Figure 3.10. *Cytochrome P450 activity in the homogenate and S9 fractions generated by enterocytes elution and scraping methods in the same HN-ileum tissue.*

3.4.4. Characterization of the TransCAT

For the TransCAT purity assessment, the SDS-PAGE was conducted in house. Figure 3.11 shows clear band within the expected molecular weight with no other dominant intense bands. The overall molecular weight ~ 100 kDa indicated by the marker band, which is similar to the molecular weight of the synthesised TransCAT 100.111 kDa provided by PolyQuant®.

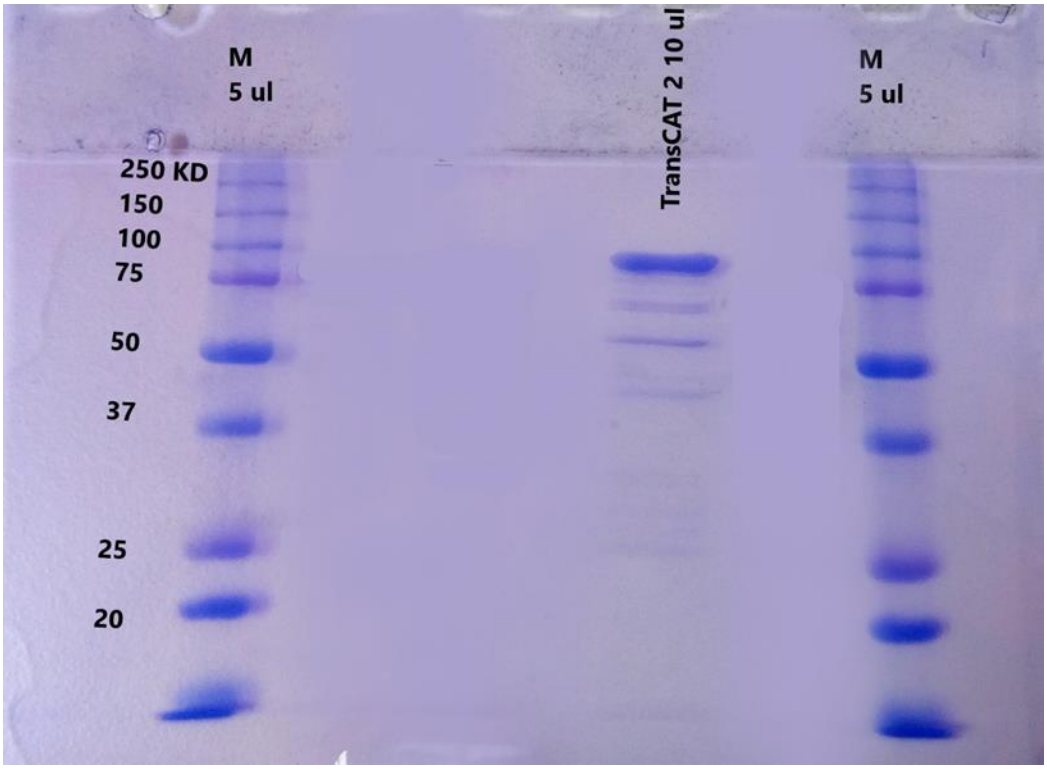

Figure 3.11. *SDS-polyacrylamide gel electrophoresis (SDS-PAGE) of TransCAT, M = molecular weight marker on the right and the left.*

TransCAT mean protein concentrations from in house Bradford assay (0.79±0.02 mg/ml) and LC-MS/MS analysis using the NNOP known abundance (1.20±0.15 mg/ml) are on agreement with the PolyQuant® results (0.78 mg/ml and 1.15 mg/ml from Bradford and LC-MS/MS analysis, respectively). 61 out of 66 peptides were identified (92% recovery) using LC-MS/MS analysis. The TransCAT sequence with all detected peptides are shown in Figure S3.2 The total number of amino acids in TransCAT sequence is 912 including the his-tag and the ribosomal core. Around 16% of all the detected peptides were miscleaved (301 out of 1827), where, the target peptides showed 34% misscleaveges. The identified peptides have been detected under variable intensities at different retention times (Figure S3.3).

The 13C-labelling efficiency of lysine (K)-ending peptides was (98.5 ± 0.54%, n = 35), which is higher than arginine (R)-ending peptides (95.5 ± 0. 62%, n = 34) as shown in Figure 3.12.

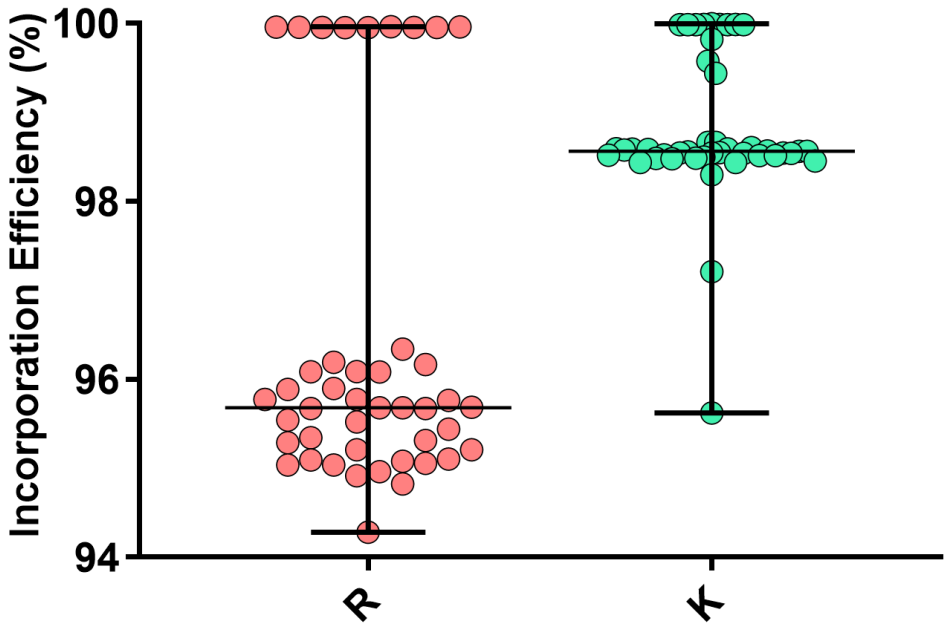

Figure 3.12. *Scatter graph showing incorporation of [13C6]-lysine (K) and [13C6]-arginine (R) in the fused TransCAT. Higher incorporation of labelled K than R is observed in the expressed QconCAT (R-incorporation = 95.5± 0.62% (mean±SD), n= 34 peptides; K-incorporation = 98.5± 0.54% (mean±SD), n = 35 peptides). Horizontal lines representing median and maximum and minimum rang.*

3.4.5. Liquid Chromatography Tandem Mass Spectrometry (LC-MS/MS)

Proteins and peptides of the identified DMETs generated using Elite and QE spectrometers were compared from the same HN-ileum sample digested by FASP. QE was found to outweigh the results generated by Elite in terms of the number of identified peptides and proteins (16342 and 2939, respectively for QE) (6406 and 1543, respectively for Elite). Furthermore, in terms of quantification of detected DMETs, QE was capable to provide information of 43 metabolising enzymes (24 CYPs & UGTs and 19 non-CYP-non-UGT) and 57 transporters. For the Elite, 29 metabolising enzymes (17 CYPs & UGTs and 12 non-CYP-non-UGT) and 38 transporters were detected (Figure 3.13).

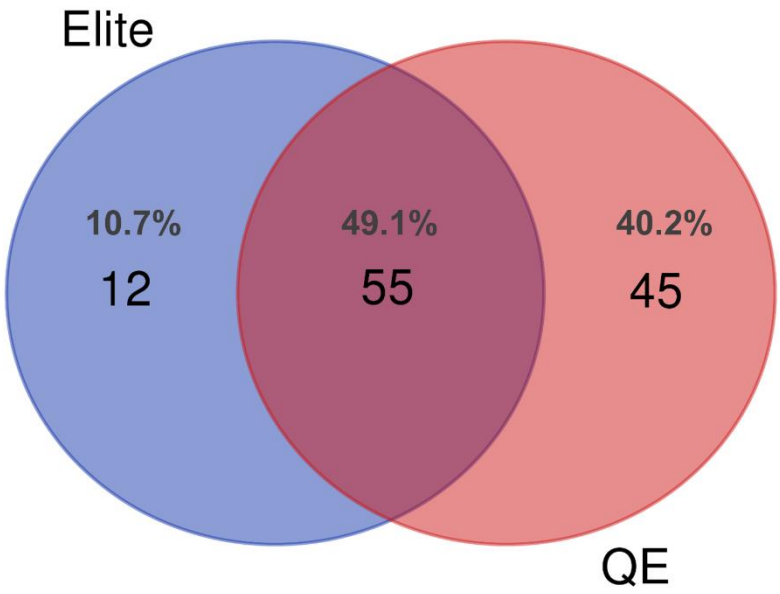

Figure 3.13. *Comparison of identified DMETs (CYPs, UGTs, non-CYP-non-UGT enzymes and transporters) generated from Elite and QE spectrometers. The same homogenate sample from HN-ileum tissue was digested by FASP and enterocytes isolated by EDTA elution method.*

3.5.Discussion

Different LC-MS/MS proteomic methodologies carry a substantial amount of potential variations which are represented in DMETs abundance levels. Thus, the variable profiles resulted as a result of these procedures could be due to any stage of the following methods: tissue isolation, homogenization, fraction extraction, digestion, LC-MS instrument and data analysis software.[11] There are no ideal procedures applied through different stages of LC-MS/MS proteomics. Determination of the most suitable proteomic methodology to be applied on the sourced intestinal samples from ileum and colon (inflamed CD, normal CD and healthy) was performed on the following steps: enterocyte isolation, subcellular fraction, digestion and LC-MS/MS spectrometer.

The use of the different LC-MSMS approaches is to ensure that we are able to quantify the desired targets based on our samples nature, small size and laboratory facilities within the available budget without compensation for quality. These steps are necessary to be taken as the available literature data of DMETs expression from CD samples are mainly mRNA or immunoblotting, hence, no prior investigation of the different approaches in a similar set of samples. Additionally, here we wanted to cover a large number of DMETs, thus, selecting a method that can cover targets located in different subcellular fractions and can be detected and analysed in the same run is crucial. This only can be done after applying the different techniques to select an isolation method and a fraction that has low contaminants, cause minimal loss of the starting material and achieve sample enrichment and separation for the main targeted proteins in the different subcellular fractions where the desired proteins are present. The best internal standard option and most cost effective to use when targeting a large number of proteins should allow incorporation of a large number of proteins that can be analysed and preferably digested with the sample at the same time. The digestion method most be combatable with the complex nature of the samples and ensure the sample purification, protein denaturing, solubilisation, complete digestion and peptides recovery.

The focus of our work is to quantify phase I and phase II metabolising enzymes, as well as uptake and efflux transporters, in intestinal tissue. These proteins are expressed in different subcellular fractions of the enterocytes which are needed to be isolated to allow for reliable DMETs absolute quantification. Assessment of the impact of enterocyte isolation methodology on DMETs abundance is carried out, based on the nature and the size of the different available intestine samples to obtain homogenate fraction and further subcellular fractionation if needed.

Comparison between the enterocytes isolation methods showed superiority of the elution by calcium chelating agent EDTA over the scraping method with our sample in terms of the detected desired proteins and their abundance. Sufficient material was produced from elution method to obtain homogenate fraction and further subcellular fractionation from most of the samples, only few samples with starting tissue size (<50 mg; insufficient mucosa/surface area) were limited to obtaining a homogenate fraction sufficient for proteomics analysis work required.

In comparative studies, the activity of CYP450 and UGT enzymes measured in the enterocytes isolated by the EDTA elution and scraping methods, favoured the elution method.[22,27] Previous studies used EDTA concentration of 5mM,[27,91] while 30 mM EDTA was used in our study as a previous report showed higher yield of enterocyte and villus material[24] specifically with colon tissue as it harder to deal with.[92] Our samples are fresh frozen, come in a variety of sizes, and there is no physical equipment available to bend the samples, especially the small ones, exposing only the mucosal surface to the elution solution. Therefore, using high concentration of EDTA after sodium citrate buffer facilitates isolation of more enterocytes and minimise contamination from material liberated from the serosal, fat and muscle layer.[93] Contamination with other cell types dilutes the obtained sample, lowering the chance of identify low abundance proteins. The enterocytes accounts for ~25% of mucosal wet weight[94] and 90% of the epithelium surface.[95] Thus, such contamination is not uncommon and should be considered.[96,97] Because of its severe mechanical nature, scraping is believed to cause higher loss in protein content[98], as a result, when comparing the protein concentrations of elution and scraping methods, it's only fair to account for such loss in the process in order to fairly compare between methods. This is achieved by scaling up the total protein content in the small intestine based on the initial mucosal weight used for the preparation of the homogenate fraction for each method. The relative difference between CYP3A4 expressions in homogenate by elution to homogenate by scraping decreased from ~57 to ~17 after scaling up, resulting in more accurate protein abundance results. The ratios of CYP3A4 expression between the two methods are ~3.4.

In two studies where CYP3A4 expression was measured in different fraction extracted by elution (210 pmol/mg microsomal protein)[25] and scraping (53.2 pmol/mg microsomal protein)[90] the ratio of CYP3A content was 3.9; when only considering the same intestine regions (duodenum and jejunum). After scaling back to the mucosal weight (homogenate),

applying the microsomal recovery calculation and calculating its total content in the small intestine the expression relative difference dropped to 1.4 (65.7 nmol; by elution and 48.1 nmol; by scraping).[89] Making CYP3 expression difference between the two methods' ratios ~3. Nonetheless, the general number of detected peptides and protein in scraped sample was higher than elution sample, the desired DMETs number and abundance were higher in elution sample. This suggests that protein abundance determination in the intestine may depend on enterocyte isolation method for certain proteins based on their expression location.

The FASP protocol uses urea that allows adequate proteins disruption in a series of steps. After that, there are processes to efficiently remove urea and detergent, in addition to, dual enzymatic cleavage on the filter.[37] These steps ensure that sufficient peptides are recovered, low artificial modifications and complete protein digestion. The same is done in the S-Trap protocol. The SDS in the SDS-protein suspension is adequately solubilised in a methanol solution to be filtered out prior of the trapped proteins are subjected to dual enzymatic digestion.[39,50] Both methods are capable of covering hydrophilic and hydrophobic proteins (Cytosolic, membrane and nuclear, etc.). When compared to S-Trap, FASP showed higher number of total identified proteins and DMETs, as well as better digestion efficiency as indicated by the misscleaved peptides, this is most probably due to the complex nature of the intestine tissue.

FASP repetitive centrifugation steps and using a molecular weight cut off (MWCO) filter may be more suitable for decreasing the complexity and more efficiently digesting and recovering protein and peptides in such a complex biological sample. S-Trap was found to be superior to FASP method in total number of identified proteins and quantitative reproducibility utilising SW480 colon cancer cell line.[49] Another study utilised bacterial lysate (*Klebsiella pneumoniae*), showed similarity in the number and abundance of the identified peptides and proteins with significant overlaps after S-trap digestion compared to FASP. Also, a comparable peptides miscleavage percent between FASP and S-Trap digestion was found.[51] Published intestine proteomic studies are mostly conducted on human intestine microsomal (HIM) and membrane (total and plasma membrane) fractions as they focus on major DMEs (CYP450s and UGTs)[45,90,99,100] and drug transporters[18,23,24,99,101]; only a few publications have included homogenates and S9 fractions and none has investigated the difference between the two.

The homogenate samples were utilised to quantify CYP3A4, P-gp abundance.[25] From S9 fraction, CES1, CES2, UGT1A1, UGT1A10, UGT2B7, UGT2B17, SULT1A1, SULT1A3, SULT1B1, and SULT2A1 were quantified.[32,33] The available information of DMETs

abundance in CD intestine is based on gene expression or immunoassay utilising tissue lysate, thus, the use of the previous mentioned fractions was not reported. The absence of comparative quantitative analysis of the intestine homogenate and S9 DMETs and lack of investigation of their proteins abundance contributes to uncertainty when choosing the most suitable fraction. In our HN and CD ileum and colon samples, homogenate fraction compared to the S9 fraction showed higher number of detected DMETs and, generally, higher abundance except for the cytosolic proteins. This is due to cellular localisation of the DMETs as the S9 fraction preserves the microsomal and cytosolic proteins while it discard the mitochondrion, peroxisome, lysosomal and nuclear proteins. Higher purification of the fraction will give better results for the proteins embedded in it, but also mean loss of targets that are not primary localised in the extracted fraction. Our primary targeted DMETs are expressed in the membrane, microsomes and cytoplasm, therefore, it is important to estimate their enrichment is the fraction used, as the fractionation process affects the protein's yield and activity. Cytochrome P450 enzymes activity used as an indicator of their enrichments, displayed a slight reduction of the microsomal marker CCR in the homogenate compared to S9 fraction. The homogenate fraction contains all intracellular proteins so it has a more complex nature and low purity. The slight enrichment difference in the Cytochrome P450 activity in the two fractions indicates that the homogenate fraction is not highly diluted compared to the more purified S9 fraction. Thus, homogenate fraction is the fraction of choice to use with our intestine samples to determine DMETs abundance.

The QconCAT technique minimises the variability caused by different processing of the analyte and the internal standard, as it is spiked with the biological sample at the same time and digested under the same conditions.[53,55] Designed surrogate peptides should follow a construction criteria that will ensure their optimal digestion, high flyability, ionisation, and detectability by LC-MS/MS.[73] Successful expression of a QconCAT is indicated by its detectability, purity, and labelling efficiency of the heavy peptides.[56] The designed TransCAT showed excellent labelling efficiency and high recovery for all the resulting K and R peptides after digestion. The remaining residue of the unlabelled peptides can be corrected for by deducting their ratios while quantifying. The resultant incorporation and recovery levels are sufficient for the development of quantitative assays using TransCAT.[54] Undetected peptides are mostly long hydrophobic peptides that are less readily eluted from the column.

The work to be carried out in this research targets a wide range of DMETs localised in different subcellular fractions, therefore, this necessitate the use of an LC-MS/MS instrument that provides a wide proteome coverage. Orbitrap Elite and QE comparison was conducted to determine their proteome coverage. QE was superior compared to Elite in the number of identified proteins and DMETs, thus, it is the chosen spectrometer for subsequent proteomic analysis work. The QE features (low detection limits, high sensitivity, rapid fragmentation and high mass accuracy)[62–64] qualifies it to be the suitable instrument for analysis of complex biological samples such as the intestine.

In conclusion, the current study allows identification of the most appropriate protocol/technique for enterocyte isolation, proteolytic digestion, subcellular fraction and mass spectrometer instrument for DMETs absolute quantification. This is to be applied with the ileum and colon tissues from different histological origins including diseased samples. The chosen methods are enterocyte harvesting by EDTA elution, FASP for protein digestion, homogenate fraction and QE spectrometer. Additionally, QconCAT design and construction of intestine relevant transporters is achieved.

3.6.References

1. Ladumor MK., Thakur A., Sharma S., Rachapally A., Mishra S., Bobe P., et al. A repository of protein abundance data of drug metabolizing enzymes and transporters for applications in physiologically based pharmacokinetic (PBPK) modelling and simulation. *Sci Rep* 2019;**9**(1):9709. Doi: 10.1038/s41598-019-45778-9.

2. Rostami-Hodjegan A. Physiologically Based Pharmacokinetics Joined With In Vitro–In Vivo Extrapolation of ADME: A Marriage Under the Arch of Systems Pharmacology. *Clin Pharmacol Ther* 2012;**92**(1):50–61. Doi: 10.1038/clpt.2012.65.

3. Harwood MD., Achour B., Neuhoff S., Russell MR., Carlson G., Warhurst G., et al. In Vitro-In Vivo Extrapolation Scaling Factors for Intestinal P-glycoprotein and Breast Cancer Resistance Protein: Part I: A Cross- Laboratory Comparison of Transporter Protein Abundances and Relative Expression Factors in Human Intestine and Caco-2 Cell. *Drug Metab Dispos* 2016;**44**(3):297–307. Doi: 10.1124/dmd.115.067371.

4. Couto N., Al-Majdoub ZM., Gibson S., Davies PJ., Achour B., Harwood MD., et al. Quantitative Proteomics of Clinically Relevant Drug-Metabolizing Enzymes and Drug Transporters and Their Intercorrelations in the Human Small Intestine. *Drug Metab Dispos* 2020;**48**(4):245–54. Doi: 10.1124/dmd.119.089656.

5. Erdmann P., Bruckmueller H., Martin P., Busch D., Haenisch S., Müller J., et al. Dysregulation of Mucosal Membrane Transporters and Drug-Metabolizing Enzymes in Ulcerative Colitis. *J Pharm Sci* 2019. Doi: 10.1016/j.xphs.2018.09.024.

6. Effinger A., O'Driscoll CM., McAllister M., Fotaki N. Predicting budesonide performance in healthy subjects and patients with Crohn's disease using biorelevant in vitro dissolution testing and PBPK modeling. *Eur J Pharm Sci* 2020:105617. Doi: 10.1016/j.ejps.2020.105617.

7. Johnson TN., Boussery K., Rowland-Yeo K., Tucker GT., Rostami-Hodjegan A. A Semi-Mechanistic Model to Predict the Effects of Liver Cirrhosis on Drug Clearance. *Clin Pharmacokinet* 2010;**49**(3):189–206. Doi: 10.2165/11318160-000000000-00000.

8. El-Khateeb E., Burkhill S., Murby S., Amirat H., Rostami-Hodjegan A., Ahmad A. Physiological-based pharmacokinetic modeling trends in pharmaceutical drug development over the last 20-years; in-depth analysis of applications, organizations, and platforms. *Biopharm Drug Dispos* 2021;**42**(4):107–17. Doi: 10.1002/bdd.2257.

9. Choudhuri S., Klaassen CD. Structure, Function, Expression, Genomic Organization, and Single Nucleotide Polymorphisms of Human ABCB1 (MDR1), ABCC (MRP), and ABCG2 (BCRP) Efflux Transporters. *Int J Toxicol* 2006;**25**(4):231–59. Doi: 10.1080/10915810600746023.

10. Hagenbuch B., Gui C. Xenobiotic transporters of the human organic anion transporting

polypeptides (OATP) family. *Xenobiotica* 2008;**38**(7–8):778–801. Doi: 10.1080/00498250801986951.

11. Bhatt DK., Prasad B. Critical Issues and Optimized Practices in Quantification of Protein Abundance Level to Determine Interindividual Variability in DMET Proteins by LC-MS/MS Proteomics. *Clin Pharmacol Ther* 2018;**103**(4):619–30. Doi: 10.1002/cpt.819.

12. Pond SM., Tozer TN. First-pass elimination. Basic concepts and clinical consequences. *Clin Pharmacokinet* 1984;**9**(1):1–25. Doi: 10.2165/00003088-198409010-00001.

13. van de Waterbeemd H., Gifford E. ADMET in silico modelling: towards prediction paradise? *Nat Rev Drug Discov* 2003;**2**(3):192–204. Doi: 10.1038/nrd1032.

14. Wegler C., Gaugaz FZ., Andersson TB., Wiśniewski JR., Busch D., Gröer C., et al. Variability in Mass Spectrometry-based Quantification of Clinically Relevant Drug Transporters and Drug Metabolizing Enzymes. *Mol Pharm* 2017;**14**(9):3142–51. Doi: 10.1021/acs.molpharmaceut.7b00364.

15. KA N., NA A., S M., M M., M M., G A., et al. Less label, more free: approaches in label-free quantitative mass spectrometry. *Proteomics* 2011;**11**(4):535–53. Doi: 10.1002/PMIC.201000553.

16. Ballad ST. The Regulation of Tight Junction Permeability During Nutrient Absorption Across the Intestinal Epithelium. *Annu Rev Nutr* 1995;**15**(1):35–55. Doi: 10.1146/annurev.nutr.15.1.35.

17. Giacomini KM., Huang S-M. Transporters in Drug Development and Clinical Pharmacology. *Clin Pharmacol Ther* 2013;**94**(1):3–9. Doi: 10.1038/clpt.2013.86.

18. Drozdzik M., Gröer C., Penski J., Lapczuk J., Ostrowski M., Lai Y., et al. Protein Abundance of Clinically Relevant Multidrug Transporters along the Entire Length of the Human Intestine. *Mol Pharm* 2014;**11**(10):3547–55. Doi: 10.1021/mp500330y.

19. Bradbury M., Stamler D., Baillie T., Sidhu S., Wood SG., Teva IS., et al. Protein abundance of pharmacokinetically relevant transporter proteins and metabolizing enzymes along the human intestine and in the liver: A comparative intra-subject study. *Drug Metab Pharmacokinet* 2018;**33**(1):S76–7. Doi: 10.1016/j.dmpk.2017.11.252.

20. Basit A., Neradugomma NK., Wolford C., Fan PW., Murray B., Takahashi RH., et al. Characterization of Differential Tissue Abundance of Major Non-CYP Enzymes in Human. *Mol Pharm* 2020;**17**(11):4114–24. Doi: 10.1021/acs.molpharmaceut.0c00559.

21. Tucker TGHA., Milne AM., Fournel-Gigleux S., Fenner KS., Coughtrie MWH. Absolute immunoquantification of the expression of ABC transporters P-glycoprotein, breast cancer resistance protein and multidrug resistance-associated protein 2 in human liver and duodenum. *Biochem Pharmacol* 2012;**83**(2):279–85. Doi:

10.1016/j.bcp.2011.10.017.

22. Galetin A., Houston JB. Intestinal and Hepatic Metabolic Activity of Five Cytochrome P450 Enzymes: Impact on Prediction of First-Pass Metabolism. *J Pharmacol Exp Ther* 2006;**318**(3):1220–9. Doi: 10.1124/JPET.106.106013.

23. Gröer C., Brück S., Lai Y., Paulick A., Busemann A., Heidecke CD., et al. LC–MS/MS-based quantification of clinically relevant intestinal uptake and efflux transporter proteins. *J Pharm Biomed Anal* 2013;**85**:253–61. Doi: 10.1016/j.jpba.2013.07.031.

24. Harwood MD., Achour B., Russell MR., Carlson GL., Warhurst G., Rostami-Hodjegan A. Application of an LC-MS/MS method for the simultaneous quantification of human intestinal transporter proteins absolute abundance using a QconCAT technique. *J Pharm Biomed Anal* 2015;**110**:27–33. Doi: 10.1016/j.jpba.2015.02.043.

25. Vonrichter O., Burk O., Fromm M., Thon K., Eichelbaum M., Kivisto K. Cytochrome P450 3A4 and P-glycoprotein expression in human small intestinal enterocytes and hepatocytes: a comparative analysis in paired tissue specimens. *Clin Pharmacol Ther* 2004;**75**(3):172–83. Doi: 10.1016/j.clpt.2003.10.008.

26. Bruyère A., Declèves X., Bouzom F., Proust L., Martinet M., Walther B., et al. Development of an optimized procedure for the preparation of rat intestinal microsomes: comparison of hepatic and intestinal microsomal cytochrome P450 enzyme activities in two rat strains. *Xenobiotica* 2009;**39**(1):22–32. Doi: 10.1080/00498250802517714.

27. Hatley OJD., Jones CR., Galetin A., Rostami-hodjegan A. Optimization of intestinal microsomal preparation in the rat : A systematic approach to assess the in fl uence of various methodologies on metabolic activity and scaling factors 2017;**208**(August 2016):187–208. Doi: 10.1002/bdd.2070.

28. Lin JH., Chiba M., Baillie T a. Is the role of the small intestine in first-pass metabolism overemphasized? *Pharmacol Rev* 1999;**51**(2):135–58.

29. Kaminsky LS., Zhang QY. The small intestine as a xenobiotic metabolizing organ. *Drug Metab Dispos* 2003;**31**(12):1520–5. Doi: 10.1124/dmd.31.12.1520.

30. Raza H. Dual localization of glutathione S-transferase in the cytosol and mitochondria: implications in oxidative stress, toxicity and disease. *FEBS J* 2011;**278**(22):4243–51. Doi: 10.1111/j.1742-4658.2011.08358.x.

31. Vuckovic D., Dagley LF., Purcell AW., Emili A. Membrane proteomics by high performance liquid chromatography-tandem mass spectrometry: Analytical approaches and challenges. *Proteomics* 2013;**13**(3–4):404–23. Doi: 10.1002/pmic.201200340.

32. Zhang H., Wolford C., Basit A., Li AP., Fan PW., Murray BP., et al. Regional Proteomic Quantification of Clinically Relevant Non-Cytochrome P450 Enzymes along the Human

Small Intestine. *Drug Metab Dispos* 2020;**48**(7):528–36. Doi: 10.1124/DMD.120.090738.

33. Rouleau M., Audet-Delage Y., Desjardins S., Rouleau M., Girard-Bock C., Guillemette C. Endogenous Protein Interactome of Human UDP-Glucuronosyltransferases Exposed by Untargeted Proteomics. *Front Pharmacol* 2017;**8**(FEB):23. Doi: 10.3389/fphar.2017.00023.

34. Wang X., He B., Shi J., Li Q., Zhu H-J. Comparative Proteomics Analysis of Human Liver Microsomes and S9 Fractions. *Drug Metab Dispos* 2020;**48**(1):31–40. Doi: 10.1124/dmd.119.089235.

35. Uchida Y., Ohtsuki S., Katsukura Y., Ikeda C., Suzuki T., Kamiie J., et al. Quantitative targeted absolute proteomics of human blood–brain barrier transporters and receptors. *J Neurochem* 2011;**117**(2):333–45. Doi: 10.1111/J.1471-4159.2011.07208.X.

36. Ohtsuki S., Ikeda C., Uchida Y., Sakamoto Y., Miller F., Glacial F., et al. Quantitative Targeted Absolute Proteomic Analysis of Transporters, Receptors and Junction Proteins for Validation of Human Cerebral Microvascular Endothelial Cell Line hCMEC/D3 as a Human Blood–Brain Barrier Model. *Mol Pharm* 2013;**10**(1):289–96. Doi: 10.1021/mp3004308.

37. Wiśniewski JR., Zougman A., Nagaraj N., Mann M. Universal sample preparation method for proteome analysis. *Nat Methods* 2009;**6**(5):359–62. Doi: 10.1038/nmeth.1322.

38. Prasad B., Unadkat JD. Comparison of Heavy Labeled (SIL) Peptide versus SILAC Protein Internal Standards for LC-MS/MS Quantification of Hepatic Drug Transporters. *Int J Proteomics* 2014;**2014**:1–11. Doi: 10.1155/2014/451510.

39. Zougman A., Selby PJ., Banks RE. Suspension trapping (STrap) sample preparation method for bottom-up proteomics analysis. *Proteomics* 2014;**14**(9):1006–1000. Doi: 10.1002/pmic.201300553.

40. Manza LL., Stamer SL., Ham AJL., Codreanu SG., Liebler DC. Sample preparation and digestion for proteomic analyses using spin filters. *Proteomics* 2005;**5**(7):1742–5. Doi: 10.1002/PMIC.200401063.

41. Wiśniewski JR. Filter-Aided Sample Preparation. *Methods in Enzymology*, vol. 585. Academic Press Inc.; 2017. p. 15–27.

42. Fallon JK., Neubert H., Hyland R., Goosen TC., Smith PC. Targeted quantitative proteomics for the analysis of 14 UGT1As and -2Bs in human liver using NanoUPLC-MS/MS with selected reaction monitoring. *J Proteome Res* 2013;**12**(10):4402–13. Doi: 10.1021/pr4004213.

43. Sato Y., Nagata M., Tetsuka K., Tamura K., Miyashita A., Kawamura A., et al. Optimized methods for targeted peptide-based quantification of human uridine 59-diphosphate-glucuronosyltransferases in biological specimens using liquid chromatography-tandem mass spectrometry. *Drug Metab Dispos* 2014;**42**(5):885–9. Doi: 10.1124/dmd.113.056291.

44. Chen Y., Zane NR., Thakker DR., Wang MZ. Quantification of flavin-containing monooxygenases 1, 3, and 5 in human liver microsomes by UPLC-MRM-based targeted quantitative proteomics and its application to the study of ontogeny. *Drug Metab Dispos* 2016;**44**(7):975–83. Doi: 10.1124/dmd.115.067538.

45. Gröer C., Busch D., Patrzyk M., Beyer K., Busemann A., Heidecke CD., et al. Absolute protein quantification of clinically relevant cytochrome P450 enzymes and UDP-glucuronosyltransferases by mass spectrometry-based targeted proteomics. *J Pharm Biomed Anal* 2014;**100**:393–401. Doi: 10.1016/j.jpba.2014.08.016.

46. Kamiie J., Ohtsuki S., Iwase R., Ohmine K., Katsukura Y., Yanai K., et al. Quantitative atlas of membrane transporter proteins: Development and application of a highly sensitive simultaneous LC/MS/MS method combined with novel in-silico peptide selection criteria. *Pharm Res* 2008;**25**(6):1469–83. Doi: 10.1007/S11095-008-9532-4.

47. Kawakami H., Ohtsuki S., Kamiie J., Suzuki T., Abe T., Terasaki T. Simultaneous Absolute Quantification of 11 Cytochrome P450 Isoforms in Human Liver Microsomes by Liquid Chromatography Tandem Mass Spectrometry with In Silico Target Peptide Selection. *J Pharm Sci* 2011;**100**(1):341–52. Doi: 10.1002/JPS.22255.

48. Al-Majdoub ZM., Couto N., Achour B., Harwood MD., Carlson G., Warhurst G., et al. Quantification of Proteins Involved in Intestinal Epithelial Handling of Xenobiotics. *Clin Pharmacol Ther* 2021;**109**(4):1136–46. Doi: 10.1002/cpt.2097.

49. Ludwig KR., Schroll MM., Hummon AB. Comparison of In-Solution, FASP, and S-Trap Based Digestion Methods for Bottom-Up Proteomic Studies. *J Proteome Res* 2018;**17**(7):2480–90. Doi: 10.1021/ACS.JPROTEOME.8B00235.

50. Elinger D., Gabashvili A., Levin Y. Suspension Trapping (S-Trap) Is Compatible with Typical Protein Extraction Buffers and Detergents for Bottom-Up Proteomics. *J Proteome Res* 2019;**18**(3):1441–5. Doi: 10.1021/ACS.JPROTEOME.8B00891.

51. HaileMariam M., Eguez RV., Singh H., Bekele S., Ameni G., Pieper R., et al. S-Trap, an Ultrafast Sample-Preparation Approach for Shotgun Proteomics. *J Proteome Res* 2018;**17**(9):2917–24. Doi: 10.1021/ACS.JPROTEOME.8B00505.

52. Ohtsuki S., Uchida Y., Kubo Y., Terasaki T. Quantitative targeted absolute proteomics-based ADME research as a new path to drug discovery and development: Methodology, advantages, strategy, and prospects. *J Pharm Sci* 2011;**100**(9):3547–59. Doi: 10.1002/jps.22612.

53. El-Khateeb E., Vasilogianni A-M., Alrubia S., Al-Majdoub ZM., Couto N., Howard M., et al. Quantitative mass spectrometry-based proteomics in the era of model-informed drug development: Applications in translational pharmacology and recommendations for best practice. *Pharmacol Ther* 2019;**203**:107397. Doi: 10.1016/j.pharmthera.2019.107397.

54. Russell MR., Achour B., Mckenzie EA., Lopez R., Harwood MD., Rostami-Hodjegan A., et al. Alternative Fusion Protein Strategies to Express Recalcitrant QconCAT Proteins for Quantitative Proteomics of Human Drug Metabolizing Enzymes and Transporters. *J Proteome Res* 2013;**12**(12):5934–42. Doi: 10.1021/pr400279u.

55. Simpson DM., Beynon RJ. QconCATs: design and expression of concatenated protein standards for multiplexed protein quantification. *Anal Bioanal Chem* 2012;**404**(4):977–89. Doi: 10.1007/s00216-012-6230-1.

56. Achour B., Al-Majdoub ZM., Al Feteisi H., Elmorsi Y., Rostami-Hodjegan A., Barber J. Ten years of QconCATs: Application of multiplexed quantification to small medically relevant proteomes. *Int J Mass Spectrom* 2015;**391**:93–104. Doi: 10.1016/j.ijms.2015.08.003.

57. Howard M., Achour B., Al-Majdoub Z., Rostami-Hodjegan A., Barber J. GASP and FASP are Complementary for LC-MS/MS Proteomic Analysis of Drug-Metabolizing Enzymes and Transporters in Pig Liver. *Proteomics* 2018;**18**(24):1800200. Doi: 10.1002/pmic.201800200.

58. Al-Majdoub ZM., Achour B., Couto N., Howard M., Elmorsi Y., Scotcher D., et al. Mass spectrometry-based abundance atlas of ABC transporters in human liver, gut, kidney, brain and skin. *FEBS Lett* 2020;**594**(23):4134–50. Doi: 10.1002/1873-3468.13982.

59. Scigelova M., Hornshaw M., Giannakopulos A., Makarov A. Fourier Transform Mass Spectrometry. *Mol Cell Proteomics* 2011;**10**(7):M111.009431. Doi: 10.1074/mcp.M111.009431.

60. Michalski A., Damoc E., Lange O., Denisov E., Nolting D., Müller M., et al. Ultra High Resolution Linear Ion Trap Orbitrap Mass Spectrometer (Orbitrap Elite) Facilitates Top Down LC MS/MS and Versatile Peptide Fragmentation Modes. *Mol Cell Proteomics* 2012;**11**(3):O111.013698. Doi: 10.1074/mcp.O111.013698.

61. Kalli A., Smith GT., Sweredoski MJ., Hess S. Evaluation and Optimization of Mass Spectrometric Settings during Data-dependent Acquisition Mode: Focus on LTQ-Orbitrap Mass Analyzers. *J Proteome Res* 2013;**12**(7):3071–86. Doi: 10.1021/pr3011588.

62. Michalski A., Damoc E., Hauschild J-P., Lange O., Wieghaus A., Makarov A., et al. Mass Spectrometry-based Proteomics Using Q Exactive, a High-performance Benchtop

Quadrupole Orbitrap Mass Spectrometer. *Mol Cell Proteomics* 2011;**10**(9):M111.011015. Doi: 10.1074/mcp.M111.011015.

63. Kelstrup CD., Young C., Lavallee R., Nielsen ML., Olsen J V. Optimized Fast and Sensitive Acquisition Methods for Shotgun Proteomics on a Quadrupole Orbitrap Mass Spectrometer. *J Proteome Res* 2012;**11**(6):3487–97. Doi: 10.1021/pr3000249.

64. Nagaraj N., Alexander Kulak N., Cox J., Neuhauser N., Mayr K., Hoerning O., et al. System-wide Perturbation Analysis with Nearly Complete Coverage of the Yeast Proteome by Single-shot Ultra HPLC Runs on a Bench Top Orbitrap. *Mol Cell Proteomics* 2012;**11**(3):M111.013722. Doi: 10.1074/mcp.M111.013722.

65. Komura H., Iwaki M. Species Differences in In Vitro and In Vivo Small Intestinal Metabolism of CYP3A Substrates. *J Pharm Sci* 2008;**97**(5):1775–800. Doi: 10.1002/jps.21121.

66. Ganapathy V. Protein Digestion and Absorption. *Physiology of the Gastrointestinal Tract*, vol. 2. Elsevier; 2012. p. 1595–623.

67. Weiser MM. Intestinal epithelial cell surface membrane glycoprotein synthesis. I. An indicator of cellular differentiation. *J Biol Chem* 1973;**248**(7):2536–41. Doi: 10.1016/S0021-9258(19)44141-0.

68. Weingartl HM., Derbyshire JB. Binding of porcine transmissible gastroenteritis virus by enterocytes from newborn and weaned piglets. *Vet Microbiol* 1993;**35**(1–2):23–32. Doi: 10.1016/0378-1135(93)90113-L.

69. Panorchan P., Thompson MS., Davis KJ., Tseng Y., Konstantopoulos K., Wirtz D. Single-molecule analysis of cadherin-mediated cell-cell adhesion. *J Cell Sci* 2006;**119**(1):66–74. Doi: 10.1242/jcs.02719.

70. Couto N., Al-Majdoub ZM., Gibson S., Davies PJ., Achour B., Harwood MD., et al. Quantitative Proteomics of Clinically Relevant Drug-Metabolizing Enzymes and Drug Transporters and Their Intercorrelations in the Human Small Intestine. *Drug Metab Dispos* 2020;**48**(4):245–54. Doi: 10.1124/dmd.119.089656.

71. Vasilogianni A., Al-Majdoub ZM., Achour B., Peters SA., Rostami-Hodjegan A., Barber J. Proteomics of colorectal cancer liver metastasis: A quantitative focus on drug elimination and pharmacodynamics effects. *Br J Clin Pharmacol* 2021. Doi: 10.1111/bcp.15098.

72. Zamek-Gliszczynski MJ., Taub ME., Chothe PP., Chu X., Giacomini KM., Kim RB., et al. Transporters in Drug Development: 2018 ITC Recommendations for Transporters of Emerging Clinical Importance. *Clin Pharmacol Ther* 2018;**104**(5):890–9. Doi: 10.1002/cpt.1112.

73. Prasad B., Unadkat JD. Optimized Approaches for Quantification of Drug Transporters in Tissues and Cells by MRM Proteomics. *AAPS J* 2014;**16**(4):634–48. Doi: 10.1208/s12248-014-9602-y.

74. Balakrishnan A., Polli JE. Apical Sodium Dependent Bile Acid Transporter (ASBT, SLC10A2): A Potential Prodrug Target. *Mol Pharm* 2006;**3**(3):223–30. Doi: 10.1021/mp060022d.

75. Grosser G., Müller SF., Kirstgen M., Döring B., Geyer J. Substrate Specificities and Inhibition Pattern of the Solute Carrier Family 10 Members NTCP, ASBT and SOAT. *Front Mol Biosci* 2021;**8**:430. Doi: 10.3389/fmolb.2021.689757.

76. Foley D., Rajamanickam J., Bailey P., Meredith D. Bioavailability Through PepT1: The Role of Computer Modelling in Intelligent Drug Design. *Curr Comput Aided-Drug Des* 2010;**6**(1):68–78. Doi: 10.2174/157340910790980133.

77. Brodin B., Nielsen CU., Steffansen B., Frøkjaer S. Transport of Peptidomimetic Drugs by the Intestinal Di/tri-peptide Transporter, PepT1. *Pharmacol Toxicol* 2002;**90**(6):285–96. Doi: 10.1034/j.1600-0773.2002.900601.x.

78. Vijay N., Morris M. Role of Monocarboxylate Transporters in Drug Delivery to the Brain. *Curr Pharm Des* 2014;**20**(10):1487–98. Doi: 10.2174/13816128113199990462.

79. Choi J-S., Jin MJ., Han H-K. Role of monocarboxylic acid transporters in the cellular uptake of NSAIDs. *J Pharm Pharmacol* 2010;**57**(9):1185–9. Doi: 10.1211/jpp.57.9.0013.

80. Barot M., Gokulgandhi MR., Agrahari V., Pal D., Mitra AK. Monocarboxylate transporter mediated uptake of moxifloxacin on human retinal pigmented epithelium cells. *J Pharm Pharmacol* 2014;**66**(4):574–83. Doi: 10.1111/jphp.12139.

81. Kalliokoski A., Niemi M. Impact of OATP transporters on pharmacokinetics. *Br J Pharmacol* 2009;**158**(3):693–705. Doi: 10.1111/j.1476-5381.2009.00430.x.

82. Wire MB., Shelton MJ., Studenberg S. Fosamprenavir Clinical Pharmacokinetics and Drug Interactions of the Amprenavir Prodrug. *Clin Pharmacokinet* 2006;**45**(2):137–68.

83. Lo WY., Balasubramanian A., Helsby NA. Hydrolysis of dinitrobenzamide phosphate prodrugs: The role of alkaline phosphatase. *Drug Metabol Drug Interact* 2009;**24**(1):1–16. Doi: 10.1515/DMDI.2009.24.1.1.

84. Prabha M. Hydrolytic Enzymes Targeting to Prodrug / Drug Metabolism for Translational Application in Cancer. *J Clin Sci Transl Med* 2019;**1**(1):000102.

85. Jornada DH., dos Santos Fernandes GF., Chiba DE., de Melo TRF., dos Santos JL., Chung MC. The Prodrug Approach: A Successful Tool for Improving Drug Solubility. *Molecules* 2015;**21**(1):42. Doi: 10.3390/molecules21010042.

86. Al-Majdoub ZM., Carroll KM., Gaskell SJ., Barber J. Quantification of the Proteins of the Bacterial Ribosome Using QconCAT Technology. *J Proteome Res* 2014;**13**(3):1211–22. Doi: 10.1021/pr400667h.

87. Al-Majdoub ZM., Al Feteisi H., Achour B., Warwood S., Neuhoff S., Rostami-Hodjegan A., et al. Proteomic Quantification of Human Blood–Brain Barrier SLC and ABC Transporters in Healthy Individuals and Dementia Patients. *Mol Pharm* 2019;**16**(3):1220–33. Doi: 10.1021/acs.molpharmaceut.8b01189.

88. MM B. A rapid and sensitive method for the quantitation of microgram quantities of protein utilizing the principle of protein-dye binding. *Anal Biochem* 1976;**72**(1–2):248–54. Doi: 10.1006/ABIO.1976.9999.

89. Yang J., Tucker G., Rostami Hodjegan A. Cytochrome P450 3A expression and activity in the human small intestine. *Clin Pharmacol Ther* 2004;**76**(4):391–391. Doi: 10.1016/j.clpt.2004.07.001.

90. Paine MF., Khalighi M., Fisher JM., Shen DD., Kunze KL., Marsh CL., et al. Characterization of interintestinal and intraintestinal variations in human CYP3A-dependent metabolism. *J Pharmacol Exp Ther* 1997;**283**(3):1552–62.

91. JR D., JW B. Intestinal microsomal drug metabolism. A comparison of rat and guinea-pig enzymes, and of rat crypt and villous tip cell enzymes. *Biochem Pharmacol* 1981;**30**(17):2415–20. Doi: 10.1016/0006-2952(81)90335-X.

92. Sandle GI., McNicholas CM., Lomax RB. Potassium channels in colonic crypts. *Lancet* 1994;**343**(8888):23–5. Doi: 10.1016/S0140-6736(94)90878-8.

93. M B., H C. Methods for the isolation of intact epithelium from the mouse intestine. *Anat Rec* 1981;**199**(4):565–74. Doi: 10.1002/AR.1091990412.

94. EG van de K., AL U., AK S., MH de J., C H., IA de G., et al. Innovative methods to study human intestinal drug metabolism in vitro: precision-cut slices compared with ussing chamber preparations. *Drug Metab Dispos* 2006;**34**(11):1893–902. Doi: 10.1124/DMD.106.011148.

95. TT K. Comparison of the gastrointestinal anatomy, physiology, and biochemistry of humans and commonly used laboratory animals. *Biopharm Drug Dispos* 1995;**16**(5):351–80. Doi: 10.1002/BDD.2510160502.

96. A D., SR M., D B. Preparation and characterization of rodent intestinal microsomes: comparative assessment of two methods. *Indian J Pharm Sci* 2009;**71**(1):75–7. Doi: 10.4103/0250-474X.51968.

97. Pacifici GM., Franchi M., Bencini C., Repetti F., Di Lascio N., Muraro GB. Tissue distribution of drug-metabolizing enzymes in humans. *Xenobiotica* 1988;**18**(7):849–56.

Doi: 10.3109/00498258809041723.

98. Hatley OJD., Jones CR., Galetin A., Rostami-Hodjegan A. Quantifying gut wall metabolism: methodology matters. *Biopharm Drug Dispos* 2017;**38**(2):155–60. Doi: 10.1002/bdd.2062.

99. Miyauchi E., Tachikawa M., Declèves X., Uchida Y., Bouillot JL., Poitou C., et al. Quantitative Atlas of Cytochrome P450, UDP-Glucuronosyltransferase, and Transporter Proteins in Jejunum of Morbidly Obese Subjects. *Mol Pharm* 2016;**13**(8):2631–40. Doi: 10.1021/acs.molpharmaceut.6b00085.

100. Lloret-Linares C., Miyauchi E., Luo H., Labat L., Bouillot JL., Poitou C., et al. Oral Morphine Pharmacokinetic in Obesity: The Role of P-Glycoprotein, MRP2, MRP3, UGT2B7, and CYP3A4 Jejunal Contents and Obesity-Associated Biomarkers. *Mol Pharm* 2016;**13**(3):766–73. Doi: 10.1021/acs.molpharmaceut.5b00656.

101. Vaessen SFC., van Lipzig MMH., Pieters RHH., Krul CAM., Wortelboer HM., van de Steeg E. Regional Expression Levels of Drug Transporters and Metabolizing Enzymes along the Pig and Human Intestinal Tract and Comparison with Caco-2 Cells. *Drug Metab Dispos* 2017;**45**(4):353–60. Doi: 10.1124/dmd.116.072231.

3.7.Supplementary material – Methodology

3.7.1. QconCAT design and characterization

Extra exclusion criteria of QconCAT surrogates peptides design were applied whenever possible. Continues aspartate (D) and Glutamate (E) (DE & ED) sequence as they are susceptible to missed cleavages, dibasic-tribasic forms of (K, R and H (histidine)) (e.g. HK, KH, HR, RH,HH), N-terminal glutamine (Q), asparagine (N) and Q, aspartic acid when paired with (glycine (G), P or serine (S)), can undergo hydrolysis and cause peptide cleavage in acidic environment, and (W) Tryptophan and H residues are also prone to chemical degradation.

Exclude peptides with:

- NG, DP, KP, NQ (prone to deamination),
- A series of glutamine, isoleucine (I), leucine (L), Phenylalanine (F), threonine (T), tyrosine (Y), or valine (V) can form β sheets that result in incomplete solvation in the LCMS, No C- and N-terminal peptide
- Check if the nominated peptide has a K or R amino acid near it in the protein sequence (at least 2 amino acids must be separating between the last K or R and the start of the new peptides) as it cause PTM and misclevage of the peptide
- A peptide containing multiple (S) serine or (P) proline residues is also difficult to synthesize,

Check LCMS parameters:

- Retention time (RT) in the LCMS column of the peptides were checked in http://hs2.proteome.ca/SSRCalc/Slope/, peptides with hydrophilicity index (HI) < 7 are not considered as they wouldn't retain in the column.
- Prediction of relative MS response: The MRM signal intensity depends on the MS response of parent as well as product ions. Fragmentation pattern with relative intensities of product ions predicted by SRMAtlas and PeptideART

Table S3.1. TransCAT target proteins with their surrogate peptides.

Transporter	Protein Name	Surrogate Peptide
ABCB1 (P-gp, MDR1)	MultiDrug Resistance protein 1 (MDR1), P-glycoprotein 1 (P-gp)	FYDPLAGK
		AGAVAEEVLAAIR
ABCB11 (BSEP)	Bile Salt Export Pump	STALQLIQR
		AADTIIGFEHGTAVER
ABCB4 (MDR3)	MultiDrug Resistance protein 3	IATEAIENIR
		GAAYVIFDIIDNNPK
ABCC2 (MRP2)	Multidrug Resistance-associated Protein 2	LTIIPQDPILFSGSLR
		YLGGDDLDTSAIR
		AFEHQQR
ABCC3 (MRP3)	Multidrug Resistance-associated Protein 3	AEGEISDPFR
		IDGLNVADIGLHDLR
ABCC4 (MRP4)	Multidrug Resistance-associated Protein 4	AEAAALTETAK
		APVLFFDR
ABCC6 (MRP6)	Multidrug Resistance-associated Protein 6	SSLPSALLGELSK
		APETEPFLR
		SSLASGLLR
ABCG2 (BCRP)	Breast Cancer Resistance Protein	VIQELGLDK
		SSLLDVLAAR
		ENLQFSAALR
ATP1A1	sodium/potassium-transporting ATPase subunit Alpha-1	IVEIPFNSTNK
		SPDFTNENPLETR
Cadherin-17 (CDH17)	Liver-Intestine cadherin	AENPEPLVFGVK
		QNSRPGK
Cadherin-23 (CDH23)	Otocadherin	ATDADEGEFGR
		DAYVGALR
SLC51A (OST-α)	Solute Carrier family 51 subunit Alpha	YTADLLEVLK
		VGYETFSSPDLDLNLK
	Solute Carrier family 51 subunit Beta	DHNSLNNLR

SLC51B (OST-β)		ETPEVLHLDEAK
SLC22A1 (OCT1)	Octamer-binding protein 1	MLSLEEDVTEK
		GVALPETMK
		ENTIYLK
SLC22A3 (OCT3)	Octamer-binding protein 3	GIALPETVDDVEK
		FLQGVFGK
SLC22A5 (OCTN2)	Organic Cation/Carnitine Transporter 2	TWNIR
		DYDEVTAFLGEWGPFQR
SLC22A7 (OAT2)	Organic Anion Transporter 2	WLLTQGHVK
		NVALLALPR
SLC22A9 (OAT4)	Organic Anion Transporter 4	DTLTLEILK
		ISLLSFTR
SLC47A1 (MATE1)	Multidrug and Toxin Extrusion protein 1	GGPEATLEVR
		DHVGYIFTTDR
SLCO1A2 (OATP1A2)	Organic Anion-Transporer Polypeptide 1	EGLETNADIIK
		IYDSTTFR
SLCO1B1 (OATP1B1)	Sodium-independent Organic Anion-Transporter Polypeptide 2	YVEQQYGQPSSK
		MFLAALSLSFIAK
		LNTVGIAK
SLCO1B3 (OATP1B3)	Organic Anion-Transporter Polypeptide 8	NVTGFFQSLK
		IYNSVFFGR
SLCO2B1 (OATP2B1)	Organic Anion Transporter Polypeptide-related protein 2	VLLQTLR
		SSPAVEQQLLVSGPGK
		AHLWKPK
SLCO4C1 (OATP4C1)	Organic Anion Transporter M1	SPEPSLPSAPPNVSEEK
		DFPAALK
SLC10A1 (NTCP)	Sodium/Taurocholate Cotransporter Polypeptide	GIYDGDLK
		GIVISLVLVLIPCTIGIVLK
		HLPGTAEIQAGK
	Intestinal H+/Peptide Cotransporter	GNEVQIK

SLC15A1 (PEPT1)		TLPVFPK
		HTLLVWAPNHYQVVK
SLC10A2 (ASBT)	Apical Sodium-dependent Bile acid Transporter	IAGLPWYR
		LWIIGTIFPVAGYSLGFLLAR
SLC16A1 (MCT1)	MonoCarboxylate Transporter1	SITVFFK
		DLHDANTDLIGR
SLCO4A1 (OATP4A1)	Organic Anion Transporter Polypeptide-related protein 1	YEVELDAGVR
		ILGGIPGPIAFGWVIDK
GluFib		EGVNDNEEGFFSAR
NNOP-1		VGFLPDGVIK

3.8.Supplementary material - Results

3.8.1. Enterocyte isolation method

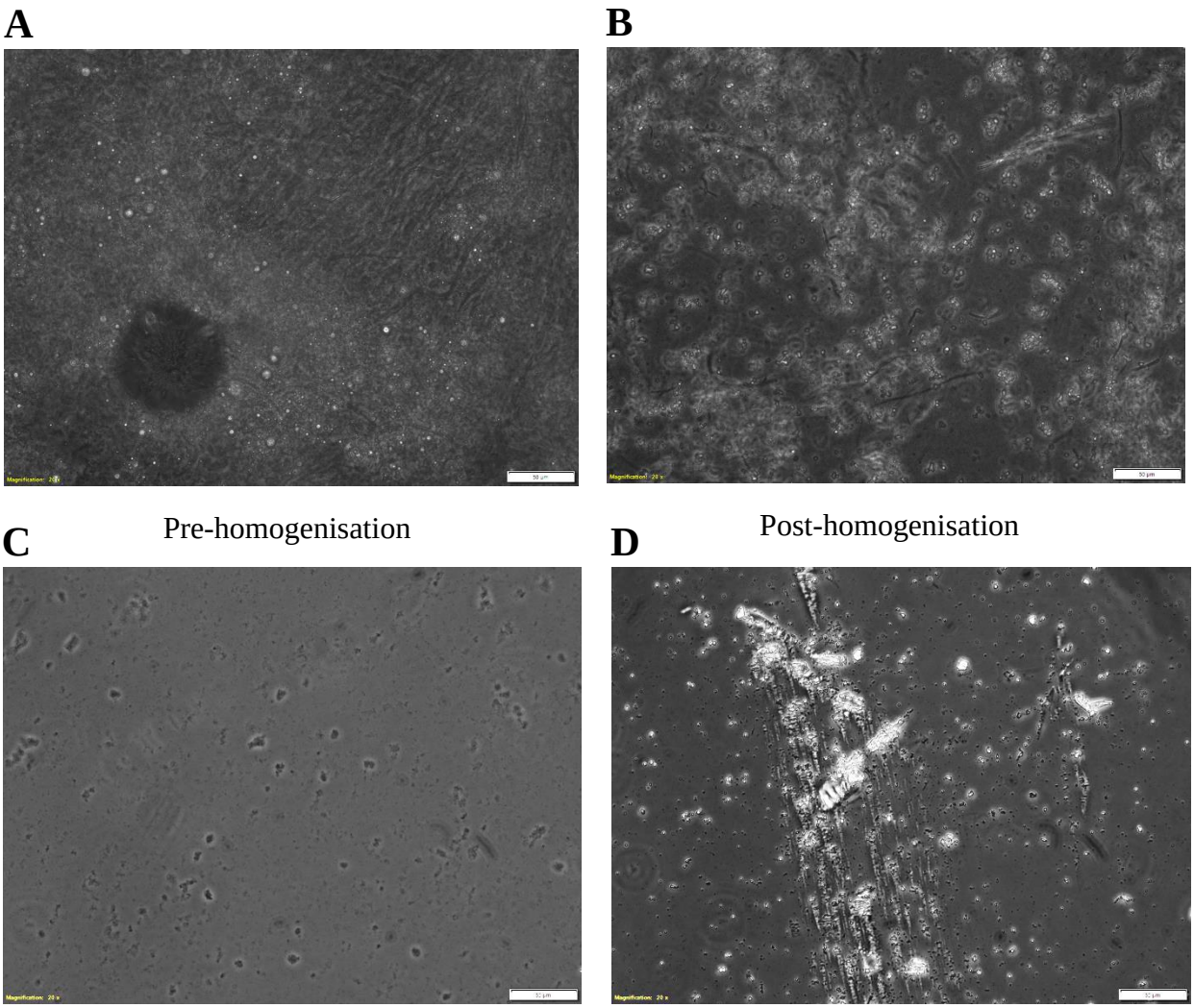

Figure S3.1. *Visual confirmation of enterocytes isolation after detachment from the lamina propria and release of its content by disruption with scraping and EDTA elution protocols.* ***(A)*** *Pre-homogenisation isolation by scraping,* ***(B)*** *Pre-homogenisation isolation by elution,* ***(C)*** *Post-homogenisation isolation by scraping and* ***(D)*** *Post-homogenisation isolation by elution. Images are ×20 original magnification and 50 µm.*

3.8.2. Characterization of the TransCAT

MGTKTFTAKPETVKRDWYVVDATGKSMALRLANELSDAAENKFGSELLAKVEGDTKPELELTLKS
DLSADINEHLIVELYSKGVNDNEEGFFSAKLEPGRLEYDPNRSAGTYVQIVARDAQSALTVSETTFGR
DFNEALVHQVVVAYAAGARLDNVVYRAVVESIQR (Ribosomal core) / LAAALEHHHHHH (His-tag)

1	GAIETEPAVK	FYDPLAGKYV	EQQYGQPSSK	TLPVFPKSTA	LQLIQRSSPA
51	VEQQLLVSGP	GKIATEAIEN	IRGVALPETM	KLTIIPQDPI	LFSGSLRNVA
101	LLALPRGIYD	GDLKAEGEIS	DPFRISLLSF	TRAEAAALTE	TAKQNSRPGK
151	FLQGVFGKIY	NSVFFGRVIQ	ELGLDKSSLA	SGLLREGLET	NADIIKSITV
201	FFKIVEIPFN	STNKLNTVGI	AKAENPEPLV	FGVKAPVLFF	DRATDADEGE
251	FGRGNEVQIK	LWIIGTIFPV	AGYSLGFLLA	RVGYETFSSP	DLDLNLKDHN
301	SLNNLRDHVG	YIFTTDRMLS	LEEDVTEKGA	AYVIFDIIDN	NPKDFPAALK
351	GIALPETVDD	VEKSSLPSAL	LGELSKTWNI	RDAYVGALRW	LLTQGHVKGG
401	PEATLEVRDT	LTLEILKILG	GIPGPIAFGW	VIDKIDGLNV	ADIGLHDLRE
451	NLQFSAALRE	TPEVLHLDEA	KIYDSTTFRA	GAVAEEVLAA	IRMFLAALSL
501	SFIAKSPDFT	NENPLETRNV	TGFFQSLKAP	ETEPFLRAHL	WKPKAADTII
551	GFEHGTAVER	VLLQTLRENT	IYLKHLPGTA	EIQAGKDYDE	VTAFLGEWGP
601	FQRAFEHQQR	HTLLVWAPNH	YQVVKAGAVA	EEVLAAVRYT	ADLLEVLKIA
651	GLPWYRSSLL	DVLAARDLHD	ANTDLIGRYE	VELDAGVRY	LGGDDLDTSA
701	IREGVNDNEE	GFFSARVGFL	PDGVIKVGYD	LPGKLAAALE	HHHHHH

Figure S3.2. *Sequence of TransCAT showing detected peptides in green, the red amino acid is where the enzymes cleaves. Blue sequences represent the ribosomal core and the His-tag sequence. The black sequences are the undetectable parts in the analysis.*

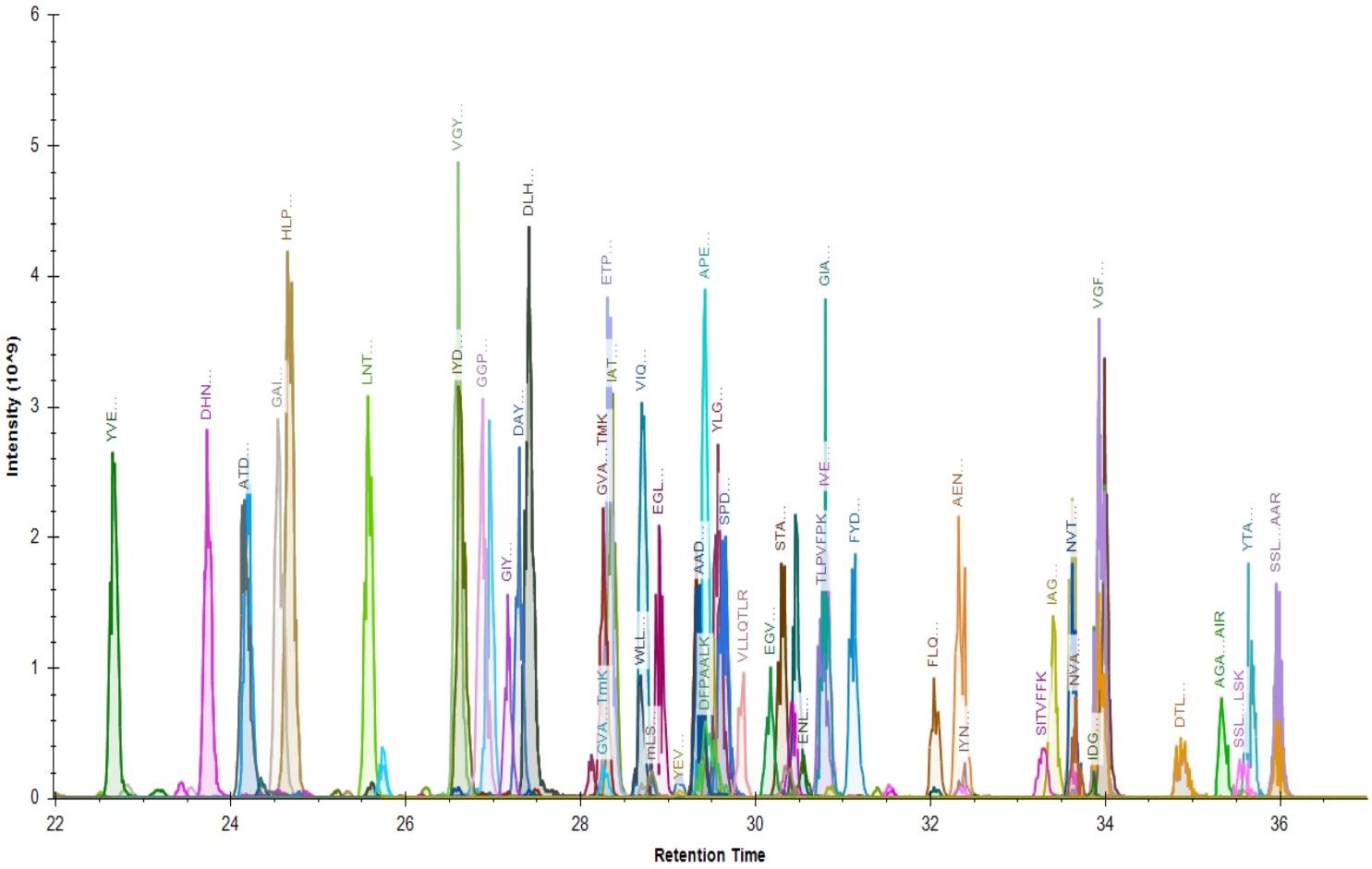

Figure S3.3. *The full chromatogram of TransCAT peptides showing the retention time at which each peptide was detected. Peptides were annotated with the first three letters and different colours.*

Chapter Four: Quantitative Assessment of the Impact of Crohn's Disease on Protein Expression of Human Intestinal Drug Metabolising Enzymes and Transporters

Declaration

This chapter constitutes an article submitted for publication to the Journal of Pharmaceutical Sciences

Sarah Alrubia, Zubida M. Al-Majdoub, Brahim Achour, Amin Rostami-Hodjegan, Jill Barber. (n.d). Quantitative Assessment of the Impact of Crohn's Disease on Protein Expression of Human Intestinal Drug Metabolising Enzymes and Transporters. *Journal of Crohn's and Colitis***.** Under review.

I carried out the literature search, generation and analysis of data, contributed to the study design and wrote the manuscript. Dr Zubida M. Al-Majdoub and Dr Brahim Achour reviewed and edited the manuscript. Dr Jill Barber and Prof. Amin Rostami- Hodjegan contributed to the study design, provided guidance and suggested edits to the manuscript. I retained editorial control.

4.1.Abstract

Background and Aims: Crohn's disease affects predominantly the mucosal layer of the intestine, ileum and colon segments. In addition to formulation impact of the dosage forms, oral drug bioavailability is determined by the interaction of the active drug moiety with intestinal drug-metabolising enzymes and transporters. Hence, alterations to intestinal enzymes and transporters in Crohn's disease is of great interest and assessed in this study.

Methods: Fresh-frozen inflamed and non-inflamed human ileum and colon tissues from Crohn's disease patients and healthy donors were processed by calcium chelation elution to isolate the enterocytes. After homogenization, the isolated homogenates pooled from individual samples in each group were analysed by liquid chromatography – mass spectrometry proteomics.

Results: Marked but non-uniform alterations were observed in the expression of various intestinal enzymes and transporters in inflamed and non-inflamed ileum and colon compared to healthy samples. In ileum, CYP3A4, CYP51A1, CYP4F12, CYP2J2, MCT1, ALDH1B1, CES1, ALPI, SULT1A2, SULT1B1 and SULT2B1 showed ≥10 fold reduction in expression in Crohn's patients. By contrast, only expression of MGST1 and SULT1B1 showed ≥10 fold reduction in the colon. Ileal UGT1A1, MGST1, MGST2, and MAOA levels increased by ≥2 fold in Crohn's patients, while only ALPI showed ≥2 fold increase in colon. Counter-intuitively, non-inflamed ileum had a higher magnitude of fold change than inflamed tissue for the target proteins when compared to healthy tissue.

Conclusions: Significantly altered expression in intestinal enzymes and transporters was quantified in Crohn's disease. The insight to these values allows improved understanding of variable effects of Crohn's disease on bioavailability of different orally administered drugs to patients with a view to predict the clinical impact and potential dose adjustment.

4.2.Introduction

As an idiopathic inflammatory bowel disease (IBD), aetiology of Crohn's disease (CD) is associated with a combination of genetic, microbial and environmental factors.[1] Patients with CD are prone to kidney, liver, cardiovascular and respiratory disease,[2] hence they may receive multiple oral drugs other than the ones used to control CD itself.

A large number of orally administered drugs undergo first-pass metabolism in the intestine and liver before reaching the systemic circulation. Moreover, efflux transporters residing in the enterocytes play a significant role in modulating the bioavailability of the drugs which are substrates for such transporters.[3] Hence, any changes in the expression of drug-metabolising enzymes and transporters (DMETs) localised in the enterocytes would influence the fate of drug absorption. Some studies have established that inflammation can alter the function and expression of intestinal DMETs, affecting oral drug absorption, activation and clearance.[4,5] Importantly, CD can affect any part of the gastrointestinal tract (GIT) but the ileum and colon are predominantly affected.[1] The ileum plays a more significant role in determining drug bioavailability than the colon owing to its high surface area and the presence of enzymes and transporters expressed in its epithelial cells.[6–8] Understanding the quantitative changes of these proteins helps with the prediction of alterations in exposure and effect of oral drugs, which may lead to unfavourable clinical outcomes.

Clinical data related to the fate of drugs in patient populations, such as CD, are scarce, particularly for new drugs coming onto market because of the lack of representation of such patients in clinical studies during drug development. Regulatory authorities have advocated inclusion of diverse patient populations in clinical studies[9], which may take a while before being fully implemented. In the absence of such data, application of physiological-based pharmacokinetic (PBPK) models to predict oral drug kinetics based on attributes of the patient population can improve dosing in different grades of the disease.[10] Therefore, collecting quantitative proteomic measurements of DMETs in CD is an essential step to inform PBPK models, which will facilitate *in vitro* to *in vivo* extrapolation (IVIVE) of available knowledge on drugs to clinical outcomes in CD. A meta-analysis of available system parameters to build a CD PBPK population demonstrated a gap in the availability of intestinal DMET expression/activity data (Chapter one).

In most previous studies on human GIT of CD patients, either mRNA was measured as an indirect indicator of protein abundance or semi-quantitative immunoassays were employed. Several reports demonstrated up or downregulation of ATP-binding cassette (ABC) transporters[11–13] and solute carriers (SLCs) in CD.[14,15] Genetic mutation of OCTN1 and 2 have been linked to increased risk of CD.[16] Mutation and downregulation of ASBT have been associated with diarrhoea in CD patients.[17] Among cytochrome P450 (CYP) enzymes, CYP3A4 was the most studied, with reports of lower expression in CD patients relative to control groups.[12,18] In addition, significant alterations were reported in the expression of other phase 1 and 2 drug-metabolising enzymes (DMEs) of adults with CD.[18–21] However, in these studies, the control groups were not always healthy subjects.

Liquid chromatography-mass spectrometry (LC-MS) based proteomics is a quantitative approach that offers greater proteome coverage and more accurate measurements compared to other techniques used previously to characterise CD samples.[22] In this study, we aimed to quantify the absolute abundance of DMETs involved in oral drug biotransformation of various drugs using LC-MS proteomics. This was carried out in both inflamed and histologically normal CD ileum and colon, with subsequent comparison against healthy baseline. In addition, we were able to generate disease perturbation factors (DPF) for each protein in CD. This reports alteration in protein expression due to disease as a ratio relative to healthy expression.[23]

4.3.Materials and methods

4.3.1. Materials

Unless otherwise indicated, all chemicals were supplied by Sigma-Aldrich (Poole, UK). All solvents were high performance liquid chromatography (HPLC) grade and supplied by Thermo Fisher Scientific (Paisley, UK). Lysyl endopeptidase (Lys-C) was purchased from Wako (Osaka, Japan). Sequencing-grade modified trypsin was supplied by Promega (Southampton, UK). Complete Mini, EDTA-free protease inhibitor cocktail tablets were supplied by Roche (Mannheim, Germany). BCA protein concentration measuring kit was obtained from ThermoFisher Scientific (Hemel Hempstead, UK).

4.3.2. Human intestine tissue samples

The fresh-frozen human intestine mucosal samples included inflamed ileum (n = 6), inflamed colon (n = 7) (I-CD), histologically normal ileum (n = 2), histologically normal colon (n = 5) (HN-CD) from active CD patients undergoing ileocolonic resection. Tissues were obtained with informed consent and supplied by Manchester Biomedical Research Centre (BRC) Biobank, Manchester University NHS Foundation Trust, Manchester, UK. Prior ethics approval was granted by NRES Committee North West - Haydock (19/NW/0644). The histologically normal tissues were taken from macroscopically normal regions away from the inflamed bowel regions. Healthy ileum (n = 5) and colon (n = 5) mucosal samples obtained from healthy deceased subjects were supplied by Caltag Medsystems Limited (Buckingham, UK). Prior ethics approval was granted by University research ethics committee (UREC), UK (2019-8120-12392). Demographic information is provided in Table S4.1 in the Supplement.

4.3.3. Enterocyte isolation and subcellular fractionation

Enterocytes were isolated from mucosal tissues by calcium chelation elution. The enterocyte isolation and homogenate fraction processing was adapted from Harwood et al (2015)[24] with minor modifications. Briefly, the process was done on ice and solutions were equilibrated at pH 7.4. The base buffer for all solutions used for chelation was 112 mM NaCl, 5 mM KCl, 20 mM HEPES. The mucosa was washed twice in the base buffer and immersed in 27 mM sodium citrate solution with a protease inhibitor cocktail (PI) for 30 min, followed by incubation in EDTA buffer (30 mM EDTA, 10 U/mL heparin, 1 mM dithiothreitol (DTT) and PI) with

stirring at 250 rpm for 40 min to initiate chelation. The chelated enterocytes were collected from the mucosa by repeated flushing with EDTA buffer. The chelated material was washed by centrifugation twice at 2000 x g for 10 min. The resulting enterocyte pellet was re-suspended in homogenisation buffer (10 mM Tris–HCl, 250 mM sucrose, 0.1 mM EGTA, 0.5 mM $MgCl_2$, 5 mM histidine and PI) at 3 ml per g of cells. Homogenisation was carried out with a Dounce hand-held homogeniser for a minimum of 75 strokes, followed by treatment with an ultrasonication probe (30 W) for two 10 s bursts to disrupt cell membranes. The formed homogenate fraction was stored in aliquots at -80°C until further processing.

4.3.4. Sample preparation and proteolytic digestion

Pooled human ileum and colon homogenates (n = 6) were processed and grouped based on the nature of the tissue. The 6 pooled samples are classified as follows: I-CD colon, I-CD ileum, HN-CD colon, HN-CD ileum, healthy colon and healthy ileum. Homogenate protein content was determined using BCA assay for individual samples and after pooling in triplicate using bovine serum albumin (BSA) as a standard. Individual samples in each group were mixed in equivalent concentration (20 µg/µl for each group, except HN-CD ileum at 50 µg/µl). 70 µg pooled homogenate protein in each sample was spiked with 0.126 µg BSA as internal standard. The 6 pooled homogenate samples were prepared for proteomics based on filter-aided sample preparation (FASP), as previously described,[25] using Amicon Ultra 0.5 mL centrifugal filters at 10-kDa molecular weight cut-off (Merck Millipore, Nottingham, UK).

4.3.1. LC-MS/MS data analysis and protein quantification

Digested samples were diluted to a final concentration of 0.5 µg/µl with water containing 0.1% (v/v) formic acid and 3% (v/v) acetonitrile. 10 µl of each sample was injected into an UltiMate® 3000 rapid separation liquid chromatography (RSLC, Dionex Corporation, Sunnyvale, CA) coupled online to a Q Exactive HF Hybrid Quadrupole Orbitrap mass spectrometer (ThermoFisher Scientific, Waltham, MA). Peptides were eluted over 90 min gradient following the LC/MS methodology as previously described.[23]

Data analysis was carried out using MaxQuant version 1.6.1.0. (Max Planck Institute for Biochemistry, Munich, Germany), and absolute protein quantification was executed using Hi-N label-free method based on obtained proteomic data.[26] The database search was applied against a UniProtKB human proteome fasta file of 71599 protein entries (UniProt, May 2017) in addition to BSA. The average intensity of the three most abundant non-conflicting unique

peptides were used to quantify the identified targeted proteins in relation to BSA at known abundance in each sample. Where three unique peptides were not available in a sample, the average intensity of two unique peptides were used for quantification. Shared sequences specific for more than one protein isoform from the same family were used when no unique peptides for the individual proteins were available. This was the case with CYP3A4 where the shared peptide between CYP3A4 and 3A7 was used to measure CYP3A4 abundance only. This is because CYP3A7 was the lowest abundance (< 1 fmol/μg protein) CYP3A isoform detected by LC/MS-MS in one previous study on human intestine,[27] while CYP3A4 is the highest detected CYP in human intestine.[28] The peptide sequences used for quantification are provided in Table S4.2.

The calculated ileum and colon mucosal abundances were expressed in units of pmol/g of mucosal tissue. This was done by scaling up protein concentrations in homogenates (pmol/mg homogenate) using the amount of tissue prepared for homogenisation (mucosal weight).

4.3.2. Statistical data analysis

Statistical data analyses and abundance comparisons (ratios relative to healthy control) were performed using Microsoft Excel and GraphPad Prism version 8 (La Jola, CA). To assess technical variability of target quantification, two samples representing the disease group (CD ileum and colon samples), were prepared in triplicate and analysed by LC-MS/MS under the same conditions. The variability was evaluated using the coefficient of variation (CV) of replicates which was between 20 and 30% (data not shown). Based on this only changes ≥2 fold increase/decrease are considered and reported here as the result of CD impact.

4.4.Results

4.4.1. Proteomic analysis of pooled intestine homogenate fractions

In pooled I-CD ileum, a total of 13214 peptides, translating to 2510 proteins, were identified. Out of these, 7 CYPs, 5 UGTs, 21 non-CYP non-UGT drug-metabolising enzymes (DMEs), 6 ABC transporters and 43 SLCs were quantified. In HN-CD ileum, 10064 peptides, translating to 2155 proteins, were identified, which included 8 CYPs, 3 UGTs, 21 non-CYP non-UGT DMEs, 3 ABC transporters and 39 SLCs. In the healthy ileum pool, 16373 peptides and 3113 proteins were identified, allowing quantification of 12 CYPs, 4 UGTs, 27 non-CYP non-UGT DMEs, 10 ABC transporters and 46 SLCs. On the other hand, for colon, 12966 peptides, translating to 2503 proteins, were identified in the pooled I-CD sample, allowing quantification of 4 CYPs, 4 UGTs, 22 non-CYP non-UGT DMEs, 5 ABC transporters and 39 SLCs. In HN-CD colon, 12720 peptides and 2414 proteins were identified, and 5 CYPs, 4 UGTs, 19 non-CYP non-UGT DMEs, 2 ABC transporters and 39 SLCs were quantified. In healthy colon, 16933 peptides and 2959 proteins were identified, allowing quantification of 5 CYPs, 3 UGTs, 23 non-CYP non-UGT DMEs, 7 ABC transporters and 41 SLCs.

In total, the protein levels of 10 ABC transporters, 48 SLCs, 13 CYPs, 5 UGTs and 28 non-CYP non-UGT drug-metabolising enzymes were measured in the two intestinal regions. The expression of DMETs protein levels were compared in ileum (Figure 4.1) and colon (Figure 4.2) as fold change in inflamed CD tissue (I-CD/HV) and in non-inflamed CD tissue (HN-CD/HV) from healthy control. Out of the quantified 48 SLCs, only PEPT1 (SLC15A1), MCT1 (SLC16A1) and OST-α (SLC51A) were of interest in this study for their known clinical involvement in oral drug bioavailability (see Table S4.3), but several SLCs showed a large expression difference relative to healthy tissue (Table S4.4).

4.4.2. Expression of DMETs in ileum of CD patients compared to healthy tissue

The total number of quantified DMETs in healthy ileum was 99 compared to 81 and 74 in I-CD and HN-CD, respectively. Expression of DMEs in I-CD and HN-CD ileum was generally lower than in healthy control, their fold decrease ranged from 2 (CYP4F12) to 96 (SULT1A2) in I-CD. Of the transporters detected, only SLC25A5, showed higher expression in I-CD ileum compared to healthy tissue with a fold change >2. The fold decrease for SLCs ranged from 2 (SLC51A (OST-α)) to 41 (SLC39A5). For the HN-CD ileum, the magnitude of the reduction

or increase was not consistent for the same protein with inflamed samples. The fold decrease was in the range 2 (CES2 and SLC25A24) to 117.7 (SULT1A2) and increased in a range of 2.3 (SLC25A5, MAOA and MGST2) to 8.2 (SLC25A6). Not all identified DMETs in I-CD or HN-CD were present in healthy tissue. UGT2B7, SLC1A5, SLC26A2, SLC35A1, SLC30A1, and ADH1C were detected in CD and/or HN-CD but not in healthy tissue, while CYP2D6, CYP3A5, CYP4F11, CYP4F2, ABCE1, ABCF1, ABCF2, ABCF3, SLC23A1, NAT1, CES3, FMO5, SULT1E1 and SULT2A1 are only detected in healthy ileum.

Figure 4.1A showed that expression of CYP51A1 in I-CD tissue showed the highest difference among DMEs (23-fold reduction) compared to healthy control. Expression of CYP3A4 had a similar 10 fold reduction in expression in both inflamed and histologically normal CD tissue. The lowest reduction in expression was observed with CYP4F12 in I-CD tissue. Fold change in UGT expression (Figure 4.1B) revealed that UGT1A10 had the highest expression difference in I-CD (7-fold reduction) compared to healthy control. Other UGT expression changes >2 were UGT2B17 (2.2 fold reduction) and UGT1A1 (2.1 increase) (Figure 4.1B). In Figure 4.1E, SULT1A2 showed the highest fold decrease in both I-CD and HN-CD ileum compared to healthy control with ~96- and 118-fold reduction in I-CD and HN-CD, respectively.

The most remarkable downregulation of ABC transporters in HN-CD was seen for ABCB7 by ~24 fold (Figure 4.1C) compared to healthy tissue. I-CD showed a lower fold change magnitude with all other quantified ABC transporters, except for ABCD1, MRP3 and BCRP, which were not detected in HN-CD tissue. In Figure 4.1D, MCT1 showed the highest fold decrease in both I-CD and HN-CD ileum compared to healthy control. MCT1 showed ~9- and 13-fold reduction in I-CD and HN-CD, respectively.

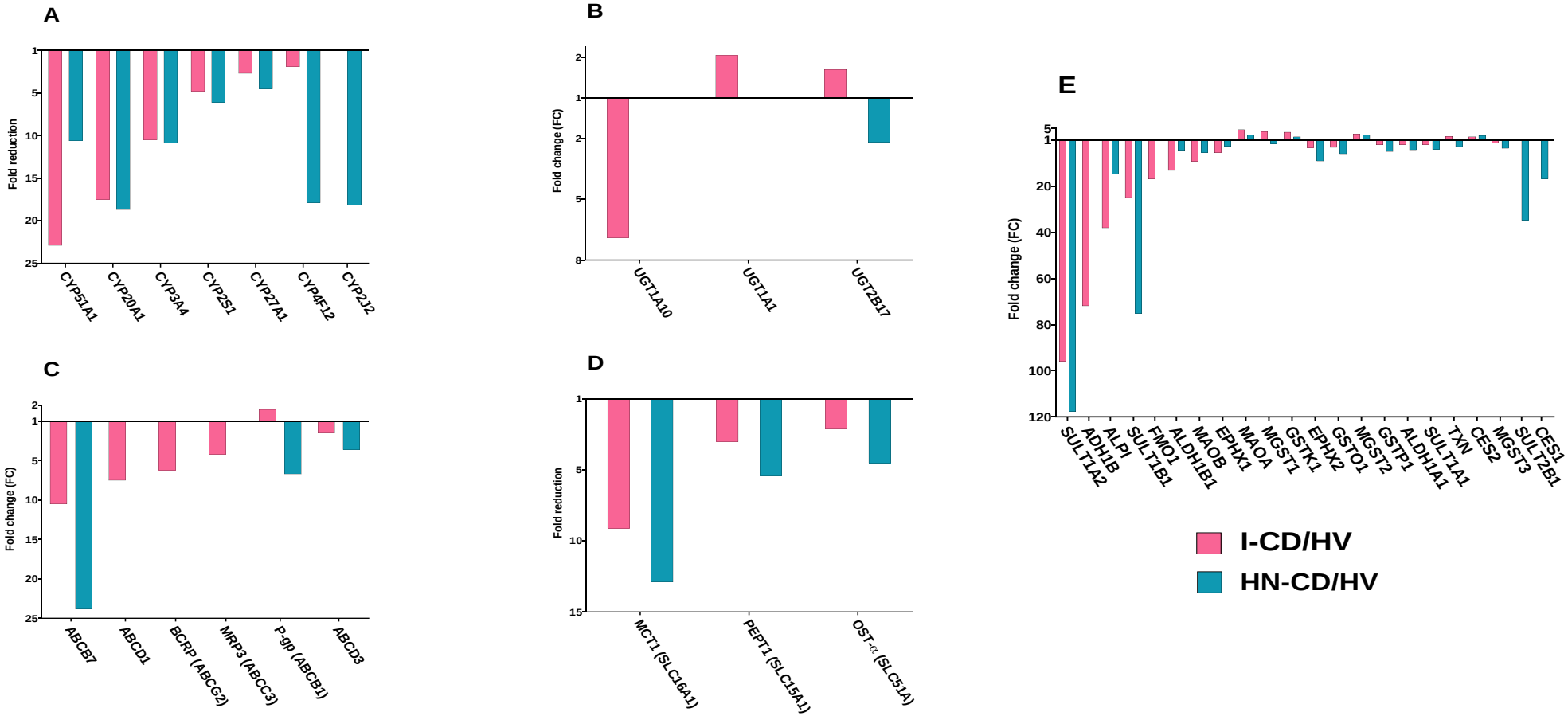

Figure 4.1. *Relative change of expression of DMETs from healthy pooled sample (n=5) in pooled inflamed CD ileum (n=6) (I-CD/HV) and non-inflamed CD ileum (n=2) (HN-CD/HV). Change in expression is shown for* ***(A)*** *CYP enzymes,* ***(B)*** *UGT enzymes,* ***(C)*** *ABC transporters,* ***(D)*** *SLCs of interest (PEPT1, MCT1 and OST-α) and* ***(E)*** *non-CYP, non-UGT drug-metabolising enzymes (DMEs). Whenever there are no data, the protein was not detected in the diseased samples.*

4.4.3. Expression of DMETs in colon of CD patients compared to healthy tissue

A total of 77 DMETs were quantified in healthy colon compared to 73 and 65 in I-CD and HN-CD colon, respectively. Similar to the ileum, expression of DMETs in I-CD and HN-CD colon was lower than healthy tissue (Figure 4.2). The fold decrease in expression of DMETs in I-CD tissue compared to healthy control was in the range of 2 (CYP51A1, ABCB7, SLC1A5 and SLC25A24) to 27.2 (MGST1). A small number of targets showed higher levels, such as SLC2A1 and ALPI. Compared to healthy tissues, nearly all quantified DMETs showed reduction in their expression in HN-CD colon. The fold decrease ranged between 2 (ALDH1B1, ADH1B, SLC35A4 and SLC44A2) and 35.4 (MGST1)). Only SLC44A2 showed 2 fold increase. .

Several DMETs were not detected in healthy colon; UGT2B7, SLC25A22, SLC16A3, OST-α (SLC51A), SLC35A1 and SLC5A1 were only detected in CD and/or HN-CD. On the other hand, ABCF2, ABCF3, SLC35C1, SLC43A2, and SLC2A13 were only detected in healthy tissue. The decrease in CYP2S1 expression was 2.6 and 4 fold (Figure 4.2A) in I-CD and HN-CD colon, respectively, compared to healthy colon. For UGTs, UGT2A3 showed the highest fold change, returning a 7-fold decrease in I-CD and 6-fold decrease in HN-CD. By contrast, UGT1A10 showed the lowest change in UGTs, with ~3 fold decrease in both I-CD and HN-CD from healthy control (Figure 4.2B). Among non-CYP non-UGT enzymes, MGST1 was the most downregulated protein in both inflamed and histologically normal CD colon compared to healthy tissue, returning a ~27- and 35-fold reduction, respectively (Figure 4.2D).

ABCD3 and MRP3 showed the most reduction among ABC transporters (~5.5 fold change in ABCD3 expression in I-CD and ~7.5 fold reduction in MRP3 in HN-CD) (Figure 4.2C).

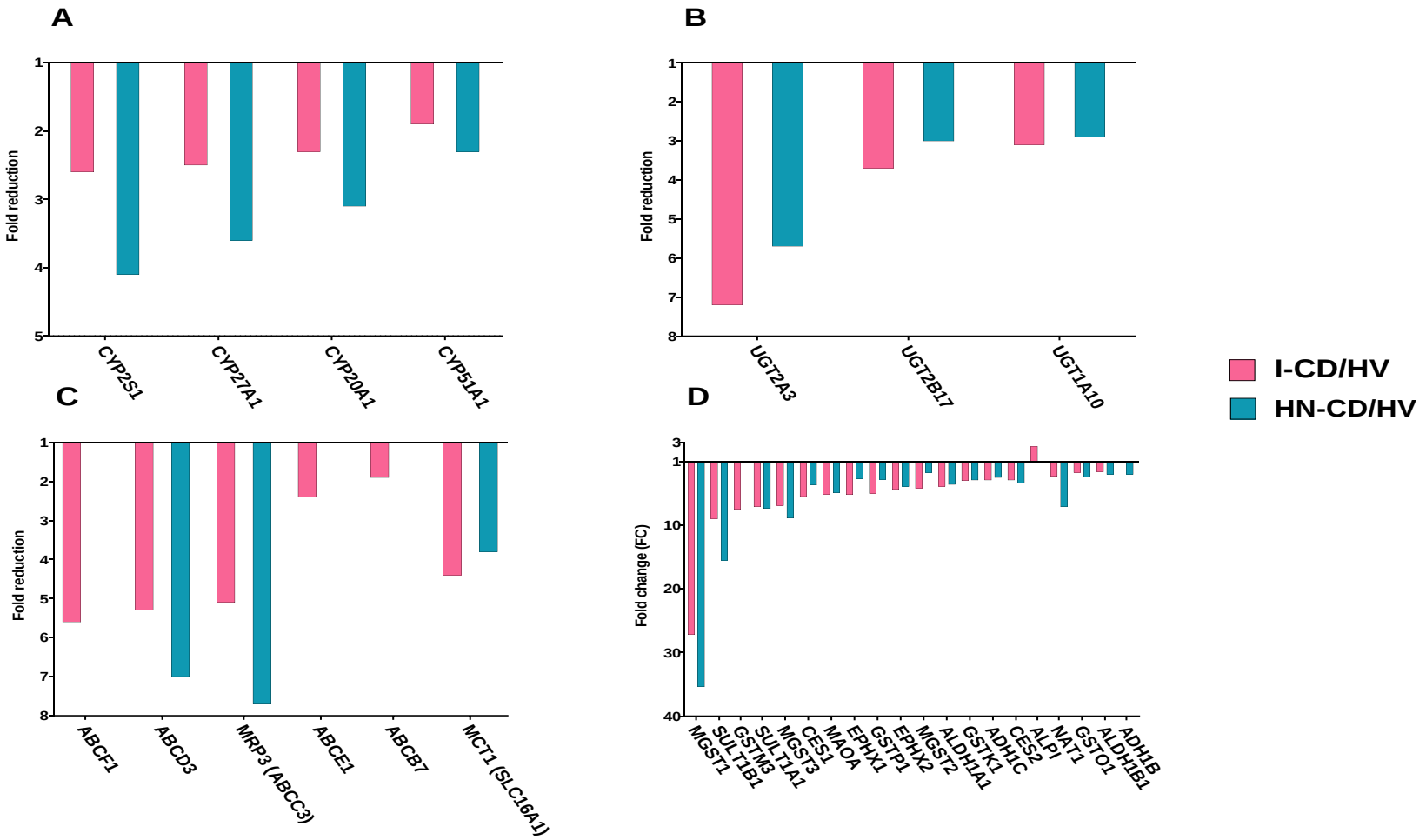

Figure 4.2. *Relative change of expression of DMETs from healthy pooled sample (n=5) in pooled inflamed CD colon (n=7) (I-CD/HV) and non-inflamed CD colon (n=5) (HN-CD/HV). Change in expression is shown for* ***(A)*** *CYP enzymes,* ***(B)*** *UGT enzymes,* ***(C)*** *ABC transporters and SLCs of interest (MCT1) and* ***(D)*** *non-CYP, non-UGT drug-metabolising enzymes (DMEs). Whenever there are no data, the protein was not detected in the diseased sample.*

4.4.4. Relative distribution of DMET expression in CD ileum and colon

Differences in expression of enzymes and transporters in CD between inflamed and histologically normal tissue from the same intestinal segment were observed. In many cases, the same protein had a different trend of expression based on the nature of the tissue. The presence and absence of some DMETs in one tissue but not the other was also observed. In I-CD ileum, 81 DMET proteins were quantified compared to 74 in matching histologically normal tissue (HN-CD). In colon, the number was 73 in I-CD tissue compared to 66 in matching histologically normal tissue (HN-CD). The pie charts in Figures 4.3 and 4.4 show changes in relative distribution of the abundance of DMETs in I-CD and HN-CD ileum and colon, respectively, with reference to healthy tissue. Only proteins that represent at least 3% of total abundance in each tissue were included in the charts of non-CYP non-UGT DMEs and SLCs.

The ileum showed higher, non-uniform relative changes in expression of DMETs in I-CD and HN-CD samples from healthy control compared to the colon. In ileum, CYP27A1 was the most abundant CYP in both I-CD and HN-CD (37% and 24%, respectively) while this was CYP20A1 in healthy samples (18%) (Figure 4.3A). UGT2B17 was the most abundant UGT in healthy and I-CD ileum (38% and 50%, respectively), while UGT2A3 was highest in HN-CD tissue (47%) (Figure 4.3B). For other DMEs, MAOA was the most abundant in I-CD and HN-CD samples (23% in both), while ALPI and SULT1B1 were highest expressed in healthy ileum (14%) (Figure 4.3C). ABCD3 was the most abundant ABC transporter in I-CD and HN-CD samples (50% and 82%, respectively), and ABCF3 was highest in healthy tissue (23%) (Figure 4.3D). SLC25A3 was the most abundant SLC in healthy and HN-CD ileum (35% and 21%, respectively), while this was SLC25A5 in I-CD tissue (27%) (Figure 4.3E).

Colon relative abundance data in I-CD and HN-CD were more consistent compared to healthy expression. For CYPs in all studied tissue groups, CYP2S1 was the highest expressed (39% in I-CD, 26% in HN-CD and 38% in healthy tissue) (Figure 4.4A). UGT2B17 was the highest expressed UGT in all three groups (70% in I-CD, 75% in HN-CD and 66% in healthy) (Figure 4.4B). Non-uniform relative change was observed with non-CYP non-UGT enzymes; the highest expressed enzymes were MAOA in I-CD (15%), TXN in HN-CD (20%) and MGST1 (47%) in healthy colon (Figure 4.4C). ABCD3 was the highest expressed ABC transporter (39% in I-CD, 65% in HN-CD and 42% in healthy) (Figure 4.4D). The case was different with

SLCs; SLC25A5 was the highest expressed in I-CD and healthy tissue (21% and 23%, respectively), while SLC25A6 was the most abundant in HN-CD colon (20%) (Figure 4.4E).

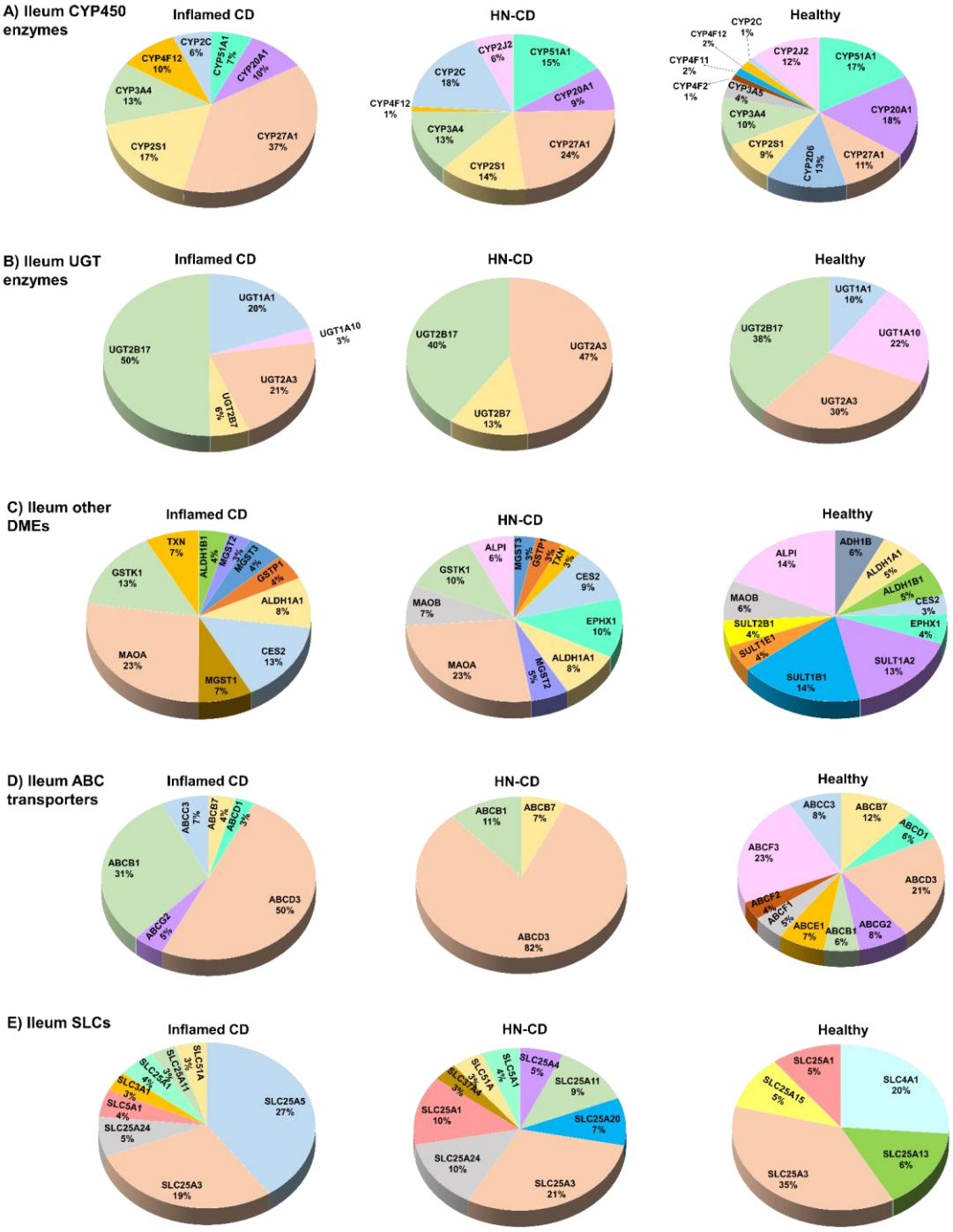

Figure 4.3. *Relative distribution of drug-metabolising enzymes and transporters (DMETs) in inflamed CD ileum, non-inflamed CD ileum and healthy ileum pooled samples, showing changes in* ***(A)*** *CYP enzymes,* ***(B)*** *UGT enzymes,* ***(C)*** *non-CYP, non-UGT drug-metabolising enzymes (DMEs),* ***(D)*** *ABC transporters, and* ***(E)*** *SLCs. For the SLCs and non-CYP non-UGT DMEs, only proteins present at ≥3% of total protein in each group are included in the pie charts.*

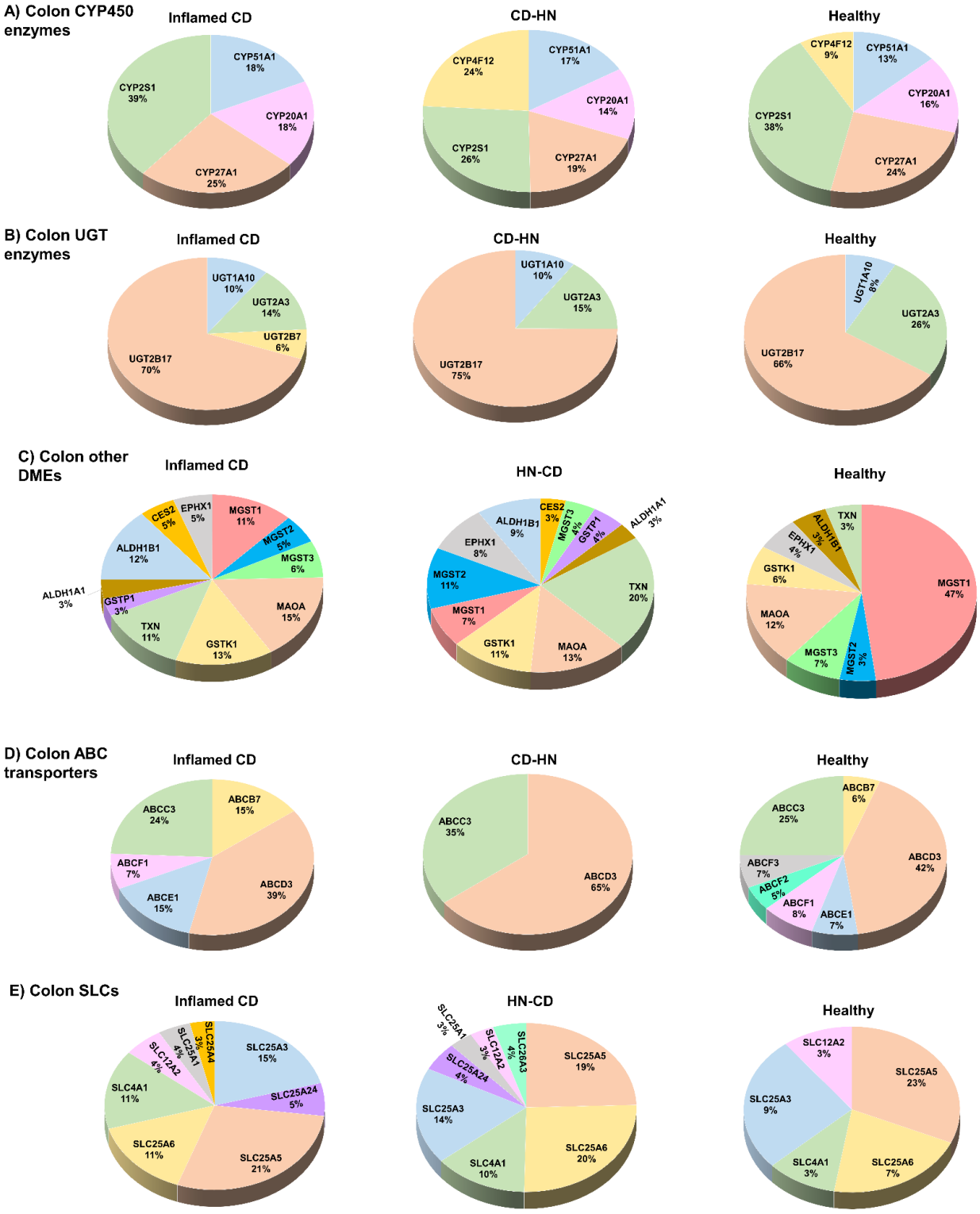

Figure 4.4. *Relative distribution of drug-metabolising enzymes and transporters (DMETs) in inflamed CD colon, non-inflamed CD colon and healthy colon pooled samples, showing changes in* ***(A)*** *CYP enzymes,* ***(B)*** *UGT enzymes,* ***(C)*** *non-CYP, non-UGT drug-metabolising enzymes (DMEs),* ***(D)*** *ABC transporters, and* ***(E)*** *SLCs. For the SLCs and non-CYP non-UGT DMEs, only proteins present at ≥3% of total protein in each group are included in the pie charts.*

4.4.5. DMETs abundance in pmol per g ileum and colon mucosa of CD patients

In total, the protein levels of 13 CYPs, 5 UGTs, 28 non-CYP non-UGT DMEs, 10 ABC transporters and 48 SLCs were measured in the two intestinal regions. Table 4.1 and Table 4.2 show the expression levels in pmol/g of mucosal tissue in I-CD, HN-CD and healthy pooled ileum and colon samples, respectively. The expression levels of other SLCs in the ileum and colon are listed in Table S4.4 and Table S4.5, respectively.

Table 4.1. Abundance (pmol/g of mucosal tissue) of CYP enzymes, UGT enzymes, other enzymes, ABC transporters, SLCs of interest (PEPT1, MCT1 and OST-α) in inflamed Crohn's disease (I-CD), histologically normal Crohn's disease (HN-CD) and healthy ileum pooled samples.

Protein	I-CD	HN-CD	Healthy
Cytochrome P450 enzymes			
CYP51A1	2.1	4.6	48.3
CYP20A1	2.9	2.7	50.5
CYP27A1	11.4	6.9	31.2
CYP2D6	ND	ND	38
CYP2S1	5.2	4.1	25
CYP3A4	ND	4	30
CYP3A4**	4	3.8	41.6
CYP3A5	ND	ND	11.4
CYP4F2	ND	ND	3.7
CYP4F11	ND	ND	4.4
CYP4F12	2.9	0.3	5.5
CYP2C*	1.9	5.2	3
CYP2J2	ND	1.9	34.1
Uridine-5′-diphospho (UDP)-glucuronosyltransferases (UGT)			
UGT1A1	13.7	ND	6.4
UGT1A10	2	ND	14
UGT2A3	15	13	19.4
UGT2B7	4.1	3.4	ND
UGT2B17	35.1	11.1	24.9

Sulfotransferases (SULT)			
SULT1A1	8.5	4.4	18
SULT1A2	2	1.6	191.9
SULT1B1	8.5	2,8	211.3
SULT1E1	ND	ND	59.1
SULT2A1	ND	ND	20.7
SULT2B1	ND	1.7	57.7
Other transferase, phosphatase and thioredoxin enzymes			
GSTK1	60.5	24.2	17.8
GSTO1	9.1	4.9	29.2
GSTP1	19.7	8.3	41.7
MGST1	31.6	5.3	8.6
MGST2	13	11.9	5.1
MGST3	21.2	6.9	25
NAT1	ND	ND	11.9
ALPI	5.7	14.6	216.6
TXN	31.5	6.7	19.5
Dehydrogenase, hydrolase and esterase enzymes			
ADH1B	1.2	ND	85.8
ADH1C	6.1	3.3	ND
ALDH1A1	38.7	19.5	83.2
ALDH1B1	17.17	6	79.2
EPHX1	11.9	24.7	65.7
EPHX2	7.1	2.5	23.1
CES1	ND	1.1	18.7
CES2	61.2	22.3	44.2
CES3	ND	ND	30.7
Flavin-containing monooxygenases and amine oxidase enzymes			
FMO1	0.8	ND	12.8
FMO5	ND	ND	6.1
MAOA	110.8	55.4	24.6
MAOB	9.8	16.8	90.2

ATP-binding cassette (ABC) transporters			
ABCB7	1.8	0.8	18.5
ABCD1	1.3	ND	9.5
ABCD3	21.7	9.2	33.5
BCRP (ABCG2)	2	ND	12.6
P-gp (ABCB1)	13.4	1.3	8.7
ABCE1	ND	ND	11.5
ABCF1	ND	ND	7.9
ABCF2	ND	ND	5.8
ABCF3	ND	ND	35.9
MRP3 (ABCC3)	3.1	ND	13.3
Solute carriers (SLC)			
MCT1 (SLC16A1)	1.9	1.3	17
OST-α (SLC51A)	19.3	9	40.9
PEPT1 (SLC15A1)	5	2.8	15.3

*Group specific as no specific peptides for each enzyme were detected; ** Based on CYP3A4 and 7 unique peptides; ND, Not detected.

Table 4.2. Abundance (pmol/g of mucosal tissue) of CYP enzymes, UGT enzymes, other enzymes, ABC transporters, SLCs of interest (MCT1 and OST-α) in inflamed Crohn's disease (I-CD), histologically normal Crohn's disease (HN-CD) and healthy colon pooled samples.

Protein	I-CD	HN-CD	Healthy
Cytochrome P450 enzymes			
CYP51A1	2.6	2.2	5
CYP20A1	2.5	1.9	5.9
CYP27A1	3.6	2.5	9.1
CYP2S1	5.5	3.5	14.3
CYP4F12	ND	3.2	3.2
Uridine-5′-diphospho (UDP)-glucuronosyltransferase (UGT)			
UGT1A10	3.2	3.5	9.9
UGT2A3	4.4	5.5	31.5
UGT2B7	2	ND	ND
UGT2B17	21.8	26.9	79.7
Sulfotransferases (SULT)			
SULT1A1	3	2.8	20.9
SULT1B1	4.7	2.7	41.9
Other transferase, phosphatase and thioredoxin enzymes			
GSTK1	39.3	40.7	117.1
GSTO1	4.9	3.5	8.2
GSTP1	9.1	16.4	45
GSTM3	1	ND	7.5
MGST1	33.3	25.6	905.9
MGST2	15.2	39.1	64.5
MGST3	19.4	14.9	133
NAT1	3.6	1.2	8.4
ALPI	4.5	ND	1.8
TXN	35.4	74	63.3
Dehydrogenase, hydrolase and esterase enzymes			
ADH1B	ND	2.5	5
ADH1C	4.2	4.8	12.2

ALDH1A1	10.1	10.8	39.1
ALDH1B1	38.9	31.6	62.4
EPHX1	15.8	30.2	82.3
EPHX2	2.3	2.5	9.9
CES1	1.4	2.1	7.8
CES2	14.5	12.4	41.9
CES3	3.6	ND	5.3
Flavin-containing monooxygenases and amine oxidase enzymes			
FMO5	2.4	ND	3.6
MAOA	45.6	48.2	237.9
ATP-binding cassette (ABC) transporters			
ABCB7	2.5	ND	4.7
ABCD3	6.5	4.9	34.4
ABCE1	2.4	ND	5.9
ABCF1	1.2	ND	6.9
ABCF2	ND	ND	4.1
ABCF3	ND	ND	5.5
MRP3 (ABCC3)	4	2.7	20.4
Solute carriers (SLC)			
MCT1 (SLC16A1)	2.6	2.9	11.2
OST-α (SLC51A)	2.3	3.3	ND

ND, Not detected.

4.4.6. Expression profile of DMETs in ileum and colon of CD patients

The expression pattern based on the abundance of the detected proteins in ileum and colon in all three studied groups is represented in a heatmap format (Figure 4.5). CYPs expression pattern showed higher abundance in ileum for all the three examined groups compared to colon (Figure 4.5A). A noticeable exceptions is CYP4F12 in HN-CD colon vs ileum. UGTs were more abundant in HN-CD and healthy colon than ileum, except for UGT2A3 in HN-CD and UGT1A10 in healthy colon (Figure 4.5B). While the opposite is seen within I-CD group, except for UGT1A10. Healthy and I-CD ileum showed a higher abundance of other DMEs for most of the targets vs colon, but the opposite is seen with HN-CD group (Figure 4.5C). Noticeably, CES2 and ALDH1A1 expression was highly different between I-CD ileum and colon, with

ileal expression being higher. For the healthy group, MGST1 and ALPI showed the highest inter-segment difference, with the former being expressed more abundantly in the colon while the latter was more abundant in the ileum.

Healthy and HN-CD ileum showed higher expression of ABCs and lower in I-CD group compared to colon for most of the targets (Figure 4.5D). Exception were ABCC3 and ABCD3 higher in healthy colon and ABCD3 in I-CD ileum. SLCs of interest were more abundant in ileum compared to colon in all three groups, except MCT1 which was higher in HN and I-CD colon than ileum (Figure 4.5E).

In addition to difference in expression in each segment, the presence of some proteins was restricted to only one segment. CYP2C, CYP2D6, CYP2J2, CYP3A4, CYP3A5, CYP4F2 and CYP4F11 were only detected in ileum (Figure 4.5A). From the detected UGTs only UGT1A1 was not detected colon (Figure 4.5B). The only undetected DME in ileum was GSTM3, while FMO1, MAOB, SULT1A2, SULT1E1, SULT2A1 and SULT2B1 were not detected in colon (Figure 4.5C). For transporters, ABCB1, ABCD1, ABCG2 and PEPT1 (SLC15A1) were not detected in the colon (Figure 4.5D and E).

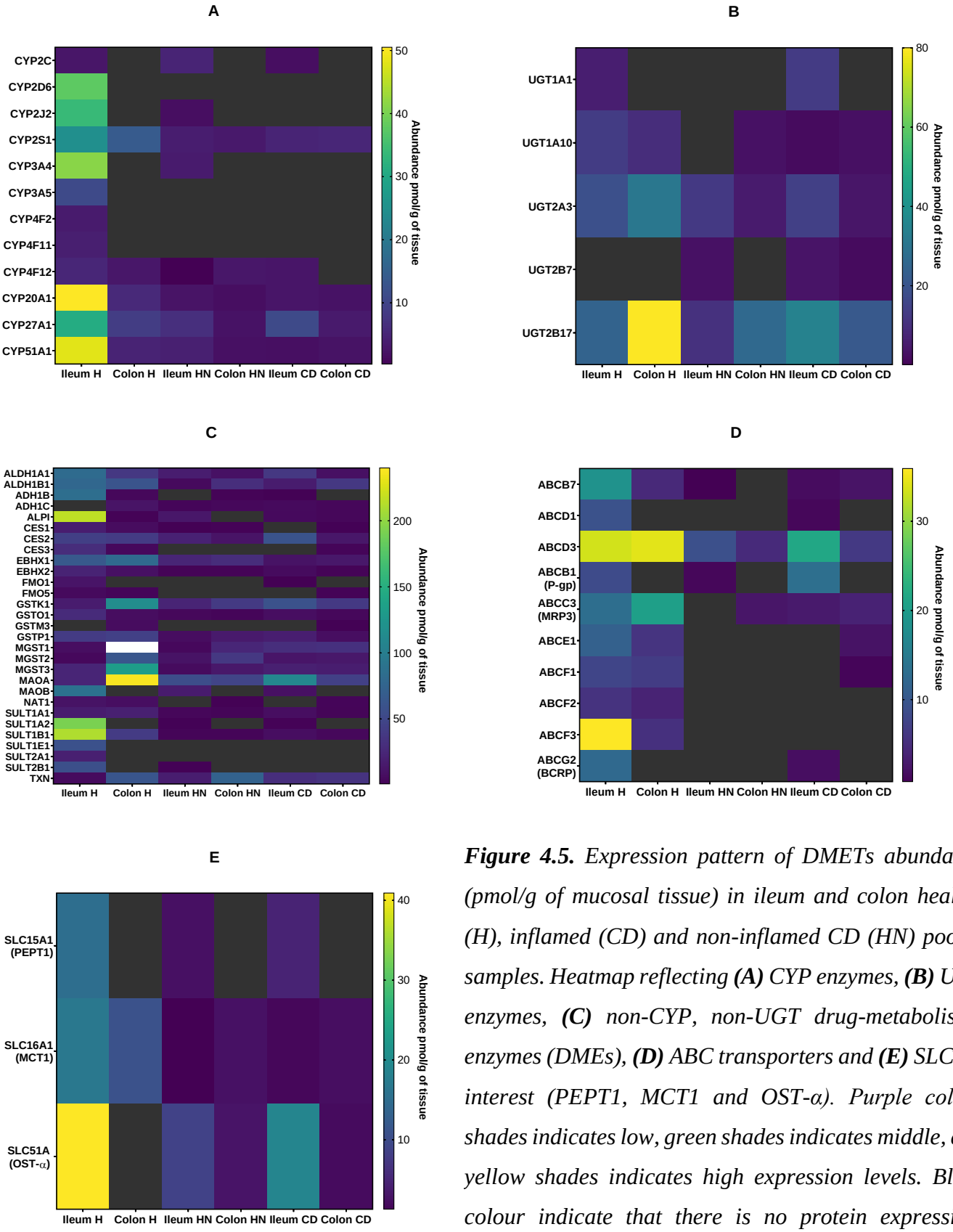

Figure 4.5. *Expression pattern of DMETs abundance (pmol/g of mucosal tissue) in ileum and colon healthy (H), inflamed (CD) and non-inflamed CD (HN) pooled samples. Heatmap reflecting* ***(A)*** *CYP enzymes,* ***(B)*** *UGT enzymes,* ***(C)*** *non-CYP, non-UGT drug-metabolising enzymes (DMEs),* ***(D)*** *ABC transporters and* ***(E)*** *SLCs of interest (PEPT1, MCT1 and OST-α). Purple colour shades indicates low, green shades indicates middle, and yellow shades indicates high expression levels. Black colour indicate that there is no protein expression. MGST1 in the healthy colon group is not included in this figure as it has the highest expression at 905.9 pmol/g of tissue and coloured weight.*

4.5.Discussion

Crohn's disease impact the PK of oral drugs used to control the disease itself, such as budesonide[29] and mesalamine[30], and other medications administered for other medical conditions, such as verapamil[31], midazolam[32] and propranolol.[33] Crohn's population are susceptible to many other diseases due to its chronic effect and young age of onset. Furthermore, 80% of CD patients require a surgery after 20 years of disease onset and approximately 30% within 5 years,[2] reflecting a considerable rate of treatment failure. The incidence of CD has increased steadily in the last 25 years.[34] However, available *in vivo* and *in vitro* data on the effect of CD on pharmacologically relevant intestinal proteins are scarce, which hinders model-based prediction of changes in drug kinetics in CD, with implications for appropriate dose adjustment in these patients.

The protein and gene expression profile of DMETs in CD has previously been reported and compared with control groups in different systems including tissue and cell lines, using mRNA and immunohistochemistry techniques.[15,35] Several reports on SLCs demonstrated upregulation of ENT1, ENT2, CNT2, PEPT1, OATP4A1 and OATP2B1 in CD, whereas ASBT, MCT1 and OCTN2 were downregulated.[14,15] Among ABC transporters, significant upregulation of MRP1 and downregulation of P-gp (MDR1) and MRP3 in CD have been observed,[11–13] but the data related to P-gp were conflicting, with some reports showing unchanged or increased expression levels in CD from normal samples.[18–20] In addition, significant alterations were reported in the expression of DMEs, such as CYP2C9, CYP2B6, CYP2E1, CYP1A1, UGT, GST in colon and rectum[18,19] and SULT2A1 in ileum.[20] Some studies reported no change in the expression of CYP3A5, MRP2, MRP3, BCRP and OSTα/β in CD relative to control.[11,18,20]

Proteomic data in this study show that there are clear differences in expression of most DMETs between adult CD and healthy tissue. The largest change in CYP abundance was observed for CYP51A1 and CYP20A1 in inflamed CD ileum. CYP20A1 is an orphan enzyme, which does not have a known role in drug metabolism,[36] while CYP51A1 is involved in steroid biosynthesis and is an antifungal drug target[37] (Table S4.3). Expression levels of these enzymes in CD intestine have not been reported previously.

CYP3A4 expression was 10 fold lower in inflamed and histologically-normal CD ileum compared with healthy control, confirming previous reports of CYP3A4 mRNA and relative

protein expression (decreased expression by up to 10, ~5 and 2 fold in rectum, colon and ileum, respectively, relative to control).[12,18] Other conflicting immunohistochemistry data were reported, reflecting significantly increased levels (by ~2 fold) in inflamed CD colon compared to control.[19] This may be dependent on the severity of inflammation, disease state of enrolled subjects and the techniques used for measurement.[12,18,19]

Despite the importance of UGT enzymes in drug clearance, their expression was reported in a very limited number of IBD studies.[19,21] Our data demonstrated a significant reduction in expression of UGT1A10 and UGT2A3 (by ~7 fold) in inflamed CD ileum. Anticancer drugs (e.g. irinotecan, flavopiridol and genistein) and cardiovascular agents (e.g. losartan, candesartan, and zolarsartan) are substrates of UGT1A10.[38–40] UGT2A3 has no known substrate or biological role (Table S4.3). Previous studies reported a slight increase in UGT1A1 relative expression (~1.4 fold) in CD colon,[19] in line with the (2 fold) increase in UGT1A1 expression in inflamed CD ileum in the current study. UGT1A1 was not detected in colon in our study. Similar to UGT1A10, UGT1A1 participates in metabolising anticancer and cardiovascular agents (Table S4.3).

SULT1A2 showed the largest reduction among non-CYP non-UGT DMEs in CD ileum samples. This transferase facilitates renal excretion of compounds through sulfonation. Like other SULT enzymes (Table S4.3), SULT1A2 has a wide range of substrates, including steroids, bile acids and phenol- and alcohol-containing compounds.[41] A non-significant reduction in SULT1A2 gene expression was reported in CD ileum and colon.[21] ADH1B and ALPI were considerably reduced in CD ileum by ~70 and ~40 fold, respectively. Similar trends for ALPI were observed using mRNA measurments.[42] ALPI activates several prodrugs (Table S4.3) by removing phosphate groups,[43] while ADH1B participates in retinoid catabolism.[44] Abundance of ADH1B is reported herein for the first time.

ABCB7 showed the highest alteration among ABC transporters. This protein transports heme in the cell, therefore reduced expression can contribute to anaemia.[45] P-gp is the most extensively studied transporter because of its role in efflux of a wide range of substrates.[46,47] Its mRNA and relative expression have been reported to significantly decrease in CD ileum and colon.[11–13] In our data, P-gp levels increased by 1.5 fold in inflamed CD ileum but decreased by ~7 fold in histologically-normal CD ileum. As a limitation of this study, the significance level of alteration was not assessed because each pooled sample was analysed only once. We only detected BCRP in inflamed CD ileum, reflecting a 6 fold reduction from healthy

baseline. A similar finding was previously reported by *Jahnel et al.* who showed that BCRP mRNA expression was significantly reduced (~2 fold) in CD ileum.[20] BCRP is a major multidrug resistance transporter, with mitoxantrone, topotecan, irinotecan, flavopiridol, and methotrexate being some of its anticancer substrates.[48] ABCD3 is the highest expressed in all tissues except for the healthy ileum, it transports long and branched chain fatty acids and bile acid intermediates.[49] In a previous report, ABCD3 was found to be very abundant throughout healthy and diseased tissues from multiple organs including the intestine.[50]

We selected three SLCs of interest (PEPT1, MCT1, OST-α) for their role in pharmacology. Expression of all three transporters decreased in CD samples. MCT1 showed the largest reduction in both CD ileum and colon. Lactate, pyruvate, butyrate, acetoacetate, β-hydroxybutyrate and γ-Hydroxybutyric acid (GHB) are transported by MCT1.[51] Levels of mRNA and relative protein expression were reported to significantly decrease in CD colon and the reduction was linked to butyrate deficiency in IBD patients.[15] PEPT1 relative abundance alteration was in the range of 6 fold and the transporter was only detected in the ileum. PEPT1 transports peptide-like substrates, such as β-lactam antibiotics and angiotensin-converting enzyme inhibitors.[52] A previous survey reported a non-significant increase in PEPT1 in CD ileum and a significant increase in CD colon.[14] Expression of the bile acid and steroids transporter[53] OST-α was shown to be reduced in CD samples in this study. Non-significant mRNA reduction was also previously reported.[20] A meta-analysis of SLC expression in distal ileum showed that PEPT1 represents a higher relative proportion in healthy Caucasian population compared to OST-α, [7] while in our pooled healthy ileum sample, OST-α and PEPT1 accounted for 3% and 1%, respectively, of the identified SLCs.

The significant alteration in various DMETs in this study might be the result of compromised integrity of the epithelium layer due to inflammation. Over the course of disease, enterocytes undergo functional and morphological modifications.[54] This can lead to increased intestine permeability and alteration to its cellular composition.[55] Moreover, the activity and/or expression reduction in CYP2C, CYP3A4, UGT1A1, UGT2B17, P-gp, and BCRP and upregulation of MRP3 are correlated with increased inflammatory biomarkers (ILs, TNF-α, and INF-γ) in inflammatory conditions.[56–58] Treatment of human Caco-2 cell line with pro-inflammatory cytokines caused downregulation of CYP3A4 and upregulation of P-gp mRNA expression.[59] This is seen with our abundance data in inflamed ileum, where CYP3A4 dropped by ~10 fold and P-gp increased by ~1.5 fold relative to healthy baseline. This correlation was

only observed in our ileum samples as CYP3A4 and P-gp were not detected in colon samples. In inflammatory conditions other than IBD, CYP3A4 expression in the liver was reported to be reduced with increased IL-2, IL-1β, IL-6, TNF-α, and INF-α and γ,[57,60,61] while a reduction in liver CYP2C activity was associated with high levels of IL-2.[62] CYP3A4 and CYP2S1 both play a role in controlling inflammatory conditions as they metabolise eicosanoids classes, such as prostaglandins.[63,64] CYP2S1 was the highest expressed CYP in healthy colon and its abundance was downregulated in all CD tissues we examined. Reduction in activity of GSTs was previously linked to increased risk of IBD.[65] All of the detected GSTs in our colon and ileum CD tissues were downregulated except GSTK1 in ileum, which was higher in inflamed and non-inflamed CD tissue. GSTK1 is essential to maintain mitochondrial function and homeostasis. Its deficiency induces inflammation and it is upregulated under oxidative stress.[66] Thus, its increase can be the result of a defence mechanism against inflammation. Similar to GSTs, reduction in ALPI activity increases the risk of IBD as it can lead to altered intestine microbiome, inflammation, and changed permeability.[67] Our data show a large drop in ALPI expression in inflamed and non-inflamed CD ileum (38 and 15 fold, respectively), while in the colon, it increases by 2.5 fold in inflamed relative to healthy colon; it was not detected in non-inflamed CD colon. Expression of transporters is also affected by inflammation; treatment of the intestinal epithelial cell line HT-29 with IFN-γ and TNF-α resulted in downregulation of MCT1 mRNA expression in a dose dependent manner.[15]

The regulatory pathway of DMETs expression can be affected by the inflammation caused by CD. The focus here is on pregnane X receptor (PXR) nuclear receptors as it is responsible for up-regulation of several DMETs including CYP3A4, UGT1A1 and P-gp in human.[68–70] Additionally, it is expressed in the cytoplasm of the intestine cells.[71] In Figure 4.6 an illustration of the regulatory pathway of DMETs expression is shown, the nuclear factor-κB (NF-κB) and PXR compete to bind with DNA-response element in the nucleus to activate the targeted gene transcription and signals the production of the desired proteins.[72] In inflammatory conditions, lipopolysaccharides (LPS) bind to immune receptors in the intestinal epithelial cells (IECs) activating NF-Kβ which stimulate the transcription of pro-inflammatory cytokines and inhibit the activity of PXR nuclear receptor shifting the production from DMETs to cytokines.[73] The impact of the long-standing CD chronic inflammation can explain the high reduction of DMETs expression seen in our HN-CD samples because of the creation of an inflammatory environment in the patient. The continuous production of cytokines and their increase presence in the circulation can affect the nuclear receptors such as PXR in the adjacent non-inflamed

tissue to encounter a similar response to the inflamed tissue while the inflamed tissue is trying to recover and compensate for the low expression of DMETs. It must be noticed that our samples are pooled and the number of non-inflamed ileum samples is low (only two), thus, further investigation based on individual samples and on larger set of samples is required.

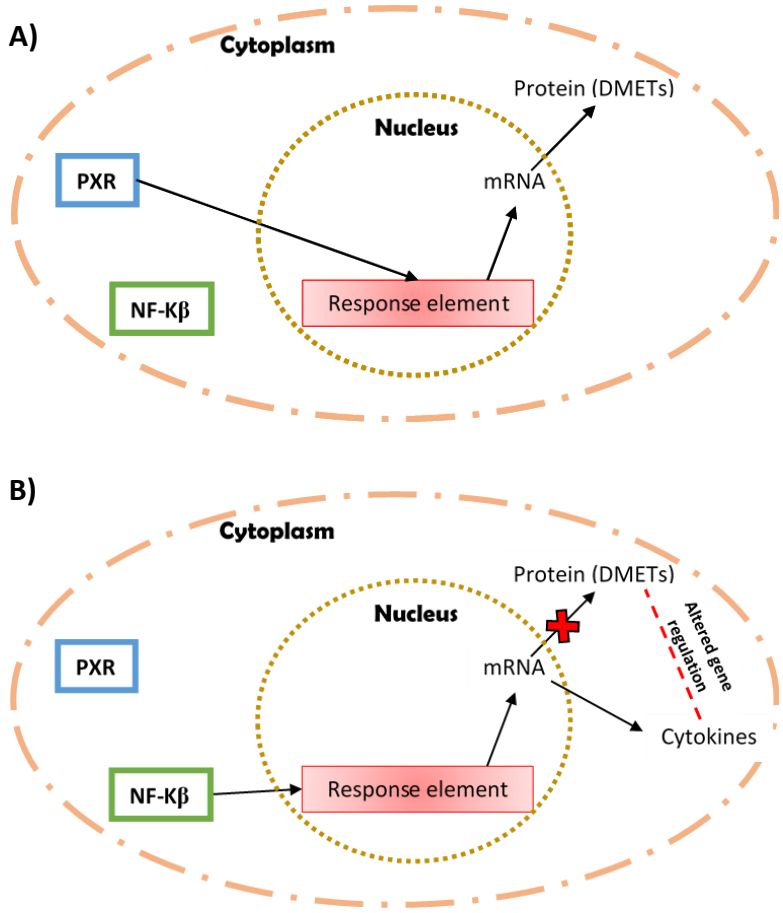

Figure 4.6. *Rough diagram of the general concept of DMETs gene regulation pathway through nuclear receptors specifically PXR.* ***(A)*** *Regulatory pathway under normal conditions* ***(B)*** *Regulatory pathway under inflammation conditions. PXR: pregnane X receptor; NF-kB: nuclear factor-kB.*

Differences observed between inflamed and histologically-normal CD samples are in general agreement with previous reports. Inflamed CD tissue was reported to show larger changes in expression of CYP3A4,[18] P-gp,[13,18] and MCT1[15] compared to non-inflamed tissue. The degree in alteration correlates proportionally with the severity of mucosal inflammation. Mild and moderate mucosal inflammation exhibited non-significant difference in expression of CYP3A4, P-gp[18] and MCT1[15], while a significant reduction was recorded with severely inflamed mucosa compared with non-inflamed mucosa. Such comparison was not possible with our samples as different grades of inflammation severity were not available. Two studies reported alteration of several DMETs in non-inflamed ileum and colon mucosa from CD patients; a significant downregulation in the expression of CYP3A4, SULT2A1, CES2, P-gp

and MRP3 was reported compared with control.[12,21] This is similar to the trends revealed by our data.

The highest abundance alteration in our data was observed in the ileum. Many of the DMETs with high impact on drug PK, such as CYP3A4, CYP3A5, UGT1A1, SULT1A2, SULT2A1, SULT1E1, SULT2B1, P-gp, BCRP and PEPT1 were only detected in the ileum. In general, proteins detected in both the ileum and colon had smaller change in abundance in CD colon compared with the ileum. Such observed difference in abundance of DMETs might be attributed to functional and anatomical properties of each segment. The ileum has a large surface area caused by the abundant presence of villi, which expand the surface area by 30–600 fold, allowing it to play a more prominent role in xenobiotic absorption and biotransformation compared to the colon.[74]

The generated data present, for the first time, quantitative profiles of all detected DMETs in CD ileum and colon using LC-MS/MS methodology. The complexity of CD-driven protein alterations is demonstrated with the impact of disease on inflamed and adjacent non-inflamed tissue. The magnitude of change from healthy expression was variable between the different proteins, regions and conditions. Further studies on the upper segments of the intestine and on individual CD subjects, to establish inter-segment and inter-patient variability, are warranted. This should allow correlation of trends with demographic characteristics, severity of inflammation and medication history for better prediction of drug exposure using PBPK models.

4.6.References

1. Chen L., Deng H., Cui H., Fang J., Zuo Z., Deng J., et al. Inflammatory responses and inflammation-associated diseases in organs. *Oncotarget* 2018. Doi: 10.18632/oncotarget.23208.

2. Feuerstein JD., Cheifetz AS. Crohn Disease: Epidemiology, Diagnosis, and Management. *Mayo Clin Proc* 2017;**92**(7):1088–103. Doi: 10.1016/j.mayocp.2017.04.010.

3. Jones CR., Hatley OJD., Ungell A-L., Hilgendorf C., Peters SA., Rostami-Hodjegan A. Gut Wall Metabolism. Application of Pre-Clinical Models for the Prediction of Human Drug Absorption and First-Pass Elimination. *AAPS J* 2016;**18**(3):589–604. Doi: 10.1208/s12248-016-9889-y.

4. Coutant DE., Hall SD. Disease-Drug Interactions in Inflammatory States via Effects on CYP-Mediated Drug Clearance. *J Clin Pharmacol* 2018;**58**(7):849–63. Doi: 10.1002/jcph.1093.

5. Ghishan FK., Kiela PR. Epithelial Transport in Inflammatory Bowel Diseases. *Inflamm Bowel Dis* 2014;**20**(6):1. Doi: 10.1097/MIB.0000000000000029.

6. Doherty MM., M., Pang KS. First-Pass Effect: Significance of the Intestine for Absorption and Metabolism. *Drug Chem Toxicol* 1997;**20**(4):329–44. Doi: 10.3109/01480549709003891.

7. Harwood MD., Zhang M., Pathak SM., Neuhoff S. The Regional-Specific Relative and Absolute Expression of Gut Transporters in Adult Caucasians: A Meta-Analysis. *Drug Metab Dispos* 2019;**47**(8):854–64. Doi: 10.1124/dmd.119.086959.

8. Bradbury M., Stamler D., Baillie T., Sidhu S., Wood SG., Teva IS., et al. Protein abundance of pharmacokinetically relevant transporter proteins and metabolizing enzymes along the human intestine and in the liver: A comparative intra-subject study. *Drug Metab Pharmacokinet* 2018;**33**(1):S76–7. Doi: 10.1016/j.dmpk.2017.11.252.

9. FDA. Enhancing the Diversity of Clinical Trial Populations — Eligibility Criteria, Enrollment Practices, and Trial Designs Guidance for Industry. 2020.

10. Darwich AS., Ogungbenro K., Vinks AA., Powell JR., Reny JL., Marsousi N., et al. Why has model-informed precision dosing not yet become common clinical reality? lessons from the past and a roadmap for the future. *Clin Pharmacol Ther* 2017;**101**(5):646–56. Doi: 10.1002/cpt.659.

11. Blokzijl H., van Steenpaal A., Borght S Vander., Bok LIH., Libbrecht L., Tamminga M., et al. Up-regulation and Cytoprotective Role of Epithelial Multidrug Resistance-associated Protein 1 in Inflammatory Bowel Disease. *J Biol Chem* 2008;**283**(51):35630–

7. Doi: 10.1074/jbc.M804374200.

12. Wilson A., Urquhart BL., Ponich T., Chande N., Gregor JC., Beaton M., et al. Crohn's Disease Is Associated with Decreased CYP3A4 and P-Glycoprotein Protein Expression. *Mol Pharm* 2019;**16**(9):4059–64. Doi: 10.1021/acs.molpharmaceut.9b00459.

13. Blokzijl H., Borght S Vander., Bok LIH., Libbrecht L., Geuken M., van den Heuvel FAJ., et al. Decreased P-glycoprotein (P-gp/MDR1) expression in inflamed human intestinal epithelium is independent of PXR protein levels. *Inflamm Bowel Dis* 2007;**13**(6):710–20. Doi: 10.1002/ibd.20088.

14. Wojtal KA., Eloranta JJ., Hruz P., Gutmann H., Drewe J., Staumann A., et al. Changes in mRNA Expression Levels of Solute Carrier Transporters in Inflammatory Bowel Disease Patients. *Drug Metab Dispos* 2009;**37**(9):1871–7. Doi: 10.1124/dmd.109.027367.

15. Thibault R., De Coppet P., Daly K., Bourreille A., Cuff M., Bonnet C., et al. Down-Regulation of the Monocarboxylate Transporter 1 Is Involved in Butyrate Deficiency During Intestinal Inflammation. *Gastroenterology* 2007;**133**(6):1916–27. Doi: 10.1053/j.gastro.2007.08.041.

16. Peltekova VD., Wintle RF., Rubin LA., Amos CI., Huang Q., Gu X., et al. Functional variants of OCTN cation transporter genes are associated with Crohn disease. *Nat Genet* 2004;**36**(5):471–5. Doi: 10.1038/ng1339.

17. Jung D. Human ileal bile acid transporter gene ASBT (SLC10A2) is transactivated by the glucocorticoid receptor. *Gut* 2004;**53**(1):78–84. Doi: 10.1136/gut.53.1.78.

18. Thörn M., Finnström N., Lundgren S., Rane A., Lööf L. Expression of cytochrome P450 and MDR1 in patients with proctitis. *Ups J Med Sci* 2007;**112**(3):303–12. Doi: 10.3109/2000-1967-203.

19. Plewka D., Plewka A., Szczepanik T., Morek M., Bogunia E., Wittek P., et al. Expression of selected cytochrome P450 isoforms and of cooperating enzymes in colorectal tissues in selected pathological conditions. *Pathol - Res Pract* 2014;**210**(4):242–9. Doi: 10.1016/j.prp.2013.12.010.

20. Jahnel J., Fickert P., Hauer AC., Högenauer C., Avian A., Trauner M. Inflammatory Bowel Disease Alters Intestinal Bile Acid Transporter Expression. *Drug Metab Dispos* 2014;**42**(9):1423–31. Doi: 10.1124/dmd.114.058065.

21. Langmann T., Moehle C., Mauerer R., Scharl M., Liebisch G., Zahn A., et al. Loss of detoxification in inflammatory bowel disease: dysregulation of pregnane X receptor target genes. *Gastroenterology* 2004;**127**(1):26–40. Doi: 10.1053/j.gastro.2004.04.019.

22. El-Khateeb E., Vasilogianni A-M., Alrubia S., Al-Majdoub ZM., Couto N., Howard M.,

et al. Quantitative mass spectrometry-based proteomics in the era of model-informed drug development: Applications in translational pharmacology and recommendations for best practice. *Pharmacol Ther* 2019;**203**:107397. Doi: 10.1016/j.pharmthera.2019.107397.

23. El-Khateeb E., Al-Majdoub ZM., Rostami-Hodjegan A., Barber J., Achour B. Proteomic Quantification of Changes in Abundance of Drug-Metabolizing Enzymes and Drug Transporters in Human Liver Cirrhosis: Different Methods, Similar Outcomes. *Drug Metab Dispos* 2021;**49**(8):610–8. Doi: 10.1124/dmd.121.000484.

24. Harwood MD., Achour B., Russell MR., Carlson GL., Warhurst G., Rostami-Hodjegan A. Application of an LC-MS/MS method for the simultaneous quantification of human intestinal transporter proteins absolute abundance using a QconCAT technique. *J Pharm Biomed Anal* 2015;**110**:27–33. Doi: 10.1016/j.jpba.2015.02.043.

25. Couto N., Al-Majdoub ZM., Gibson S., Davies PJ., Achour B., Harwood MD., et al. Quantitative Proteomics of Clinically Relevant Drug-Metabolizing Enzymes and Drug Transporters and Their Intercorrelations in the Human Small Intestine. *Drug Metab Dispos* 2020;**48**(4):245–54. Doi: 10.1124/dmd.119.089656.

26. Chevreux G., Tilly N., Bihoreau N. Quantification of proteins by data independent acquisition: Performance assessment of the Hi3 methodology. *Anal Biochem* 2018;**549**:184–7. Doi: 10.1016/j.ab.2018.03.019.

27. Miyauchi E., Tachikawa M., Declèves X., Uchida Y., Bouillot JL., Poitou C., et al. Quantitative Atlas of Cytochrome P450, UDP-Glucuronosyltransferase, and Transporter Proteins in Jejunum of Morbidly Obese Subjects. *Mol Pharm* 2016;**13**(8):2631–40. Doi: 10.1021/acs.molpharmaceut.6b00085.

28. Al-Majdoub ZM., Couto N., Achour B., Harwood MD., Carlson G., Warhurst G., et al. Quantification of Proteins Involved in Intestinal Epithelial Handling of Xenobiotics. *Clin Pharmacol Ther* 2021;**109**(4):1136–46. Doi: 10.1002/cpt.2097.

29. Edsbäcker S., Bengtsson B., Larsson P., Lundin P., Nilsson Å., Ulmius J., et al. A pharmacoscintigraphic evaluation of oral budesonide given as controlled-release (Entocort) capsules. *Aliment Pharmacol Ther* 2003;**17**(4):525–36. Doi: 10.1046/j.1365-2036.2003.01426.x.

30. Norlander B., Gotthard R., Strom M. Pharmacokinetics of a 5-aminosalicylic acid enteric-coated tablet in patients with Crohn's disease or ulcerative colitis and in healthy volunteers. *Aliment Pharmacol Ther* 1990;**4**(5):497–505. Doi: 10.1111/j.1365-2036.1990.tb00496.x.

31. Sanaee F., Clements JD., Waugh AWG., Fedorak RN., Lewanczuk R., Jamali F. Drug−disease interaction: Crohn's disease elevates verapamil plasma concentrations but reduces response to the drug proportional to disease activity. *Br J Clin Pharmacol*

2011;**72**(5):787–97. Doi: 10.1111/j.1365-2125.2011.04019.x.

32. Wilson A., Tirona RG., Kim RB. CYP3A4 Activity is Markedly Lower in Patients with Crohn's Disease. *Inflamm Bowel Dis* 2017;**23**(5):804–13. Doi: 10.1097/MIB.0000000000001062.

33. Schneider R., Bishop H., Hawkins C. Plasma propranolol concentrations and the erythrocyte sedimentation rate. *Br J Clin Pharmacol* 1979;**8**(1):43–7. Doi: 10.1111/j.1365-2125.1979.tb05907.x.

34. Ng SC., Shi HY., Hamidi N., Underwood FE., Tang W., Benchimol EI., et al. Worldwide incidence and prevalence of inflammatory bowel disease in the 21st century: a systematic review of population-based studies. *Lancet* 2017;**390**(10114):2769–78. Doi: 10.1016/S0140-6736(17)32448-0.

35. Rodrigues AD., Rowland A. Profiling of Drug-Metabolizing Enzymes and Transporters in Human Tissue Biopsy Samples: A Review of the Literature. *J Pharmacol Exp Ther* 2020;**372**(3):308–19. Doi: 10.1124/jpet.119.262972.

36. Guengerich FP. Cytochrome P450 and Chemical Toxicology. *Chem Res Toxicol* 2008;**21**(1):70–83. Doi: 10.1021/tx700079z.

37. Strushkevich N., Usanov SA., Park H-W. Structural Basis of Human CYP51 Inhibition by Antifungal Azoles. *J Mol Biol* 2010;**397**(4):1067–78. Doi: 10.1016/j.jmb.2010.01.075.

38. Gagné J-F., Montminy V., Belanger P., Journault K., Gaucher G., Guillemette C. Common Human UGT1A Polymorphisms and the Altered Metabolism of Irinotecan Active Metabolite 7-Ethyl-10-hydroxycamptothecin (SN-38). *Mol Pharmacol* 2002;**62**(3):608–17. Doi: 10.1124/mol.62.3.608.

39. Alonen A., Finel M., Kostiainen R. The human UDP-glucuronosyltransferase UGT1A3 is highly selective towards N2 in the tetrazole ring of losartan, candesartan, and zolarsartan. *Biochem Pharmacol* 2008;**76**(6):763–72. Doi: 10.1016/j.bcp.2008.07.006.

40. Tripathi SP., Prajapati R., Verma N., Sangamwar AT. Predicting substrate selectivity between UGT1A9 and UGT1A10 using molecular modelling and molecular dynamics approach. *Mol Simul* 2016;**42**(4):270–88. Doi: 10.1080/08927022.2015.1044451.

41. Gamage N., Barnett A., Hempel N., Duggleby RG., Windmill KF., Martin JL., et al. Human Sulfotransferases and Their Role in Chemical Metabolism. *Toxicol Sci* 2006;**90**(1):5–22. Doi: 10.1093/toxsci/kfj061.

42. Tuin A., Poelstra K., de Jager-Krikken A., Bok L., Raaben W., Velders MP., et al. Role of alkaline phosphatase in colitis in man and rats. *Gut* 2009;**58**(3):379–87. Doi: 10.1136/gut.2007.128868.

43. Yang Y., Aloysius H., Inoyama D., Chen Y., Hu L. Enzyme-mediated hydrolytic activation of prodrugs. *Acta Pharm Sin B* 2011;**1**(3):143–59. Doi: 10.1016/j.apsb.2011.08.001.

44. Gallego O., Belyaeva O V., Porté S., Ruiz FX., Stetsenko A V., Shabrova E V., et al. Comparative functional analysis of human medium-chain dehydrogenases, short-chain dehydrogenases/reductases and aldo-keto reductases with retinoids. *Biochem J* 2006;**399**(1):101–9. Doi: 10.1042/BJ20051988.

45. Allikmets R., Raskind WH., Hutchinson A., Schueck ND., Dean M., Koeller DM. Mutation of a Putative Mitochondrial Iron Transporter Gene (ABC7) in X-Linked Sideroblastic Anemia and Ataxia (XLSA/A). *Hum Mol Genet* 1999;**8**(5):743–9. Doi: 10.1093/hmg/8.5.743.

46. van Helvoort A., Smith AJ., Sprong H., Fritzsche I., Schinkel AH., Borst P., et al. MDR1 P-Glycoprotein Is a Lipid Translocase of Broad Specificity, While MDR3 P-Glycoprotein Specifically Translocates Phosphatidylcholine. *Cell* 1996;**87**(3):507–17. Doi: 10.1016/S0092-8674(00)81370-7.

47. Chen G., Durán GE., Steger KA., Lacayo NJ., Jaffrézou J-P., Dumontet C., et al. Multidrug-resistant Human Sarcoma Cells with a Mutant P-Glycoprotein, Altered Phenotype, and Resistance to Cyclosporins. *J Biol Chem* 1997;**272**(9):5974–82. Doi: 10.1074/jbc.272.9.5974.

48. Robey RW., Polgar O., Deeken J., To KW., Bates SE. ABCG2: determining its relevance in clinical drug resistance. *Cancer Metastasis Rev* 2007;**26**(1):39–57. Doi: 10.1007/s10555-007-9042-6.

49. Morita M., Imanaka T. Peroxisomal ABC transporters: Structure, function and role in disease. *Biochim Biophys Acta - Mol Basis Dis* 2012;**1822**(9):1387–96. Doi: 10.1016/j.bbadis.2012.02.009.

50. Al-Majdoub ZM., Achour B., Couto N., Howard M., Elmorsi Y., Scotcher D., et al. Mass spectrometry-based abundance atlas of ABC transporters in human liver, gut, kidney, brain and skin. *FEBS Lett* 2020;**594**(23):4134–50. Doi: 10.1002/1873-3468.13982.

51. Vijay N., Morris M. Role of Monocarboxylate Transporters in Drug Delivery to the Brain. *Curr Pharm Des* 2014;**20**(10):1487–98. Doi: 10.2174/13816128113199990462.

52. Foley D., Rajamanickam J., Bailey P., Meredith D. Bioavailability Through PepT1: The Role of Computer Modelling in Intelligent Drug Design. *Curr Comput Aided-Drug Des* 2010;**6**(1):68–78. Doi: 10.2174/157340910790980133.

53. Ballatori N., Christian W V., Wheeler SG., Hammond CL. The heteromeric organic solute transporter, OSTα–OSTβ/SLC51: A transporter for steroid-derived molecules.

Mol Aspects Med 2013;**34**(2–3):683–92. Doi: 10.1016/j.mam.2012.11.005.

54. Barbara G., Stanghellini V., Cremon C., De Giorgio R., Corinaldesi R. What is the effect of inflammation on intestinal function? *Inflamm Bowel Dis* 2008. Doi: 10.1002/ibd.20701.

55. Sartor RB. Current concepts of the etiology and pathogenesis of ulcerative colitis and Crohn's disease. *Gastroenterol Clin North Am* 1995.

56. Cressman AM., Petrovic V., Piquette-Miller M. Inflammation-mediated changes in drug transporter expression/activity: Implications for therapeutic drug response. *Expert Rev Clin Pharmacol* 2012:69–89. Doi: 10.1586/ecp.11.66.

57. Morgan E. Impact of Infectious and Inflammatory Disease on Cytochrome P450–Mediated Drug Metabolism and Pharmacokinetics. *Clin Pharmacol Ther* 2009;**85**(4):434–8. Doi: 10.1038/clpt.2008.302.

58. Coutant DE., Kulanthaivel P., Turner PK., Bell RL., Baldwin J., Wijayawardana SR., et al. Understanding disease-drug interactions in cancer patients: Implications for dosing within the therapeutic window. *Clin Pharmacol Ther* 2015;**98**(1):76–86. Doi: 10.1002/cpt.128.

59. Bertilsson PM., Olsson P., Magnusson K-E. Cytokines influence mRNA expression of cytochrome P450 3A4 and MDRI in intestinal cells. *J Pharm Sci* 2001;**90**(5):638–46. Doi: 10.1002/1520-6017(200105)90:5<638::AID-JPS1020>3.0.CO;2-L.

60. Morgan ET., Goralski KB., Piquette-Miller M., Renton KW., Robertson GR., Chaluvadi MR., et al. Regulation of Drug-Metabolizing Enzymes and Transporters in Infection, Inflammation, and Cancer. *Drug Metab Dispos* 2008;**36**(2):205–16. Doi: 10.1124/dmd.107.018747.

61. Dickmann LJ., Patel SK., Rock DA., Wienkers LC., Slatter JG. Effects of Interleukin-6 (IL-6) and an Anti-IL-6 Monoclonal Antibody on Drug-Metabolizing Enzymes in Human Hepatocyte Culture. *Drug Metab Dispos* 2011;**39**(8):1415–22. Doi: 10.1124/dmd.111.038679.

62. Elkahwaji J., Robin MA., Berson A., Tinel M., Lettéron P., Labbe G., et al. Decrease in hepatic cytochrome P450 after interleukin-2 immunotherapy. *Biochem Pharmacol* 1999;**57**(8):951–4. Doi: 10.1016/S0006-2952(98)00372-4.

63. Nebert DW., Plastaras JP., Guengerich FP., Marnett LJ. Xenobiotic-metabolizing Cytochromes P450 Convert Prostaglandin Endoperoxide to Hydroxyheptadecatrienoic Acid and the Mutagen, Malondialdehyde. *J Biol Chem* 2000;**275**(16):11784–90. Doi: 10.1074/jbc.275.16.11784.

64. Bui P., Imaizumi S., Beedanagari SR., Reddy ST., Hankinson O. Human CYP2S1

Metabolizes Cyclooxygenase- and Lipoxygenase-Derived Eicosanoids. *Drug Metab Dispos* 2011;**39**(2):180–90. Doi: 10.1124/dmd.110.035121.

65. Broekman MMTJ., Bos C., te Morsche RHM., Hoentjen F., Roelofs HMJ., Peters WHM., et al. GST Theta null genotype is associated with an increased risk for ulcerative colitis: a case–control study and meta-analysis of GST Mu and GST Theta polymorphisms in inflammatory bowel disease. *J Hum Genet* 2014;**59**(10):575–80. Doi: 10.1038/jhg.2014.77.

66. Oniki K., Nohara H., Nakashima R., Obata Y., Muto N., Sakamoto Y., et al. The DsbA-L gene is associated with respiratory function of the elderly via its adiponectin multimeric or antioxidant properties. *Sci Rep* 2020;**10**(1):1–12. Doi: 10.1038/s41598-020-62872-5.

67. Bilski J., Mazur-Bialy A., Wojcik D., Zahradnik-Bilska J., Brzozowski B., Magierowski M., et al. The Role of Intestinal Alkaline Phosphatase in Inflammatory Disorders of Gastrointestinal Tract. *Mediators Inflamm* 2017;**2017**:1–9. Doi: 10.1155/2017/9074601.

68. Lehmann JM., McKee DD., Watson MA., Willson TM., Moore JT., Kliewer SA. The human orphan nuclear receptor PXR is activated by compounds that regulate CYP3A4 gene expression and cause drug interactions. *J Clin Invest* 1998;**102**(5):1016–23. Doi: 10.1172/JCI3703.

69. Tien ES., Negishi M. Nuclear receptors CAR and PXR in the regulation of hepatic metabolism. *Xenobiotica* 2006;**36**(10–11):1152–63. Doi: 10.1080/00498250600861827.

70. Geick A., Eichelbaum M., Burk O. Nuclear Receptor Response Elements Mediate Induction of Intestinal MDR1 by Rifampin. *J Biol Chem* 2001;**276**(18):14581–7. Doi: 10.1074/jbc.M010173200.

71. Kliewer SA., Moore JT., Wade L., Staudinger JL., Watson MA., Jones SA., et al. An Orphan Nuclear Receptor Activated by Pregnanes Defines a Novel Steroid Signaling Pathway. *Cell* 1998;**92**(1):73–82. Doi: 10.1016/S0092-8674(00)80900-9.

72. Oladimeji PO., Chen T. PXR: More Than Just a Master Xenobiotic Receptor. *Mol Pharmacol* 2018;**93**(2):119–27. Doi: 10.1124/mol.117.110155.

73. Wu K-C., Lin C-J. The regulation of drug-metabolizing enzymes and membrane transporters by inflammation: Evidences in inflammatory diseases and age-related disorders. *J Food Drug Anal* 2019;**27**(1):48–59. Doi: 10.1016/j.jfda.2018.11.005.

74. Kiela PR., Ghishan FK. Physiology of Intestinal Absorption and Secretion. *Best Pract Res Clin Gastroenterol* 2016;**30**(2):145–59. Doi: 10.1016/j.bpg.2016.02.007.

4.7.Supplementary material – Methodology

Table S4.1. Demographic and tissue details of Crohn's disease (CD) patients and healthy subjects.

Sample ID	Tissues source	Gender	Age	Ethnicity	Tissue classification	Pooled Sample
156	Colon	Male	39	Caucasian-Irish	Diseased	Inflamed CD colon
974	Colon	Male	18	N/A	Diseased	Inflamed CD colon
1569	Colon	Female	31	Caucasian-British	Diseased	Inflamed CD colon
328a	Colon	Female	38	N/A	Diseased	Inflamed CD colon
1942a	Colon	Female	25	N/A	Diseased	Inflamed CD colon
2055	Colon	Male	30	Pakistani	Diseased	Inflamed CD colon
2003a	Colon	Male	68	Caucasian-Irish	Diseased	Inflamed CD colon
844a	Ileum	Female	51	N/A	Diseased	Inflamed CD ileum
917	Ileum	Male	23	Caucasian-Irish	Diseased	Inflamed CD ileum
1265a	Terminal Ileum	Male	46	Caucasian-British	Diseased	Inflamed CD ileum
304	Ileum	Female	27	Caucasian-British	Diseased	Inflamed CD ileum
1004a	Ileum	Female	19	Caucasian-British	Diseased	Inflamed CD ileum
1940a	Ileum	Female	62	Caucasian-British	Diseased	Inflamed CD ileum

328b	Colon	Female	38	N/A	Histologically normal	HN-CD colon
844b	Colon	Female	51	N/A	Histologically normal	HN-CD colon
1265b	Colon	Male	46	Caucasian-British	Histologically normal	HN-CD colon
1942b	Colon	Female	25	N/A	Histologically normal	HN-CD colon
2003b	Colon	Male	68	Caucasian-Irish	Histologically normal	HN-CD colon
1004b	Ileum	Female	19	Caucasian-British	Histologically normal	HN-CD ileum
1940b	Ileum	Female	62	Caucasian-British	Histologically normal	HN-CD ileum
F-28	Colon	Female	50	Caucasian	Healthy	Healthy colon
208A	Colon	Female	78	Caucasian	Healthy	Healthy colon
S3-13	Colon	Male	30	Caucasian	Healthy	Healthy colon
S4-12	Colon	Male	30	Caucasian	Healthy	Healthy colon
M-28	Colon	Male	54	Caucasian	Healthy	Healthy colon
1C-10	Ileum	Male	33	Caucasian	Healthy	Healthy ileum
S13-20	Ileum	Male	48	Caucasian	Healthy	Healthy ileum
S3-26	Ileum	Male	30	Caucasian	Healthy	Healthy ileum
208A	Ileum	Female	78	Caucasian	Healthy	Healthy ileum
90-12-23A	Ileum	Female	65	Caucasian	Healthy	Healthy ileum

Table S4.2. Distinct peptides (unique peptides) sequences with highest intensity assigned to each DMET to quantify their levels in pooled inflamed, histologically normal CD and healthy samples based on Hi-N label-free methodology.

Protein target	Peptide sequence	Peptide sequence	Peptide sequence	Subcellular fraction localisation	Detected in ileum/colon
CYP51A1	EYFESWGESGEK	NEDLNAEDVYSR	CIGENFAYVQIK	Endoplasmic reticulum, microsomes	Both
CYP20A1	NHGTVWSEIGK	LTPVSAQLQDIEGK	TFSSLGFSGTQECPELR		Both
CYP2D6	AFLTQLDELLTEHR	DIEVQGFRIPK			Ileum
CYP2S1	QVQQHQGNLDASGPAR	DLVDAFLLK	LLALVPMGIPR		Both
CYP3A4	VWGFYDGQQPVLAITDPDMIK	GFCMFDMECHK	GVVVMIPSYALHRDPK		Ileum
CYP3A4*	EAETGKPVTLK	DVEINGMFIPK	LFPIAMR		Ileum
CYP3A5	DSIDPYIYTPFGTGPR	YWTEPEEFRPER			Ileum
CYP4F2	NWFWGHQGMVNPTEEGMR	VWMGPISPLLSLCHPDIIR			Ileum
CYP4F11	TLTQLVTTYPQGFK	ACHLVHDFTDAVIQER			Ileum
CYP4F12	TLPTQGIDDFFK	SYITIFNK	SITNASAAIAPK		Both
CYP2C**	VQEEIECVVGR	DFIDCFLIK			Ileum
CYP2J2	VQAEIDRVIGQGQQPSTAAR	DFIDAYLK	LLDEVTYLEASK		Ileum
CYP27A1	LYPVVPTNSR	IQHPFGSVPFGYGVR	DFAHMPLLK	Mitochondrion	Both
UGT1A1	DSAMLLSGCSHLLHNK	DGAFYTLK	ESFVSLGHNVFENDSFLQR	Endoplasmic reticulum membrane	Ileum
UGT1A10	TYSTSYTLEDQNR	GHEVVVVMPEVSWQLER			Both
UGT2A3	GHEVTVLTHSK	GAAVEINFK	ALGRPTTLCETVGK		Both
UGT2B7	TELENFIMQQIK	ANVIASALAQIPQK			Both

UGT2B17	WTYSISK	NDLEDFFMK	MFDRWTYSISK		Both
ADH1B	GAVYGGFK	KPFSIEDVEVAPPK		Cytoplasm	Both
ADH1C	GAIFGGFK	PIHHFVGVSTFSQYTVVDENAVAK		Cytoplasm	Both
ALDH1A1	MSGNGRELGEYGFHEYTEVK	PAEQTPLTALHVASLIK	YILGNPLTPGVTQGPQIDK	Cytosol	Both
ALDH1B1	EEIFGPVQPLFK	TFVEESIYNEFLER	VAFTGSTEVGHLIQK	Mitochondrion	Both
NAT1	EQYIPNEEFLHSDLLEDSK	LDLETLTDILQHQIR	SYQMWQPLELISGK	Cytoplasm	Both
CES1	TVIGDHGDELFSVFGAPFLK	DAGAPTYMYEFQYRPSFSSDMK	TTTSAVMVHCLR	Endoplasmic reticulum	Both
CES2	APVYFYEFQHQPSWLK	SFFGGNYIK	FTEEEEQLSR		Both
CES3	NTIYPLTVDGTVFPK	DSGSPVFFYEFQHRPSSFAK			Both
FMO1	PLGSMIPTGETQAR	INNWLNHANYGLIPEDR	VEDGQASLYK	Endoplasmic reticulum	Ileum
FMO5	KQPDFATSGQWEVVTESEGK	SVIINTSK	ALSQHPTLNDDLPNR		Both
EPHX1	EDDSIRPFK	ENLGQGWMTQK	EETLPLEDGWWGPGTR	Endoplasmic reticulum	Both
EPHX2	ILIPALMVTAEK	AVASLNTPFIPANPNMSPLESIK	ASDESVLSMHK		Both
MGST1	VFANPEDCVAFGK	IYHTIAYLTPLPQPNR		Endoplasmic reticulum	Both
MGST2	VTPPAVTGSPEFER	HLYFWGYSEAAK			Both
MGST3	IASGLGLAWIVGR	VEYPIMYSTDPENGHIFNCIQR	VLYAYGYYTGEPSK		Both
ALPI	QVPDSAATATAYLCGVK	IDHGHHEGVAYQALTEAVMFDDAIER	YEIHRDPTLDPSLMEMTEAALR	Plasma membrane	Both

SULT1A1	VHPEPGTWDSFLEK	THLPLALLPQTLLDQK		Cytoplasm	Both
SULT1A2	YFAEALGPLQSFQARPDDLLISTYPK	SLPEETVDLMVEHTSFK	VYPHPGTWESFLEK		Ileum
SULT1B1	MIYLAR	RGFITEK	NLNDEILDR		Both
SULT1E1	NHFTVALNEK	QLDEMNSPR	NNPSTNYTTLPDEIMNQK		Ileum
SULT2A1	SPWVESEIGYTALSETESPR	LFSSHLPIQLFPK	WIQSVPIWER		Ileum
SULT2B1	ICGFLGRPLGK	GEVQFGSWFDHIK		Cytoplasm, Nucleus and Endoplasmic reticulum	Ileum
MAOA	IFFAGTETATK	DVPAVEITHTFWER	EIPTDAPWEAQHADK	Mitochondrion membrane	Both
MAOB	HLPSVPGLLR	LERPVIYIDQTR	IMDLLGDRVK	Mitochondrion membrane	Ileum
GSTK1	DFLSVMLEK	FLTAVNLEHPEMLEK	GLYMANDLK	Peroxisome	Both
GSTM3	FSWFAGEK	CLDEFPNLK	LLLEFTDTSYEEK	Cytoplasm	Colon
GSTO1	LLPDDPYEK	EDPTVSALLTSEK	VPSLVGSFIR	Cytosol	Both
GSTP1	DQQEAALVDMVNDGVEDLR	YISLIYTNYEAGK	MLLADQGQSWK	Nucleus and Mitochondrion	Both
TXN	PFFHSLSEK	CMPTFQFFK	TAFQEALDAAGDK	Nucleus and Cytoplasm	Both
ABCB7	VLSGISFEVPAGK	LQEEIVNSVK	LAGLHDAILR	Mitochondrion membrane	Both

ABCD1	DQVIYPDSVEDMQR	VHEMFQVFEDVQR		Membrane protein	Ileum
ABCD3	VGITLFTVSHR	IANPDQLLTQDVEK	LITNSEEIAFYNGNK	Peroxisome membrane	Both
ABCG2 (BCRP)	LFDSLTLLASGR	TIIFSIHQPR	LLSDLLPMR	Plasma membrane	Ileum
ABCB1 (P-gp)	FYDPLAGK	NVHFSYPSRK	SEIDALEMSSNDSR		Ileum
ABCE1	ADIFMFDEPSSYLDVK	GTVGSILDRK	NTVANSPQTLLAGMNK	Mitochondrion membrane	Both
ABCF1	FGLESHAHTIQICK	NLDFGIDMDSR	NQDEESQEAPELLK	Nucleus and cytoplasm	Both
ABCF2	SMLLSAIGK	LMELYERLEELDADK	TPLHCVMEVDTER	Membrane protein	Both
ABCF3	LLLGDLAPVR	TSNPLVLEEASASQAGSRK			Both
ABCC3 (MRP3)	SQLTIIPQDPILFSGTLR	IDGLNVADIGLHDLR	SPIYSHFSETVTGASVIR	Plasma membrane	Both
SLC3A2	DLLLTSSYLSDSGSTGEHTK	GLVLGPIHK	IGDLQAFQGHGAGNLAGLK	Membrane protein	Both
SLC1A5	EVLDSFLDLAR	LGPEGELLIR		Plasma membrane	Both
SLC33A1	LLWAPLVDAVYVK	YTAGPQPLNTFYK	TPDAVELCK	Endoplasmic reticulum membrane	Both
SLC25A4	EFHGLGDCIIK	QLFLGGVDR	EQGFLSFWR	Mitochondrion membrane	Both
SLC25A5	GTDIMYTGTLDCWR	AAYFGIYDTAK	KGTDIMYTGTLDCWR		Both
SLC25A6	HTQFWR	DFLAGGIAAAISK			Both

SLC4A1	IFQDHPLQK	ADFLEQPVLGFVR	AAATLMSER	Plasma membrane	Both
SLC25A12	ILREEGPSAFWK	IVQLLAGVADQTK	LATATFAGIENK	Mitochondrion membrane	Both
SLC25A13	VTAIDFR	NGEFFMSPNDFVTR	STGSFVGELMYK		Both
SLC44A1	NLPFTPILASVNR	LVSGYDSYGNICGQK	LPVPASAPIPFFHR	Membrane protein	Both
SLC44A2	NDGSAERPYFMSSTLK	CQFAFYGGESGYHR	DFEYYK		Both
SLC44A4	NAFMLLMR	YDPSFRGPIK	NEFSQTVGEVFYTK	Plasma membrane	
SLC25A10	VHLQTQQEVK	VLLGSVSGLAGGFVGTPADLVNVR	FAIYETVR	Mitochondrion membrane	Both
SLC35C1	YLLDSPSLR	VLPAVDGSIWR		Golgi apparatus membrane	Both
SLC37A4	AGLSNYGNPR	FVSGVLSDQMSAR	DDLGFITSSQSAAYAISK	Endoplasmic reticulum membrane	Both
SLC25A22	VYTSMSDCLIK	SRGIAGLYK	GVNEDTYSGILDCAR	Mitochondrion membrane	Both
SLC2A1	FLLINRNEENR	GRTFDEIASGFR	KVTILELFR	Plasma membrane	Both
SLC2A2	HVLGVPLDDRK	SFEEIAAEFQK	LGPSHILIIAGR		Ileum
SLC43A2	FSWLGFDHK	FLVSGDQK		Membrane protein	Both
SLC25A11	ITREEGVLTLWR	NVFNALIR	LGIYTVLFER	Mitochondrion membrane	Both

SLC25A20	LQTQPPSLPGQPPMYSGTFDCFR	LQTQPPSLPGQPPMYSGTFDCFRK	CLLQIQASSGESK	Mitochondrion membrane	Both
SLC16A1 (MCT1)	SITVFFK	DLHDANTDLIGRHPK	DLHDANTDLIGR	Plasma membrane	Both
SLC16A3	AVSVFFK	GGAVVDEGPTGVK		Plasma membrane	Both
SLC25A3	IQTQPGYANTLR	GVAPLWMR	FACFER	Mitochondrion membrane	Both
SLC25A15	MQTFPDLYR	IQVLSMSGK	NEGITALYSGLK	Mitochondrion membrane	Ileum
SLC51A (OST-α)	LHLGEQNMGAK	NTLCPIK	VGYETFSSPDLDLNLK	Plasma and Endoplasmic reticulum membrane	Both
SLC2A13	EVGSAGPVICR	STVIDSSCVPVNK		Plasma membrane	Both
SLC12A2	LSGVEDHVK	SPGWRPAFK	PALLHLVHDFTK	Plasma membrane	Both
SLC15A1 (PEPT1)	CGFNFTSLK	HTLLVWAPNHYQVVK	WTLQATTMSGK	Membrane protein	Ileum
SLC22A18	TDAQAPLPGGPR	ASVFDLK	TLGPTVGGLLYR	Plasma membrane	Both
SLC23A1	LAGAPPPPVHAINR	FDMLYK	AYGFQAR	Plasma membrane	Ileum

SLC25A40	FGAVTVISPLELIR	KPGNFQGTLDAFFK		Mitochondrion membrane	Colon
SLC26A2	QTVNPILIK	DSAEGNDSYPSGIHLELQR	FVAPLYYINK	Plasma membrane	Both
SLC26A3	SVLAALALGNLK	GFICTVDTIK	QGLLQVTPK	Plasma membrane	Both
SLC27A2	MTLVEEGFNPAVIK	SLLHCFQCCGAK	VDEVSTEPIPESWR	Membrane protein	Both
SLC27A4	ILSFVYPIR	TALIFEGTDTHWTFR	AGMAAVASPTGNCDLER	Endoplasmic reticulum membrane	Both
SLC35A3	YLSSTAVVVAELLK	VLHDEILNK		Golgi apparatus membrane	Both
SLC35B2	FVSFPTQVLAK	AVPVESPVQK	TEAAETTPMWQALK	Golgi apparatus membrane	Both
SLC35A4	RVEDEVNSGVGQDGSLLSSPFLK	GFLAGYVVAK	NQLESLQR	Golgi apparatus membrane	Both
SLC39A14	ALLNHLDVGVGR	IGSSELQEFCPTILQQLDSR		Membrane protein	Both
SLC4A4	PLISPAAER	AIATLMSDEVFHDIAYK	LADYYPINSNFK	Plasma membrane	Both

SLC6A19	GSLGVWSSIHPALK	SSPVDYFWYR	IPSLAELETIEQEEASSRPK	Plasma membrane	Ileum
SLC5A1	IACVVPSECEK	EERIDLDAEEENIQEGPK	AGVVTMPEYLRK	Membrane protein	Both
SLC5A12	TWPLPLSTDQCIK	EFLVGGR	SGITSTYEYLQLR	Plasma membrane	Ileum
SLC25A24	VLPAVGISYVVYENMK	FWAYEQYK	TSTAPLDRLK	Mitochondrion membrane	Both
SLC3A1	GEGLIFEHNTK	LYQDLSLLHANELLLNR	FMGTEAYAESIDR	Membrane protein	Ileum
SLC25A1	MQGLEAHK	FFVMTSLR	NTWDCGLQILK	Mitochondrion membrane	Both
SLC30A1	ESALILLQTVPK	CEDPTSYMEVAK		Plasma membrane	Both
SLC30A7	LIVAPDADAR	TPPLLENSLPQCYQR		Golgi apparatus membrane	Both
SLC30A9	TPEELETFMLK	LTELLENDPSVR		Membrane protein	Colon

* Based on CYP3A4 and CYP3A7 unique peptides **Group specific as no specific peptides of each isoform is detected

4.8.Supplementary material – Results

Table S4.3. List of DMEs and transporters detected/quantified in the investigated pooled colon and ileum samples. The list includes proteins with 10 or more fold change in inflamed CD or HN-CD samples from healthy pooled ileum and colon controls.

Gene name	Other names	Substrate Specificity/importance	Detection in the examined colon/ileum tissues	References
CYP51A1	LDM, CYPLI	Involved in sterols biosynthesis which are an essential membrane component, and precursors to various hormones, vitamin D, and bile acids. It is involved in cholesterol biosynthesis in humans and ergosterol in fungi. Thus, CYP51A is an important drug target. Its inhibition in fungi by azole drugs is used to prevent of fungal growth. In addition, CYP51 is a potential target for cholesterol-lowering drug in human. CYP51 is also responsible for production of the follicular fluid meiosis-activating sterol (MAS) in mammals. MAS contributes to gametogenesis in an unknown mechanism.	All investigated samples	1
CYP20A1	-----	Has no known substrate or biological role (orphan CYP enzyme).		2

CYP27A1	CYP27	Hydroxylises cholesterol, cholesterol derivatives and vitamin D3 to its active form and is involved in cholesterol homeostasis by catalysing its conversion to bile acids.		3,4
CYP2S1	CYPIIS1	Metabolises retinoids and eicosanoids that are used to treat skin conditions.		5
CYP3A4	CYPIIIA3, CYPIIIA4	Contributes to 30-40% of xenobiotic metabolism.	All ileum (Inflamed CD, HN-CD and Healthy)	6
CYP3A5	CYPIIIA5	Metabolises steroids and vitamins.	Healthy ileum	7
CYP4F2	CYPIVF2	Metabolises fatty acids, eicosanoids and vitamins.	Healthy ileum	8
CYP4F11	CYPIVF11		Healthy ileum	9,10
CYP4F12	CYPIVF12	Metabolises polyunsaturated fatty acids, arachidonate and antihistamine drugs. It has different xenobiotic substrates from other CYP4F isoforms.	All ileum (Inflamed CD, HN-CD and Healthy) HN-CD colon Healthy colon	11,12
CYP2J2	CYPIIJ2	Metabolises albendazole and fenbendazole anthelmines, danazol, amiodarone, terfenadine, astemizole, thioridazine, tamoxifen, cyclosporin A and nabumetone.	HN-CD ileum Healthy ileum	13,14
UGT1A1	hUG-BR1	Metabolise estrogen hormones, bilirubin, anticancer and cardiovascular agents.	Inflamed CD ileum Healthy ileum	15–18
UGT1A10	UGT-1J		All colon (Inflamed CD, HN-CD and Healthy)	

			Inflamed CD ileum Healthy ileum	
UGT2A3	UDPGT 2A3	No identified substrate or biological role. Its function is assumed to be the same as other UGTs.	All investigated samples	
UGT2B7	UDPGT 2B9	Metabolises steroid hormones, bile acid, angiotensin receptor antagonist and mycophenolate. It also regulates retinoic acid levels.	Inflamed CD colon Inflamed CD ileum HN-CD ileum	16,19–21
UGT2B17	UDPGT 2B17	Metabolises estrogen hormones and androgens.	All investigated samples	22
ADH1B	ADH2	Participates in retinoid catabolism	Inflamed CD ileum HN-CD colon Healthy colon Healthy ileum	23
ALDH1B1	ALDH5, ALDHX	Metabolizes aliphatic and aromatic aldehydes including acetaldehyde, and is also involved in metabolism of corticosteroids, amines and lipids. Increased expression and/or activity of ALDH1A1 and ALDH1B1 can be a potential biomarker for human colon cancer.	All investigated samples	24,25
NAT1	ARY1, AAC1	Catalyses N-Acetylation and O-acetylation, and metabolises aromatic and heterocyclic amines. Can activate carcinogenesis.	All colon (Inflamed CD, HN-CD and healthy) Healthy ileum	26

CES1	SES1, ACAT, CE-1, hCE-1	Metabolises ester, thioester, carbamate and amide containing drugs.	All colon (Inflamed CD, HN-CD and healthy) HN-CD ileum Healthy ileum	27
FMO1	—	Metabolises nucleophilic nitrogen, sulfur, selenium, and phosphorous containing drugs. Chlorpromazine, promethazine, brompheniramine, cimetidine, ranitidine, and itopride are some of its substrates.	Inflamed CD ileum Healthy ileum	28
EPHX1	mEH, EPOX, HYEP	Metabolises epoxides to diols. Converts xenobiotics faster than endogenous substrates compared to EPHX2. Mainly detoxifies rather than activates its substrates.	All investigated samples	29
EPHX2	CEH, sEH	Hydrolyses cholesterol and epoxyeicosatrienoic acids (anti-inflammatory and vasodilator metabolite) to less active metabolites.	All investigated samples	30
MGST1	GST12	Detoxifying enzymes that conjugate glutathione to hydrophobic electrophilic compounds. Also, participate in lipids metabolism.	All investigated samples	31,32
MGST3	GST-3			
ALPI		Catalyses the removal of phosphate groups from a diverse class of compounds, including nucleotides, proteins and alkaloids.	All ileum (Inflamed CD, HN-CD and healthy) Inflamed CD colon	33

		It activates several prodrugs to their active form, including oxymethylphosphate prodrugs of lopinavir, oxyethylphosphate prodrugs of ritonavir, fosamprenavir phosphate prodrug of amprenavir and dinitrobenzamide mustards, a prodrug group of anticancer medications.	Healthy colon	
SULT1A1	ST1A1, STP1, HAST1	Catalyse sulfate conjugation of compounds with hydroxyl or amine groups. The sulfonation process facilitates the compounds' renal excretion by increasing their water solubility. They work on a broad range of endogenous and xenobiotic substrates, including steroids, bile acids and compounds containing phenol and alcohol. These include paracetamol. Also, they can activate other substrates to their active metabolites.	All investigated samples	34,35
SULT1A2	ST1A2, STP2		All ileum (Inflamed CD, HN-CD and healthy)	
SULT1B1	ST1B1		All investigated samples	
SULT2B1	ST2B1, HSST2		HN-CD ileum Healthy ileum	
ABCB1	MDR1, P-gp	Translocates phospholipids across the membrane. Decreases drug accumulation in multidrug resistance cells.	All ileum (Inflamed CD, HN-CD and Healthy)	36,37
ABCB7	ABC7	Participates in heme and fatty acid transport; polymorphism can causes abnormal iron, fatty acid metabolism and sideroblastic anemia.	All ileum (Inflamed CD, HN-CD and Healthy) Inflamed CD colon Healthy colon	38

ABCC3	MRP3, CMOAT2, MLP2	Transports a wide range of substrates, such as anticancer drugs, cyclic peptides and cyclic nucleotides. It has a high affinity to glucuronide conjugate compounds, which aid in removal of toxic organic anions.	All colon (Inflamed CD, HN-CD and Healthy) Inflamed CD ileum Healthy ileum	39
ABCD1	ALD	Transports very long chain fatty acids (VLCFAs) and their co-esters	Inflamed CD ileum Healthy ileum	40
ABCD3	PMP70	Transports long and branched chain fatty acids and bile acid intermediates.	All investigated samples	41
ABCE1	RLI, RNASEL1, RNASELI	Participates in ribosomal recycling mechanisms.	Inflamed CD colon Healthy colon Healthy ileum	42
ABCF1	ABC50	Participates in innate immunity regulation.	Inflamed CD colon Healthy colon Healthy ileum	43
ABCF2	HUSSY-18	Role in uterine cancer prognosis.	Healthy colon Healthy ileum	44
ABCF3		Assumed to have an antiviral effect against flaviviruses.	Healthy colon Healthy ileum	
ABCG2	BCRP, MXR	One of the major multidrug resistance transporters. Anticancer drugs, mitoxantrone, topotecan, irinotecan, flavopiridol, and methotrexate are some of its substrates.	Inflamed CD ileum Healthy ileum	45

SLC16A1	MCT1	Transports monocarboxylate, including lactate, pyruvate, butyrate, acetoacetate, β-hydroxybutyrate and γ-Hydroxybutyric acid (GHB) substrates	All investigated samples	46
SLC51A	OST-α	Transports bile acids and steroids, as well as structurally-related compounds	All ileum (Inflamed CD, HN-CD and Healthy) Inflamed CD colon HN- CD colon	47
SLC15A1	PEPT1	Transports peptide-like substrates, such as β-lactam antibiotics, angiotensin-converting enzyme inhibitors, antivirals and renin inhibitors	All ileum (Inflamed CD, HN-CD and Healthy)	48
SLC16A3	MCT4	Transports monocarboxylate, which include lactate, pyruvate, acetoacetate and β- hydroxybutyrate substrates	Inflamed CD colon Inflamed CD ileum Healthy ileum	49,50
SLC33A1	ACATN, AT1	Transports acetyl–CoA	All investigated samples	51
SLC25A3	PTP, PHC	Transports phosphate and copper	All investigated samples	52
SLC25A10	DIC	Transports dicarboxylate substrates malonate, malate and succinate	All investigated samples	53

SLC25A12	ARALAR1, AGC1	Calcium binding transports that are aspartate and glutamate carriers from mitochondria to cytosol	All colon (Inflamed CD, HN-CD and healthy) Inflamed CD ileum Healthy ileum	54
SLC25A13	ARALAR2, AGC2		All investigated samples	
SLC25A15	ORC1, ORNT1	Transports mitochondrial ornithine and participates in urea cycle, ammonium detoxification and arginine synthesis	HN-CD ileum Healthy ileum	55
SLC27A2	ACSVL1, FACVL1, FATP2, VLACS	Transports long chain and very long chain fatty acids. It affects various pathways of lipid and bile metabolism	All investigated samples	56
SLC27A4	ACSVL4, FATP4	Transports long chain and very long chain fatty acids. FATP transporters are considered one of the main fatty acid transporter families in small intestinal enterocytes.	All ileum (Inflamed CD, HN-CD and healthy) HN-CD colon Healthy colon	57
SLC30A7	ZNT7, ZNTL2	Transports zinc to Golgi apparatus. Participates in activation of alkaline phosphatases.	All investigated samples	58
SLC35A4	__	Transports nucleotide sugar.	All investigated samples	59

SLC39A5	ZIP5	Transports zinc. Participates in regulation of bone morphogenetic protein transforming growth factor-beta and eye development.	All ileum (Inflamed CD, HN-CD and healthy)	60
SLC35B2	PAPST1, PSEC0149	Transports adenosine 3'-phospho 5'-phosphosulfate (PAPS).	All investigated samples	61
SLC3A1	RBAT	Transports neutral and basic amino acids.	All ileum (Inflamed CD, HN-CD and healthy)	62
SLC4A1	AE1, DI, EPB3	Transports bicarbonates across the cell membrane. Involved in cells maintenance as it regulates intracellular pH and acid-base balance.	All investigated samples	63
SLC5A12	SMCT2	Transports monocarboxylates, such as acetate and pyruvate substrates	Inflamed CD ileum Healthy ileum	64
SLC12A2	NKCC1	Cotransports electroneutral ions (chloride, potassium and sodium). Involved in cells maintenance as it regulates ionic balance and cell volume.	All investigated samples	65
SLC22A18	BWR1A, BWSCR1A, HET, IMPT1, ITM, ORCTL2	Might participate in transport of cations, chloroquine and quinidine compounds.	All investigated samples	66

Table S4.4. Abundance (pmol/g mucosa) of SLC transporters in adult ileum inflamed Crohn's disease (I-CD), histologically normal Crohn's disease (HN-CD) and healthy pooled samples.

DMET name	I-CD	HN-CD	Healthy
SLC3A2	5.1	4.5	22.9
SLC1A5	6.3	3.3	ND
SLC33A1	2.2	0.9	39.1
SLC25A4	13.4	12.4	55
SLC25A5	164.3	68.6	30.1
SLC25A6	8	61.4	7.4
SLC4A1	24.1	11	371.9
SLC25A12	1.5	ND	42.1
SLC25A13	9.5	3.1	188
SLC44A1	3.8	3.1	4.6
SLC44A2	1.9	1.7	4.6
SLC44A4	6	ND	5.1
SLC25A10	8.8	5.2	63
SLC35C1	7.2	ND	11.6
SLC37A4	4.3	6.9	7.3
SLC25A22	ND	5.8	15.1
SLC2A1	3.5	1.7	9.5
SLC2A2	ND	1.3	5.2
SLC43A2	ND	1.7	6.5
SLC25A11	15.2	22.9	15.3
SLC25A20	14.1	17.8	31.3
SLC16A3	0.9	ND	10.9
SLC25A3	116.6	56.3	1047.6
SLC25A15	ND	5.4	136.6
SLC2A13	0.8	ND	4.7
SLC12A2	13.5	3.6	52.5
SLC22A18	7.1	2.9	52.3
SLC23A1	ND	ND	61.9
SLC26A2	2.3	ND	ND

SLC26A3	5.2	NDND	21.4
SLC27A2	4.4	2.1	29.2
SLC27A4	1.9	1	44.4
SLC35A3	2.5	1.7	5.7
SLC35B2	1.2	1.6	23.6
SLC35A4	2.9	2.7	44.7
SLC39A14	ND	4.7	15.5
SLC4A4	2.2	0.9	6.5
SLC6A19	5.6	ND	8.4
SLC5A1	22	11.1	30.4
SLC5A12	1.4	ND	21
SLC25A24	31.6	26	49.3
SLC3A1	15.4	4.9	63
SLC25A1	23.2	25.8	140
SLC30A1	1.7	2.4	ND
SLC30A7	1.4	0.4	22.7

ND, Not detected.

Table S4.5. Abundance (pmol/g of mucosal tissue) of SLC transporters in adult colon inflamed Crohn's disease (I-CD), histologically normal Crohn's disease (HN-CD) and healthy pooled samples.

DMET name	I-CD	HN-CD	Healthy
SLC3A2	4.6	2.3	6
SLC1A5	10.8	9	21
SLC33A1	1.6	2	7.5
SLC25A4	13.6	10.9	23.1
SLC25A5	106.9	85.9	448.5
SLC25A6	56.4	90.4	143.1
SLC4A1	57.2	48.1	48.7
SLC25A12	3.1	2.1	11.2
SLC25A13	5.3	5.2	20.2
SLC44A1	6.8	6.2	22.6
SLC44A2	2	2.8	1.4

SLC44A4	4.4	3.2	9.3
SLC25A10	8	8.7	37.8
SLC35C1	6.5	51.8	23.7
SLC37A4	ND	ND	3.6
SLC25A22	2.6	3	ND
SLC2A1	8.2	3.7	4
SLC43A2	ND	ND	1.6
SLC25A11	10	6.4	28
SLC25A20	9.2	5.9	22.3
SLC16A3	2.3	ND	ND
SLC25A3	77.8	64.8	179.8
SLC2A13	ND	ND	1.2
SLC12A2	21.8	12.4	50.6
SLC22A18	4.4	2.5	6.8
SLC25A40	0.8	ND	3
SLC26A2	3.9	6.2	27.3
SLC26A3	6.6	17.2	45.9
SLC27A2	7.3	2.6	16.7
SLC27A4	ND	0.8	6.8
SLC35A3	4.6	1.5	7.9
SLC35B2	3.6	1.1	4.1
SLC35A4	3.4	3.8	7.1
SLC39A14	1.5	3.9	5.9
SLC4A4	2.1	ND	17.9
SLC5A1	2.6	ND	ND
SLC25A24	23.6	19.5	46.3
SLC25A1	18	12.1	39.7
SLC30A1	1.5	1.3	3.6
SLC30A7	1.7	1.1	2.2
SLC30A9	ND	1.3	3.9

ND, Not detected.

4.9.Supplementary material-References

1. Strushkevich N., Usanov SA., Park H-W. Structural Basis of Human CYP51 Inhibition by Antifungal Azoles. *J Mol Biol* 2010;**397**(4):1067–78. Doi: 10.1016/j.jmb.2010.01.075.

2. Guengerich FP. Cytochrome P450 and Chemical Toxicology. *Chem Res Toxicol* 2008;**21**(1):70–83. Doi: 10.1021/tx700079z.

3. Shinkyo R., Sakaki T., Kamakura M., Ohta M., Inouye K. Metabolism of vitamin D by human microsomal CYP2R1. *Biochem Biophys Res Commun* 2004;**324**(1):451–7. Doi: 10.1016/j.bbrc.2004.09.073.

4. Pikuleva IA., Babiker A., Waterman MR., Björkhem I. Activities of Recombinant Human Cytochrome P450c27 (CYP27) Which Produce Intermediates of Alternative Bile Acid Biosynthetic Pathways. *J Biol Chem* 1998;**273**(29):18153–60. Doi: 10.1074/jbc.273.29.18153.

5. Smith G., Wolf CR., Deeni YY., Dawe RS., Evans AT., Comrie MM., et al. Cutaneous expression of cytochrome P450 CYP2S1: individuality in regulation by therapeutic agents for psoriasis and other skin diseases. *Lancet* 2003;**361**(9366):1336–43. Doi: 10.1016/S0140-6736(03)13081-4.

6. Xie F., Ding X., Zhang Q-Y. An update on the role of intestinal cytochrome P450 enzymes in drug disposition. *Acta Pharm Sin B* 2016;**6**(5):374–83. Doi: 10.1016/j.apsb.2016.07.012.

7. Lee AJ., Cai MX., Thomas PE., Conney AH., Zhu BT. Characterization of the Oxidative Metabolites of 17β-Estradiol and Estrone Formed by 15 Selectively Expressed Human Cytochrome P450 Isoforms. *Endocrinology* 2003;**144**(8):3382–98. Doi: 10.1210/en.2003-0192.

8. Fer M., Corcos L., Dréano Y., Plée-Gautier E., Salaün J-P., Berthou F., et al. Cytochromes P450 from family 4 are the main omega hydroxylating enzymes in humans: CYP4F3B is the prominent player in PUFA metabolism. *J Lipid Res* 2008;**49**(11):2379–89. Doi: 10.1194/jlr.M800199-JLR200.

9. Edson KZ., Prasad B., Unadkat JD., Suhara Y., Okano T., Peter Guengerich F., et al. Cytochrome P450-dependent catabolism of vitamin K: ω-hydroxylation catalyzed by human CYP4F2 and CYP4F11. *Biochemistry* 2013. Doi: 10.1021/bi401208m.

10. KALSOTRA A. Expression and characterization of human cytochrome P450 4F11: Putative role in the metabolism of therapeutic drugs and eicosanoids. *Toxicol Appl Pharmacol* 2004;**199**(3):295–304. Doi: 10.1016/j.taap.2003.12.033.

11. Stark K., Wongsud B., Burman R., Oliw EH. Oxygenation of polyunsaturated long chain fatty acids by recombinant CYP4F8 and CYP4F12 and catalytic importance of Tyr-125 and Gly-328 of CYP4F8. *Arch Biochem Biophys* 2005;**441**(2):174–81. Doi:

10.1016/j.abb.2005.07.003.

12. Bylund J., Bylund M., Oliw EH. cDNA Cloning and Expression of CYP4F12, a Novel Human Cytochrome P450. *Biochem Biophys Res Commun* 2001;**280**(3):892–7. Doi: 10.1006/bbrc.2000.4191.

13. Lee CA., Neul D., Clouser-Roche A., Dalvie D., Wester MR., Jiang Y., et al. Identification of Novel Substrates for Human Cytochrome P450 2J2. *Drug Metab Dispos* 2010;**38**(2):347–56. Doi: 10.1124/dmd.109.030270.

14. Wu Z., Lee D., Joo J., Shin J-H., Kang W., Oh S., et al. CYP2J2 and CYP2C19 Are the Major Enzymes Responsible for Metabolism of Albendazole and Fenbendazole in Human Liver Microsomes and Recombinant P450 Assay Systems. *Antimicrob Agents Chemother* 2013;**57**(11):5448–56. Doi: 10.1128/AAC.00843-13.

15. Sneitz N., Vahermo M., Mosorin J., Laakkonen L., Poirier D., Finel M. Regiospecificity and Stereospecificity of Human UDP-Glucuronosyltransferases in the Glucuronidation of Estriol, 16-Epiestriol, 17-Epiestriol, and 13-Epiestradiol. *Drug Metab Dispos* 2013;**41**(3):582–91. Doi: 10.1124/dmd.112.049072.

16. Alonen A., Finel M., Kostiainen R. The human UDP-glucuronosyltransferase UGT1A3 is highly selective towards N2 in the tetrazole ring of losartan, candesartan, and zolarsartan. *Biochem Pharmacol* 2008;**76**(6):763–72. Doi: 10.1016/j.bcp.2008.07.006.

17. Gagné J-F., Montminy V., Belanger P., Journault K., Gaucher G., Guillemette C. Common Human UGT1A Polymorphisms and the Altered Metabolism of Irinotecan Active Metabolite 7-Ethyl-10-hydroxycamptothecin (SN-38). *Mol Pharmacol* 2002;**62**(3):608–17. Doi: 10.1124/mol.62.3.608.

18. Joseph TB., Wang SWJ., Liu X., Kulkarni KH., Wang J., Xu H., et al. Disposition of Flavonoids via Enteric Recycling: Enzyme Stability Affects Characterization of Prunetin Glucuronidation across Species, Organs, and UGT Isoforms. *Mol Pharm* 2007;**4**(6):883–94. Doi: 10.1021/mp700135a.

19. Perreault M., Gauthier-Landry L., Trottier J., Verreault M., Caron P., Finel M., et al. The Human UDP-Glucuronosyltransferase UGT2A1 and UGT2A2 Enzymes Are Highly Active in Bile Acid Glucuronidation. *Drug Metab Dispos* 2013;**41**(9):1616–20. Doi: 10.1124/dmd.113.052613.

20. Samokyszyn VM., Gall WE., Zawada G., Freyaldenhoven MA., Chen G., Mackenzie PI., et al. 4-Hydroxyretinoic Acid, a Novel Substrate for Human Liver Microsomal UDP-glucuronosyltransferase(s) and Recombinant UGT2B7. *J Biol Chem* 2000;**275**(10):6908–14. Doi: 10.1074/jbc.275.10.6908.

21. Picard N., Ratanasavanh D., Prémaud A., Le Meur Y., Marquet P. IDENTIFICATION OF THE UDP-GLUCURONOSYLTRANSFERASE ISOFORMS INVOLVED IN

MYCOPHENOLIC ACID PHASE II METABOLISM. *Drug Metab Dispos* 2005;**33**(1):139–46. Doi: 10.1124/dmd.104.001651.

22. Itäaho K., Mackenzie PI., Ikushiro S., Miners JO., Finel M. The Configuration of the 17-Hydroxy Group Variably Influences the Glucuronidation of β-Estradiol and Epiestradiol by Human UDP-Glucuronosyltransferases. *Drug Metab Dispos* 2008;**36**(11):2307–15. Doi: 10.1124/dmd.108.022731.

23. Gallego O., Belyaeva O V., Porté S., Ruiz FX., Stetsenko A V., Shabrova E V., et al. Comparative functional analysis of human medium-chain dehydrogenases, short-chain dehydrogenases/reductases and aldo-keto reductases with retinoids. *Biochem J* 2006;**399**(1):101–9. Doi: 10.1042/BJ20051988.

24. Vasiliou V., Pappa A., Estey T. Role of Human Aldehyde Dehydrogenases in Endobiotic and Xenobiotic Metabolism. *Drug Metab Rev* 2004;**36**(2):279–99. Doi: 10.1081/DMR-120034001.

25. Chen Y., Orlicky DJ., Matsumoto A., Singh S., Thompson DC., Vasiliou V. Aldehyde dehydrogenase 1B1 (ALDH1B1) is a potential biomarker for human colon cancer. *Biochem Biophys Res Commun* 2011;**405**(2):173–9. Doi: 10.1016/j.bbrc.2011.01.002.

26. Hein DW. Molecular genetics and function of NAT1 and NAT2: role in aromatic amine metabolism and carcinogenesis. *Mutat Res* 2002;**506**–**507**:65–77. Doi: 10.1016/s0027-5107(02)00153-7.

27. Wang D., Zou L., Jin Q., Hou J., Ge G., Yang L. Human carboxylesterases: a comprehensive review. *Acta Pharm Sin B* 2018;**8**(5):699–712. Doi: 10.1016/j.apsb.2018.05.005.

28. Koukouritaki SB., Simpson P., Yeung CK., Rettie AE., Hines RN. Human Hepatic Flavin-Containing Monooxygenases 1 (FMO1) and 3 (FMO3) Developmental Expression. *Pediatr Res* 2002;**51**(2):236–43. Doi: 10.1203/00006450-200202000-00018.

29. Václavíková R., Hughes DJ., Souček P. Microsomal epoxide hydrolase 1 (EPHX1): Gene, structure, function, and role in human disease. *Gene* 2015;**571**(1):1–8. Doi: 10.1016/j.gene.2015.07.071.

30. Spector AA., Fang X., Snyder GD., Weintraub NL. Epoxyeicosatrienoic acids (EETs): Metabolism and biochemical function. *Prog Lipid Res* 2004;**43**(1):55–90. Doi: 10.1016/S0163-7827(03)00049-3.

31. Kuang Q., Purhonen P., Ålander J., Svensson R., Hoogland V., Winerdal J., et al. Dead-end complex, lipid interactions and catalytic mechanism of microsomal glutathione transferase 1, an electron crystallography and mutagenesis investigation. *Sci Rep* 2017;**7**(1):1–10. Doi: 10.1038/s41598-017-07912-3.

32. Uno Y., Murayama N., Kunori M., Yamazaki H. Short Communication Characterization of Microsomal Glutathione S -Transferases. *Drug Metab Dispos* 2013;**41**:1621–5.

33. Yang Y., Aloysius H., Inoyama D., Chen Y., Hu L. Enzyme-mediated hydrolytic activation of prodrugs. *Acta Pharm Sin B* 2011;**1**(3):143–59. Doi: 10.1016/j.apsb.2011.08.001.

34. Gamage N., Barnett A., Hempel N., Duggleby RG., Windmill KF., Martin JL., et al. Human Sulfotransferases and Their Role in Chemical Metabolism. *Toxicol Sci* 2006;**90**(1):5–22. Doi: 10.1093/toxsci/kfj061.

35. Hebbring SJ., Moyer AM., Weinshilboum RM. Sulfotransferase gene copy number variation: Pharmacogenetics and function. *Cytogenet Genome Res* 2009;**123**(1–4):205–10. Doi: 10.1159/000184710.

36. van Helvoort A., Smith AJ., Sprong H., Fritzsche I., Schinkel AH., Borst P., et al. MDR1 P-Glycoprotein Is a Lipid Translocase of Broad Specificity, While MDR3 P-Glycoprotein Specifically Translocates Phosphatidylcholine. *Cell* 1996;**87**(3):507–17. Doi: 10.1016/S0092-8674(00)81370-7.

37. Chen G., Durán GE., Steger KA., Lacayo NJ., Jaffrézou J-P., Dumontet C., et al. Multidrug-resistant Human Sarcoma Cells with a Mutant P-Glycoprotein, Altered Phenotype, and Resistance to Cyclosporins. *J Biol Chem* 1997;**272**(9):5974–82. Doi: 10.1074/jbc.272.9.5974.

38. Allikmets R., Raskind WH., Hutchinson A., Schueck ND., Dean M., Koeller DM. Mutation of a Putative Mitochondrial Iron Transporter Gene (ABC7) in X-Linked Sideroblastic Anemia and Ataxia (XLSA/A). *Hum Mol Genet* 1999;**8**(5):743–9. Doi: 10.1093/hmg/8.5.743.

39. Zelcer N., Saeki T., Reid G., Beijnen JH., Borst P. Characterization of Drug Transport by the Human Multidrug Resistance Protein 3 (ABCC3). *J Biol Chem* 2001;**276**(49):46400–7. Doi: 10.1074/jbc.M107041200.

40. Roermund CWT., Visser WF., IJlst L., Cruchten A., Boek M., Kulik W., et al. The human peroxisomal ABC half transporter ALDP functions as a homodimer and accepts acyl–CoA esters. *FASEB J* 2008;**22**(12):4201–8. Doi: 10.1096/fj.08-110866.

41. Morita M., Imanaka T. Peroxisomal ABC transporters: Structure, function and role in disease. *Biochim Biophys Acta - Mol Basis Dis* 2012;**1822**(9):1387–96. Doi: 10.1016/j.bbadis.2012.02.009.

42. Pisarev A V., Skabkin MA., Pisareva VP., Skabkina O V., Rakotondrafara AM., Hentze MW., et al. The Role of ABCE1 in Eukaryotic Posttermination Ribosomal Recycling. *Mol Cell* 2010;**37**(2):196–210. Doi: 10.1016/j.molcel.2009.12.034.

43. Wilcox SM., Arora H., Munro L., Xin J., Fenninger F., Johnson LA., et al. The role of

the innate immune response regulatory gene ABCF1 in mammalian embryogenesis and development. *PLoS One* 2017;**12**(5):e0175918. Doi: 10.1371/journal.pone.0175918.

44. Nishimura S., Tsuda H., Miyagi Y., Hirasawa A., Suzuki A., Kataoka F., et al. Can ABCF2 protein expression predict the prognosis of uterine cancer? *Br J Cancer* 2008;**99**(10):1651–5. Doi: 10.1038/sj.bjc.6604734.

45. Robey RW., Polgar O., Deeken J., To KW., Bates SE. ABCG2: determining its relevance in clinical drug resistance. *Cancer Metastasis Rev* 2007;**26**(1):39–57. Doi: 10.1007/s10555-007-9042-6.

46. Vijay N., Morris M. Role of Monocarboxylate Transporters in Drug Delivery to the Brain. *Curr Pharm Des* 2014;**20**(10):1487–98. Doi: 10.2174/13816128113199990462.

47. Ballatori N., Christian W V., Wheeler SG., Hammond CL. The heteromeric organic solute transporter, OSTα–OSTβ/SLC51: A transporter for steroid-derived molecules. *Mol Aspects Med* 2013;**34**(2–3):683–92. Doi: 10.1016/j.mam.2012.11.005.

48. Foley D., Rajamanickam J., Bailey P., Meredith D. Bioavailability Through PepT1: The Role of Computer Modelling in Intelligent Drug Design. *Curr Comput Aided-Drug Des* 2010;**6**(1):68–78. Doi: 10.2174/157340910790980133.

49. Halestrap AP., Meredith D. The SLC16 gene family?from monocarboxylate transporters (MCTs) to aromatic amino acid transporters and beyond. *Pfl*[illegible]*gers Arch Eur J Physiol* 2004;**447**(5):619–28. Doi: 10.1007/s00424-003-1067-2.

50. DIMMER K-S., FRIEDRICH B., LANG F., DEITMER JW., BRÖER S. The low-affinity monocarboxylate transporter MCT4 is adapted to the export of lactate in highly glycolytic cells. *Biochem J* 2000;**350**(1):219. Doi: 10.1042/0264-6021:3500219.

51. Mao F., Li Z., Zhao B., Lin P., Liu P., Zhai M., et al. Identification and functional analysis of a SLC33A1: c.339T>G (p.Ser113Arg) Variant in the Original SPG42 Family. *Hum Mutat* 2015. Doi: 10.1002/humu.22732.

52. Boulet A., Vest KE., Maynard MK., Gammon MG., Russell AC., Mathews AT., et al. The mammalian phosphate carrier SLC25A3 is a mitochondrial copper transporter required for cytochrome c oxidase biogenesis. *J Biol Chem* 2018;**293**(6):1887–96. Doi: 10.1074/jbc.RA117.000265.

53. Fiermonte G., Palmieri L., Dolce V., Lasorsa FM., Palmieri F., Runswick MJ., et al. The Sequence, Bacterial Expression, and Functional Reconstitution of the Rat Mitochondrial Dicarboxylate Transporter Cloned via Distant Homologs in Yeast and Caenorhabditis elegans. *J Biol Chem* 1998;**273**(38):24754–9. Doi: 10.1074/jbc.273.38.24754.

54. Thangaratnarajah C., Ruprecht JJ., Kunji ERS. Calcium-induced conformational changes of the regulatory domain of human mitochondrial aspartate/glutamate carriers. *Nat*

Commun 2014;**5**(1):5491. Doi: 10.1038/ncomms6491.

55. Fiermonte G., Dolce V., David L., Santorelli FM., Dionisi-Vici C., Palmieri F., et al. The Mitochondrial Ornithine Transporter. *J Biol Chem* 2003;**278**(35):32778–83. Doi: 10.1074/jbc.M302317200.

56. Falcon A., Doege H., Fluitt A., Tsang B., Watson N., Kay MA., et al. FATP2 is a hepatic fatty acid transporter and peroxisomal very long-chain acyl-CoA synthetase. *Am J Physiol Metab* 2010;**299**(3):E384–93. Doi: 10.1152/ajpendo.00226.2010.

57. Mitchell RW., On NH., Del Bigio MR., Miller DW., Hatch GM. Fatty acid transport protein expression in human brain and potential role in fatty acid transport across human brain microvessel endothelial cells. *J Neurochem* 2011:no-no. Doi: 10.1111/j.1471-4159.2011.07245.x.

58. Suzuki T., Ishihara K., Migaki H., Ishihara K., Nagao M., Yamaguchi-Iwai Y., et al. Two Different Zinc Transport Complexes of Cation Diffusion Facilitator Proteins Localized in the Secretory Pathway Operate to Activate Alkaline Phosphatases in Vertebrate Cells. *J Biol Chem* 2005;**280**(35):30956–62. Doi: 10.1074/jbc.M506902200.

59. Sosicka P., Maszczak-Seneczko D., Bazan B., Shauchuk Y., Kaczmarek B., Olczak M. An insight into the orphan nucleotide sugar transporter SLC35A4. *Biochim Biophys Acta - Mol Cell Res* 2017;**1864**(5):825–38. Doi: 10.1016/j.bbamcr.2017.02.002.

60. Guo H., Jin X., Zhu T., Wang T., Tong P., Tian L., et al. SLC39A5 mutations interfering with the BMP/TGF-β pathway in non-syndromic high myopia. *J Med Genet* 2014;**51**(8):518–25. Doi: 10.1136/jmedgenet-2014-102351.

61. Kamiyama S., Suda T., Ueda R., Suzuki M., Okubo R., Kikuchi N., et al. Molecular Cloning and Identification of 3′-Phosphoadenosine 5′-Phosphosulfate Transporter. *J Biol Chem* 2003;**278**(28):25958–63. Doi: 10.1074/jbc.M302439200.

62. Mizoguchi K., Cha SH., Chairoungdua A., Kim DK., Shigeta Y., Matsuo H., et al. Human cystinuria-related transporter: Localization and functional characterization. *Kidney Int* 2001;**59**(5):1821–33. Doi: 10.1046/j.1523-1755.2001.0590051821.x.

63. Shnitsar V., Li J., Li X., Calmettes C., Basu A., Casey JR., et al. A Substrate Access Tunnel in the Cytosolic Domain Is Not an Essential Feature of the Solute Carrier 4 (SLC4) Family of Bicarbonate Transporters. *J Biol Chem* 2013;**288**(47):33848–60. Doi: 10.1074/jbc.M113.511865.

64. Srinivas SR., Gopal E., Zhuang L., Itagaki S., Martin PM., Fei Y-J., et al. Cloning and functional identification of slc5a12 as a sodium-coupled low-affinity transporter for monocarboxylates (SMCT2). *Biochem J* 2005;**392**(3):655–64. Doi: 10.1042/BJ20050927.

65. Yang X., Wang Q., Cao E. Structure of the human cation–chloride cotransporter

NKCC1 determined by single-particle electron cryo-microscopy. *Nat Commun* 2020;**11**(1):1016. Doi: 10.1038/s41467-020-14790-3.

66. Reece M., Prawitt D., Landers J., Kast C., Gros P., Housman D., et al. Functional characterization of ORCTL2 - an organic cation transporter expressed in the renal proximal tubules. *FEBS Lett* 1998;**433**(3):245–50. Doi: 10.1016/S0014-5793(98)00907-7.

Chapter Five: Quantitative Targeted Proteomics of Drug-Metabolizing Enzymes and Drug Transporters in Human Intestine of Crohn's Disease Patients

Declaration

Sarah Alrubia, Brahim Achour, Zubida M. Al-Majdoub, Amin Rostami-Hodjegan and Jill Barber

I carried out the literature search, generation and analysis of data, contributed to the study design and wrote the manuscript. Dr Brahim Achour reviewed and edited the manuscript. Dr Brahim Achour and Dr Zubida M. Al-Majdoub were consulted on experimental methodology and statistical analysis. Dr Jill Barber and Prof. Amin Rostami- Hodjegan contributed to the study design, provided guidance and suggested edits to the manuscript. I retained editorial control.

5.1.Abstract

Background and Aims: Crohn's disease (CD) is an intestine localized chronic inflammatory disease. The inflammation caused by the disease alters the expression of drug-metabolizing enzymes and transporters. These proteins play a vital role in first pass metabolism of many orally administered drugs. Lack of reliable abundance data for these proteins is a major obstacle to development of physiologically-based pharmacokinetic (PBPK) models, precluding accurate prediction of oral drug bioavailability in Crohn's population. This study aimed to determine the absolute abundances of enzymes and transporters in Crohn's disease inflamed and histologically normal ileum and colon tissues compared to healthy tissue.

Methods: Fresh-frozen inflamed ileum (n=6), inflamed colon (n=7), histologically normal ileum (n=2), histologically normal colon (n=5) tissue from CD patients and healthy subjects (n=10; 5 ileum and 5 colon) were processed by calcium chelation elution to isolate enterocytes. The isolated homogenates from individual samples were prepared for liquid chromatography–mass spectrometry proteomics using quantitative concatemers (QconCAT) as standards for targeted quantification. The data were processed by MaxQuant and Progenesis, and detection of target proteins by each software was compared.

Results: The number of the targets identified by MaxQuant (16 enzymes and 3 transporters) was higher compared to Progenesis (13 enzymes and 3 transporters). The number of the quantified protein targets (5 CYPs, 4 UGTs, 3 non-CYP and non-UGT enzymes, and 3 transporters) by the QconCAT technique in a sufficient number of samples was not large enough to determine the impact of CD on the abundance of drug-metabolizing enzymes and transporters. However, the generated data for the quantified targets showed varying up and down regulation in their expression compared to healthy expression.

Conclusion: MaxQuant provided a wider coverage of protein targets than Progenesis, and therefore, MaxQuant was used to carry out subsequent proteomic analysis. The generated targeted proteomic data did not provide reliable expression data applicable to PBPK modelling. Therefore, a label-free approach is to be carried out subsequently in order to generate the required data to allow prediction of the impact of CD on oral drug systemic exposure.

5.2.Introduction

Crohn's disease (CD) is a chronic inflammatory bowel disease (IBD) predominately affecting the ileum and colon segments of the intestine.[1] CD aetiology is not fully understood, but it has been linked to genetic and environmental factors. Epidemiological studies show that CD is more common in the Western younger population (15-35 years), females, smokers and populations of urban areas.[1] CD patients usually receive several oral drugs during their prolonged therapy. Moreover, due to the young onset of the disease, CD population can also receive non-CD drugs to control other conditions. Inflammation caused by CD could potentially lead to alteration of oral drug pharmacokinetics (PK). Inflammation does not only affect the inflamed part of the intestine; its effect can also reach adjacent histologically normal tissue.[2] Extended inflammation can cause large changes in drug handling in CD population, leading to altered efficacy and safety profiles. CD population is a heterogeneous population where the PK profiles of oral drugs may differ from healthy population due to alterations in a wide range of system parameters, such as blood protein levels,[3,4] intestine blood flow rate,[5–7] and activity of liver drug metabolising enzymes and transporters (DMETs),[8] abundance of intestinal enzymes[9–11] and transporters,[9,10,12–16] as well as other intestine related parameters (Chapter One).

DMETs are responsible for activation (e.g. aldehyde oxidase, AOX1, activates azathioprine to its active metabolite, mercaptopurine[17,18]), metabolic clearance (e.g. N-acetyltransferase 1, NAT1, metabolizes oral 5-aminosalicylic acid, 5-ASA,[19] and CYP3A4 metabolizes budesonide and prednisone[20,21]), and absorption (e.g. P-gp is involved in the absorption of budesonide[20]) of oral drugs used to control CD. Therefore, if these key proteins are reduced due to CD inflammatory effect,[22,23] patients with CD are susceptible to decreased capacity of intestinal first pass metabolism, hence bioavailability of oral drugs is affected, which might necessitate dosage adjustment for specific drugs.

CD patients currently receive drugs with no dosage guidance as dedicated PK studies are not conducted in CD populations during drug development. Alternatively, the use of physiologically-based pharmacokinetic (PBPK) models can be used to predict alterations in the PK of oral drugs and guide dose adjustment if needed in CD population. PBPK models of special populations are increasingly incorporated in regulatory submissions and guiding drug labels in various therapeutic areas, such as oncology,[24] liver impairment[25] and chronic kidney disease.[26] Building and refining such models requires abundance data together with other

system parameters to be incorporated with drug data.[27] PBPK models in CD are not well established and are usually specific to a certain drug/condition.[28,29] This is due to lack of system-specific data in this population, including robust quantitative measurements of DMETs in CD patients using liquid chromatography and tandem mass spectrometry (LC-MS/MS) based proteomics. Available quantitative data are generated by immunohistochemistry[9,11,15,30,31] and mRNA[2,10,12,13,15,16] based expression strategies, which are limited to protein targets that have specific antibodies or are indirect measurements of expression.[32,33] Available data, which are scarce, showed significant upregulation of solute carriers (SLCs) PEPT1, OATP4A1 and OATP2B1, whereas ASBT and MCT1 were downregulated in CD compared to control.[13,15,30] Among ATP-binding cassette (ABC) transporters significant upregulation of MRP1 and downregulation of P-gp and MRP3 in CD has been observed.[9,14,16] The reports on CYP3A4 enzyme shows its lower expression in colon[10] and ileum of CD patients relative to healthy subjects.[9]

Quantitative are still scarce, and expression of key enzymes, such as uridine 5'-diphosphate glucuronosyltransferases (UGT) and sulfotransferases (SULT), has not been reported in inflamed tissue. Moreover, only few studies reported the expression of DMETs in histologically normal tissue from CD patients.[2,10] Such lack of information, together with the high variability caused by the differences between intestine segments,[34] hinders building reliable PBPK models for CD.

Additionally, data analysis software packages are associated with differences in identified proteins due to different algorithms used to assign peptide and fragment peaks. MaxQuant and Progenesis are commonly used proteomic analysis tools which were previously found to have 65% overlap in detected peptides from human liver samples.[35]

In this study, we aimed to determine the abundance of DMETs in the individual ileum and colon of healthy, histologically normal and inflamed tissues from CD patients, using QconCAT-based targeted proteomics.

In addition, a comparison of the proteomics data output from MaxQuant and Progenesis was carried out to determine which software provides wider coverage of the targeted proteins.

5.3.Materials and Methods

5.3.1. Materials

Unless otherwise indicated, all chemicals were supplied by Sigma-Aldrich (Poole, UK). All solvents were high performance liquid chromatography (HPLC) grade and supplied by Thermo Fisher Scientific (Paisley, UK). Lysyl endopeptidase (Lys-C) was purchased from Wako (Osaka, Japan). Sequencing-grade modified trypsin was supplied by Promega (Southampton, UK). Complete Mini, EDTA-free protease inhibitor cocktail tablets were supplied by Roche (Mannheim, Germany). BCA protein assay kit was obtained from ThermoFisher Scientific (Hemel Hempstead, UK).

5.3.2. Intestine Samples and Donor Demographics

Samples were fresh-frozen human intestine samples representing inflamed (I-CD) and histologically normal (HN-CD) areas of the ileum (n = 6 and 2, respectively) and colon (n = 7 and 5, respectively). Samples were taken from active CD patients undergoing ileocolonic resection where the histologically normal tissues were taken from macroscopically normal regions away from the inflamed bowel regions. Tissues were obtained with informed consent and supplied by Manchester Biomedical Research Centre (BRC) Biobank, Manchester University NHS Foundation Trust, Manchester, UK. Prior ethics approval was granted by NRES Committee North West - Haydock (19/NW/0644). The average age of Crohn's patients at surgery was 40 years (range 18-68 years). Percentage of female subjects was 54% and their body mass index (BMI) ranged from 17 to 34.3 kg/m^2. Detailed demographic and clinical data are summarised in Supplementary Table S5.1.

A control group of healthy mucosal samples (ileum n=5, colon =5) obtained from healthy deceased donors were supplied by Caltag Medsystems Limited (Buckingham, UK). Prior ethics approval was granted by University Research Ethics Committee (UREC), UK (2019-8120-12392). The average age of healthy subjects was 48.5 years (range 30-70 years). The percentage of female subjects was 40%. The average post mortem interval (PMI) was 4.4 hrs (range 1-9 hrs). Available demographic information is summarised in Table S5.2.

5.3.3. Enterocyte Isolation and Subcellular Fractionation

Harvesting of enterocytes from the underlying lamina propria was done using elution by chelation. Ethylenediaminetetraacetic acid (EDTA) calcium chelation elution was adapted

from Harwood et al (2015)[36] with few modifications. The process was done on ice and all solutions were equilibrated at pH 7.4. The base buffer for all solutions used for chelation was 112 mM NaCl, 5 mM KCl, 20 mM HEPES. The mucosa was washed twice in the base buffer and immersed for 30 min in 27 mM sodium citrate solution with protease inhibitor cocktail (PI), followed by incubation in EDTA buffer (30 mM EDTA, 10 U/mL heparin, and 1 mM dithiothreitol (DTT)) with stirring at 250 rpm for 40 min to initiate chelation. The chelated enterocytes were collected from the mucosa by repeated flushing with EDTA buffer. The formed material was washed by centrifugation twice at 2000 x g for 10 min. The resulting enterocyte pellet was weighted (mucosal weight) then re-suspended in homogenisation buffer (10 mM Tris–HCl, 250 mM sucrose, 0.1 mM EGTA, 0.5 mM $MgCl_2$, 5 mM histidine and 0.2% SDS) at 3 ml per g of cells. Homogenisation was carried out with a Dounce hand-held homogeniser with a minimum of 75 strokes, followed by treatment with ultrasonication probe (30 W) for two 10 s bursts to disrupt cell membranes. The formed homogenate fraction was stored in aliquots at -80°C until further processing.

5.3.4. Sample Preparation and Proteolytic Digestion

Protein content in ileum and colon homogenates (n = 30) was determined using BCA assay in triplicate with bovine serum albumin (BSA) as a standard. Three stable isotope labelled quantitative concatemers (QconCATs)[37] were spiked with 70 µg homogenate protein from each sample. The added QconCATs are MetCAT (QconCAT standard for CYP and UGT enzymes),[38,39] NuncCAT (QconCAT for non-CYP, non-UGT enzymes)[38] and TransCAT (QconCAT for ABC transporters and SLCs), (see Chapter Three), to enable targeted quantification of intestinal DMETs. The amount of NuncCAT and TransCAT added to ileum and colon homogenates was 0.3 µg (from 1.5 mg/ml original concentration) and 0.24 µg (from 1.2 mg/ml original concentration), respectively. For MetCAT, the amount added to ileum and colon homogenates was 0.18 µg and 0.09 µg (from 0.27 mg/ml original concentration), respectively. The targeted proteins and sequences of their surrogate peptides in the three QconCATs as well as the non-naturally occurring peptide (NNOP) added for the quantification of the QconCAT standards are summarized in Table S5.3.

The 30 samples were prepared for proteomics using filter-aided sample preparation (FASP), as previously described,[40] with Amicon Ultra 0.5 mL centrifugal filters at 3-kDa molecular weight cut-off (Merck Millipore, Nottingham, UK). Briefly, homogenate proteins were incubated with 10% (w/v) sodium deoxycholate at room temperature for 10 min, followed by incubation at

56°C for 30 min with 100 mM dithiothreitol (DTT) to reduce disulphide bonds. The samples were then transferred to the filter unit and centrifuged at 14000*g* at room temperature for 30 min. The samples were incubated with 100 µl of 50 mM iodoacetamide (IAA) in the dark for 30 min at room temperature for alkylation, followed by double wash step with 200 µl of 8 M urea in the Tris buffer. A buffer exchange was performed by two washes with 200 µl of 1 M urea in 50 mM ammonium bicarbonate (pH 8.5). For each wash, the samples were centrifuged at 14000*g* at room temperature for 20 min. The filtrate was transferred into a new collection tube and 80 µl 1 M urea in 50 mM ammonium bicarbonate was added. Protein digestion was achieved by adding LysC (enzyme to protein ratio 1:50, for 3-4 hours, at 30°C), followed by trypsin (enzyme to protein ratio 1:25 for 12 hours at 37°C). After digestion, peptides were recovered from the filter unit by centrifugation at 14000*g* for 20 min, followed by addition of 100 µl of 500 mM sodium chloride to the filter and centrifugation (14000*g*, 20 min) for a second collection. The collected peptides were acidified with trifluoroacetic acid, and then desalted using C18 spin columns, according to the manufacturer's instructions (Nest group, USA). The peptides were lyophilised to dryness using a vacuum concentrator at 30ºC and with vacuum in aqueous mode then stored at -80°C until mass spectrometric analysis.

5.3.5. Liquid Chromatography and Tandem Mass Spectrometry (LC-MS/MS)

Digested samples were diluted to a final concentration of 0.5 µg/µl with HPLC water containing 0.1% (v/v) formic acid and 3% (v/v) acetonitrile. 10 µl of each sample was injected into an UltiMate® 3000 rapid separation liquid chromatography (RSLC, Dionex Corporation, Sunnyvale, CA) coupled online to a Q Exactive HF Hybrid Quadrupole Orbitrap mass spectrometer (ThermoFisher Scientific, Waltham, MA). Peptides were eluted over 90 min gradient, as previously described[38], with mobile phase A (0.1% formic acid in water) and mobile phase B (0.1% formic acid in acetonitrile). Peptides were resolved on Charged Surface Hybrid (CSH) C18 analytical column (75 mm x 250 µm inner diameter, 1.7 µm particle size) (Waters, UK). A 1 µl aliquot of each sample was transferred to a 5 µl loop and loaded onto the column at a flow rate of 300 nl/min for 5 min at 5% B. The loop was then taken out of line and the flow was reduced to 200 nl/min in 0.5 min. Peptides were separated using a gradient from 5% to 18% B in 63.5 min, then from 18% to 27% B in 8 min, and finally from 27% B to 60% B in 1 min. The column was washed at 60% B for 3 min before re-equilibration to 5% B in 1 min. At 85 min, the flow was increased to 300 nl/min until the end of the run. Peptides were selected for fragmentation automatically by data-dependant acquisition (DDA) with an MS scan window between m/z 300 and 1750. The top 12 peptides with a charge state of 2+ to 4+

were selected with dynamic exclusion set at 15 seconds. The MS resolution was set at 120,000 with an AGC target of 3E6 and a maximum fill time set at 20 ms. The MS2 resolution was set to 30,000, with an AGC target of 2E5, a maximum fill time of 45 ms, isolation window of 1.3 and a collision energy of 28 eV.

5.3.6. Data Analysis and Protein Quantification

To identify target peptides and proteins, data analysis was carried out on MaxQuant version 1.6.1.0. (Max Planck Institute for Biochemistry, Munich, Germany) and Progenesis QI v4.0 (Nonlinear Dynamics, Newcastle-upon-Tyne, UK) as previously described.[38,41] This was done to compare between the outcomes of the two software and determine which one to use for our analysis. The performance of each software was evaluated based on the number of identified targeted peptides and proteins. For MaxQuant, the database search was applied against UniProtKB human proteome fasta file of 74788 protein entries (UniProt, May 2017, http://www.uniprot.org/) with inclusion of QconCAT sequences (MetCAT, NuncCAT and TransCAT). Identified peptides with scores <40 were removed. Only proteins with at least one identified surrogate peptide and with a reliable quantification in at least 2 samples (within the whole set) were considered. Detailed parameters of the MaxQuant search are listed in Table S5.4.

Progenesis assesses peaks lists from the MS/MS scan raw data, where the precursor ions are automatically aligned based on retention time; data exported as Mascot generic files (mgf). The generated mgf files are used for peptide search and identification by an in-house Mascot server (Matrix Science, London, UK). Mascot MS/MS ions search was performed against a reference human proteome database (SwissProt and QconCAT) containing 75004 protein sequences. Progenesis parameters are listed in Table S5.4. The resulting .xml files were re-imported into Progenesis QI. The resulting peptides with score of <15 were removed. The score of 15 with Mascot is equivalent to a score of 40 by MaxQuant as previously determined based on human liver tissue samples.[35] Only proteins with at least one identified surrogate peptide and with a reliable quantification in at least 2 samples (within the whole set) were considered.

QconCAT-based targeted quantification was carried out as previously described.[36,38] The three QconCATs included 10 CYPs, 5 UGTs, 21 non-CYP non-UGT enzymes, 8 ABC transporters and 11 SLCs considered in this study. A protein was considered quantifiable in intestine homogenate samples if it was identified by at least one surrogate peptide and detected in any

number of samples per segment. The abundance of each targeted protein was calculated using the equations previously reported,[38] as follows:

$$[Prtein] = [QconCAT] \times I_{i,L}/I_{i,H} \qquad \textbf{(1)}$$

Where [Protein] is protein abundance based on surrogate peptide *i*. [QconCAT] is the abundance of the labelled internal standard added measured using Equation 2. Abundance of the QconCAT internal standard and the targeted protein are measured in pmol/mg homogenate protein. $Ii,_L/Ii,_H$ is the ratio of the intensity of the light (analyte) to the heavy (QconCAT-derived) surrogate peptide.

$$[QconCAT] = [\mathrm{NNOP}] \times I_{i,H}/I_{i,L} \qquad \textbf{(2)}$$

Where [QconCAT] is the abundance of the labelled QconCAT standard. [NNOP] is the concentration of the NNOP peptide standard. QconCAT and NNOP are both measured in pmol/mg homogenate protein. $Ii,_H/Ii,_L$ is the ratio of the intensity of the heavy (QconCAT-derived) to the light (spiked in) NNOP standard peptide.

All intensity ratios were corrected for isotope labelling efficiency prior to use in the equations.[37,42] Unlabelled NNOP peptide GVNDNEEGFFSAR was added at 0.13 pmol for ileum and 0.065 pmol for colon, while AEGVNDNEEGFFSAR and EGVNDNEEGFFSAR were added at 0.25 pmol for all samples to quantify MetCAT, NuncCAT and TransCAT, respectively. The calculated ileum and colon mucosal abundances were then converted to units of pmol/g tissue by scaling up using protein content of homogenates for each sample.

5.3.7. Comparison of DMET Absolute Abundances across Sample Groups

DMET absolute abundance values in ileum and colon of inflamed CD (I-CD) and histologically normal CD (HN-CD) tissue were compared to healthy expression. Targets that were detected in more than one sample in at least two groups (I-CD, HN-CD and healthy) of each segment (ileum and colon) were included in the comparison. Targets only detected in one sample in one group were excluded. Based on technical variability, only changes of at least 2 fold were considered and reported as a disease effect.

5.3.8. Assessment of Technical and Analytical Variability

To assess technical variability, eight samples representing all groups (1 healthy ileum, 1 HN-CD ileum, 2 I-CD ileum, 1 healthy colon, 1 HN-CD colon and 1 I-CD colon), were prepared

in triplicate and analysed under the same LC-MS/MS conditions. For the assessment of between and within batch variability, a pool of healthy colon samples (n = 5) was prepared once and analysed at the start and end of each batch run (8 runs). The coefficient of variation (CV) was used to assess the technical and batch-to-batch variability between the replicates for the DMET targets.

5.3.9. Statistical Data Analysis

Statistical data analyses were carried out by GraphPad Prism version 8 (La Jola, CA, USA) and Microsoft Excel. Expression data were presented as means ± standard deviation and coefficient of variation (CV). The data were found not to follow normal distribution based on Shapiro-Wilk normality test. Statistical difference was assessed by Kruskal-Wallis ANOVA with statistical significance set at *p*-value of 0.05 or lower. If a difference was detected across groups, then a non-parametric post-hoc Mann-Whitney test was used for pairwise comparison.

5.4.Results

5.4.1. Assessment of Technical and Analytical Variability

Technical variability in ileum and colon were within 30% (CV) for 90% and 93% of targets, respectively. The targets that exhibited the highest variability (>30% CV) in ileum and colon replicate samples were not detected consistently. Batch to batch analytical variability was within 30% for 90% of targets (Figure S5.1).

5.4.2. Protein content of ileum and colon homogenates

Protein concentration was measured in the homogenate fractions. In ileum (Figure 5.1), protein concentration was highest in healthy tissue samples (2.3-11.6 mg/ml) compared to samples from normal (0.73-1.95 mg/ml) and inflamed (0.45-3.6 mg/ml) tissues. The lowest concentration was measured in inflamed sample 1940a (0.45 mg/ml) while its matched histologically normal sample 1940b had higher protein concentration (0.73 mg/ml). The other matched ileum samples 1004a and b showed slightly lower concentration in inflamed tissue (1.2 mg/ml) compared to its matched histologically normal sample (1.95 mg/ml).

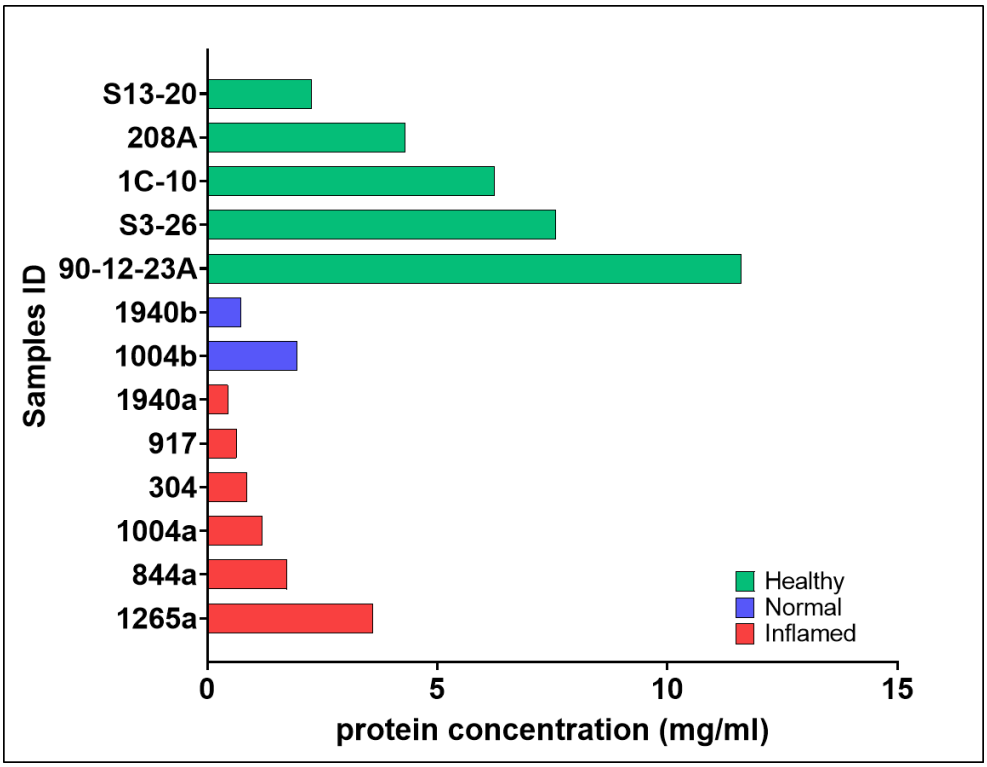

Figure 5.1. *The protein content (mg/ml) of the 13 homogenate samples from healthy (n=5), histologically normal (n=2) and inflamed (n=6) ileum. The presented mean values are obtained from BCA assay.*

For colon samples, there was no considerable difference between the protein concentrations from the different colon tissue groups (Figure 5.2). Three matched inflamed and normal samples were included. The protein concentration of the inflamed tissue of two of these (328a and 1942a) showed lower concentration (0.1 and 3.9 mg/ml, respectively) compared to their matched normal (328b and 1942b) counterparts (1.1 and 4.7 mg/ml, respectively). The opposite was observed with third set of matched samples as inflamed tissue 2003a showed higher protein concentration (3.5 mg/ml) compared to its matched normal tissue 2003b (3.0 mg/ml).

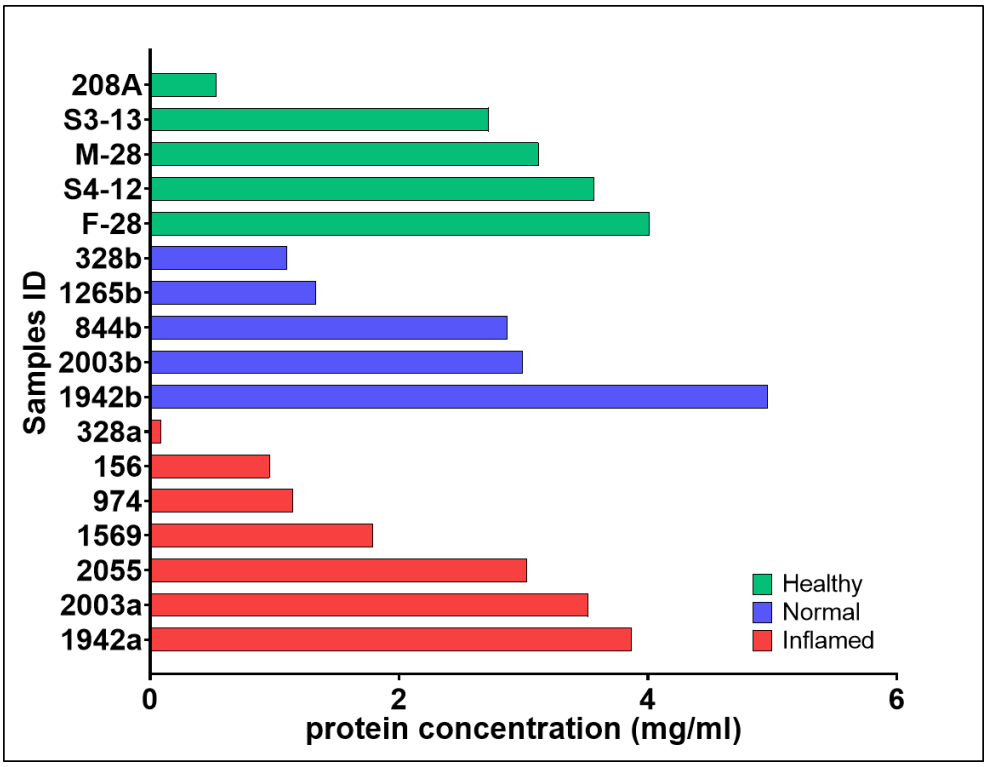

Figure 5.2. *The protein content (mg/ml) of the 17 homogenate samples from healthy (n=5), histologically normal (n=5) and inflamed (n=7) colon. The presented mean values are obtained from BCA assay.*

The range of protein concentration in inflamed ileum (0.4-3.6 mg/ml) was comparable to inflamed colon (0.1-3.9 mg/ml). On the other hand, healthy ileum samples showed higher protein concentration (2.3-11.6 mg/ml) compared to healthy colon samples (2.7-4.0 mg/ml).

5.3.2 Comparison of the Output of Protein Quantification Software

The average number of identified peptides after filtering based on low score, modification and miscleavage in the 13 ileum samples was 21270 (range 20119-22023) by Progenesis and 14208 (range 8269-17581) by MaxQuant. For the 17 colon samples, the average number of identified peptides was 21173 (range 19518-22086) by Progenesis and 15444 (range 12932-18173) by MaxQuant. In total, 20% of the peptides identified by Progenesis were miscleaved and 13%

were modified, while in the case of MaxQuant, 17.5% were miscleaved and 10% were modified.

When accounting for targeted proteins of interest, MaxQuant detected a higher number of targets in total (6 CYPs, 5 UGTs, 5 non-CYPs non-UGTs and 3 transporters) compared to the total number of targets detected by Progenesis (4 CYPs, 4 UGTs, 5 non-CYPs non-UGTs and 3 transporters). These targets were identified by at least one surrogate peptide each and quantified in at least 2 samples of the total number of samples. For these proteins, a summary of the numbers of identified surrogate peptides is shown in Table S5.5. Figure 5.3 shows abundance of CYPs, UGTs, non-CYP non-UGT enzymes, and transporters quantified by the two software packages. Interestingly, some targets were only found exclusively in one of the software packages. A larger number of targets were exclusively detected by MaxQuant (CYP1A2, CYP3A5, CYP3A43, CYP2C18, CYP2D6, CYP4F2, UGT1A1, PEPT1, MGST1 and SULT1A1). UGT1A6, OST-α, MGST2, SULT2A1 and AOX1 were only detected by Progenesis. MaxQuant was used henceforth for targets quantification.

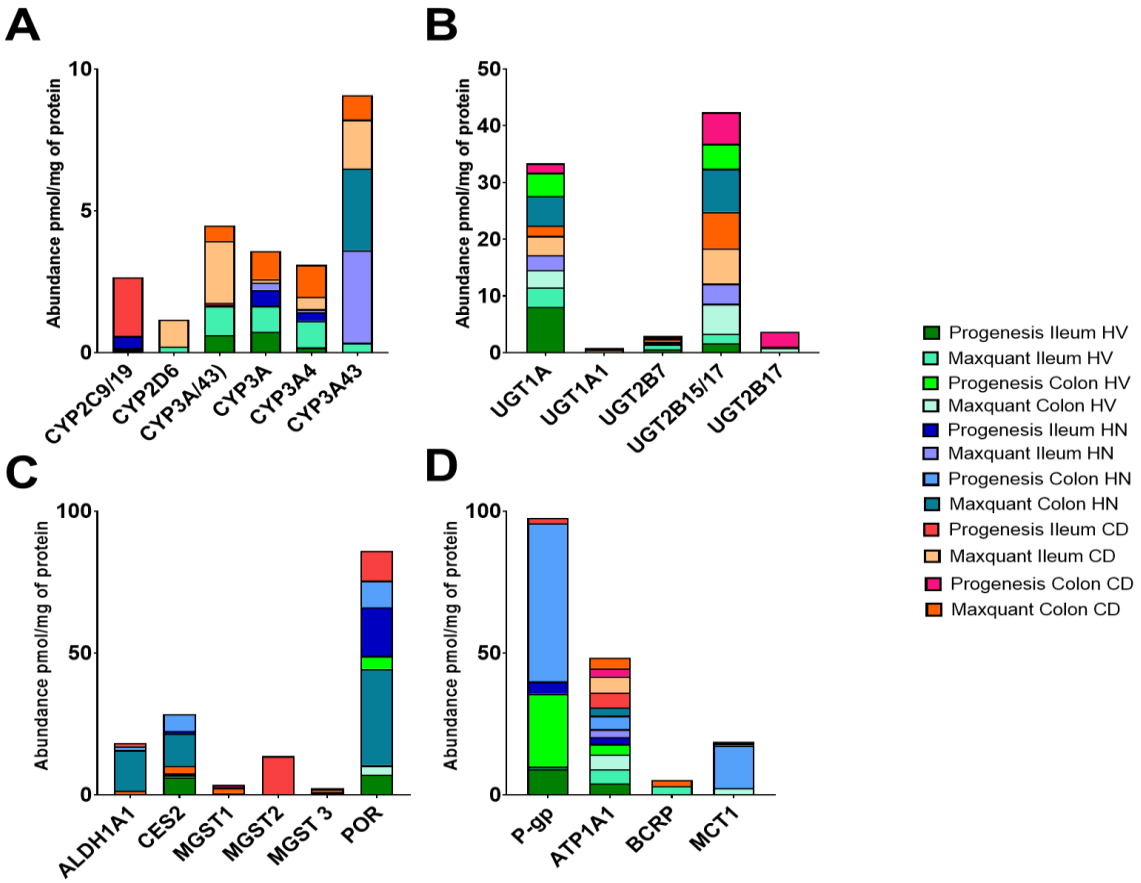

***Figure 5.3**. Comparison of quantified target proteins (in pmol/mg), **(A)** CYPs, **(B)** UGTs, **(C)** non-CYP non-UGT enzymes and **(D)** transporters by MaxQuant and Progenesis in homogenate samples from healthy (HV), normal (HN) and inflamed (CD) ileum and colon samples.*

5.4.3. Absolute Abundance of DMETs in Crohn's Groups Compared to Healthy Control

Targets included in the comparison were detected in at least one sample in two groups (inflamed, normal and healthy) of the same segment (ileum or colon). Changes in DMET abundance in I-CD and HN-CD ileum and colon from healthy baseline was assessed. In total, the list of quantified targets included 5 CYPs, 4 UGTs, 3 non-CYP non-UGT enzymes, and 3 transporters. Table 5.1 presents abundance data in pmol/g of mucosal tissue in each tissue group per segment. Only targets with change of at least 2 fold were considered as altered by disease.

Table 5.1. Abundance (pmol/g mucosal tissue) of CYP enzymes, UGT enzymes, non-CYP non-UGT enzymes and transporters in inflamed Crohn's disease (I-CD), histologically normal Crohn's disease (HN-CD) and healthy ileum and colon. Data presented as mean, standard deviation (SD) and coefficient of variation (%CV).

Ileum Target (pmol/g mucosal tissue)	**Surrogate peptide**	**Healthy**		**Inflamed Crohn's disease (I-CD)**		**Histologically normal Crohn's disease (HN-CD)**	
		Mean±SD	**CV (%)**	**Mean±SD**	**CV (%)**	**Mean±SD**	**CV (%)**
Ileum							
CYP2D6	AFLTQLDELLTEHR	3± N/A	N/A	10.2± N/A	N/A	N/A	
CYP3A	SLLSPTFTSGK	13.2±14.8	112.2	1.4±2	141.2	0.8±0.1	18.7
CYP3A4	LSLGGLLQPEK	10.4±8.6	82.5	3.1± 3	96.8	0.6± N/A	N/A
CYP3A43	DVTHFLK	6.2±2.5	40.6	6.1± N/A	N/A	19.1±N/A	N/A
CYP3A/43	ETQIPLK	16.8±17.1	101.6	22.4± N/A	N/A	0.3± N/A	N/A
UGT1A	IPQTVLWR	37.6±23.8	63.4	23.8±20.1	84.5	9.4±4	42.3
UGT2B7	ADVWLIR	15.5± N/A	N/A	2.3±1.3	58.2	0.5± N/A	N/A
UGT2B15/17	SVINDPIYK	18.5±11.5	62.1	32.3±18.3	56.7	17±17.9	104.9
CES2	ADHGDELPFVFR	2.5± N/A	N/A	3.2±3.5	82.2	1.1± N/A	N/A

MGST3	IASGLGLAWIVGR	2.9±3.9	133.9	0.8±0.7	93.4	N/A	
ATP1A1	IVEIPFNSTNK	44.4±10.9	32.8	27.7±10.1	36.6	8.8±1.3	14.7
Colon							
CYP3A43	DVTHFLK	N/A		15.2± N/A	N/A	25.9±N/A	N/A
UGT1A	IPQTVLWR	34.8±25.1	72.3	10.4±11.5	110.7	8.3±8.9	106.7
UGT2B17	WTYSISK	8.4± N/A	N/A	N/A		11.6± N/A	N/A
UGT2B15/17	SVINDPIYK	50.1±44.2	88.3	43.6±49.4	113.3	28.6±29.9	104.4
MGST1	VFANPEDCVAFGK	1.7± 0.3	19	13.6±16.1	118.4	3.8± 4.8	125.9
MGST3	IASGLGLAWIVGR	1.9± N/A	N/A	5.2± N/A	N/A	N/A	
ATP1A1	IVEIPFNSTNK	48.3±32.3	54.7	30.7±29.6	87.7	20.7±18.4	88.8
MCT1	DLHDANTDLIGR	23.3±22.5	96.6	N/A		2.7±2.3	83.5

N/A, no available data as the value could not be calculated due to insufficient data points (reported in only one sample in the group) or not detected.

5.4.4. Comparison of Absolute Abundance of DMETs in ileum

Only CYP3A (group specific not isoform specific, common between CYP3A4, 5 & 7) was detected in more than one sample in diseased and healthy ileum groups. A significant difference (p=0.0185) was detected across the three groups using Kruskal-Wallis ANOVA test. Comparing I-CD and HN-CD samples to the healthy set and to each other using post-hoc Mann-Whitney test yielded no statistical significance (p=0.0952 (for both CD and HN-CD compared to HV) and p>0.999, respectively). Expression of ATP1A1 showed statistically significant difference (p=0.0019) across the three groups and between I-CD and healthy samples (p=0.0286). ATP1A1 abundance in HN-CD samples was not significantly different from healthy and I-CD (p=0.1333 for both). The expression of the rest of the targets (UGT1A and UGT2B15/17; group specific not isoform specific) were not significantly different (p>0.05) across the three groups or between any two of the groups of ileum. Kruskal-Wallis ANOVA test was not possible to perform with (CYP3A4, CYP3A/43 (group specific not isoform specific, common between CYP3A4, 5, 7 & 43) and MGST3) as there were not enough data points in the three groups. These targets showed no statistical significance (p>0.05) for

disease relative to healthy expression (post-hoc Mann-Whitney test). Figures 5.4-5.6 show abundance values for CYPs, UGTs, non-CYP non-UGT enzymes and transporters.

Inter-individual variability of the quantified targets in each group is presented as CV% (Table 5.1). In healthy samples (n=5), the highest inter-individual variability was assigned to MGST3 (134%, detected in 3 samples). The lowest was assigned to ATP1A1 (CV 33%, detected in 5 samples). The highest inter-individual variation in I-CD samples (n=6) was assigned to CYP3A (141%, detected in 2 samples) and the lowest was assigned to ATP1A1 (CV 37%, detected in 4 samples). For HN-CD samples (n=2), UGT2B15/17 showed the highest variability (105%), while ATP1A1 (CV 15%) showed the lowest variability.

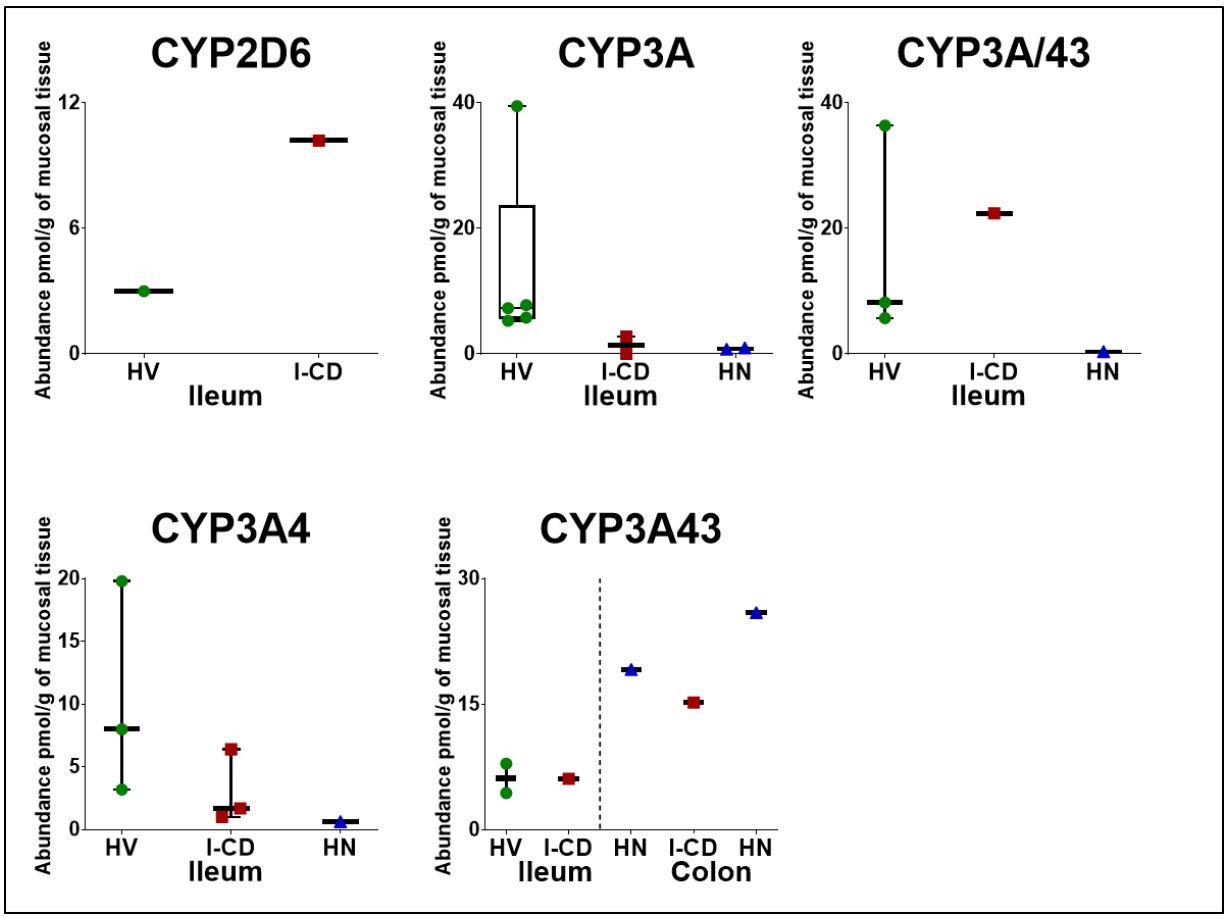

Figure 5.4. *Individual abundance values of cytochrome P450 enzymes (CYPs) in pmol per g of mucosal tissue from healthy, inflamed and non-inflamed Crohn's ileum and colon samples (HV: Healthy, I-CD: inflamed and HN: histologically normal). Horizontal lines represent means and bars represent max and min values.*

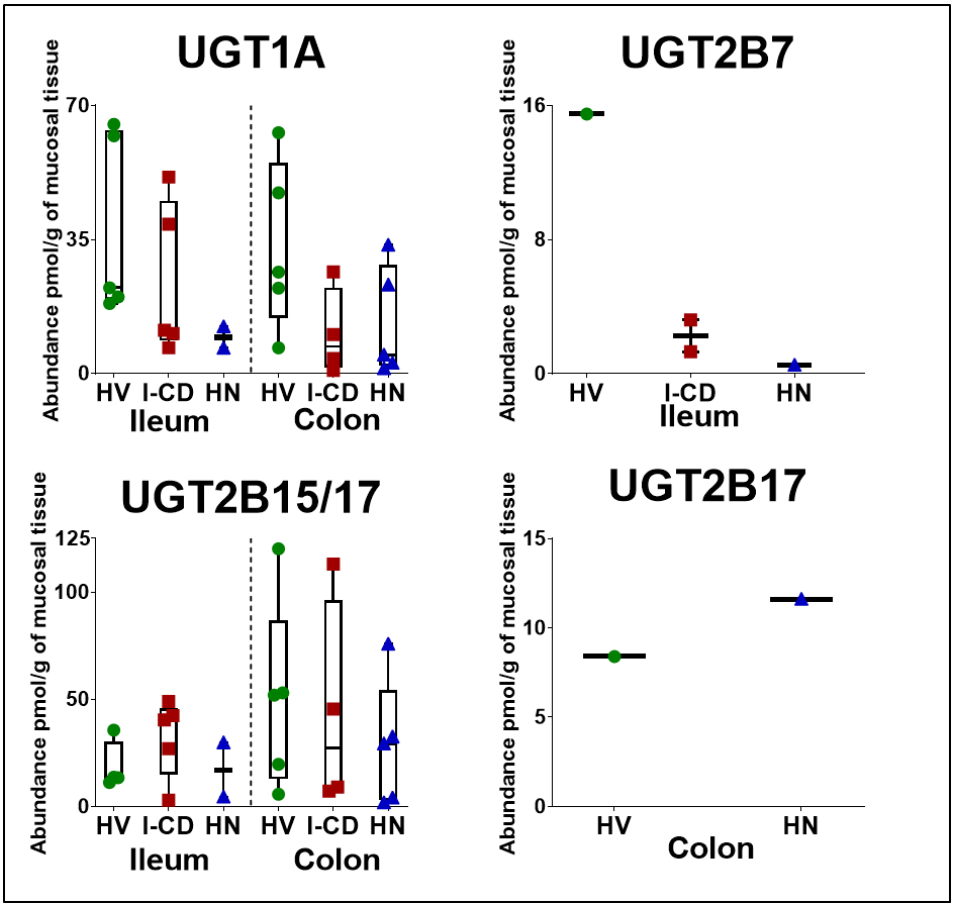

Figure 5.5. *Individual abundance values of uridine-5'-diphospho-glucuronosyltransferase enzymes (UGTs) in pmol per g of mucosal tissue from healthy, inflamed and non-inflamed Crohn's ileum and colon (HV: Healthy, I-CD: inflamed and HN: histologically normal). Horizontal lines represent means and bars represent max and min values.*

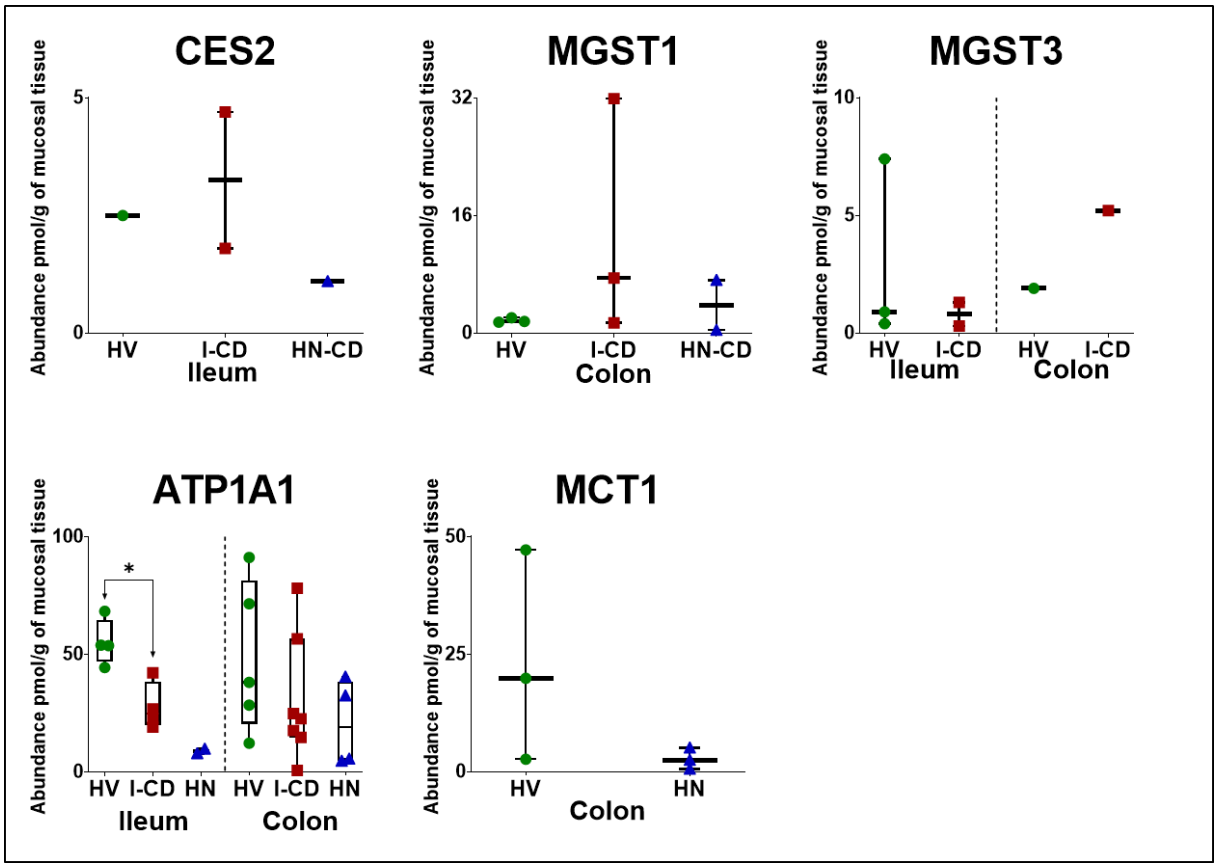

Figure 5.6. *Individual abundance values of non-CYP and non-UGT enzymes and transporters in pmol per g of mucosal tissue from healthy, inflamed and non-inflamed Crohn's ileum and colon (HV: Healthy, I-CD: inflamed and HN: histologically normal). Horizontal lines represent means and bars represent max and min values. Stars (*) represent statistical significance (*p<0.05 and **p <0.01) for comparisons between inflamed and non-inflamed with healthy.*

The fold change in abundance in Crohn's disease groups compared to healthy control and to each other is presented in Figure 5.7. Fold reduction in abundance of DMETs in I-CD ranged from 3.4 (CYP3A4) to 7 (UGT2B7) fold compared to healthy expression. Only one target (CYP2D6) reported a fold increase (3.3 fold) in expression. When expression in I-CD was compared to that in HN-CD tissue, only one target (CYP3A43) showed fold reduction (3.1 fold). The rest of the targets showed a fold increase ranging from 2.5 fold (UGT1A) to 85.3 fold (CYP3A/43). A reduction in most of the quantified targets was recorded for HN-CD compared to healthy tissue. This ranged from 4 fold (UGT1A) to 64 fold (CYP3A/43). CYP3A43 and CES2 were the only targets to show a fold increase at 3.1 and 2.3 fold, respectively.

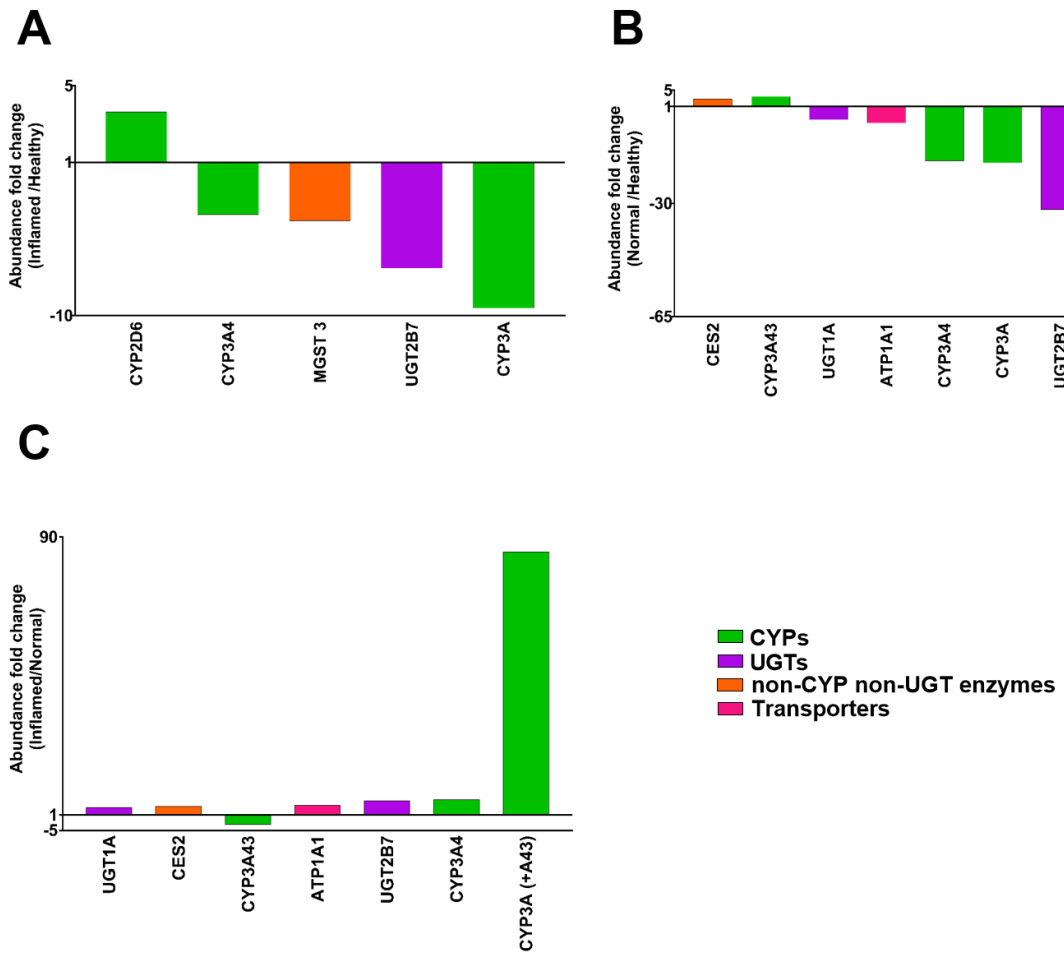

Figure 5.7. *Relative change in expression of DMETs (CYPs, UGTs, non-CYP non-UGT enzymes and transporters) in inflamed CD ileum (n=6) and histologically normal CD ileum (n=2) relative to healthy ileum (n=5). Change in expression is shown for* ***(A)*** *inflamed relative to healthy,* ***(B)*** *histologically normal relative to healthy and* ***(C)*** *inflamed relative to histologically normal. Only fold change ≥2 is considered.*

5.4.5. Comparison of Absolute Abundance of DMETs in Colon

Comparison of UGT1A, UGT2B15/17, MGST1, ATP1A1 and MCT1 across the three examined groups show no significant difference (p>0.05). No statistical significance was observed in post-hoc analysis between I-CD and healthy, HN-CD and healthy and I-CD and HN-CD samples. CYP3A43, UGT2B17 and MGST3 were only detected in one sample per group. Figures 5.4-5.6 show abundance of enzymes and transporters in the colon.

Inter-individual variability assessed as a CV% is shown in Table 5.1. In healthy tissue samples (n=5), the highest inter-individual variation was assigned to MCT1 (97%, detected in 3 samples). The lowest was assigned to MGST1 (19%, detected in 3 samples). The highest variability in I-CD samples (n=7) was recorded for MGST1 (118%, detected in 3 samples) and the lowest was that of ATP1A1 (88%, detected in 5 samples). For HN-CD samples (n=5), MGST1 had the highest variability (126%, detected in 2 samples), while MCT1 showed the lowest variation (84%, detected in 3 samples).

Fold change in Crohn's disease groups compared to healthy control and to each other is presented in Figure 5.8. Only UGT1A in I-CD tissue showed a reduction by 3.4 fold compared to healthy expression. MGST1 and MGST3 showed a fold increase by 7.9 and 4.6 fold, respectively, in I-CD tissue compared to healthy control. When compared to HN-CD, MGST1 and MGST3 targets showed a fold increase by 3.6 and 2.8 fold, respectively. The rest of the targets showed no difference between the groups. In HN-CD tissue samples, fold reduction ranged from 8.6 fold (MCT1) to 2.3 fold (ATP1A1) compared to healthy tissue. MGST1 reported a fold increase of 2.2 fold.

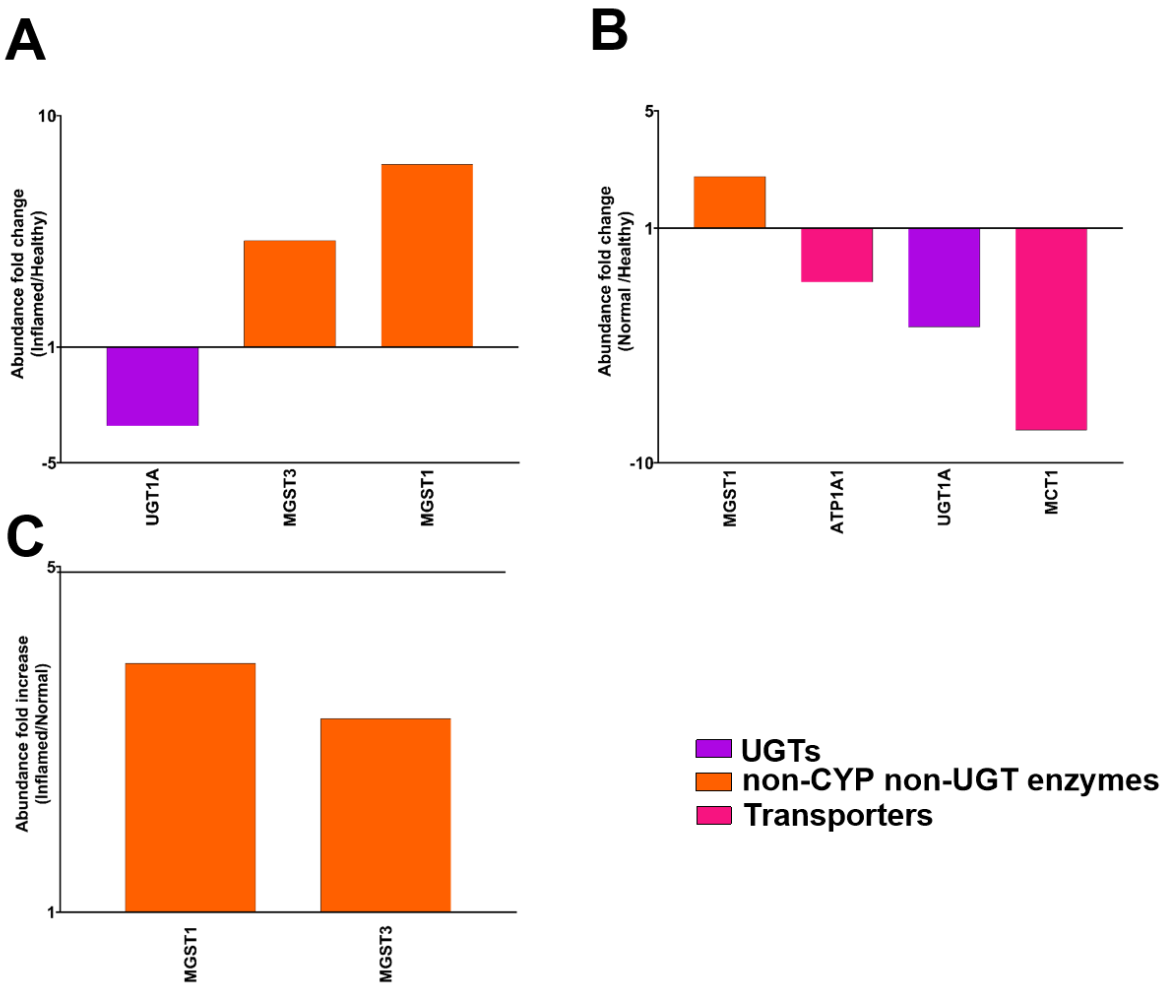

Figure 5.8. *Relative change of DMETs (UGTs, non-CYP non-UGT enzymes and transporters) expression from healthy colon individual samples (n=5), inflamed CD colon (n=7) and histologically normal CD colon (n=5). Change in expression is shown for* ***(A)*** *inflamed relative to healthy,* ***(B)*** *histologically normal relative to healthy and* ***(C)*** *inflamed relative to histologically normal. Only fold change ≥2 is considered.*

5.5.Discussion

Crohn's disease is a chronic bowel disease with a local and systemic inflammatory effect. Inflammation caused by the disease can affect the PK of oral drugs used to control the disease itself or other co-morbidities. In the intestine, inflammation causes alteration in expression and activity of DMETs, among other altered physiological parameters. To assess the impact of CD on oral drug bioavailability, reliable abundance data are needed to refine PBPK models that allow prediction of the fate of drugs in the body. In this study, we applied targeted proteomics for the quantification of different DMETs in ileum and colon from inflamed and non-inflamed CD relative to healthy tissue.

We first investigated difference in the output of two commonly used proteomic analysis tools, MaxQuant and Progenesis. This was carried out in order to determine the software package that provides better coverage of the target proteins. MaxQuant showed higher coverage of the targets (19) compared to Progenesis (16) in human intestine. CYP and UGT enzymes and transporters were more readily detectable by MaxQuant; however, no significant difference in counts were uncovered by the two software.

QconCAT-based proteomics allowed detection of a low number of targets (3 CYPs, 2 UGTs, 3 non-CYP non-UGT and 2 transporters); these were compared to healthy baseline. This could be due to the used LC-MS peptide selection strategy, LC-MS selectivity and specificity can be enhanced in targeted proteomics by pre-selection of precursor ions of the surrogate peptides.[43,44] This reduces ionic complexity enabling quantification of targeted peptides with low abundance in a complex biological sample. With our samples peptides were selected for fragmentation automatically, where the peptides with the most intense signals will be captured primarily. LC-MS automatic selection of peptides was successfully applied with quantitative targeted proteomics, utilising intestine samples from healthy and histologically normal jejunum and ileum tissues.[45] The main difference between our study and the previous intestine study is that it used 180 minutes gradient while in our current study we used 90 minutes gradient. Additionally, the fraction used in the previous study was crude membrane fraction which is more purified compared to our non-enriched fraction (homogenate) fraction. The homogenate fraction consists of all the cellular components (mitochondria, endoplasmic reticulum, cytoplasm, nucleus, and plasma membrane) which dilutes the signal from the desired targets.[46] Soluble proteins are more amenable to digestion and therefore present a major interference risk to membrane embedded targets such as enzymes and transporters.[47] Thus, purification of the

subcellular fraction of interest is advantageous to provide enrichment of target proteins (microsomal fraction for CYP and UGT enzymes, S9 for cytosolic enzymes, and membrane fraction for transporters).[48] This is particularly useful when measuring UGT enzymes and transporters because of their membrane topology, high sequence homology and low expression levels.[49,50]

Label-free global proteomics presents an alternative approach which is adopted together with or independently from targeted proteomics; we have demonstrated its utility with pooled samples in Chapter Four. Label-free quantification uses non-labelled protein standards added at known concentrations to enable quantification of a large number of proteins in complex biological samples. This makes it cost-effective compared to the use of stable isotope labelled peptide and protein standards,[37,51] while being nearly as accurate as targeted proteomics.[52]

The proteins that were quantified in the healthy and Crohn's samples include group specific enzymes (CYP3A, CYP3A/43, UGT1A and UGT2B15/17) and individual targets (CYP2D6, CYP3A4, CYP3A43, UGT2B7, UGT2B17, CES2, MGST1, MGST3, ATP1A1 and MCT1). Abundant targets included UGY2B17, which is the most abundant UGT in both segments (ileum: 38%-50%, and colon: 66%-75%), and MGST1, which is the most abundant enzyme in healthy colon (47%), based on analysis of pooled samples (Chapter Four). CYP3A4 is the most important and most abundant CYP enzyme in the intestine (approximately 80% of intestinal CYP).[53] In the ileum, all quantified targets showed lower expression in inflamed and histologically normal tissue compared to healthy control. Suppression of CYP3A4 and MGST3 is in line with previous reports.[9] The exception was observed with CYP2D6, CES2 and CYP3A43, where diseased tissue expression was higher. These three enzymes are reported here for the first time. Only CES2 showed the same trend in pooled samples (~2.3-fold reduction in healthy tissue compared to tissue from CD subjects) (Chapter Four). CES2 is a carboxylesterase, which is involved in the metabolism of a wide range of drugs, including acetylsalicylic acid, angiotensin-receptor blockers (candesartan, olmesartan and azilsartan) and antiviral agents (tenofovir, adefovir and valacyclovir).[54] In the colon, MCT1 was lower in histologically normal CD tissue compared to healthy control, consistent with the literature.[15] Other targets (MGST1 and MGST3) displayed lower abundance in healthy tissue compared to tissue from CD subjects. Again, this trend is reported here for the first time, while the results from the pooled samples show the opposite trend. Microsomal glutathione S-transferases are

detoxifying enzymes that conjugate glutathione to hydrophobic electrophilic compounds and participate in lipids metabolism.[55,56]

Inter-individual variability in the detected targets was generally higher in ileum compared to colon. The inflamed CD ileum set displayed the highest variability (36.6%-141.2%) and the histologically normal exhibited the lowest variability (14.7%-104.9%). In the colon, the highest variability (36.6%-141.2%) was observed in the histologically normal group, while the lowest variability (19%-96.6%) was recorded for the healthy group. This variation can be attributed to the differences in protein distribution across the intestinal segments due to their different physiological functions. Another contributor to this finding is the high turnover rate of the enterocytes which are the cellular units where DMETs reside.[53,57,58] Nevertheless, the number of the targets quantified in this study and the number of samples in which they are detected is very small to determine the true inter-individual variability in CD. It is important to note that capturing the abundance and its variability in a population should be performed in a sufficient number of individuals across the different conditions of the investigated populations.[59,60]

To conclude, MaxQuant showed a better coverage of the intestinal targets compared to Progenesis, and therefore, it was used to analyse the proteomic data. Only a limited number of the target proteins were detected, most likely due to the unsuitability of the LC-MS strategy when considering the complexity of the sample fraction under study. The targets that were quantified generated interesting observations of differential expression in CD, which will be expanded by label-free global quantification.

5.6.References

1. Hart AL., Ng SC. Crohn's disease. *Medicine (Baltimore)* 2011;**39**(4):229–36. Doi: 10.1016/j.mpmed.2011.01.004.

2. Langmann T., Moehle C., Mauerer R., Scharl M., Liebisch G., Zahn A., et al. Loss of detoxification in inflammatory bowel disease: dysregulation of pregnane X receptor target genes. *Gastroenterology* 2004;**127**(1):26–40. Doi: 10.1053/j.gastro.2004.04.019.

3. Ricci G., Ambrosi A., Resca D., Masotti M., Alvisi V. Comparison of serum total sialic acid, C-reactive protein, α1-acid glycoprotein and β2-microglobulin in patients with non-malignant bowel diseases. *Biomed Pharmacother* 1995;**49**(5):259–62. Doi: 10.1016/0753-3322(96)82632-1.

4. Nguyen GC., Du L., Chong RY., Jackson TD. Hypoalbuminaemia and Postoperative Outcomes in Inflammatory Bowel Disease: the NSQIP Surgical Cohort. *J Crohn's Colitis* 2019;**13**(11):1433–8. Doi: 10.1093/ecco-jcc/jjz083.

5. Yekeler E., Danalioglu A., Movasseghi B., Yilmaz S., Karaca C., Kaymakoglu S., et al. Crohn disease activity evaluated by Doppler ultrasonography of the superior mesenteric artery and the affected small-bowel segments. *J Ultrasound Med* 2005;**24**(1):59–65. Doi: 10.7863/jum.2005.24.1.59.

6. van Oostayen JA., Wasser MNJM., van Hogezand RA., Griffioen G., de Roos A. Activity of Crohn disease assessed by measurement of superior mesenteric artery flow with Doppler US. *Radiology* 1994;**193**(2):551–4. Doi: 10.1148/radiology.193.2.7972778.

7. van Oostayen J. Diagnosis of Crohn's ileitis and monitoring of disease activity: value of Doppler ultrasound of superior mesenteric artery flow. *Am J Gastroenterol* 1998;**93**(1):88–91. Doi: 10.1016/S0002-9270(97)00029-4.

8. Wilson A., Tirona RG., Kim RB. CYP3A4 Activity is Markedly Lower in Patients with Crohn's Disease. *Inflamm Bowel Dis* 2017;**23**(5):804–13. Doi: 10.1097/MIB.0000000000001062.

9. Wilson A., Urquhart BL., Ponich T., Chande N., Gregor JC., Beaton M., et al. Crohn's Disease Is Associated with Decreased CYP3A4 and P-Glycoprotein Protein Expression. *Mol Pharm* 2019;**16**(9):4059–64. Doi: 10.1021/acs.molpharmaceut.9b00459.

10. Thörn M., Finnström N., Lundgren S., Rane A., Lööf L. Expression of cytochrome P450 and MDR1 in patients with proctitis. *Ups J Med Sci* 2007;**112**(3):303–12. Doi: 10.3109/2000-1967-203.

11. Plewka D., Plewka A., Szczepanik T., Morek M., Bogunia E., Wittek P., et al. Expression of selected cytochrome P450 isoforms and of cooperating enzymes in

colorectal tissues in selected pathological conditions. *Pathol - Res Pract* 2014;**210**(4):242–9. Doi: 10.1016/j.prp.2013.12.010.

12. Jahnel J., Fickert P., Hauer AC., Högenauer C., Avian A., Trauner M. Inflammatory Bowel Disease Alters Intestinal Bile Acid Transporter Expression. *Drug Metab Dispos* 2014;**42**(9):1423–31. Doi: 10.1124/dmd.114.058065.

13. Wojtal KA., Eloranta JJ., Hruz P., Gutmann H., Drewe J., Staumann A., et al. Changes in mRNA Expression Levels of Solute Carrier Transporters in Inflammatory Bowel Disease Patients. *Drug Metab Dispos* 2009;**37**(9):1871–7. Doi: 10.1124/dmd.109.027367.

14. Blokzijl H., Borght S Vander., Bok LIH., Libbrecht L., Geuken M., van den Heuvel FAJ., et al. Decreased P-glycoprotein (P-gp/MDR1) expression in inflamed human intestinal epithelium is independent of PXR protein levels. *Inflamm Bowel Dis* 2007;**13**(6):710–20. Doi: 10.1002/ibd.20088.

15. Thibault R., De Coppet P., Daly K., Bourreille A., Cuff M., Bonnet C., et al. Down-Regulation of the Monocarboxylate Transporter 1 Is Involved in Butyrate Deficiency During Intestinal Inflammation. *Gastroenterology* 2007;**133**(6):1916–27. Doi: 10.1053/j.gastro.2007.08.041.

16. Blokzijl H., van Steenpaal A., Borght S Vander., Bok LIH., Libbrecht L., Tamminga M., et al. Up-regulation and Cytoprotective Role of Epithelial Multidrug Resistance-associated Protein 1 in Inflammatory Bowel Disease. *J Biol Chem* 2008;**283**(51):35630–7. Doi: 10.1074/jbc.M804374200.

17. Wright S. Clinical significance of azathioprine active metabolite concentrations in inflammatory bowel disease. *Gut* 2004;**53**(8):1123–8. Doi: 10.1136/gut.2003.032896.

18. Choughule K V., Barnaba C., Joswig-Jones CA., Jones JP. In Vitro Oxidative Metabolism of 6-Mercaptopurine in Human Liver: Insights into the Role of the Molybdoflavoenzymes Aldehyde Oxidase, Xanthine Oxidase, and Xanthine Dehydrogenase. *Drug Metab Dispos* 2014;**42**(8):1334–40. Doi: 10.1124/dmd.114.058107.

19. Akobeng AK., Zhang D., Gordon M., MacDonald JK. Oral 5-aminosalicylic acid for maintenance of medically-induced remission in Crohn's disease. *Cochrane Database Syst Rev* 2016;**9**(9):CD003715. Doi: 10.1002/14651858.CD003715.pub3.

20. Ufer M., Dilger K., Leschhorn L., Daufresne LM., Mosyagin I., Rosenstiel P., et al. Influence of CYP3A4, CYP3A5, and ABCB1 genotype and expression on budesonide pharmacokinetics: a possible role of intestinal CYP3A4 expression. *Clin Pharmacol Ther* 2008;**84**(1):43–6. Doi: 10.1038/SJ.CLPT.6100505.

21. Imani S., Jusko WJ., Steiner RW. Diltiazem retards the metabolism of oral prednisone

with effects on T-cell markers. *Pediatr Transplant* 1999;**3**(2):126–30. Doi: 10.1034/J.1399-3046.1999.00027.X.

22. Aitken AE., Richardson TA., Morgan ET. REGULATION OF DRUG-METABOLIZING ENZYMES AND TRANSPORTERS IN INFLAMMATION. *Annu Rev Pharmacol Toxicol* 2006;**46**(1):123–49. Doi: 10.1146/annurev.pharmtox.46.120604.141059.

23. Morgan ET. Impact of infectious and inflammatory disease on cytochrome P450-mediated drug metabolism and pharmacokinetics. *Clin Pharmacol Ther* 2009;**85**(4):434. Doi: 10.1038/CLPT.2008.302.

24. Yoshida K., Budha N., Jin JY. Impact of physiologically based pharmacokinetic models on regulatory reviews and product labels: Frequent utilization in the field of oncology. *Clin Pharmacol Ther* 2017;**101**(5):597–602. Doi: 10.1002/CPT.622.

25. Edginton AN., Willmann S. Physiology-based simulations of a pathological condition: prediction of pharmacokinetics in patients with liver cirrhosis. *Clin Pharmacokinet* 2008;**47**(11):743–52. Doi: 10.2165/00003088-200847110-00005.

26. Huang W., Isoherranen N. Novel Mechanistic PBPK Model to Predict Renal Clearance in Varying Stages of CKD by Incorporating Tubular Adaptation and Dynamic Passive Reabsorption. *CPT Pharmacometrics Syst Pharmacol* 2020;**9**(10):571–83. Doi: 10.1002/PSP4.12553.

27. Rostami-Hodjegan A. Physiologically Based Pharmacokinetics Joined With In Vitro–In Vivo Extrapolation of ADME: A Marriage Under the Arch of Systems Pharmacology. *Clin Pharmacol Ther* 2012;**92**(1):50–61. Doi: 10.1038/clpt.2012.65.

28. Effinger A., O'Driscoll CM., McAllister M., Fotaki N. Predicting budesonide performance in healthy subjects and patients with Crohn's disease using biorelevant in vitro dissolution testing and PBPK modeling. *Eur J Pharm Sci* 2020:105617. Doi: 10.1016/j.ejps.2020.105617.

29. Wang L., Chen Y., Zhou W., Miao X., Zhou H. Utilization of physiologically-based pharmacokinetic model to assess disease-mediated therapeutic protein-disease-drug interaction in immune-mediated inflammatory diseases. *Clin Transl Sci* 2021. Doi: 10.1111/cts.13164.

30. Jung D. Human ileal bile acid transporter gene ASBT (SLC10A2) is transactivated by the glucocorticoid receptor. *Gut* 2004;**53**(1):78–84. Doi: 10.1136/gut.53.1.78.

31. Girardin M., Dionne S., Goyette P., Rioux J., Bitton A., Elimrani I., et al. Expression and functional analysis of intestinal organic cation/l-carnitine transporter (OCTN) in Crohn's Disease. *J Crohn's Colitis* 2012;**6**(2):189–97. Doi: 10.1016/j.crohns.2011.08.003.

32. Berggren S., Gall C., Wollnitz N., Ekelund M., Karlbom U., Hoogstraate J., et al. Gene and Protein Expression of P-Glycoprotein, MRP1, MRP2, and CYP3A4 in the Small and Large Human Intestine. *Mol Pharm* 2007;**4**(2):252–7. Doi: 10.1021/mp0600687.

33. Hayeshi R., Hilgendorf C., Artursson P., Augustijns P., Brodin B., Dehertogh P., et al. Comparison of drug transporter gene expression and functionality in Caco-2 cells from 10 different laboratories. *Eur J Pharm Sci* 2008;**35**(5):383–96. Doi: 10.1016/J.EJPS.2008.08.004.

34. Sjögren E., Abrahamsson B., Augustijns P., Becker D., Bolger MB., Brewster M., et al. In vivo methods for drug absorption - comparative physiologies, model selection, correlations with in vitro methods (IVIVC), and applications for formulation/API/excipient characterization including food effects. *Eur J Pharm Sci* 2014;**57**(1):99–151. Doi: 10.1016/J.EJPS.2014.02.010.

35. Vasilogianni A-M., El-Khateeb E., Alrubia S., Al-Majdoub ZM., Couto N., Achour B., et al. Complementarity of MaxQuant and Progenesis in Identification of Drug-Metabolising Enzymes and Transporters in Human Liver. *Unpublished* n.d.

36. Harwood MD., Achour B., Russell MR., Carlson GL., Warhurst G., Rostami-Hodjegan A. Application of an LC-MS/MS method for the simultaneous quantification of human intestinal transporter proteins absolute abundance using a QconCAT technique. *J Pharm Biomed Anal* 2015;**110**:27–33. Doi: 10.1016/j.jpba.2015.02.043.

37. Russell MR., Achour B., Mckenzie EA., Lopez R., Harwood MD., Rostami-Hodjegan A., et al. Alternative Fusion Protein Strategies to Express Recalcitrant QconCAT Proteins for Quantitative Proteomics of Human Drug Metabolizing Enzymes and Transporters. *J Proteome Res* 2013;**12**(12):5934–42. Doi: 10.1021/pr400279u.

38. El-Khateeb E., Al-Majdoub ZM., Rostami-Hodjegan A., Barber J., Achour B. Proteomic Quantification of Changes in Abundance of Drug-Metabolizing Enzymes and Drug Transporters in Human Liver Cirrhosis: Different Methods, Similar Outcomes. *Drug Metab Dispos* 2021;**49**(8):610–8. Doi: 10.1124/dmd.121.000484.

39. Achour B., Al-Majdoub ZM., Al Feteisi H., Elmorsi Y., Rostami-Hodjegan A., Barber J. Ten years of QconCATs: Application of multiplexed quantification to small medically relevant proteomes. *Int J Mass Spectrom* 2015;**391**:93–104. Doi: 10.1016/j.ijms.2015.08.003.

40. Couto N., Al-Majdoub ZM., Gibson S., Davies PJ., Achour B., Harwood MD., et al. Quantitative Proteomics of Clinically Relevant Drug-Metabolizing Enzymes and Drug Transporters and Their Intercorrelations in the Human Small Intestine. *Drug Metab Dispos* 2020;**48**(4):245–54. Doi: 10.1124/dmd.119.089656.

41. Al-Majdoub ZM., Al Feteisi H., Achour B., Warwood S., Neuhoff S., Rostami-Hodjegan A., et al. Proteomic Quantification of Human Blood–Brain Barrier SLC and

ABC Transporters in Healthy Individuals and Dementia Patients. *Mol Pharm* 2019;**16**(3):1220–33. Doi: 10.1021/acs.molpharmaceut.8b01189.

42. Achour B., Dantonio A., Niosi M., Novak JJ., Al-Majdoub ZM., Goosen TC., et al. Data generated by quantitative liquid chromatography-mass spectrometry proteomics are only the start and not the endpoint: Optimization of quantitative concatemer-based measurement of hepatic uridine-59-diphosphate–glucuronosyltransferase enzymes with ref. *Drug Metab Dispos* 2018;**46**(6):805–12. Doi: 10.1124/dmd.117.079475.

43. Jonsson AP. Mass spectrometry for protein and peptide characterisation. *Cell Mol Life Sci* 2001;**58**(7):868–84. Doi: 10.1007/PL00000907.

44. Ohtsuki S., Uchida Y., Kubo Y., Terasaki T. Quantitative targeted absolute proteomics-based ADME research as a new path to drug discovery and development: Methodology, advantages, strategy, and prospects. *J Pharm Sci* 2011;**100**(9):3547–59. Doi: 10.1002/jps.22612.

45. Couto N., Al-Majdoub ZM., Gibson S., Davies PJ., Achour B., Harwood MD., et al. Quantitative Proteomics of Clinically Relevant Drug-Metabolizing Enzymes and Drug Transporters and Their Intercorrelations in the Human Small Intestine. *Drug Metab Dispos* 2020;**48**(4):245–54. Doi: 10.1124/dmd.119.089656.

46. Vuckovic D., Dagley LF., Purcell AW., Emili A. Membrane proteomics by high performance liquid chromatography-tandem mass spectrometry: Analytical approaches and challenges. *Proteomics* 2013;**13**(3–4):404–23. Doi: 10.1002/pmic.201200340.

47. Helbig AO., Heck AJR., Slijper M. Exploring the membrane proteome—Challenges and analytical strategies. *J Proteomics* 2010;**73**(5):868–78. Doi: 10.1016/j.jprot.2010.01.005.

48. El-Khateeb E., Vasilogianni A-M., Alrubia S., Al-Majdoub ZM., Couto N., Howard M., et al. Quantitative mass spectrometry-based proteomics in the era of model-informed drug development: Applications in translational pharmacology and recommendations for best practice. *Pharmacol Ther* 2019;**203**:107397. Doi: 10.1016/j.pharmthera.2019.107397.

49. Harwood MD., Achour B., Neuhoff S., Russell MR., Carlson G., Warhurst G., et al. In Vitro-In Vivo Extrapolation Scaling Factors for Intestinal P-glycoprotein and Breast Cancer Resistance Protein: Part I: A Cross- Laboratory Comparison of Transporter Protein Abundances and Relative Expression Factors in Human Intestine and Caco-2 Cell. *Drug Metab Dispos* 2016;**44**(3):297–307. Doi: 10.1124/dmd.115.067371.

50. Achour B., Al-Majdoub ZM., Rostami-Hodjegan A., Barber J. Mass Spectrometry of Human Transporters. *Annu Rev Anal Chem* 2020;**13**(1):223–47. Doi: 10.1146/annurev-anchem-091719-024553.

51. Al Feteisi H., Achour B., Barber J., Rostami-Hodjegan A. Choice of LC-MS Methods for the Absolute Quantification of Drug-Metabolizing Enzymes and Transporters in Human Tissue: a Comparative Cost Analysis. *AAPS J* 2015;**17**(2):438–46. Doi: 10.1208/s12248-014-9712-6.

52. Wegler C., Gaugaz FZ., Andersson TB., Wiśniewski JR., Busch D., Gröer C., et al. Variability in Mass Spectrometry-based Quantification of Clinically Relevant Drug Transporters and Drug Metabolizing Enzymes. *Mol Pharm* 2017;**14**(9):3142–51. Doi: 10.1021/acs.molpharmaceut.7b00364.

53. Paine MF., Hart HL., Ludington SS., Haining RL., Rettie AE., Zeldin DC. THE HUMAN INTESTINAL CYTOCHROME P450 "PIE." *Drug Metab Dispos* 2006;**34**(5):880–6. Doi: 10.1124/dmd.105.008672.

54. Casey Laizure S., Herring V., Hu Z., Witbrodt K., Parker RB. The role of human carboxylesterases in drug metabolism: have we overlooked their importance? *Pharmacotherapy* 2013;**33**(2):210–22. Doi: 10.1002/PHAR.1194.

55. Kuang Q., Purhonen P., Ålander J., Svensson R., Hoogland V., Winerdal J., et al. Dead-end complex, lipid interactions and catalytic mechanism of microsomal glutathione transferase 1, an electron crystallography and mutagenesis investigation. *Sci Rep* 2017;**7**(1):1–10. Doi: 10.1038/s41598-017-07912-3.

56. Uno Y., Murayama N., Kunori M., Yamazaki H. Short Communication Characterization of Microsomal Glutathione S -Transferases. *Drug Metab Dispos* 2013;**41**:1621–5.

57. Darwich AS., Aslam U., Ashcroft DM., Rostami-Hodjegan A. Meta-analysis of the turnover of intestinal epithelia in preclinical animal species and humans. *Drug Metab Dispos* 2014;**42**(12):2016–22. Doi: 10.1124/DMD.114.058404.

58. Darwich AS., Burt HJ., Rostami-Hodjegan A. The nested enzyme-within-enterocyte (NEWE) turnover model for predicting dynamic drug and disease effects on the gut wall. *Eur J Pharm Sci* 2019;**131**:195–207. Doi: 10.1016/j.ejps.2019.02.017.

59. Drozdzik M., Busch D., Lapczuk J., Müller J., Ostrowski M., Kurzawski M., et al. Protein Abundance of Clinically Relevant Drug-Metabolizing Enzymes in the Human Liver and Intestine: A Comparative Analysis in Paired Tissue Specimens. *Clin Pharmacol Ther* 2019;**105**(5):1204–12. Doi: 10.1002/cpt.967.

60. Harwood MD., Zhang M., Pathak SM., Neuhoff S. The Regional-Specific Relative and Absolute Expression of Gut Transporters in Adult Caucasians: A Meta-Analysis. *Drug Metab Dispos* 2019;**47**(8):854–64. Doi: 10.1124/dmd.119.086959.

5.7.Supplementary material – Methodology

Table S5.1. Demographic and clinical details of Crohn's disease (CD) patients.

Sample ID	Tissues source	Gender	Age at surgery (year)	Ethnicity	Height (m)	Weight (kg)	BMI	Smoking	Drinking	Tissue classification	Medical history	Medication history
328a	Colon	Female	38	N/A	1.74	53	17.51	Yes (recent ex)	Yes occasionally	Diseased	Crohn's disease	Methotrexate 4 years ago
328b										Histologically normal		
1942a	Colon	Female	25	N/A	1.57	42	17.04		N/A	Diseased-Active CD with extensive ulceration	Crohn's diagnosed in 2003. Failure to all medications including adalimumab, infliximab, tacrolimus, vedolizumab, ustekinumab and anti-MAP therapy	Azathioprine
1942b										Histologically normal		
1940a	Ileum	Female	62	Caucasian-British	1.65	58.06	21.33	No	N/A	Diseased-Patchy mild to moderate transmural chronic	Bowel resection (2013), bile salt malabsorption, reflux	Ustekinumab, iron tablets, B12 injections, cholestyramine, omeprazole, azathioprine, fortisip
1940b										Histologically normal		
974	Colon	Male	18	N/A	1.8	55.2	17.04	No	No	Diseased	Crohn's disease, recently treated for latent Tuberculosis	Laxido, adalimumab, azathioprine

156	Colon	Male	39	Caucasian-Irish	1.8	111	34.26	No	Yes 25 units per week	Diseased	Crohn's disease, laprotomy (2005), reversal ileostomy (2005), gout wrist	Candesartan, salbutamol, luperamide, buscupan, mesalazine, allupurinol
1569	Colon	Female	31	Caucasian-British	1.65	74	27.18	Ex - stopped 6yrs ago. E-cig currently	No	Diseased	Anorectal strictoplasty (2016), c-section x2 (2008 & 2009), drainage of fistula (2006), rectal abscess (2005), abdominal pain, heart murmur (as child), heartburn (reflux), low BP, tonsillectomy, vit. D deficiency	Omeprazole, azathioprine
1265b	Colon	Male	46	Caucasian-British	1.84	110	32.14	Yes	N/A	Histologically normal	post-traumatic stress disorder, Crohn's disease with stricture formation (ileum)	Quetiapine, mirtazapine, co-codamol, zopiclone
1265a	Terminal Ileum									Diseased		
2055	Colon	Male	30	Pakistani	1.87	120	34.32	Cannabis for pain relief	N/A	Diseased	Anxiety, low mood	Loperamide, octasa
917	Ileum	Male	23	Caucasian-Irish	1.87	84.6	24.19	No	Occasionally	Diseased	Mild asthma, heartburn, ileal Crohn's disease	Prednisolone, ciprofloxacin, metronidazole,

												omeprazole, tramadol
304	Ileum	Female	27	Caucasian-British	N/A	78	N/A	Yes	No	Diseased	Terminal ileal Crohn's disease	Azathioprine, movicol, docusate sodium
844b	Colon	Female	51	N/A	1.62	61	23.24	N/A	N/A	Histologically normal	IBD, Ileal Crohn's disease	Seretide, folic acid
844a	Ileum									Diseased		
1004a	Ileum	Female	19	Caucasian-British	1.62	46	17.53	No	No	Diseased-mild CD	Ileal Crohn's disease	Azathioprine, adalimumab
1004b										Histologically normal		
2003a	Colon	Male	68	Caucasian-Irish	1.8	91.2	28.14	Ex	N/A	Diseased	Piles tied (2016), HTN, hypercholesterolaemia, heartburn, anaemia, diverticulitis, Crohn's	Amlodipine
2003b										Histologically normal		

N/A, No available information; BP, blood pressure; IBD, inflammatory bowel disease; HTN, hypertension.

Table S5.2. Demographic details of healthy subjects.

Sample ID	Tissues source	Gender	Age (year)	Ethnicity	Tissue classification	Cause of death	Post mortem interval (PMI) (hrs)
F-28	Colon, Descending	Female	50	Caucasian	Healthy	Car accident	4
208A	Colon, Transverse	Female	78	Caucasian	Healthy	Cardiovascular disease, unspecified	5
S3-13	Colon, Sigmoid	Male	30	Caucasian	Healthy	Car accident	4
S4-12	Colon, Descending	Male	30	Caucasian	Healthy	Car accident	4
M-28	Colon, Descending	Male	54	Caucasian	Healthy	Injuries in the abdomen	4
1C-10	Ileum	Male	33	Caucasian	Healthy	Traumatic injury	4
S13-20	Ileum	Male	48	Caucasian	Healthy	Mechanical trauma	1
S3-26	Ileum	Male	30	Caucasian	Healthy	Car accident	4
208A	Ileum	Female	78	Caucasian	Healthy	Cardiovascular disease, unspecified	5
90-12-23A	Ileum	Female	65	Caucasian	Healthy	Acute myocardial infarction	9

Table S5.3. Targets and their surrogate peptides in each QconCAT standard, NuncCAT, MetCAT and TransCAT.

NuncCAT		MetCAT		TransCAT	
Target	**Surrogate peptide**	**Target**	**Surrogate peptide**	**Target**	**Surrogate peptide**
CES1	EGYLQIGANTQAAQK	**CYP1A2**	ASGNLIPQEK	**P-gp, (ABCB1)**	FYDPLAGK§
	FLSLDLQGDPR		YLPNPALQR		AGAVAEEVLAAIR
CES2	ADHGDELPFVFR	**CYP2A6**	DPSFFSNPQDFNPQHFLNEK	**BSEP (ABCB11)**	STALQLIQR
	SFFGGNYIK		GTGGANIDPTFFLSR		AADTIIGFEHGTAVER
	TTHTGQVLGSLVHVK	**CYP2B6**	ETLDPSAPR	**MDR3 (ABCB4)**	IATEAIENIR
FMO3	LVGPGQWPGAR		GYGVIFANGNR		GAAYVIFDIIDNNPK
	NNLPTAISDWLYVK	**CYP2C18**	GSFPVAEK	**MRP2 (ABCC2)**	LTIIPQDPILFSGSLR
			SLTNFSK		
FMO5	WATQVFK	**CYP2C19**	GHFPLAER		YLGGDDLDTSAIR
	TDDIGGLWR				
	LTHFIWK				
EPHX1	IIPLLTDPK	**CYP2C8**	SFTNFSK		AFEHQQR
	FSTWTNTEFR	**CYP2C9/19**	GIFPLAER	**MRP3 (ABCC3)**	AEGEISDPFR
			LPPGPTPLPVIGNILQIGIK		IDGLNVADIGLHDLR
EPHX2	GLLNDAFQK	**CYP2D6**	AFLTQLDELLTEHR	**MRP4 (ABCC4)**	AEAAALTETAK
	WLDSDAR		DIEVQGFR		APVLFFDR
MGST1	VFANPEDCVAFGK	**CYP2E1**	FITLVPSNLPHEATR	**MRP6 (ABCC6)**	SSLPSALLGELSK
	IYHTIAYLTPLPQPNR		GIIFNNGPTWK		APETEPFLR
					SSLASGLLR
MGST2	HLYFWGYSEAAK	**CYP2J2**	FEYQDSWFQQLLK	**BCRP (ABCG2)**	VIQELGLDK
			VIGQGQQPSTAAR		
MGST 3	IASGLGLAWIVGR	**CYP3A4**	EVTNFLR		SSLLDVLAAR
	VLYAYGYYTGEPSK		LSLGGLLQPEK		ENLQFSAALR
UGT2B17	WTYSISK	**CYP3A/43**	ETQIPLK	**ATP1A1**	IVEIPFNSTNK
		CYP3A	SLLSPTFTSGK		

	GHEVIVLTSSASILVNASK	**CYP3A43**	YIPFGAGPR		SPDFTNENPLETR
UGT2B15/17	SVINDPIYK		DVTHFLK	**Cadherin-17**	AENPEPLVFGVK
					QNSRPGK
ADH1A	GAILGGFK	**CYP3A5**	DTINFLSK	**Cadherin-23**	ATDADEGEFGR
	NDVSNPQGTLQDGTSR		YWTEPEEFRPER		DAYVGALR
	KPIHHFLGISTFSQYTVVDENAVAK			**OST-α (SLC51A)**	YTADLLEVLK
ADH1B	AAVLWEVK	**CYP3A7**	FGGLLLTEK		VGYETFSSPDLDLNLK
	GAVYGGFK		FGGLLLTEKPIVLK	**OST-β (SLC51B)**	DHNSLNNLR
ADH1C	FSLDALITNILPFEK		FNPLDPFVLSIK		ETPEVLHLDEAK
ALDH1A1	IFVEESIYDEFVR	**CYP4F2**	HVTQDIVLPDGR	**OCT1 (SLC22A1)**	MLSLEEDVTEK
	IFINNEWHDSVSGK				GVALPETMK
	TIPIDGNFFTYTR	**UGT1A**	IPQTVLWR		ENTIYLK
		UGT1A1	DGAFYTLK		
AOX	LILNEVSLLGSAPGGK		TYPVPFQR	**OCT3 (SLC22A3)**	GIALPETVDDVEK
	GLHGPLTLNSPLTPEK	**UGT1A3**	HVLGHTQLYFETEHFLK		FLQGVFGK
NAT1	DNTDLIEFK		YLSIPTVFFLR	**OCTN2 (SLC22A5)**	TWNIR
	NYIVDAGFGR	**UGT1A4**	GTQCPNPSSYIPK		DYDEVTAFLGEWGPFQR
NAT2	TLTEEEVEEVLK		YIPCDLDFK	**OAT2 (SLC22A7)**	WLLTQGHVK
					NVALLALPR
	DNTDLVEFK	**UGT1A6**	SFLTAPQTEYR		
SULT1E1	KPSEELVDR		VSVWLLR	**OAT4 (SLC22A9)**	DTLTLEILK
	NHFTVALNEK	**UGT1A9**	AFAHAQWK		ISLLSFTR
SULT1A1	VHPEPGTWDSFLEK		ESSFDAVFLDPFDNCGLIVAK	**MATE1 (SLC47A1)**	GGPEATLEVR
SULT1A2	VYPHPGTWESFLEK	**UGT2B4**	FSPGYAIEK		DHVGYIFTTDR
SULT2A1	DEDVIILTYPK	**UGT2B7**	ADVWLIR	**OATP1A2 (SLCO1A2)**	EGLETNADIIK
	TLEPEELNLILK	**UGT2B4/7**	TILDELIQR		IYDSTTFR

TPMT	NQVLTLEEWQDK	**UGT2B10**	GHEVTVLASSASILFDPNDSSTLK	**OATP1B1 (SLCO1B1)**	YVEQQYGQPSSK
	TSLDIEEYSDTEVQK	**UGT2B11**	GHEVTVLASSASILFDPNDASTLK		MFLAALSLSFIAK
POR	QYELVVHTDIDAAK	**UGT2B15**	ASGNLIPQEK		LNTVGIAK
	YYSIASSSK			**OATP1B3 (SLCO1B3)**	NVTGFFQSLK
	IQTLTSSVR				IYNSVFFGR
NNOPs	AEGVNDNEEGFFSAR		WIYGVSK	**OATP2B1 (SLCO2B1)**	VLLQTLR
	TEGVNDNEEGFFSAR	**NNOPs**	GVNDNEEGFFSAR		SSPAVEQQLLVSGPGK
	SLLAVGITEVIGDFR		VGFAFDLPWGSIK		AHLWKPK
				OATP4C1 (SLCO4C1)	SPEPSLPSAPPNVSEEK
					DFPAALK
				NTCP (SLC10A1)	GIYDGDLK
					GIVISLVLVLIPCTIGIVLK
					HLPGTAEIQAGK
				PEPT1 (SLC15A1)	GNEVQIK
					TLPVFPK
					HTLLVWAPNHYQVVK
				ASBT (SLC10A2)	IAGLPWYR
					LWIIGTIFPVAGYSLGFLLAR
				MCT1 (SLC16A1)	SITVFFK
					DLHDANTDLIGR
				OATP4A1 (SLCO4A1)	YEVELDAGVR
					ILGGIPGPIAFGWVIDK
				NNOPs	EGVNDNEEGFFSAR
					VGFLPDGVIK

Table S5.4. Processing parameters applied with MaxQuant and Progenesis (Mascot).

Parameter description	**Parameter setting**
Labelling	label 13C (6) (K) & label 13C (6) (R)
Max. missed cleavage	1
Multiplicity	1
Digestion Enzyme	Trypsin/P
Variable Modifications	Oxidation (M) & Deamidation (NQ)
Fixed modifications	Carbamidomethyl (C)
Max number of modifications per peptide	11
Max charge	(up to 7 with MaxQuant) , (+ 2, + 3 & + 4 with Progenesis)
Main search peptide tolerance	5 ppm
Max peptide length	25
Min peptide length	7
Min peptide length for unspecific	70
Max peptide mass [Da]	6000 Da
Peptides for quantification	Unique + razor
MS/MS match tolerance	0.5 Da
False discovery rate (FDR)	1%

5.8.Supplementary material – Results

Table S5.5. Comparison of the total number of samples and surrogate peptides of the targeted proteins identified by MaxQuant and Progenesis.

MaxQuant			Progenesis		
Targets	**Surrogate peptides**	**Number of samples**	**Targets**	**Surrogate peptides**	**Number of samples**
CYP3A4	1	7 ileum & 1 colon	CYP3A4	1	3 ileum
CYP3A43	1	4 ileum & 2 colon	---	---	---
CYP3A	1	9 ileum & 1 colon	CYP3A	1	2 ileum
CYP3A/43	1	5 ileum & 1 colon	CYP3A/43	1	2 ileum
CYP2C9/19	1	2 ileum & 1 colon	CYP2C9/19	1	3 ileum & 3 colon
CYP2D6	2	2 ileum	---	---	---
UGT1A	1	12 ileum & 13 colon	UGT1A	1	11 ileum & 12 colon
UGT1A1	1	1 ileum & 1 colon	---	---	---
UGT2B7	1	4 ileum & 1 colon	UGT2B7	1	4 ileum & 2 colon
UGT2B15/17	2	11 ileum & 14 colon	UGT2B15/17	1	12 ileum & 14 colon
UGT2B17	1	1 ileum & 2 colon	---	---	---
CES2	3	4 ileum & 2 colon	CES2	3	5 ileum & 7 colon
MGST 1	1	2 ileum & 8 colon	---	---	---
---	---	---	MGST 2	1	1 ileum & 1 colon
MGST 3	2	5 ileum & 2 colon	MGST 3	2	1 ileum & 3 colon
ALDH1A1	1	2 colon	ALDH1A1	2	1 ileum & 2 colon
POR	1	1 ileum & 1 colon	POR	1	4 ileum & 4 colon
---	---	---	P-gp	1	4 ileum & 2 colon
BCRP	1	2 ileum & 1 colon	---	---	---
ATP1A1	2	13 ileum & 17 colon	ATP1A1	1	12 ileum & 17 colon
MCT1	1	6 colon	MCT1	1	2 ileum & 3 colon

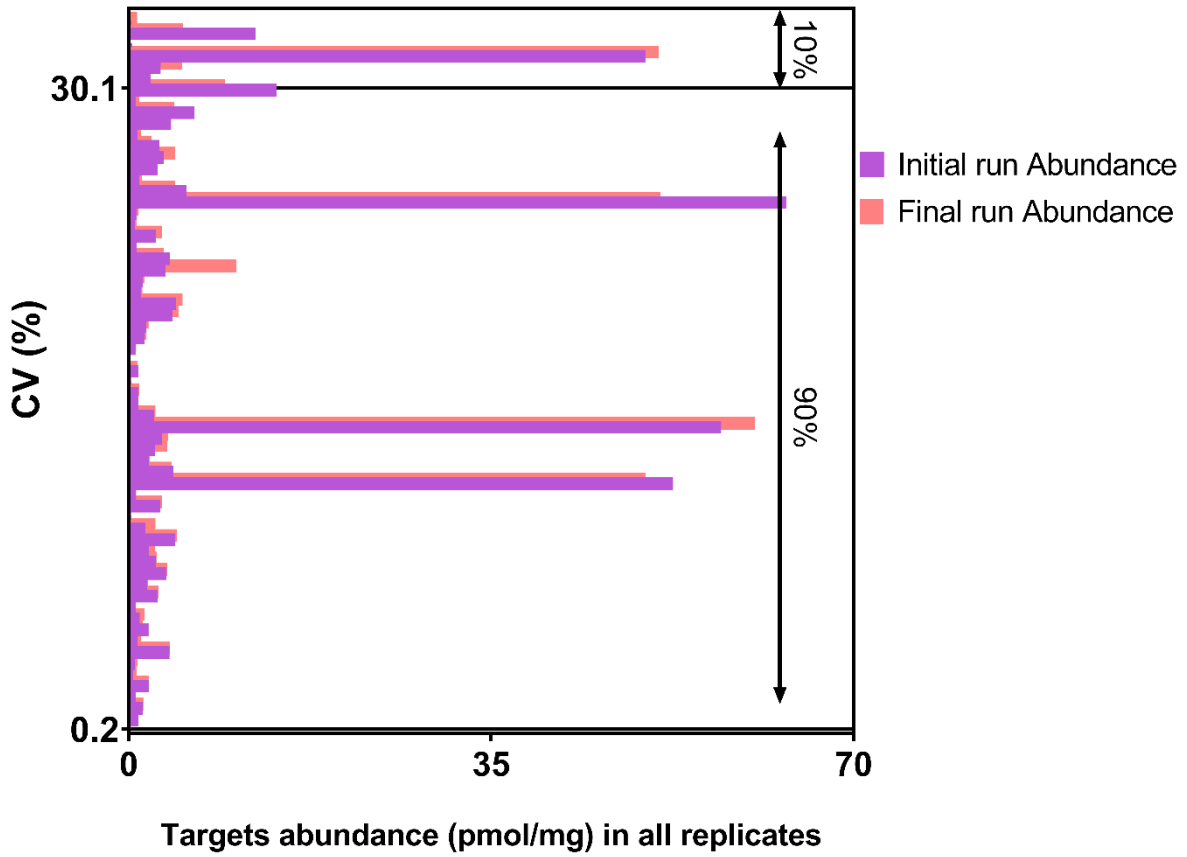

Figure S5.1. *Batch to-batch (analytical) variability represented by percent coefficient of variations (%CV) for different targets in a set of QC samples (8 runs of same sample; at the start and end of each batch run).*

Chapter Six: Quantitative Proteomics of Drug Metabolising Enzymes and Drug Transporters Using Label Free Method in Adult Human Intestine of Crohn's Disease and PBPK Modelling Application for Prediction of Oral Drugs Behaviour in Crohn's Population

Declaration

Sarah Alrubia, Zubida M. Al-Majdoub, Brahim Achour, Amin Rostami-Hodjegan, Jill Barber

I carried out the literature search, generation and analysis of data, contributed to the study design and wrote the manuscript. Dr Jill Barber reviewed and edited the manuscript. Dr Brahim Achour and Dr Zubida M. Al-Majdoub were consulted on experimental methodology and statistical analysis. Dr Jill Barber and Prof. Amin Rostami- Hodjegan contributed to the study design, provided guidance and suggested edits to the manuscript. Prof. Amin Rostami-Hodjegan was consulted on PBPK modelling I retained editorial control.

6.1.Abstract

Background and Aims: Crohn's disease is a chronic inflammatory disease that affects the intestine mucosal layer. Inflammation causes changes in the structure of the epithelial layer cells, in the permeability of the epithelium and in the expression of drug metabolising enzymes and transporters. These changes are more severe in active disease than in the remission state. Reliable prediction of the bioavailability of oral drugs in Crohn's disease using physiologically-based pharmacokinetic models is dependent on knowing the expression levels of enzymes and transporters in diseased as well as healthy tissue, yet this information is surprisingly lacking. This study aimed to determine for the first time the absolute abundances of ileum and colon enzymes and transporters in active Crohn's disease inflamed and non-inflamed tissues and their applicability in physiologically-based pharmacokinetic models.

Methods: Fresh-frozen inflamed (n=13; 6 ileum and 7 colon) and non-inflamed (n=7; 2 ileum and 5 colon) adult human tissues from Crohn's disease patients and healthy (n=10; 5 ileum and 5 colon) deceased subjects were processed by calcium chelation elution to isolate the enterocytes. The isolated homogenates from individual samples was prepared for liquid chromatography – mass spectrometry proteomics. The abundance values were scaled up to the tissue volume to compare their levels in the diseased and normal tissues with healthy levels using label free based proteomics.

Results: All enzymes and transporters showed reduction of expression in the inflamed and non-inflamed Crohn's tissues, relative to healthy tissue. Significant downregulation (p<0.05) was observed with clinically relevant enzymes and transporters (CYP3A4, AOX1, NAT1, SULT1A1, SULT1A2, SULT1B1, SULT1E1 and SULT2A1 in inflamed ileum compared to healthy samples. In inflamed and non-inflamed colon significant downregulation was observed with UGT1A10, SULT1A1, SULT1A2, SULT1B1, NAT1 and BCRP (ABCG2) compared to healthy samples. Inter-individual variability of ileal samples was high in all studied tissues for the majority of the proteins targets (up to 146 % CV with SULT1A1 in inflamed tissues) and the inter-individual variability of colon samples was higher among the Crohn's samples compared to healthy (up to 169 % CV with ABCB3 in histologically normal tissues). Enzymes strong inter-correlations (Rs > 0.60, p-value <0.05) were found between MAOA-TXN, MAOA-AOX1, AOX1-TXN and within SULT (1A1-1A2) in ileum and between MAOA-CES2 in colon. Strong inter-correlations were found between ABC transporters (B1-D3), (B3-B11), (B3-C4) and (B11-C4) in colon only. None of the assessed demographics showed strong

correlation with proteins abundance, except that age (19-62 years, n=5) correlated with UGT2B7 and ALPI ileum expression.

Integration of the abundance alteration data into Crohn's disease physiologically-based pharmacokinetic models to measure the disease effect on 12 oral drugs showed a considerable change of the oral drugs systemic exposure (≥2 fold) with some of the drugs.

Conclusion: Crohn's disease inflammation induces significant reduction in expression of intestinal drug metabolising enzymes and transporters. Alteration in these enzymes and transporters abundance profile causes alteration in oral drug pharmacokinetics. Abundance data generated in this study was used to simulate the impact of these changes in Crohn's patients along with other system parameters on oral drug exposure. Integration of expression data in physiologically-based pharmacokinetic models will facilitate prediction of the fate of oral drugs and enhance dosing accuracy in Crohn's population.

6.2.Introduction

Crohn's disease (CD) is an inflammatory disease localized in the intestine affecting any of its upper or lower segments, with ileum and colon be the predominantly affected segments.[1] CD goes between active phase where patients suffer from sever symptomatic episodes or relapses and inactive phase where patients are in remission state with little or no symptoms.[2] Certain demographics have a higher rate of CD over others; this can be linked to either genetic or environmental factors or a combination of both as its aetiology not fully understood. Epidemiological studies show that CD is more common in the western younger population (15-35 years), females, smokers and urban dwellers.[1]

CD patients usually receive prolonged therapy where orally administered small molecules are important. Treatment is rarely curative and patients suffer from relapses. Measurement of prolonged response in corticosteroid treated CD patients showed that 32% of the patients have a complete remission while 38% eventually require surgery.[3] Orally administered glucorticoids, budesonide and prednisone, fail in 47% and 34% of active CD patients, respectively.[4] Moreover, due to the young onset of the disease CD patients are more susceptible to receive non-CD drugs to control conditions other than CD.

Clinical studies on oral drugs given to CD patients showed alteration in their pharmacokinetics (PK) profile due to the disease effect on a combination of system variables (intestine and liver DMETs, albumin, blood flow, etc.). S and R verapamil tablets (CYP3A4 and P-gp substrate)[5], midazolam oral solution (CYP3A4 substrate)[6], propranolol tablets (CYP1A2, 2C19, 2D6 and P-gp substrate)[7] and mesalamine controlled release formulation (NAT1 and NAT2 substrate)[8] showed >2 fold increase in their bioavailability in CD patients compared to control group.

Loss of response and altered PK profile of oral drugs in CD patients compel the use of the model-informed precision dosing (MIPD) approach in order to improve the clinical outcomes in regards to drug efficacy and safety in this population. This can be facilitated by physiologically based pharmacokinetic (PBPK) models where prediction of drug disposition based on changes in different body compartments in the disease state can be carried out to guide a better dosing approach in the CD population. Inflammation of the intestine mucosa can extend to any of the epithelial layer cells causing morphological and/or structural changes to their inner composition, which include but are not limited to changes in drug metabolising enzymes and transporter protein (DMETs) abundances. Mucosal layer damage caused by CD

leads to activation of T cells and macrophages releasing inflammatory cytokines (TNFα, INF-γ, IL-6, IL-12 and others) that are connected to destruction to the epithelial barrier and cellular tight junctions which increases the intestine permeability.[9–11] This might also be linked to loss of the activity/abundance of the membrane transporters that function as gate keepers, leading to higher absorption of orally administered drugs in CD patients.[12]

Data on DMETs in acute inflammation and inflammatory conditions other than CD have been reported.[13,14] However, in adult CD patients, few studies have been conducted to investigate the abundance of the intestine DMETs. All of the available abundance information is based on mRNA and immunohistochemistry techniques. Most previous studies are concerned only with the colon, which contributes less than the ileum to drug metabolism, while fewer studies assessed the ileum tissue.[15–19] Tandem liquid chromatography - mass spectrometry (LC-MS) delivers good proteome coverage and more accurate quantification[20] yet it has not been used to measure DMETs absolute abundance in CD population.

In inflamed tissue samples CYP3A4 showed reduction of its abundance in rectum of CD patients.[21] One study on CD colon reported its upregulation[22] but the inflammation severity, activity state of enrolled patients and the methodology used to measure the abundance is not unified with the other studies, which might be the cause of such data conflict. Other CYPs[22] and SULT2A1[15] expression are reported to change significantly in CD patients' intestine relative to control. The studied ABC transporters and SLCs showed both upregulation (MRP1, ENT1, ENT2, CNT2, PEPT1, OATP4A1 and OATP2B1) and downregulation (MRP3 ASBT, MCT1 and OCTN2) compared to the control group with varying ratios between the different studies for the same target.[15,17,23,24] There is some conflict of data observed with P-gp (ABCB1) expression. [18,21,22]

In histologically normal ileum and colon tissue, expression of CYP (3A4, 3A7, and 2C9), CES2, UGT1A3 and SULT (1A1, 1A2, 1A3, 2A1 and 2B1) showed mix of up and downregulation relative to control. The same was observed with the studied ABC transporters (P-gp, MRP1, MRP2 and MRP3).[16,25]

CD inflammation can cause extra-intestinal effects which influence other system parameters that are involved in oral drug bioavailability. Up to 30% of the CD population exhibit abnormal liver function, where liver function enzymes (ALT, AST and bilirubin) increases.[26,63] A 5 fold reduction in hepatic CYP3A4 activity in active CD patients using IV and oral midazolam was

reported.[6] A mouse induced colitis model showed reduction in hepatic CYP1A2, 2E1, 2C11 and 3A2.[27,28] Albumin and α1-AGP showed change in their systemic level during the course of CD.[29–32]

Demographics can contribute to inter-individual variability. Age and gender influence the expression of several DMEs in the liver,[33–38] while their association with transporter expression was not significant.[39,40] In the intestine, however, no correlation is reported for the expression of most of the studied CYPs, UGTs and transporters in jejunum and ileum tissue with age, sex, smoking and weight of the assessed subjects.[41,42]

Further determination of DMET abundance in CD patients is warranted. Control groups used in the previously mentioned studies were not always healthy subjects, majority of the abundance data are based on relative methods and many of the DMETs are not studied before. These gaps in the literature hamper the prediction of CD impact on oral drug bioavailability. So far only one study applied PBPK modelling to predict budesonide response in CD.[43] This application cannot be generalised at the moment because of lack of system-specific fundamental information in CD patients that are required for accurate PK prediction. Identifying CD impact on the intestine DMETs abundance can allow better predictability of oral drugs' fate and improves MIPD outcomes.

Therefore, the primary aim of this study was to identify expression changes in ileum and colon proteins associated with oral drug disposition from individual inflamed (I-CD) and histologically normal (HN-CD) tissues relative to healthy. To our knowledge, this is the first comprehensive study of DMETs levels in CD. This is to incorporate the generated abundance data into a PBPK CD model and investigate the difference in oral drug exposure between CD and healthy population. A secondary aim was to assess DMET inter-individual variability in diseased tissue samples and association with patients' characteristics that are linked to the disease susceptibility (sex, age and smoking) as well as BMI. Among the sources of variability between the expression results for the same protein between different studies is the nature of the control group recruited. Few of the studies that measured inflammatory bowel diseases (IBD) proteins expression used non-IBD diseased group as a control group from which normal tissue from cancerous patients where used.[44,45] Here we investigated the abundance difference in ileal tissue from this group compared to healthy and normal CD to identify its relevance to be utilized as a control group in CD studies.

6.3.Materials and methods

6.3.1. Materials

Unless otherwise indicated, all chemicals were supplied by Sigma-Aldrich (Poole, UK). All solvents were high performance liquid chromatography (HPLC) grade and supplied by Thermo Fisher Scientific (Paisley, UK). Lysyl endopeptidase (Lys-C) was purchased from Wako (Osaka, Japan). Sequencing-grade modified trypsin was supplied by Promega (Southampton, UK). Complete Mini, EDTA-free protease inhibitor cocktail tablets were supplied by Roche (Mannheim, Germany). BCA protein concentration measuring kit was obtained from ThermoFisher Scientific (Hemel Hempstead, UK).

6.3.2. Intestine samples and donor demographics

Sourced fresh-frozen human intestine mucosal samples representing inflamed (I-CD) and histologically normal (HN-CD) areas from ileum (n = 6 and 2, respectively), and from colon (n = 7 and 5, respectively). Samples were taken from active CD patients undergoing ileocolonic resection where the histologically normal tissues were taken from macroscopically normal regions away from the inflamed bowel regions. From theses sample 3 of the I-CD colon were matched while 2 of the I-CD ileum were matched with their HN-CD. Tissues were obtained with informed consent and supplied by Manchester Biomedical Research Centre (BRC) Biobank, Manchester University NHS Foundation Trust, Manchester, UK. Prior ethics approval was granted by NRES Committee North West - Haydock (19/NW/0644). The average age of Crohn's patients at surgery was 40 years (range 18-68 years). Percentage of female subjects was ~54% and the body mass index (BMI) ranged from 17 to 34.3 kg/m^2. Further detailed demographic and clinical data are summarised in Supplementary Table S6.1. A set of 4 histologically normal ileum from adenocarcinoma patients (HN-cancer) (Table S6.2) were sourced just as Crohn's samples to allow a comparison of its DMETs abundance to healthy subjects' and HN-CD.

The control group was represented by healthy mucosal samples (ileum n=5, colon =5) obtained from healthy deceased subjects and were supplied by Caltag Medsystems Limited (Buckingham, UK). Prior ethics approval was granted by University research ethics committee (UREC), UK (2019-8120-12392). The average age of healthy subjects was 48.5 years (range 30-70 years). The percentage of female subjects was 40%. The average post mortem interval

(PMI) was 4.4 hrs (range 1-9 hrs), available demographic information are summarised in Table S6.3.

6.3.3. Enterocyte isolation and subcellular fractionation

Enterocytes were isolated from mucosal tissues by calcium chelation elution. The enterocyte isolation and homogenate fraction processing was adapted from *Harwood et al* (2015)[46] with minor modifications. Briefly, the process was done on ice and solutions were equilibrated at pH 7.4. The base buffer for all solutions used for chelation was 112 mM NaCl, 5 mM KCl, 20 mM HEPES. The mucosa was washed twice in the base buffer and immersed in 27 mM sodium citrate solution with a protease inhibitor cocktail (PI) for 30 min, followed by incubation in EDTA buffer (30 mM EDTA, 10 U/mL heparin, 1 mM dithiothreitol (DTT) and PI) with stirring at 250 rpm for 40 min to initiate chelation. The chelated enterocytes were collected from the mucosa by repeated flushing with EDTA buffer. The chelated material was washed by centrifugation twice at 2000 x g for 10 min. The resulting enterocyte pellet was re-suspended in homogenisation buffer (10 mM Tris–HCl, 250 mM sucrose, 0.1 mM EGTA, 0.5 mM $MgCl_2$, 5 mM histidine, 0.2% SDS and PI) at 3 ml per g of cells. Homogenisation was carried out with a Dounce hand-held homogeniser for a minimum of 75 strokes, followed by treatment with an ultrasonication probe (30 W) for two 10 s bursts to disrupt cell membranes. The formed homogenate fraction was stored in aliquots at -80°C until further processing.

6.3.4. Sample preparation and proteolytic digestion

The protein content of ileum and colon homogenates (n = 17 for each segment) was determined using BCA assay in triplicate using bovine serum albumin (BSA) as a standard. 70 µg homogenate protein in each sample was spiked with 0.126 µg BSA as internal standard. The 34 samples were prepared for proteomics based on filter-aided sample preparation (FASP), as previously described,[41] using Amicon Ultra 0.5 mL centrifugal filters at 10-kDa molecular weight cut-off (Merck Millipore, Nottingham, UK).

6.3.5. Liquid Chromatography and Tandem Mass Spectrometry (LC-MS/MS)

Digested samples were diluted to a final concentration of 0.5 µg/µl with water containing 0.1% (v/v) formic acid and 3% (v/v) acetonitrile. 10 µl of each sample was injected into an UltiMate® 3000 rapid separation liquid chromatography (RSLC, Dionex Corporation, Sunnyvale, CA) coupled online to a Q-Exactive HF Hybrid Quadrupole Orbitrap mass spectrometer (ThermoFisher Scientific, Waltham, MA). Peptides were eluted over 90 min gradient following

the LC/MS methodology as previously described.[47] Details of the methods are found in Chapter Five.

6.3.6. Data analysis and protein quantification

To identify the targeted proteins data analysis was carried out using MaxQuant version 1.6.1.0. (Max Planck Institute for Biochemistry, Munich, Germany). The peptide MS/MS database search was applied against a UniProtKB human proteome fasta file of 74788 protein entries (UniProt, May 2017 (http://www.uniprot.org/)) in addition to BSA. Label free absolute protein quantification was executed using Hi-N method using BSA as an internal standard to measure the abundance of identified CYPs, UGTs, non-CYP/non-UGT drug-metabolising enzymes, ABC transporters and SLCs. The average intensity of the three most abundant non-conflicting unique peptides were used to quantify the identified targeted proteins in relation to BSA at known abundance in each sample. Where three unique peptides were not available in a sample, the average intensity of two unique peptides were used for quantification. A protein was considered quantifiable in intestine homogenate samples if it was identified by at least two unique peptides and it was detected in a sufficient number of samples (at least 2 samples/group/segment (except for HN-CD ileum as there are only 2 samples in this group; even if the protein was not detected in this group but detected in an adequate number of samples in the other groups from the same segment then it is included)). List of the detected DMETs and the peptides sequences used for their quantification are provided in Table S6.4.

The abundance of each target protein was calculated using Equation 1.[47]

$$[prtein] = [BSA] \times {\left(\sum_{i=1}^{n} I_{rank(i)} /n\right)} \Big/ {\left(\sum_{j=1}^{n} I_{rank(j)} /m\right)} \qquad \textbf{(1)}$$

Where [Protein] is the targeted protein abundance and [BSA] is the abundance of the BSA internal standard added, both measured in pmol/mg homogenate protein. The fractions reflects the ratio of the average intensity of the n; highest expressed unique peptides for each protein relative to the reference BSA. Known concentration of BSA is used in all samples (26 pmol/mg of homogenate protein). The calculated ileum and colon mucosal abundances were then expressed in units of pmol/g of mucosal tissue. This was done by scaling up protein concentrations in homogenates (pmol/mg homogenate) using the amount of tissue prepared for homogenisation (mucosal weight in grams) for each sample.

6.3.7. DMETs absolute abundance comparison among sample groups and covariates correlation

Ileum and colon DMET absolute abundance values of I-CD, HN-CD and HN-cancer samples were compared to healthy samples. Additionally, ileum HN-CD samples were compared to HN-cancer samples. Only fold change differences ≥2 between the groups are reported and considered to be due to the disease effect as lower values can result from variability caused by operator or/and the machine. Inter-correlation between protein expression levels was evaluated in each ileum and colon sample group. The impact of Inter-individual variations (age, sex, BMI and smoking) on DMETs expression in CD was examined by measuring the effect of presence and absence of inflammation against each covariate.

6.3.8. Assessment of technical and analytical variability

To assess the quantitative technical variability eight samples, representing all groups (1 healthy ileum, 1 HN-CD ileum, 2 I-CD ileum, 1 HN-cancer ileum, 1 healthy colon, 1 HN-CD colon and 1 I-CD colon samples), were prepared in triplicate and analysed under the same LC-MS/MS conditions. For the assessment of between and within batches variability a pool of healthy colon samples (n = 5) was prepared once and analysed at the start and end of each batch run (8 runs). The % CV was used to assess the technical and analytical variability between the replicates. Lower limit of quantification (LLOQ) was estimated based on the resulted %CV for ileum and colon targets.

6.3.9. Statistical data analysis

Statistical data analyses were carried out by GraphPad Prism version 8 (La Jola, CA, USA) and R v3.6.1. Data normality of distribution was tested by Shapiro-Wilk normality test. The data found to follow non-normal distribution hence non-parametric statistics were used. Expression data were presented as means ± standard deviation and coefficient of variation (%CV). Targeted DMETs abundance statistical difference between the healthy and Crohn's disease groups (I-CD and HN-CD) was assessed by Kruskal-Wallis ANOVA test with *p*-value 0.05 been the statistical significance cut off value. If a statistical significance was detected then a post-hoc Mann-Whitney test was used to assess the statistical difference between two groups based on the segment (ileum and colon). In addition, a post-hoc Mann-Whitney test was used to test the DMETs expression difference between the healthy and HN-cancer group and the later with HN-CD group. The cut off statistical significance was 0.05 *p*-value. The %CV was

used to calculate the inter-individual variability in DMETs abundance levels in ileum and colon healthy, I-CD and HN-CD tissue samples.

Correlations within targeted CYPs, UGTs, non-CYP-UGT enzymes, ABCs and SLCs expression among each group in ileum and colon was assessed using Spearman correlation (Rs) test with t-distribution of the p-value. A significant correlation is determined when the Rs values > 0.60 and *p*-value ≤0.05. Due to the small number of the samples in each group protein expression correlations were only considered if it was found in at least two groups per intestinal segment. Rs correlation was used with age and BMI-disease related changes (with I-CD and HN-CD tissues). Linear regression analysis was utilised to assess the linearity and scatter of the relationship (R^2). Correlations were considered significant if Rs followed the same significance criteria above with addition of data scatter (R^2) > 0.30. Analysis of sex and smoking habits changes related to disease was performed using a Mann-Whitney test where *p*-value ≤0.05 is considered significant.

Principal components analysis (PCA) was used to anticipate the biological and technical variations and similarities within the sample groups (healthy, I-CD, HN-CD and HN-cancer) for ileum and colon. This analysis was done utilising percentage identical peptide (PIP) and percentage identical protein (PIPr) which were calculated as previously described.[48,49]

6.3.10. Physiologically Based Pharmacokinetic (PBPK) simulations

The utility of the generated DMETs abundance data in predicting the disposition of oral drugs in CD population was assessed using PBPK modelling on Simcyp® Simulator V19 (Certara, Sheffield, UK). Abundance values from I-CD and HN-CD group were applied on Simcyp created active CD populations by changing the default healthy population based on the relative changes in CD patients from the generated literature data analysis in Chapter One. Details of changed system parameters in Simcyp to create the active CD population are in Table S6.5. A Total of 12 oral drugs was chosen primarily based on the availability of dissolution, absorption, and metabolism (ADAM) or Multilayer-ADAM (M-ADAM) as the absorption model of the substrate. The reason to limit the selection of the drugs to the drugs with ADAM or M-ADAM absorption models is that these models allow investigating the impact of the change in the intestine physiology and DMTs proteomic profile in the different intestine segments of CD population. 10 drugs were from Simcyp substrates and inhibitors library built using ADAM absorption model and 2 created substrates, as in Chapter One, built in Simcyp using M-ADAM

absorption model with available clinical systemic exposure data in CD. Details of the drugs, their protein binding, their corresponding enzymes and/or transporters and formulation are in Table 6.1.

PBPK simulations were performed using Sim-Healthy volunteers virtual populations and the created active CD population with incorporating the intestine DMETs abundance using the ileum and colon data generated in this study (whenever applicable). These changes were based on the relative changes of DMETs between healthy and I-CD or HN-CD samples proteomic profile and the relative changes of their CV percentages. Whenever a protein was not detected in colon tissues but detected in ileum and its abundance level was available in Simcyp then assumption of its reduction is made based on the reduction detected in ileum tissues from the same tissue nature (I-CD and HN-CD). Also, if a protein was not detected or its expression change was not ≥2 fold from healthy in either ileum or colon tissue then the original abundance, data in Simcyp was used without change. Details of the incorporated abundance values and their %CV from I-CD and HN-CD tissues for the relevant enzymes/transporters to the oral drugs simulated in this study are in Table S6.6. This simulation was carried out according to 4 scenarios creating 4 models as follows:

Model 1 (M-1): CD population with intestine DMETs abundance data from I-CD tissues and normal albumin level

Model 2 (M-2): CD population with intestine DMETs abundance data from I-CD tissues and reduced albumin level

Model 3 (M-3): CD population with intestine DMETs abundance data from HN-CD tissues and normal albumin level

Model 4 (M-4): CD population with intestine DMETs abundance data from HN-CD tissues and reduced albumin level

For each model and drug, the trial design had the following parameters: 10 trials with 10 virtual individuals (100 virtual subjects), female to male ratio (0.5), age range (18-65 years), duration of study: 24 h and done under fasted conditions. Only budesonide and midazolam had a trial design that matches the clinical trial specifications (Table S6.7). The effects of the changes of DMETs abundance and other system parameters in CD on drug exposure following oral administration were assessed by comparing the mean of the systemic exposure parameters; area

under the curve (AUC) from time 0 to 24 hours and maximum drug plasma concentrations (C_{max}) values from the plotted mean systemic concentration (Csys)-time profiles.

Table 6.1. Oral drugs from Simcyp V19 library with ADAM absorption model and created midazolam and budesonide drug profiles with M-ADAM absorption model used for physiologically based pharmacokinetic (PBPK) simulations with active CD population.

Drug	**Oral Formulation**	**Intestine Metabolising Enzyme/ Transporter ***	**Binding to Blood Proteins (Albumin or α1-AGP)****
Budesonide	Controlled Release solid formulation	CYP3A4, CYP2C9 & P-gp	80-90% bound to Albumin[50]
Celecoxib	Solution	CYP2C9 & CYP3A4	~95% bound to Albumin[51]
Crizotinib	Immediate Release solid formulation	CYP3A4 & P-gp	~91% bound to Albumin[52]
Digoxin	Solution	P-gp	~25% bound to Albumin[53]
Dabigatran etexilate	Solution	CES1, CES2 & P-gp	~35% bound to Albumin[54]
Gemfibrozil	Solution	UGT2B7	~98% bound to Albumin[55]
Midazolam	Solution	CYP3A4& CYP3A5	~95% bound to Albumin[56]
Pravastatin	Solution	MRP2	~50% bound to Albumin[57]
Ritonavir	Immediate Release solid formulation	CYP2D6, CYP3A4 & CYP3A5	~99% bound to α1-AGP[58]
Rosuvastatin	Solution	BCRP & OATP2B1	~90% bound to Albumin[59]
Valsartan	Immediate Release solid formulation	CYP2C9 & MRP2	~95% bound to Albumin[60]
Verapamil	Solution	CYP2C8, CYP3A4, CYP3A5, P-gp & MRP2	~90% bound to Albumin[61]

* based on the incorporated enzymes and transporters in Simcyp drug profile; ** the protein mentioned is based on what Simcyp drug profile used as the primary protein bound to the drug

6.4.Results

6.4.1. Assessment of technical and analytical variability

Technical variabilities of ileum and colon were within 35% (CV) for 90% and 81% of the targets, respectively, (Figure S6.7). The targets that reflected the highest variability (>35% CV) in ileum samples are CYP51A1, CYP2S1, CYP4F2, CYP4F11, UGT2B7, SULT1A1, SULT1A2, SULT1B1, SULT2A1, CES1, EPHX2, ABCB7, ABCB8, MRP3 (ABCC3) and BCRP. In colon samples, CYP4F2, CYP51A1, SULT1A1, SULT1B1, CES1, CES2, EPHX1, EPHX2, MAOA, ABCB7, ABCE1, MCT1 and OST-α showed the highest variability (>35% CV). Of these targets CYP51A1, CYP4F11, SULT1A1, CES1, EPHX2, ABCB8, MRP3 and BCRP were not consistently detected in ileum and CYP51A1, SULT1A1, ABCB7, ABCE1, MCT1, and OST-α were not consistently detected in colon.

Ileum consistent targets lower limit of quantification (LLOQ) based on 35% CV was 0.11 pmol/mg protein which is around 1.22 pmol/g of mucosal tissue. Colon consistent targets LLOQ was 0.09 pmol/mg protein which is around 0.85 pmol/g of mucosal tissue based on a cut-off technical variability of 35% in quality control samples.

To determine batch to batch variation analytical variabilities were within 35% for 91% of the targets. The targets that reflected the highest variability (>35%) (CYP4F2, UGT2B7, NAT1, MAOB, MGST2, MGST3, ABCB1, ABCB7, ABCB8).

6.4.2. Ileum DMETs absolute abundance in Crohn's disease sample groups compared to healthy group

Changes in DMETs absolute abundance in the ileum of I-CD and HN-CD from healthy group were assessed. Quantified targets were 13 CYPs, 5 UGTs, 22 non-CYP and non-UGT enzymes, 14 ABC transporters and 7 SLCs in I-CD and healthy samples. For the HN-CD group, the only difference was with CYPs and non-CYP and non-UGT enzymes, as 12 CYPs and 21 non-CYP and non-UGT enzymes were quantified. Figures (6.1-6.5) show the abundance values of CYP, UGT, non-CYP non-UGT, ABC and SLC targets, respectively, presented as individual points, mean and max-min range where statistical significance between the groups are indicated. A summary of the mean value of DMETs quantified in each ileum group expressed in pmol/g of mucosal tissue ±SD and (%CV) is presented in Table 6.2.

Since the data were not normally distributed Kruskal-Wallis ANOVA test was used where a significant difference ($p \leq 0.05$) detected across the three groups for CYP3A4 (p = 0.015), CYP3A5 (p = 0.0357), CYP4F2 (p = 0.0186), UGT2A3 (p = 0.0357), AOX1 (p = 0.0034*), EPHX1 (p = 0.0126), MAOA (p = 0.0027*), MAOB (p = 0.0082*), MGST2 (p = 0.0369), MGST3 (p = 0.0369), NAT1 (p = 0.0032*), SULT1A1 (p = 0.0062*), SULT1A2 (p = 0.0027*), SULT1B1 (p = 0.0103), SULT1E1 (p = 0.0055*), SULT2A1 (p = 0.002*), ABCB7 (p = 0.006**), ABCB8 (p = 0.0028*), ABCD3 (p = 0.0386), ABCE1 (p = 0.0357). The rest of the targets showed no significant difference. For targets that showed a significant difference or was not detected in HN-CD group (doesn't qualify for Kruskal-Wallis ANOVA test) post-hoc Mann-Whitney tests was used to assess the statistical significance between healthy and I-CD, healthy and HN-CD and I-CD and HN-CD samples.

For ileum I-CD group, 2 CYPs; CYP3A4 (p = 0.0159) and CYP4F2 (p = 0.0317), only 1 UGT; UGT2A3 (p = 0.0317) and 12 non-CYP non-UGT; AOX1 (p = 0.0043*), EPHX1 (p = 0.0173), FMO3 (p = 0.0476), MAOA (p = 0.0043*), MAOB (p = 0.0087*), MGST2 (p = 0.0303) and NAT1 (p = 0.0043*), from which 5 are SULTs SULT1A1 (p = 0.0087*), SULT1A2 (p = 0.0043*), SULT1B1 (p = 0.0159), SULT1E1 (p = 0.0079*) and SULT2A1 (p = 0.0043*) showed significant reduction in their expression compared to healthy. For ABC transporters; ABCB7 (p = 0.0159), ABCB8 (p = 0.0179), and ABCD3 (p = 0.0159) showed a significant reduction in their expression compared to healthy. The fold change of Crohn's disease sample groups compared to healthy group and to each other is presented in Figure S (6.1 and 6.2). DMETs fold reduction in I-CD group compared to healthy ranged from 2 (CES1, ABCD3 and BCRP) to 28.5 (SULT2A1) fold. Few of the targets with ≥5 fold reduction (CYP3A5, CYP4F11, ABCD1 and ABCE1) didn't show statistical significant. None of the targets showed higher expression in I-CD compared to healthy. When compared to HN-CD, fold reduction ranged from 2.4 (MAOB) to 5.7 (MRP6) fold, while higher expression ranged from 2 (TPMT) to 28.7 (UGT1A1) fold.

The HN-CD group showed no significant difference in any of the targets when compared to healthy and I-CD group. This might be due to the small number of the samples (n=2) available. Their fold reduction ranges between 2 (CYP20A1, EPHX1, MGST2 and OST-α) and 128.3 (CYP3A5) compared to healthy, while no DMET encountered increase in their expression compared to healthy. CYP3A5 and ABCE1 didn't show statistically significant difference in any of the Crohn's disease groups compared to healthy despite their statistical significance

across groups using the Kruskal-Wallis ANOVA test (p = 0.0159 and 0.0357, respectively). CYP3A5 was detected in only 3 of the I-CD samples (p = 0.0571 compared to healthy) and 1 of the HN-CD while ABCE1 was detected in only 2 samples of the I-CD samples (p = 0.0952 compared to healthy) and 1 of the HN-CD.

Ileum quantified targets in each group inter-individual variability were assessed by means of %CV (Table 6.2). In healthy tissue samples (n=5) the highest inter-individual variation across CYPs, UGTs, non-CYP and non-UGT enzymes, ABC transporters and SLCs abundance levels was: CYP2C19 (CV = 140%, detected in 3 samples), UGT1A10 (CV = 113.7%, detected in all 5 samples), ALPI (CV = 96%, detected in 3 samples), ABCD1 (CV = 106.8%, detected in all 5 samples), and PEPT1 (CV = 80.3%, detected in all 5 samples). The highest inter-individual variation in 6 I-CD samples was: CYP3A5 (CV = 111.6%, detected in 3 samples), UGT2B7 (CV = 96.6%, detected in 5 samples), SULT1A1 (CV = 145.9%, detected in all 6 samples), ABCB10 (CV = 118.5%, detected in 4 samples), and PEPT1 (CV = 102.9%, detected in 4 samples). As for HN-CD samples only 2 samples were available and inter-individual variation was assessed in targets whenever they were detected in both samples. The highest variation was: CYP1A2 (CV = 133.5%), UGT1A1 (CV = 113.5%), MGST1 (CV = 136.2%), MRP3 (CV = 139.6%), and OST-α (CV = 121.3%). In general, higher variation range of non-CYP and non-UGT enzymes, ABC transporters and SLCs abundance levels is observed with CD ileum sample groups compared to healthy. While the variation range of CYPs and UGTs enzymes was higher in healthy samples, but the difference in variability range between CD groups and healthy is not high indicating that disease state is not the major factor of the observed DMETs heterogeneity.

Table 6.2. Abundance (pmol/g of mucosal tissue) of CYP enzymes, UGT enzymes, non-CYP and non-UGT enzymes, ABC transporters and SLCs in inflamed Crohn's disease (I-CD, n=6), histologically normal Crohn's disease (HN-CD, n=2) and healthy ileum (n=5) individual samples. Data represented by the mean, the standard deviation of the mean (SD) and the coefficient of variation (%CV)

Ileum Target (pmol/g of mucosal tissue)	Healthy (n=5)		Inflamed Crohn's disease (I-CD, n=6)		Histologically normal (HN-CD, n=2)	
	Mean±SD	CV (%)	Mean±SD	CV (%)	Mean±SD	CV (%)
CYP1A2	2±1.5	73.7	0.9±0.5	53.3	1.1±1.4	133.5
CYP20A1	4.5±2.1	46.7	2.1±0.7	35.3	2.2±1.6	70
CYP27A1	38±14.8	39	15.5±13.4	86	13.7±13.3	97.5
CYP51A1	6.3±2.7	41.9	2.4±2.3	98.2	1±0.6	64.6
CYP2C18	3.9±3.2	82	0.8±0.7	84.3	2±1.9	95
CYP2C19	2.2±3.1	140	0.7±0.2	32.3	0.8±0.5	57.5
CYP2D6	6.3±5.5	87.2	2.2±1.5	67.5	N/A	
CYP2S1	12.9±6.7	51.7	5.6±2.5	44	5.6±6.9	122.1
CYP3A4	50.8±38.4	75.6	6.7±5	75.3	12.1±9.9	81.4
CYP3A5	18±12.7	70.5	1.9±2.1	111.6	0.1±N/A	N/A
CYP4F2	25.6±26.1	102	3.5±2.9	81.2	1.7±1.5	86.6
CYP4F11	5.5±4	72.8	1.1±0.4	39.1	5.9±N/A	N/A
CYP4F12	9.9±12.4	125.6	2±1.8	89.3	1.6±0.9	57.8
UGT1A1	32.5±34.4	105.7	10.5±5.5	51.9	0.4±0.4	113.5
UGT1A10	9±10.2	113.7	2.3±1.9	82.4	2.7±N/A	N/A
UGT2A3	56.5±25.5	45.1	14.1±13.4	95.2	23.3±23.4	100.6
UGT2B7	13.6±11.4	84.2	3.8±3.7	96.6	4.7±3.1	65.1
UGT2B17	309±239.4	77.5	222.6±160.7	72.2	201.1±220.3	109.6
ALPI	26.8±25.7	96	6.4±4.4	68.7	15.9±9	56.8
AOX1	6.2±2.9	46	1.5±0.8	50.9	1.4±1.7	122.4
CES1	3.1±2.2	71.7	1.6±1.4	90.6	2±2	100.3
CES2	67.4±51.3	76	56.6±65.7	116.1	59.3±72.7	122.6
EPHX1	37.1±17.4	46.8	10.8±7.1	65.5	18.8±4.5	24.1
EPHX2	7.5±3.1	41.4	7±6.8	97.5	3.3±2.5	75
FMO3	1.5±1.2	76.5	0.6±0.6	99.7	0.4±0.4	93.2
FMO5	5.4±2.8	51.4	2.2 ±1.7	76.8	2.6±3.5	135
MAOA	482.9±153.4	31.8	94.5±63.3	67	128.3±100.4	78.3
MAOB	156.1±97.3	62.3	26.4±23.8	90.1	64±10.2	15.9
MGST1	49.4±32.3	65.4	26.4±17.3	65.4	12±16.4	136.2

MGST2	25.9±10.2	39.4	10.5±6.4	61.5	13.1±10.3	79
MGST3	60.1±47.3	78.7	17.4±17.6	101.5	9.6±13	135.8
NAT1	7.1±4.3	60.5	0.9±0.6	63.2	0.8±1	123.5
NAT2	2.1±1.6	79.2	0.6±0.1	23.7	N/A	
SULT1A1	45.5±23.6	51.8	5.9±8.7	145.9	3.1±N/A	N/A
SULT1A2	156±75.5	48.4	10.6±13.8	130.5	9.7±1	10.1
SULT1B1	59.4±45.2	76.1	9.3±10.1	108	5.1±6	118.2
SULT1E1	10.9±7.4	67.6	0.5±0.5	92.8	0.3±0.3	111.5
SULT2A1	17.9±16.4	91.5	0.6±0.4	63	0.9±0.3	32.5
TPMT	2.5±1.5	59.2	1.1±1.1	99.9	0.6±0.6	114
TXN	50.6±21.1	41.7	36.1±28.4	78.6	14.8±12.2	82.2
ABCB1 (P-gp)	20.3±16	78.7	6±5.3	88.2	3.8±2.4	61.7
ABCB3 (TAP2)	13.9±5.5	39.6	9.3±6.1	65.6	1.3±N/A	N/A
ABCB7	5±2.4	49.1	1.4±0.8	55.4	0.7±0.2	25.7
ABCB8	3.6±0.5	14.9	0.9±0.7	73.5	0.3±0.1	16
ABCB10	1.5±1.4	91.3	1±1.2	118.5	1.1±0.4	33.3
ABCB11 (BSEP)	4.3±3.2	75	1.2±0.7	60.6	0.8±0.9	110.2
ABCC2 (MRP2)	1.7±1.8	103.8	0.4±0.2	43.7	0.7±N/A	N/A
ABCC3 (MRP3)	4±2.6	65.6	4.5±1.3	28.4	1.5±2.1	139.6
ABCC4 (MRP4)	0.8±0.7	87.3	0.3±0.2	65.3	0.3±0.3	111
ABCC6 (MRP6)	3±2.2	74.4	1±0.6	61.9	5.5±7.6	137
ABCD1	6.2±6.6	106.8	0.7±0.2	36.7	0.2±N/A	N/A
ABCD3	30.6±17	55.5	15.3±5	32.6	11.7±15.4	131.2
ABCE1	5.7±4.8	85.3	0.9±0.7	74.7	0.2±N/A	N/A
ABCG2 (BCRP)	6.3±4.9	77.9	3.1±1.8	58.2	1.9±0.2	11.3
SLC15A1 (PEPT1)	9.6±7.7	80.3	4.6±4.7	102.9	0.8±0.1	15.1
SLC16A1 (MCT1)	1.4±0.9	61.6	0.8±0.4	54.9	0.6±0.04	5.9
SLC51A (OST-α)	7.8±4.2	53.7	3.8±2.2	59.3	4.1±4.9	121.3
SLC51B (OST-β)	1±0.5	52.7	0.9±0.4	47.4	1.1±N/A	N/A
SLCO1A2 (OATP1A2)	1.1±0.8	74.7	0.4±0.3	72.4	0.7±N/A	N/A
SLCO1B1 (OATP1B1)	0.3±0.1	18.7	0.1±0.03	28.3	0.1±N/A	N/A
SLCO2B1 (OATP2B1)	3±1.7	57.5	1.1±0.9	79.9	1.1±N/A	N/A

N/A, no available data as the value can't be calculated due to insufficient data points (reported in only one sample in the group) or not detected

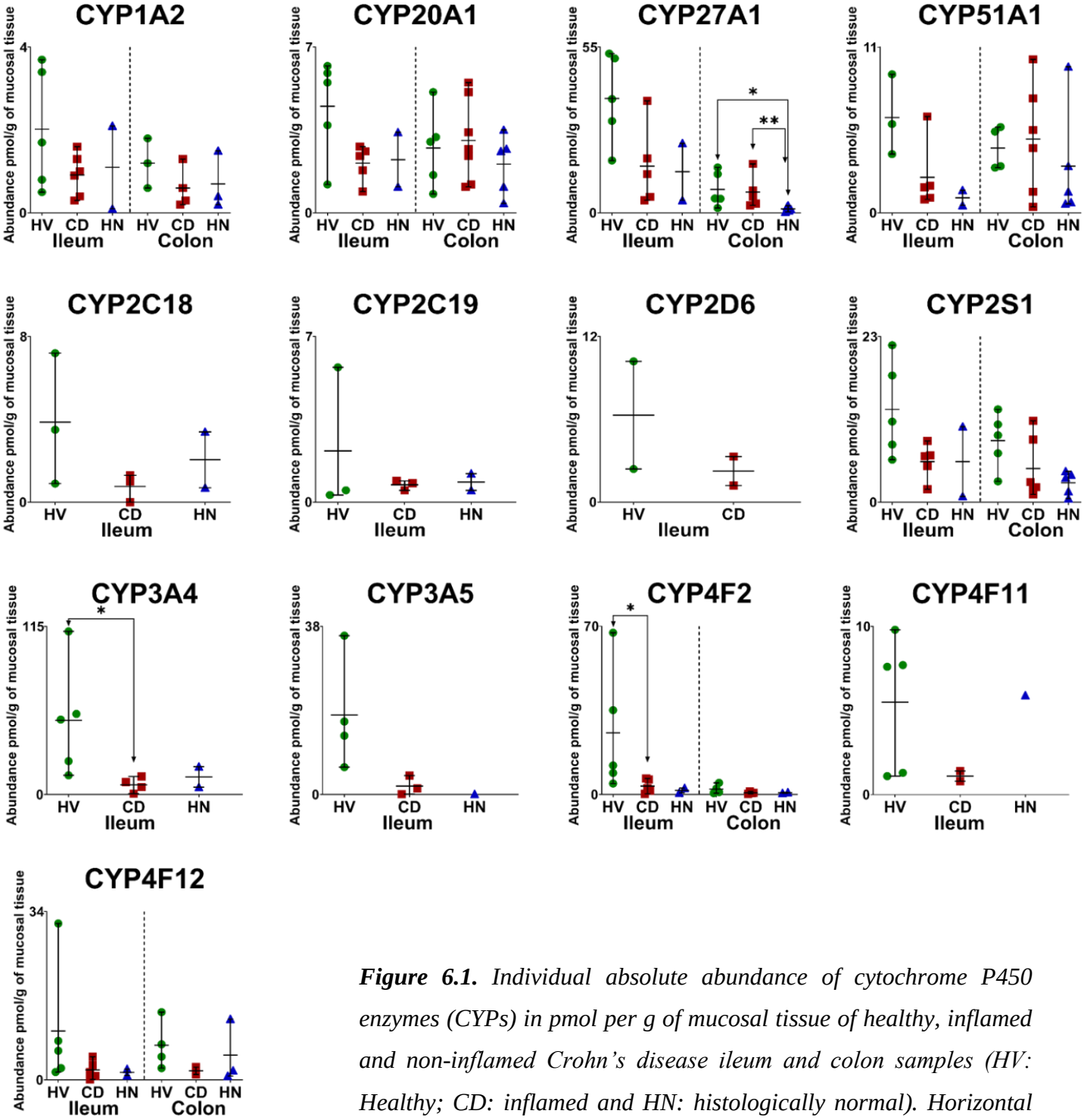

Figure 6.1. *Individual absolute abundance of cytochrome P450 enzymes (CYPs) in pmol per g of mucosal tissue of healthy, inflamed and non-inflamed Crohn's disease ileum and colon samples (HV: Healthy; CD: inflamed and HN: histologically normal). Horizontal lines represent means and bars represent maximum and minimum values. Stars (*) represent statistical significance (*p=<0.05 and **p <0.0087) comparisons between inflamed, non-inflamed and healthy.*

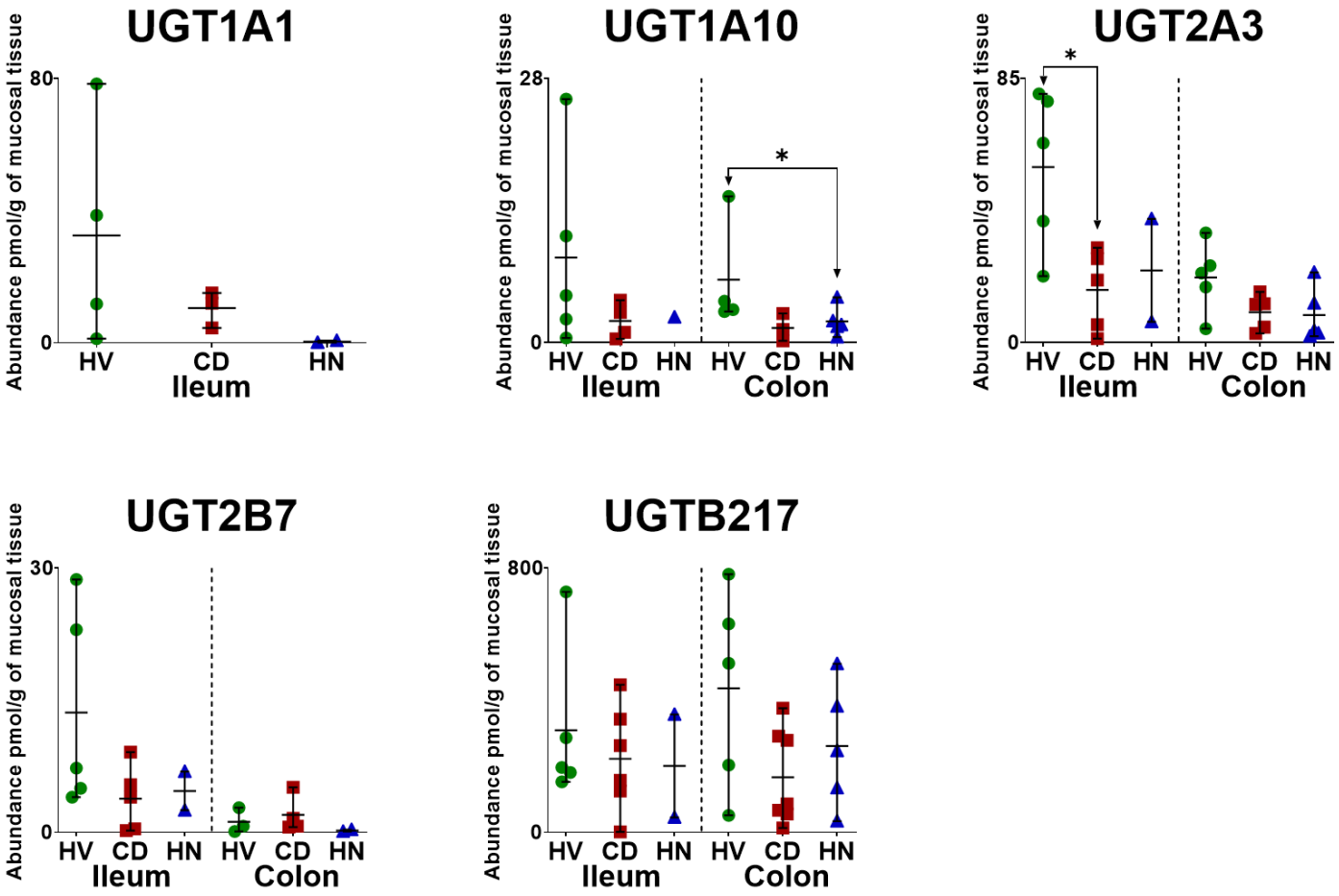

Figure 6.2. *Individual absolute abundance of uridine-5'-diphospho-glucuronosyltransferase enzymes (UGTs) in pmol per g of mucosal tissue of healthy, inflamed and non-inflamed Crohn's disease ileum and colon samples (HV: Healthy; CD: inflamed and HN: histologically normal). Horizontal lines represent means and bars represent maximum and minimum values. Stars (*) represent statistical significance (*p=<0.05) comparisons between inflamed and non-inflamed with healthy.*

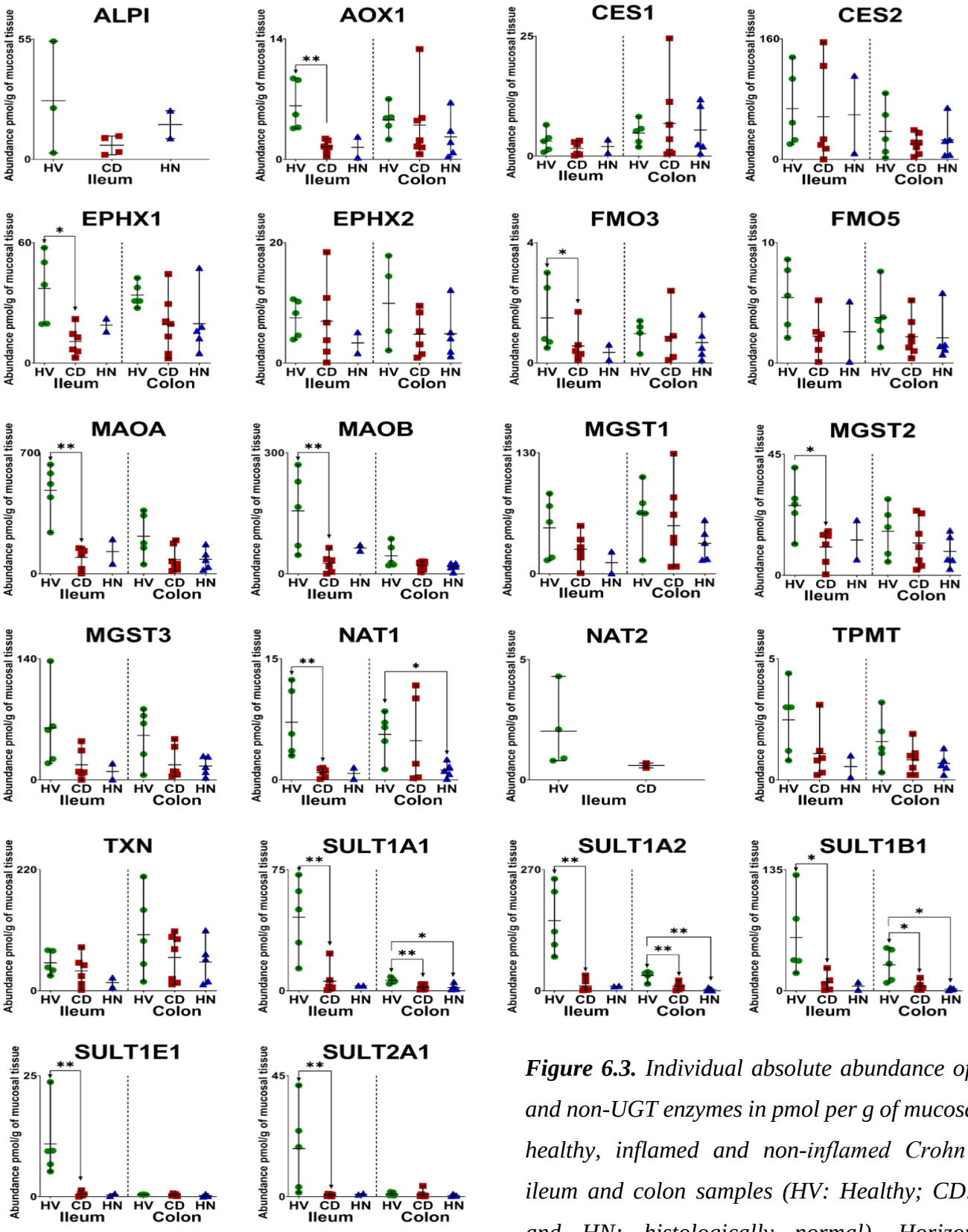

Figure 6.3. *Individual absolute abundance of non-CYP and non-UGT enzymes in pmol per g of mucosal tissue of healthy, inflamed and non-inflamed Crohn's disease ileum and colon samples (HV: Healthy; CD: inflamed and HN: histologically normal). Horizontal lines represent means and bars represent maximum and minimum values. Stars (*) represent statistical significance (*p=<0.05 and **p <0.0087) comparisons between inflamed and non-inflamed with healthy.*

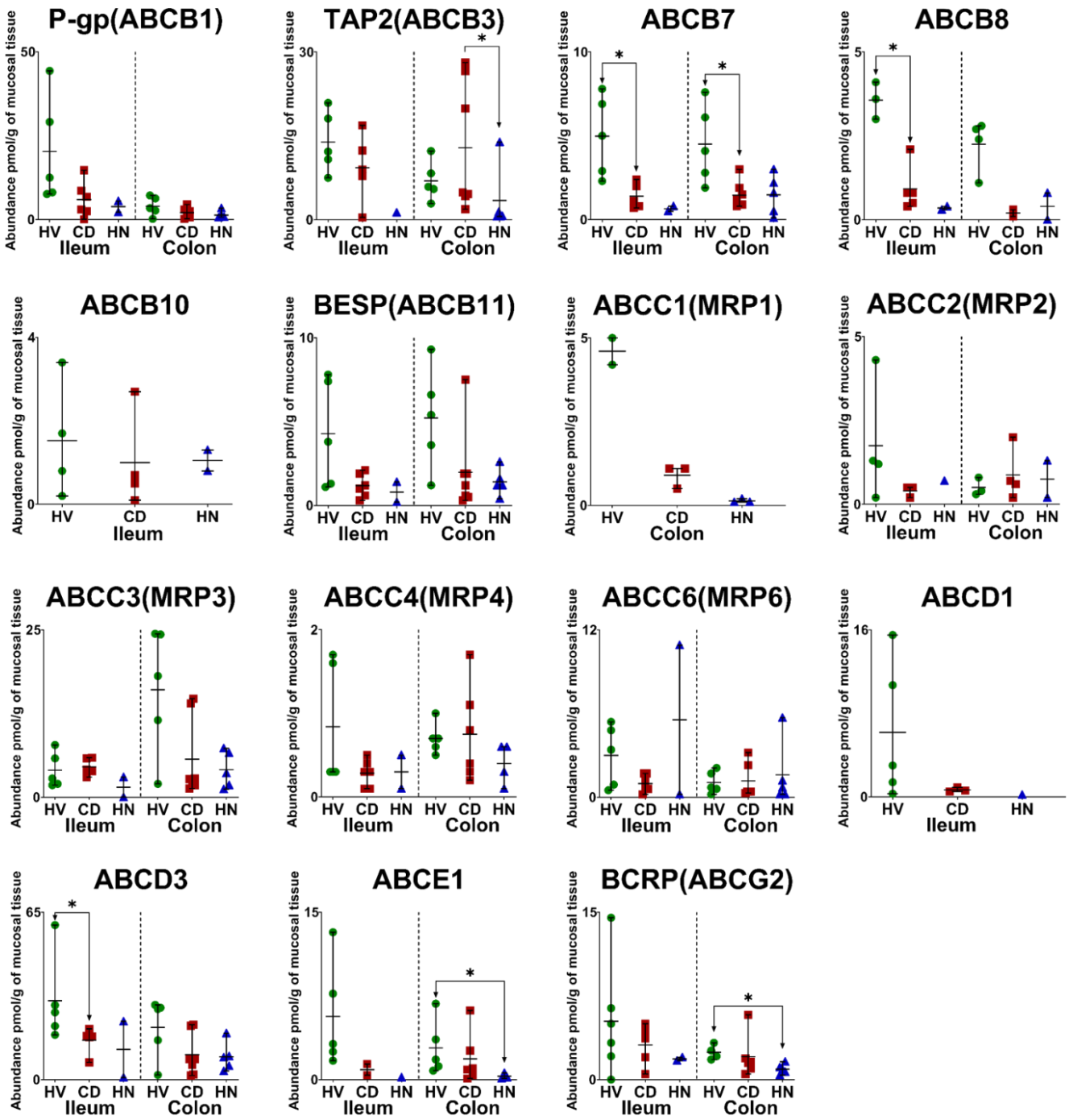

Figure 6.4. *Individual absolute abundance of ATP-binding cassette (ABC) transporters in pmol per g of mucosal tissue of healthy, inflamed and non-inflamed Crohn's disease ileum and colon samples (HV: Healthy; CD: inflamed and HN: histologically normal). Horizontal lines represent means and bars represent maximum and minimum values. Stars (*) represent statistical significance (*p=<0.05 and **p <0.0087) comparisons between inflamed, non-inflamed and healthy.*

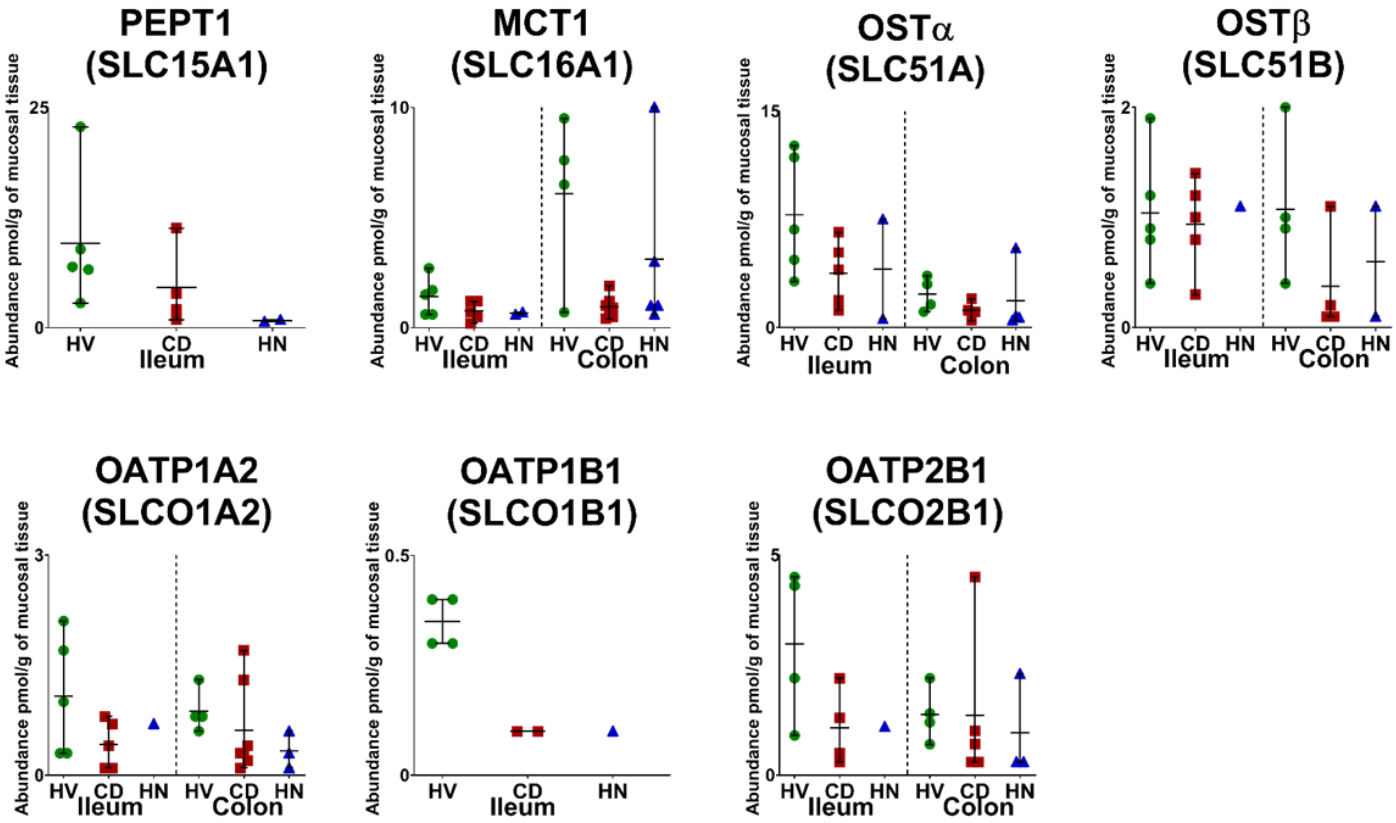

Figure 6.5. *Individual absolute abundance of solute carrier (SLC) in pmol per g of mucosal tissue of healthy, inflamed and non-inflamed Crohn's disease ileum and colon samples (HV: Healthy; CD: inflamed and HN: histologically normal). Horizontal lines represent means and bars represent maximum and minimum values.*

The percent of identical peptides (PIP) and identical proteins (PIPr) were calculated between ileum samples and their results analysed by means of PCA individually (Figure 6.6). Healthy samples tends to cluster close to each other indicating homogeneity within the identified peptides and proteins between the group samples. I-CD and HN-CD groups formed cluster are very closely to each other indicating less distinguishable proteomic profile between the two groups. PC1 and PC2 reflects the divergence between healthy and CD ileum PIP at 28.8% and 16%, respectively and at 33.2% and 22.1%, respectively for PIPr. This makes disease and histology explains a total of ~45% and 55% for PIP and PIPr variation among the ileum samples. One sample of I-CD group was distant from the rest of the samples; the donor of this sample is the only donor to have had a previous bowel resection a few years before obtaining the sample used in this study. This might have contributed to protein distribution and abundance.

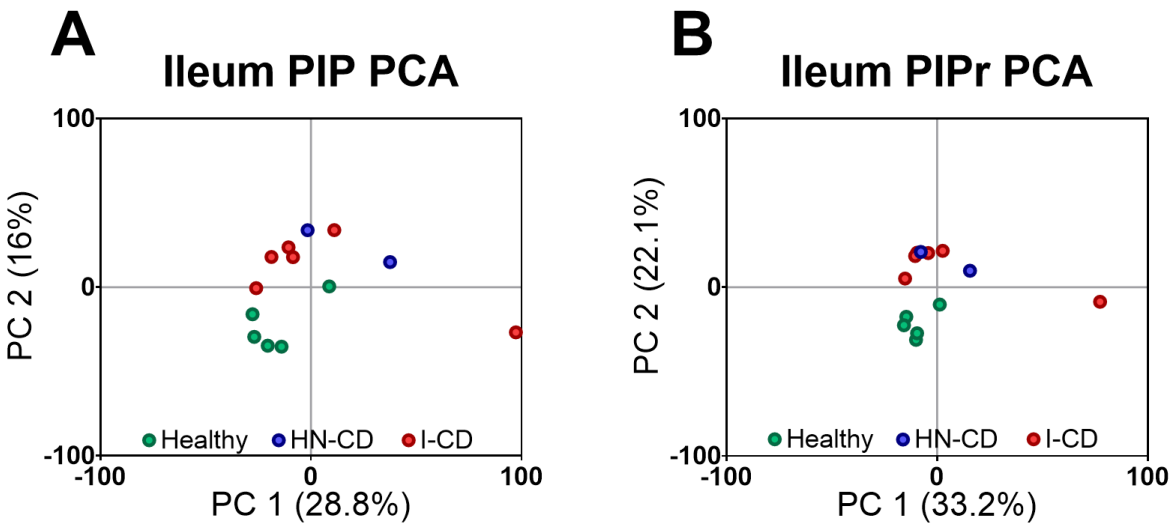

Figure 6.6. *Principal components analysis (PCA) similarity data based on* ***(A)*** *percentage identical peptides (PIP) and* ***(B)*** *percentage identical proteins (PIPr). Identified peptides and proteins from 13 ileum samples of healthy, inflamed from Crohn's disease (I-CD) and non-inflamed from Crohn's disease (HN-CD) ileum tissues.*

The relative abundance between two histologically normal and their inflamed matched ileum samples are presented in Figure S6.3 for individual targets that were detected in the paired set. From the graph no observed consistency and relationship in the relative abundance of the individual targets between the matched samples.

6.4.3. Colon DMETs absolute abundance comparison among sample groups

Assessment of the change in DMETs absolute abundance in the colon of I-CD and HN-CD from healthy group was applied on 7 CYPs, 4 UGTs, 20 non-CYP and non-UGT enzymes, 13 ABC transporters and 5 SLCs. Summary of the mean value of the quantified DMETs in each colon group expressed in pmol/g of mucosal tissue ±SD and (%CV) is presented in Table 6.3.

Statistical analysis was performed using non-parametric statistics as the data were not normally distributed. Kruskal-Wallis ANOVA test was used a cross groups for each target where significant difference ($p \leq 0.05$) detected with CYP27A1 ($p = 0.0105$), UGT1A10 ($p = 0.0262$), NAT1 ($p = 0.0317$) SULT1A1 ($p = 0.034$*), SULT1A2 ($p = 0.0011$*), SULT1B1 ($p = 0.0094$), ABCB7 ($p = 0.027$), ABCB8 ($p = 0.0333$), MRP1 ($p = 0.0107$), ABCE1 ($p = 0.022$) and BCRP ($p = 0.0222$). Mann-Whitney tests was used with the previous targets to assess their significance ($p \leq 0.05$) between healthy and I-CD, healthy and HN-CD and I-CD and HN-CD

colon samples. Figures (6.1-6.5) show the abundance values of CYP, UGT, non-CYP non-UGT, ABC and SLC targets, respectively, presented as individual points, mean and max-min range where statistical significance between the groups are indicated.

In HN-CD group, higher number of targets; 1 CYP, 4 non-CYP non-UGT and 2 ABC transporters showed statistical significance in their absolute abundance compared to healthy. While 1 UGT, 3 non-CYP non-UGT and 1 ABC transporters in I-CD group showed statistical significance compared to healthy. For I-CD group, UGT1A10 (p = 0.0286), SULT1A1 (p = 0.0013*), SULT1A2 (p = 0.0087*), SULT1B1 (p = 0.0173) and ABCB7 (p = 0.0126) showed a significant reduction in their expression compared to healthy. Their fold reduction ranged from 2 (CYP1A2, TPMT, P-gp and OST-α) to 10.1 (ABCB8). MPR1, ABCB8 and MCT1 of the assessed targets didn't have a statistical significance while their fold change reduction was between 5 and 10 fold.

Significant difference was detected with CYP27A1 (p = 0.0317), NAT1 (p = 0.0317), SULT1A1 (p = 0.0159), SULT1A2 (p = 0.0079*), SULT1B1 (p = 0.0159), ABCE1 (p = 0.0357) and BCRP (p = 0.0159) in HN-CD group compared to healthy. Some targets (UGT2B7, ABCB8 and MRP1) with > 5 fold reduction in HN-CD relative to healthy did not demonstrate significant difference ($p \leq 0.05$) using Mann-Whitney tests. The highest fold reduction in HN-CD group compared to healthy was 26.9 fold (MRP1) while the lowest was 2 (MGST1, TXN, TAP2 (ABCB3) and MCT1). None of the DMET targets showed higher expression in I-CD and HN-CD samples group compared to healthy.

CYP27A1 (p = 0.0079**), UGT2B7, NAT1, SULT1A2, SULT2A1, SULT1B1, TAP2 (p = 0.029), MRP1, MRP4, ABCE1 and BCRP exhibited higher expression in I-CD compared to HN-CD group. Fold change of the colon Crohn's disease sample groups compared to healthy and to each other is presented in Figure S(6.4 and 6.5). ABCB8 and MRP1 didn't show statistically significant difference in any of the Crohn's disease groups compared to healthy despite their statistical significance across groups using the Kruskal-Wallis ANOVA test. ABCB8 was detected in only 2 of the I-CD and HN-CD samples (p = 0.1333 in both groups compared to healthy). MRP1 was detected in 3 samples of the I-CD and HN-CD samples and 2 of the healthy group (p = 0.2 in I-CD and HN-CD groups compared to healthy).

Inter-individual variability were assessed for each protein target in each group by means of % CV (Table 6.3).The highest inter-individual variation across CYPs, UGTs, non-CYP and non-

UGT enzymes, ABC transporters and SLCs abundance levels in 5 healthy samples was: CYP4F2 (CV = 85.7%, detected in 4 samples), UGT2B7 (CV = 117.6%, detected in 3 samples), CES2 (CV = 96.7%, detected in all 5 samples), ABCE1 (CV = 87%, detected in all 5 samples), and OST-β (CV = 62.8%, detected in 4 samples). The highest inter-individual variation in 7 I-CD samples was: CYP2S1 (CV = 90.5%, detected in 6 samples), UGT2B7 (CV = 105.8%, detected in 4 samples), SULT2A1 (CV = 156.5%, detected in all 7 samples), BSEP (ABCB11) (CV = 125.2%, detected in all 7 samples), and OST-β (CV = 135.4%, detected in 4 samples). In 5 HN-CD samples, the highest inter-individual variation was with CYP4F12 (CV = 127%, detected in 3 samples), UGT2A3 (CV = 98.8%, detected in all 5 samples), SULT1E1 (CV = 116.8%, detected in 3 samples), TAP2 (CV = 169.3%, detected in all 5 samples), and OST-α (CV = 129.9%, detected in 4 samples). The observed higher range of abundance variation among the CD colon sample groups compared to healthy indicates higher DMETs heterogeneity in disease state.

Table 6.3. Abundance (pmol/g of mucosal tissue) of CYP enzymes, UGT enzymes, non-CYP and non-UGT enzymes, ABC transporters, SLCs in inflamed Crohn's disease (I-CD, n=7), histologically normal Crohn's disease (HN-CD, n=5) and healthy (n=5) colon individual samples. Data represented by the mean, the standard deviation of the mean (SD) and the coefficient of variation (%CV)

Colon Target (pmol/g of mucosal tissue)	Healthy (n=5)		Inflamed Crohn's disease (I-CD, n=7)		Histologically normal (HN-CD, n=5)	
	Mean±SD	% CV	Mean±SD	% CV	Mean±SD	% CV
CYP1A2	1.2±0.6	50.7	0.6±0.5	81.4	0.7±0.7	102.3
CYP20A1	2.7±1.7	61.6	3.1±1.7	56.8	2±1.3	63
CYP27A1	7.8±5.8	74.6	6.9±5.6	80.9	1.3±0.9	65.6
CYP51A1	4.3±1.4	33.3	4.9±3.7	75.1	3.1±3.8	122.5
CYP2S1	8.5±3.9	45.3	4.7±4.2	90.5	2.7±1.6	59.9
CYP4F2	2.3±1.9	85.7	0.7±0.4	63.2	0.7±0.2	30.4
CYP4F12	7±4.9	69.6	1.8 ±1.1	58.7	5±6.3	127.1
UGT1A10	6.7±5.9	88.4	1.6±1.5	94.1	2.3±1.5	67.8
UGT2A3	21±11.5	53.3	9.8±5.6	57	8.9±8.8	98.8
UGT2B7	1.2±1.4	117.6	2±2.1	105.8	0.2±0.2	64.3
UGT2B17	435.9±302	69.3	166.7±143.6	86.1	261.4±190.2	72.7
AOX1	4.6±1.7	37.2	4±4.2	106.1	2.6±2.5	97.1

CES1	4.8±2.5	51.1	6.8±8.7	128.2	5.4±5.2	96.2
CES2	37±35.8	96.7	20.6±13.3	64.3	25.7±25.6	99.7
EPHX1	33.9±6	17.8	19.2±14.5	75.7	19.6±16.2	82.3
EPHX2	9.9±7.4	74.8	4.8±3.6	75.1	4.9±4.4	89.4
FMO3	1±0.5	46.9	0.9±0.9	103.5	0.7±0.6	87.5
FMO5	3.8±61.4	61.4	2.2±1.6	74.8	2.1±2.1	100.4
MAOA	217.2±131.5	60.5	83±72.4	87.2	84.3±59	70
MAOB	44.7±29.8	66.6	20.5±10.4	50.6	17.5±9.3	53.3
MGST1	65±32.4	49.8	51.7±43.7	84.5	32.8±18.2	55.5
MGST2	16.3±9.8	59.9	12±9.1	75.6	8.9±6.1	69.2
MGST3	51.3±32.5	63.3	17.4±17.6	100.8	16±11	68.6
NAT1	5.6±2.7	48.8	4.9±5.6	115.1	1.2±0.9	76
SULT1A1	6.4±1.6	24.9	2.4±1.6	67.7	2±1.9	94.1
SULT1A2	33.8±10.9	32.2	9.6±8	83.9	2.6±2.5	97.9
SULT1B1	28.9±18.2	62.7	4.9±5.1	103.1	1.8±1.2	64.3
SULT1E1	0.4±0.1	18.3	0.3±0.2	71	0.2±0.2	116.8
SULT2A1	1±0.6	60.6	0.9±1.4	156.5	0.4±0.3	78
TPMT	1.6±1.1	69.1	0.8±0.6	72.3	0.7±0.4	56.9
TXN	101.8±76.4	75.1	60.4±42.8	70.9	52±39.9	76.7
ABCB1 (P-gp)	3.9±2.9	72.2	2.1±1.5	73.6	1.3±1.1	86.1
ABCB3 (TAP2)	7±3.5	50.3	12.9±11.5	89.5	3.4±5.8	169.3
ABCB7	4.5±2.3	52.3	1.5±0.8	53	1.5±1.2	79.4
ABCB8	2.2±0.8	35.4	0.2±0.2	77.9	0.4±0.6	136.8
ABCB11 (BESP)	5.2±3.1	59.1	2±2.5	125.2	1.4±0.8	57.8
ABCC1 (MRP1)	4.6±0.5	11.1	0.9±0.3	38.7	0.2±0.1	40.8
ABCC2 (MRP2)	0.5±0.3	56.1	0.9±0.8	86.2	0.8±0.8	103.3
ABCC3 (MRP3)	16.1±9.5	59.2	5.7±6	105.1	4.1±2.8	67.7
ABCC4 (MRP4)	0.7±0.2	23.3	0.8±0.6	76.6	0.4±0.3	66
ABCC6 (MRP6)	1±0.8	76.8	1.2±1.3	105.7	1.6±2.3	144.1
ABCD3	20.3±11.7	57.9	9.6±8.2	85.2	8.8±5.6	63.9
ABCE1	2.8±2.5	87.1	1.9±2.3	121.4	0.3±0.3	93.4
ABCG2 (BCRP)	2.5±0.7	27.7	2.1±1.9	91.8	0.9±0.5	48
SLC16A1 (MCT1)	6.1±3.8	62.4	0.9±0.5	53.6	3.1±4	127.1
SLC51A (OST-α)	2.3±1.2	50.8	1.2±0.6	52.1	1.9±2.4	129.9
SLC51B (OST-β)	1.1±0.7	62.8	0.4±0.5	135.4	0.6±0.7	110.1
SLCO1A2 (OATP1A2)	0.9±0.3	35.9	0.6±0.6	98.1	0.3±0.3	76.1
SLCO2B1 (OATP2B1)	1.4±0.6	45.7	1.4±1.8	130.7	1±1.2	118.1

PIP and PIPr calculated for colon samples and the results analysed by means of PCA individually (Figure 6.7). Healthy samples tends to cluster creating its own pattern away from the inflamed and normal CD samples. However, the inflamed and normal CD samples clusters very closely to each other indicating a similar proteomic profile between the two groups. PC1 of PIP and PIPr is 19.8% and 26.2%, respectively, while PC2 is 12% and 18%, respectively, reflecting the difference between healthy and CD colon. This makes disease and histology explains a total of ~32% and 44% for PIP and PIPr variation among the colon samples.

The relative abundance of three histologically normal and their inflamed matched colon samples for individual targets detected in the paired set are presented in Figure S6.3. From the graph no observed consistency and relationship in the relative abundance of the individual targets between the matched samples.

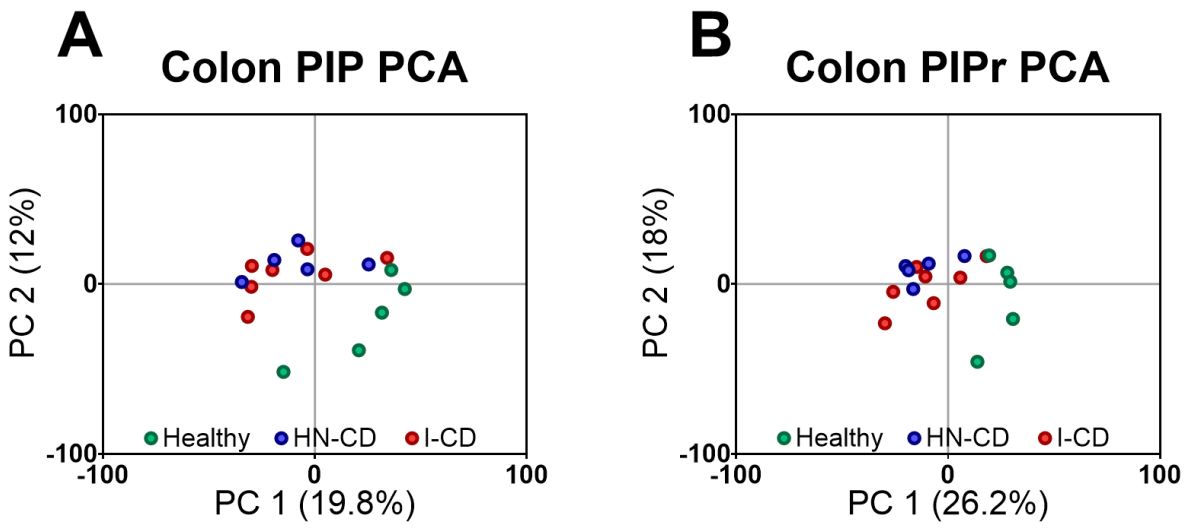

Figure 6.7. *Principal components analysis (PCA) similarity data based on* ***(A)*** *percentage identical peptides (PIP) and* ***(B)*** *percentage identical proteins (PIPr). Identified peptides and proteins from 17 colon samples of healthy, inflamed from Crohn's disease (I-CD) and non-inflamed from Crohn's disease (HN-CD) colon tissues.*

6.4.4. Ileum and colon DMETs abundance inter-correlation

Pairwise expression correlation within CYPs, UGTs, non-CYP non-UGT, ABC transporters and SLCs was assessed with the Spearman correlation (Rs) test among ileum and colon healthy, I-CD and HN-CD samples whenever possible (based on the number of the samples where a

certain protein is quantified). A strong correlation was considered if Rs > 0.60, *p*-value ≤0.05 and this significant correlation was seen in at least two groups of the three groups under investigation in ileum or colon.

In healthy and I-CD ileum samples (Figure 6.8) strong correlations were found between MAOA-TXN, MAOA-AOX1, AOX1-TXN and SULT1A1-SULT1A2 (Rs=1, *p*=0.017; in all healthy samples and Rs=0.886, *p*=0.033, Rs=0.943, *p*=0.017; in I-CD samples). No strong correlation was found within any of the targeted CYPs and transports detected in the ileum.

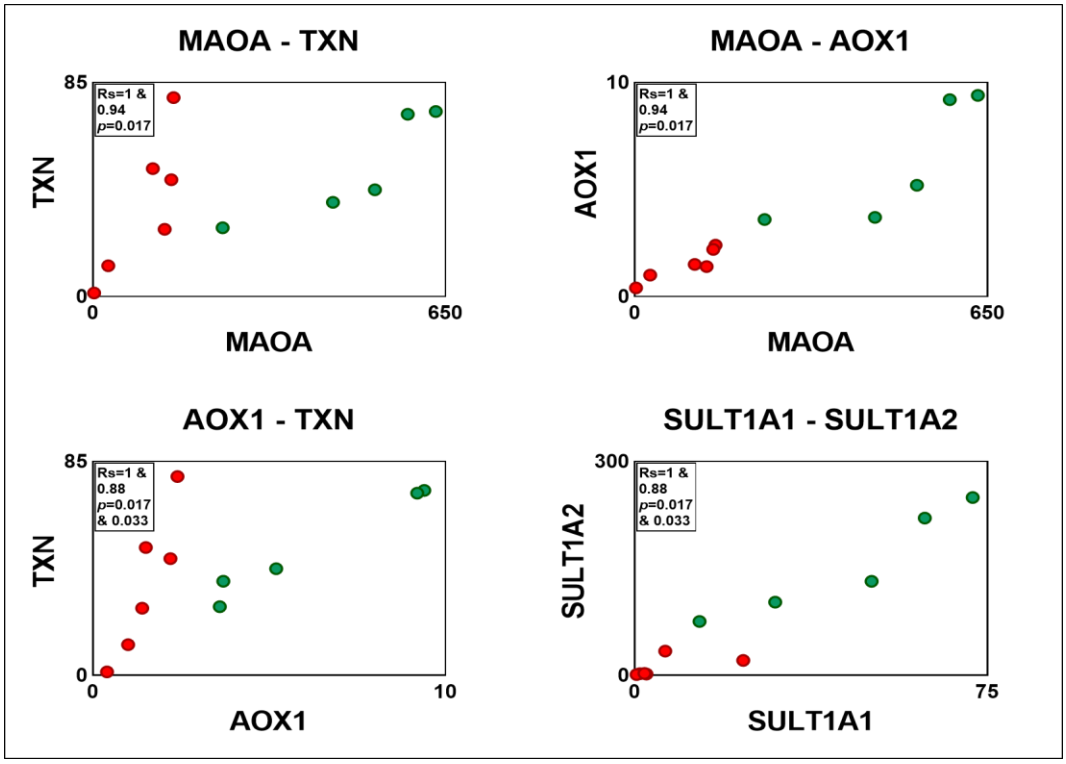

Figure 6.8. *Observed strong correlations (Rs > 0.60 and p-value < 0.05) in ileum protein abundances between non-CYP non-UGT enzymes. Green circles correspond to protein abundance in the healthy ileum and red circles correspond to protein abundance in the inflamed Crohn's disease (I-CD) ileum.*

In colon (Figure 6.9) only MAOA-CES2 showed a strong correlation within healthy and HN-CD tissues (Rs=1, *p*=0.017, in both groups). For transporters TAP2-BSEP, TAP2-MRP4 and BSEP-MRP4 showed strong correlation in their abundance within healthy (Rs=1, *p*=0.017 and Rs=0.975, *p*=0.033, respectively) and I-CD (Rs=0.821, *p*=0.034 and Rs=0.943, *p*=0.017, respectively) tissue samples. A strong correlation was detected between P-gp-ABCD3 within

I-CD (Rs=0.893, *p*=0.012) and HN-CD (Rs=1, *p*=0.017) tissue samples. No significant correlation was detected within CYPs, UGTs and targeted SLCs in the colon.

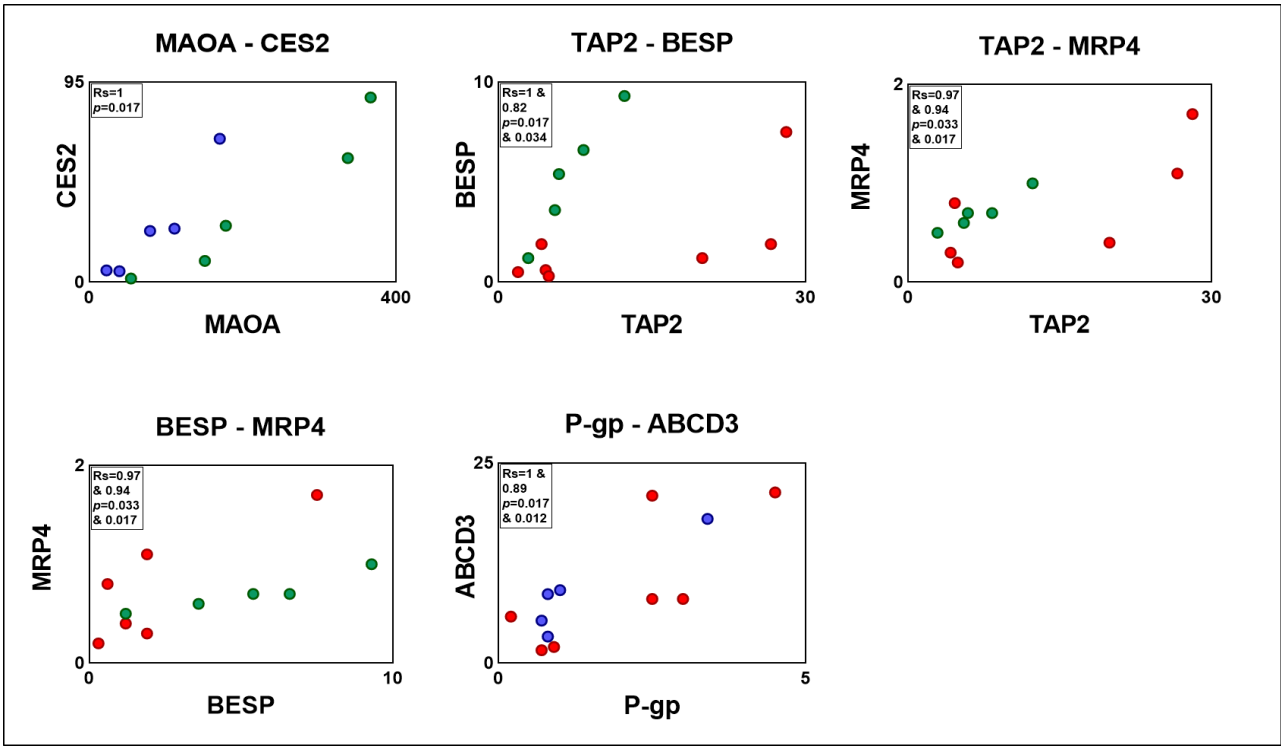

Figure 6.9. *Observed strong correlations (Rs > 0.60 and p-value < 0.05) in colon protein abundances between non-CYP non-UGT enzymes and between ABC transporters. Green circles correspond to protein abundance in the healthy, blue circles correspond to protein abundance in the non-inflamed Crohn's disease (HN-CD) and red circles correspond to protein abundance in the inflamed Crohn's disease (I-CD) colon.*

6.4.5. Covariates and DMETs abundance correlation

Correlation of patient demographics with CYPs, UGTs, non-CYP non-UGT enzymes, ABC transporters and SLCs expression in ileum and colon from I-CD and HN-CD tissue samples were assessed. A strong age (19-62 years, n=5) correlation was detected with just two targets (Figure 6.10) UGT2B7 (Rs=1, *p*=0.0167 & R^2=0.9348) and ALPI (Rs=1, *p*=0.0348 & R^2=0.9814) in I-CD ileum tissue. No other age related correlation was detected with HN-CD ileum, not surprisingly as there were only two samples. No strong correlation with age was detected in I-CD colon (18-68 years, n=7) or HN-CD colon (25-68 years, n=5). No correlation with BMI was detected with any of the targets in ileum (n=5 and 2 of I-CD and HN-CD, respectively) and colon (n=6 and n=3 of I-CD and HN-CD, respectively) tissues.

Association difference of sex (Figure S6.6) and smoking habit with DMETs expression in I-CD and HN-CD ileum and colon tissues was investigated using Mann-Whitney test where $p \leq 0.05$ is considered significant. There was no statistical significant difference detected between female (n=4) and male (n=2) from I-CD ileum tissues, while a comparison based on HN-CD group were not possible because there were no samples from male donors. Similar results observed with female (n=3) and male (n=5) I-CD and female (n=3) and male (n=2) HN-CD colon tissues. Smokers (n=2) and non-smokers (n=3) showed no significant difference with any of the proteins expression in I-CD ileum. Similar to I-CD ileum results smokers (n=4) and non-smokers (n=2) from I-CD colon samples showed no significant difference. Assessing the effect of smoking habit in HN-CD group from ileum and colon was not possible as no enough samples with known history of smoking were available.

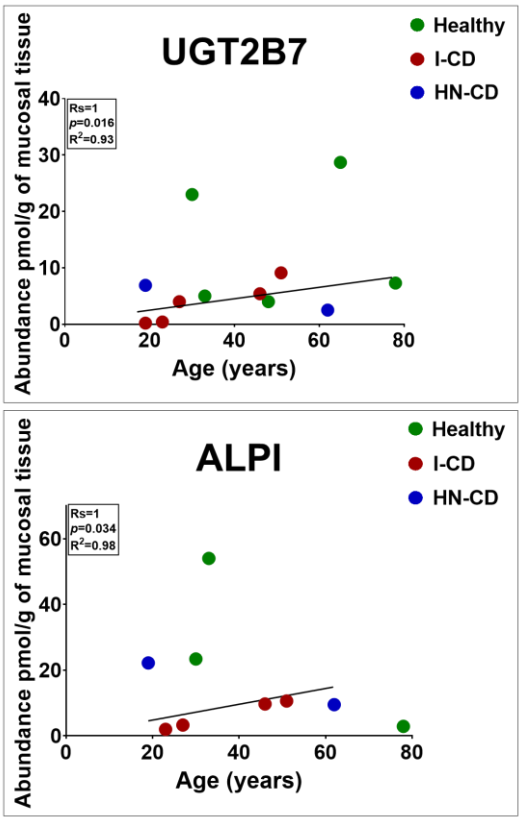

Figure 6.10. *Age effect on UGT2B7 and ALPI abundance of healthy, histologically normal Crohn's disease (HN-CD) and inflamed Crohn's disease (I-CD) ileal tissues. The solid line represents the linear regression. Strong correlation (Rs > 0.60, p-value < 0.05 and R2=>0.30) presented in the boxes, was only found with inflamed Crohn's disease (I-CD) ileal samples.*

6.4.6. Impact of Crohn's disease related system changes and intestine DMETs abundance on oral drugs PBPK models

A good quality model for Crohn's disease should allow the intestine to be considered as several segments rather than as a single entity. We therefore chose the ADAM (Advanced Dissolution Absorption and Metabolism) absorption model in the Simcyp Simulator, which allows for 9

segments, as a starting point.[62] 10 oral drugs were in the library associated with the ADAM model (Table 6.1). The Crohn's population used in this study is described in Chapter One. Four Crohn's disease population models derived from protein levels of enzymes and transporters data generated in this study were now created. These are shown in Table 6.4.

Table 6.4. Four Crohn's disease population models created in Simcyp simulator.

CD population models	Protein abundance data from Inflamed tissue	Protein abundance data from Histologically normal tissue
Normal albumin	M-1	M-3
Reduced albumin	M-2	M-4

The four CD models were validated by running midazolam and budesonide created based on available clinical data; the clinical data on midazolam were derived from active CD patients, those on budesonide were from a mixed active and inactive population. The clinical AUC and Cmax values for budesonide were close to those generated by M-2 (Figure 6.11 A and Table S6.8), where CYP3A4, 2C9 and P-gp abundance data were derived from I-CD tissues and albumin levels were reduced. The ratio of the predicted $AUC_{0-\infty}$ to the observed was 1.7 and 1.57 for Cmax. For midazolam, the best fit was M-1, where CYP3A4 abundance data was derived from I-CD tissues and normal albumin levels were applied. The ratio of the predicted $AUC_{0-\infty}$ to the observed was 0.68 with 0.48 for Cmax. Comparison of the PK variables values from the observed clinical data to the predicted values from the simulations of active CD population models is in Table S6.9 and Figure 6.11 B.

After evaluating the performance of the created population models each of the 10 oral drugs selected from Simcyp library was run through each model (M-1 to M-4), in order to generate a picture of drug metabolism and disposition in the Crohn's population. Both expression values from the inflamed and normal tissues were used assuming the intestine absorption and metabolism capacity in CD patients is in between the two states. Predicted AUC and Cmax results of the simulated oral drugs with the different CD population models relative to the Simcyp healthy population are shown in Figure 6.12. Verapamil shows the greatest changes in AUC and Cmax with all tested models (AUC: 2.8 fold increase with M-1 & M-3 and 2 fold increase with M2&M-4; Cmax: 2.9 fold increase with M-1, 2 fold increase with M-2&M-4 and 2.7 with M-3). Similarly ritonavir shows increases in both AUC and Cmax (AUC: 2.4 fold

increase; Cmax: 2.1 fold increase with all models). Some of the other drugs show a reduction in AUC and Cmax. The highest AUC and Cmax fold reduction was observed with valsartan (AUC: 1.9 and Cmax: 1.6 fold) and celecoxib (AUC: 1.8 and Cmax: 2.1 fold) in M-2 and M-4, respectively. Dabigatran and rosuvastatin showed 2.33 and 2 fold increase in Cmax, respectively, with M-1 and M-3. For the other drugs their AUC and Cmax relative change to healthy varied between the four models but did not exceed 2 fold difference.

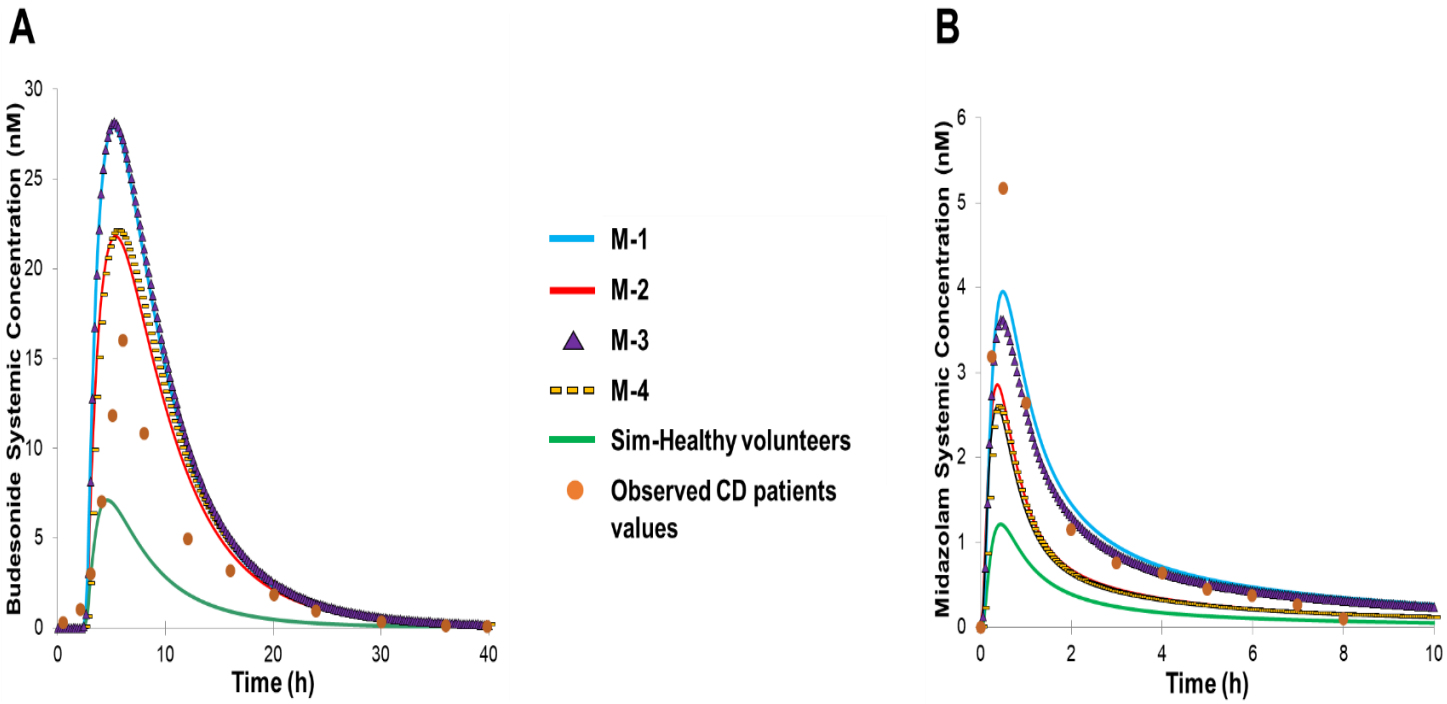

Figure 6.11. *Simulated plasma concentration-time profiles of* ***(A)*** *budesonide and* ***(B)*** *midazolam using Crohn's disease metabolising enzymes and transporters abundance values generated in this study and other system changes to create CD population (**M-1**; intestine DMETs abundance data from I-CD tissues and normal albumin level, **M-2**; intestine DMETs abundance data from I-CD tissues and reduced albumin level, **M-3**; intestine DMETs abundance data from HN-CD tissues and normal albumin level, **M-4**; intestine DMETs abundance data from HN-CD tissues and reduced albumin level and Simcyp V19 default healthy population) compared to the observed in-vivo data in Crohn's disease patients.*

.

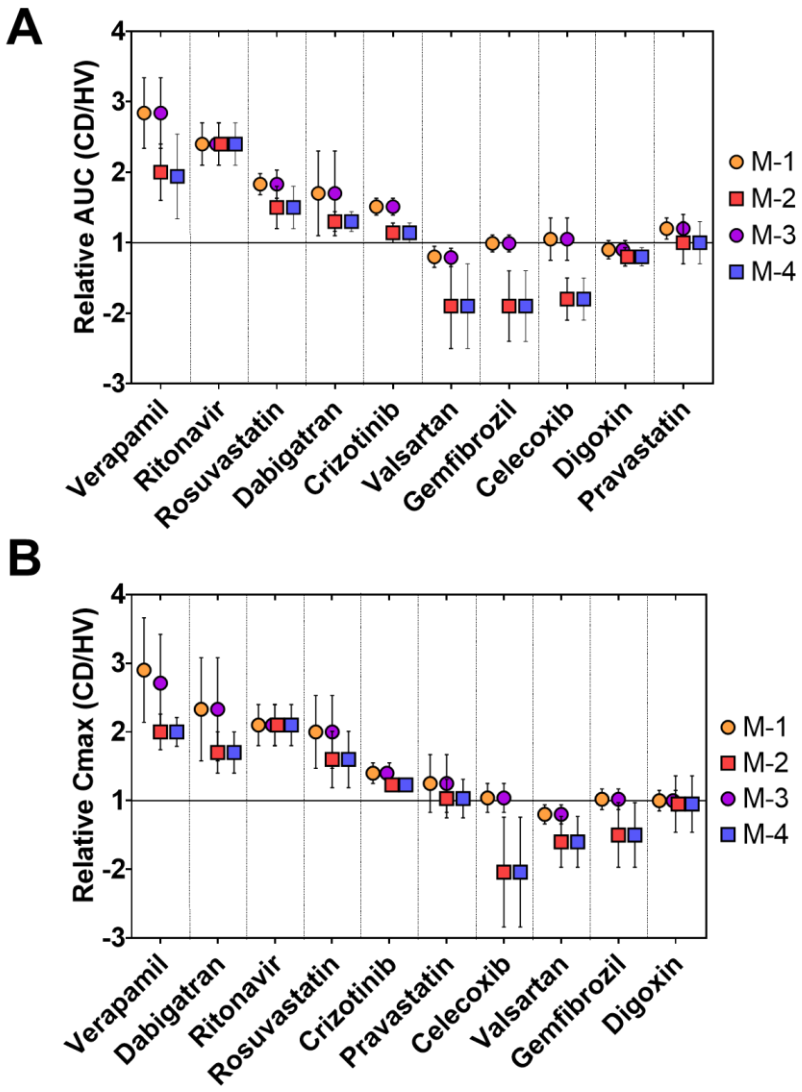

Figure 6.12. *Simulated relative* ***(A)*** *AUC and* ***(B)*** *Cmax between Crohn's disease (CD) and healthy (HV) populations of 10 oral substrates. The markers represent the mean relative values and the lines represent the ± standard deviation (SD). The applied Crohn's population models:* ***M-1*** *(intestine DMETs abundance data from I-CD tissues and normal albumin level),* ***M-2*** *(intestine DMETs abundance data from I-CD tissues and reduced albumin level),* ***M-3*** *(intestine DMETs abundance data from HN-CD tissues and normal albumin level) and* ***M-4*** *(intestine DMETs abundance data from HN-CD tissues and reduced albumin level).*

6.4.7. Ileum DMETs absolute abundance in HN-cancer sample group compared to HN-CD and healthy group

The HN-cancer samples group were only included in the abundance comparison to healthy and HN-CD samples in order to assess its feasibility to be used as a control group for CD studies when healthy samples are not available. Calculated PIP and PIPr analysed by PCA (Figure 6.13) for the three compared groups. The analysis shows that the identified proteins in HN-cancer samples are clustering more closely to HN-CD samples rather than healthy for both PIP and PIPr. PC1 and PC2 indicates the difference between the identified peptides and protein in healthy, HN-CD and HN-cancer ileum at 26.7% and 19.4%, respectively, for PIP. For PIPr PC1 and PC2 were at 36.2% and 23.8%, respectively. This makes disease and histology explains a total of ~46% and 60% for PIP and PIPr variation among the three groups.

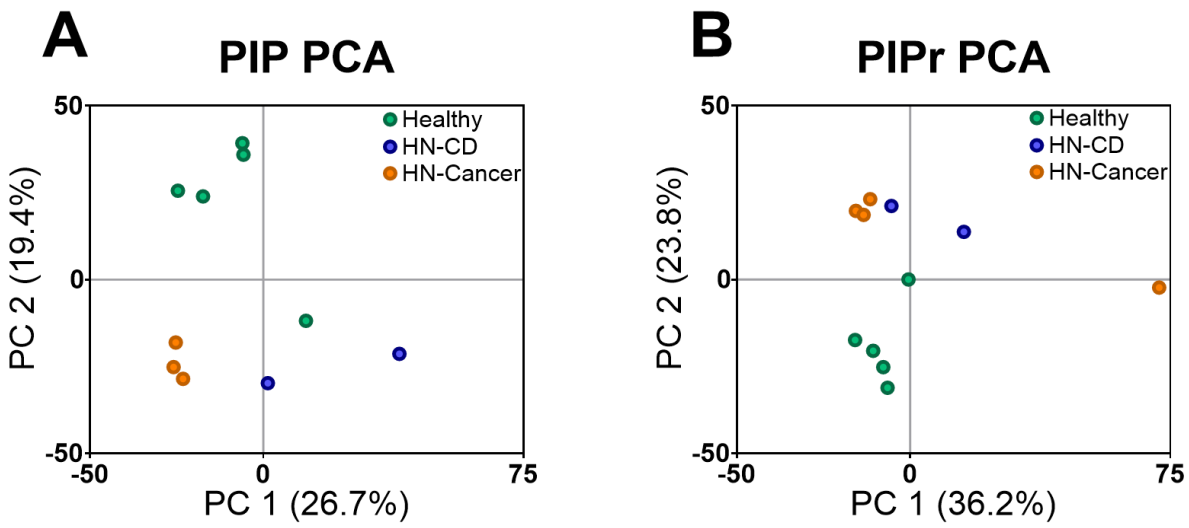

Figure 6.13. *Principal components analysis (PCA) similarity data based on* ***(A)*** *percentage identical peptides (PIP) and* ***(B)*** *percentage identical proteins (PIPr). Identified peptides and proteins from 10 ileum samples of healthy, histologically normal from Crohn's disease (HN-CD) and histologically normal from cancer patients (HN-Cancer) ileum tissues.*

SULT1E1, TXN and MRP3 in HN-cancer samples shows statistical significant with post-hoc Mann-Whitney tests (p =0.0159 for all) compared to healthy (Figure 6.14). No statistical significance was detected when compared to HN-CD (only two samples available). Other targets (EPHX2, NAT1, SULT1A1, P-gp and BCRP) reported statistical significance across the three groups ($p \leq 0.05$) using Kruskal-Wallis ANOVA test, but no significance detected when post-hoc Mann-Whitney tests pairwise comparison performed. The average expression values of HN-cancer samples are generally higher than the healthy and the HN-CD. In Figure S (6.8 and 6.9) fold change of their mean abundance to healthy and to HN-CD samples are reported where fold reduction ranged from 2.2 (ABCE1) to 6.4 (SULT1E1) fold and fold increase ranged from 2 (P-gp and PEPT1) to 7.3 (CES2) fold relative to healthy. When compared to HN-CD samples only MRP6 (ABCC6) showed fold reduction with 2.8 fold while the rest showed fold increased ranging from 2 (EPHX1) to 61.4 (UGT1A1) fold.

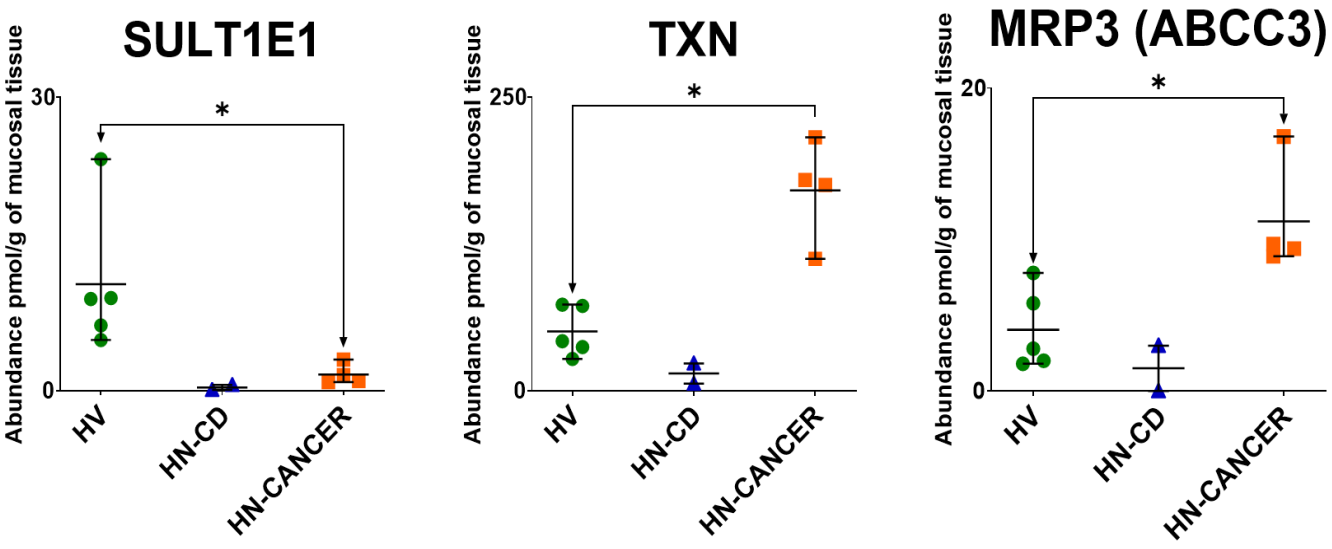

Figure 6.14. *Individual absolute abundance in pmol per g of mucosal tissue of DMETs with significant difference from healthy, normal Crohn's disease and normal cancer ileum samples (HV: Healthy; HN-CD: histologically normal from Crohn's subjects and HN-cancer: histologically normal from cancer subjects). Horizontal lines represent means and bars represent maximum and minimum values. Stars (*) represent statistical significance (*p=<0.05) comparisons between inflamed and non-inflamed with healthy.*

6.5.Discussion

Crohn's disease is a chronic disease of all ages where inflammation of the bowel occurs and patients undergo recurring active and remission phases. During both phases of the disease, patients may be exposed to many oral drugs, both to control the disease itself and to treat other conditions. Intestinal inflammation brought about by active CD causes alteration in DMETs of the inflamed segment and of nearby tissue. Systemic responses are also induced, such as induction of liver injury in CD patients.[26,63] The active phase generally sees more aggressive alterations in body system measures relevant to oral drug disposition.[30,64–69] There is surprisingly little quantitative information available about the expression of DMETs in CD. Here, we conducted for the first time a study to explore different DMETs absolute abundance in ileum and colon of active CD patients to enable more reliable and better predictable PBPK models applications of the fate of oral drugs in CD population.

We demonstrated a downregulation of all quantified DMETs in inflamed and histologically normal CD tissues in both ileum and colon relative to healthy. Generally, for the same targets, downregulation in ileum tissue samples was higher than colon in both I-CD and HN-CD relative to healthy expression. When the downregulation is translated into statistical data, significance was reported with some of the quantified DMETs in inflamed ileum and colon segments and normal from colon.

Of these proteins, CYP3A4 is the most important as it is involved in the metabolism of up to 30% of drugs used clinically.[70] Orally administered glucocorticoids (prednisone and budesonide) are substrates of CYP3A4[71,72] and are commonly used to treat CD. Up to 62% of IBD patients receive oral glucocorticoids within 10 years of the diagnosis.[73] The CYP3A family represents approximately 80% of the intestinal CYP enzymes and CYP3A4 is the most highly expressed.[74] In our samples, CYP3A4 & 3A5 were detected in the ileum tissue only and below LLOQ in the colon (0.85 pmol/g of mucosal tissue). The observed significant downregulation of CYP3A4 (~ 8 and ~ 4 fold in I-CD and HN-CD, respectively) and CYP3A5 (~ 9 and ~128 fold in I-CD and HN-CD, respectively) in our CD ileum tissue samples can be attributed to several inflammation related mechanisms. Inflammatory cytokines (TNF-α, INF-γ IL-1β and IL-6) that are found to be upregulated in CD[75] are linked to CYP3A downregulation.[13,76] Other CYPs such as CYP1A2 and CYP2C were also downregulated during inflammation[14] and found to be downregulated in our samples. Another mechanism that could have contributed in the CYP3A downregulation, is the change of pregnancy X receptor

(PXR) regulation in CD[77] and other inflammatory conditions.[78] As PXR is a known transcription factor signalling the induction pathway of CYP3A expression. The observed reduction in our abundance data is in line with previous gene and relative protein abundance data, with varying levels of reduction.[16,21,25] Moreover, drug-disease interaction studies reported a significant alteration of the PK profile of CYP3A4 substrates' budesonide, midazolam and verapamil oral formulation in CD patients.[5,6,79]

The downregulation of phase II metabolising enzymes, UGTs and SULTs, can be explained similarly. Reduced mRNA expression and enzymatic activity of several UGT and SULT isoforms in response to elevation of inflammatory cytokines has been reported.[80,81] The same expression response of UGT and SULT isoforms has been linked to the dysregulation of their relevant nuclear receptors and transcription factors in inflammatory conditions other than IBD.[80,82–84] However, very limited information available on UGTs and SULTs expression in IBD population.[44] > 2 fold reduction in UGT1A3 gene expression in the ileum and colon of CD patients was reported.[25] UGT1A3 was below the limit of detection in all of our CD ileum and colon samples. A slight increase in UGT1A1 relative expression in CD colon was reported.[22] A significant reduction of SULT1A2 and SULT2A1 mRNA expression was reported in ileum and colon samples from CD patients compared to the control group.[15,25] We have demonstrated a significant reduction in colon UGT1A10 (~ 4 and 3 fold in I-CD and HN-CD, respectively) at the protein level. UGT1A10 is involved in the metabolism of oral anticancer (genistein) and cardiovascular (losartan, candesartan, and zolarsartan) agents.[85,86] SULTs in our data were significantly reduced in both ileum (SULT1A1, SULT1A2, SULT1B1, SULT1E1 and SULT2A1) and colon (SULT1A1, SULT1A2, and SULT1B1) CD tissue samples. These enzymes catalyse sulfate conjugation in a broad range of endogenous and xenobiotic substrates, including oral paracetamol and minoxidil.[87,88]

Other non-CYP and non-UGT enzymes displaying significant reduction in their expression include: AOX1, FMO3, MAOA, MAOB and NAT1. There are no previous studies on their expression level or activity in CD patients. Aldehyde oxidase (AOX1) is found to be significantly reduced in ileum CD tissue (~4 fold in both I-CD and HN-CD) relative to control. This enzyme is involved in the metabolism of two oral immunosuppressant drugs (methotrexate and azathioprine) prescribed to control refractory CD.[89,90] Azathioprine is an immunosuppressant prodrug metabolised to its active metabolite, mercaptopurine, which is further metabolised by AOX1.[91] Additionally, azathioprine is further metabolised by thiopurine

methyltransferase (TPMT) which is found to be reduced in our CD samples from ileum and colon segments, up to 4.5 fold in HN-CD from ileum. TPMT deficiency and genetic variation causes serious toxicity, such as thrombocytopenia and myelotoxicity related to azathioprine and its metabolite mercaptorpurine accumulation.[92,93] Around 17% of IBD patients cannot tolerate treatment with azathioprine or mercaptopurine and dose reduction might be warranted.[94]

Flavin-containing monooxygenases (FMOs) metabolise nucleophilic nitrogen, sulfur, selenium, and phosphorous containing drugs and oral chlorpromazine, promethazine, brompheniramine, cimetidine, ranitidine, and itopride are some of their substrates.[95] In ileum tissue FMO3 and FMO5 expression was downregulated in all CD samples, while no change observed in colon expression relative to healthy tissue. Hepatic FMO activity in human has been reported to decline in inflammatory conditions other than IBD[96] because of increased nitric oxide production.[97,98]

In our study, monoamine oxidase (MAOA and MAOB) were significantly reduced in CD ileum relative to healthy levels. There is no previous literature data available for MAO enzymes in the IBD population. MAOA and B catalyse the degradation of serotonin, norepinephrine, dopamine, phenylethylamine and benzylamine.[99] MAO inhibitors are drugs for the treatment of several neurological diseases. In some cases these drugs are given by routes other than oral; for example, selegiline is given by the transdermal route to avoid its inactivation by intestinal and hepatic MAOA and B.[100,101] In other cases, the oral formulation of a pro-drug slowly converts to its active moiety to avoid interaction with intestinal MAOs, as the case with ladostigil.[102]

N-Acetyltransferase 1 (NAT1) was significantly decreased in CD ileum (8 and 9 fold in I-CD and HN-CD, respectively) and colon HN-CD samples (~5 fold). It catalyses N-acetylation and O-acetylation, and metabolises aromatic and heterocyclic amines.[103] It metabolises oral aminosalicylate (5-ASA) agents which are used to control CD. In a systemic review, 5-ASA effectiveness in CD subjects was not superior to placebo.[104] In in-vivo settings, mesalamine exhibited a higher systemic exposure in CD patients compared to healthy and ulcerative colitis (UC) patients.[8] In another study, lower bioavailability of mesalmine was reported in CD patients in remission compared to healthy subjects.[105]

For clinically relevant transporters a high reduction (≥5 fold) was observed with P-gp and PEPT1 in histologically normal CD ileum samples. In the colon, MRP1, BCRP and MCT1 showed high reduction (≥5 fold) in tissue samples from CD patients. Previous literature data on CD patients focus on P-gp because of its efflux excretion role on a broad range of drugs.[106,107] P-gp mRNA level showed a significant reduction in CD ileum and colon.[16,18,24] Similarly, BCRP mRNA expression was reported to significantly decrease in CD ileum;[15] this is one of the major multidrug resistance transporters involved in the efflux of oral flavopiridol and methotrexate.[108] MCT1 a lactate, pyruvate, butyrate, acetoacetate, β-hydroxybutyrate and γ-hydroxybutyric acid (GHB) transporter [109] was also reported to have significantly reduced mRNA expression in the CD colon.[23] PEPT1 was the only transporter reported to be upregulated in CD ileum colon.[17] Oral β-lactam antibiotics and angiotensin-converting enzyme inhibitors are substrates of PEPT1 as it transports peptide-like compounds.[110] The mechanisms by which several transporters encounter alteration in their expression during inflammation is significantly linked to the increase of inflammatory mediators (ILs, TNF-α, and INF-γ).[23,111,112]Most of the data report downregulation of intestinal and hepatic transporters. Only a few studies showed disagreement where upregulation of P-gp and MRP3 expression was found to increase as inflammatory biomarkers concentration increased.[76,111] Moreover, mRNA expression of ABC transporters was found to correlate with PXR activation, which impacts the intestine epithelial barrier function, hence the intestine permeability.[113]

In contrast to the commonly observed correlation between inflammation severity and the alteration of protein abundance, some targets like CYP3A5, UGT1A1, ABCB3 and PEPT1 showed a higher reduction in HN-CD ileal samples (~14, 29, 7 and 5.5 fold, respectively) compared to I-CD tissue reduction. In colon samples, CYP27A1, UGT2B7, NAT1, TAP2, ABCE1 and MRP1 abundance were lower in HN-CD tissues (~5, 8, 4, 4, 6 and 5 fold, respectively) compared to their abundance in I-CD tissues. In both ileum and colon segments, the observed higher reduction of DMETs abundance in HN-CD tissues compared to I-CD tissues indicates that the impact of inflammation magnitude is not restricted to where it is localised. In a study comparing CYP3A4, 3A5 and P-gp gene expression in inflamed and non–inflamed rectum tissues from CD patients, CYP3A4 was the only one to show a significant lower expression in inflamed tissue.[21] MCT1 mRNA level was significantly decreased in both inflamed and non-inflamed colon tissues (n=14) from CD patients compared to control. A significantly higher reduction was observed with the inflamed tissue vs the non-inflamed.[23] OATP2B1 and 4A1 mRNA expression displayed no difference between inflamed and non-

inflamed ileum tissues. When compared to healthy OATP2B1 and 4A1 levels were significantly higher in CD patients.[17] Whereas, ASBT expression in ileum and colon tissues (n=49) from CD patients was significantly lower than healthy expression.[17] The literature reports a direct relationship between inflammation severity and changes of DMETs expression.[21,23] Such comparison between our inflamed tissue samples was not possible, as the inflammation severity scale for each patient was not provided. It is important to note that in our study and the referenced studies non-inflamed tissue was actually tissue adjacent to the inflamed tissue. This limits further generalisation of this finding on the expression behaviour of non-inflamed upper intestine segments (duodenum and jejunum) in CD patients.

In the ileum, strong inter-correlations were found between UGT enzymes, SULT enzymes, and between other non-CYP non-UGT enzymes. In the colon, inter-correlations were found between non-CYP non-UGT enzymes and between ABC transporters. Incorporation of correlation information in PBPK models aid in creating more reliable predictions. For example, such correlation data were shown to enhance the prediction of population and drug-drug interaction PBPK models for liver and kidney.[114,115] The Focus here is on the paired enzymes with known impact on oral substrates (SULT1A1-SULT1A2), (MAOA-TXN), (MAOA-AOX1), (AOX1-TXN) and (MAOA-CES2). The strong correlation between these enzymes might be attributed to a common transcriptional pathway, where they share the same regulatory nuclear receptor.[116,117] SULT1A1 and SULT1A2 expression was found to be regulated by hepatocyte nuclear factor 4α (HNF4α), constitutive androstane receptor (CAR) and PXR in the liver and hepatic cell lines.[118–120] Oxidase enzymes: AOX1 and MAOA along with thioredoxin (TXN) are regulated by the transcription factor nuclear factor E2-related factor 2 (Nrf2) pathway.[121–123] The causes of the detected strong correlation between MAOA and CES2 are unclear.

Inter-individual variability including variability in abundances of DMETs can affect individuals' response to the same medication. This might lead to negative outcomes such as adverse reactions, resistance to treatments, and lower efficacy profile. The impact of the inter-individual variability is seen in CD patients receiving non-oral drugs.[125–128] For oral drugs, azathioprine and mercaptopurine (TPMT and AOX1 substrates), response and toxicity were evaluated based on the inter-individual variation of IBD patients in thiopurine metabolism. Dosage adjustment based on these enzymes improved the response rate and decreased haematological adverse events.[129] Our inter-individual variability data from ileum and colon

tissue samples, measured by coefficient of variation (%CV), showed that the variation of AOX1 and TMPT abundance was higher in tissues sourced from CD patients compared to healthy. The PK profile of oral budesonide (CYP3A4 and P-gp substrate) exhibited variability in CD patients receiving the same formulation in different studies.[79,130,131] Other studies on budesonide and prednisolone (CYP3A4 and P-gp substrate) showed high variability in CD patients' response and adverse events.[4,132,133] CYP3A4 and P-gp abundance variation in our ileum and colon samples showed relatively similar variation in tissues sourced from CD and healthy subject. In a previous study, inter-individual variation, measured by (%CV), of CYP3A4 and P-gp relative expression in CD patients were significant in ileal and colonic tissues between CD and control group.[16]

In disease, some demographic and/or medication history variables correlate with changes in protein expression.[20] No significant correlation found between the demographical covariates (sex, age, smoking and BMI) of our CD subjects and DMETs abundance. The only exception was correlation of age (19-62 years, n=5) with UGT2B7 and ALPI abundance in ileal I-CD tissues. In a study on CD patients (n=23), age and sex correlation with CYP3A4 and P-gp expression was assessed and no strong correlation was observed, except with colonic P-gp in both CD and control subjects (n=60).[16]

Abundance data generated in this study was integrated into the Simcyp simulator V19 to assess the impact of DMET alteration on oral drug bioavailability. The selection of drugs from the Simcyp library was restricted to drugs built using the ADAM absorption model, to allow investigation of the variability of the intestine physiology in relation to the drug absorption and first pass metabolism. The ADAM absorption model accounts for the intestine upper (duodenum, jejunum 1&2 and ileum 1–4) and lower (colon) segments' anatomical and physiological characteristics (i.e., transit time, pH, surface area, blood flows, food effect, etc.). In this model, absorption and metabolism of drugs is carried out in the enterocyte compartment, where metabolising enzymes and transporters are distributed based on their abundance in each segment.[62,134] The drug fraction that escapes the intestine first pass metabolism is transferred to the liver by the blood flow though the portal vein before it reaches the systemic circulation. Assessment of CD impact on the systemic exposure of 10 oral drugs was carried out with alteration of the proteins involved in their metabolism/absorption (CYP3A4, CYP3A5, CYP2D6, UGT2B7, P-gp, MRP2, BCRP and OATP2B1) in the intestine based on our generated data. The simulated AUC outcomes varied, two substrates (ritonavir and verapamil)

encountered >2 fold change in their AUC in the CD population relative to healthy population. This is most probably due to their metabolism by CYP3A4, which is downregulated in both liver and intestine in the CD population and their high affinity for blood proteins (ritonavir bound ~99% to α1-AGP while verapamil bound ~90% to albumin). Although celecoxib and crizotinib are also metabolised by CYP3A4 and are highly bound to albumin (95% and 91%, respectively) the change of their CD population AUC relative to healthy population was 1.8 fold reduction and 1.5 fold increase, respectively. This might be due to their low (celecoxib EH ~ 0.04-0.2) and intermediate (crizotinib E_H ~ 0.44) extraction ratio.[52,135] Alteration of the drugs' AUC was not different when protein abundance data from I-CD tissue were applied compared to HN-CD data (M-1 and M-3), while the change in albumin level caused higher AUC alteration in the applied models (M-2 and M-4). Change in Cmax value from healthy to CD population was generally greater than the change seen with AUC. Five drugs (celecoxib, crizotinib, dabigatran, rosuvastatin, ritonavir and verapamil) encountered >2 fold change in their Cmax of CD population with the different models. CYPs and/or efflux transporters are involved in the disposition of these drugs, where their abundance is reduced in the intestine tissue of CD patients. Cmax can indicate the extent of drug absorption by the intestine secondary to AUC. In general, change in Cmax was only slightly higher when protein abundance data from I-CD tissue were applied compared to HN-CD (M-1 and M-3).

Furthermore, our intestine DMETs data were used to simulate the clinical exposure of midazolam and budesonide in CD patients. The two drugs were chosen mainly due to the availability of oral and systemic PK profile in clinical setting in CD and healthy subjects to allow for model verification. They are metabolised by CYP3A4 (altered in intestine and liver of CD patients) and are relevant to the CD population. Simulation of midazolam based on the M-1 model (CYP3A4 is reduced based on I-CD ileum abundance and albumin level is normal) showed that the high change of bioavailability (~5 fold in AUC) observed clinically in CD subjects compared to healthy was mainly due to the alteration in CYP3A4 expression. This is supported by the improved prediction of midazolam PK parameters (AUC, Cmax and Tmax) when using direct protein abundance data (M-1 and M-2 models) compared to prediction based on simulation using available relative or gene expression data (Chapter One). For budesonide, the M-2 model (reduction of both CYP3A4 based on I-CD ileum abundance and albumin level) showed that the change of bioavailability (~2 fold in AUC) observed clinically in CD subjects compared to healthy was mainly due to combination of the different altered system parameters during the disease course. Additionally, performance of M-1 and M-2 models using direct

protein abundance did not improved the prediction of budesonide AUC, Cmax and Tmax variables compared to simulation prediction based on available relative or gene abundance data (Chapter One). Unfortunately, substrates of UGTs or SULTs have no available PK in-vivo data in CD patients in order to assess the impact of their abundance changes observed in our CD tissues.

Using different control groups is one of the sources of the variability detected between different studies assessing DEMT expression in IBD tissue samples. Few studies utilised normal tissue from cancer patients as their control group.[44,45] Our assessment of protein abundance in histologically normal tissue form adenocarcinoma patients showed significant alteration in SULT1E1 (6.4 fold reduction), TXN and MRP3 (3.4 and 2.8 fold increase, respectively) compared to the abundance in healthy tissue. Thus, when using normal (not diseased) tissue from a diseased population as the control group caution should be practised.

In summary, a lack of information regarding the physiological changes encountered during disease makes it difficult to build a reliable PBPK population and drug models. For active CD population, many of the physiological changes encountered are directly related to the drug systemic availability. Some DMET expression were reported in this disease phase, yet the available information are far from been adequate to build a reliable PBPK model. In this study, the impact of CD on DMETs absolute abundance is reported for the first time using LC-MS based proteomics quantification. Downregulation of all quantified CYP enzymes, UGT enzymes, non-CYP and non-UGT enzymes, ABC transports and SLCs was reported in I-CD and HN-CD ileal and colon samples compared to healthy. Inter-individual variability showed contribution in the extent of the findings between CD and healthy. Collection of the physiological changes in CD from the literature and our DMET proteomics data allowed enhancement of the created CD population to be used in PBPK models. More information are needed; as the observations in this study regarding the DMETs expression are to be confirmed for the intestine upper segments. The extent of the liver involvement is hard to resolve as sourcing liver tissue biopsies from CD patients is challenging. Liquid biopsy (blood samples)[136] is an attractive technology to measure the proteins expression when the access to the tissue is limited. Measuring DMETs expression in CD patients relative to healthy provides disease perturbation factor (DPF) which can be incorporated into PBPK applications to enhance dose accuracy of oral medications, by predicting the drug PK during CD active phase.

6.6.References

1. Hart AL., Ng SC. Crohn's disease. *Medicine (Baltimore)* 2011;**39**(4):229–36. Doi: 10.1016/j.mpmed.2011.01.004.

2. Peyrin-Biroulet L., Panés J., Sandborn WJ., Vermeire S., Danese S., Feagan BG., et al. Defining Disease Severity in Inflammatory Bowel Diseases: Current and Future Directions. *Clin Gastroenterol Hepatol* 2016;**14**(3):348-354.e17. Doi: 10.1016/j.cgh.2015.06.001.

3. Faubion WA., Loftus E V., Harmsen WS., Zinsmeister AR., Sandborn WJ. The natural history of corticosteroid therapy for inflammatory bowel disease: A population-based study. *Gastroenterology* 2001;**121**(2):255–60. Doi: 10.1053/gast.2001.26279.

4. Rosell R., Gomez-Codina J., Camps C., Maestre JA., Padille J., Cantó A., et al. A Comparison of Budesonide with Prednisolone for Active Crohn's Disease. *N Engl J Med* 1994;**330**(3):153–8.

5. Sanaee F., Clements JD., Waugh AWG., Fedorak RN., Lewanczuk R., Jamali F. Drug−disease interaction: Crohn's disease elevates verapamil plasma concentrations but reduces response to the drug proportional to disease activity. *Br J Clin Pharmacol* 2011;**72**(5):787–97. Doi: 10.1111/j.1365-2125.2011.04019.x.

6. Wilson A., Tirona RG., Kim RB. CYP3A4 Activity is Markedly Lower in Patients with Crohn's Disease. *Inflamm Bowel Dis* 2017;**23**(5):804–13. Doi: 10.1097/MIB.0000000000001062.

7. Schneider R., Bishop H., Hawkins C. Plasma propranolol concentrations and the erythrocyte sedimentation rate. *Br J Clin Pharmacol* 1979;**8**(1):43–7. Doi: 10.1111/j.1365-2125.1979.tb05907.x.

8. Norlander B., Gotthard R., Strom M. Pharmacokinetics of a 5-aminosalicylic acid enteric-coated tablet in patients with Crohn's disease or ulcerative colitis and in healthy volunteers. *Aliment Pharmacol Ther* 1990;**4**(5):497–505. Doi: 10.1111/j.1365-2036.1990.tb00496.x.

9. Fries W., Belvedere A., Vetrano S. Sealing the Broken Barrier in IBD: Intestinal Permeability, Epithelial Cells and Junctions. *Curr Drug Targets* 2013;**14**(12):1460–70. Doi: 10.2174/1389450111314120011.

10. Raddatz D., Bockem??hl M., Ramadori G. Quantitative measurement of cytokine mRNA in inflammatory bowel disease: relation to clinical and endoscopic activity and outcome. *Eur J Gastroenterol Hepatol* 2005;**17**(5):547–57. Doi: 10.1097/00042737-200505000-00012.

11. Andrews C., McLean MH., Durum SK. Cytokine Tuning of Intestinal Epithelial

Function. *Front Immunol* 2018;**9**(JUN):1270. Doi: 10.3389/fimmu.2018.01270.

12. Epel D., Luckenbach T., Stevenson CN., Macmanus-Spencer LA., Hamdoun A., Smital T. EFFLUX TRANSPORTERS: Newly Appreciated Roles in Protection against Pollutants: Cellular "bouncers" help keep toxicants out of cells, but anthropogenic chemicals can circumvent or overwhelm this defense. *Environ Sci Technol* 2008;**42**(11):3914–20.

13. Coutant DE., Hall SD. Disease-Drug Interactions in Inflammatory States via Effects on CYP-Mediated Drug Clearance. *J Clin Pharmacol* 2018;**58**(7):849–63. Doi: 10.1002/jcph.1093.

14. Morgan E. Impact of Infectious and Inflammatory Disease on Cytochrome P450–Mediated Drug Metabolism and Pharmacokinetics. *Clin Pharmacol Ther* 2009;**85**(4):434–8. Doi: 10.1038/clpt.2008.302.

15. Jahnel J., Fickert P., Hauer AC., Högenauer C., Avian A., Trauner M. Inflammatory Bowel Disease Alters Intestinal Bile Acid Transporter Expression. *Drug Metab Dispos* 2014;**42**(9):1423–31. Doi: 10.1124/dmd.114.058065.

16. Wilson A., Urquhart BL., Ponich T., Chande N., Gregor JC., Beaton M., et al. Crohn's Disease Is Associated with Decreased CYP3A4 and P-Glycoprotein Protein Expression. *Mol Pharm* 2019;**16**(9):4059–64. Doi: 10.1021/acs.molpharmaceut.9b00459.

17. Wojtal KA., Eloranta JJ., Hruz P., Gutmann H., Drewe J., Staumann A., et al. Changes in mRNA Expression Levels of Solute Carrier Transporters in Inflammatory Bowel Disease Patients. *Drug Metab Dispos* 2009;**37**(9):1871–7. Doi: 10.1124/dmd.109.027367.

18. Blokzijl H., Borght S Vander., Bok LIH., Libbrecht L., Geuken M., van den Heuvel FAJ., et al. Decreased P-glycoprotein (P-gp/MDR1) expression in inflamed human intestinal epithelium is independent of PXR protein levels. *Inflamm Bowel Dis* 2007;**13**(6):710–20. Doi: 10.1002/ibd.20088.

19. Jung D. Human ileal bile acid transporter gene ASBT (SLC10A2) is transactivated by the glucocorticoid receptor. *Gut* 2004;**53**(1):78–84. Doi: 10.1136/gut.53.1.78.

20. El-Khateeb E., Vasilogianni A-M., Alrubia S., Al-Majdoub ZM., Couto N., Howard M., et al. Quantitative mass spectrometry-based proteomics in the era of model-informed drug development: Applications in translational pharmacology and recommendations for best practice. *Pharmacol Ther* 2019;**203**:107397. Doi: 10.1016/j.pharmthera.2019.107397.

21. Thörn M., Finnström N., Lundgren S., Rane A., Lööf L. Expression of cytochrome P450 and MDR1 in patients with proctitis. *Ups J Med Sci* 2007;**112**(3):303–12. Doi: 10.3109/2000-1967-203.

22. Plewka D., Plewka A., Szczepanik T., Morek M., Bogunia E., Wittek P., et al. Expression of selected cytochrome P450 isoforms and of cooperating enzymes in colorectal tissues in selected pathological conditions. *Pathol - Res Pract* 2014;**210**(4):242–9. Doi: 10.1016/j.prp.2013.12.010.

23. Thibault R., De Coppet P., Daly K., Bourreille A., Cuff M., Bonnet C., et al. Down-Regulation of the Monocarboxylate Transporter 1 Is Involved in Butyrate Deficiency During Intestinal Inflammation. *Gastroenterology* 2007;**133**(6):1916–27. Doi: 10.1053/j.gastro.2007.08.041.

24. Blokzijl H., van Steenpaal A., Borght S Vander., Bok LIH., Libbrecht L., Tamminga M., et al. Up-regulation and Cytoprotective Role of Epithelial Multidrug Resistance-associated Protein 1 in Inflammatory Bowel Disease. *J Biol Chem* 2008;**283**(51):35630–7. Doi: 10.1074/jbc.M804374200.

25. Langmann T., Moehle C., Mauerer R., Scharl M., Liebisch G., Zahn A., et al. Loss of detoxification in inflammatory bowel disease: dysregulation of pregnane X receptor target genes. *Gastroenterology* 2004;**127**(1):26–40. Doi: 10.1053/j.gastro.2004.04.019.

26. Silva J., Brito BS., Silva IN de N., Nóbrega VG., da Silva MCSM., Gomes HDDN., et al. Frequency of Hepatobiliary Manifestations and Concomitant Liver Disease in Inflammatory Bowel Disease Patients. *Biomed Res Int* 2019;**2019**:7604939. Doi: 10.1155/2019/7604939.

27. Masubuchi Y., Horie T. Endotoxin-mediated disturbance of hepatic cytochrome P450 function and development of endotoxin tolerance in the rat model of dextran sulfate sodium-induced experimental colitis. *Drug Metab Dispos* 2004;**32**(4):437–41. Doi: 10.1124/dmd.32.4.437.

28. Chaluvadi MR., Nyagode BA., Kinloch RD., Morgan ET. TLR4-dependent and -independent regulation of hepatic cytochrome P450 in mice with chemically induced inflammatory bowel disease. *Biochem Pharmacol* 2009;**77**(3):464–71. Doi: 10.1016/j.bcp.2008.10.029.

29. Ricci G., Ambrosi A., Resca D., Masotti M., Alvisi V. Comparison of serum total sialic acid, C-reactive protein, α1-acid glycoprotein and β2-microglobulin in patients with non-malignant bowel diseases. *Biomed Pharmacother* 1995;**49**(5):259–62. Doi: 10.1016/0753-3322(96)82632-1.

30. Suzuki Y., Matsui T., Ito H., Ashida T., Nakamura S., Motoya S., et al. Circulating Interleukin 6 and Albumin, and Infliximab Levels Are Good Predictors of Recovering Efficacy After Dose Escalation Infliximab Therapy in Patients with Loss of Response to Treatment for Crohn's Disease. *Inflamm Bowel Dis* 2015;**21**(9):2114–22. Doi: 10.1097/MIB.0000000000000475.

31. Liu X., Wu X., Zhou C., Hu T., Ke J., Chen Y., et al. Preoperative hypoalbuminemia is

associated with an increased risk for intra-abdominal septic complications after primary anastomosis for Crohn's disease. *Gastroenterol Rep* 2017;**5**(4):298–304. Doi: 10.1093/gastro/gox002.

32. Nguyen GC., Du L., Chong RY., Jackson TD. Hypoalbuminaemia and Postoperative Outcomes in Inflammatory Bowel Disease: the NSQIP Surgical Cohort. *J Crohn's Colitis* 2019;**13**(11):1433–8. Doi: 10.1093/ecco-jcc/jjz083.

33. Bhatt DK., Gaedigk A., Pearce RE., Leeder JS., Prasad B. Age-dependent protein abundance of cytosolic alcohol and aldehyde dehydrogenases in human liver. *Drug Metab Dispos* 2017;**45**(9):1044–8. Doi: 10.1124/dmd.117.076463.

34. Boberg M., Vrana M., Mehrotra A., Pearce RE., Gaedigk A., Bhatt DK., et al. Age-dependent absolute abundance of hepatic carboxylesterases (CES1 and CES2) by LC-MS/MS proteomics: Application to PBPK modeling of oseltamivir in vivo pharmacokinetics in infants. *Drug Metab Dispos* 2017;**45**(2):216–23. Doi: 10.1124/dmd.116.072652.

35. Bhatt DK., Mehrotra A., Gaedigk A., Chapa R., Basit A., Zhang H., et al. Age- and Genotype-Dependent Variability in the Protein Abundance and Activity of Six Major Uridine Diphosphate-Glucuronosyltransferases in Human Liver. *Clin Pharmacol Ther* 2019;**105**(1):131–41. Doi: 10.1002/cpt.1109.

36. Ladumor MK., Bhatt DK., Gaedigk A., Sharma S., Thakur A., Pearce RE., et al. Ontogeny of hepatic sulfotransferases and prediction of age-dependent fractional contribution of sulfation in acetaminophen metabolism. *Drug Metab Dispos* 2019;**47**(8):818–31. Doi: 10.1124/dmd.119.086462.

37. Song G., Sun X., Hines RN., McCarver DG., Lake BG., Osimitz TG., et al. Determination of human hepatic CYP2C8 and CYP1A2 age-dependent expression to support human health risk assessment for early ages. *Drug Metab Dispos* 2017;**45**(5):468–75. Doi: 10.1124/dmd.116.074583.

38. Wolbold R., Klein K., Burk O., Nüssler AK., Neuhaus P., Eichelbaum M., et al. Sex is a major determinant of CYP3A4 expression in human liver. *Hepatology* 2003;**38**(4):978–88. Doi: 10.1053/jhep.2003.50393.

39. Prasad B., Lai Y., Lin Y., Unadkat JD. Interindividual Variability in the Hepatic Expression of the Human Breast Cancer Resistance Protein (BCRP/ABCG2): Effect of Age, Sex, and Genotype. *J Pharm Sci* 2013;**102**(3):787–93. Doi: 10.1002/jps.23436.

40. Prasad B., Evers R., Gupta A., Hop CECA., Salphati L., Shukla S., et al. Interindividual Variability in Hepatic Organic Anion-Transporting Polypeptides and P-Glycoprotein (ABCB1) Protein Expression: Quantification by Liquid Chromatography Tandem Mass Spectroscopy and Influence of Genotype, Age, and Sex. *Drug Metab Dispos* 2014;**42**(1):78–88. Doi: 10.1124/dmd.113.053819.

41. Couto N., Al-Majdoub ZM., Gibson S., Davies PJ., Achour B., Harwood MD., et al. Quantitative Proteomics of Clinically Relevant Drug-Metabolizing Enzymes and Drug Transporters and Their Intercorrelations in the Human Small Intestine. *Drug Metab Dispos* 2020;**48**(4):245–54. Doi: 10.1124/dmd.119.089656.

42. Miyauchi E., Tachikawa M., Declèves X., Uchida Y., Bouillot JL., Poitou C., et al. Quantitative Atlas of Cytochrome P450, UDP-Glucuronosyltransferase, and Transporter Proteins in Jejunum of Morbidly Obese Subjects. *Mol Pharm* 2016;**13**(8):2631–40. Doi: 10.1021/acs.molpharmaceut.6b00085.

43. Effinger A., O'Driscoll CM., McAllister M., Fotaki N. Predicting budesonide performance in healthy subjects and patients with Crohn's disease using biorelevant in vitro dissolution testing and PBPK modeling. *Eur J Pharm Sci* 2020:105617. Doi: 10.1016/j.ejps.2020.105617.

44. Erdmann P., Bruckmueller H., Martin P., Busch D., Haenisch S., Müller J., et al. Dysregulation of Mucosal Membrane Transporters and Drug-Metabolizing Enzymes in Ulcerative Colitis. *J Pharm Sci* 2019. Doi: 10.1016/j.xphs.2018.09.024.

45. Girardin M., Dionne S., Goyette P., Rioux J., Bitton A., Elimrani I., et al. Expression and functional analysis of intestinal organic cation/l-carnitine transporter (OCTN) in Crohn's Disease. *J Crohn's Colitis* 2012;**6**(2):189–97. Doi: 10.1016/j.crohns.2011.08.003.

46. Harwood MD., Achour B., Russell MR., Carlson GL., Warhurst G., Rostami-Hodjegan A. Application of an LC-MS/MS method for the simultaneous quantification of human intestinal transporter proteins absolute abundance using a QconCAT technique. *J Pharm Biomed Anal* 2015;**110**:27–33. Doi: 10.1016/j.jpba.2015.02.043.

47. El-Khateeb E., Al-Majdoub ZM., Rostami-Hodjegan A., Barber J., Achour B. Proteomic Quantification of Changes in Abundance of Drug-Metabolizing Enzymes and Drug Transporters in Human Liver Cirrhosis: Different Methods, Similar Outcomes. *Drug Metab Dispos* 2021;**49**(8):610–8. Doi: 10.1124/dmd.121.000484.

48. Al Feteisi H., Al-Majdoub ZM., Achour B., Couto N., Rostami-Hodjegan A., Barber J. Identification and quantification of blood-brain barrier transporters in isolated rat brain microvessels. *J Neurochem* 2018;**146**(6):670–85. Doi: 10.1111/jnc.14446.

49. Al-Majdoub ZM., Al Feteisi H., Achour B., Warwood S., Neuhoff S., Rostami-Hodjegan A., et al. Proteomic Quantification of Human Blood–Brain Barrier SLC and ABC Transporters in Healthy Individuals and Dementia Patients. *Mol Pharm* 2019;**16**(3):1220–33. Doi: 10.1021/acs.molpharmaceut.8b01189.

50. Pharmacology C. Entocort EC. *Metab Clin Exp* 2005:3–17.

51. Han D-G., Kwak J., Seo S-W., Kim J-M., Yoo J-W., Jung Y., et al. Pharmacokinetic

Evaluation of Metabolic Drug Interactions between Repaglinide and Celecoxib by a Bioanalytical HPLC Method for Their Simultaneous Determination with Fluorescence Detection. *Pharmaceutics* 2019;**11**(8):382. Doi: 10.3390/pharmaceutics11080382.

52. Zhao D., Chen J., Chu M., Long X., Wang J. Pharmacokinetic-Based Drug-Drug Interactions with Anaplastic Lymphoma Kinase Inhibitors: A Review. *Drug Des Devel Ther* 2020;**14**:1663–81. Doi: 10.2147/DDDT.S249098.

53. Iisalo E. Clinical Pharmacokinetics of Digoxin. *Clin Pharmacokinet* 1977;**2**(1):1–16. Doi: 10.2165/00003088-197702010-00001.

54. Blech S., Ebner T., Ludwig-Schwellinger E., Stangier J., Roth W. The Metabolism and Disposition of the Oral Direct Thrombin Inhibitor, Dabigatran, in Humans. *Drug Metab Dispos* 2008;**36**(2):386–99. Doi: 10.1124/dmd.107.019083.

55. Hamberger C., Barre J., Zini R., Taiclet A., Houin G., Tillement JP. In vitro binding study of gemfibrozil to human serum proteins and erythrocytes: Interactions with other drugs. *Int J Clin Pharmacol Res* 1986;**6**(6):441–9.

56. Allonen H., Ziegler G., Klotz U. Midazolam kinetics. *Clin Pharmacol Ther* 1981;**30**(5):653–61. Doi: 10.1038/clpt.1981.217.

57. Quion A V., Jones PH. Clinical Pharmacokinetics of Pravastatin. *Clin Pharmacokinet* 1994;**27**(2):94–103. Doi: 10.2165/00003088-199427020-00002.

58. Patterson KB., Dumond JB., Prince HA., Jenkins AJ., Scarsi KK., Wang R., et al. Protein Binding of Lopinavir and Ritonavir During 4 Phases of Pregnancy. *JAIDS J Acquir Immune Defic Syndr* 2013;**63**(1):51–8. Doi: 10.1097/QAI.0b013e31827fd47e.

59. Martin P. Absolute oral bioavailability of rosuvastatin in healthy white adult male volunteers. *Clin Ther* 2003;**25**(10):2553–63. Doi: 10.1016/S0149-2918(03)80316-8.

60. Wu Q., Wang X., Chen Q., Zou Y., Xu X., Li T., et al. Pharmacokinetics and Bioequivalence of Two Formulations of Valsartan 80 mg Capsules: A Randomized, Single Dose, 4-Period Crossover Study in Healthy Chinese Volunteers Under Fasting and Fed Conditions. *Drug Des Devel Ther* 2020;**14**:4221–30. Doi: 10.2147/DDDT.S253078.

61. Keefe DL., Yee Y-G., Kates RE. Verapamil protein binding in patients and in normal subjects. *Clin Pharmacol Ther* 1981;**29**(1):21–6. Doi: 10.1038/clpt.1981.4.

62. Jamei M., Marciniak S., Feng K., Barnett A., Tucker G., Rostami-Hodjegan A. The Simcyp ® Population-based ADME Simulator. *Expert Opin Drug Metab Toxicol* 2009;**5**(2):211–23. Doi: 10.1517/17425250802691074.

63. Cappello M., Randazzo C., Bravatà I., Licata A., Peralta S., Craxì A., et al. Liver Function Test Abnormalities in Patients with Inflammatory Bowel Diseases: A Hospital-

based Survey. *Clin Med Insights Gastroenterol* 2014;**7**:CGast.S13125. Doi: 10.4137/CGast.S13125.

64. Press AG., Hauptmann IA., Hauptmann L., Fuchs B., Fuchs M., Ewe K., et al. Gastrointestinal pH profiles in patients with inflammatory bowel disease. *Aliment Pharmacol Ther* 1998;**12**(7):673–8. Doi: 10.1046/j.1365-2036.1998.00358.x.

65. van Oostayen J. Diagnosis of Crohn's ileitis and monitoring of disease activity: value of Doppler ultrasound of superior mesenteric artery flow. *Am J Gastroenterol* 1998;**93**(1):88–91. Doi: 10.1016/S0002-9270(97)00029-4.

66. Yekeler E., Danalioglu A., Movasseghi B., Yilmaz S., Karaca C., Kaymakoglu S., et al. Crohn disease activity evaluated by Doppler ultrasonography of the superior mesenteric artery and the affected small-bowel segments. *J Ultrasound Med* 2005;**24**(1):59–65. Doi: 10.7863/jum.2005.24.1.59.

67. Hultén L., Lindhagen J., Lundgren O., Fasth S., Ahrén C. Regional intestinal blood flow in ulcerative colitis and Crohn's disease. *Gastroenterology* 1977;**72**(3):388–96. Doi: 10.1016/S0016-5085(77)80245-X.

68. Di Sabatino A., Fulle I., Ciccocioppo R., Ricevuti L., Tinozzi FP., Tinozzi S., et al. Doppler Enhancement After Intravenous Levovist Injection in Crohn's Disease. *Inflamm Bowel Dis* 2002;**8**(4):251–7. Doi: 10.1097/00054725-200207000-00003.

69. Vagianos K., Bector S., McConnell J., Bernstein CN. Nutrition Assessment of Patients With Inflammatory Bowel Disease. *J Parenter Enter Nutr* 2007;**31**(4):311–9. Doi: 10.1177/0148607107031004311.

70. Zanger UM., Schwab M. Cytochrome P450 enzymes in drug metabolism: Regulation of gene expression, enzyme activities, and impact of genetic variation. *Pharmacol Ther* 2013;**138**(1):103–41. Doi: 10.1016/j.pharmthera.2012.12.007.

71. Jönsson G., Aström A., Andersson P. Budesonide is metabolized by cytochrome P450 3A (CYP3A) enzymes in human liver. *Drug Metab Dispos* 1995;**23**(1):137–42.

72. Varis T., Kivistö KT., Neuvonen PJ. The effect of itraconazole on the pharmacokinetics and pharmacodynamics of oral prednisolone. *Eur J Clin Pharmacol* 2000;**56**(1):57–60. Doi: 10.1007/s002280050720.

73. Targownik LE., Nugent Z., Singh H., Bernstein CN. Prevalence of and Outcomes Associated with Corticosteroid Prescription in Inflammatory Bowel Disease. *Inflamm Bowel Dis* 2014;**20**(4):622–30. Doi: 10.1097/MIB.0000000000000008.

74. Paine MF., Hart HL., Ludington SS., Haining RL., Rettie AE., Zeldin DC. THE HUMAN INTESTINAL CYTOCHROME P450 "PIE." *Drug Metab Dispos* 2006;**34**(5):880–6. Doi: 10.1124/dmd.105.008672.

75. Strober W., Fuss IJ. Proinflammatory Cytokines in the Pathogenesis of Inflammatory Bowel Diseases. *Gastroenterology* 2011;**140**(6):1756-1767.e1. Doi: 10.1053/j.gastro.2011.02.016.

76. Bertilsson PM., Olsson P., Magnusson K-E. Cytokines influence mRNA expression of cytochrome P450 3A4 and MDRI in intestinal cells. *J Pharm Sci* 2001;**90**(5):638–46. Doi: 10.1002/1520-6017(200105)90:5<638::AID-JPS1020>3.0.CO;2-L.

77. Iwamoto J., Saito Y., Honda A., Miyazaki T., Ikegami T., Matsuzaki Y. Bile Acid Malabsorption Deactivates Pregnane X Receptor in Patients with Crohn's Disease. *Inflamm Bowel Dis* 2013;**19**(6):1278–84. Doi: 10.1097/MIB.0b013e318281f423.

78. Aitken AE., Richardson TA., Morgan ET. REGULATION OF DRUG-METABOLIZING ENZYMES AND TRANSPORTERS IN INFLAMMATION. *Annu Rev Pharmacol Toxicol* 2006;**46**(1):123–49. Doi: 10.1146/annurev.pharmtox.46.120604.141059.

79. Edsbäcker S., Bengtsson B., Larsson P., Lundin P., Nilsson Å., Ulmius J., et al. A pharmacoscintigraphic evaluation of oral budesonide given as controlled-release (Entocort) capsules. *Aliment Pharmacol Ther* 2003;**17**(4):525–36. Doi: 10.1046/j.1365-2036.2003.01426.x.

80. Congiu M., Mashford ML., Slavin JL., Desmond P V. UDP Glucuronosyltransferase mRNA Levels in Human Liver Disease. *Drug Metab Dispos* 2002;**30**(2):129–34. Doi: 10.1124/dmd.30.2.129.

81. Shimada M., Watanabe E., Iida Y., Nagata K., Yamazoe Y. Alteration of Hepatic Sulfation by Endotoxin. *Jpn J Pharmacol* 1999;**80**(4):371–4. Doi: 10.1254/jjp.80.371.

82. Barbier O., Duran-Sandoval D., Pineda-Torra I., Kosykh V., Fruchart J-C., Staels B. Peroxisome Proliferator-activated Receptor α Induces Hepatic Expression of the Human Bile Acid Glucuronidating UDP-glucuronosyltransferase 2B4 Enzyme *. *J Biol Chem* 2003;**278**(35):32852–60. Doi: 10.1074/JBC.M305361200.

83. Barbier O., Girard H., Inoue Y., Duez H., Villeneuve L., Kamiya A., et al. Hepatic Expression of the UGT1A9 Gene Is Governed by Hepatocyte Nuclear Factor 4α. *Mol Pharmacol* 2005;**67**(1):241–9. Doi: 10.1124/MOL.104.003863.

84. Song CS., Jung MH., Kim SC., Hassan T., Roy AK., Chatterjee B. Tissue-specific and Androgen-repressible Regulation of the Rat Dehydroepiandrosterone Sulfotransferase Gene Promoter. *J Biol Chem* 1998;**273**(34):21856–66. Doi: 10.1074/jbc.273.34.21856.

85. Alonen A., Finel M., Kostiainen R. The human UDP-glucuronosyltransferase UGT1A3 is highly selective towards N2 in the tetrazole ring of losartan, candesartan, and zolarsartan. *Biochem Pharmacol* 2008;**76**(6):763–72. Doi: 10.1016/j.bcp.2008.07.006.

86. Tripathi SP., Prajapati R., Verma N., Sangamwar AT. Predicting substrate selectivity between UGT1A9 and UGT1A10 using molecular modelling and molecular dynamics approach. *Mol Simul* 2016;**42**(4):270–88. Doi: 10.1080/08927022.2015.1044451.

87. Gamage N., Barnett A., Hempel N., Duggleby RG., Windmill KF., Martin JL., et al. Human Sulfotransferases and Their Role in Chemical Metabolism. *Toxicol Sci* 2006;**90**(1):5–22. Doi: 10.1093/toxsci/kfj061.

88. Hebbring SJ., Moyer AM., Weinshilboum RM. Sulfotransferase gene copy number variation: Pharmacogenetics and function. *Cytogenet Genome Res* 2009;**123**(1–4):205–10. Doi: 10.1159/000184710.

89. Wright S. Clinical significance of azathioprine active metabolite concentrations in inflammatory bowel disease. *Gut* 2004;**53**(8):1123–8. Doi: 10.1136/gut.2003.032896.

90. Herfarth HH., Kappelman MD., Long MD., Isaacs KL. Use of Methotrexate in the Treatment of Inflammatory Bowel Diseases. *Inflamm Bowel Dis* 2016;**22**(1):224–33. Doi: 10.1097/MIB.0000000000000589.

91. Choughule K V., Barnaba C., Joswig-Jones CA., Jones JP. In Vitro Oxidative Metabolism of 6-Mercaptopurine in Human Liver: Insights into the Role of the Molybdoflavoenzymes Aldehyde Oxidase, Xanthine Oxidase, and Xanthine Dehydrogenase. *Drug Metab Dispos* 2014;**42**(8):1334–40. Doi: 10.1124/dmd.114.058107.

92. Lennard L., Van Loon JA., Weinshilboum RM. Pharmacogenetics of acute azathioprine toxicity: Relationship to thiopurine methyltransferase genetic polymorphism. *Clin Pharmacol Ther* 1989;**46**(2):149–54. Doi: 10.1038/clpt.1989.119.

93. Nguyen CM., Mendes MAS., Ma JD. Thiopurine methyltransferase (TPMT) genotyping to predict myelosuppression risk. *PLoS Curr* 2011;**3**:RRN1236. Doi: 10.1371/currents.RRN1236.

94. Chaparro M., Ordás I., Cabré E., Garcia-Sanchez V., Bastida G., Peñalva M., et al. Safety of Thiopurine Therapy in Inflammatory Bowel Disease. *Inflamm Bowel Dis* 2013;**19**(7):1404–10. Doi: 10.1097/MIB.0b013e318281f28f.

95. Koukouritaki SB., Simpson P., Yeung CK., Rettie AE., Hines RN. Human Hepatic Flavin-Containing Monooxygenases 1 (FMO1) and 3 (FMO3) Developmental Expression. *Pediatr Res* 2002;**51**(2):236–43. Doi: 10.1203/00006450-200202000-00018.

96. Rossner R., Kaeberlein M., Leiser SF. Flavin-containing monooxygenases in aging and disease: Emerging roles for ancient enzymes. *J Biol Chem* 2017;**292**(27):11138–46. Doi: 10.1074/jbc.R117.779678.

97. Majano PL., García-Monzón C., López-Cabrera M., Lara-Pezzi E., Fernández-Ruiz E., García-Iglesias C., et al. Inducible nitric oxide synthase expression in chronic viral hepatitis. Evidence for a virus-induced gene upregulation. *J Clin Invest* 1998;**101**(7):1343–52. Doi: 10.1172/JCI774.

98. Ryu S-D., Yi H-G., Cha Y-N., Kang J-H., Kang J-S., Jeon Y-C., et al. Flavin-containing monooxygenase activity can be inhibited by nitric oxide-mediated S-nitrosylation. *Life Sci* 2004;**75**(21):2559–72. Doi: 10.1016/j.lfs.2004.05.018.

99. Ma J., Yoshimura M., Yamashita E., Nakagawa A., Ito A., Tsukihara T. Structure of Rat Monoamine Oxidase A and Its Specific Recognitions for Substrates and Inhibitors. *J Mol Biol* 2004;**338**(1):103–14. Doi: 10.1016/j.jmb.2004.02.032.

100. Mawhinney M., Cole D., Azzaro AJ. Daily transdermal administration of selegiline to guinea-pigs preferentially inhibits monoamine oxidase activity in brain when compared with intestinal and hepatic tissues. *J Pharm Pharmacol* 2003;**55**(1):27–34. Doi: 10.1111/j.2042-7158.2003.tb02430.x.

101. Clarke A., Johnson ES., Mallard N., Corn TH., Johnston A., Boyce M., et al. A new low-dose formulation of selegiline: clinical efficacy, patient preference and selectivity for MAO-B inhibition. *J Neural Transm* 2003;**110**(11):1257–71. Doi: 10.1007/s00702-003-0042-6.

102. Finberg JPM., Rabey JM. Inhibitors of MAO-A and MAO-B in Psychiatry and Neurology. *Front Pharmacol* 2016;**7**(OCT):340. Doi: 10.3389/fphar.2016.00340.

103. Hein DW. Molecular genetics and function of NAT1 and NAT2: role in aromatic amine metabolism and carcinogenesis. *Mutat Res* 2002;**506**–**507**:65–77. Doi: 10.1016/s0027-5107(02)00153-7.

104. Akobeng AK., Zhang D., Gordon M., MacDonald JK. Oral 5-aminosalicylic acid for maintenance of medically-induced remission in Crohn's disease. *Cochrane Database Syst Rev* 2016;**9**(9):CD003715. Doi: 10.1002/14651858.CD003715.pub3.

105. Gionchetti P., Campieri M., Belluzzi A., Boschi S., Brignola C., Miglioli M., et al. Bioavailability of single and multiple doses of a new oral formulation of 5-ASA in patients with inflammatory bowel disease and healthy volunteers. *Aliment Pharmacol Ther* 1994;**8**(5):535–40. Doi: 10.1111/j.1365-2036.1994.tb00327.x.

106. van Helvoort A., Smith AJ., Sprong H., Fritzsche I., Schinkel AH., Borst P., et al. MDR1 P-Glycoprotein Is a Lipid Translocase of Broad Specificity, While MDR3 P-Glycoprotein Specifically Translocates Phosphatidylcholine. *Cell* 1996;**87**(3):507–17. Doi: 10.1016/S0092-8674(00)81370-7.

107. Chen G., Durán GE., Steger KA., Lacayo NJ., Jaffrézou J-P., Dumontet C., et al. Multidrug-resistant Human Sarcoma Cells with a Mutant P-Glycoprotein, Altered

Phenotype, and Resistance to Cyclosporins. *J Biol Chem* 1997;**272**(9):5974–82. Doi: 10.1074/jbc.272.9.5974.

108. Robey RW., Polgar O., Deeken J., To KW., Bates SE. ABCG2: determining its relevance in clinical drug resistance. *Cancer Metastasis Rev* 2007;**26**(1):39–57. Doi: 10.1007/s10555-007-9042-6.

109. Vijay N., Morris M. Role of Monocarboxylate Transporters in Drug Delivery to the Brain. *Curr Pharm Des* 2014;**20**(10):1487–98. Doi: 10.2174/13816128113199990462.

110. Foley D., Rajamanickam J., Bailey P., Meredith D. Bioavailability Through PepT1: The Role of Computer Modelling in Intelligent Drug Design. *Curr Comput Aided-Drug Des* 2010;**6**(1):68–78. Doi: 10.2174/157340910790980133.

111. Cressman AM., Petrovic V., Piquette-Miller M. Inflammation-mediated changes in drug transporter expression/activity: Implications for therapeutic drug response. *Expert Rev Clin Pharmacol* 2012:69–89. Doi: 10.1586/ecp.11.66.

112. Lee G., Piquette-Miller M. Cytokines Alter the Expression and Activity of the Multidrug Resistance Transporters in Human Hepatoma Cell Lines; Analysis Using RT-PCR and cDNA Microarrays. *J Pharm Sci* 2003;**92**(11):2152–63. Doi: 10.1002/jps.10493.

113. Shah YM., Ma X., Morimura K., Kim I., Gonzalez FJ. Pregnane X receptor activation ameliorates DSS-induced inflammatory bowel disease via inhibition of NF-κB target gene expression. *Am J Physiol Liver Physiol* 2007;**292**(4):G1114–22. Doi: 10.1152/ajpgi.00528.2006.

114. Melillo N., Darwich AS., Magni P., Rostami-Hodjegan A. Accounting for inter-correlation between enzyme abundance: a simulation study to assess implications on global sensitivity analysis within physiologically-based pharmacokinetics. *J Pharmacokinet Pharmacodyn* 2019;**46**(2):137–54. Doi: 10.1007/s10928-019-09627-6.

115. Doki K., Darwich AS., Achour B., Tornio A., Backman JT., Rostami-Hodjegan A. Implications of intercorrelation between hepatic CYP3A4-CYP2C8 enzymes for the evaluation of drug-drug interactions: a case study with repaglinide. *Br J Clin Pharmacol* 2018;**84**(5):972–86. Doi: 10.1111/bcp.13533.

116. Urquhart BL., Tirona RG., Kim RB. Nuclear Receptors and the Regulation of Drug-Metabolizing Enzymes and Drug Transporters: Implications for Interindividual Variability in Response to Drugs. *J Clin Pharmacol* 2007;**47**(5):566–78. Doi: 10.1177/0091270007299930.

117. Runge-Morris M., Kocarek TA., Falany CN. Regulation of the cytosolic sulfotransferases by nuclear receptors. *Drug Metab Rev* 2013;**45**(1):15–33. Doi: 10.3109/03602532.2012.748794.

118. Radović B., Hussong R., Gerhäuser C., Meinl W., Frank N., Becker H., et al. Xanthohumol, a prenylated chalcone from hops, modulates hepatic expression of genes involved in thyroid hormone distribution and metabolism. *Mol Nutr Food Res* 2010;**54**(S2):S225–35. Doi: 10.1002/mnfr.200900489.

119. Hwang-Verslues WW., Sladek FM. HNF4α—role in drug metabolism and potential drug target? *Curr Opin Pharmacol* 2010;**10**(6):698–705. Doi: 10.1016/j.coph.2010.08.010.

120. Westerink WMA., Schoonen WGEJ. Phase II enzyme levels in HepG2 cells and cryopreserved primary human hepatocytes and their induction in HepG2 cells. *Toxicol Vitr* 2007;**21**(8):1592–602. Doi: 10.1016/j.tiv.2007.06.017.

121. Maeda K., Ohno T., Igarashi S., Yoshimura T., Yamashiro K., Sakai M. Aldehyde oxidase 1 gene is regulated by Nrf2 pathway. *Gene* 2012;**505**(2):374–8. Doi: 10.1016/j.gene.2012.06.010.

122. Thimmulappa RK., Mai KH., Srisuma S., Kensler TW., Yamamoto M., Biswal S. Identification of Nrf2-regulated genes induced by the chemopreventive agent sulforaphane by oligonucleotide microarray. *Cancer Res* 2002;**62**(18):5196–203.

123. Tonelli C., Chio IIC., Tuveson DA. Transcriptional Regulation by Nrf2. *Antioxid Redox Signal* 2018;**29**(17):1727–45. Doi: 10.1089/ars.2017.7342.

124. Al-Majdoub ZM., Couto N., Achour B., Harwood MD., Carlson G., Warhurst G., et al. Quantification of Proteins Involved in Intestinal Epithelial Handling of Xenobiotics. *Clin Pharmacol Ther* 2021;**109**(4):1136–46. Doi: 10.1002/cpt.2097.

125. Feagan BG., Rochon J., Fedorak RN., Irvine EJ., Wild G., Sutherland L., et al. Methotrexate for the Treatment of Crohn's Disease. *N Engl J Med* 1995;**332**(5):292–7. Doi: 10.1056/NEJM199502023320503.

126. Hanauer SB., Feagan BG., Lichtenstein GR., Mayer LF., Schreiber S., Colombel JF., et al. Maintenance infliximab for Crohn's disease: the ACCENT I randomised trial. *Lancet* 2002;**359**(9317):1541–9. Doi: 10.1016/S0140-6736(02)08512-4.

127. Ternant D., Berkane Z., Picon L., Gouilleux-Gruart V., Colombel J-F., Allez M., et al. Assessment of the Influence of Inflammation and FCGR3A Genotype on Infliximab Pharmacokinetics and Time to Relapse in Patients with Crohn's Disease. *Clin Pharmacokinet* 2015;**54**(5):551–62. Doi: 10.1007/s40262-014-0225-3.

128. Rosario M., Dirks NL., Milch C., Parikh A., Bargfrede M., Wyant T., et al. A Review of the Clinical Pharmacokinetics, Pharmacodynamics, and Immunogenicity of Vedolizumab. *Clin Pharmacokinet* 2017;**56**(11):1287–301. Doi: 10.1007/s40262-017-0546-0.

129. Chouchana L., Narjoz C., Beaune P., Loriot M-A., Roblin X. Review article: the benefits of pharmacogenetics for improving thiopurine therapy in inflammatory bowel disease. *Aliment Pharmacol Ther* 2012;**35**(1):15–36. Doi: 10.1111/j.1365-2036.2011.04905.x.

130. Lundin P., Naber T., Nilsson M., Edsbacker S. Effect of food on the pharmacokinetics of budesonide controlled ileal release capsules in patients with active Crohn's disease. *Aliment Pharmacol Ther* 2001. Doi: 10.1046/j.1365-2036.2001.00910.x.

131. Lundin PDP., Edsbäcker S., Bergstrand M., Ejderhamn J., Linander H., Högberg L., et al. Pharmacokinetics of budesonide controlled ileal release capsules in children and adults with active Crohn's disease. *Aliment Pharmacol Ther* 2003. Doi: 10.1046/j.1365-2036.2003.01386.x.

132. Greenberg GR., Feagan BG., Martin F., Sutherland LR., Thomson A., Williams CN., et al. Oral Budesonide for Active Crohn's Disease. *N Engl J Med* 1994;**331**(13):836–41. Doi: 10.1056/NEJM199409293311303.

133. Tremaine WJ., Hanauer SB., Katz S., Winston BD., Levine JG., Persson T., et al. Budesonide Cir Capsules (Once Or Twice Daily Divided-Dose) in Active Crohn's Disease: A Randomized Placebo-Controlled Study in The United States. *Am J Gastroenterol* 2002;**97**(7):1748–54. Doi: 10.1111/j.1572-0241.2002.05835.x.

134. Jamei M., Turner D., Yang J., Neuhoff S., Polak S., Rostami-Hodjegan A., et al. Population-Based Mechanistic Prediction of Oral Drug Absorption. *AAPS J* 2009;**11**(2):225–37. Doi: 10.1208/s12248-009-9099-y.

135. SEEDHER N., BHATIA S. Reversible binding of celecoxib and valdecoxib with human serum albumin using fluorescence spectroscopic technique. *Pharmacol Res* 2006;**54**(2):77–84. Doi: 10.1016/j.phrs.2006.02.008.

136. Achour B., Al-Majdoub ZM., Grybos-Gajniak A., Lea K., Kilford P., Zhang M., et al. Liquid Biopsy Enables Quantification of the Abundance and Interindividual Variability of Hepatic Enzymes and Transporters. *Clin Pharmacol Ther* 2021;**109**(1):222–32. Doi: 10.1002/CPT.2102.

6.7.Supplementary material – Methodology

Table S6.1. Demographic and clinical details of Crohn's disease (CD) patients.

Sample ID	Tissues source	Gender	Age at surgery (year)	Ethnicity	Height (m)	Weight (kg)	BMI	Smoking	Drinking	Tissue classification	Medical history	Medication history
328a	Colon	Female	38	N/A	1.74	53	17.51	Yes (recent ex)	Yes occasionally	Diseased	Crohn's disease	Methotrexate 4 years ago
328b										Histologically normal		
1942a	Colon	Female	25	N/A	1.57	42	17.04		N/A	Diseased-Active CD with extensive ulceration	Crohn's diagnosed in 2003. Failure to all medications including adalimumab, infliximab, tacrolimus, vedolizumab, ustekinumab and anti-MAP therapy	Azathioprine
1942b										Histologically normal		
1940a	Ileum	Female	62	Caucasian-British	1.65	58.06	21.33	No	N/A	Diseased-Patchy mild to moderate transmural chronic	Bowel resection (2013), bile salt malabsorption, reflux	Ustekinumab, iron tablets, B12 injections, cholestyramine, omeprazole, azathioprine, fortisip
1940b										Histologically normal		

974	Colon	Male	18	N/A	1.8	55.2	17.04	No	No	Diseased	Crohn's disease, recently treated for latent Tuberculosis	Laxido, adalimumab, azathioprine
156	Colon	Male	39	Caucasian-Irish	1.8	111	34.26	No	Yes 25 units per week	Diseased	Crohn's disease, laprotomy (2005), reversal ileostomy (2005), gout wrist	Candesartan, salbutamol, luperamide, buscupan, mesalazine, allupurinol
1569	Colon	Female	31	Caucasian-British	1.65	74	27.18	Ex - stopped 6yrs ago. E-cig currently	No	Diseased	Anorectal strictoplasty (2016), c-section x2 (2008 & 2009), drainage of fistula (2006), rectal abscess (2005), abdominal pain, heart murmur (as child), heartburn (reflux), low BP, tonsillectomy, vit. D deficiency	Omeprazole, azathioprine
1265b	Colon	Male	46	Caucasian-British	1.84	110	32.14	Yes	N/A	Histologically normal	post-traumatic stress disorder, Crohn's disease with stricture formation (ileum)	Quetiapine, mirtazapine, co-codamol, zopiclone
1265a	Terminal Ileum									Diseased		

2055	Colon	Male	30	Pakistani	1.87	120	34.32	Cannabis for pain relief	N/A	Diseased	Anxiety, low mood	Loperamide, octasa
917	Ileum	Male	23	Caucasian-Irish	1.87	84.6	24.19	No	Occasionally	Diseased	Mild asthma, heartburn, ileal Crohn's disease	Prednisolone, ciprofloxacin, metronidazole, omeprazole, tramadol
304	Ileum	Female	27	Caucasian-British	N/A	78	N/A	Yes	No	Diseased	Terminal ileal Crohn's disease	Azathioprine, movicol, docusate sodium
844b	Colon	Female	51	N/A	1.62	61	23.24	N/A	N/A	Histologically normal	IBD, Ileal Crohn's disease	Seretide, folic acid
844a	Ileum									Diseased		
1004a	Ileum	Female	19	Caucasian-British	1.62	46	17.53	No	No	Diseased-mild CD	Ileal Crohn's disease	Azathioprine, adalimumab
1004b										Histologically normal		
2003a	Colon	Male	68	Caucasian-Irish	1.8	91.2	28.14	Ex	N/A	Diseased	Piles tied (2016), HTN, hypercholesterolaemia, heartburn, anaemia, diverticulitis, Crohn's	Amlodipine
2003b										Histologically normal		

N/A, No available information; BP, blood pressure; IBD, inflammatory bowel disease; HTN, hypertension.

Table S6.2. Demographic and clinical details of adenocarcinoma patients.

Sample ID	Tissues source	Gender	Age at surgery (year)	Ethnicity	Height (m)	Weight (kg)	BMI	Smoking	Drinking	Tissue classification	Medical history	Medication history
2097 (16502)	Ileum-Small bowel	Male	55	Caucasian-British	N/A	N/A	N/A	N/A	N/A	Normal (adenocarcinoma)	Metastatic Colon cancer (Moderately differentiated pT4a), Pulmonary embolism (resolved 2019)	No regular medications
2104 (16537)	Ileum-Small bowel	Female	79	Caucasian-British	1.58	71.6	28.7	No	Rarely	Normal (adenocarcinoma)	Caecal cancer (Moderate to poorly differentiated pT4a pN1a), HTN, Type 2 diabetes, acid reflux, hypercholesterolaemia, right knee replacement	Atorvastatin, bendroflumethiazide, lansoprazole, paracetamol, valsartan
2057 (16366)	Ileum-Small bowel	Female	88	Caucasian-Irish	1.49	65	29.3	N/A	N/A	Normal (adenocarcinoma)	Caecal cancer (Well differentiated pT3), Asthma, anaemia, right knee replacement,	Relvar inhaler, calcichew D3 forte, montelukast, bendroflumethiazid

											bilateral shoulder replacement, cholecystectomy, hypertension, back pain	e, ramipril, aspirin, ivabradine
2077 (16432)	Ileum-Small bowel	Female	59	Caucasian-British	1.63	88	33.1	N/A	N/A	Normal (adenocarcinoma)	Colon cancer (Moderately well differentiated pT1 pN1a), GORD, left breast lymphectomy, discectomy, fibromyalgia, colorectal polyps, osteoarthritis (hands and spine)	Omeprazole, celecoxib

N/A, No available information; HTN, hypertension; GORD, Gastro-oesophageal reflux disease.

Table S6.3. Demographic details of healthy subjects.

Sample ID	Tissues source	Gender	Age (year)	Ethnicity	Tissue classification	Cause of death	Post mortem interval (PMI) (hrs)
F-28	Colon, Descending	Female	50	Caucasian	Healthy	Car accident	4
208A	Colon, Transverse	Female	78	Caucasian	Healthy	Cardiovascular disease, unspecified	5
S3-13	Colon, Sigmoid	Male	30	Caucasian	Healthy	Car accident	4
S4-12	Colon, Descending	Male	30	Caucasian	Healthy	Car accident	4
M-28	Colon, Descending	Male	54	Caucasian	Healthy	Injuries in the abdomen	4
1C-10	Ileum	Male	33	Caucasian	Healthy	Traumatic injury	4
S13-20	Ileum	Male	48	Caucasian	Healthy	Mechanical trauma	1
S3-26	Ileum	Male	30	Caucasian	Healthy	Car accident	4
208A	Ileum	Female	78	Caucasian	Healthy	Cardiovascular disease, unspecified	5
90-12-23A	Ileum	Female	65	Caucasian	Healthy	Acute myocardial infarction	9

Table S6.4. Unique peptides sequences with highest intensity assigned to each DMET to quantify their levels in inflamed, histologically normal CD, histologically normal cancer and healthy samples based on Hi-N label-free methodology.

Protein target	Peptide sequence	Peptide sequence	Peptide sequence	Subcellular fraction localisation	Detected in ileum/colon
CYP1A2	IGSTPVLVLSR	YLPNPALQR		Endoplasmic reticulum, microsomes	Both
CYP20A1	NHGTVWSEIGK	LTPVSAQLQDIEGK	TFSSLGFSGTQECPELR		Both
CYP27A1	LYPVVPTNSR	IQHPFGSVPFGYGVR	DFAHMPLLK	Mitochondrion	Both
CYP51A1	EYFESWGESGEK	NEDLNAEDVYSR	CIGENFAYVQIK	Endoplasmic reticulum, microsomes	Both
CYP2C18	YIDLLPTNLPHAVTCDVK	SLTNFSK	EHQESLDMNSAR		Ileum
CYP2C19	NLAFMESDILEK	GHFPLAER			Ileum
CYP2D6	AFLTQLDELLTEHR	DIEVQGFRIPK			Ileum
CYP2S1	QVQQHQGNLDASGPAR	DLVDAFLLK	LLALVPMGIPR		Both
CYP3A4	VWGFYDGQQPVLAITDPDMIK	GFCMFDMECHK	GVVVMIPSYALHRDPK		Ileum
CYP3A5	DSIDPYIYTPFGTGPR	YWTEPEEFRPER			Ileum
CYP4F2	NWFWGHQGMVNPTEEGMR	VWMGPISPLLSLCHPDIIR			Both
CYP4F11	TLTQLVTTYPQGFK	ACHLVHDFTDAVIQER			Ileum
CYP4F12	TLPTQGIDDFFK	SYITIFNK	SITNASAAIAPK		Both
UGT1A1	DSAMLLSGCSHLLHNK	DGAFYTLK	ESFVSLGHNVFENDSFLQR	Endoplasmic reticulum membrane	Ileum
UGT1A10	TYSTSYTLEDQNR	GHEVVVVMPEVSWQLER			Both
UGT2A3	GHEVTVLTHSK	GAAVEINFK	ALGRPTTLCETVGK		Both

UGT2B7	TELENFIMQQIK	ANVIASALAQIPQK			Both
UGT2B17	WTYSISK	NDLEDFFMK	MFDRWTYSISK		Both
ALPI	QVPDSAATATAYLCGVK	IDHGHHEGVAYQALTEAVMFDDAIER	YEIHRDPTLDPSLMEMTEAALR	Plasma membrane	Ileum
AOX1	GLHGPLTLNSPLTPEK	LILNEVSLLGSAPGGK	VFFGEGDGIIR	Cytoplasm and Cytosol	Both
CES1	TVIGDHGDELFSVFGAPFLK	DAGAPTYMYEFQYRPSFSSDMK	TTTSAVMVHCLR	Endoplasmic reticulum	Both
CES2	APVYFYEFQHQPSWLK	SFFGGNYIK	FTEEEEQLSR		Both
EPHX1	EDDSIRPFK	ENLGQGWMTQK	EETLPLEDGWWGPGTR		Both
EPHX2	ILIPALMVTAEK	AVASLNTPFIPANPNMSPLESIK	ASDESVLSMHK		Both
FMO3	LVGPGQWPGAR	NNLPTAISDWLYVK	IQEYIIAFAK		Both
FMO5	KQPDFATSGQWEVVTESEGK	SVIINTSK	ALSQHPTLNDDLPNR		Both
MAOA	IFFAGTETATK	DVPAVEITHTFWER	EIPTDAPWEAQHADK	Mitochondrion membrane	Both
MAOB	HLPSVPGLLR	LERPVIYIDQTR	IMDLLGDRVK		Both
MGST1	VFANPEDCVAFGK	IYHTIAYLTPLPQPNR		Endoplasmic reticulum	Both
MGST2	VTPPAVTGSPEFER	HLYFWGYSEAAK			Both
MGST3	IASGLGLAWIVGR	VEYPIMYSTDPENGHIFNCIQR	VLYAYGYYTGEPSK		Both
NAT1	EQYIPNEEFLHSDLLEDSK	LDLETLTDILQHQIR	SYQMWQPLELISGK	Cytoplasm and Cytosol	Both
NAT2	DNTDLVEFK	TLTEEEVEEVLK			Ileum
SULT1A1	VHPEPGTWDSFLEK	THLPLALLPQTLLDQK			Both

SULT1A2	YFAEALGPLQSFQARPDDLLISTYPK	SLPEETVDLMVEHTSFK	VYPHPGTWESFLEK		Both
SULT1B1	MIYLAR	RGFITEK	NLNDEILDR		Both
SULT1E1	NHFTVALNEK	QLDEMNSPR	NNPSTNYTTLPDEIMNQK		Both
SULT2A1	SPWVESEIGYTALSETESPR	LFSSHLPIQLFPK	WIQSVPIWER		Both
TPMT	NQVLTLEEWQDK	TSLDIEEYSDTEVQK	SWGIDCLFEK		Both
TXN	PFFHSLSEK	CMPTFQFFK	TAFQEALDAAGDK	Nucleus and Cytoplasm	Both
ABCB1 (P-gp, MDR1)	FYDPLAGK	NVHFSYPSRK	SEIDALEMSSNDSR	Plasma membrane	Both
ABCB3 (TAP2)	EAVGGLQTVR	SFGAEEHEVCR	QDLGFFQETK	Endoplasmic reticulum	Both
ABCB7	VLSGISFEVPAGK	LQEEIVNSVK	LAGLHDAILR	Mitochondrion membrane	Both
ABCB8	IVALVGQSGGGK	FYDPTAGVVMLDGR	AMGVADEALGNVR		Both
ABCB10	VTQDSLAQATQLAEER	SFQGALEFK	TSLFSSILR		Ileum
ABCB11 (BSEP)	AADTIIGFEHGTAVER	STALQLIQR		Plasma membrane	Both
ABCC1 (MRP1)	EDTSEQVVPVLVK	GYIQMTPLNK	SPVYSHFNETLLGVSVIR		Colon
ABCC2 (MRP2)	YLGGDDLDTSAIR	LTIIPQDPILFSGSLR			Both
ABCC3 (MRP3)	SQLTIIPQDPILFSGTLR	IDGLNVADIGLHDLR	SPIYSHFSETVTGASVIR		Both

ABCC4 (MRP4)	APVLFFDR	AEAAALTETAK	ILTTEIGLHDLR		Both
ABCC6 (MRP6)	SSLASGLLR	APETEPFLR			Both
ABCD1	DQVIYPDSVEDMQR	VHEMFQVFEDVQR		Peroxisome membrane	Ileum
ABCD3	VGITLFTVSHR	IANPDQLLTQDVEK	LITNSEEIAFYNGNK		Both
ABCE1	ADIFMFDEPSSYLDVK	GTVGSILDRK	NTVANSPQTLLAGMNK	Mitochondrion and Cytoplasm	Both
ABCG2 (BCRP)	LFDSLTLLASGR	TIIFSIHQPR	LLSDLLPMR	Plasma membrane	Both
SLC15A1 (PEPT1)	CGFNFTSLK	HTLLVWAPNHYQVVK	WTLQATTMSGK	Membrane protein	Ileum
SLC16A1 (MCT1)	SITVFFK	DLHDANTDLIGRHPK	DLHDANTDLIGR	Plasma membrane	Both
SLC51A (OST-α)	LHLGEQNMGAK	NTLCPIK	VGYETFSSPDLDLNLK	Plasma membrane	Both
SLC51B (OST-β)	ETPEVLHLDEAK	DHNSLNNLR	PNLAQVELELK		Both
SLCO1A2 (OATP1A2)	IYDSTTFR	EGLETNADIIK		Plasma membrane	Both
SLCO1B1 (OATP1B1)	LNTVGIAK	YVEQQYGQPSSK			Ileum
SLCO2B1 (OATP2B1)	VLLQTLR	SSPAVEQQLLVSGPGK			Both

Table S6.5. Summary of input system parameters alterations in active CD population in relation to healthy/control based on literature collected data.

Physiological parameter	Active CD population
pH Proximal small intestine (fasted)	Duodenum = 6.8 Jejunum I & II = 6.9 & 7
pH Terminal small intestine (fasted)	Ileum (I-IV) = 7, 7.1, 7.2 & 7.4
pH Large intestine (fasted)	Colon = 6.7
Small intestine transit time (hr)	2.96
Colonic transit time (hr) (fasted)	Unaltered from normal values*
Gastric emptying time (hr) (fasted)	0.41
Small Intestine blood flow (% of cardiac output)	Male = 31 Female = 34
Liver blood flow (Q_H) (% of cardiac output)	Male= 25 Female = 27
Liver CYP3A4 [pmol/mg protein]	Male = 63 Female = 91.5
Serum Albumin (g/L)**	Unaltered from normal values in one simulation Female = 25.2 Male = 30.13
α1-AGP (g/L)	Female = 1.18 Male = 1.3

*No available information that support their alteration from normal values so Simcyp HV population values are used; ** Only around 20 % of CD population suffer from albumin drop based on the collected literature data so two simulations are carried out once with reduced albumin level and once with normal albumin level

Table S6.6. Input drug metabolising enzymes and transporters abundance values in Simcyp simulator, in the created active CD population in relation to healthy based on this study generated data.

Metabolising enzyme/ transporter	Small intestine (SI) (nmol/SI)				Colon (nmol/colon)			
	Inflamed CD	CV (%)	Histologically normal CD	CV (%)	Inflamed CD	CV (%)	Histologically normal CD	CV (%)
CYP3A4	8.6	75.3	15.6	81.4	Change was assumed to be similar to the changed detected in ileum as it was below LLOQ in our colon tissues			
CYP3A5	2.48	100	0.18	N/A				
CYP2D6	0.39	67.5	N/A	N/A				
UGT2B7	1.28	96.6	1.6	65.1	Not applicable			
P-gp*	0.11	88.2	0.08	61.7	0.3	73.6	0.19	89.1
MRP2*	0.19	43.7	0.35	N/A	No change from default healthy			
BCRP*	0.17	58.2	0.1	11.3	No change from default healthy		0.22	48
OATP2B1*	0.15	79.9	0.15	N/A	No change from default healthy			

N/A, no data as the value can't be calculated due to insufficient data points or been not detected, thus default healthy values are used; *The ileum and colon transporters distribution are incorporated and expressed relative to the abundance in the jejunum.

Table S6.7. Demographics of the virtual individuals of budesonide and midazolam implemented in Simcyp simulator, PBPK-based simulation workflow and their corresponding trial design parameters.

Trial parameter	Budesonide [1]	Midazolam [2]
Oral Dose	18 mg	100 µg
Number of individuals/ trials	10 trials with 10 virtual individuals (100 virtual subjects)	
CD population age range	21–63 years	25–65 years
CD female / male	50% female (3/3) 3 active and 3 inactive	87% (7/1) all active
Duration of the study (hr)	40	10
Fed/ fasted	Fed	Fasted

6.8.Supplementary material – Results

Table S6.8. Comparison of predicted and observed PK parameters and their fold change in active CD populations with the different applied models (M-1, M-2, M-3 & M-4) of oral budesonide controlled release formulation under fed conditions.

Parameter	**$AUC_{0-\infty}$ (nmol*h/L)**			**Cmax (nM)**			**Tmax (h)**			**F (%)**		
Model	Predicted	Observed Mean, 95% CI	Predicted/ Observed	Predicted	Observed Mean, 95% CI	Predicted/ Observed	Predicted	Observed Mean, 95% CI	Predicted/ Observed	Predicted	Observed Mean, 95% CI	Predicted/ Observed
M-1	235.6	114, (81.4-159.5)	2.1	28.67	14.3, (6-13.7)	2	5.23	6, (3-8)	0.87	38	20.5, (8.8-15)	1.85
M-2	195		1.71	22.43		1.57	5.38		0.9	27		1.32
M-3	243.6		2.14	29.2		2.04	5.23		0.87	35		1.71
M-4	202.9		1.78	22.93		1.6	5.37		0.9	26		1.27

M-1, Model 1 CD population with intestine DMETs abundance data from I-CD tissues and normal albumin level; M-2, Model 2 CD population with intestine DMETs abundance data from I-CD tissues and reduced albumin level; M-3, Model 3 CD population with intestine DMETs abundance data from HN-CD tissues and normal albumin level; M-4, Model 4 CD population with intestine DMETs abundance data from HN-CD tissues and reduced albumin level.

Table S6.9. Comparison of predicted and observed PK parameters and their fold change in active CD populations with the different applied models (M-1, M-2, M-3 & M-4) of oral midazolam solution formulation under fasted conditions.

Parameter	**AUC0-∞ (nM*h)**			**Cmax (nM)**			**Tmax (h)**			**F (%)**		
Model	Predicted	Observed Mean ±SD	Predicted/ Observed	Predicted	Observed Mean ±SD	Predicted/ Observed	Predicted	Observed Mean ±SD	Predicted/ Observed	Predicted	Observed Mean ±SD	Predicted/ Observed
M-1	9.52	14±6.38	0.68	4.04	8.4±5.13	0.48	0.5	0.53± 1.3	0.94	52	31±22	0.6
M-2	5.18		0.37	2.92		0.35	0.38		0.72	40		0.78
M-3	8.61		0.62	3.71		0.44	0.49		0.92	47		0.66
M-4	4.67		0.32	2.65		0.32	0.37		0.7	36		0.86

M-1, Model 1 CD population with intestine DMETs abundance data from I-CD tissues and normal albumin level; M-2, Model 2 CD population with intestine DMETs abundance data from I-CD tissues and reduced albumin level; M-3, Model 3 CD population with intestine DMETs abundance data from HN-CD tissues and normal albumin level; M-4, Model 4 CD population with intestine DMETs abundance data from HN-CD tissues and reduced albumin level.

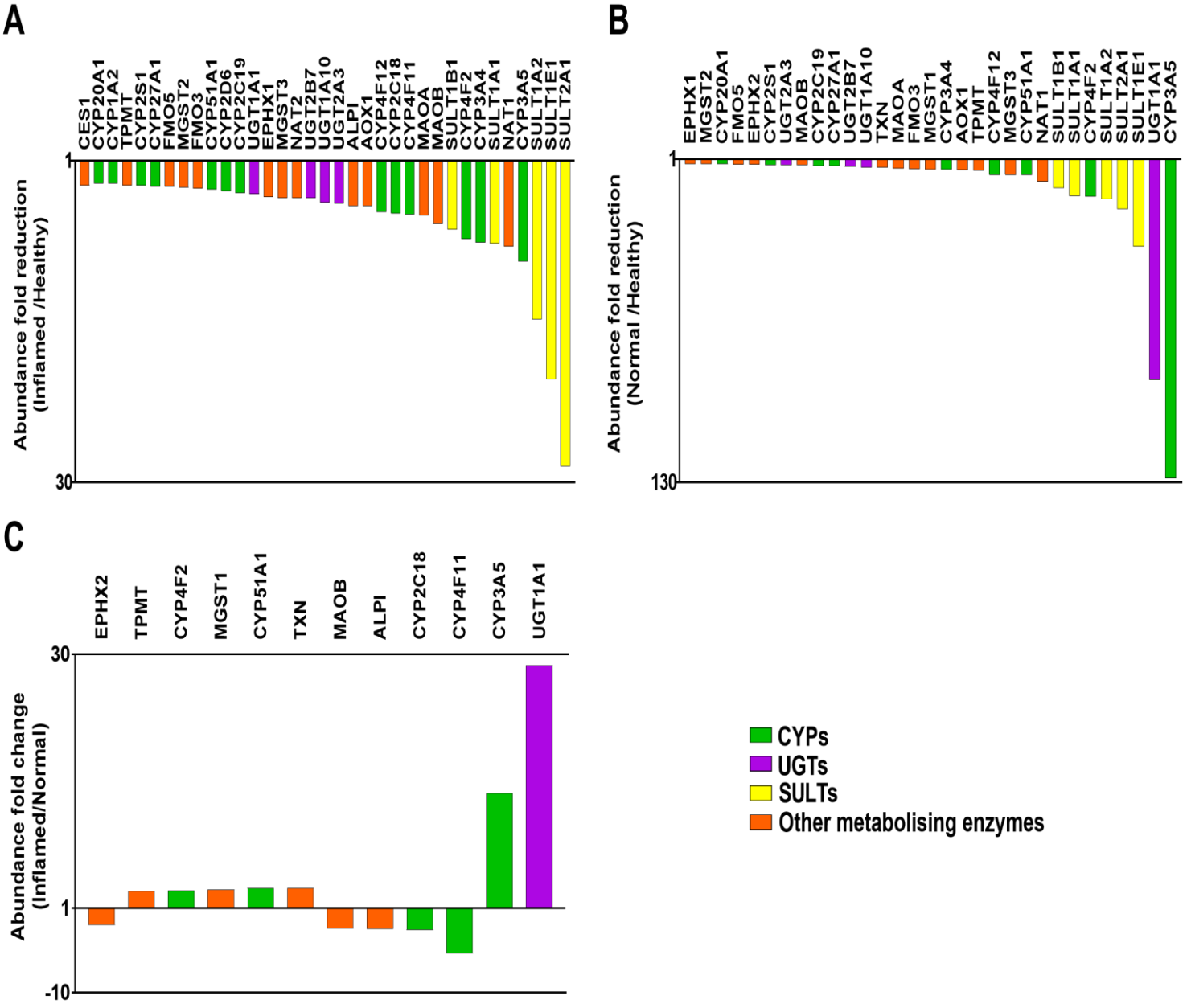

Figure S6.1. *Relative change of DMEs (CYPs, UGTs, SULTs and other enzymes) expression from healthy ileum individual samples (n=5), inflamed CD ileum (n=6) and histologically normal CD ileum (n=2). Change in expression is shown for* ***(A)*** *inflamed relative to healthy,* ***(B)*** *histologically normal relative to healthy and* ***(C)*** *inflamed relative to histologically normal. Only fold change ≥2 is considered.*

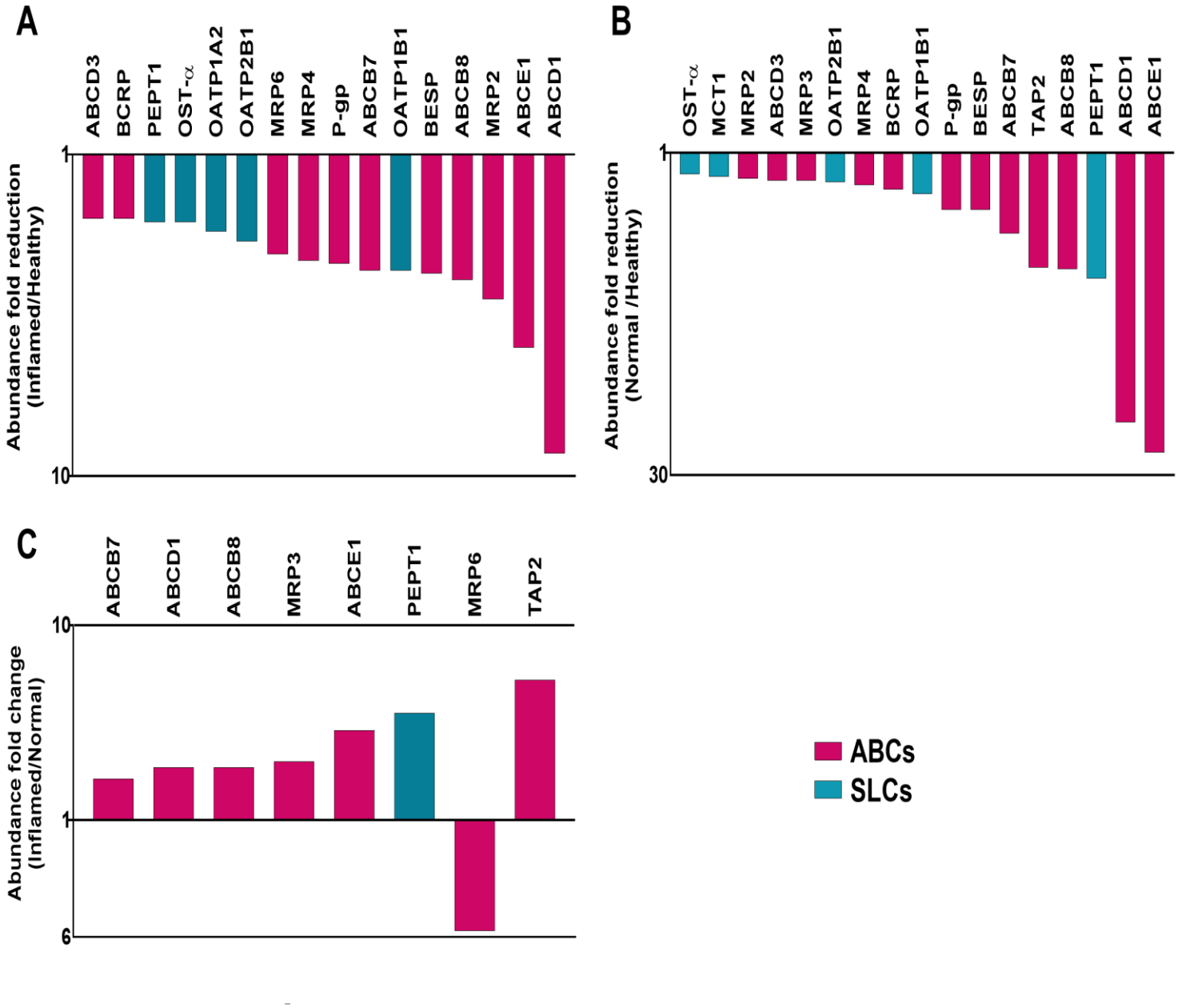

Figure S6.2. *Relative change of Drug transporters (ABC and SLC) expression from healthy ileum individual samples (n=5), inflamed CD ileum (n=6) and histologically normal CD ileum (n=2). Change in expression is shown for* ***(A)*** *inflamed relative to healthy,* ***(B)*** *histologically normal relative to healthy and* ***(C)*** *inflamed relative to histologically normal. Only fold change ≥2 is considered.*

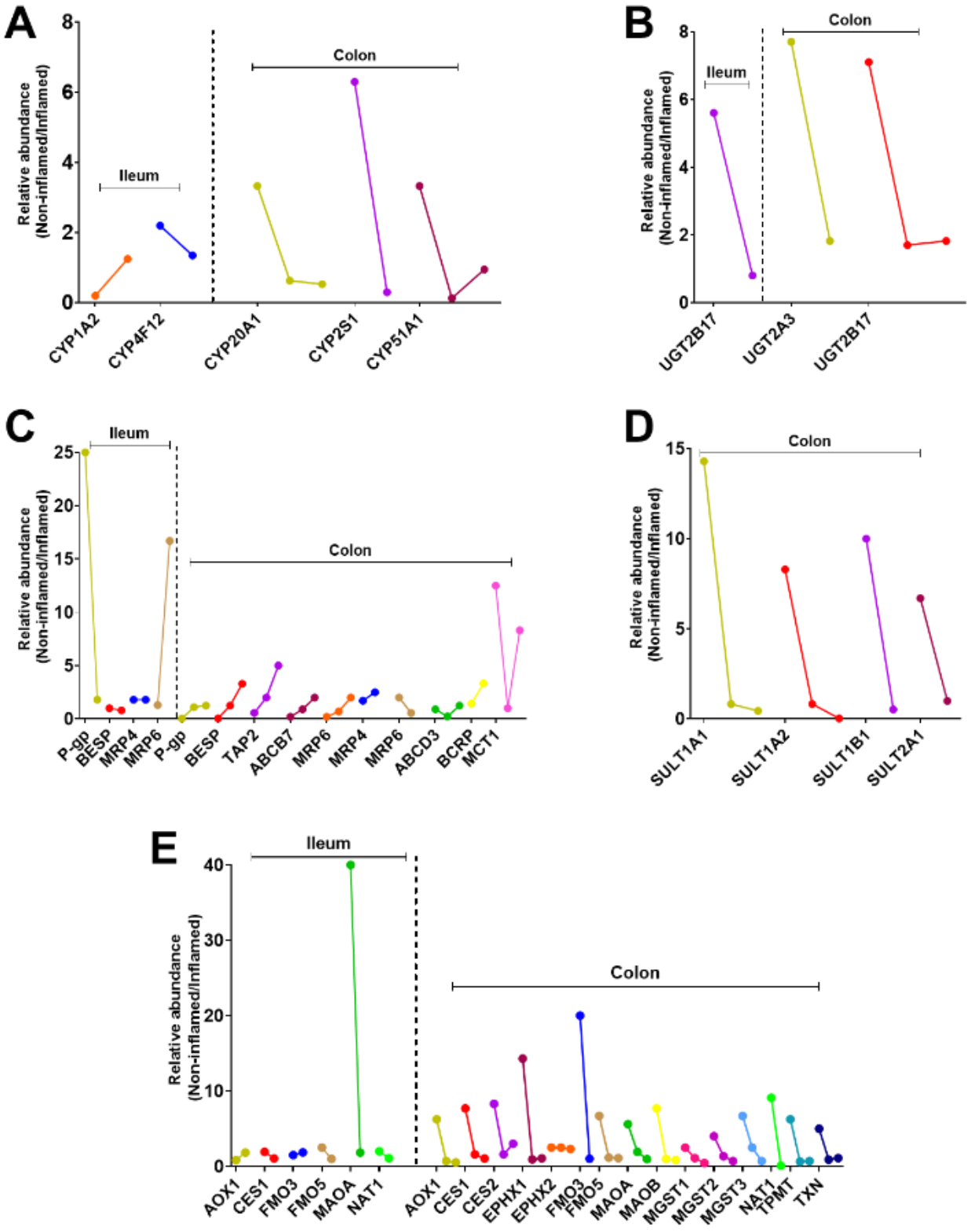

Figure S6.3. *Relative abundance of* ***(A)*** *CYPs, (B) UGTs,* ***(C)*** *transporters,* ***(D)*** *SULTs and* ***(E)*** *other metabolising enzymes in histologically normal ileum (n=2) and colon (n=3) to their matched inflamed samples.*

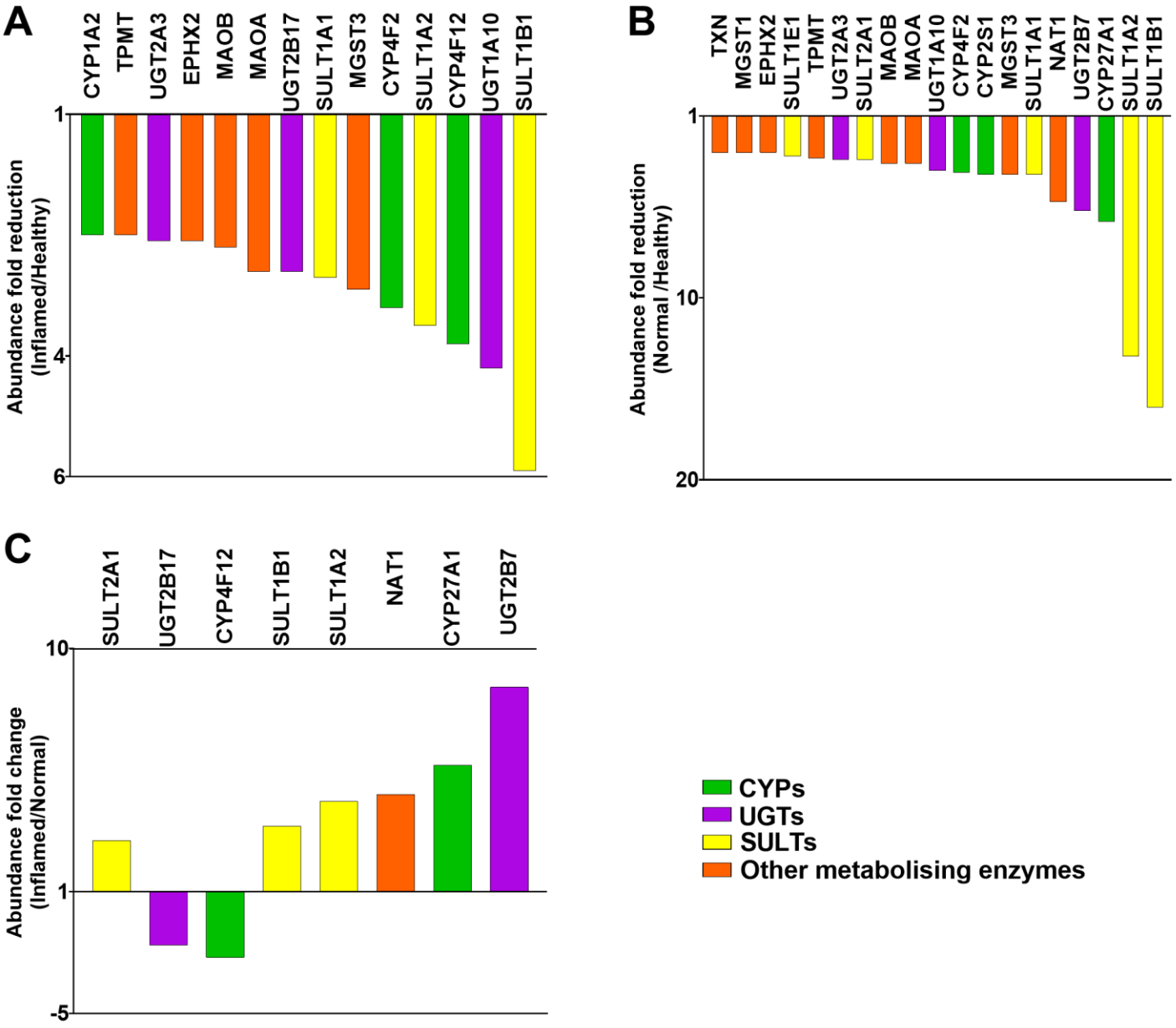

Figure S6.4. *Relative change of DMEs (CYPs, UGTs, SULTs and other enzymes) expression from healthy colon individual samples (n=5), inflamed CD colon (n=7) and histologically normal CD colon (n=5). Change in expression is shown for* ***(A)*** *inflamed relative to healthy,* ***(B)*** *histologically normal relative to healthy and* ***(C)*** *inflamed relative to histologically normal. Only fold change ≥2 is considered.*

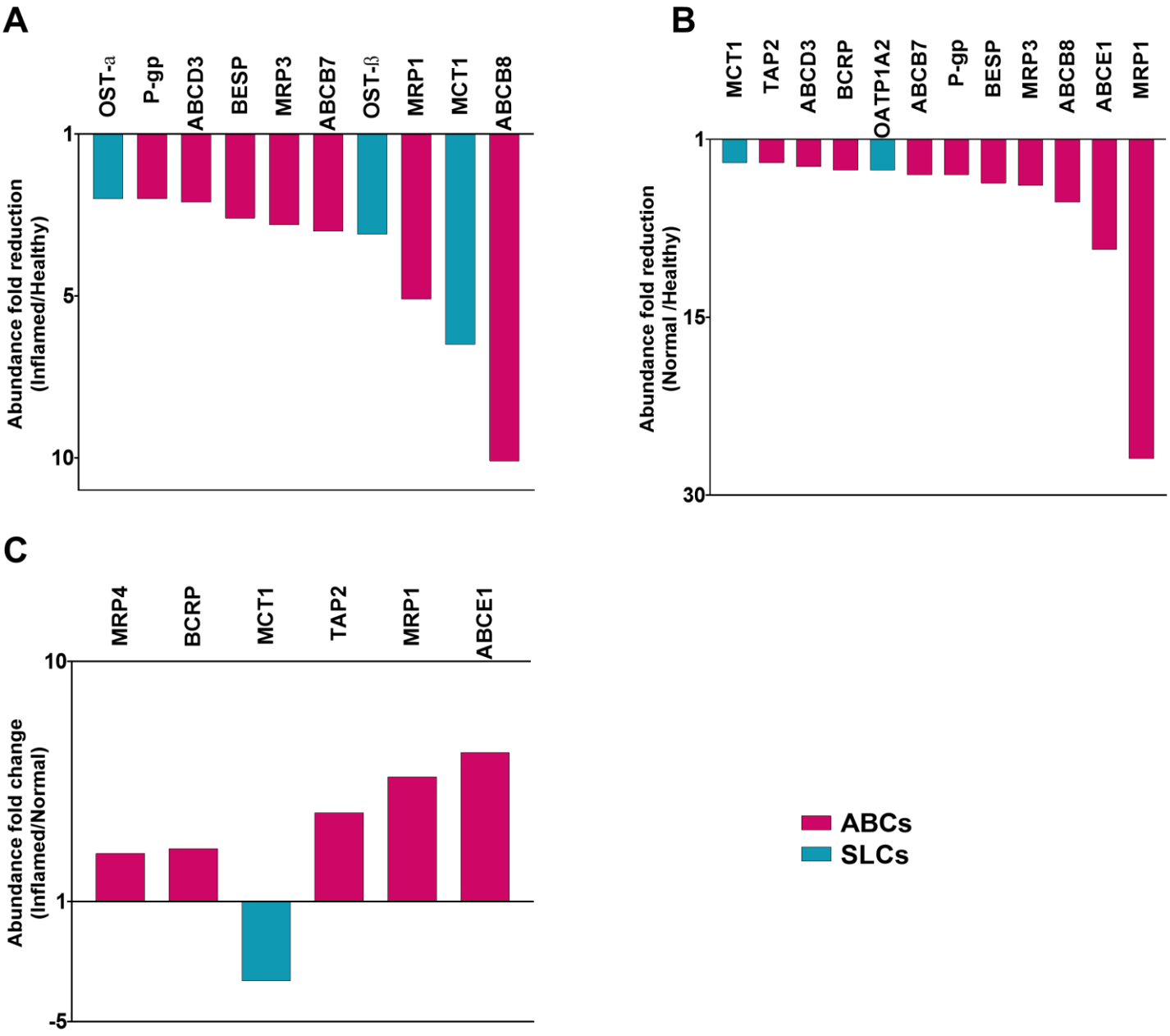

Figure S6.5. *Relative change of Drug transporters (ABC and SLC) expression from healthy colon individual samples (n=5), inflamed CD colon (n=7) and histologically normal CD colon (n=5). Change in expression is shown for* ***(A)*** *inflamed relative to healthy,* ***(B)*** *histologically normal relative to healthy and* ***(C)*** *inflamed relative to histologically normal. Only fold change ≥2 is considered.*

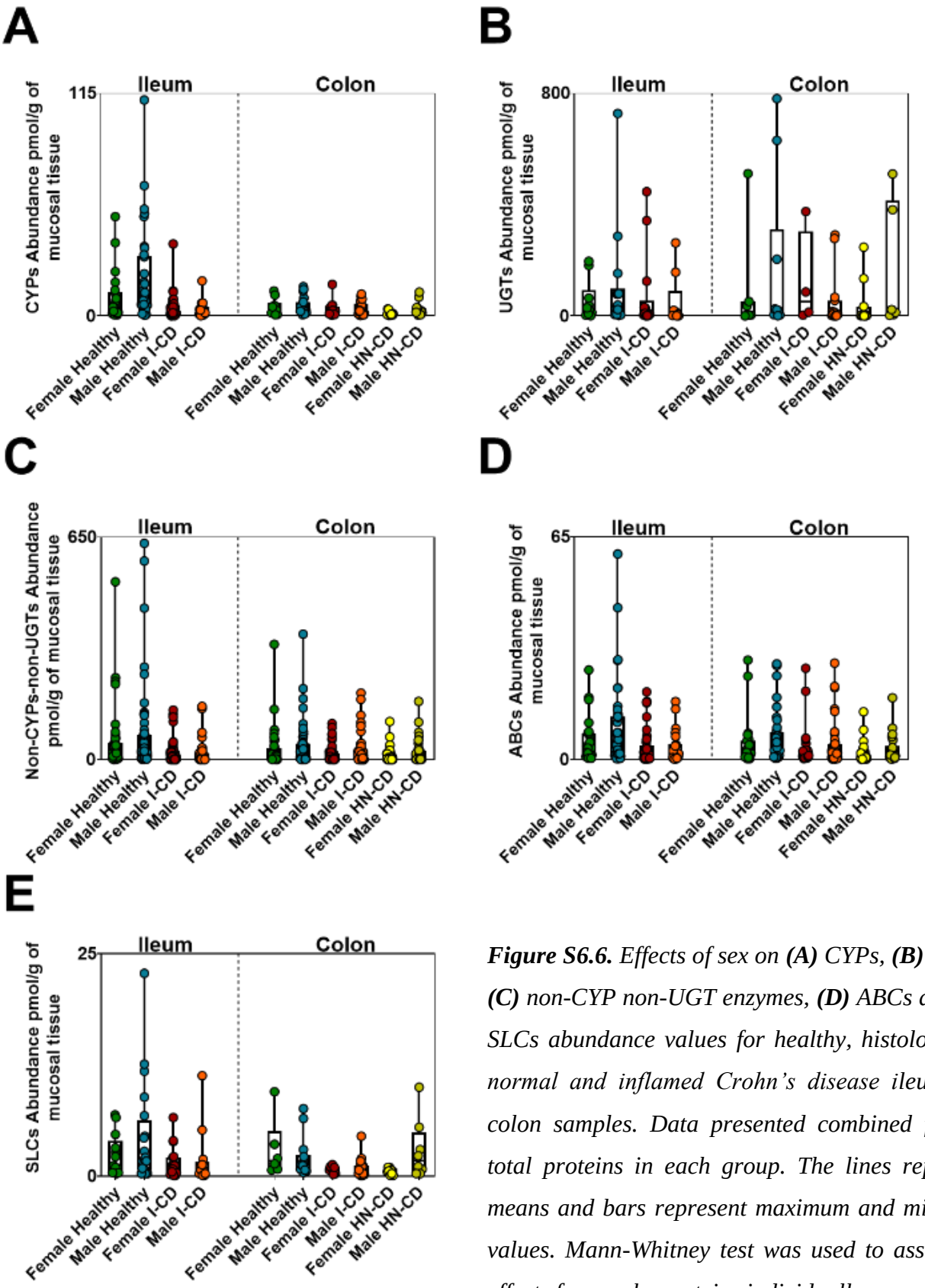

Figure S6.6. *Effects of sex on* ***(A)*** *CYPs,* ***(B)*** *UGTs,* ***(C)*** *non-CYP non-UGT enzymes,* ***(D)*** *ABCs and* ***(E)*** *SLCs abundance values for healthy, histologically normal and inflamed Crohn's disease ileum and colon samples. Data presented combined for the total proteins in each group. The lines represent means and bars represent maximum and minimum values. Mann-Whitney test was used to assess the effect for each protein individually per sample where no significant relation ($p > 0.05$) was found.*

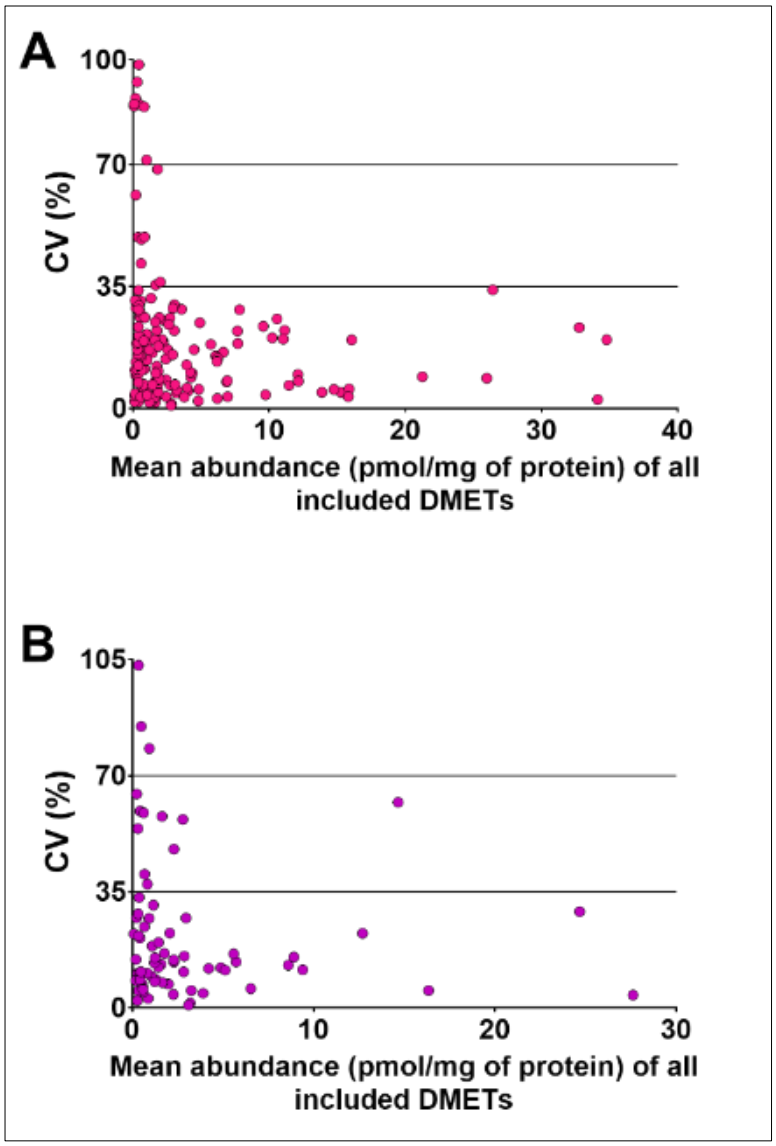

Figure S6.7. *Technical variability of* ***(A)*** *Ileum DMETs and* ***(B)*** *Colon DMETs represented by percent coefficient of variations (%CV) for different targets in a set of 5 ileum and 3 colon samples (prepared in triplicates).*

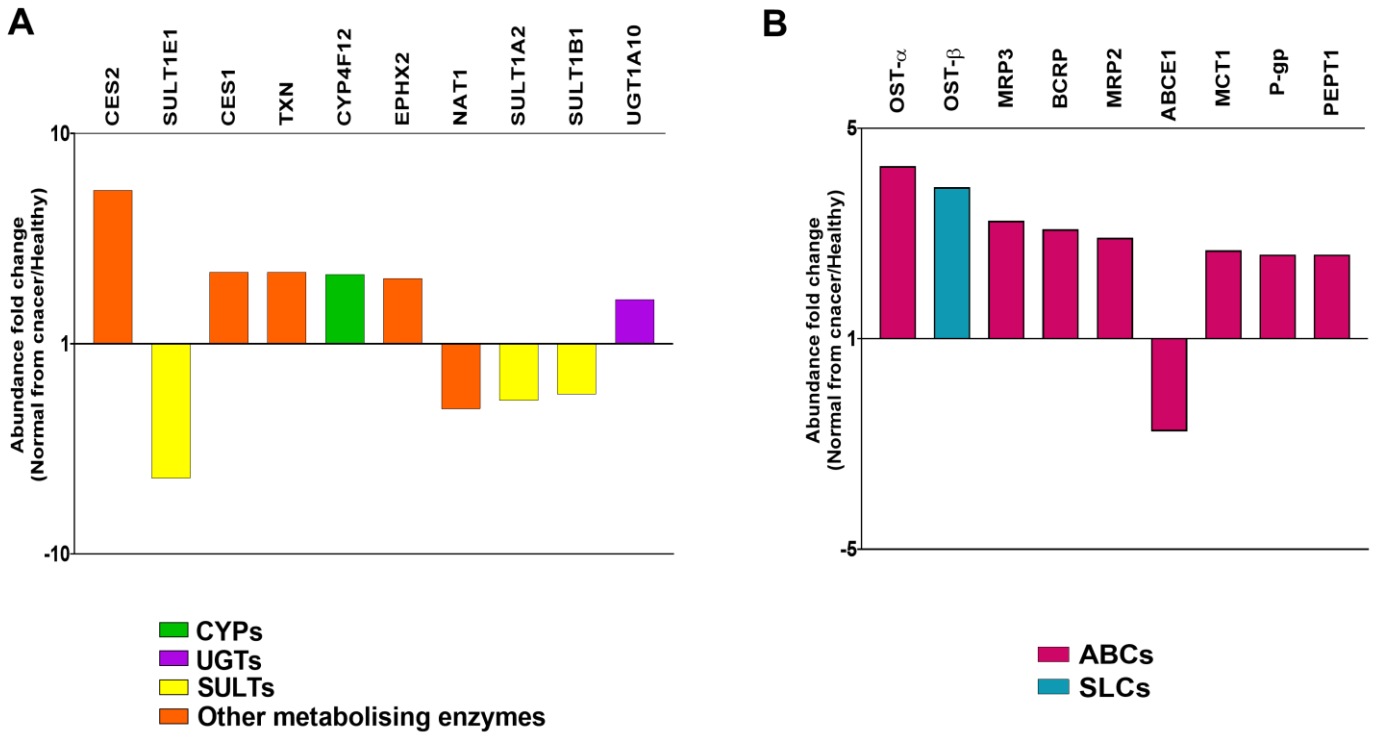

Figure S6.8. *Relative change of DMETs (CYPs, UGTs, SULTs, other enzymes, ABCs and SLCs) expression from healthy ileum individual samples (n=5) and histologically normal ileum from cancer patients (n=4). Change in expression is shown for* ***(A)*** *DMEs (CYPs, UGTs, SULTs and other enzymes) and* ***(B)*** *ABC transporters and SLCs. Only fold change ≥2 is considered.*

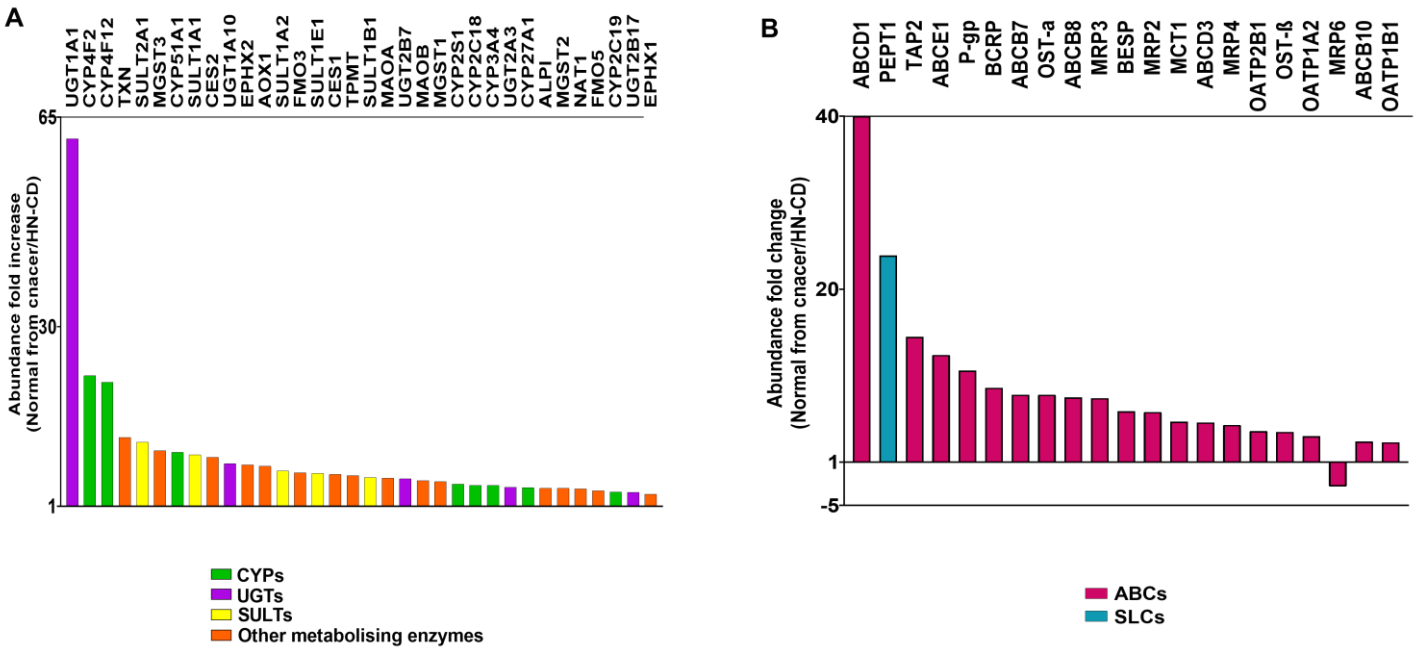

Figure S6.9. *Relative change of DMETs (CYPs, UGTs, SULTs, other enzymes, ABCs and SLCs) expression from histologically normal CD ileum individual samples (n=2) and histologically normal ileum from cancer patients (n=4). Change in expression is shown for* ***(A)*** *DMEs (CYPs, UGTs, SULTs and other enzymes) and* ***(B)*** *ABC transporters and SLCs. Only fold change ≥2 is considered.*

6.9.Supplementary material-References

1. Edsbäcker S., Bengtsson B., Larsson P., Lundin P., Nilsson Å., Ulmius J., et al. A pharmacoscintigraphic evaluation of oral budesonide given as controlled-release (Entocort) capsules. *Aliment Pharmacol Ther* 2003;**17**(4):525–36. Doi: 10.1046/j.1365-2036.2003.01426.x.

2. Wilson A., Tirona RG., Kim RB. CYP3A4 Activity is Markedly Lower in Patients with Crohn's Disease. *Inflamm Bowel Dis* 2017;**23**(5):804–13. Doi: 10.1097/MIB.0000000000001062.

Chapter Seven: Conclusion and Future Work

7.1.Defining the needs for Crohn's disease population

The intestine is an important organ for absorption and first-pass metabolism of oral drugs. The upper (duodenum, jejunum and ileum) and the colon segments of the intestine participate largely in the determination of oral drugs bioavailability. The extent of the influence by each segment on the drug bioavailability is governed by the drug physiochemical properties and formulation. In Crohn's disease (CD) population the intestine endures physiological and structural modifications caused by the inflammatory nature of the disease. These modifications causes alteration of the absorption and first-pass metabolism process of oral drugs, hence their pharmacokinetic (PK) profile from healthy population. The intestine pH, motility, hemodynamic, secretions, wall thickness, epithelial cells turnover rate and cellular compositions encounter changes in CD. Some of these changes correlate with the severity if the disease like the superior mesenteric artery (SMA) blood flow. The ileum and colon segments are the most commonly affected segments by Crohn's disease and changes in their morphology due to inflammation causes change in their function which affect the absorptive and metabolic capacity of the intestine. Moreover, the inflammatory effect is not localised but rather systemically distributed. The liver and blood proteins (known to bind to the drug in the systemic circulation) like albumin and α1-AGP are shown to be altered in CD patients. [1–5] The degree of the change in the physiological parameters varies based on the activity state of the disease. This results in high variations in drug PK response between active and inactive CD patients and when compared with healthy subjects, which add to the challenge of precision dosing and optimising the clinical outcome. To minimise none evidence-based practice of oral drugs dosing in CD patients, a dedicated clinical studies on CD patients should be included. This practice would take a long time to be implemented, as it requires great effort, time and resources. Thus, a convenient and cost effective alternative is the use of physiological based pharmacokinetic (PBPK) models for prediction of pharmacokinetic parameters. In order to build a reliable and reproducible model a population-specific systems parameters are required which can be generated from *in vitro* assays. *In vitro-in vivo extrapolation* (IVIVE) approach, have been increasingly used for the prediction of drug PK over the last two decades.[6]

Little is known about the intestine drug related parameters in CD patients; especially the expression of drug metabolising enzyme and transporter proteins (DMETs). Generalising the current knowledge on the whole population can result in misleading predictions. DMETs are

major contributors in oral drugs PK behaviour. These proteins reside in the mucosal layer of the gut wall with varying distribution of abundance. Changes of the DMETs in the inflamed intestine during the course of the disease are essential to be addressed and identified at this stage. This is in order to measure the extent of the effect of the altered abundance of DMETs on oral drug PK. Although the upper intestine segments, specifically the jejunum, play a major role in oral drug disposition, they are not usually inflamed hindering the feasibility to source such tissue samples. The focus here is on the ileum and colon segments from inflamed and normal tissues from CD patients. This to achieve the main aim of this project, to fill the gap in regard to the intestine drug related parameters to create an active CD population with a more reliable predictability.

7.2.What this project adds to the previous knowledge

In the current thesis, an extensive literature search was carried out in Chapter One, to identify the current knowledge of drug related system parameters in CD population. To allow prediction of oral drug bioavailability in CD patients, the literature data were critically analysed and the gaps were identified and prioritised to be filled in order to build a CD population-based PBPK model. Previous reviews are available on the same topic but none of the reviews considered segregation between the active and inactive phases of the disease and focused on the two phases as different CD populations. The reports regarding the investigated system parameters (intestine related; pH, small and large intestine transit time, intestine blood flow, etc., and none intestine related; albumin level, etc.) are highly different between the two states of the disease. The previews knowledge reports the reduction of the intestine blood flow but without linking it to the drug PK in this disease population, although, its effect is pronounced on drugs with high extraction ratio as the case with budesonide. From this literature gap analysis, two main gaps are identified and need to be covered, the drug enzymes and transporters abundance/activity of the intestine and liver in CD patients. This is in both phases the active and the inactive. The observed heterogeneity of CD population either between the active and inactive phases of the disease or between patients during the same phase makes it very challenging to create a unified CD population model. Our focus is on the active stage of the disease since the patients in this stage suffer from uncontrolled disease symptoms, usually end up requiring surgery and the alteration of the reported system parameters are more severe than the inactive stage when compared with healthy population. In general, change in the drugs PK profile from *in vivo* studies was significant in active CD patients,[1,7,8] while inactive did not report significant changes from control group.

To measure the DMETs abundance in the ileum and colon tissues, LC-MS/MS quantitative proteomics is used. This method has successfully provided proteins expression data in various tissues including the intestine. The abundance data extracted are based on the protein level rather than the gene level and a large number of output data are given in a single run, which allow for a wider coverage of several desired proteins. This method is comprehensively reviewed in Chapter Two, in this chapter the different quantitative proteomic techniques, basic guidance of the technique to be used based on the samples nature and the method application in translational pharmacology are highlighted. From the information provided in this review a decision was made to use the QconCAT methodology for quantifying the protein targets. Unfortunately, this method was not successful with our samples for several reasons (Chapter Five). The most important reason was the lack of an equipped LC-MS instrument with the targeted proteomic approach that supports the pre-selection of the surrogate peptides despite their intensity and the complexity of the used sample. Therefore, quantification of the desired proteins was carried out by the label free method using unlabelled standard.

Several techniques used in each step of LC-MS based quantitative proteomics, which might lead to variation in the results by the different methods. The performance of the different techniques with our diseased and normal tissue samples in terms of the quantity and quality of the resultant data is unknown. Some of these methods have been applied and optimised in previous studies utilising tissue samples from none disease donors, which caused uncertainty at the start of this project. Thus, in Chapter Three a comparative analysis between the different techniques used in proteomics methodology steps are carried out using inflamed and normal ileum and colon tissues. This included enterocytes isolation; as the DMETs are impeded in the enterocytes, proteolytic digestion, subcellular fractionation, the LC-MS instrument, and the analysing software which was determined in Chapter Five. The results gives more confidence in using the elected methods (EDTA enterocytes elution, FASP digestion, homogenate fraction, QE mass spectrometer and MaxQuant data analysis software) with the diseased samples, which bare different amounts and concentrations. The detection and quantification of the primary targeted proteins (CYP and UGT enzymes, ABC transporters and SLCs) was the ruling end point in regards to the methods to be used.

The quality of the data generated after applying the selected methods based on Chapter Three was tested in Chapter Four. A pilot study of CD impact on DMETs using pooled samples from inflamed, histologically normal and healthy ileum and colon tissues. This study highlighted what to expect from such set of samples and provided for the first time abundance data of

DMETs in CD patients relative to healthy abundance. The results showed a marked reduction of several important enzymes; CYP3A4, CYP2J2, CES1, MGST1 ALPI, SULT1A2, SULT1B1 and SULT2B1 and MCT1 transporter. The reduction of some of targets was up to ≥10 fold in inflamed and non-inflamed ileum and colon compared to healthy samples. Few of the targets showed fold increase in CD samples compared to healthy. This increase was up to ≥2 fold with UGT1A1, MGST1, MGST2, MAOA and ALPI. Also, a wider coverage of the Solute carriers (SLC) and none CYP & none UGT enzymes was provided. These proteins can serve purposes other than directly being involved in drugs PK; such as cell maintenance and regulation of its ionic, pH and acid-base balance which affects cells growth and detoxification.

The absorption and first-pass metabolism by the intestine is an important parameter for the prediction of oral drug exposure. *In vitro* data relevant to drug clearance and bioavailability need to be extrapolated from inflamed tissue and the surrounding normal tissue of CD patients. In Chapter Six, such data are extracted for the first time from individual samples by measuring the absolute abundance of DMETs. The use of individual tissue samples allowed statistical, inter-individual variability and proteins & demographics covariates correlation analysis of the abundance data. In addition to absolute expression levels, disease perturbation factor (DPF) was provided. This represents alteration in protein expression due to disease as a ratio relative to what is observed in healthy individuals, which Increases the confidence in the generated results regarding the disease effect on DMETs expression. All the quantified enzymes and transporters were lower in Crohn's disease ileum and colon relative to healthy. This indicates a potential reduction in their substrates' metabolism and/or absorption in CD patients. Significant reduction was reported with important enzymes and transporters; CYP3A4, UGT1A10, AOX1, NAT1, SULT1A1, SULT1A2, SULT1B1, SULT1E1, SULT2A1 and BCRP, MRP4. Inter-individual variability of ileal and colon samples was high in all studied tissues for the majority of the proteins targets, but slightly higher among the Crohn's samples compared to healthy. The generated abundance data of relevant DMETs was integrated along with other identified system parameters in the created active CD population in order to improve the PBPK simulation and prediction for Crohn's disease patients. The disease effect showed differences in drug systemic exposure when using CD-specific abundance data instead of the healthy population data on 10 oral drugs using Simcyp simulator. From these 10 drugs verapamil showed the highest alteration in its exposure which is in agreement with the clinical observation when it was given to active CD patients.[7] The simulated clinical data of 2 oral drugs in CD patients showed a ≤ 2 fold predicted-to-observed ratio of PK parameters outcomes.

Changes in DMETs expressions with Crohn's disease in inflamed and normal tissues, and application of the multiple parameters together in PBPK models were extensively investigated in this thesis. By providing this data the intestine contribution and causative factors in the observed alterations of oral drugs PK in CD patients are now clearer than ever. Nevertheless, the true influence of the duodenum, jejunum and the liver are yet to be explored and identified.

7.3.Future work

The abundance data of the different DMETs can be measured again by the QconCAT targeted proteomic method, after applying the required modifications of increasing the spiked amount of the QconCATs, increasing the running time of the LC-MS to three hours instead of the used 90 minutes and further fractionation of the homogenate to a more pure factions to enrich the presence of the targeted DMETs. Details of the recommended modifications are mentioned in Chapter Five, this is to confirm the feasibility of the constructed QconCATs with the intestine samples from CD and healthy tissues. The homogenate samples bear the advantage of reserving all the subcellular fractions, thus, it can be used to further investigate the presence of inflammatory and other CD biomarkers reside in any of the cell components. This can go beyond the application of proteomics in PBPK, as it might allow for better understanding of the disease manifestation and differentiation from other form of bowel inflammation as well as discovery and development of pharmacology targets. Additionally, more purified fractions can be generated by further centrifugation to enrich the desired DMETs which were masked by the complexity of the homogenate fraction. The fractions that can be generated and contain DMETs of significance to our research purpose are microsomal fraction for CYPs and UGTs, cytosolic fraction for SULTs and other non-CYP non-UGT enzymes and membrane fraction for ABC and SLC transporters. Other cellular components result from the fractionation process, such as mitochondria and nucleus, can be preserved for further analysis and exploring of CD markers that cannot be detected in the homogenate. Further fractionation of the homogenate can be executed to generate fractions more specific for a set of protein targets where disease scaling factors can be measured in protein per whole intestine (PPI) (MPPI; from microsomal fraction, CPPI; from cytosolic fraction and TMePPI; from total membrane fraction). The scaling factors can be used for IVIVE of the intestine drug metabolism and absorption, and reflects its absorptive and metabolic capacity in the disease state. The availability of the intestine scaling factors from CD patients allow determination of the intestine intrinsic clearance, which improves the prediction outcome of oral drug exposure in this population.

It is important to measure the catalytic or absorptive activity of the main drug metabolising enzymes and transporters in the intestine tissue from CD patients compared to healthy. Using a specific probe for the targeted protein, the activity assay measures the actual metabolic or absorptive activity of the enzyme/transporter in the diseased and healthy samples. This can be done using the available homogenate samples used for measuring the abundance in this project. Also this allows for examining the degree of correlation between the protein activity and its abundance, which enhance the confidence in the results of the PBPK applications based on the proteomics data. Although PBPK applications were carried out in this project, it was limited to the drugs with available ADAM absorption model which allows testing of the intestine different segments. These drugs are not diverse in term of the formulation, physiochemical properties and their substrate/inhibitor nature. Thus, it would be useful to assess the impact of the observed reduction of the DMETs in CD on oral drugs with varying formulations other than solution and immediate release formulations. Also application on drugs metabolised by enzymes other than CYPs are warranted to have a wider coverage and better view of CD impact. To do so creation of oral drug profiles in Simcyp simulator with ADAM or M-ADAM absorption model is encouraged.

To have a complete picture of the intestine physiological alterations in the active and remission states of CD, inflamed and non-inflamed tissue samples from patients in each CD activity state, would allow a clearer differentiation between the proteomic profiles of the two disease states. An even better situation would be sourcing theses samples from the same patient when going through the two disease states. Sourcing inflamed and non-inflamed tissue samples from the same patient wold be very beneficial to investigate the actual magnitude of change of DMETs abundance compared with healthy when excluding the external factors that can affect the protein abundance profile such as patient's age, nutrition and medical history. It would be helpful to source a larger number of inflamed and normal tissues with known levels of inflammation severity to be able to link the degree of CD severity to the observed reduction of the DMETs expression. Little is known about the expression of DMETs in the upper (duodenum and jejunum) none inflamed intestinal segments and the liver, hence, their impact on oral drug pharmacokinetics and the simulation outcome. Liquid biopsy is a promising technique that allows quantification of desired proteins where sourcing tissue biopsies is challenging. The intestine permeability should be addressed separately by measuring the disruption of the tight junction due to the inflammatory effect caused by CD. This disruption can lead to a leaky intestine which can impact the oral drug absorption and bioavailability. If

these applications are to be carried out, the whole picture of Crohn's disease impact on the fate of the oral drugs and their PK behaviour will be clear and will lead to a better implementation of precision dosing practice and better clinical outcomes in this population.

7.4.References

1. Wilson A., Tirona RG., Kim RB. CYP3A4 Activity is Markedly Lower in Patients with Crohn's Disease. *Inflamm Bowel Dis* 2017;**23**(5):804–13. Doi: 10.1097/MIB.0000000000001062.

2. Ricci G., Ambrosi A., Resca D., Masotti M., Alvisi V. Comparison of serum total sialic acid, C-reactive protein, α1-acid glycoprotein and β2-microglobulin in patients with non-malignant bowel diseases. *Biomed Pharmacother* 1995;**49**(5):259–62. Doi: 10.1016/0753-3322(96)82632-1.

3. Suzuki Y., Matsui T., Ito H., Ashida T., Nakamura S., Motoya S., et al. Circulating Interleukin 6 and Albumin, and Infliximab Levels Are Good Predictors of Recovering Efficacy After Dose Escalation Infliximab Therapy in Patients with Loss of Response to Treatment for Crohn's Disease. *Inflamm Bowel Dis* 2015;**21**(9):2114–22. Doi: 10.1097/MIB.0000000000000475.

4. Liu X., Wu X., Zhou C., Hu T., Ke J., Chen Y., et al. Preoperative hypoalbuminemia is associated with an increased risk for intra-abdominal septic complications after primary anastomosis for Crohn's disease. *Gastroenterol Rep* 2017;**5**(4):298–304. Doi: 10.1093/gastro/gox002.

5. Nguyen GC., Du L., Chong RY., Jackson TD. Hypoalbuminaemia and Postoperative Outcomes in Inflammatory Bowel Disease: the NSQIP Surgical Cohort. *J Crohn's Colitis* 2019;**13**(11):1433–8. Doi: 10.1093/ecco-jcc/jjz083.

6. Rostami-Hodjegan A. Physiologically Based Pharmacokinetics Joined With In Vitro–In Vivo Extrapolation of ADME: A Marriage Under the Arch of Systems Pharmacology. *Clin Pharmacol Ther* 2012;**92**(1):50–61. Doi: 10.1038/clpt.2012.65.

7. Sanaee F., Clements JD., Waugh AWG., Fedorak RN., Lewanczuk R., Jamali F. Drug−disease interaction: Crohn's disease elevates verapamil plasma concentrations but reduces response to the drug proportional to disease activity. *Br J Clin Pharmacol* 2011;**72**(5):787–97. Doi: 10.1111/j.1365-2125.2011.04019.x.

8. Edsbäcker S., Bengtsson B., Larsson P., Lundin P., Nilsson Å., Ulmius J., et al. A pharmacoscintigraphic evaluation of oral budesonide given as controlled-release (Entocort) capsules. *Aliment Pharmacol Ther* 2003;**17**(4):525–36. Doi: 10.1046/j.1365-2036.2003.01426.x.